“Insights into the interplay between sumoylation of chromatin-associated proteins and DNA”

Nicola Zilio

University College London

and

Cancer Research UK London Research Institute

Ph.D. supervisor: Helle Ulrich

A thesis submitted for the degree of

Doctor of Philosophy

University College London

December 2010

Declaration

I, Nicola Zilio, confirm that the work presented in this thesis is my own. Where information has been derived from other sources, I confirm that this has been indicated in the thesis.

Abstract

The maintenance of correct genome sequence is an essential cellular process in which the small ubiquitin-like modifier SUMO plays an important role, probably because its post-translational conjugation to certain proteins can regulate DNA metabolism. The identities of these proteins remain largely unknown, as do how their sumoylation is controlled or what effects their modification has. I was therefore interested in identifying such factors and studying the upstream signals and downstream consequences of their sumoylation, with a particular focus on how DNA may be involved in these processes.

To address this problem, I initially used *Xenopus laevis* egg extracts to isolate and identify SUMO conjugates from replicating chromatin, as it should be enriched for proteins involved in DNA metabolism. I found that progression through S phase, but not genotoxic stress, altered the abundance of chromatin-associated SUMO conjugates. A proteomic analysis of these species during unperturbed and disrupted S phase identified several proteins with a role in DNA metabolism as putative sumoylation substrates. Some of these modification events were confirmed by western blotting and were also shown to be conserved in the budding yeast *Saccharomyces cerevisiae*.

By further investigating the modification of one of the candidates I discovered, *i.e.* ORC1, the largest subunit of the six-membered origin recognition complex (ORC), I found that all of the ORC subunits were sumoylated. I, however, also observed that manipulating the general levels of sumoylation in either egg extracts or budding yeast did not affect the recognized functions of ORC in DNA replication, thus indicating that sumoylation does not play a significant role in such a process.

I therefore focused on the sumoylation of another candidate I found in my screen, the DNA-break sensor poly(ADP-Ribose) polymerase 1, PARP-1. *In vitro*, I found that sumoylation of both the full-length protein and its DNA-binding domain alone depended on the presence of intact DNA and was strongly inhibited by nicks in the double helix. *In vivo*, two main sites of sumoylation in PARP-1 were identified. By mutating them and creating a linear PARP-1-SUMO fusion, to mimic a constitutively sumoylated polymerase, I investigated the functions of PARP-1 sumoylation in human cells. I found that the sumoylation of PARP-1 did not affect the protein's catalytic activity, localization or binding to intact chromatin or nicked DNA. Instead, sumoylation appeared to accelerate PARP-1's ubiquitylation and subsequent degradation.

These observations exemplify how DNA and sumoylation can interplay with each other to control the properties of chromatin-associated proteins. They also suggest that when

PARP-1 is associated to single-stranded DNA breaks, and is therefore engaged in DNA repair, it becomes refractory to sumoylation and subsequent degradation. Thus, sumoylation may help cells to distinguish between two functionally distinct sub-populations of PARP-1: one that is not sumoylated because it is bound to, and in the process of repairing, DNA nicks, and one that is sumoylated because it is bound to intact DNA, which could be involved in other processes in which the polymerase plays a role, such as transcription regulation.

Acknowledgements

It is my pleasure to thank all of the people who have helped, supported, advised and encouraged me in the longest journey on which I have ever embarked, my *Ph.D*.

First and foremost I would like to thank Helle Ulrich, for her supervision, advice and suggestions, whenever I needed. Thank you, Helle, for believing in most of my crazy ideas and allowing me to grow scientifically. I would also like to thank my second supervisor Tim Hunt and my thesis committee member Vincenzo Costanzo for their guidance.

A big thanks goes to the past and present members of the Ulrich laboratory for making it such an enjoyable workplace, for their support, and for being able to stand me most of the time: Diana Huttner, Andrea Bucceri, Liz Colby, Kai Zhao, Laure Gonzalez, Magda Morawska, Olivier Santt, Yasu Daigaku, Irene Saugar, Jo Parker and Adelina Davies. Thank you Kai for coping with my insistent questions about your possible girlfriends, we have shared a very long journey together. Thank you Irene for Friday evening “The X factor” sessions, talks about the size of lighthouse light bulbs and cheap philosophy about science, I was lucky to have you around during almost all of my *Ph.D*. Thank you Jo for teaching me how to purify proteins and do real biochemistry, you have been the only one that has managed to get a grasp of my ramblings. Thank you Addie for your friendship and for listening to my complaints about science and life in general, I would have not been able to do this without your help.

This work would have not been possible without the assistance of many other people throughout the years. Thank you Kristina Trenz for teaching me how to work with frog egg extracts. Thank you Claudia Cosentino for your vast knowledge about mammalian cells. A big thanks is also owed to the Core Technology Facilities and the Administration team of the London Research Institute for their incredible help. I would also like to thank Sebastian Eustermann because without him the PARP-1 project would have never been possible. I really enjoyed discussing about PARP-1 and DNA with you. Thank you very much Rajvee Shah for sharing your results about PARP-1 sumoylation and for always encouraging me to continue my scientific journey.

The Boehringer Ingelheim Fonds and Cancer Research UK are greatly acknowledged for the funding.

A huge thanks also goes to my friends. Thank you Blanca for always clawing your way back into my life, I do not think I would have been able to do this without your unconditional friendship. I also want to thank my LPC-UWC and university friends in London because you have constantly reminded me how important it is to have fun.

Grazie ai miei nonni, in particolare, alle nonne Adriana e Milde, perché non vi siete mai dimenticate di me. Il più grande ringraziamento va però a Sabrina e Tiziano, i miei genitori, perché non avete mai smesso di incoraggiarmi e credere in me. Questa tesi è dedicata a voi.

Table of contents

List of figures

List of tables

Abbreviations

3-AB	3-aminobenzamide
5-FOA	5-fluoroorotic acid
$A_{260/280}$	Absorbance at 260/280 nm
aa	Amino acid
AAA	ATPases associated with diverse cellular activities
AD for PARP-1	Auto-modification domain
AD for yeast two-hybrid	Gal4 activation domain
ADP	Adenosine 5'-diphosphate
AIF	Apoptosis-inducing factor
ALC1	Amplified in liver cancer 1
AMP	Adenosine 5'-monophosphate
ANK	Ankyrin repeat
AOS1	Activation of Smt3
AP	Abasic site
APE1	AP endonuclease 1
APLF	Aprataxin- and PNK-like factor
ARH3	ADP-ribosylhydrolase 3
ARS	Autonomously replicating sequence
ASC2	Activating signal co-integrator 2
AT-rich	Adenine- and thymine-rich
ATCC	American Type Culture Collection
ATG	Autophagy-related protein
ATP	Adenosine 5'-triphosphate
ATR	Ataxia-telangiectasia mutated- and Rad3-related
BCL	B-cell lymphoma
BD	Gal4 DNA-binding domain
BER	Base excision repair
bp	Base pair
BRCA	Breast cancer
BRCT	Breast cancer susceptibility protein (BRCA1) C-terminus
BSA	Bovine serum albumin
CAT for PARP-1	Catalytic domain
CAT1	Cationic amino acid transporter 1
CBP	Calcium-binding protein
CD	Catalytic domain
CDC	Cell division cycle
CDK	Cyclin-dependent kinase
CDT1	Cdc10-dependent transcript 1
CENP	Centromeric protein
CHD	Chromodomain-helicase-DNA-binding protein
ChIP	Chromatin immunoprecipitation
CHX	Cycloheximide
CR-UK	Cancer Research UK
CTBP	C-terminal-binding protein
CTCF	CCCTC-binding factor
CTP	Cytosine 5' triphosphate
CXCL1	CXC chemokine 1
Da	Dalton
dATP	Deoxyadenosine 5'-triphosphate
DAPI	4,6-diamidino-2-phenylindole

DAXX	Death domain-associated protein 6
DBD	DNA-binding domain
DBF4	Dumbbell former 4
dCTP	Deoxycytidine 5’-triphosphate
DDK	Dbf-dependent kinase
DMEM	Dulbecco’s modified Eagle medium
DMSO	Dimethyl sulfoxide
DN	Dominant negative
DNA	Deoxy-ribonucleic acid
DNA-PK	DNA-dependent protein kinase
DNA-PKcs	DNA protein kinase catalytic subunit
DNMT1	DNA (cytosine-5)-methyltransferase 1
DOX	Doxycycline
ds	Double-stranded
DSB	Double-stranded break
DTT	Dithiothreitol
EB	Egg buffer
ECL	Enhanced chemiluminescence
EDTA	Ethylenediaminetetraacetic acid
eGFP	Enhanced GFP
EGTA	Ethylene glycol tetraacetic acid
ELB	Egg lysis buffer
ELG1	Enhanced levels of genome instability protein 1
EMSA	Electrophoretic mobility shift assay
FAT10	Leukocyte antigen F-associated transcript 10
FEN1	FLAP-endonuclease 1
FSC	Forward scatter
FUB1	Fau ubiquitin-like protein 1
g	Gravity of Earth
GAL	Galactose
GFP	Green fluorescent protein
GG	Di-glycine
GINS	Go, Ichi, Nii, and San; five, one, two, and three in Japanese
GMP1	GAP-modifying protein 1
GST	Glutathione S-transferase
GTP	Guanosine 5’-triphosphate
HAT	Histone acetyl transferase
HDAC	Histone deacetylase
HECT	Homologous to the E6-AP Carboxyl Terminus
HES1	Hairy and enhancer of split 1
HIC1	Hypermethylated in cancer 1
HIPK2	Homeodomain-interacting protein kinase 2
HML	Mating type cassette - left
HMR	Mating type cassette - right
HP1	Heterochromatin protein 1
HPS	Homopolymeric runs of histidine
HRP	Horse radish peroxidase
HSF	Heat shock factor
HSP	Heat shock protein
HT	Herring testis
HTLV	Human T-lymphotropic virus
HU	Hydroxyurea
IgG	Immunoglobulin isotype G

IL	Interleukin
IPTG	Isopropyl-1-thio-β-D-galactopyranoside
IR	Internal repeat
ISG15	Interferon-induced 15 kDa protein
IUR	Immediate upstream region
IκBα	Nuclear factor of κ light polypeptide gene enhancer in B-cells inhibitor α
JAK STAT	Janus kinase signal transducer and transcription activator
KO	Knock out
LB	Luria broth
LC	Liquid chromatography
m/z	Mass to charge ratio
MBR	Major breakpoint region
MCM	Mini-chromosome maintenance
MEC1	Mitosis entry checkpoint 1
MEF2	Myocyte-specific enhancer factor 2
MHC	Major histocompatibility complex
Miz	Myc-interacting zinc
MLS	Mitochondrial localization signal
MMS	Methyl methanesulfonate
MNNG	1-Methyl-3-nitro-1-nitrosoguanidine
MNSFα	Monoclonal nonspecific suppressor factor α
MNU	N-Nitroso-N-methylurea
MOI	Multiplicity of infection
MOPS	3-(N-Morpholino)propanesulfonic acid
MRC LMB	Medical Research Council - Laboratory of Molecular Biology
mRNA	Messenger RNA
MS	Mass spectrometry
MVP-BD	Major vault protein binding site
MWCO	Molecular weight cut-off
NAD	Nicotinamide adenine dinucleotide
NCoR	Nuclear receptor co-repressor
NDSM	Negatively charged residue-dependent sumoylation motif
NEDD8	Neural precursor cell expressed developmentally down-regulated protein 8
NES	Nuclear export signal
NFAT	Nuclear factor of activated T-cells
NFκB	Nuclear factor κ-light-chain-enhancer of activated B cells
NLS	Nuclear localization signal
NMR	Nuclear magnetic resonance
NoLS	Nucleolar localization signal
Nt	Nucleotide
NTA	Nitrilotriacetic acid
NuMA	Nuclear mitotic apparatus protein 1
OAc	Acetate
OCT1	Octamer-binding protein 1
OD_{600}	Optical density at 600 nm
ORC	Origin recognition complex
ORF	Open reading frame
PAGE	Polyacrylamide gel electrophoresis
PAR	Poly(ADP-ribose)
PARG	Poly(ADP-ribose) glycohydrolase
PARP	Poly(ADP-ribose) polymerase

PBS	Phosphate buffered saline
PBS-T	PBS with Tween 20
PBS-Tx	PBS with Triton X-100
PBZ	PAR-binding Zn finger
PC	Polycomb
PCNA	Proliferating cell nuclear antigen
PCR	Polymerase chain reaction
PDSM	Phosphorylation-dependent sumoylation motif
PEG	Polyethylene glycol
PES	Polyethersulfone
Pfu	*Pyrococcus furiosus*
pfu	Plaque forming unit
PGC1α	Peroxisome proliferator-activated receptor gamma 1α
PGK	3-phosphoglycerate kinase
P_i	Phosphate group
PIAS	Protein inhibitor of activated STAT protein
PIC1	PML-interacting clone 1
PLK1	Polo-like kinase protein 1
PML	Promyelocytic leukemia
PMSF	Phenylmethanesulfonyl fluoride
POL	Polymerase
PP_i	Pyrophosphate group
ppm	Part per million
Pre-RC	Pre-replication complex
PrSc	Prescission protease (Human Rhinovirus 3C protease)
PVDF	Polyvinylidene Fluoride
RAD	Radiation sensitive
RANBP2	Ran-binding protein 2
RANGAP1	Ran GTPase-activating protein 1
RBBP7	Retinoblastoma-binding protein
REC	Recombination
REG	Regenerating protein 1
REP	Replication
RFC	Replication factor C
RFP	Ring finger protein
RING	Really interesting new gene
RIPA	Radio-immunoprecipitation assay
RNA	Ribonucleic acid
RNF4	RING finger protein 4
RPA	Replication protein A
RRM	RNA-recognition motif
RSUME	RWD-containing sumoylation enhancer
RTEL1	Regulator of telomere elongation helicase 1
SALL1	Sal-like protein 1
SAM	Sterile α-motif
SAP	SAF-A/B, Acinus and PIAS
SAXS	Small-angle X-ray scattering
SC	Synthetic complete
SCID	Severe combined immunodeficiency
SDS	Sodium dodecyl sulfate
SENP	Sentrin-specific protease
SFC	Skp1-Cul1-F-box
SILAC	Stable isotope labelling with amino acids in cell culture

SIM	SUMO-interacting motif
SIN3A	SWI-independent protein 3A
SIP1	Smad-interacting protein 1
SIZ	SAP and Miz-finger domain-containing protein
SLD	Synthetically lethal with Dpb11
SLX	Synthetic lethal of unknown function
SML1	Suppressor of *mec1* lethality
SMT3	Suppressor of *mif-two* 3
SP	Specificity protein
SP-RING	SIZ/PIAS RING
SREBP-2	Sterol regulatory element-binding protein 2
SRS2	Suppressor of *rad-six* 2
ss	Single-stranded
SSB	Single-stranded break
SSC	Side scatter
STAT	Signal transducer and transcription activator
STE	Saline/Tris/EDTA
Su-DBD	Sumoylated PARP-1's DBD
Su-PARP-1	Sumoylated PARP-1
SUMO	Small ubiquitin-like modifier
SuNaSp	Sucrose sodium spermidine
TAB2	TGF-beta-activated
TAE	Tris acetate EDTA
Taq	*Thermus aquaticus*
TAT1	Trypanosome tubulin 1
TBE	Tris borate EDTA
TCA	Trichloroacetic acid
TDG	Thymine DNA glycosylase
TE	Tris EDTA
TEF1	Transcriptional enhancer factor 1
TEP1	Telomerase protein component 1
tiPARP	2,3,7,8-tetrachlorodibenzo-p-dioxin-inducible PARP
TLE1	Transducin-like enhancer protein 1
TNF	Tumour necrosis factor
TOPBP1	DNA topoisomerase II binding protein 1
TOPORS	Topoisomerase I-binding RING finger protein
TOR	Target of rapamycin
TRF	Telomeric repeat-binding factor
TRRAP	Transformation/transcription domain-associated protein
TXRE	Tax-responsive element
U	Unit
UBA	Ubiquitin activating
UBC	Ubiquitin conjugating
UBE1I	Ubiquitin-activating enzyme E1-like
UBL	Ubiquitin-like
UIM	Ubiquitin-interacting motif
ULP	Ubiquitin-like-specific protease
UPLC	High performance liquid chromatography
URM	Ubiquitin-related modifier
UTR	Untranslated region
UV	Ultra-violet
v/v	Volume by volume
VIT	Vault inter-α-trypsin

vPARP	Vault PARP
vWA	Von Willebrand factor type A
w/v	Weight by volume
WDHD1	WD repeat and HMG-box DNA-binding protein 1
WGR	Tryptophan, glycine and arginine
WRN	Werner's
WT	Wild type
WWE	Tryptophan, tryptophan and glutamate
Xcorr	Cross-correlation
XP	Xeroderma pigmentosum
XRCC1	X-ray repair cross-complementing
YP	Yeast peptone
YPD	Yeast peptone dextrose (glucose)
YY1	Ying-yang protein 1
β-ME	β-mercaptoethanol

Chapter 1. Introduction

Recent estimates suggest that humans (~25,000 genes) have slightly more genes than the puffer fish *Fugu rubripens* (~26,000 genes) and the mustard weed *Arabidopsis thaliana* (~25,500 genes), and only about twice as many as the fruit fly *Drosophila Melanogaster* (~13,600 genes) and the worm *Caenorhabditis elegans* (~17,000 genes). This does not however mean that we are twice as complicated as a worm or a plant. In fact, it is not the number of genes that determines the complexity of an organism but rather the size and regulation of its proteome, which cannot be easily predicted on the basis of genomic sequence only. Eukaryotes can expand and control the complexity of their proteomes through a variety of mechanisms, including alternative splicing of messenger RNAs (mRNAs) and the post-translational modification of proteins with small chemical groups, such as phosphate, acetyl, methyl and ADP-ribose groups, and/or polypeptides, such as ubiquitin.

Post-translational modifiers usually change, in a controlled manner, the biological properties of their targets. They can do so very quickly because their actions do not require the re-synthesis of substrate proteins or the production of additional factors, which allows cells to rapidly respond to specific cues. The first and best-characterized example of a polypeptide modifier is ubiquitin, which is well known for targeting proteins for degradation by the proteasome but it also plays non-degradative functions. Since the discovery of ubiquitin, several ubiquitin-like proteins have been found and demonstrated to also act as post-translational modifiers. One of these factors is the small ubiquitin-like modifier SUMO, which has been the main focus of my research.

1.1 Ubiquitin and ubiquitin-like proteins as post-translation modifiers

1.1.1 Ubiquitin

Ubiquitin is a protein of 76 amino acids that is very well conserved in all eukaryotes. It adopts a particular structure, known as β-grasp fold, which consists of a four-stranded anti-parallel β-sheet holding onto an α-helix (**Figure 1.1**B). Ubiquitin is produced as a longer inactive precursors (*e.g.* head-to-tail tetra-ubiquitin chains) that needs to be processed by specific peptidases to expose a C-terminal di-glycine motif to become competent for conjugation (Jentsch and Pyrowolakis, 2000).

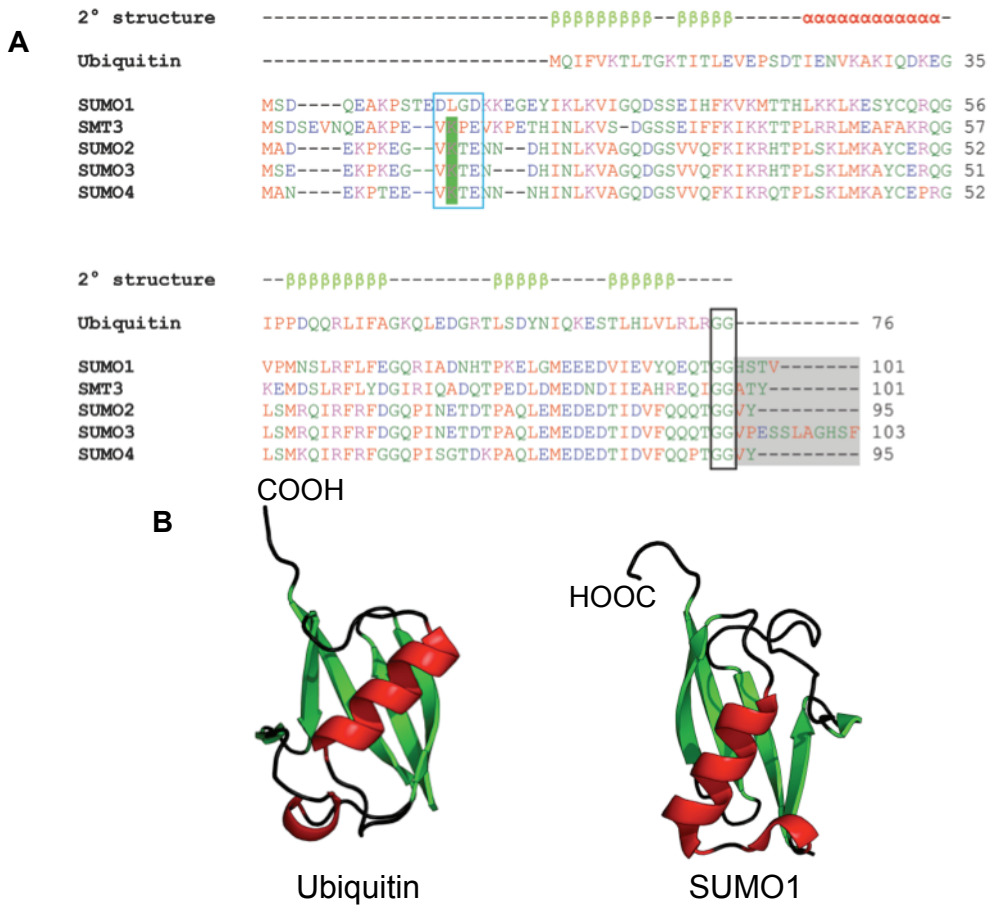

Figure 1.1 - Similarities between ubiquitin and SUMO. (A) Alignment of the primary sequences of the human ubiquitin, the *S. cerevisiae* protein Smt3 and the human SUMO1-4 proteins (ClustalW2, Larkin *et al.*, 2007). The alignment is coloured according to the chemical properties of amino acids, as follows: purple, basic; blue, acidic; red, hydrophobic; green, polar or small. The secondary structure of the presented sequences is indicated above the alignment itself (α = α-helix, β = β-strand). The consensus motif used to form poly-SUMO chains is boxed in blue. The C-terminal di-glycine motif is boxed in black. (B) Cartoon representations of the tertiary structures of the human ubiquitin and SUMO1 proteins. Secondary structure elements are colour in red, for α-helices, and green, for β-strands. The images were created with PyMOL (http://pymol.sourceforge.net/).

Once ubiquitin has been processed, it is attached to its substrates by covalently linking the carboxyl group of its C-terminal most glycine with the ε-amino group of a lysine found within a specific target protein. This process is brought about by the successive actions of three classes of enzymes: an E1 or ubiquitin-activating enzyme, an E2 or ubiquitin-conjugating enzyme and E3 or ubiquitin protein ligase. There exist one main ubiquitin E1 enzyme in all eukaryotes, but many E2s and even more E3s. The latter two enzymes, and in particular the E3s, are responsible for defining the target specificity of a particular ubiquitylation event. Ubiquitin can modify its substrates as a single moiety and also as polymeric chains because it is itself a substrate of

ubiquitylation, through any of the seven lysines it contains (Jentsch and Pyrowolakis, 2000).

Ubiquitylation is involved in many processes in a cell; its specific functions depend on the nature of a particular modification event. For instance, mono-ubiquitylation is involved in controlling protein trafficking throughout the cell (Hicke and Dunn, 2003). K48- and K11-linked ubiquitin chains target proteins for degradation by the 26S proteasome, while those linked through K63 act as signalling molecules in various pathways, such as DNA repair and cell signalling (Bergink and Jentsch, 2009; Jentsch and Pyrowolakis, 2000).

1.1.2 The ubiquitin-like modifiers

Ubiquitin is the founding member of a class of polypeptides known as ubiquitin-like proteins (UBLs). They share a similar β-grasp structure with ubiquitin but show little sequence identity with it. Like ubiquitin, these factors need to be processed to yield a C-terminal di-glycine motif. Such residues are ligated to lysines in certain target proteins through enzymatic cascades that are analogous, but usually distinct, from that of ubiquitin (Welchman *et al.*, 2005). Nine different UBLs have been identified so far, however, more are likely to exist. Their salient features will be briefly highlighted below.

NEDD8 is a 9-kDa protein that shares considerable sequence (60%) and structural identity with ubiquitin. It is conjugated to its substrates through its own E1 (NAE1-UBA3), E2 (UBC12 and UBE2F) and E3 (DCN1) enzymes (Huang *et al.*, 2009; Welchman *et al.*, 2005). NEDD8 targets p53, inhibiting its transcriptional activity (Xirodimas *et al.*, 2004), and almost all the members of the cullin family of proteins. These proteins act as scaffolding subunits for SFC-type ubiquitin ligases and their neddylation regulates the activity of such enzymes (Hori *et al.*, 1999).

FAT10 is an 18-kDa protein that consists of two ubiquitin-like domains ~30% identical to ubiquitin. It is encoded by a gene located within the MHC I locus and is expressed in mature B cells, dendritic cells and other cell types upon exposure to specific immunological signals (Raasi *et al.*, 1999). Under these conditions, FAT10 becomes conjugated to certain proteins, including a 35-kDa species that is targeted to the 26S proteasome and thereby degraded (Raasi *et al.*, 2001).

Like FAT10, ISG15 is an 18-kDa protein that contains two ubiquitin-like domains. It is activated by a dedicated E1 (UBE1L) but then it is attached to its substrates through the ubiquitin E2 enzyme UBCH8 (Welchman *et al.*, 2005). *ISG15* is also induced by

specific cellular signals, thus leading to the modification of several proteins, and it plays an important role in the regulation of interferon-related immune responses (D'Cunha *et al.*, 1996).

ATG8 and ATG12 are 15-kDa proteins that share 10-15% identity with ubiquitin and have a single C-terminal glycine residue. The E1-like enzyme ATG7 activates them both. The E2-like enzymes ATG10 and ATG3 then catalyze the transfer of ATG12 to ATG5 and that of ATG8 to phosphatidylethanolamine, respectively. ATG8 and ATG12 play a critical role in autophagy, the process by which cell degrade their own cytoplasmic materials (Ichimura *et al.*, 2000; Mizushima *et al.*, 1998).

URM1 is 11 kDa in size and although it shares only 12% identity with ubiquitin it contain a β-grasp fold. In budding yeast, it is activated by the E1-like enzyme Uba4 and it is believed to be conjugated to proteins; the fact that a double knockout mutant of *URM1* and *UBA4* is sensitive to rapamycin indicates that Urm1 must be involved in the TOR (target of rapamycin) pathway, which is activated in response to nutrient starvation (Mizushima *et al.*, 1998). Interestingly, URM1 has also been shown to act as a sulphur carrier in thiolation of eukaryotic transfer RNA (Leidel *et al.*, 2009).

FUB1 is 8 kDa in size and shares 37% identity with ubiquitin. It targets the T-cell-receptor-α-like protein MNSFα, which probably acts as a stabilization factor for FUB1 itself given that it appears to be rather prone to aggregation *in vivo* (Nagata *et al.*, 1998). FUB1 also modifies the B-cell lymphoma-G, a pro-apoptotic factor of the BCL2 family of proteins (Nakamura and Tanigawa, 2003).

UBL5 is an 8-kDa protein that shares 22% identity with ubiquitin. It folds into a ubiquitin-type β-grasp fold but it bears a tyrosine, instead of a glycine, at its C-terminus. In addition, unlike ubiquitin's unstructured C-terminal domain, UBL5's one forms a β-sheet, thus suggesting that it may not be conjugatable (Ramelot *et al.*, 2003). Yet, in budding yeast Ubl5 has been reported to modify Sph1, a protein that plays a role in bud site selection and cellular morphogenesis during mating (Dittmar *et al.*, 2002).

1.1.3 The small ubiquitin-like modifier SUMO

SUMO, also known as Smt3 in budding yeast and PIC1, sentrin, GMP1 and UBL1 in mammalian cells, is a well-conserved post-translational modifier of about 90 aminoacids and 11 kDa. A single SUMO gene exists in lower eukaryotes, but four paralogues, SUMO1-4, have been reported in higher organisms. SUMO2/3 seem to constitute a greater percentage of total cellular sumoylation than does SUMO1 (Saitoh

and Hinchey, 2000). Although SUMO folds into a β-grasp structure very similar to that of ubiquitin, it shares only 18% sequence identity with this protein (**Figure 1.1**). It also contains a unique N-terminal extension of about 20 amino acid, which is involved in the formation of SUMO chains (see 1.2.6).

Amongst the SUMO genes, SUMO4 remains somewhat of enigma for two reasons. Firstly, although it was initially thought to be a pseudo-gene given that it is located within an intron of the *TAB2* gene, it has been found to be expressed, particularly in immune tissues, such as the kidneys and the pancreas (Bohren *et al.*, 2004; Guo *et al.*, 2005; Su and Li, 2002). Secondly, ectopically producing a mature form of SUMO4 in cells leads to its incorporation into high molecular weight species, thus indicating that it must be competent for conjugation (Guo *et al.*, 2005; Owerbach *et al.*, 2005). Yet, the presence of a proline residue at position 90 of SUMO4, instead of the glutamine normally found in the other SUMO paralogues, has been shown to prevent the processing of the immature form of such protein, both *in vivo* and *in vitro* (Owerbach *et al.*, 2005). Thus, it would appear that although SUMO4 can potentially be conjugated to proteins, it may not normally do so *in vivo* because it cannot be converted into its mature form. SUMO4 may nevertheless still have certain biological functions, which could be mediated through non-covalent protein-protein interactions (Owerbach *et al.*, 2005). SUMO4 has in fact been proposed to play a role in immune responses because a spontaneously occurring point mutation within this gene, which exchanges M55 for a valine residue in the corresponding protein, has been associated with an increased susceptibility to the auto-immune, type I, diabetes (Bohren *et al.*, 2004; Guo *et al.*, 2004; Park *et al.*, 2005; Qu *et al.*, 2005; Smyth *et al.*, 2005).

1.2 The SUMO conjugation pathway

SUMO is conjugated to its substrates through an enzymatic pathway that is analogous to, but distinct from, that of ubiquitylation: it involves the successive activities of a SUMO E1 (AOS1/UBA2), a SUMO E2 (UBC9) and one of several SUMO E3s (**Figure 1.2**). *In vitro*, sumoylation of many, but not all substrates, can be achieved in the presence of the E1 and E2 enzymes only, but *in vivo* an E3 is usually required. Sumoylation is a reversible mode of post-translational modification: desumoylation is achieved by specific SUMO isopeptidases known as ULPs, which are also involved in process of SUMO maturation.

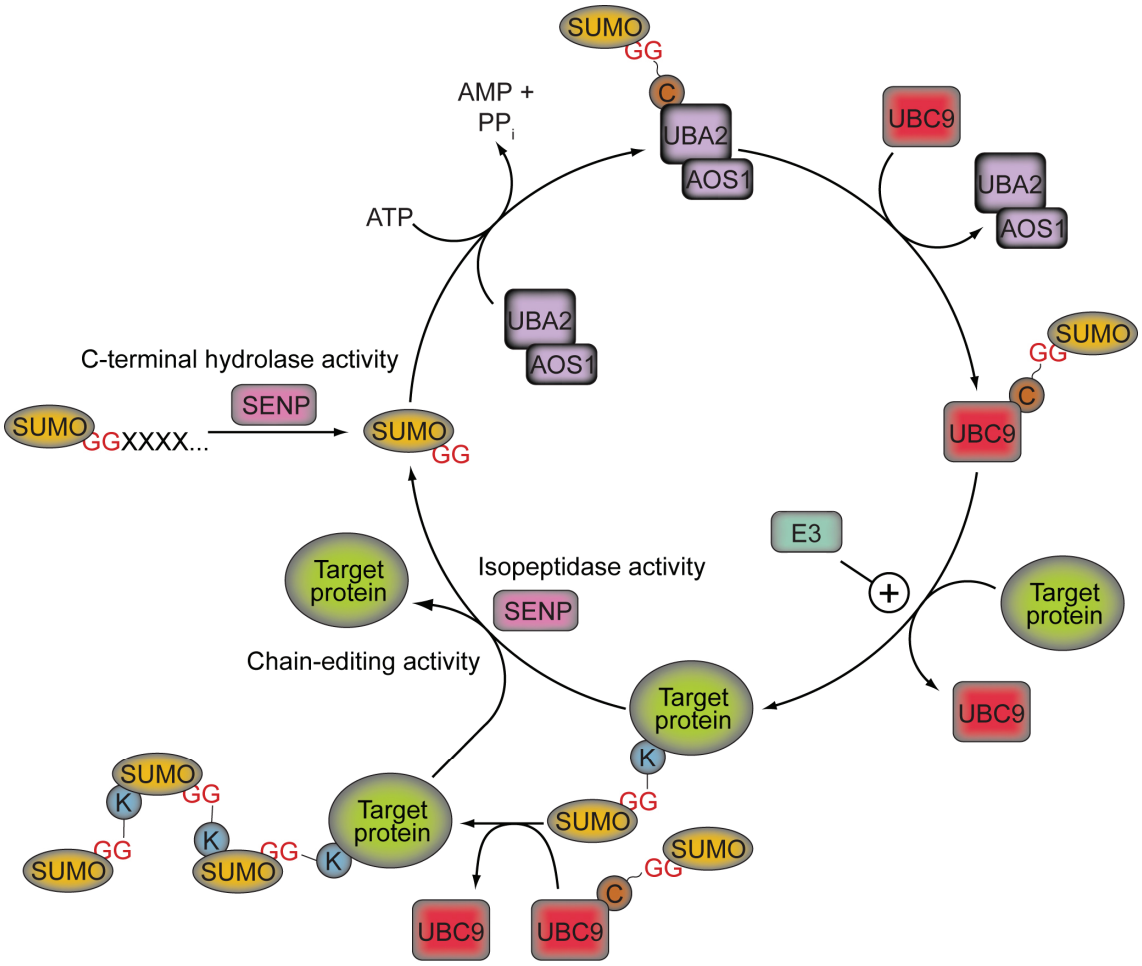

Figure 1.2 - The mechanism of reversible sumoylation. SUMO is produced as a longer, inactive, precursor that is proteolytically cleaved to reveal a C-terminal GG motif by SUMO proteases called sentrin-specific proteases, or SENPs. The mature SUMO is initially activated by the hetero-dimeric E1 enzyme AOS1/UBA2 in an ATP-dependent manner and then transferred to the E2 SUMO conjugating enzyme UBC9. Aided by one of several SUMO E3 ligases, UBC9 transfers SUMO to specific lysines (K) within a target protein. UBC9 can sumoylate SUMO itself, thus leading to the formation of poly-SUMO chains. SUMO-conjugated proteins can be de-sumoylated by SENPs. C = cysteine, PP_i = pyrophosphate. Adapted from Geiss-Friedlander and Melchior (2007).

1.2.1 The SUMO E1 (AOS1/UBA2)

A single SUMO-activating enzyme has been found in both lower and higher eukaryotes, where it is mainly localized within the nucleus. It exists as a hetero-dimer of AOS1 and UBA2, which share sequence similarity to the N- and C-terminal domains of the ubiquitin activating enzyme, respectively (Desterro *et al.*, 1999; Johnson *et al.*, 1997). In budding yeast, *AOS1* and *UBA2* are essential genes for viability, thus indicating that sumoylation must play vital functions in this organism (Johnson *et al.*, 1997).

Like the E1s for ubiquitin and other UBLs, the SUMO-activating enzyme performs two functions: 1) it activates SUMO through adeylation and thiolation, and subsequently 2) it transfers the modifier to UBC9. Initially, AOS1/UBA2 binds to ATP and SUMO exclusively through its UBA2 subunit, which contains a typical G-X-G-X-X-G ATP-binding motif that is also found in other E1 enzymes (Lois and Lima, 2005). It then catalyzes the attack of the C-terminal carboxyl group of SUMO itself to ATP to form a SUMO-AMP adenylate intermediate that concomitantly releases pyrophosphate. This reaction occurs in the so-called adenylation domain, a pocket formed by surfaces of both AOS1 and, mostly, UBA2, which strongly resembles the catalytic motif of bacterial adenylating enzymes (Lois and Lima, 2005). A conserved zinc-binding motif in UBA2 has also been proposed to help this protein holding onto SUMO during adenylation and preventing the resulting SUMO-AMP intermediate to dissociate from the E1 before the formation of the thioester conjugate (Wang and Chen, 2010). Next, the thiol group of UBA2's active site cysteine attacks the SUMO-AMP intermediate, releasing AMP and simultaneously forming a high energy thioester linkage between the E1 and SUMO. At the same time, the E1 is loaded with a second SUMO molecule, which is adenylated while the enzyme still carries the first thioester-bound modifier (Walden *et al.*, 2003). The fact that the ATP-binding site and catalytic cysteine of the SUMO E1 are more than 3 nm away from each other made it hard to explain how the SUMO adenylate could be attacked by the active site thiol group. This mystery has been recently cracked by solving the structures of AOS1/UBA2 bound to mimics of the adenylation- and thioester-bound forms of SUMO (Olsen *et al.*, 2010). Such structures show that when the E1 binds to the SUMO-thioester analogue the α-helix containing the active site undergoes a dramatic 130° rotation, which juxtaposes the catalytic cysteine next to where the SUMO adenylate would be. Finally, the activated SUMO is transferred to the active site cysteine of UBC9, through a ubiquitin-like domain found at the C-terminus of UBA2 (Lee and Schindelin, 2008; Lois and Lima, 2005).

1.2.2 The SUMO E2 (UBC9)

Unlike the ubiquitylation pathway, which features several conjugating enzymes, only one E2, *i.e.* UBC9, has been identified for SUMO (Desterro *et al.*, 1997). It is a very well conserved protein, being 56% identical between yeast and humans, and it is essential in all systems tested. UBC9 shares a significant amount of sequence identity with ubiquitin E2s, and accordingly it also folds into a structure consisting of four α-

helices and a four-stranded anti-parallel β sheet that conforms to the typical UBC superfold αββββ(βββ)ααα (Giraud *et al.*, 1998).

UBC9 must contain functionally-important binding surfaces for at least four proteins: AOS1/UBA2, SUMO ligases, substrates of sumoylation and SUMO itself.

UBC9 and AOS1/UBA2 contact with each other through at least two sites. The first one involves a surface of the E2 consisting of its α_1 helix and the $\alpha_1\beta_2$ loop and the C-terminal ubiquitin-like domain of UBA2. Although this interaction has not been directly proven for the SUMO enzymes, it occurs between the closely related neddylation enzymes UBC12 and UBA3 (Huang *et al.*, 2007). Interestingly, in this system the thiolation of NEDD8 induces a conformational change within UBA3 that moves the UBC12 molecule bound to its C-terminal ubiquitin-like domain to a position where their catalytic cysteines face each other (Huang *et al.*, 2007). Additionally, UBC9 also interacts with the catalytic pocket of UBA2 through a region surrounding its catalytic site (Wang *et al.*, 2007). These observations therefore provide a possible mechanism for how the E1-bound SUMO could be directly transferred to the E2 enzyme.

UBC9 and SUMO ligases may also associate with each other through multiple surfaces. The structure of the SUMO-1-UBC9-RANBP2–RANGAP1 complex revealed that the four-stranded β-sheet of UBC9 binds to the E3 RANBP2 (Reverter and Lima, 2005; Tatham *et al.*, 2005). In addition, given that ubiquitin E2s generally associate with their cognate E3s through a region formed by their $\beta_2\beta_3$ and $\beta_6\alpha_2$ loops (Zheng *et al.*, 2000), it is possible that an analogous surface could also be involved in the interactions between UBC9 and the relevant ligases.

SUMO often targets lysines that fall within the consensus motif ΨKXD/E (see 1.2.5). This phenomenon depends on the ability of a patch surrounding the catalytic cysteine of UBC9 (C93), which is located in middle of its $\beta_4\alpha_2$ extended loop, to directly recognize such a consensus, which consequently becomes buried in a hydrophobic groove of this enzyme (Bernier-Villamor *et al.*, 2002; Tatham *et al.*, 2003b).

UBC9 interacts with SUMO through both covalent and non-covalent interactions. The transfer of the activated SUMO from the E1 enzyme to UBC9 leads to the formation of a thioester bond between these proteins. Additionally, UBC9 is also auto-sumoylated (Knipscheer *et al.*, 2008). In the mammalian enzyme, this event targets K14 and has been shown to be critical for the modification of some sumoylation targets, such as the transcription factor SP100, in a manner that depends on its ability to non-covalently interact with SUMO. Thus, the auto-sumoylated UBC9 modifies SP100 more efficiently

than the unmodified E2 enzyme probably because this transcription factor contains an additional binding surface for UBC9 itself, *i.e.* SUMO (Knipscheer *et al.*, 2008). Interestingly, not all of the sumoylation substrates that non-covalently interact with SUMO are preferentially modified by the auto-sumoylated UBC9. Thus, it has been proposed that in addition to the presence of a SUMO-interacting motif (see 1.3.1) in a protein, the particular position of such a domain with respect to the target lysine is also important to enable the auto-sumoylated UBC9 to preferentially modify it (Knipscheer *et al.*, 2008). SUMO also interacts non-covalently with UBC9, through at least two sites. One of these regions (D100 and K101) is located close to the enzyme's catalytic cysteine (Tatham *et al.*, 2003a). Mutating D100 and K101 inhibits the transfer of the activated SUMO from the E1 and increases the association rate and decreases the dissociation rate of binding of the SUMO-loaded UBC9 to define model substrates (Tatham *et al.*, 2003a). Since D100 and K101 are not conserved in other E2s, it is possible that these residues could underlie the specificity that UBC9 shows for SUMO, in comparison to other UBLs (Tatham *et al.*, 2003a). In addition, SUMO also non-covalently associates with UBC9 through the β-sheet of this enzyme, distantly from its active site, which is important for its chain-building activity (Capili and Lima, 2007; Knipscheer *et al.*, 2007).

1.2.3 The SUMO E3 enzymes

E3 ligases function by increasing the efficiency and defining the substrate specificity of a particular post-translational event. SUMO ligases can be classified into three categories, which are described below.

1.2.3.1 The PIAS/SIZ family of SUMO E3 enzymes

The largest class of SUMO ligases are the PIAS/SIZ proteins. This family includes: PIAS1, PIASx (PIAS2), PIAS3 and PIASy (PIAS4) in mammals, which were initially described as protein inhibitors of the activated JAK-STAT signaling pathway, Siz1 and Siz2 in budding yeast as well as Pli1 and Nse2 in fission yeast (Watts *et al.*, 2007). Interestingly, the modification of many SUMO substrates can be stimulated by more than one PIAS or SIZ protein both *in vitro* and *in vivo*, thus indicating that there is a significant amount of redundancy amongst these enzymes (Martin *et al.*, 2009; Reindle *et al.*, 2006).

PIAS/SIZ proteins share a common modular structure that consists of four domains. An N-terminal SAP domain, which mediates interactions with DNA but is not essential for

catalytic activity (Okubo *et al.*, 2004; Parker *et al.*, 2008; Suzuki *et al.*, 2009; Takahashi and Kikuchi, 2005). A “PINIT” motif, which mediates both the target protein- and target site- selectivity of some sumoylation event by directly contacting sumoylation substrates (Takahashi and Kikuchi, 2005; Yunus and Lima, 2009b), but it also seems to play a role in the localization of PIAS/SIZ ligases (Duval *et al.*, 2003). A Miz-type zinc finger fold, also known as SIZ/PIAS RING domain (SP-RING), which is essential for the SUMO ligase activity of PIAS/SIZ proteins (Kotaja *et al.*, 2002; Takahashi and Kikuchi, 2005; Yunus and Lima, 2009b). This domain is related, both in terms of sequence and structure, to the classical RING-type zinc fingers found in ubiquitin ligases and thus, like such motifs, it probably mediates the E2:E3 contacts necessary to transfer the modifier from the E2 to its substrates (Yunus and Lima, 2009b). It therefore seems likely that PIAS/SIZ proteins stimulate sumoylation by acting as adaptors between the loaded E2 and its targets. The C-terminus of PIAS/SIZ proteins contains a classical SUMO-interacting motif (see 1.3.1), which is dispensable for catalytic activity (Takahashi and Kikuchi, 2005; Yunus and Lima, 2009b), and an acidic domain, which is instead essential for efficient SUMO conjugation, possibly by contacting basic residues in the SUMO moiety of the charged UBC9 (Yunus and Lima, 2009b).

SUMO ligases that contain an SP-RING, but do not belong to the PIAS/SIZ family of proteins, also exist and include: MMS21, which is part of a complex that is involved in DNA damage sensing and repair as well as telomere homeostasis (Zhao and Blobel, 2005), and the meiosis-specific yeast enzyme Zip3 (Cheng *et al.*, 2006a).

1.2.3.2 RANBP2

RANBP2 defines a second class of SUMO ligases. It is a large vertebrate-specific protein that localizes to the cytoplasmic fibrils of the nuclear pore, a big protein complex that controls the shuttling of materials across the nuclear envelope, where it mainly plays a role in protein import. This role of RANBP2 depends on its ability to bind, and thereby recruit to the nuclear pore complex, the RAN GTPase activator protein RANGAP1, which only occurs when the latter protein is sumoylated (Mahajan *et al.*, 1997; Matunis *et al.*, 1996; Matunis *et al.*, 1998).

RANBP2 has been shown to enhance the modification of several proteins *in vitro*, including HDAC4, SP100, borealin and PML (Kirsh *et al.*, 2002; Klein *et al.*, 2009; Pichler *et al.*, 2002; Tatham *et al.*, 2005). To date, only topoisomerase II has been identified as a substrate of RANBP2 *in vivo*, at least in mouse cells (Dawlaty *et al.*, 2008). In fact, in *Xenopus* egg extracts and possibly in some human cell lines

topoisomerase II sumoylation seems to depend on PIASy (Azuma *et al.*, 2005; Diaz-Martinez *et al.*, 2006).

The E3 ligase activity of RANBP2 is mediated through a ~300-amino acid domain, which contains two internal repeats (IR1 and IR2) of a 50-amino acid sequence separated by a 25-amino acid middle (M) domain that share no similarity with any other known protein. A region encompassing the IR1 and the M motifs binds to UBC9 and is able to recapitulate the activity of the full-length RANBP2, although the IR1 motif alone is also functional (Pichler *et al.*, 2002; Pichler *et al.*, 2004; Saitoh *et al.*, 2002; Tatham *et al.*, 2005). The IR1+M region also appears to be mostly unstructured in its free form but becomes more compact upon binding to UBC9 (Pichler *et al.*, 2004). Conversely, the IR2 and M domains show no activity on their own, but they are somewhat active in combination (Pichler *et al.*, 2004; Tatham *et al.*, 2005). Together, the IR2 and M motifs can bind SUMO1 but not SUMO2 (Tatham *et al.*, 2005). Yet, RANBP2 enhances the modification of model substrates by both SUMO1 and SUMO2, albeit with different kinetics, thus indicating that its ligase activity is probably brought about through two different mechanisms (Tatham *et al.*, 2005).

Biochemical and structural data suggest a possible mechanism for how RANBP2 brings about SUMO ligase activity. Firstly, there is no evidence for this enzyme being able to directly contact its substrates (Pichler *et al.*, 2004; Reverter and Lima, 2005). Thus, unlike PIAS/SIZ proteins, it probably does not act as a bridging factor between the SUMO-charged UBC9 and a substrate. Secondly, the evidence that RANBP2's catalytic core does not require cysteines to enhance sumoylation means that it does not function like HECT-type ubiquitin ligases, where the E3 enzyme itself forms a thioester bond with ubiquitin before transferring it to a substrate (Pichler *et al.*, 2004). Finally, the crystal structure of the sumoylated RANGAP1 in complex with UBC9 and RANBP2's catalytic core shows that RANBP2 contacts both SUMO1 and UBC9 (Reverter and Lima, 2005). By doing so, RANBP2 has been proposed to position the SUMO-UBC9 thioester for optimal attack by a target lysine, which would consequently accelerate the rate of SUMO transfer to such residue (Reverter and Lima, 2005).

1.2.3.3 Other SUMO ligases

In addition to PIAS/SIZ proteins and RANBP2, two other SUMO ligases have been identified, *i.e.* PC2 and TOPORS, for which, however, the mechanisms of action remain unknown.

PC2 is a member of the polycomb group family of proteins, which form large nuclear complexes that mediate the stable and heritable repression of several genes by modifying histones (Kagey *et al.*, 2003). Given its highly confined localization, PC2 is likely to have a more limited range of targets compared to other SUMO ligases (Kagey *et al.*, 2005). In fact, so far this enzyme has been shown to enhance the sumoylation of only four proteins, both *in vivo* and *in vitro*, including the transcriptional regulators CtBP (Kagey *et al.*, 2003), SIP1 (Long *et al.*, 2005) and HIPK2 (Roscic *et al.*, 2006), which all co-localize with PC2 at polycomb complexes. How PC2 exerts its SUMO ligase activity remains poorly understood. A mutant of PC2 that binds CtBP and UBC9 and localizes to polycomb complexes, but lacks its N-terminal domain, is unable to stimulate CtBP modification, thus indicating that these interactions are necessary, but not sufficient, for PC2's SUMO ligase activity (Kagey *et al.*, 2005). The N-terminus of this protein stimulates sumoylation *in vitro*, but not *in vivo*, where it needs either to be fused to a CtBP-binding motif or the concomitant production of PC2's C-terminal domain (Kagey *et al.*, 2005). In addition, the SUMO ligase activity of PC2 has been shown to depend on two SUMO-interacting motifs found in this enzyme, one located within its N-terminal domain and the other in its C-terminus (Merrill *et al.*, 2010; Yang and Sharrocks, 2010).

The topoisomerase I-interacting protein TOPORS also has SUMO ligase activity. It stimulates the sumoylation of topoisomerase I itself, p53, SIN3A and possibly several other proteins, which appear to be mainly involved in chromatin modification and transcription regulation (Pungaliya *et al.*, 2007; Weger *et al.*, 2005). Interestingly, TOPORS contains a typical RING-type zinc finger domain, which confers to it ubiquitin E3 ligase activity (Rajendra *et al.*, 2004).

1.2.4 SUMO deconjugation

SUMO proteases are enzymes that catalyze the processing of SUMO to its mature form (C-terminal hydrolase activity), its removal from target substrates (isopeptidase activity) and the length of polymeric SUMO chains (chain editing activity). These proteins belong to the C48 cysteine protease superfamily of proteins and share a conserved ~200-amino acid catalytic region, known as ULP domain (Li and Hochstrasser, 1999, 2000; Mossessova and Lima, 2000). This domain is generally found close to the C-terminus of SUMO proteases, while their N-terminal regions are often important for their correct sub-cellular localization. In budding yeast, two such proteins exist (Ulp1 and Ulp2), while six have been identified in mammals (SENP1-3, SENP5 and SENP6).

1.2.4.1 The yeast SUMO proteases

Budding yeast Ulp1 has C-terminal hydrolase and isopeptidase activities, both of which are essential for cell viability (Li and Hochstrasser, 1999). As a SUMO isopeptidase, Ulp1 is important for cell cycle progression, in particular at the G_2/M transition (Li and Hochstrasser, 1999). It is found at nuclear pore complexes in budding yeast (Li and Hochstrasser, 1999), but it delocalizes to the nucleoplasm during mitosis in fission yeast (Taylor *et al.*, 2002). The targeting of Ulp1 to nuclear pores requires its N-terminus and is essential for maintaining its functions (Panse *et al.*, 2003). An Ulp1 mutant that lacks its N-terminal region is found throughout the nucleus and shows reduced isopeptidase activity towards its own substrates but an increased one towards those proteins normally desumoylated through Ulp2 (Li and Hochstrasser, 2003). Consequently, this Ulp1 mutant exhibits several phenotypes including increased DNA-damage sensitivity (Li and Hochstrasser, 2003; Panse *et al.*, 2003; Zhao *et al.*, 2004a).

Ulp2 possesses only isopeptidase activity and it localizes throughout the nucleus (Li and Hochstrasser, 2000). It is not an essential gene but in its absence cells cannot properly segregate chromosomes because of impaired topoisomerase II sumoylation (Bachant *et al.*, 2002). Additionally, Ulp2 is also important for resuming cell cycle progression following exposure to DNA damaging agents (Schwartz *et al.*, 2007). Mutants of *ULP2* also accumulate SUMO chains in a way that depends on lysines important for the formation of such polymers (see 1.2.6), thus suggesting that Ulp2 may have SUMO chain-editing activity (Bylebyl *et al.*, 2003).

1.2.4.2 The mammalian SUMO proteases

The mammalian SENPs can be classified into three categories: 1) SENP1 and SENP2, which have C-terminal hydrolase activity and act as isopeptidases towards all three SUMO paralogues, 2) SENP3 and SENP5, which prefer SUMO2/3 over SUMO1 and localize to the nucleolus, and 3) SENP6 and SENP7, which show a preference for trimming SUMO2/3 chains and contain a 50-200 amino acid insertion in their ULP domains, the functional significance of which remains unclear (Yeh, 2009). From a phylogenetic point of view SENP1-3 and SENP5 are more similar to Ulp1, while SENP6 and SENP7 are more related to Ulp2. The basic properties of these enzymes are summarized in **Table 1.1**.

		Localization	Activity		
			C-terminal hydrolase	Isopeptidase	Chain-editing
Ulp1-like	SENP1	Nucleus but not nucleolus[1]	SUMO1>>SUMO2 >SUMO3[1,2]	SUMO2/3 > SUMO-1[2]	Yes, but due to general iso-peptidase activity
	SENP2	Nuclear pore and uncharacterized nuclear speckles[3,4]	SUMO2>>SUMO1 >SUMO3[3,5]	SUMO2/3 > SUMO1[5]	
	SENP3	Nucleolus[6]	No[6]	SUMO2/3>> SUMO1[6]	
	SENP5				
Ulp2-like	SENP6	Nucleus[7,8]	Poor[8,9]	SUMO2/3> SUMO1[8,9]	Yes[8,9,10]
	SENP7				

Table 1.1 - Summary of the properties of mammalian SUMO proteases. The sub-cellular localization and enzymatic activities of the six mammalian SUMO proteases are summarized. [1] - Gong *et al.* (2000), [2] - Shen *et al.* (2006a), [3] - Hang and Dasso (2002), [4] - Itahana *et al.* (2006), [5] - Reverter and Lima (2006), [6] - Gong and Yeh (2006), [7] - Cheng *et al.* (2006b), [8] - Shen *et al.* (2009), [9] - Lima and Reverter (2008), [10] - Mukhopadhyay *et al.* (2006).

1.2.4.3 The enzymatic activities of SUMO proteases

The catalytic domains of ULPs and SENPs fold into a similar structure consisting of seven α-helices and one two-stranded and one four-stranded β-sheets. Residues present in α_6, β_4 and β_5 of this structure come together to form the catalytic triad cysteine, histidine and asparagine (Lima and Reverter, 2008; Mossessova and Lima, 2000; Reverter and Lima, 2004; Shen *et al.*, 2006a). The C-terminal hydrolase and isopeptidase activities of these enzymes have been analyzed from both biochemical and structural perspectives and will be described below.

1.2.4.3.1 C-terminal hydrolase activity

C-terminal hydrolase activity involves the cleavage of the peptide bond between the C-terminal glycine of SUMO and the first amino acid in its C-terminal tail. SENP1 and SENP2 are the only mammalian SUMO proteases known to efficiently process SUMO precursors, which they do in a paralogue-specific manner (**Table 1.1**). This specificity depends on the length and sequence of the regions C-terminal to the di-glycine motif of such modifiers, rather than their affinity for SENPs *per se* (Mikolajczyk *et al.*, 2007; Reverter and Lima, 2004; Shen *et al.*, 2006a). In particular, it is the proline residue (P94) found two amino acids after the di-glycine motif of SUMO3 that hinders its ability to be processed by SENP1 (Xu and Au, 2005), and probably by SENP2 as well.

Similarly, in SUMO1, it is H98 located adjacent to its C-terminal glycine that makes it an efficient substrate for maturation by SENP-1 (Xu and Au, 2005). It is now clear that these amino acid requirements depends on how SENPs catalyze SUMO maturation. When inactive mutants of SENP1's and SENP2's catalytic domains bind to the immature forms of SUMO, they bring about isomerisation of the modifier's scissile peptide bond to an unstably kinked *cis*-configuration (Reverter and Lima, 2006; Shen *et al.*, 2006a). This conformational change moves the C-terminal tail of SUMO into a position such that in SUMO1 its H98 residue is able to form a hydrogen bond with SENP1's G600 (Shen *et al.*, 2006a), thus stabilizing the resulting transition state complex. This stabilizing effect cannot occur for SUMO3 because it bears a proline at an equivalent position of SUMO1'S H98, which is probably detrimental to isomerisation given its rigidity (Shen *et al.*, 2006a). These structural studies also provide a possible explanation for why SENP2 is a much more efficient isopeptidase than C-terminal hydrolase (Reverter and Lima, 2006). When SUMO2 was crystallized with SENP2, in only one of three different configurations was SENP2's catalytic domain in an appropriate position for attacking to SUMO2's scissile bond (Reverter and Lima, 2006). It is therefore possible that the process of SUMO maturation, unlike deconjugation, may go through a series of non-productive intermediates. In addition, upon peptide bond-isomerization the residues in the C-terminal tail of SUMO adopt a position that may hinder interactions with SENP2's catalytic centre (Reverter and Lima, 2006).

1.2.4.3.2 Isopeptidase activity

Isopeptidase activity involves the cleavage of the peptide bond between the C-terminal glycine of SUMO and the ε-amino group of a target lysine. The structures of inactive mutants of SENP1's and SENP2's catalytic domain bound to a sumoylated fragment of RANGAP1 show that, like SUMO processing, SUMO deconjugation also proceeds through isomerisation of the scissile isopeptide bond, which positions such a linkage in a productive arrangement for its cleavage (Reverter and Lima, 2006; Shen *et al.*, 2006a). Nevertheless, a SUMO-conjugated lysine presents higher flexibility and fewer steric impediments in the catalytic pocket of SENPs in comparison to the more rigid modifier's C-terminal tail (see 1.2.4.3.1 and Reverter and Lima, 2006). This observation therefore puts forward an additional explanation for why SENP2 works preferentially as an isopeptidase.

The structures presented by Reverter and Lima (2006) and Shen *et al.* (2006a) also provide some insight on how these enzymes specifically desumoylate a certain

lysine/protein or SUMO paralogue (Gong and Yeh, 2006). Firstly, these properties are unlikely to depend on a direct interaction between the catalytic domain of a SENP and a substrate protein itself because SENP1's and SENP2's catalytic regions bind the sumoylated RanGAP1 mostly through SUMO and make very few contacts with RanGAP1 itself (Shen *et al.*, 2006a). Thus, other determinants may be involved in enabling SENPs to recognize a specific substrate, such as the regions flanking their catalytic domains. Secondly, it has been shown that SENP2 makes greater contact with SUMO2 than SUMO1 when they are conjugated to RANGAP1 and that, consistently, it desumoylates RANGAP1-SUMO2 more efficiently than RANGAP1-SUMO1 (Reverter and Lima, 2006). Conversely, although SENP1 binds SUMO1 and SUMO2 equally well, it processes RANGAP1-SUMO2 twice as well as RANGAP1-SUMO1 (Shen *et al.*, 2006a). These observations therefore suggest that the ability of SENPs to discriminate amongst SUMO paralogues may not be simply dependent on binding affinities.

1.2.5 The SUMO acceptor sites

Unlike ubiquitylation, for which no consensus modification sequence has been yet identified, SUMO typically targets lysines that fall within the motif ΨKXD/E, where Ψ is an aliphatic branched residue and X is any amino acid (Rodriguez *et al.*, 2001), although a hydrophobic residues at this position also improves sumoylation efficiency (Schwamborn *et al.*, 2008). At least partly, this phenomenon depends on the fact that sumoylation is brought about through a single E2, UBC9, which directly recognizes the motif ΨKXD/E (Bernier-Villamor *et al.*, 2002; Tatham *et al.*, 2003a), while ubiquitylation relies upon many different conjugating enzymes. Several lysines that do not fall within this motif can, however, be also sumoylated (Blomster *et al.*, 2009; Blomster *et al.*, 2010), indicating that other determinants, such as SUMO E3s, may be important for targeting SUMO to a particular substrate. For instance, in budding yeast the E3 enzyme Siz1 mediates the sumoylation of PCNA at the non-consensus lysine K164 (see 1.3.3). On the other hand, the evidence that not all lysines found within a ΨKXD/E sequence are sumoylated may depend on the fact that UBC9 can bind to this motif only when it is found in an extended loop or an unstructured region, but not when it is located in an α-helix (Bernier-Villamor *et al.*, 2002; Pichler *et al.*, 2005).

Several extensions of this basic ΨKXD/E sumoylation sequence have been identified. The first two types introduce a negative charge near such a consensus motif and thereby increase its likelihood/efficiency of being targeted by UBC9. The

phophorylation-dependent sumoylation motif (PDSM) was initially identified in the heat shock factor HSF1, but since then it has also been found in several other proteins (Hietakangas *et al.*, 2003; Hietakangas *et al.*, 2006; Yang and Gregoire, 2006). It conforms to the sequence ΨKX(D/E)XX(S/T)P, which can be efficiently sumoylated only when its serine/threonine is phosphorylated (Hietakangas *et al.*, 2006; Mohideen *et al.*, 2009; Yang and Gregoire, 2006). Thus, the PDSM provides cells with a way to control the sumoylation of specific proteins. This phenomenon is directly mediated by UBC9 through the presence of a positively-charged patch located close to its active site (K65, K74 and K76, Mohideen *et al.*, 2009), which is in an ideal position to accommodated the phosphorylated serine/threonine of a PDSM. A second extended sumoylation motif consists of the ΨKXD/E sequence followed by negatively charged amino acids, called negatively charged residue-dependent sumoylation motif (NDSM), and it has been found in several transcription factors (Yang *et al.*, 2006b). These acidic amino acids probably perform an analogous function to, and therefore substitute, the phosphorylated serine/threonine side chains found in the PDSM. Mutating the basic patch of UBC9 formed by K65, K74 and K76 inhibited the modification of a model NDSM only slightly (Mohideen *et al.*, 2009). This observation indicates that other residues within UBC9 may be important to mediate the enhanced modification of a NDSM in comparison to the PDSM, *e.g.* K59 and R61 (Yang *et al.*, 2006b). The recent identification of a large number of endogenous SUMO2-modified peptides in human cells by mass spectrometry has also revealed that clusters of basic or hydrophobic residues are often found C-terminal to the core sumoylation motif ΨKXD/E and are important for its efficient modification (Matic *et al.*, 2010; Schimmel *et al.*, 2010). Interestingly, Matic *et al.* (2010) also found that several human protein are modified at sites that conform to an inverted core sumoylation motif, that is, E/DXKΨ.

1.2.6 Formation and functions of SUMO chains

The N-terminal tails of the yeast Smt3 protein (^{10}AKPE$_{13}$, ^{13}VKPE$_{16}$ and ^{18}VKPE$_{21}$) and the higher eukaryotic SUMO2/3/4 (^{10}VKTE$_{13}$) contain classic SUMO attachment motifs, which can be sumoylated both *in vitro* and *in vivo*, leading to the formation of polymeric SUMO chains. Although SUMO1 lacks such sequences, it can still polymerize *in vitro*, mainly through K7, K16 and K17 (Pedrioli *et al.*, 2006). *In vivo* poly-SUMO1 chains have not been detected (Matic *et al.*, 2008), however they may exist given that a lysine in SUMO1's N-terminus, which conforms to an inverted sumoylation motif (^{5}EAKP$_{8}$), can be conjugated to SUMO2 in human cells (Matic *et al.*, 2010). SUMO1 has also

been found at the end of SUMO2/3 chains, thus suggesting that it may act as a chain-terminator (Matic *et al.*, 2008; Tatham *et al.*, 2008). Although the SUMO E1 and E2 enzymes alone are sufficient to generate SUMO chains *in vitro*, E3s can stimulate this process (Johnson and Gupta, 2001; Pichler *et al.*, 2002; Tatham *et al.*, 2001).

Unlike mono-sumoylation events, for which a downstream function cannot be generally predicted (see 1.3), poly-SUMO chains are poly-ubiquitylated, which therefore targets them, and the substrates attached to them, for proteasome-mediated degradation. In both budding and fission yeasts the key player in this process is a protein called Slx8. It contains a RING domain that mediates both ubiquitin ligase activity and binding to Slx5 in budding yeast, and Rfp1 (or the redundant Rfp2) in fission yeast (Ii *et al.*, 2007a; Mullen and Brill, 2008; Prudden *et al.*, 2007; Sun *et al.*, 2007; Uzunova *et al.*, 2007; Xie *et al.*, 2007). The presence of multiple SUMO-interacting motifs in Slx5 and Rfp1/2 enables Slx8 to preferentially bind, and thereby poly-ubiquitylate, poly-SUMO chains (Uzunova *et al.*, 2007). In humans, Slx8 and Slx5/Rfp1/Rfp2 have converged into a single protein called RNF4, which contains both a RING domain and multiple SUMO-interaction motifs, and it also mediates the poly-ubiquitylation of poly-sumoylated species (Lallemand-Breitenbach *et al.*, 2008; Sun *et al.*, 2007; Tatham *et al.*, 2008). *In vivo*, sumoylated proteins that are simultaneously ubiquitylated have been detected (Tatham *et al.*, 2008; Uzunova *et al.*, 2007). The levels of these species increase upon loss of the Slx8 complex in yeast or RNF4 in mammalian cells, but also when the proteasome is inhibited (Prudden *et al.*, 2007; Sun *et al.*, 2007; Tatham *et al.*, 2008; Uzunova *et al.*, 2007). In addition, Slx8/RNF4 proteins can catalyze the formation of K11- and K48-linked ubiquitin chains (Mullen and Brill, 2008; Tatham *et al.*, 2008), which have degradative functions. Proof that Slx8/RNF4 proteins target poly-sumoylated species for degradation came from the finding that PML is a target of RNF4. Exposure to arsenic trioxide leads to the recruitment of RNF4 and the proteasome to PML nuclear bodies and the degradation of PML itself (Lallemand-Breitenbach *et al.*, 2008; Shao *et al.*, 1998). The latter phenomenon depends on the ability PML to be sumoylated, on the presence of RNF4 and an active proteasome (Lallemand-Breitenbach *et al.*, 2008; Lallemand-Breitenbach *et al.*, 2001; Tatham *et al.*, 2008; Weisshaar *et al.*, 2008). In addition, *in vitro* RNF4 efficiently poly-ubiquitylates PML only when it has been previously poly-sumoylated (Tatham *et al.*, 2008; Weisshaar *et al.*, 2008).

The ability of Slx8/RFN4 proteins to target sumoylated species for degradation appears to be important for maintaining genome stability. In budding and fission yeasts, *SLX8*

mutants are hypersensitive to the fork-stalling agents hydroxyurea and the DNA alkylating agent MMS (Ii *et al.*, 2007b; Kosoy *et al.*, 2007; Mullen and Brill, 2008; Mullen *et al.*, 2001; Prudden *et al.*, 2007; Sun *et al.*, 2007; Xie *et al.*, 2007; Zhang *et al.*, 2006). They also exhibit a high frequency of gross chromosomal rearrangements, gene conversion events and small point mutations, which are likely to arise because of aberrant repair of double-stranded breaks (DSBs, Burgess *et al.*, 2007; Prudden *et al.*, 2007; Zhang *et al.*, 2006). In fission yeast a hypomorphic *slx8-1* allele is also synthetically lethal with deletions of genes involved in homologous recombination (Prudden *et al.*, 2007).

1.2.7 Regulation of SUMO conjugation

Sumoylation is not a static post-translational protein modification system but it is often regulated by specific factors such as environmental/cellular signals or the cell cycle. Mechanistically, sumoylation could be controlled by changing the rate of conjugation and/or removal of SUMO, globally or more specifically at a certain location in a cell or at a particular stage of the cell cycle. All of these scenarios have been reported and will be described below.

Firstly, environmental stimuli affect sumoylation levels. Unlike SUMO1, which is mostly found conjugated during unperturbed cell growth, SUMO2/3 mainly exist in their free forms under normal conditions but are quickly attached to cellular substrates in response to cellular insults such as excessive heat, metabolic stress, osmotic shock, hypoxia, *etc.* (Blomster *et al.*, 2009; Golebiowski *et al.*, 2009; Saitoh and Hinchey, 2000; van Hagen *et al.*, 2010,Sramko, 2006 #790). How cellular stresses upregulate the modification by SUMO2/3 is unknown but, at least in part, it could involve controlling the enzyme of the sumoylation pathway. For instance, during keratinocyte differentiation, Ca^{2+} signalling transiently induces transcription of *SAE1*/*SAE2*, *UBC9*, *SUMO2/3*, and *PIASx* (Deyrieux *et al.*, 2007). In addition, hypoxia stimulates the expression of *SUMO1* and the sumoylation enhancer RSUME (Carbia-Nagashima *et al.*, 2007). RSUME binds UBC9 and increases the non-covalent association between this enzyme and SUMO, which enhances UBC9~SUMO thioester formation and consequently SUMO conjugation (Carbia-Nagashima *et al.*, 2007). Sumoylation can also be regulated by signal-dependent changes in the sub-cellular localization of sumoylation pathway enzymes. Pro-inflammatory stimuli lead to the phosphorylation of PIAS1, which causes it to re-localize to, and therefore inhibit, PIAS1-responsive promoters, probably by promoting the modification of specific proteins at such locations

(Liu *et al.*, 2007). Environmental cues do not always stimulate the attachment of SUMO but they can also inhibit it. For example, moderate-to-low amounts of oxidative stress reduce sumoylation levels (Bossis and Melchior, 2006). This inhibitory effect is caused by the formation of a disulphide bond at the catalytic residues of UBA2 and UBC9, which effectively inactivates them (Bossis and Melchior, 2006). *In vivo*, the oxidative burst that accompanies the activation of macrophages also results in loss of sumoylation, indicating that the oxidation-dependent inhibition of sumoylation is a physiologically relevant phenomenon (Bossis and Melchior, 2006).

Secondly, the cell cycle has also been shown to affect sumoylation. In mammalian cells, SUMO1- and SUMO2-modified species are present throughout interphase, largely disappear at metaphase but their levels rise again during mitosis (Zhang *et al.*, 2008). Conversely, in *Xenopus* egg extracts substrates of SUMO2/3 can be detected in mitosis but hardly during interphase (Azuma *et al.*, 2003). The importance of the cell cycle in regulating sumoylation has also been demonstrated for specific SUMO substrates, such as PCNA (see 1.3.3), topoisomerase II (Agostinho *et al.*, 2008; Azuma *et al.*, 2003; Bachant *et al.*, 2002; Dawlaty *et al.*, 2008) and the bud neck-associated yeast septins (Johnson and Blobel, 1999). The modification of PCNA is restricted to S phase probably because it is efficiently sumoylated only when loaded onto DNA, that is, during DNA replication (Parker *et al.*, 2008). Conversely, the sumoylation of septins occurs only during mitosis and on the mother-side of the bud neck because their modification strictly depends on Siz1, which specifically re-localizes to the mother-cell side of a bud neck during mitosis (Johnson and Blobel, 1999; Johnson and Gupta, 2001). Regulating the sub-cellular localization of SUMO proteases, instead of SUMO ligases, during the cell cycle could also help restricting the modification of certain proteins at a specific cell cycle stage. This could be the case for the fission yeast Ulp1, which is found at the nuclear periphery during interphase but delocalizes throughout the nucleus at M phase (Taylor *et al.*, 2002), hence possibly leading to the loss/acquisition of defined sumoylation events specifically at mitosis.

Interestingly, it is becoming increasingly clear that the regulation of several cell cycle- or environmentally-controlled sumoylation events could depend on crosstalk between sumoylation and other post-translational modification events. For instance, phosphorylation can enhance sumoylation of a protein, generally by targeting a PDSM (see 1.2.5), but it can also inhibit it, as it seems to be the case for c-JUN, PML, IκBα and SREBP-2 (Arito *et al.*, 2008; Desterro *et al.*, 1998; Everett *et al.*, 1999; Muller *et al.*, 2000). Sumoylation can also be controlled by other post-translational modifiers that

target lysines, *e.g.* ubiquitylation, acetylation, methylation, *etc.*, potentially as a result of competition for the same cojugation site. For example, sumoylation competes with TNFα-, IL-1β- or okadaic acid-induced poly-ubiquitylation of IκBα at K21, thereby preventing its proteasome-mediated degradation (Desterro *et al.*, 1998). Additionally, SUMO also competes with acetylation, as in the case of histones H2A and H2B and transcription factors SP3, PGC1α, MEF2 and HIC1 (Gregoire *et al.*, 2006; Muller *et al.*, 2000; Nathan *et al.*, 2006; Rytinki and Palvimo, 2009; Sapetschnig *et al.*, 2002). For the latter two proteins, the acetylation-sumoylation switch is controlled by phosphorylation (Shalizi *et al.*, 2006; Stankovic-Valentin *et al.*, 2007).

1.3 Molecular consequences of sumoylation of DNA-associated proteins

Unlike ubiquitylation, which often targets proteins for degradation, the functional outcomes of sumoylation are impossible to predict because they can be as varied as changing the activity, localization and stability of a specific protein.

However diverse, the molecular consequences of different sumoylation events have been often traced back to a common molecular mechanism, that is, the ability of SUMO to alter the interactions of its substrates with other macromolecules. In fact, conjugating this modifier to proteins typically either occludes or creates specific binding sites in them. In most cases, sumoylation is likely to bring about these changes simply by adding an extra surface, *i.e.* SUMO, at a particular position along a protein, without significantly affecting its structure. Yet, in some instances sumoylation has been shown to alter the interaction properties of its targets by inducing them to undergo conformational changes (Geiss-Friedlander and Melchior, 2007). Although SUMO seems to exert its actions mainly by modulating the binding properties of its targets, exceptions to this rule have been reported. For instance, sumoylation has been shown to obstruct the post-translational modification of certain lysines by other post-translational modifiers, *e.g.* IκBα (see 1.2.7).

Here, I will initially present the general features of how sumoylation can bring about its functions. I will then contextualize these properties by describing the way in which SUMO affects the functions of two proteins, *i.e.* the DNA polymerase processivity factor PCNA and thymidine DNA glycosylase. I chose these two proteins because the roles of their modification are well understood, but also because they exemplify how DNA and sumoylation can regulate each other, which has been the main focus of my research.

1.3.1 The SUMO-interacting motif (SIM)

It is becoming increasingly clear that the ability of SUMO to change the binding properties of its targets is brought about through a motif that specifically recognizes SUMO itself. The best-characterized SUMO-interacting motif (SIM) consists of an essential hydrophobic core of four amino acids ([IVL]-X-[IVL]-[IVL] or [IVL]-[IVL]-X-[IVL]), which is often, but not always, flanked by a cluster of negatively charged amino acids or serines/threonines (Hannich *et al.*, 2005; Minty *et al.*, 2000; Song *et al.*, 2004). The latter residues have been proposed to allow the controlled introduction of a negative charge into a SIM, by being reversibly phosphorylated (Hecker *et al.*, 2006). These residues are not essential for the SUMO-SIM interactions, yet, they are important in modulating its strength, orientation and, possibly, paralogue specificity (see below).

Structural studies have shown that a SIM adopts an extended β-strand conformation and uses its hydrophobic core to bind SUMO within a groove that occurs between the α-helix and β_2 strand of this modifier. In addition, they have also revealed that SIMs can wedge into this site either in a parallel or an anti-parallel orientation with respect to the sense of the β_2 strand of SUMO (Baba *et al.*, 2005; Reverter and Lima, 2005; Song *et al.*, 2005). The specific orientation that a SIM adopts when binding SUMO is influenced by at least two factors: 1) the particular amino acid composition of its hydrophobic core, and 2) the presence of negatively charged residues around it (Kerscher, 2007). The latter of these two factors seems particularly important because the hydrophobic groove of SUMO is lined with basic amino acids, such as K39 of SUMO1 (Chupreta *et al.*, 2005; Song *et al.*, 2005). This residue occupies a favourable position to interact with the acidic residues of a SIM, and there is some evidence suggesting that it may actually do so (Hecker *et al.*, 2006). Thus, if such interaction existed, then it would bias the biding of a SIM to SUMO towards one orientation rather than the other because these motifs can carry negatively charged residues either N- or C-terminal to their hydrophobic core. Another residue that may be important to favour the binding of a SIM to SUMO is K78 of SUMO1. Unlike K39, which is conserved amongst all SUMO paralogues, K78 is unique to SUMO1 and therefore could account for the paralogue specificity that some SIMs exhibit (Hecker *et al.*, 2006). This specificity could also depend on the somewhat different positions that the hydrophobic grooves adopt with respect to the surrounding basic residues in SUMO1 and SUMO2/3 (Kerscher, 2007).

Since SIMs and SUMO can bind to each other on their own and with rather low affinity, it follows that the high-affinity/high-specificity binding with which SIM-containing factors must be targeted to the appropriate sumoylated proteins *in vivo* probably depends on additional elements. These elements could represent extra sites within the sumoylated protein that bind to the SIM-containing factor (Geiss-Friedlander and Melchior, 2007). Accordingly, although the effector of sumoylated PCNA in budding yeast, *i.e.* Srs2, can bind both SUMO and PCNA on their own, these interactions are significantly weaker than the one Srs2 exhibits for the modified PCNA (see 1.3.3 and Papouli *et al.*, 2005).

In addition to enabling a protein to recognize the modified form of a certain sumoylation target SIMs also play other roles. Firstly, many SIM-containing proteins known to date have also been found to be sumoylated, in a manner that depends on an intact SIM (Lin *et al.*, 2006; Meulmeester *et al.*, 2008; Takahashi *et al.*, 2005). Secondly, SIMs have also been identified in, and appear to be important for the activity of, some of the enzymes involved in the sumoylation pathway, such as UBA2, RANBP2 and PIAS-family E3s (Reverter and Lima, 2005; Song *et al.*, 2004).

To date, at least sixteen different domains have been shown to non-covalently bind ubiquitin (Grabbe and Dikic, 2009). It is therefore likely that SIMs other than the one described here exist. A variant of such a motif has in fact recently been discovered in mammals. It conforms to the consensus sequence [I/V/L]-[D/E]-[I/V/L]-[D/E]-[I/V/L], it is flanked to its N-terminus by negatively charged residues and it specifically recognizes SUMO-2/3 (Ouyang *et al.*, 2009).

1.3.2 How do low levels of sumoylation significantly affect the functions of a protein?

RANGAP1 is the only known example of a sumoylation target that is quantitatively modified (Mahajan *et al.*, 1997; Matunis *et al.*, 1996). In fact, most other substrates are sumoylated at surprisingly low levels (~1-2% or even less). Yet, eliminating even such small levels of sumoylation from these proteins often has a major effect on their properties. How can these apparently contradictory observations be explained? I will put forward two non-mutually exclusive models. They are similar to those already proposed by Geiss-Friedlander and Melchior (2007) and Johnson (2004), but they have been revisited on the basis of more recent findings. The first one of these two models speculates that sumoylation may occur, and thereby have an effect, only on a functionally active sub-population of a given protein. This scenario could happen if, for instance, such a protein sub-population exhibits properties that are different from the

general pool, such as sub-cellular localization or structure. Thus, under these conditions inhibiting the low sumoylation levels of a protein would be converted into a large effect on its functions because it would specifically affect only those molecules that are carrying out in a certain function (*e.g.* PCNA). The second model postulates that the entire pool of certain SUMO substrates is being constantly sumoylated. However, these proteins normally show low steady-state levels of modification probably because they undergo such rapid cycles of sumoylation and desumoylation that their modified forms exist only briefly. For some sumoylation events, such a short existence may be sufficiently long to exert their functions directly, while for others long-lasting effects may be brought about by their persistence even after SUMO has been removed. Thus, under these conditions abolishing the sumoylation of a certain protein would have a big effect on its properties simply because most of it is sumoylated during its normal life (*e.g.* thymidine DNA glycosylase).

1.3.3 The sumoylation of PCNA

PCNA forms a homotrimeric ring that encircles DNA and acts as a processivity factors for DNA polymerases during DNA synthesis. In *Saccharomyces cerevisiae*, PCNA is sumoylated mainly at K164 by Siz1, and to a lesser degree at K127 by Siz2 (Hoege *et al.*, 2002; Parker *et al.*, 2008; Stelter and Ulrich, 2003). The sumoylation of PCNA normally occurs at S phase (Hoege *et al.*, 2002), which is consistent with the fact that this protein is efficiently modified only when associated with DNA Parker *et al.* (2008). On the basis of these results and the fact that only a small amount of the total pool of PCNA is loaded onto DNA even during replication, (Parker *et al.*, 2008) have proposed that a large proportion, if not all, of the DNA-bound trimer could be modified.

PCNA's K164 is not only conjugated to SUMO: in response to genotoxic stress it is also mono- and poly-ubiquitylated by a group of enzymes known as the *RAD6* pathway (Hoege *et al.*, 2002). Mono-ubiquitylated PCNA allows stalled replication forks to bypass DNA lesions by recruiting damage-tolerant polymerases, while the poly-ubiquitylated one activates a damage avoidance pathway that relies on homologous recombination (Ulrich, 2005). Although SUMO and ubiquitin are attached to the same site on PCNA, they do not seem to compete or act antagonistically with each other. Instead, PCNA sumoylation has been proposed to divert DNA repair away from homologous recombination and into the *RAD6* pathway (Papouli *et al.*, 2005).

The first clue to the roles of PCNA sumoylation came from the observation that the helicase Srs2 and PCNA sumoylation belong to the same genetic pathway. An

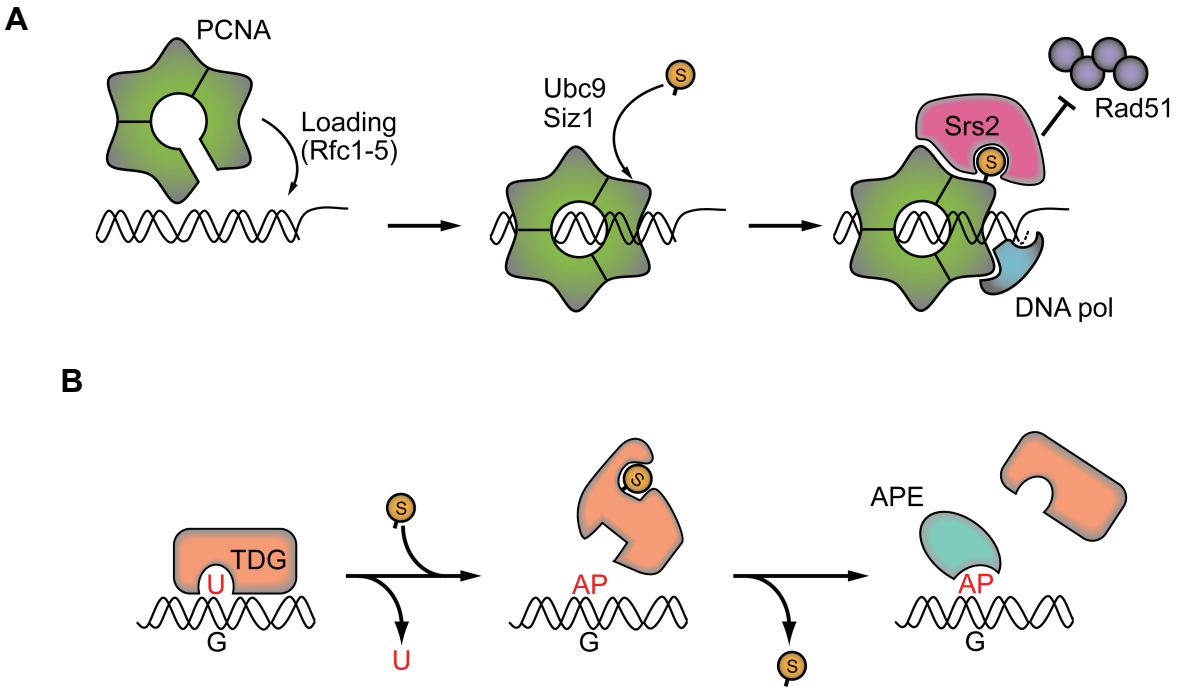

Figure 1.3 - Molecular consequences of sumoylation of DNA-associated proteins. A) At S phase PCNA is loaded onto DNA by the Rfc1-5 complex, thereby becoming a suitable substrate for sumoylation. The resulting PCNA-SUMO conjugate recruits the Srs2 helicase to replication forks, where it prevents the formation of recombinogenic Rad51 filaments. B) TDG binds and cleaves mismatched uracils (U) or thymidines from DNA, producing an abasic site (AP). TDG strongly binds to AP sites and to disassociate from them it needs to undergo a sumoylation-induced conformational change. Once TDG detaches from the DNA, it is probably quickly de-sumoylated, allowing it to bind damaged DNA again. DNA pol = DNA polymerase, G = guanine, APE = AP endonuclease, S = SUMO.

unsumoylatable PCNA mutant (*pol30*$^{K127/164R}$) or a deletion of *SIZ1* or *SRS2* all suppress equally well the DNA damage sensitivity of *rad18Δ* cells, where PCNA cannot be ubiquitylated. Additionally, deleting *SRS2* in *rad18*Δ *siz1*Δ or *rad18*Δ *pol30*$^{K127/164R}$ cells does not suppress their damage sensitivity any further. As expected, given the anti-recombinogenic properties of Srs2, such suppressor phenotypes have also been shown to depend on the presence of an intact homologous recombination pathway (Papouli *et al.*, 2005; Pfander *et al.*, 2005). Homologous recombination involves the exchange or replacement of genetic information between two homologous DNA regions. This genetic relationship was taken a step forward by demonstrating that Srs2 preferentially interacts with the sumoylated PCNA both *in vivo* and *in vitro*, probably because it contains a SIM at its C-terminus (Papouli *et al.*, 2005; Pfander *et al.*, 2005). It has therefore been proposed that the sumoylated PCNA recruits Srs2 to replication forks, where this enzyme counteracts homologous recombination. Conversely, when PCNA cannot be modified, Srs2 is unable to associate with replication forks efficiently,

thus explaining the increased rate of homologous recombination that cells demonstrate under these conditions (Robert *et al.*, 2006).

Overall, these observations suggest that sumoylated PCNA, by means of recruiting Srs2, prevents stalled replication forks from being repaired by possibly harmful homologous recombination, and consequently promotes damage bypass through PCNA ubiquitylation (**Figure 1.3**A, Papouli *et al.*, 2005; Pfander *et al.*, 2005).

The sumoylation of PCNA is not specific to budding yeast, but it has also been seen in *Xenopus* egg extracts, chicken DT40 cells and human cells (Arakawa *et al.*, 2006; Leach and Michael, 2005; Stephen West, personal communication). Its downstream functions in these systems remain, however, unclear because although helicases with some sequence similarity to Srs2 have been found in higher eukaryotes, none has yet been demonstrated to impinge on the *RAD6* pathway like Srs2.

Sumoylation appears to modulate the interactions of PCNA not only with Srs2 but also with other proteins. One such factor is Elg1, which plays a role in the maintenance of various aspects of genome stability. It binds to Rfc2-5 to form a PCNA-loading complex that is functionally distinct from the canonical Rfc1-5 complex. Elg1, through SIMs that are located in its N-terminus, preferentially interacts with the sumoylated PCNA (Parnas *et al.*, 2010). Although the functional implications of this observation presently remain unclear, it has been shown that knocking out *ELG1* results in higher levels of sumoylated PCNA and Srs2 on chromatin and synthetic sickness in the *srs2Δ* background. In addition, mutating Elg1's SIMs recapitulates, to a partial degree, the genome stability phenotype that is observed in *ELG1* knockout cells (Parnas *et al.*, 2010). On the other hand, sumoylation also seems to interfere with the binding of PCNA to at least two of its known interaction partners, *i.e.* Rfc1 and Eco1. In budding yeast, K127 is found within a region of PCNA that acts as its main partner-interaction site. The sumoylation of such residue has therefore been proposed to have a general effect on the association of PCNA with its partners, essentially acting as an "off-switch" to clear the clamp (Moldovan *et al.*, 2006).

1.3.4 The sumoylation of thymidine DNA glycosylase

Thymidine DNA glycosylase (TDG) binds and removes thymine or uracil within the G•T and G•U mismatches that are formed from the deamination of 5-methyl-cytosine or cytosine, respectively (Barnes and Lindahl, 2004). It is part of a family of enzymes that recognize and cleave a narrow spectrum of damaged or modified nitrogenous bases.

The abasic sites produced by these enzymes feed into a common pathway that involves the initial disassociation of the glycosylase from the DNA and the nicking of its damaged strand by the APE1 endonuclease. Subsequently, DNA polymerase β removes the baseless sugar backbone and polymerizes across the resulting gap. Finally, the XRCC1-ligase III complex seals the patched DNA (Barnes and Lindahl, 2004). This pathway of DNA repair is known as base excision repair (BER).

Human TDG is sumoylated at K330 and it contains two SIMs, one N- and one C-terminal to its central catalytic core (Baba *et al.*, 2005; Hardeland *et al.*, 2002; Mohan *et al.*, 2007; Steinacher and Schar, 2005; Takahashi *et al.*, 2005). The crystal structures of the central region of TDG conjugated to either SUMO1 or SUMO3 suggest that the covalent and non-covalent (through the C-terminal SIM) interactions SUMO makes with TDG may extrude a helix from the surface of the glycosylase. When DNA is fitted into such a structure, this protruding helix sterically clashes with the duplex, thus indicating that a SUMO-induced conformational change may force the enzyme to dissociate from DNA (Baba *et al.*, 2005, 2006). In fact, sumoylating TDG strongly reduces its affinity for DNA, thereby stimulating its catalytic turnover (Hardeland *et al.*, 2002). The ability of SUMO to interact with the N-terminal domain of TDG, which is necessary for tight binding to mismatched G•T, may also be involved in reducing its affinity for DNA because deleting such domain enhances TDG turnover in a way that is “epistatic” with SUMO modification. Consistently, the N-terminus of TDG appears to undergo a conformational change when the enzyme becomes sumoylated (Steinacher and Schar, 2005). Altogether, these observations indicate that conjugating SUMO to TDG changes the structure of its central catalytic and N-terminal domains, thereby reducing its affinity for DNA allowing it to dissociate from the abasic site and promoting catalytic turnover (**Figure 1.3**B, Hardeland *et al.*, 2002; Steinacher and Schar, 2005; Takahashi *et al.*, 2005). Given that *in vivo* DNA glycosylases quickly turn over on damaged DNA (Barnes and Lindahl, 2004), it follows that TDG probably exists as a SUMO conjugate for a very short period of time during its catalytic cycle.

What happens to the sumoylated TDG after it disassociates from the DNA? It is probably quickly desumoylated. This event appears to be an essential pre-requisite to allow TDG to translocate to PML bodies. In fact, in exponentially growing cells TDG is enriched within PML nuclear bodies (Mohan *et al.*, 2007). Mutating either PML’s sumoylation sites or TDG’s SIMs abolishes this co-localization, indicating that it relies on the interaction between TDG’s SIMs and sumoylated PML (Mohan *et al.*, 2007; Takahashi *et al.*, 2005). Consistently, TDG preferentially binds to sumoylated PML *in*

vitro (Takahashi *et al.*, 2005). The reasons for why TDG would need to localize within PML nuclear bodies are unknown but it could involve the acetyl-transferase CBP/p300. CBP/p300 localizes to PML bodies and it can acetylate TDG, but only when it is unmodified (Tini *et al.*, 2002), thus suggesting that the ability of the glycosylase to localize within PML bodies may promote its acetylation (Mohan *et al.*, 2007).

1.4 Poly(ADP-ribosyl)ation

In addition to being targeted by SUMO and other common types of protein post-translational modifiers, proteins can also be covalently conjugate to chains of ADP-ribose units linked together by glycosidic bonds. Poly(ADP-ribose), or PAR, chains are synthesized from NAD^+ by members of the poly(ADP-ribose) polymerase (PARP) family of enzymes and they are degraded by the combined actions of specific glycosylases and lyases.

1.4.1 The poly(ADP-ribosyl)ation reaction

The mechanism of PAR formation by PARP-1, the founding member of the PARP family of proteins (see 1.5), and probably by the other members of such family, involves three enzymatic steps (**Figure 1.4**B, Alvarez-Gonzalez and Mendoza-Alvarez, 1995; Alvarez-Gonzalez *et al.*, 1994).

Initially, PARP-1 hydrolyzes NAD^+ (**Figure 1.4**A) to produce nicotinamide, one proton and an ADP-ribose unit, which this enzyme then transfers directly to a substrate. PAR can be attached to the side chains of glutamates and, less commonly, aspartates through a relatively labile ester linkage as well as that of lysines through a more stable peptide bond (Altmeyer *et al.*, 2009; Burzio *et al.*, 1979; Messner *et al.*, 2010; Riquelme *et al.*, 1979; Suzuki *et al.*, 1986; Tao *et al.*, 2009).

In the second reaction, known as elongation step, PARP-1 catalyzes the transfer of ADP-ribose moieties onto a mono(ADP-rybosyl)ated protein by linking the 1'-OH group of the "nicotinamide" ribose of the second ADP-ribose moiety to the 2'-OH group of the "adenine" ribose of the previous ADP-ribose unit via a (1''-2') glycosydic bond (**Figure 1.4**B). Multiple rounds of this reaction produce chains that can reach up to 200 units in length both *in vitro* and *in vivo* (Alvarez-Gonzalez and Jacobson, 1987; Alvarez-Gonzalez *et al.*, 1994; Hayashi *et al.*, 1983). Once a PAR polymer is 20 or more units long, PARP-1 can branch it every 20-40 ADP-ribose moieties by catalyzing the formation of a (1'''-2'') glycosydic bond between the 2''-OH group of the "nicotinamide"

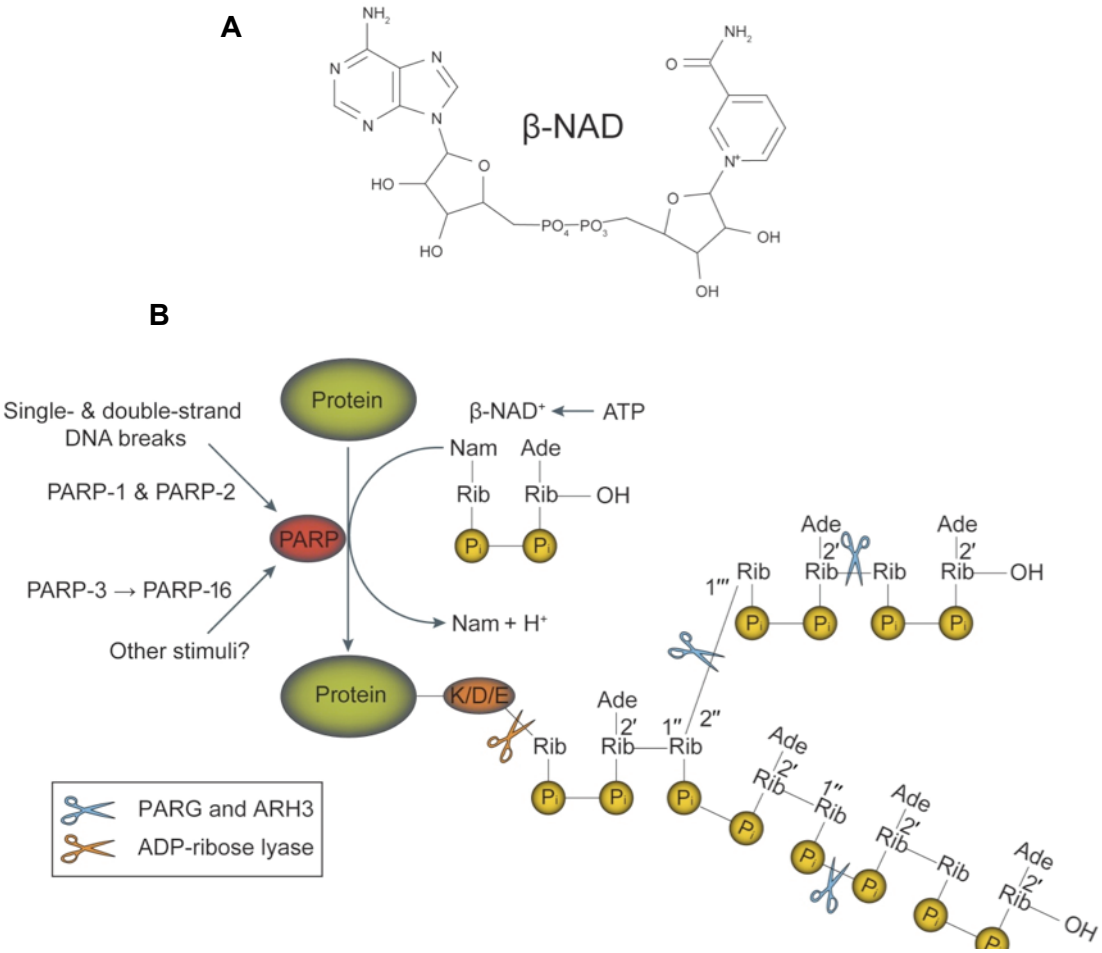

Figure 1.4 - The mechanism of reversible parylation. (A) The chemical structure of β-NAD. (B) Upon stimulation by a relevant signal, PARPs hydrolyze β-NAD$^+$ to ADP-ribose and subsequently attach this molecule to specific lysine (K), glutamate (E) or aspartate (D) residues within a target protein. PARPs can further elongate mono(ADP-ribosyl)ated amino acids by catalyzing the formation of a 2'-1'' glycosidic bond between ADP-ribose moieties. Glycosidic bonds of the 2''-1''' type can also be generated by PARPs, thus leading to the branching of PAR chains. Such polymers are degraded by the combined actions of PARG and ARH. ADP-ribose-lyase is responsible for cleaving the bond that occurs between the side chain of an amino acid and the ADP-ribose moiety attached to it. Ade = adenine, Rib = ribose, P_i = phosphate group. Adapted from Schreiber *et al.* (2006).

ribose of a PAR chain and the 1'''-OH group of the "nicotinamide" ribose of an ADP-ribose unit (**Figure 1.4**B, Hayashi *et al.*, 1983; Juarez-Salinas *et al.*, 1982).

1.4.2 Poly(ADP-ribose) catabolism

In mammalian cells, the half-life of PAR is very short; it ranges from 30 s to 5 min (Alvarez-Gonzalez and Althaus, 1989), which means that it must be quickly degraded. PAR degradation depends on at least three different enzymes: poly(ADP-ribose)

glycohydrolase (PARG), (ADP-ribosyl)arginine hydrolase-3 (ARH3) and ADP-ribose lyase.

1.4.2.1 PARG

PARG is the best characterized amongst the PAR-degrading enzymes. It hydrolyzes the glycosidic linkage between ADP-ribose units both exo- and endo-glycoytically, eventually yielding free ADP-ribose (Braun *et al.*, 1994; Brochu *et al.*, 1994; Hatakeyama *et al.*, 1986). On the basis of the time-dependent changes that the length and abundance of PAR chains undergo *in vitro* in the presence of PARG, it has been proposed that such an enzyme degrades these polymers in a two-step process (Braun *et al.*, 1994; Brochu *et al.*, 1994; Davidovic *et al.*, 2001; Hatakeyama *et al.*, 1986). Initially, PARG quickly reduces the overall size of the polymers by attacking them using both its endo- and exo-glycosidic activities, the latter of which seems to act processively (Braun *et al.*, 1994; Hatakeyama *et al.*, 1986). When these oligomers reach a critically small size, PARG switches to a slow exo-glycosidic mode of action, which appears to proceed distributively (Braun *et al.*, 1994; Hatakeyama *et al.*, 1986). These observations are consistent with *in vivo* data showing that PAR is processed through an initial rapid degradation step followed by a slower one (Wielckens *et al.*, 1983).

In mammals, several isoforms of PARG have been detected, which appear to be generated by alternative splicing and have different properties (Meyer *et al.*, 2007; Meyer-Ficca *et al.*, 2004; Niere *et al.*, 2008; Whatcott *et al.*, 2009). One of the two main forms is 110 kDa in size and it is exclusively found in the nucleus (Meyer-Ficca *et al.*, 2004). The other main form of PARG is 65 kDa in size and it localizes to the cytoplasm and mitochondria (Mueller-Dieckmann *et al.*, 2006; Whatcott *et al.*, 2009). The size of such PARG isoforms can be reduced even further by the use of alternative translation start sites to produce a protein of 55 kDa, which localizes only to the mitochondrial matrix (Meyer *et al.*, 2007; Niere *et al.*, 2008; Whatcott *et al.*, 2009). These mitochondrial species are therefore likely to be responsible for the PAR-degrading activity that has been detected in such organelles (Meyer *et al.*, 2007). At present the roles of a mitochondrial PAR-degrading activity remain unclear but they could be related to the proposed ability of over-activated PARP-1 to trigger the breakdown of the mitochondrial membrane potential and the consequent release of apoptosis inducing factors (see 1.5.3.2).

In mammals, PARG must have essential functions or play essential roles because *PARG*$^{-/-}$ mice die at an early embryonic stage (Koh *et al.*, 2004). Similarly, a loss-of-function allele of PARG also compromises larval survival in the fruit fly (Hanai *et al.*, 2004). At least some of PARG's roles must relate to DNA repair because depleting it slows down the repair of single-stranded breaks (SSBs) and DSBs (Ame *et al.*, 2009; Fisher *et al.*, 2007). Mice carrying a hypomorphic PARG allele, which eliminates its 110 kDa form while preserving the 60 kDa one, are also hyper-sensitive to genotoxins (Cortes *et al.*, 2004). Consistently, cells derived from these animals show several markers of altered DNA repair, such as: the formation of an unusually small number of DNA damage-induced XRCC1 foci, delayed γH2AX phosphorylation, decreased DNA break intermediates during repair, and increased cell death (Gao *et al.*, 2007). PARG-depleted cells also demonstrate DNA damage-induced amplification and fragmentation of centrosomes, aberrant mitotic cells, aneuploidy, and increased cell death by mitotic catastrophe (Ame *et al.*, 2009). The latter observations therefore suggest that PARG may impinge on other processes in a cell besides DNA repair, such as transcription (Frizzell *et al.*, 2009) and chromatin structure (Tulin *et al.*, 2006).

1.4.2.2 ARH3 and ADP-ribose lyase

ARH3 is the second PAR-degrading enzyme that has been identified in mammals (Mueller-Dieckmann *et al.*, 2006; Oka *et al.*, 2006). It is located in the mitochondrial matrix (Meyer *et al.*, 2007; Niere *et al.*, 2008), and it can also cleave O-acetyl-ADP-ribose, which is a by-product of the activity of SIR2 family of acetyl-histone deacetylases (Ono *et al.*, 2006).

Although PARG and ARH3 can hydrolyze the glycosidic linkages that hold PAR chains together, they are unable to cleave the bond that ties the first ADP-ribose moiety of these polymers to an amino acid. This activity is mediated by ADP-ribose lyase (**Figure 1.4**B, Oka *et al.*, 1984; Okayama *et al.*, 1978), which remains a poorly characterized enzyme.

1.4.3 The PARP superfamily of proteins

All seventeen members of the PARP family of proteins share a common β-α-loop-β-α-loop-β fold known as the "PARP signature" (Ame *et al.*, 2004). This motif is found at the C-terminus of all PARPs except for PARP-4, where it is located closer to its N-terminus. The PARP signature shows a fair amount of variability amongst PARPs in at least two respects. Firstly, in terms of the length and sequence of its loops, which have

Figure 1.5 - The PARP family. The domain architecture of the seventeen members of the PARP family from humans is shown. Protein domains are depicted as coloured boxes, as indicated in the figure itself. Within the hypothetical catalytic domains of these proteins (light blue boxes), the region similar to the PARP signature (aa 859-908 of PARP-1) and the amino acid corresponding to the putative catalytic residue of PARP-1, *i.e.* E988, are highlighted using a darker shade of blue. WGR = tryptophan, glycine and arginine, DBD = DNA-binding domain, RRM = RNA-recognition motif; BRCT = BRCA1 C-terminus, WWE = tryptophan, tryptophan, glutamate, ANK = ankyrin repeat, SAM = sterile α-motif, UIM = ubiquitin-interacting motif, HPS = a domain that contains homopolymeric runs of histidine, vWA = von Willebrand factor type A, VIT = vault inter-α-trypsin, MVP-BD = binding site for major vault protein, MLS = mitochondrial localization signal, NES = nuclear export signal, NoLS = nucleolar localization signal, NLS = nuclear localization signal. Adapted from Schreiber *et al.* (2006).

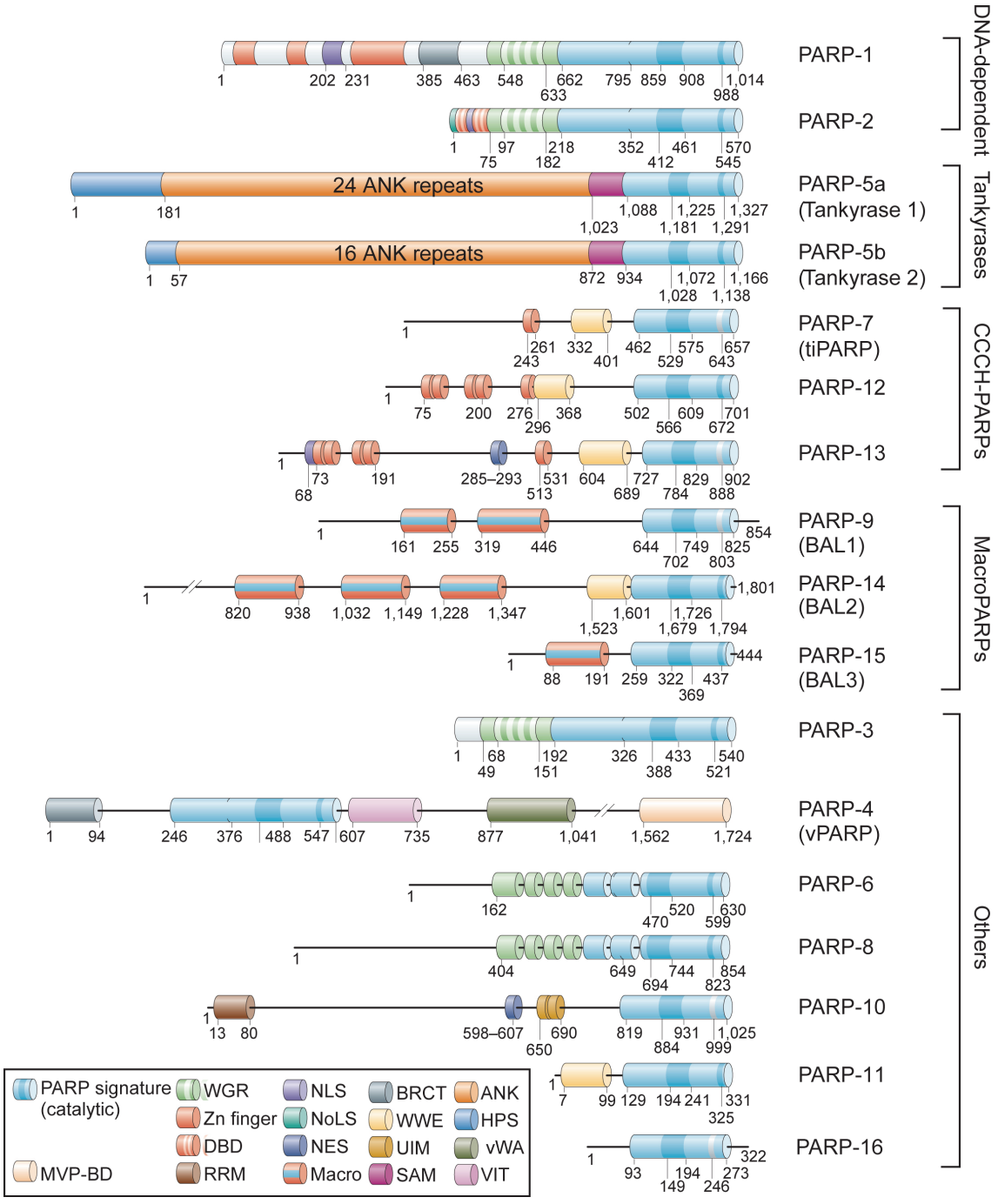

been proposed to act as protein-protein interaction sites (Ame *et al.*, 2004). Secondly, in terms of the presence and/or identity of the catalytic residue carried within such a fold. The catalytic glutamate of PARP-1, *i.e.* E988, is present in PARP-2, PARP-3, PARP-4, the tankyrases PARP-5a and 5b, PARP-5c, PARP-11, PARP-12 and PARP-14 (Ame *et al.*, 2004). They are therefore likely to be active, which has actually been shown for some of them (Ame *et al.*, 1999; Smith *et al.*, 1998). On the other hand, PARP-1's E988 appears to be substituted with an aspartate in PARP-15, but is absent from PARP-7, PARP-9, PARP-10, PARP-13 and PARP-16, thus raising the question of whether these proteins are catalytically active (Ame *et al.*, 2004). Interestingly, while PARP-9 seems to be unable to make PAR (Aguiar *et al.*, 2005), some activity has been reported for PARP-7 and PARP-10 (Ma *et al.*, 2001; Yu *et al.*, 2005).

Outside their PARP signature, the members of the PARP family are very heterogeneous with respect to the functions of the domains they contain, thus suggesting that they probably play roles in a variety of cellular processes. Some of the motifs found in these proteins are known to be involved in: nucleic acid binding (zinc fingers, SAP and RRM), protein-protein interactions (SAM, ankyrin, BRCT), ubiquitin binding (WWE and UIM), ADP-ribose binding (macro domain), and cell signalling (hormone binding domains and HPS, Ame *et al.*, 2004). The functional heterogeneity of a few of these proteins is increased even further by the controlled exclusion of some of their domains through alternative splicing (Schreiber *et al.*, 2006). On the basis of the functions of the domains they contain and/or their known roles, the proteins belonging to the PARP family have been classified into five categories (Schreiber *et al.*, 2006): DNA-activated PARPs (PARP-1 and PARP-2), tankyrases (PARP-5a and PARP-5b), CCCH-type PARPs (PARP7, PARP-12 and PARP-13), macroPARPs (PARP-9, PARP-14 and PARP-15) and other PARPs (PARP-3, PARP-4 and PARP-10).

1.4.3.1 DNA damage-activated PARPs

The most salient feature of PARP-1 and PARP-2 is that their catalytic activity is strongly induced by DNA strand breaks.

PARP-1 is a large multi-domain enzyme that plays roles in genome stability, DNA repair, cell death and transcription, which I will describe in more detail in 1.5.

PARP-2 is fairly similar to PARP-1. It was initially discovered because of the presence of residual levels of DNA damage-dependent PARP activity in *PARP-1*$^{-/-}$ mouse embryonic fibroblasts (Ame *et al.*, 1999; Shieh *et al.*, 1998). PARP-1 and PARP-2 are

likely to be, at least partly, complementary to each other because mice that lack either one of these genes are viable while the double knockout is embryonically lethal (Menissier de Murcia *et al.*, 2003). In addition, it has been shown that PARP-1 and PARP-2 hetero-dimerize and share many partners, including proteins involved in BER (*e.g.* XRCC1, DNA polymerase β and DNA ligase III, Schreiber *et al.*, 2002), hence suggesting that PARP-2, like PARP-1, might also be involved in DNA repair. In line with this hypothesis it was shown that *PARP-2*$^{-/-}$ cells repair single-stranded DNA breaks more slowly than their wild-type counterparts (Schreiber *et al.*, 2002). Such results have however been challenged by a more recent report where PARP-2-deficient cells were found to repair their DNA as well as control cells, both in the presence and absence of PARP-1 (Fisher *et al.*, 2007). Even though PARP-2 is likely to be partly redundant with PARP-1, it probably also has unique features because the phenotypes of *PARP-2*$^{-/-}$ mice are not identical to those observed in *PARP-1*$^{-/-}$ animals (Menissier de Murcia *et al.*, 2003). In fact, while PARP-1 can recognize both DNA nicks and gaps and preferentially parylates histone H1 (see 1.5), PARP-2 apparently binds only gaps and preferentially parylates histone H2B (Ame *et al.*, 2004).

1.4.3.2 Tankyrases

PARP-5a and PARP-5b, also known as tankyrase 1 and tankyrase 2, are paralogous proteins with roles in telomere homeostasis, mitotic spindle function and intracellular trafficking.

Both tankyrase 1 and tankyrase 2 include the PARP signature as well as SAM and ankyrin domains. Tankyrase 1 also comprises a HPS motif (Ame *et al.*, 2004). The SAM motif mediates the homo- and hetero-dimerization of these proteins, while the ankyrin domain allows them to interact with other proteins, including TRF1 and NuMA (Hsiao and Smith, 2008). Since tankyrase 1 and tankyrase 2 are very similar to each other and share most of their protein partners, it is likely that they play overlapping and/or redundant functions. It has in fact been recently shown that although individually knocking out one or the other tankyrase produces mice that are mostly normal, except for a reduced size in the tankyrase 2 mutant (Chiang *et al.*, 2006), the double knockout is embryonically lethal (Chiang *et al.*, 2008).

TRF1 is a negative regulator of telomere length. *In vitro*, tankyrase 1 parylates TRF1 and reduces its ability to bind telomeres (Smith *et al.*, 1998). *In vivo*, over-producing tankyrase 1 leads to the loss of TRF1 from telomeres and their consequent elongation (Smith and de Lange, 2000). Conversely, tankyrase 1 knock-down leads to telomere

shortening (Donigian and de Lange, 2007). The over-production of tankyrase 2 also causes telomere lengthening, but the relevance of this observation remains to be confirmed because such a protein does not localize to telomeres (Cook *et al.*, 2002).

Tankyrases also interact with a protein called NuMA, which is essential for the proper assembly of mitotic spindles (Chang *et al.*, 2005a; Chang *et al.*, 2005b). This interaction is probably physiologically relevant because depleting NuMA leads to the loss of tankyrase 1 from the spindle poles, while knocking down tankyrase 1 compromises the assembly of normal bipolar spindles and triggers to the formation of ectopic ones (Chang *et al.*, 2005a; Chang *et al.*, 2005b). Interestingly, NuMA itself binds PAR (Chang *et al.*, 2005b).

1.4.3.3 CCCH-type PARPs

The CCCH-type PARPs (PARP-7, PARP-12 and PARP-13) contain $CX_8CX_5CX_3$-like zinc fingers, a WWE domain and the PARP fold (Ame *et al.*, 2004). Very little is known about the properties of these proteins.

Transcription of the *PARP-7* gene, also known as *tiPARP*, is induced by the pollutant 2,3,7,8-tetrachlorodibenzo-*p*-dioxin and after prolonged long-term potentiation in the hippocampus (Ma *et al.*, 2001; Matsuo *et al.*, 2000).

PARP-13 is produced as two isoforms by alternative splicing (Ame *et al.*, 2004). The shorter one lacks the catalytic domain and confers resistance to infection by retroviruses by binding to the viral RNA genome through its CCCH motif (Gao *et al.*, 2002).

PARP-12 is closely related to PARP-13.

1.4.3.4 MacroPARPs

MacroPARPs (PARP-9, PARP-14 and PARP-15) contain the PARP catalytic motif plus 1-3 macro domains (Ame *et al.*, 2004). These domains are highly conserved in all kingdoms of life and directly recognize NAD^+ metabolites such ADP-ribose, *O*-acetyl-ADP-ribose or PAR (Karras *et al.*, 2005).

Although the exact functions of the macro domains found in the macroPARPs remain unclear, these proteins appear to act as transcription regulators. PARP-9 seems to negatively influence transcription and to play a role in lymphocyte migration *in vitro* (Aguiar *et al.*, 2005; Aguiar *et al.*, 2000). Following stimulation by interleukin 4, PARP-

14 mediates the activation of the *STAT6* gene in T cells and protects B cells against apoptosis (Cho *et al.*, 2009; Goenka and Boothby, 2006).

1.4.3.5 Other PARPs

PARP-3 is a mono-ADP-ribosylase that interacts with PARP-1 and activates it *in vitro* (Loseva *et al.*, 2010). PARP-3 localizes to the daughter centriole within centrosomes (Augustin *et al.*, 2003). Although its over-production has no discernable effect on the centriole cycle, it interferes with progression into S phase (Augustin *et al.*, 2003). PARP-3 also co-localizes with polycomb group bodies and it interacts with several proteins involved in genome stability (Rouleau *et al.*, 2007). Yet, knocking down PARP-3 does not perceivably affect cell survival in response to the genotoxic agent camptothecin (Augustin *et al.*, 2003).

PARP-4, also known as vPARP, is part of barrel-shaped ribonucleoprotein complexes called vaults, which play a role in the multi-drug resistance of human tumours (Kickhoefer *et al.*, 1999). PARP-4 associates with the vault protein TEP1, which is known to interact with telomerase (Liu *et al.*, 2004). PARP-4 knockout mice are viable and show no appreciable defect in vault structure or telomere homeostasis, but they exhibit an increased incidence of carcinogen-induced colon tumours (Liu *et al.*, 2004; Raval-Fernandes *et al.*, 2005).

PARP-10 is also a mono-ADP-ribosylase (Kleine *et al.*, 2008). It contains an RRM and a glycine-rich domain, both of which can mediate interactions with RNA (Ame *et al.*, 2004). It preferentially localizes to the nucleolus where it is phosphorylated at the G_1-S and prometaphase-to-cytokinesis transitions (Chou *et al.*, 2006). PARP-10 interacts with and strongly inhibits the cell transformation properties of the proto-oncoprotein c-MYC (Yu *et al.*, 2005).

So far, nothing is known about the functions of PARP-6, PARP-8 and PARP-11.

1.5 The poly(ADP-ribose) polymerase 1 (PARP-1)

The human PARP-1 is a modular protein of 1014 amino acids and 113 kDa. It is encoded by the *PARP-1* gene which is located at 1q41-42, is 43 kbp long, contains 23 exons and encodes for an mRNA with an open reading frame of 3042 nt. PARP-1 is present in all higher eukaryotes, but not in yeast.

PARP-1 is a chromatin-associated protein that resides mainly in the nucleus, where it is somewhat enriched in the nucleolus (Meder *et al.*, 2005) as well as at the nuclear

membrane and nuclear matrix (Fakan *et al.*, 1988; Kaufmann *et al.*, 1991; Mosgoeller *et al.*, 1996). Additionally, PARP-1 has also been found in the mitochondria (Fakan *et al.*, 1988; Rossi *et al.*, 2009). It is the most abundant member of the PARP family, it accounts for 90% of the parylation activity *in vivo* (Shieh *et al.*, 1998), and it is also the main, but not the sole, acceptor of PAR (Satoh and Lindahl, 1992). It has been estimated that between 2×10^5 to 2×10^6 molecules of the polymerase exist in a cell, depending on the type (Ludwig *et al.*, 1988; Yamanaka *et al.*, 1988), which gives about one molecule of this protein for every 1,500-15,000 bp of the human genome. PARP-1 plays a critical role in genome stability, but it also controls gene transcription and apoptosis. For some of these functions its catalytic activity is not required.

1.5.1 The structure of PARP-1

PARP-1 can be divided into three functionally distinct domains: an N-terminal DNA-binding domain (DBD), an auto-modification domain (AD) and a C-terminal catalytic domain (CAT, **Figure 1.6**, Kameshita *et al.*, 1984).

1.5.1.1 The DNA-binding domain

The DBD comprises the initial 373 aa of PARP-1 and contains three zinc fingers.

The first two fingers are similar to each other and conform to the consensus sequence $CX_2C\text{-}X_{28/30}\text{-}WHX_2C$. This kind of domain is known as PARP-type zinc finger and it has been found in other proteins such as DNA ligase III, ZDP, a DNA 3'-phosphoesterase from *A. thaliana*, and many others by bioinformatics means (Petrucco and Percudani, 2008). It folds into a structure consisting of an N-terminal three-stranded anti-parallel β-sheet, which contains a long loop joining the first and second β-strands, and a C-terminal region that includes two α-helices (Nagashima *et al.*, 2005). The extended loop and the C-terminal portion of the first α helix show significant variability amongst the PARP-type zinc fingers, and could account for their different DNA binding properties (Petrucco and Percudani, 2008). In fact, exchanging the first α helix of PARP-1's finger I motif with that of its second zinc finger imparts finger I-like DNA binding properties onto the finger II motif (Gradwohl *et al.*, 1990).

The first and second zinc fingers of PARP-1 are widely believed to recognize both altered structures in DNA, and consequently activate the polymerase, and possibly also specific DNA sequences (see 1.5.2). They bind DNA breaks independently of the remainder of PARP-1 and they may dimerize in the process of doing so (Menissier-de Murcia *et al.*, 1989; Pion *et al.*, 2003; Pion *et al.*, 2005). Additionally, the first two

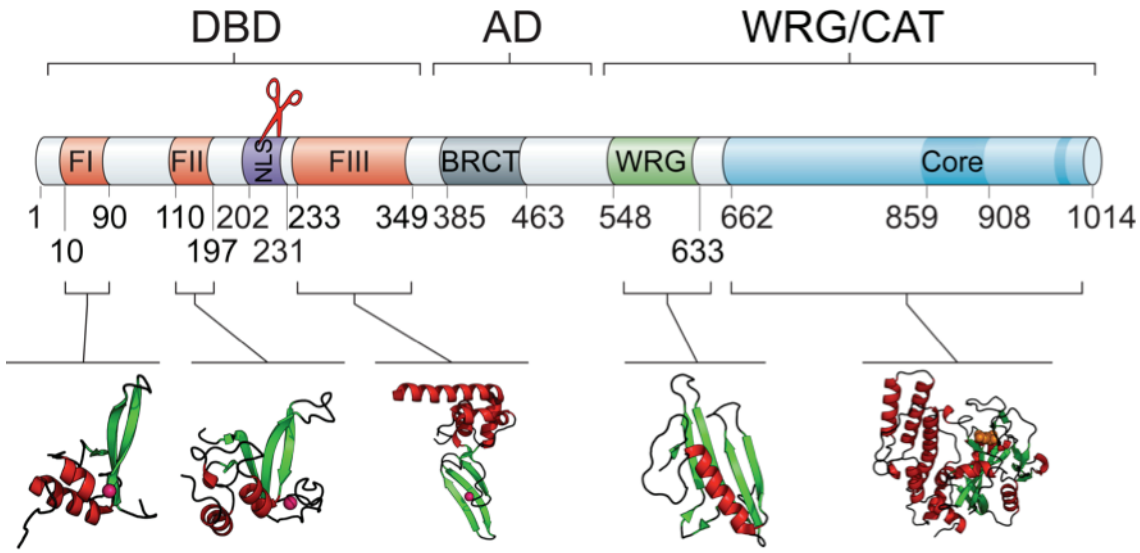

Figure 1.6 - The domain structure of the human PARP-1 protein. The domain architecture of the human PARP-1 protein is shown. Numbers indicate amino acid positions. Red scissors show the position of PARP-1's caspase cleavage site. DBD = DNA-binding domain, AD = auto-modification domain, WRG/CAT = catalytic domain, FI-III = zinc finger domains I through III, NLS = nuclear localization signal, BRCT = BRCA1 C-terminus domain, WRG = tryptophan, arginine and glycine domain, core = PARP signature. If available, the tertiary structure of individual PARP-1 domains is shown. Secondary structure elements are colour in red, for α-helices, green, for β-strands, and pink for the Zn^{2+} ion. The cartoon representations of protein structures were created with PyMOL (http://pymol.sourceforge.net/).

fingers of PARP-1 also seem to mediate interactions of the polymerase with other proteins, such as DNA polymerase α (Dantzer *et al.*, 1998), histones (Griesenbeck *et al.*, 1997), the transcription factor TEF1 (Butler and Ordahl, 1999) and the hormone receptor RXRα (Miyamoto *et al.*, 1999). It however remains to be undoubtedly confirmed that these interactions are direct and not mediated through DNA.

An intact finger I motif is essential for the activation of the polymerase in response to both single- and double-stranded breaks (Altmeyer *et al.*, 2009; Ikejima *et al.*, 1990), indicating that it is probably involved in recognizing both types of lesions. Interestingly, this domain must be able to act *in trans* to form a catalytically active complex of PARP-1 with DNA because incubating a mutant polymerase missing its first zinc finger with one lacking its finger III motif or its catalytic residue restores PAR formation *in vitro* (Altmeyer *et al.*, 2009). These *in vitro* data apparently contradict the finding that in the fruit fly a PARP-1 mutant devoid of its finger I domain is activated as well as the wild type polymerase in response to ionizing radiation (Kotova *et al.*, 2010). Instead, this mutant demonstrates an unusually strong localization within euchromatin and a concomitant decrease in that within heterochromatin, thus resulting in an increased

mobilization of the transposable elements normally found in these regions (Kotova *et al.*, 2010).

The finger II motif of PARP-1 directly recognizes SSBs and it is essential for the activation of the polymerase in their presence, but not in response to DSBs (Gradwohl *et al.*, 1990; Ikejima *et al.*, 1990). Binding of PARP-1 to nicked DNA, probably through its second zinc finger, protects 7 bp of DNA on both sides of the break (Gradwohl *et al.*, 1990; Menissier-de Murcia *et al.*, 1989).

The third zinc finger of PARP-1 is structurally and functionally different from the other two. It folds into three anti-parallel β-strands and it conforms to the consensus sequence CX_2C-X_{12}(loop)-C-X_9-C, which resembles a classic zinc ribbon motif (Langelier *et al.*, 2008; Tao *et al.*, 2008). It does not appear to bind DNA, at least on its own (Tao *et al.*, 2008), and inactivating it in the context of the full-length polymerase does not affect its binding to dsDNA oligonucleotides bearing free ends (Langelier *et al.*, 2008). Although this motif is not essential for the catalytic activity of PARP-1 *per se*, mutating or deleting it abolishes the ability of the polymerase to become activated in response to DNA damage (Altmeyer *et al.*, 2009; Langelier *et al.*, 2008; Tao *et al.*, 2008). Interestingly, incubating PARP-1 mutants with an inactive or missing zinc finger III motif together with a wild type version of this domain alone reconstituted their capacity to generate PAR. A similar effect was also observed when these mutants were mixed with a catalytically dead version of the polymerase (Altmeyer *et al.*, 2009; Langelier *et al.*, 2008; Tao *et al.*, 2008). This apparent ability of PARP-1's third zinc finger to act *in trans* has been interpreted as to mean that it must aid the DNA-dependent activation of the polymerase by mediating intra-molecular interactions between its DBD bound to damaged DNA and its catalytic domain (Langelier *et al.*, 2008). Such interactions are likely to be mediated by the extended loop that is part of the finger III domain because mutating specific residue within this region also abolishes the DNA-dependent activation of PARP-1 (Langelier *et al.*, 2010). These findings cannot be easily reconciled with the observation that the finger III motif of the polymerase does not appreciably bind any other PARP-1 domain, either in the presence or absence of DNA (Langelier *et al.*, 2008). It has however been proposed that these interactions may be either too weak to be detected or that they may occur only in the context of full-length PARP-1, when DNA and/or NAD^+ are also present (Langelier *et al.*, 2008). The crystal structure of PARP-1's third zinc finger has revealed that it can form a dimer in the crystal lattice (Langelier *et al.*, 2008). The relevance of this finding is unclear because in solution this domain exists as a monomer (Langelier

et al., 2010; Tao *et al.*, 2008). Nevertheless, mutating the residues that line this hypothetical dimerization surface between finger III motifs in the full-length PARP-1 reduces the ability of this enzyme to compact chromatin and consequently to inhibit transcription *in vitro*, but not its DNA-dependent activation (Langelier *et al.*, 2010).

The DBD also includes a bipartite nuclear localization signal of the type KRK-X_{11}-KKKSKK (aa 207-226) that targets PARP1 to the nucleus (Schreiber *et al.*, 1992).

1.5.1.2 The auto-modification domain

The AD is located between amino acids 373 and 525 of the human PARP-1. It acts as the main acceptor region for the auto-parylation activity of this enzyme, but only when it is physically linked to its catalytic domain (Kameshita *et al.*, 1986). Some auto-modification also seems to occur within the DBD (Desmarais *et al.*, 1991).

The AD is positively charged and contains 15 of the 28 glutamates that have been hypothesized to be parylated in PARP-1 (Desmarais *et al.*, 1991; Kameshita *et al.*, 1984; Kawaichi *et al.*, 1981; Mendoza-Alvarez and Alvarez-Gonzalez, 1999). The modification of some of these residues (D387, E488, and E491) has been directly proven by mass spectrometry (Tao *et al.*, 2009). Mutating them however reduces but does not abolish PARP-1 auto-modification, thus suggesting that other sites must also be modified (Tao *et al.*, 2009). Altmeyer *et al.* (2009) also showed that a PARP-1 mutant lacking its BRCT motif (see below) and all of the remaining glutamates found within its AD was auto-parylated as well as the wild-type protein. Instead, they demonstrated that mutating K498, K521 and K524 was sufficient to almost completely abolish the auto-parylation of the polymerase, thus indicating that lysines, rather than glutamates, might be the major sites of PARP-1 auto-parylation, at least *in vitro*.

In addition to acting as the main acceptor region of PAR, PARP-1's AD also functions as a binding site for a variety of proteins, such as ribosomal proteins (Koyama *et al.*, 1999), the transcription factors YY1 (Oei *et al.*, 1997), OCT1 (Nie *et al.*, 1998) and E2F1 (Simbulan-Rosenthal *et al.*, 2003), UBC9 (Masson *et al.*, 1997), p21 (Cazzalini *et al.*, 2010), the human papillomavirus type 18 E2 protein (Lee *et al.*, 2002), XRCC1 (Masson *et al.*, 1998), PARG (Keil *et al.*, 2006) and histones (Buki *et al.*, 1995). These interactions could be mediated by the BRCT domain present within the AD, which is well-known to act as a protein-protein interaction motif in other polypeptides. In fact, this appears to be the case for XRCC1 (Masson *et al.*, 1998) and the human papillomavirus type 18 E2 protein (Lee *et al.*, 2002). These binding events could alternatively be dependent on a leucine zipper that has been hypothesized to exist at

the N-terminus of PARP-1's AD (Uchida *et al.*, 1993), which has also been proposed to possibly mediate PARP-1 homo-dimerization and/or hetero-dimerization with PARP-2 (Schreiber *et al.*, 2002; Uchida *et al.*, 1993).

1.5.1.3 The catalytic domain

The CAT domain is located between amino acids 526 and 1014 of the human PARP-1, however, the minimal region that is able to support normal PAR activity maps to the C-terminal most 40 kDa of the enzyme (Simonin *et al.*, 1990). The activity of this domain is very limited and is not stimulated by damaged DNA, which means that it corresponds to the basal activity of the full-length PARP-1 (Simonin *et al.*, 1990).

The first 80-90 residues of PARP-1's CAT region form a WGR domain, which is named after its most-conserved residues: tryptophan (W), glycine (G) and arginine (R). It is essential for the DNA-dependent enzymatic activity of PARP-1 (Altmeyer *et al.*, 2009), and, on the basis of its structure, it has been proposed to bind nucleic acids (Nagashima *et al.*, 2005).

The core of PARP-1's catalytic domain is a region of approximately 50 residues that extends over amino acids 859 and 908 in the human enzyme, which corresponds to the PARP signature (Ame *et al.*, 2004). It acts as PARP-1's NAD^+-binding pocket and contains the active site (Ruf *et al.*, 1996). Its structure resembles that of the catalytic domain of bacterial mono(ADP-ribosyl)ating enzymes but not other common NAD^+-binding motifs, such as the Rossman fold (Ruf *et al.*, 1996). On account of this similarity, it has been proposed that E988 of the human PARP-1 could act as the catalytic residue (Marsischky *et al.*, 1995). Mutating it almost completely abolishes the ability of the polymerase to extent PAR chains but has a comparatively minor effect on its mono(ADP-ribosyl)ation activity (Rolli *et al.*, 1997). Thus, these observations indicate that E988 is essential for PARP-1 to extend PAR polymers, but other residues must mediate the initial mono(ADP-ribosyl)ation step. The presence of two dinucleotide-binding motifs in PARP-1's catalytic core, *i.e.* $^{892}GKG_{894}$ and $^{952}GKT_{954}$, the first one of which is important for PARP-1 activity (Kim *et al.*, 1997), also provides a rationale for how this enzyme can catalyze the formation of a glycosidic bond between two ADP-ribose moieties.

PARP-1's CAT domain also appears to play functions that are independent of its catalytic activity. Firstly, it could be involved in DNA binding because a fragment of the polymerase encompassing the C-terminal region of its DBD, AD and CAT domains bound to a DNA substrate more strongly that an equivalent construct lacking the

catalytic motif (Desmarais *et al.*, 1991). Secondly, the CAT domain may promote the dimerization of PARP-1 and thereby regulate this protein because such a motif, on its own, can form dimers, regardless of DNA being present or not (Mendoza-Alvarez and Alvarez-Gonzalez, 2004). Thirdly, the CAT domain is essential for the ability of PARP-1 to regulate chromatin structure. *In vitro*, the full-length polymerase can trigger the compaction of a nucleosomal array in a manner that depends on an intact DBD (Wacker *et al.*, 2007). Yet, although PARP-1's DBD is unable to condense chromatin on its own, it can do so when it is artificially fused to the CAT domain (Wacker *et al.*, 2007).

1.5.2 Binding of PARP-1 to DNA

The earliest recognized property of PARP-1 was its ability to become activated in response to damaged DNA both *in vitro* and *in vivo*, where this event leads to a rapid drop in the cellular pools of NAD^+ (Durkacz *et al.*, 1980; Yoshihara, 1972). Because of its ability to directly bind SSBs, PARP-1 has been long viewed by many as a molecular DNA nick sensor; yet, it can recognize other kinds of DNA damage and also intact DNA, as I will describe in more detail below.

1.5.2.1 Interactions with damaged DNA

The interactions between PARP-1 and damaged DNA occur through its DBD and have been best characterized for single- and different kinds of double-stranded breaks. Measurement of tryptophan fluorescence decay upon binding of PARP-1's DBD to different types of DNA strand interruptions (SSBs, blunt DSBs or DSBs bearing 5' or 3' overhangs) indicate that it binds to all of them equally well (Lilyestrom *et al.*, 2010; Pion *et al.*, 2005). Yet, PARP-1 is activated by 3' overhangs better than 5' ones, which in turn stimulate the polymerase more efficiently than SSBs (Benjamin and Gill, 1980; D'Silva *et al.*, 1999). The effects of blunt DSBs on PARP-1 activation are instead less clear: although a plasmid containing this type of interruption activates the polymerase more strongly than those bearing 3' or 5' ends and both 8 bp- and 201 bp-long dsDNA oligonucleotides have also been shown to stimulate it (Benjamin and Gill, 1980; D'Silva *et al.*, 1999; Hengartner *et al.*, 1991), Pion *et al.* (2005) detected no PARP-1 activation in the presence of a 66 bp-long dsDNA oligonucleotide. The phosphorylation state of DSBs also dictates how well they can activate PARP-1, as those bearing dephosphorylated ends stimulate the polymerase better than those with 3' phosphorylated termini and, in turn, 5' phosphorylated ones (Benjamin and Gill, 1980).

Although plenty of evidence shows that the binding of PARP-1 to damaged DNA activates this enzyme, only recently the first, low resolution, image of how such a phenomenon may occur at the molecular level has been reported. By using small-angle X-ray diffraction scattering (SAXS), Lilyestrom *et al.* (2010) showed that a region of PARP-1 encompassing its DBD and BRCT motif (PARP aa 1-486) seems to consist of two, or possibly more, folded domains connected by bendy hinges that make it highly flexible in its free form. In the presence of SSBs and DSBs, PARP-1(1-486) binds to them and becomes more elongated. The extent of this elongation is more pronounced for blunt DSBs than those bearing 3' overhangs or single-stranded breaks, thus indicating that PARP-1 binds to different DNA interruptions in different ways (Lilyestrom *et al.*, 2010). Upon binding to DNA breaks the two SAXS diffraction peaks shown by DNA-free PARP-1(1-486), but not those produced by a domain of the polymerase containing only its first and second zinc fingers, coalesce into one. Such observations have been interpreted to mean that PARP-1(1-486) probably undergoes a structural change in the presence of damaged DNA that involves a region outside its first two finger motifs, that is, its third zinc finger and BRCT domains. This hypothesis would be consistent with the fact that the third finger motif of PARP-1 seems to mediate inter-domain contacts that are important for the activation of the polymerase (see 1.5.1.1).

Lilyestrom *et al.* (2010) and other groups have also uncovered other aspects of how PARP-1 binds to DNA damage. Firstly, they have shown that the DBD of this enzyme protects less DNA on oligonucleotides containing blunt DSBs than those bearing SSBs or 3' overhangs (Lilyestrom *et al.*, 2010; Pion *et al.*, 2003; Pion *et al.*, 2005). For the latter type of damage, the DBD was found to bind proximally to the single-to-double-stranded region of the DNA substrate in an asymmetric manner with respect to the break itself, *i.e.* the double-stranded portion of this oligonucleotide was protected more than the single-stranded one (Lilyestrom *et al.*, 2010; Pion *et al.*, 2003; Pion *et al.*, 2005). Secondly, tryptophan fluorescence decay data suggest that PARP-1(1-214) dimerizes upon binding to 5' double-stranded breaks with positive cooperativity. This observation is consistent with the evidence that catalytically-active PARP-1 may exist as a dimer (Altmeyer *et al.*, 2009; Mendoza-Alvarez and Alvarez-Gonzalez, 1993). Having said that, the diffraction and sedimentation equilibrium ultracentrifugation data presented by Lilyestrom *et al.* (2010) indicate that PARP-1(1-486) binds to its DNA substrates as a monomer.

PARP-1 does not only recognize DNA strand interruptions but it also apparently binds, and thereby becomes activated by, other kinds of insults, such as the cross-linking type

of DNA damage caused by UV light, *e.g.* pyrimidine dimers (Vodenicharov *et al.*, 2005), or platinum, *e.g.* mostly 1,2-d(GpG) (Zhu *et al.*, 2010).

1.5.2.2 Interactions with intact DNA

In addition to its well-characterized ability to recognize DNA strand breaks, PARP-1 can also interact with intact forms of DNA, including specific sequences, non-B type DNA and possibly standard undamaged DNA duplexes.

PARP-1 can recognize specific DNA sequences. They are often, but not always, found in transcription regulatory regions where they probably help the polymerase exert some of its gene expression-related roles (see 1.5.3.3.3). These sequences include the IUR element (TCGATCTGGAACTCC) in the *CXCL1* gene (Nirodi *et al.*, 2001), the MCAT-1 sequence (CATTCCT) in the cardiac troponin T gene (Butler and Ordahl, 1999), the TxRE element (TGACGACA) in the *HTLV1* promoter (Zhang *et al.*, 2002), a *cis*-element in the *REG* promoter (TGCCCCTCCCAT, Akiyama *et al.*, 2001), the 37-bp MBR region of the *BCL2* promoter (Yang *et al.*, 2010), a silencer-binding region (GATGGGTTTCACAATTTTTCAAGCA) within the *BRCA2* promoter (Wang *et al.*, 2008a) and an intronic sequence (TTGANNACAA) at the *BCL6* locus (Ambrose *et al.*, 2007). In addition, PARP-1 also binds nuclear matrix attachment DNA sequences and certain repetitive elements found within human centromeric sequences, such as GTGAAAAAG and ATGTATATATGTGTATATAGACATAAAT (Earle *et al.*, 2000; Galande and Kohwi-Shigematsu, 1999). Interestingly, the latter interaction could explain why PARP-1 is enriched at active centromeres in human cells, especially during mitosis and replication, independently of heterochromatin nucleation (Earle *et al.*, 2000).

By using a variety of biochemical techniques, *e.g.* plasmon surface resonance, atomic force microscopy, foot-printing and electrophoretic mobility shift assays, and in many cases circular or end-protected DNA substrates, many groups have shown that PARP-1 can also bind related non-B DNA structures. These structures include stable or transiently-forming simple hairpins or loops, three-way, *i.e.* replication fork, and four-way, *i.e.* Holliday, junctions (Jorgensen *et al.*, 2009; Lonskaya *et al.*, 2005; Pion *et al.*, 2005; Potaman *et al.*, 2005; Sastry and Kun, 1990; Soldatenkov *et al.*, 2002). What feature of such DNA structures PARP-1 recognizes remains unclear. Potaman *et al.* (2005) showed that PARP-1 protects from nuclease cleavage the tip of a stable hairpin in an artificial four-way junction but not its cross-over point. Conversely, nuclease protection analysis of a cruciform that naturally occurs in plasmid pUC7 revealed that

PARP-1 protects one half of the base of this structure, but not its loops (Sastry and Kun, 1990). It is therefore possible that although the polymerase binds both loops and crossovers, it preferentially recognizes only one of these structures in a particular cruciform. Besides binding to hairpins and cruciforms, PARP-1 also seems to recognize other non-B DNA structures, such as DNA bends (Sastry *et al.*, 1989), which usually occur in AT-rich sequences, and G-quadruplexes (Soldatenkov *et al.*, 2008), which are four-stranded secondary structures that are believed to originate in regions of high densities of adjacent guanines. With the exception of DNA bends, all of the above-described DNA structures can activate PARP-1 *in vitro* (Jorgensen *et al.*, 2009; Lonskaya *et al.*, 2005; Pion *et al.*, 2005; Potaman *et al.*, 2005; Sastry and Kun, 1990; Soldatenkov *et al.*, 2002; Soldatenkov *et al.*, 2008). Altogether these observations therefore provide a possible explanation for how PARP-1 can parylate several proteins, many of which have a role in transcription (see 1.5.3.3), apparently in the absence of DNA damage. As a matter of fact, transcriptional regulatory regions are known to contain sequences prone to forming unusual non-B type DNA structures (van Holde and Zlatanova, 1994).

To date, whether PARP-1 binds standard B form DNA in a sequence-independent manner remains unclear. This hypothesis has in fact never been directly addressed and there is evidence both in its favour and against it. On the one hand, Ikejima *et al.* (1990) observed that PARP-1 shows generalized binding to both supercoiled and digested plasmids, with only a slight preference for the latter. In the case of the digested plasmid, the polymerase also preferentially bound longer DNA fragments, which would be consistent with PARP-1 being able to recognize multiple internal sites of intact DNA. PARP-1's DBD was not necessary for these binding events because a mutant lacking such a domain could still bind both the supercoiled and digested plasmids, only more weakly than the full-length protein. Additionally, Sastry *et al.* (1989) detected binding of PARP-1 to a plasmid that had been cut at a single position and then ligated to produce a relaxed circular DNA molecule. PARP-1's ability to interact with a relaxed plasmid is also further supported by the fact that this enzyme can introduce negative supercoiling in such a type of DNA (Sastry and Kun, 1988). This observation, together with the fact that PARP-1 is able to relax supercoiled plasmids (Chasovskikh *et al.*, 2005; Gradwohl *et al.*, 1987; Yung *et al.*, 2004) and to introduce significant alternations in the structure of an AT-rich bent DNA substrate (Sastry *et al.*, 1989), highlight an important property of the enzyme, *i.e.* its ability to impart structural changes onto DNA. On the other hand, Lonskaya *et al.* (2005) detected no binding of

PARP-1 to an end-protected ~300 bp dsDNA oligonucleotide, and Gradwohl *et al.* (1987) showed that the polymerase efficiently binds a plasmid only when it is supercoiled. It was hypothesized that the latter phenomenon occurred probably because in a supercoiled plasmid the torsional strain to which the DNA is subjected may promote the formation of unusual secondary structures, which may be directly recognized by PARP-1.

1.5.3 The functions of PARP-1

1.5.3.1 Roles of PARP-1 in DNA repair

Treating cells with genotoxins, such as monovalent alkylating agents (*e.g.* MMS, MNNG, MNU, etc.), H_2O_2, UV light or double-stranded break-inducing drugs (*e.g.* γ-irradiation), leads to the production of PAR during the first few minutes of exposure, in a PARP-1-dependent manner (Hagan *et al.*, 2007; Vodenicharov *et al.*, 2005; von Kobbe *et al.*, 2003). Parylation is therefore believed to be the first line of response cells trigger following DNA damage (Chatterjee and Berger, 1998), which is not surprising considering that PARP-1 can directly recognize, and thereby be activated by, broken DNA (see 1.5.2.1). The ability of PARP-1 to promptly respond to damaged DNA is important to maintain genome stability because *PARP-1*$^{-/-}$ mice show increased sensitivity to a range of genotoxins as well as higher levels of DNA damage-induced sister-chromatid exchanges, chromosome breaks and micro-nuclei, in comparison to wild type animals (de Murcia *et al.*, 1997; Masutani *et al.*, 1999; Simbulan-Rosenthal *et al.*, 1999). Many of these organismal phenotypes have also been observed at the cellular level in various types of *PARP-1*$^{-/-}$ mouse cells or chicken DT40 cells but also in human cells depleted of the polymerase (de Murcia *et al.*, 1997; Fisher *et al.*, 2007; Trucco *et al.*, 1998). At least in part, the above-described phenotypes are likely to depend on the ability of PARP-1 to promote the repair of both SSBs and DSBs.

1.5.3.1.1 PARP-1 and the repair of single-stranded DNA breaks

SSBs are the most common type of DNA damage found in a cell. They represent breakage of the deoxyribose-phosphate backbone of a DNA duplex, which can occur as result of direct attack by chemicals such as H_2O_2, aborted topoisomerase I activity and as normal intermediates of DNA repair processes.

SSBs activate PARP-1 *in vitro* and *in vivo*, where they are mainly repaired by BER (see 1.3.4 and Barnes and Lindahl, 2004). Although PARP-1 is not essential for this pathway of DNA repair, and BER can in fact be reconstituted *in vitro* without the

polymerase (Kubota *et al.*, 1996), this enzyme seems to enhance it. By employing *PARP-1*$^{-/-}$ mouse embryonic fibroblasts, *PARP-1*$^{-/-}$ chicken DT40 cells and human cells stably depleted of PARP-1, three different groups have demonstrated that in the absence of the polymerase, even though the repair of SSBs goes to completion, the rate of this process is slowed down in comparison to wild type cells (Dantzer *et al.*, 2000; Fisher *et al.*, 2007; Trucco *et al.*, 1998; Woodhouse *et al.*, 2008). An earlier report by Vodenicharov *et al.* (2000) challenges this view because the authors did not detect any difference in the repair efficiency of DNA breaks between *PARP-1*$^{-/-}$ and *PARP-1*$^{+/+}$ cells. The fact that all of the former three studies used a very sensitive technique to measure the number of DNA breaks within cells, called the comet assay, instead of relying on the incorporation of a labelled nucleotide, as did Vodenicharov *et al.* (2000), may explain such discrepancies. Inhibiting PARP activity also affects how efficiently DNA breaks are repaired *in vivo*, hence suggesting that the catalytic activity of PARP-1 may be necessary for its DNA repair-promoting properties (Atorino *et al.*, 2001; Durkacz *et al.*, 1981; Durkacz *et al.*, 1980; Smith *et al.*, 2005). This phenomenon however needs to be considered with care because it is probably the consequence of a dominant-negative effect of inactivating PARP-1. In fact, the evidence that auto-parylated PARP-1 has a lower affinity for DNA than the unmodified enzyme (D'Amours *et al.*, 1999; Wacker *et al.*, 2007), probably because of ionic repulsion between the negatively charged DNA and PAR polymers bound to it (Ferro and Olivera, 1982), has been taken to mean that parylation of PARP-1 is required for its disassociation from a DNA break (D'Amours *et al.*, 1999; Satoh and Lindahl, 1992). It follows that a catalytically inhibited PARP-1 would tightly bind to DNA breaks without being able let go of them, hence preventing other repair proteins from accessing the damaged DNA (Fisher *et al.*, 2007; Parsons *et al.*, 2005). Consistent with this hypothesis is the fact that PARP-1's DBD, which should behave similarly to a chemically-inhibited full-length enzyme, acts as a trans-dominant mutant of the polymerase when it is over-produced: it inhibits DNA damage-induced parylation, it sensitizes cells to DNA-damaging agents and it can also induce polyploid nuclei in the absence of genotoxins (Cayuela *et al.*, 2001; Kupper *et al.*, 1990; Kupper *et al.*, 1995; Molinete *et al.*, 1993; Rudat *et al.*, 2001).

1.5.3.1.2 PARP-1 and the repair of double-stranded breaks

The roles of PARP-1 in the processing of DSBs remain poorly understood and controversial. This type of DNA lesion can be repaired by either homologous

recombination, which involves the replacement of genetic information between two identical or similar DNA sequences, and/or non-homologous end joining, where broken DNA ends are directly ligated together without the need for a homologous DNA template. In mammalian cells, DSBs are repaired mostly by non-homologous end joining (Jackson, 2002).

The fact that PARP-1 binds to, and is stimulated by, DSBs *in vitro* (Benjamin and Gill, 1980) and that DSB-inducing genotoxins activate it *in vivo* (Dong *et al.*, 2010) would suggest that PARP-1 is involved in repairing this type of DNA lesion. Consistently, cells devoid of PARP-1 or PARP activity are hypersensitive to genotoxins that cause DSBs, show increased levels of DNA re-arrangements, and accumulate unusually high levels of sister chromatid exchanges, which are widely believed to result from over-activation of homologous recombination (de Murcia *et al.*, 1997; Simbulan-Rosenthal *et al.*, 1999; Trucco *et al.*, 1998; Wang *et al.*, 1997). Altered rates of trans-gene integration have also been reported following the loss of PARP-1 or PARP activity, a process that depends on the processing of DSBs, however, some studies report higher insertion rates while others lower ones than wild type cells (Dominguez-Bendala *et al.*, 2006; Farzaneh *et al.*, 1988; Waldman and Waldman, 1990). These observations would predict that cells devoid of PARP-1 or PARP activity should accumulate DSBs, which has in fact been demonstrated (Heacock *et al.*, 2010). The fact that such a phenomenon is restricted to cells in S phase of the cell cycle (Heacock *et al.*, 2010), however, suggests that it, and by inference also the above-described phenotypes, probably arise from DSB that are generated by replicating DNA over unrepaired nicks or gaps, rather than because of compromised DSB repair *per se* (Bryant and Helleday, 2006; Heacock *et al.*, 2010). This model is supported by many studies showing that *PARP-1*$^{-/-}$ cells have no significant defects in homologous recombination or non-homologous end joining in comparison to wild type cells (Noel *et al.*, 2003; Schultz *et al.*, 2003; Yang *et al.*, 2004). It has however to be mentioned that inhibition of PARP activity or loss of PARP-1 has been shown to somewhat sensitize cells to DSB-inducing genotoxins (Hochegger *et al.*, 2006) and slow down the repair of breaks induced by γ-irradiation (Mitchell *et al.*, 2009).

Although PARP-1 may not be involved in repairing DSBs in normal cells, there is some evidence indicating that it becomes important in such a process when the classical non-homologous end joining pathway is compromised. In this pathway, DNA ends are joined together by the combined actions of the KU70/80/DNA-PKcs complex, which in addition to binding and protecting free DNA termini probably also brings them in close

proximity, the nuclease Artemis, which seems to polish DNA ends, and the XRCC4-ligase IV complex, which eventually ligates them together (Jackson, 2002). Firstly, PARP-1 parylates KU70 and DNA-PKcs and is phosphorylated by DNA-PKcs (Ariumi *et al.*, 1999; Morrison *et al.*, 1997). Secondly, although neither *KU80* nor *PARP-1* is an essential gene in mice, deleting both of them is embryonically lethal (Henrie *et al.*, 2003). Thirdly, inhibiting PARP activity in cells devoid of the KU complex or where DNA-PKcs is also inactivated significantly compromises the repair of DSBs (Audebert *et al.*, 2004; Wang *et al.*, 2006). Inhibition of PARP activity also reduced the efficiency of re-ligation of plasmid containing a DSB in KU complex- and ligase IV-deficient cells (Wang *et al.*, 2006).

1.5.3.1.3 How does PARP-1 promote the repair of DNA strand breaks?

The ways in which PARP-1 cooperates with DNA repair pathways to facilitate the mending of damaged DNA have been extensively studied, but they remain poorly understood. The most important mechanism is probably dependent on PARP-1's ability to control chromatin structure, yet the polymerase has also been proposed to act as a damage sensor/protector and has been shown to have a direct function in BER and non-homologous end joining as well as to be able to recruit DNA repair factors at sites of DNA damage.

1.5.3.1.3.1 PARP-1 as a damage sensor/protector

It has been shown that cell extracts can repair damaged DNA more efficiently in the presence of NAD^+ than in its absence, in manner that depends on the presence of PARP-1. Yet, even in the presence of NAD^+, extracts devoid of PARP-1 repair DNA breaks as well as, or even better than, PARP-1-proficient ones (Allinson *et al.*, 2003; Satoh and Lindahl, 1992; Satoh *et al.*, 1993; Vodenicharov *et al.*, 2000). In addition, supplementing extracts made from *PARP-1*$^{-/-}$ cells with recombinant PARP-1 also inhibits their ability to mend DNA damage, both in the presence and absence of NAD^+ (Vodenicharov *et al.*, 2000). On the basis of these data, it has been proposed that PARP-1 could act as a damage sensor/protector (Satoh and Lindahl, 1992). This model hypothesizes that PARP-1 is detrimental to DNA repair because it competes with DNA repair factors for binding to damaged DNA, thus inhibiting their actions. In the presence of NAD^+, PARP-1 bound to DNA breaks would become auto-parylated and consequently it would disassociate from the DNA, thus allowing DNA repair to take place. In support of this model it has been shown that intermediates of SSB repair

become particularly sensitive to nuclease cleavage in extracts prepared from *PARP-1*$^{-/-}$ mouse fibroblasts and after depletion of PARP-1 from HeLa cell extracts (Parsons *et al.*, 2005).

1.5.3.1.3.2 Direct functions of PARP-1 in BER

By analyzing the repair patches generated during the repair of an abasic site, Dantzer *et al.* (2000) found that extracts prepared from *PARP-1*$^{-/-}$ cells were half as efficient as those made from *PARP-1*$^{+/+}$ cells at carrying out long-patch BER, but they were only slightly affected in short-patch BER. In BER, DNA polymerase β usually removes the 5' deoxyribose-phosphate of an incised abasic site and then fills in the resulting single nucleotide gap in a process that is known as short-patch repair. When DNA lesions cannot be repaired by this mechanism, an alternative pathway, known as long-patch repair is used. It involves the insertion of 2-10 nucleotides across the abasic site by displacement DNA synthesis, which results in the formation of a flap, and requires PCNA and either DNA polymerase β itself or the replicative DNA polymerases ε and δ (Barnes and Lindahl, 2004). These results are consistent with the observation that PARP-1 can stimulate displacement DNA synthesis by DNA polymerase β in an *in vitro* reconstituted BER system including only purified components, in a manner that depends on PARP-1 catalytic activity and the presence of the flap endonuclease FEN1 (Prasad *et al.*, 2001). The data reported by Dantzer *et al.* (2000), however, need to be considered with care because the authors did not directly analyze the rate of DNA repair, *i.e.* the resealing of DNA breaks. Instead, they quantified the incorporation of a labelled nucleotide at the abasic site and took it as a measure of DNA repair efficiency, when, in fact, it may simply represent the length of the repair patch.

1.5.3.1.3.3 Direct functions of PARP-1 in non-homologous end joining

In addition to its possible direct roles in BER, PARP-1 also seems to be directly involved in joining free DNA ends together. Depleting either the KU70/80/DNA-PKcs or XRCC4/ligase IV complexes from HeLa cell extract has barely any effect on their end joining activities (Audebert *et al.*, 2004). Instead, cell extracts prepared from either *PARP-1*$^{-/-}$ or *XRCC1*$^{-/-}$ cells are essentially incapable of performing end joining. Adding recombinant PARP-1 to such extracts restores their abilty to join DNA ends. Purified PARP-1 also promotes DNA synapsing *in vitro* between DNA molecules with free ends and consequently promotes ligation of these molecules in combination with XRCC1 and Ligase III (Audebert *et al.*, 2004). For certain kinds of DSBs, *i.e.* those bearing

unphosphorylated 5′-termini, the activity of polynucleotide kinase is required for efficient end joining by PARP-1/XRCC1/ligase III (Audebert *et al.*, 2006). The ability of ligase III to ligate DSBs is further confirmed by studies showing that this protein accounts for most of the DNA end joining activity of HeLa cell extracts and *in vivo* (Wang *et al.*, 2005a). Altogether, these observations indicate that PARP-1, XRCC1, and DNA ligase III likely define a backup non-homologous end joining pathway that is distinct from the classical one, which depends on the KU/DNA-PKcs and XRCC4/ligase IV complexes.

The roles of PARP-1 in non-homologous end joining are probably not limited to providing cells with an alternative mechanism to ligate DSBs. Loss of PARP-1 sensitizes cells to DSB-inducing drugs and impairs homologous recombination in a manner that requires the presence of the KU complex or DNA ligase IV (Hochegger *et al.*, 2006). On the basis of this observation, it has been proposed that PARP-1 could help minimizing potential negative effects of non-homologous end joining on homologous recombination (Hochegger *et al.*, 2006). Such a model could in turn explain why *PARP-1*$^{-/-}$ cells cannot efficiently restart replication forks (Sugimura *et al.*, 2008; Yang *et al.*, 2004), given that this process depends on homologous recombination.

1.5.3.1.3.4 Recruitment of DNA repair factors by PARP-1

PARP-1 and PAR also interact with DNA repair factors and in this way they may contribute to the recruitment of such proteins to DNA breaks. Several members of BER interact with PARP-1 and some of them, *e.g*. XRCC1 and DNA ligase III, have been shown to directly interact with PAR *in vitro* (Ahel *et al.*, 2008; Leppard *et al.*, 2003; Masson *et al.*, 1998; Pleschke *et al.*, 2000). APLF, a protein that interacts with factors involved in BER and non-homologous end joining and is important for the efficient repair of DNA strand breaks, has also been shown to bind PAR directly *in vitro* through a motif called PBZ domain (Ahel *et al.*, 2008). *In vivo*, both XRCC1 and APLF are quickly recruited to DNA damage-induced PAR nuclear foci in a manner that depends on their ability to recognize PAR (Ahel *et al.*, 2008; El-Khamisy *et al.*, 2003). Both APLF and XRCC1 interact preferentially with the auto-parylated PARP-1 and inhibiting PAR synthesis *in vivo* greatly reduces the binding of XRCC1 to PARP-1 (Ahel *et al.*, 2008; Masson *et al.*, 1998; Pleschke *et al.*, 2000). In addition, XRCC1 repair foci do not form in PARP-1$^{-/-}$ cells treated with genotoxins (El-Khamisy *et al.*, 2003). Interestingly, the PBZ domain has been identified by bioinformatics means in many protein with a variety of roles in genome stability (Ahel *et al.*, 2008), which suggests that the way in which

PARP-1 and PAR impinge on DNA repair is probably more complicated than we believe.

1.5.3.1.3.5 Changes in chromatin structure by PARP-1

It was recognized very early on that PARP-1 and PAR have a dramatic effect on the structure of chromatin (de Murcia *et al.*, 1986; Poirier *et al.*, 1982). Given that the compaction state of chromatin affects the efficiency of chromatin-related processes, such as DNA repair and transcription (see 1.5.3.3), this function of PARP-1 could provide an additional mechanism for how the polymerase controls genome integrity. While loosely packed DNA, known as euchromatin, is accessible to proteins and is therefore active, heterochromatin is heavily condensed and inert (Grewal and Moazed, 2003). It appears that PARP-1 and PAR control chromatin structure both directly and by regulating its composition and by recruiting chromatin-remodelling factors.

PARP-1 and PAR directly impinge on chromatin compaction by interacting with histones. In the presence of NAD^+, PARP-1 relaxes compacted chromatin in a manner that depends on its activation (de Murcia *et al.*, 1986; Poirier *et al.*, 1982). Although histone H1, which is important to fold chromatin into higher order structures, is parylated under these conditions, the above-mentioned phenomenon cannot be caused by the loss of parylated H1 from chromatin because it remains associated with the DNA (Poirier *et al.*, 1982). At the moment, it cannot be however categorically excluded that parylation of H1 may compromise the chromatin-condensing properties of this protein without affecting its binding to chromatin. It instead seems that the auto-modification of PARP-1 itself may cause chromatin relaxation because parylated PARP-1 can unfold chromatin on its own (Realini and Althaus, 1992). This property probably depends on PARP-1's ability to release core histone particles from the DNA (Panzeter *et al.*, 1993). How auto-parylated PARP-1 achieves this is unclear but it may involve a competition between PAR and DNA for binding to histones. PAR in fact non-covalently interacts with such proteins, but also with histone H1, with an affinity and specificity that cannot be explained by simple electrostatic interactions (Panzeter *et al.*, 1993). Additionally, when histones are mixed with auto-parylated PARP-1 and DNA, they bind to DNA only after PAR has been saturated with them (Realini and Althaus, 1992). It has therefore been proposed that activated PARP-1 may evict histones from chromatin, relaxing it, and subsequently act as scaffold for their sequestration (Hassa *et al.*, 2006). Adding PARG to PARP-1-relaxed chromatin causes loss of PAR, re-association of histones with DNA, and chromatin re-compaction (Realini and Althaus,

1992), thus indicating that the effects PARP-1 exerts on chromatin structure are reversible. The above-described results contrast the more recent observations reported by Kim *et al.* (2004) showing that, in the presence of NAD^+, PARP-1 can indeed relax chromatin, but without modification or loss of histones from DNA. Thus, the exact mechanism by which PARP-1 leads to chromatin de-condensation remains unclear.

In the absence of NAD^+, PARP-1 induces the condensation of relaxed chromatin (Kim *et al.*, 2004). The polymerase binds stoichiometrically with nucleosomes at their dyad axis, that is, where the DNA that enters a histone core particle meets the one that exits it, in a manner that depends on both its DNA binding and catalytic domains (Kim *et al.*, 2004; Wacker *et al.*, 2007). Adding NAD^+ to these reactions leads to PARP-1 activation and subsequent chromatin decompaction (Kim *et al.*, 2004). Given that PARP-1 shares several properties with histone H1 with respect to how it interacts with nucleosomes and induces chromatin condensation (Kim *et al.*, 2004), it is possible that these two proteins change chromatin structure through analogous mechanism.

Given that the way in which PARP-1 affects chromatin structure *in vitro* depends on its activation state, it has been proposed that PARP-1 may regulate chromatin accessibility *in vivo* by being locally inhibited. This phenomenon could occur through confined changes in the levels of ATP, which can inhibit PARP-1 (Bauer *et al.*, 2005). Thus, in the presence of local high levels of ATP, PARP-1 would bind to chromatin but remain enzymatically inactive, thus leading to chromatin compaction. Conversely, the local consumption of ATP by chromatin-related processes, such as chromatin remodelling and transcription, could lead to an increase in PARP-1 activity and consequent chromatin relaxation (Hassa *et al.*, 2006).

PARP-1 can also control chromatin structure by recruiting specific PAR-recognizing chromatin-remodelling factors, *i.e.* ALC1 and the histone-variant macroH2A1.1, at sites of DNA damage. These two proteins have been shown to localize to regions of PARP-1 activation in a manner that depends on PARP-1, PARP activity and a functional PAR-interacting macro-domain, which is present in both of these proteins (Ahel *et al.*, 2009; Gottschalk *et al.*, 2009; Timinszky *et al.*, 2009). The recruitment of macroH2A1.1 to sites of DNA damage causes a transient increase in the DNA density of these areas, which probably represents chromatin compaction (Timinszky *et al.*, 2009). ALC1 is also likely to mediate chromatin remodelling at sites of PARP-1 activation because PAR strongly stimulates the chromatin remodelling activity of this protein *in vitro* in a manner that depends on its macro-domain (Ahel *et al.*, 2009; Gottschalk *et al.*, 2009).

Importantly, *in vivo* ALC1 depletion reduces cell survival against several genotoxins and its over-production leads to the accumulation of DNA damage (Ahel *et al.*, 2009).

1.5.3.2 PARP-1 and cell death

Cells can die in two different ways: by programmed cell death, also known as apoptosis, or by necrosis. Apoptosis is the default pathway of cell death, while necrosis happens only after extreme cell-damaging conditions. This probably occurs because, unlike necrotic cells, which leak their contents into the surrounding environment leading to inflammation, apoptotic ones are cleared by macrophages thereby causing no damage to the neighbouring tissues (Fink and Cookson, 2005). A role for PARP-1 in cell death has been long known because over-activation of this enzyme, for instance by DNA damage, causes dramatic energy depletion possibly leading to cell death by "starvation" (Berger, 1985). In addition, it was shown that cells accumulate PAR in the early stages of apoptosis (Simbulan-Rosenthal *et al.*, 1998) and that under these conditions PARP-1 is cleaved, mainly by caspase 3 and caspase 7 (Kaufmann *et al.*, 1993; Lazebnik *et al.*, 1994). Caspase-mediated cleavage of PARP-1 is now widely used as a marker for cell death. In line with these results it has been shown that the loss of PARP-1 impairs hallmarks of apoptosis such as pro-caspase cleavage/activation and DNA fragmentation in cycloheximide-treated 3T3-L1 adipocytes (Smulson *et al.*, 2000), while PARP inhibition leads to increased apoptotic body formation in HL-60 cells treated with actinomycin D (Shiokawa *et al.*, 1997). In addition, *PARP-1*$^{-/-}$*, PARP-2*$^{-/-}$ mice or wild type mice exposed to PARP inhibitors are protected from several pathophysiological conditions, such as post-ischaemic damage, which causes cell death in otherwise wild type animals (Jagtap and Szabo, 2005; Shall and de Murcia, 2000). Other studies have however shown no significant differences in the levels of cell death in a range of *PARP-1*$^{-/-}$ and *PARP-1*$^{+/+}$ cell types and in response to a variety of apoptotic signals (Leist *et al.*, 1997). Thus, it is possible that the role of the polymerase in apoptosis may dependent on the specific type of cell and signals used.

How PARP-1 controls cell death has been best characterized in the cellular response to genotoxins: low-to-moderate amounts of DNA damage lead to apoptosis while more extreme levels cause necrosis (Berger, 1985; Berger *et al.*, 1983). PARP-1 regulates the balance between these two modes of cell death because inhibiting or depleting it shifts the use of necrosis towards apoptosis (Virag *et al.*, 1998a; Virag *et al.*, 1998b). This phenomenon has been explained by proposing that in the presence of abnormal

amounts of DNA damage PARP-1 over-activation causes NAD^+ to be rapidly depleted, hence forcing cells to replenish it by consuming two to four molecules of ATP per molecule of NAD^+, depending on the salvage pathway involved. The consequent loss of ATP would lead to cellular dysfunction and eventually necrosis (Berger, 1985; Berger *et al.*, 1983). In support of this model, it has been shown that inhibiting PARP activity or depleting PARP-1 significantly improves cellular energy levels and viability in response to pro-necrotic signals (Jagtap and Szabo, 2005; Shall and de Murcia, 2000). Additionally, it has been shown that cells using glycolysis to produce ATP, *i.e.* proliferating cells, are more susceptible to necrosis than non-proliferative ones, which instead generate it through oxidative phosphorylation (Zong *et al.*, 2004). This phenomenon was observed probably because cells that use the former metabolic pathway to make ATP, which takes place in the cytoplasm, would be expected to be more vulnerable to drastic changes in the nucleo-cytoplasmic levels of NAD^+ than those employing the latter one (Zong *et al.*, 2004), which instead occurs in mitochondria.

In addition to mediating cell death through starvation, PARP-1 plays a role in apoptosis by controlling the release of the pro-apoptotic factor AIF from mitochondria (Yu *et al.*, 2002). AIF is found on the inner mitochondrial membrane where it functions as an NADH oxidase (Miramar *et al.*, 2001). In response to pro-apoptotic stimuli AIF is released from these organelles into the cytoplasm where it associates with cyclophilin A to form an active nuclease (Cande *et al.*, 2004). This complex translocates into the nucleus, inducing chromatin condensation and DNA fragmentation (Susin *et al.*, 1999). Inhibiting PARP activity or loss of PARP-1 prevents the release of AIF from mitochondria, reducing susceptibility to apoptosis (Yu *et al.*, 2002). Interestingly, the fact that purified PAR alone induces release of AIF from isolated mitochondria, but also in cells, where it eventually induces apoptosis (Yu *et al.*, 2006), suggests PAR itself is sufficient for AIF-release from mitochondria. At the moment it cannot be however excluded that the PARP-1-dependent depletion of NAD^+ and ATP in response to DNA damage and/or in the presence of reactive oxygen species may also contribute to this mode of apoptosis. In fact, injecting NAD^+ into cells rescues their ATP levels, blocks the translocation of AIF from mitochondria to nuclei and eventually prevents cell death (Alano *et al.*, 2004).

1.5.3.3 PARP-1 and the regulation of gene transcription

In addition to being involved in DNA repair and cell death, PARP-1 also plays a critical role in the regulation of transcription under basal, signal-activated, and stress-induced conditions. PARP-1's transcription-related functions have been demonstrated on a single gene-basis through a large number of reports, some of which will be described below. More recently, "genome-wide" expression profiling techniques have also been applied to simultaneously compare the expression levels of a huge number of genes between various cell lines and tissues proficient in or devoid of PARP-1. Simbulan-Rosenthal *et al.* (2000) identified 91 genes amongst the 11,000 ones tested that showed at least a 2-fold change in expression between mouse embryonic fibroblasts or livers obtained from *PARP-1*$^{+/+}$ and *PARP-1*$^{-/-}$ mice. Interestingly, many of the genes down-regulated by the loss of PARP-1 in this study encode for proteins involved in cell cycle progression, DNA replication, and chromosome dynamics. In a second report, Ogino *et al.* (2007) compared the expression levels of almost 10,000 genes between *PARP*$^{-/-}$ and *PARP-1*$^{+/+}$ embryonic stem cells, embryonic fibroblasts and livers. They observed that although ~3.6% of the tested transcripts showed altered expression in all of the three systems examined, with ~70% of them being down-regulated by the loss of PARP-1, the three pools overlapped very little in terms of their constituents' identities. In the most recent study, Frizzell *et al.* (2009) compared the expression of over 20,000 genes between wild type and PARP-1-depleted MCF-7 cells. They found that the expression of 8.7% of the studied genes was affected by PARP-1 deficiency. Amongst these, 204 genes, mainly involved in metabolism and stress responses, were found to be most robustly controlled, with half of them being upregulated upon loss of PARP-1 (Frizzell *et al.*, 2009). The importance of PARP-1 in transcription demonstrated by the above-described studies is further corroborated by the observation that this enzyme is enriched at the promoter of possibly 90% of protein-coding genes in MCF-7 cells, in a way that is mutually exclusive with histone H1 (Krishnakumar *et al.*, 2008). Although the association of H1 with the promoter of a gene usually inhibits its activation, this does not mean that the presence of PARP-1 at such a location would instead stimulate it. In fact, depending on which gene is considered, the presence of PARP-1 at its promoter can either positively or negatively effect its transcription.

PARP-1 not only controls basal levels of gene transcription during normal growth but it often contributes to the regulation of transcription in response to signals, including steroid hormones (Ju *et al.*, 2006), peptide hormones, cytokines, heat shock (Ouararhni *et al.*, 2006; Tulin and Spradling, 2003), Ca^{2+} (Ju *et al.*, 2004) and other

extra-cellular signals (Hassa *et al.*, 2005; Kauppinen *et al.*, 2006). Many of these stimuli appear to impinge on the transcription-related functions of PARP-1 by inducing its post-translational modification with PAR (Cohen-Armon *et al.*, 2007), acetyl (Hassa and Hottiger, 1999) or phosphate (Kauppinen *et al.*, 2006) groups, which are likely to regulate the properties of this enzyme. For instance, activation of macrophages leads to PARP-1 acetylation by p300/CBP. This modification event allows PARP-1 to interact with, and activate, the transcription factor NFκB leading to the induction of NFκB-responsive genes (Hassa *et al.*, 2005).

The roles of PARP-1 in transcription are extremely varied and they have been classified into four categories: 1) modulation of chromatin structure, 2) direct binding to enhancer sequences, 3) co-regulation functions at specific promoters and 4) insulator functions (Kraus, 2008).

1.5.3.3.1 Regulation of chromatin structure

In 1.5.3.1.3.5, I described how PARP-1 can control chromatin structure either directly or indirectly by modulating its composition and how this property impacts on genome stability. Since the transcription of a gene is also heavily controlled by the compaction state of the chromatin in which it is found, it is unsurprising that PARP-1 can control this process as well.

Firstly, the ability of PARP-1 to compact chromatin in the absence of NAD^+ is inhibitory to transcription *in vitro*, a phenomenon that can be reversed by adding NAD^+ to the reaction (Kim *et al.*, 2004). Such an *in vitro* property is likely to be relevant *in vivo* because PARP-1 enzymatic activity has been observed at chromosomal “puffs” within *Drosophila* polytene chromosomes, which are regions of high transcriptional activity and chromatin de-condensation (Tulin and Spradling, 2003).

In addition, PARP-1 may also control chromatin structure and transcription by modulating chromatin composition. The recruitment of the chromatin-remodelling factors ALC1 and macroH2A1.1 at sites of PARP-1 activation, see 1.5.3.1.3.5, may lead to changes in the expression of certain genes, if they fall within transcriptional regulatory regions. Consistent with this model it has been shown that macroH2A1.1 interacts directly with PARP-1, they are part of the same nucleosome complex and they co-localize at the promoter of the *HSP70.1* gene (Nusinow *et al.*, 2007; Ouararhni *et al.*, 2006). Upon heat shock, both mH2A1.1 and PARP-1 leave the *HSP70.1* promoter, concomitantly several proteins that are associated with it become parylated, and gene transcription is activated in a manner that depends on the presence of

PARP-1 or mH2A1.1 (Ouararhni *et al.*, 2006). As mentioned earlier, PARP-1 also excludes histone H1 from the promoters of several genes, thereby affecting their transcription (Krishnakumar *et al.*, 2008). In the case of the oestrogen-responsive *pS2* gene, upon stimulation, the PARP-1-dependent removal of H1 from the promoter of this gene is also followed by the recruitment of, amongst other proteins, HMGB1 (Ju *et al.*, 2006). HMGB1 is an architectural protein with DNA bending properties that is often associated with chromatin remodelling and stimulation of transcription (Stros, 2010).

1.5.3.3.2 Insulator functions

PARP-1 also seems to control transcription by regulating the activity of insulators. Insulators are specific DNA sequences that bind to proteins, *e.g.* CTCF, and divide the genome into distinct regulatory units, hence reducing the effects of enhancers on promoters and preventing heterochromatin from spreading into euchromatic regions (Wallace and Felsenfeld, 2007). CTCF is parylated and it co-localizes with PARP-1 at most CTCF-binding sites. Inhibiting PARP activity or mutating CTFC's PAR attachment sites impairs its insulator functions, thus indicating that parylation plays an important role in controlling the properies of this protein (Farrar *et al.*, 2010; Yu *et al.*, 2004). Given that PAR can control the global levels of DNA methylation in a cell, probably by inhibiting the DNA methyl transferase DNMT1 (de Capoa *et al.*, 1999; Guastafierro *et al.*, 2008; Reale *et al.*, 2005), and the activity of genomic insulators generally depends on their methylation state (Reale *et al.*, 2005), it is possible that PARP-1 may regulate insulator function also by controlling DNA methylation.

1.5.3.3.3 Direct binding to enhancer sequences

In a few cases, PARP-1 appears to control transcription by acting as a classical enhancer-binding transcription factor, that is, by directly recognizing specific regulatory DNA sequences and/or structures within the promoter regions of certain genes. This appears to be case for *REG* (Akiyama *et al.*, 2001), *BCL6* (Ambrose *et al.*, 2007), *CXCL1* (Amiri *et al.*, 2006), *BRAC2* (Wang *et al.*, 2008a) and the *PARP-1* gene itself (Soldatenkov *et al.*, 2002). For instance, in its inactive form, PARP-1 binds to a specific DNA sequence within the CXCL1 promoter, thereby hindering its association with the transcription factor NF-κB and preventing its expression (Amiri *et al.*, 2006). Activation of PARP-1 evicts the polymerase itself from the CXCL1 promoter, therefore allowing it to bind NF-κB and be turned on (Amiri *et al.*, 2006). PARP-1 also binds to a specific sequence in the first intron of the *BCL6* gene and in the *BRAC2* promoter (Ambrose *et*

al., 2007; Wang *et al.*, 2008a). Although it is not known whether such binding phenomena are directly involved in controlling the expression of these two genes, it has been shown that inhibition of PARP activity or depleting PARP-1 can alter their transcription (Ambrose *et al.*, 2007; Wang *et al.*, 2008a). Interestingly, PARP-1 also recognizes its own promoter, both *in vivo* and *in vitro*, and appears to be able to down-regulate it (Soldatenkov *et al.*, 2002). This binding event has been proposed to stem from PARP-1's ability to recognize certain secondary structures such as hairpins (see 1.5.2.2), which may be present in its promoter (Soldatenkov *et al.*, 2002).

1.5.3.3.4 Transcription co-regulator functions

PARP-1 can also control gene expression by acting as a co-activator or a co-repressor, depending on the gene examined. Co-regulators are proteins that generally interact with DNA-binding transcription factors and consequently either activate or repress the transcription of a gene (Glass and Rosenfeld, 2000). PARP-1 activity is not always necessary for its co-regulator functions, *e.g.* NF-κB, B-MYB, and HTLV TAX1 (Hassa and Hottiger, 1999; Kraus and Lis, 2003; Pavri *et al.*, 2005), but when it is, *e.g.* HES1, SP1, NFAT, and ELK1 (Cohen-Armon *et al.*, 2007; Ju *et al.*, 2004; Olabisi *et al.*, 2008; Zaniolo *et al.*, 2007), one or more components of the co-regulatory complex with which the polymerase is associated are ususally parylated. It is generally believed that, as a co-regulator, PARP-1 is recruited to specific promoters by interacting with its partner DNA-binding transcription factor (Kraus, 2008). Yet, additional elements must also be involved because ChIP-on-Chip analysis shows that the promoter-associated peaks of PARP-1 enrichment can be as wide as 3 kbp (Krishnakumar *et al.*, 2008). Although the mechanisms by which PARP-1 functions as a co-regulator are poorly understood and they are likely to be gene- and/or transcription factor-specific, recent evidence suggests that PARP-1 may be involved in exchanging co-regulatory complexes at specific promoters. For instance, PARP-1 and PARP activity are necessary to mediate the exchange of a repressive complex, consisting of the co-repressor NCoR and the histone deacetylase HDAC3, for an activator complex that contains PARP-1, topoisomerase IIβ, the co-activator ASC2, and the DNA repair proteins KU70/80 and DNA-PK at the promoter of the oestrogen-inducible *pS2* gene, upon activation (Ju *et al.*, 2006). Interestingly, this PARP-1-dependent coregulator exchange event is accompanied by the formation of a topoisomerase IIβ-dependent DSB at the *pS2* promoter and it has been shown to occur at promoters of many other signal-induced genes (Ju *et al.*, 2006). Likewise, upon retinoic acid-stimulation PARP-1 is also

necessary to convert an inactive $CDK8^+$ Mediator complex to an active $CDK8^-$ one and thereby to induce transcription from retinoic acid-responsive promoters both *in vivo* and *in vitro* (Pavri *et al.*, 2005). This phenomenon does not require PARP-1's catalytic domain (Pavri *et al.*, 2005). Conversely, PARP-1 needs to be active to mediate the exchange of a PARP-1-containing TLE1 co-repressor complex for a HAT-containing co-activator one at the *HES1* promoter, upon Ca^{2+} mobilization in neurons (Ju *et al.*, 2004).

1.5.4 PARP-1 and cancer

1.5.4.1 The involvement of PARP-1 in tumourigenesis

It is generally believed that tumours and cancers develop during a long period of time from a single cell that accumulates several heritable changes, through successive rounds of mutation and natural selection, and thereby becomes able to outgrow its neighbours. Thus, it seems that a certain amount of genome instability is necessary for the development of tumours (Hanahan and Weinberg, 2000). Given the functions that PARP-1 plays in maintaining genome integrity, but also in cell death and transcription, it would be expected that its partial or complete loss could lead to an increased rate of tumour formation in an organism.

The roles of PARP-1 in tumourigenesis have been investigated in *PARP-1*$^{-/-}$ mice. Three different *PARP-1*$^{-/-}$ mice have been generated by three different groups, by deleting exon 1, 2 or 4 of the *PARP-1* gene (de Murcia *et al.*, 1997; Masutani *et al.*, 1999; Wang *et al.*, 1995). They are all viable and fertile, indicating that *PARP-1* is not an essential gene for survival under laboratory conditions. Although these mice are very susceptible to DNA-damaging agents and show a generalized genome instability phenotype (see 1.5.3.1 and Shall and de Murcia, 2000), they are not particularly prone to developing cancers spontaneously. One study did however report that *PARP-1*$^{-/-}$ mice naturally develop liver tumours after 12-24 months more frequently than wild type animals (Tong *et al.*, 2002). Another study also showed that deleting *PARP-1* in the severe combined immuno-deficiency (SCID) mouse model also leads to an unusually high frequency of spontaneous T cell lymphomas (Morrison *et al.*, 1997). In contrast to spontaneous tumour formation, it has been shown that *PARP-1*$^{-/-}$ mice exposed to DNA-damaging drugs, or additionally devoid of other factors involved in maintaining genome stability, accumulate unusually high levels of tumours in various organs

(Morrison *et al.*, 1997; Nozaki *et al.*, 2003; Tong *et al.*, 2002; Tong *et al.*, 2001; Tsutsumi *et al.*, 2001).

Altogether the observations described above suggest that PARP-1 protects against tumourigenesis. This property is evident only when *PARP-1*$^{-/-}$ mice accumulate unusually high levels of DNA damage probably because under these conditions the presence of the polymerase becomes essential for efficient DNA repair. Conversely, under normal conditions the lesions that spontaneously arise in the genome of the *PARP-1*$^{-/-}$ mice, and would normally be dealt with by PARP-1 itself, may be relatively infrequent and therefore could be repaired by some auxiliary mechanism.

1.5.4.2 PARP as a target for cancer treatment

Although PARP-1 protects cells from developing malignancies, inhibiting its enzymatic activity is one of the most heavily studied and promising strategies for the treatment of some types of cancer. At present most of the chemicals used to inhibit PARP-1 are also likely to inactivate other PARPs because they act as competitive inhibitors of NAD^+ (see below), and all PARPs share very similar catalytic cores (see 1.4.3).

The oldest PARP inhibitor is the nicotinamide analogue 3-aminobezamide (Purnell and Whish, 1980). It is not particularly potent or specific for PARP-1 (Rouleau *et al.*, 2010) and it also affects the normal functions of the cytoskeleton (Malorni *et al.*, 1995). It is therefore not surprising that 3-aminobenzamide can cause serious side effects (Horsman *et al.*, 1986). Newer inhibitors, mostly based on the benzamide or purine structures, have therefore been engineered are now in their third generation (ABT-888, AG014699, AZD2281, BSI-201, CEP-8983 and MK-4827). Although they are more potent and specific than 3-aminobenzamide, they still target PARP-1, PARP-2, and probably other members of the PARP family (Ferraris, 2010; Rouleau *et al.*, 2010).

PARP inhibitors are presently used as 1) potentiators of chemo- and radio-therapy (Tentori and Graziani, 2005) and 2) cytotoxic agents in their own right for the treatment of cancers that bear specific genetic markers, such as mutations in the *BRCA-1* or *BRCA-2* genes (Martin *et al.*, 2008).

1.5.4.2.1 Potentiation of chemo- and radio-therapy

The finding that PARP-1 inactivation sensitizes cells to genotoxins (see 1.5.3.1) suggested that inhibiting this enzyme could coadjuvate the therapeutic properties of common anti-cancer drugs, because they often act by introducing lesions in DNA. PARP-1 inhibitors have in fact been shown to potentiate the cytotoxic actions of

chemotherapeutics such temozolomide, a DNA alkylating agents, and irinotecan, a topoisomerase I poison, as well as radiotherapy, both in cultured cancer cells and in tumour xenograft models (Bowman *et al.*, 1998; Miknyoczki *et al.*, 2003).

PARP inhibition is believed to potentiate the effects of chemotherapeutics by rendering cells unable to efficiently repair the lesions inflicted to DNA by these drugs, hence causing cell death through the accumulation of unrepairable DNA damage (Martin *et al.*, 2008). In line with this model it has been shown that inhibiting PARP leads to the increased accumulation of DNA strand breaks and apoptosis in cells treated with temozolomide (Boulton *et al.*, 1995; Tentori *et al.*, 1997). These results have led to the approval of the first clinical trial for a PARP inhibitor: the use of AG014699 as a potentiator of temozolomide in metastatic myelomas (Plummer *et al.*, 2006). Such a study reported promising results in that the combined administration of these two drugs suppressed tumour development more strongly than temozolomide alone (Plummer *et al.*, 2006).

PARP inhibitors are presently undergoing analogous clinical trials for the treatment of other types of cancers, such as glioblastoma multiforme.

1.5.4.2.2 PARP inhibitors as cytotoxic agents

In addition to augmenting the cytotoxicity of cancer therapeutics, PARP inhibitors have been shown to be particularly effective in treating cancers that carry mutations in specific genes. For example, cells homozygous for mutations in the *BRCA1* and *BRCA2* genes are exquisitely sensitive to inhibition of PARP, unlike the corresponding heterozygous mutants or wild type cells (Bryant *et al.*, 2005; Farmer *et al.*, 2005). These findings are very important because 80% of the people that carry heterozygous *BRCA1* or *BRCA2* mutations lose the other functional allele of these genes during their lives in some of their cells, and thereby develop cancers, mostly of the breast in women and of the prostate in men (Venkitaraman, 2002).

The above-described results suggest that PARP inhibition could be used in $BRCA^{+/-}$ patients for “targeted chemotherapy”, that is, to specifically kill the tumour-prone $BRCA^{-/-}$ cells while leaving all the other heterozygous ones unaffected. Thus, in this particular context killing tumour cells should be so specific that the drug’s side effects would be expected to be reduced to a minimum. In fact, in a recent clinical trial, the PARP inhibitor AZD2281 was demonstrated to stabilize or regress the growth of breast, ovarian, and prostate cancers defective in BRCA1 or BRCA2, but not those that carried

functional copies of these genes, with fewer side effects for the patients than more traditional chemotherapeutic regimes (Fong *et al.*, 2009).

BRCA1 and BRCA2 are necessary for the orderly progression of homologous recombination (Venkitaraman, 2009). This pathway of DNA repair is particularly important in mending stalled or collapsed replication forks and therefore plays a critical role in cell survival (Helleday, 2010). Inhibiting PARP leads to increased levels of homologous recombination in normal cells, probably because under these conditions the lesions that would normally be repaired through PARP-1 are instead dealt with by homologous recombination (Schultz *et al.*, 2003). It has therefore been proposed that the synthetic lethal effect of combining PARP inhibition with mutation in *BRCA* genes occurs because the damaged replication forks that accumulate due to the loss of PARP activity cannot be repaired by homologous recombination, hence resulting in their irreversible, and lethal, collapse (Bryant *et al.*, 2005; Farmer *et al.*, 2005).

Importantly, PARP inhibition may not be an effective treatment only for BRCA-defective cancers but also for all those sporadic malignancies that exhibit a BRCA-like phenotype, either through the epigenetic inactivation of the *BRCA* genes or the disruption of other factors important for homologous recombination (Martin *et al.*, 2008). In addition, given that a wide range of tumours demonstrate an impaired ability to repair DNA (Martin *et al.*, 2008), it is possible that inhibiting PARP may also be useful in their treatment.

1.6 The aims of this thesis

Sumoylation and DNA heavily interplay with each other: not only can DNA stimulate the sumoylation of some proteins, *e.g.* PCNA (see 1.3.3), and *vice versa* sumoylation can affect the binding of some of its substrates to DNA, *e.g.* TDG (see 1.3.4), but also, and more importantly, the sumoylation pathway itself is crucial to maintain genomic information (see 3.1). SUMO plays a role in genome stability probably because it controls specific aspects of DNA metabolism. Until not very long ago (Dou *et al.*, 2010; Galanty *et al.*, 2009; Morris *et al.*, 2009), how SUMO impinged on DNA metabolism was largely unknown as this phenomenon had not yet been correlated to the modification of certain proteins by specific ligases. Thus, my research hoped to uncover the ways in which SUMO regulated DNA-related processes such as DNA replication, recombination and/or repair, and in particular how DNA may be involved. To begin accomplishing this objective, I aimed at systematically identifying sumoylated proteins from normal and damaged replicating chromatin, because they should be

enriched for proteins with a role in DNA metabolism. Subsequently, for a few interesting new candidates of sumoylation with a role in DNA metabolism, I aimed at characterizing two aspects of their modification. Firstly, I planned to study how it was controlled with respect to: 1) the enzymes responsible for it, 2) when and where it took place, 3) any susceptibility to cellular and/or environmental signals and 4) whether/how DNA impinged on it, because this type of information could provide clues about the functional consequences of such sumoylation events. Secondly, I aimed at investigating the roles of the sumoylation of these new sumoylation targets more directly by: 1) mapping their SUMO-attachment site and then 2) creating unsumoylatable mutants whose properties, in particular the DNA-related ones, could be compared against those of the relevant wild type proteins.

Chapter 2. Materials and methods

2.1 Reagents

2.1.1 Proteins

Protein	Source
Bovine serum albumin (BSA)	Sigma
GST-Rhinovirus 3C protease	Sven Kjaer
His_6-Geminin	Vincenzo Costanzo
His_6-Ulp1(aa 403–621)	Dale Wigley
PARP-1(aa 1-214), PARP-1(aa 103-214), PARP-1^{R122I}(aa 103-214)	Sebastian Eustermann
Phusion DNA polymerase	Finnzymes
Restriction enzymes, T4 DNA ligase, calf intestinal phosphatase	New England Biolabs
S. cerevisiae SUMO, SUMO E1 and E2, Siz1(aa 1-508) and $Siz^{G55A, K57A, L60A}$(aa 1-508)	In-house
Taq DNA polymerase	Thermo Scientific
Topoisomerase I	Invitrogen
Trypsin	Promega
Untagged PARP-1	Enzo Life Sciences
Untagged SUMO E1, SUMO1 and SUMO2	BostonBiochem
Zymolyase 20T	AMS Biotechnology

Table 2.1 - A list of the proteins used in this study.

2.1.2 Antibodies

	Specificity	Reactivity	Source (catalogue #)	Dilution
Monoclonal	3-phosphoglycerate kinase (PGK)	*S. cerevisiae*	Invitrogen (459250)	1:10,000
	c-Myc (clone 9E10)	N/A	CR-UK	1:5,000
	FLAG (clone M2)	N/A	SIGMA (F1804)	1:5,000
	Green fluorescent protein (GFP)	N/A	Roche (11814460001)	WB 1:5,000 IF 1:1000
	His_6 (clone HIS-1)	N/A	Sigma (H1029)	1:5,000
	MCM7	Metazoan	Abcam (ab2360)	1:200
	ORC1	*Xenopus laevis*	CR-UK, Tugal *et al.* (1998)	1:4,000
	Orc1 (clone SB13)	*S. cerevisiae*	Santa Cruz (sc-6674)	1:1,000
	Orc2 (clone SB46)	*S. cerevisiae*	CR-UK	1:1,000
	Orc6 (clone SB49)	*S. cerevisiae*	CR-UK	1:3,000

	PARP-1 (clone C2-10)	Mammalian species	Enzo Lifesciences (BML-SA250-0050)	1:5,000
	PARP-1 (clone F1-23)	Mammalian species	Enzo Lifesciences (ALX-804-211)	1:5,000
	PARP-1 (clone F2)	Human	Santa Cruz	1:3,000
	PCNA (clone PC-10)	Metazoan	CR-UK	1:5,000
	Poly(ADP-ribose) (clone 10H)	N/A	Trevigen (4335-MC-01K-AC)	1:1,000
	Tubulin (TAT1)	N/A	CR-UK	1:100,000
	Ubiquitin (clone P4D1)	Pan	Cell Signalling Technology (3936)	1:3,000
Polyclonal	c-Myc (A-14)	N/A	Santa Cruz (sc-789)	1:3,000
	DNA polymerase α	Metazoan species	Abcam (ab31777)	1:3,000
	Histone H3, CT	Pan	Millipore (07-690)	1:3,000
	ORC2	*X. laevis*	Tim Hunt's laboratory, Tugal *et al.* (1998)	1:3,000
	PCNA (affinity purified)	*S. cerevisiae*	In-house	1:3,000
	Promyelotic leukaemia protein (PML)	Human	Paul Freemont's laboratory	IF 1:200
	RPA70	Metazoan	Stephen West's laboratory	1:3,000
	Smt3	*S. cerevisiae*	In-house	1:5,000
	SUMO1 (affinity purified)	Metazoan	In-house	1:200
	SUMO2 (affinity purified)	Metazoan	In-house	1:200

Table 2.2 - A list of the primary antibodies used in this thesis. Dilutions are for western blotting (WB) unless otherwise stated. IF = Immunofluorescence.

Antibody	Source (catalogue #)	Dilution
HRP-conjugated anti-mouse IgG	DakoCytomation (P0447)	1:10,000
HRP-conjugated anti-rabbit IgG	DakoCytomation (P0399)	1:10,000
HRP-conjugated anti-rabbit IgG heavy-chain	Sigma (A1949)	1:10,000
HRP-conjugated anti-mouse IgG light-chain	Jackson ImmunoResearch (115-035-174)	1:10,000
HRP-conjugated anti-mouse IgG light-chain	Jackson ImmunoResearch (211-032-171)	1:10,000
Alexa Fluor 488 anti-mouse IgG	Invitrogen (A-11001)	1:500
Alexa Fluor 594 anti-rabbit IgG	Invitrogen (A-11012)	1:500

Table 2.3 - A list of the secondary antibodies used in this thesis.

2.1.3 Chemicals and reagents

Unless otherwise stated, most chemicals and reagents were obtained from Sigma, BDH Chemicals or Fisher Scientific. Those ones purchased from other companies are listed below or indicated in the relevant paragraph.

BD Biosciences: FACSFlow, FACSRinse and FACSClean

Bio-Rad: ammonium persulfate, bromophenol blue, 30% w/v acrylamide/Bis solution (37.5:1 acrylamide:N,N'-methylene-bis-acrylamide electrophoresis purity reagent)

Duchefa Biochimie: Amino acids for yeast media

Invitrogen: 0.4% w/v Trypan blue Stain

London Research Institute's Peptide Synthesis team: α factor (WHWLQLKPGQPMY)

Melford: dithiothreitol (DTT)

National Diagnostics: 20% w/v sodium dodecyl sulfate (SDS)

New England Biolabs: 10× T4 DNA ligase buffer and 10× buffers for restriction enzymes

2.2 Media and solutions

2.2.1 Media

2.2.1.1 Bacterial cells

Luria Broth (LB) medium and 10× M9 salt solution, LB agar, 4% w/v bacto-agar, 20% w/v glucose were prepared by the London Research Institute's Media Production team.

Liquid M9 medium without leucine: 1× M9 salt solution, 1 mM $MgSO_4$, 1 $\mu g \cdot ml^{-1}$ thiamine, 0.5% w/v glucose, and 1 $\mu g \cdot ml^{-1}$ tryptophan and 1 $\mu g \cdot ml^{-1}$ leucine

M9 agar without leucine: 1.5% w/v bacto-agar, 1× M9 salt solution, 1 mM $MgSO_4$, 1 $\mu g \cdot ml^{-1}$ thiamine, 0.5% w/v glucose, 1 $\mu g \cdot ml^{-1}$ tryptophan and 1 $\mu g \cdot ml^{-1}$ leucine

All antibiotics were prepared as 1000× stock solutions, stored at -20°C and then added to liquid medium or agar plates as desired for the selection of transformed bacterial cells.

	1000× stock solutions ($mg \cdot mL^{-1}$)	Solvent
Ampicillin	100	Water, filter sterilized
Chloramphenical	34	Ethanol
Kanamycin	50	Water, filter sterilized
Tetracycline	10	Ethanol
Gentamycin	7	Water, filter sterilized
Spectinomycin	100	Water, filter sterilized
Streptomycin	75	Water, filter sterilized

Table 2.4 - A list of the antibiotic stock solutions used in this thesis.

2.2.1.2 Yeast cells

Yeast Peptone (YP) medium, Yeast Peptone Glucose (YPD) medium, YPD agar and 4% w/v bacto-agar were prepared by the London Research Institute's Media Production team.

Dropout powder: 2 g of p-aminobenzoic acid and 20 g of each of alanine, arginine, asparagine, aspartic acid, cysteine, glutamine, glutamic acid, glycine, inositol, isoleucine, lysine, methionine, phenylalanine, proline, serine, threonine, tyrosine and valine were mixed overnight

Synthetic Complete (SC) powder: 36.7 g of dropout powder, 4 g of leucine, 2 g of histidine, 2 g of tryptophan, 2 g of uracil and 0.5 g of adenine were mixed overnight. Specific SC powder stocks were prepared by omitting the desired amino acid

2.5× SC medium: 5 g of SC powder, 4.25 g of yeast nitrogen base (without amino acids and ammonium sulfate, Invitrogen) and 12.5 g of ammonium sulfate were mixed with 1 L of water, stirred for 30 min and autoclaved

Liquid SC medium: 200 mL of 2.5× of SC medium, 250 mL of distilled water and 50 mL of 20% w/v glucose or galactose

SC medium agar: 200 mL of 2.5× SC medium, 250 of molten 4% w/v of bacto-agar and 50 mL of 20% w/v glucose or galactose

5-FOA SC medium agar: 200 mL of SC complete medium, 250 mL of molten 4% w/v bacto-agar, 50 mL of 20% w/v glucose supplemented with 2 $mg \cdot mL^{-1}$ of each of uracil, adenine and 5-FOA

G418 YPD agar: YPD agar supplemented with 200 $\mu g \cdot mL^{-1}$ G418

20% w/v galactose: 20 g of galactose was mixed with warm water up to 100 mL and autoclaved

100 mM $CuSO_4$: 24.97 g of copper sulphate pentahydrate was mixed with water up to 100 mL and filter-sterilized

1% w/v KOAc: 9.8 g of potassium acetate was mixed with water up to 100 mL and filter-sterilized

2.2.1.3 Insect cells

Unless otherwise stated, insect cells were grown in Grace's medium (without insect haemolymph) supplemented with 3.3 $g \cdot L^{-1}$ lactalbumin hydrolysate and 3.3 $g \cdot L^{-1}$ yeastolate (Invitrogen), 10% v/v heat-inactivated (55°C for 30 min) foetal bovine serum and, when required, antibiotics (50 $\mu g \cdot mL^{-1}$ gentamycin and 250 $ng \cdot mL^{-1}$ amphotericin B).

2.2.1.4 Mammalian cells

Unless otherwise stated, all cell lines were maintained in DMEM supplemented with 4.5 $mg \cdot mL^{-1}$ glucose, 2 mM glutamine, 15 $\mu g \cdot mL^{-1}$ phenol red (11995-040**,** Invitrogen) as well as 10% v/v heat-inactivated (30 min at 55°C) foetal bovine serum, 100 $U \cdot mL^{-1}$ penicillin, 100 $\mu g \cdot mL^{-1}$ streptomycin and, where appropriate, additional antibiotics (see 2.5.4).

2.2.2 Solutions

2.2.2.1 General

The London Research Institute's Media Production team prepared the following solutions using standard recipes: 1× and 10× PBS, TE pH 8.0, 0.5 M EDTA pH 8.0, 1 M Tris-HCl pH 7.5 and 8.0, 5 M NaCl, 1 M $MgCl_2$ and 1 M $MgSO_4$.

2.2.2.2 Bacterial cells

TbfI solution**:** 30 mM potassium acetate, 100 mM rubidium chloride, 10 mM calcium chloride, 50 mM manganese chloride, 15% (v/v) glycerol, adjusted to pH 5.8 with dilute acetic acid; autoclaved

TbfII solution**:** 10 mM MOPS, 75 mM calcium chloride, 10 mM rubidium chloride, 15% (v/v) glycerol, adjusted to pH 6.5 with dilute NaOH; autoclaved

2.2.2.3 X. laevis egg extracts

De-jellying buffer: 20 mM Tris-HCl pH 8.5, 110 mM NaCl

5× MMR buffer: 100 mM HEPES-KOH pH 7.5, 2 M NaCl, 10 mM KCl, 5 mM $MgSO_4$, 10 mM $CaCl_2$, 0.5 mM EDTA

S buffer: 50 mM HEPES-KOH pH 7.5, 50 mM KCl, 2.5 mM $MgCl_2$, 0.25 M sucrose

SuNaSp buffer: 0.25 M sucrose, 75 mM NaCl, 0.5 mM spermidine, 0.15 mM spermine

EB buffer: 50 mM HEPES-KOH pH 7.9, 50 mM KCl, 5 mM $MgCl_2$, 5 mM EGTA, 2 mM β-ME

ELB buffer: 10 mM HEPES-KOH pH 7.7, 50 mM KCl, 2.5 mM $MgCl_2$

Fixation buffer: 15 mM PIPES-KOH pH 7.2, 80 mM KCl, 15 mM NaCl, 1% v/v formalin, 2 $\mu g \cdot ml^{-1}$ Hoechst 33258, 50% v/v glycerol

STOP buffer: 80 mM Tris-HCl pH 8.0, 8 mM EDTA, 0.13% w/v phosphoric acid, 10% w/v ficoll, 5% w/v SDS, 0.2% w/v bromophenol blue

10× TBE: 0.89 M Tris, 0.89 M boric acid, 20 mM EDTA

2.2.2.4 Yeast cells

LiT buffer: 10 mM Tris-HCl, pH 7.4, 100 mM lithium acetate; autoclaved

LiT/PEG solution: 50% w/v PEG 3350 in LiT buffer; autoclaved

HT DNA solution: herring sperm DNA (type XIV, Sigma) in TE buffer was extensively sonicated, subjected to phenol/chloroform extraction followed by ethanol precipitation as described by Sambrook and Russell (2001), resuspended in TE buffer at 10 $mg \cdot mL^{-1}$ and finally boiled at 95°C for 5 min

Zymolyase solution: 50 µL of a 20 $\mu g \cdot \mu L^{-1}$ zymolyase 20T solution and 50 µL of 1 M DTT were combined with 900 µL of sterile water just before required

NaOH/β−ME solution: 925 µL of 2 M NaOH and 75 µL of 100% v/v β-ME were mixed just before required

0.5 M citrate buffer: 0.5 M sodium citrate was mixed with a few mL of 0.5 M citric acid until the pH reached a value 7

Propidium iodide stock solution: 20 $\mu g \cdot mL^{-1}$ propidium iodide in 50 mM citrate buffer

STE buffer: 1.2 M sorbitol, 25 mM Tris-HCl pH 8.0, 25 mM EDTA pH 8.0; filter-sterilized

STE-Zymolyase solution: 37 µL of STE buffer, 2 µL of 1M DTT and 1 µL of a 20 $\mu g \cdot \mu L^{-1}$ Zymolyase (20T) solution

HU buffer: 8 M urea, 5% w/v SDS, 200 mM Tris-HCl pH 6.8, 1 mM EDTA, 0.1% w/v bromophenol blue and 50 mM DTT

2.2.2.5 Mammalian cells

Trypsin/versene: 0.1% w/v trypsin, 0.7 mM EDTA, 0.2% w/v phenol red in 1× PBS (London Research Institute's Media production team)

PBS-Tx: 1× PBS + 0.1% v/v Triton X-100

100× penicillin/streptomycin solution: 10,000 $U \cdot mL^{-1}$ penicillin and 10,000 $g \cdot mL^{-1}$ streptomycin in 1× PBS (London Research Institute's Media production team)

Cell fractionation buffer A: 10 mM HEPES-KOH pH 7.5, 10 mM KCl, 1.5 mM $MgCl_2$, 0.34 M sucrose and 10% v/v glycerol with freshly supplemented 1× Complete Protease Inhibitors (Roche) and 1 mM DTT

Cell fractionation buffer B: 3 mM EDTA, 0.2 mM EGTA with freshly supplemented 1× Complete Protease Inhibitors and 1 mM DTT

2.2.2.6 General manipulation of DNA

50× TAE: 2 M Tris base, 2 M glacial acetic acid and 50 mM EDTA

10× TBE: 0.89 M Tris base, 0.89 M boric acid, 20 mM EDTA

6× DNA Loading buffer: 50% w/v sucrose, 0.1% w/v bromophenol blue and 0.1% w/v xylene cyanol FF in TE

2.2.2.7 General manipulation of proteins

5× SDS-PAGE running buffer: 125 mM Tris base, 1.25 M glycine and 0.5% w/v SDS

Coomassie Blue staining solution: 0.25% w/v Brilliant Blue R, 45% v/v methanol and 10% (v/v) glacial acetic acid; filtered

De-staining solution: 45% v/v methanol and 10% v/v glacial acetic acid

Gel Drying solution: 20% v/v methanol and 3% v/v glycerol in water

SYPRO fixing solution**:** 50% v/v ethanol and 7% v/v glacial acetic acid

SYPRO wash solution: 10% v/v ethanol and 7% v/v glacial acetic acid

Blotting buffer I**:** 300 mM Tris-HCl pH 10.4 and 15% v/v methanol

Blotting buffer II: 30 mM Tris-HCl pH 10.4 and 15% v/v methanol

Blotting buffer III: 25 mM Tris-HCl pH 9.4, 40 mM 6-aminocaproic acid and 15% v/v methanol

PBS-T: 1× PBS + 0.1% w/v Tween 20

Blocking solution**:** 5% w/v non-fat dry milk powder (Sainsbury's Basic) dissolved in PBS-T

Gentle stripping buffer: 200 mM glycine, 0.1% w/v SDS and 1% v/v Tween 20, adjusted to pH 2.2 with HCl just before required

Harsh stripping buffer: 100 mM Tris-HCl pH 7.5, 10 mM EDTA and 0.5% w/v SDS. 140 µL of 100% v/v β-ME was added per 20 mL of stripping buffer just before required

2.2.2.8 Protein purification

Ni^{2+}-NTA lysis buffer: 50 mM Tris-HCl pH 8, 300 mM, 20 mM imidazole and 2 mM freshly added β-ME

Ni^{2+}-NTA wash buffer: 50 mM Tris-HCl pH 8, 300 mM, 30 mM imidazole and 2 mM freshly added β-ME

Ni^{2+}-NTA elution buffer: 50 mM Tris-HCl pH 8, 300 mM, 250 mM imidazole and 2 mM freshly added β-ME

E1 gel filtration buffer: 50 mM Tris-HCl pH 7.5, 200 mM NaCl, 1 mM freshly added DTT

Protein storage buffer: 20 mM HEPES-KOH pH 7.5, 200 mM KCl, 10% v/v glycerol and 1 mM freshly added DTT

E2 lysis buffer: 50 mM phosphate buffer pH 6.5, 50 mM NaCl and 1 mM freshly added DTT

E2 elution buffer: 50 mM phosphate buffer pH 6.5, 300 mM NaCl and 1 mM freshly added DTT

GST wash buffer: 50 mM Tris-HCl pH 8, 300 mM and 1 mM freshly added DTT

GST elution buffer: 50 mM Tris-HCl pH 8, 300 mM, 15 mM freshly added reduced glutathione and 1 mM DTT

PARP-1 lysis buffer: 50 mM Tris-HCl pH 7.5 and 500 mM NaCl

2.2.2.9 Generation and affinity purification of polyclonal antibodies

Antibody elution buffer I: 200 mM Glycine adjusted to pH 2.8 with HCl

Antibody elution buffer II: 200 mM Glycine adjusted to pH 2.2 with HCl

Neutralization buffer: 0.5 M Tris-HCl pH 8 and 1.5 M KCl

2.2.2.10 Enzymatic reactions

Sumoylation buffer: 20 mM HEPES-KOH pH 7.5, 110 mM KOAc, 2 mM $Mg(OAc)_2$, 0.05% Tween 20, 0.2 $\mu g \cdot \mu L^{-1}$ BSA and 1 mM DTT

Auto-parylation buffer: 50 mM Tris-HCl pH 8.0, 100 mM NaCl, 4 mM $MgCl_2$, 0.1 $\mu g \cdot \mu l^{-1}$ BSA, 0.4 mM NAD^+ and 1 mM DTT

Extract buffer: 25 mM HEPES-KOH pH 7.9, 70 mM KCl and 1 mM DTT

3C Cleavage buffer: 50 mM Tris-HCl pH 7.5, 120 mM NaCl, 1 mM $MgCl_2$, 20 mM imidazole and 1 mM DTT

Su-DBD wash buffer: 50 mM Tris-HCl pH 7.5, 200 mM NaCl, 1 mM $MgCl_2$, 20 mM imidazole and 1 mM DTT

Su-DBD gel filtration buffer: 50 mM Tris-HCl pH 7.5, 200 mM NaCl, 1 mM $MgCl_2$ and 1 mM DTT

Su-PARP-1 wash buffer: 20 mM HEPES-KOH pH 7.5, 500 mM NaCl, 20 mM imidazole and 1 mM DTT

Su-PARP-1 elution buffer: 20 mM HEPES-KOH pH 7.5, 500 mM NaCl, 400 mM imidazole and 1 mM DTT

2.2.2.11 Analysis of protein-protein interactions

Hypotonic buffer: 25 mM Tris-HCl pH 7.5, 10 mM KCl, 10 mM EDTA and 0.5% v/v Triton X-100 freshly supplemented with 1× Complete Protease Inhibitors

Co-immunoprecipitation buffer: 25 mM Tris-HCl pH 7.5, 150 mM KCl, 10 mM EDTA and 0.1% v/v Triton X-100

2.2.2.12 Analysis of protein sumoylation

Ni^{2+}-NTA Buffer A: 6 M guanidine hydrochloride, 100 mM phosphate buffer pH 8, 300 mM NaCl, and 10 mM Tris-HCl pH 8 and 2 mM β-ME

Ni^{2+}-NTA Buffer C: 8 M urea, 100 mM sodium phosphate pH 6.3, and 10 mM Tris-HCl, pH 6.3. Alternatively, 8 M urea, 100 mM sodium phosphate pH 8.0, 10 mM Tris-HCl and 30 mM imidazole

RIPA buffer: 50 mM Tris-HCl pH 8.0, 150 mM NaCl, 5 mM EDTA, 1% v/v Triton X-100, 0.1% v/v sodium deoxycholate, freshly supplemented with 1× Complete Protease Inhibitors, 10 $\mu g \cdot ml^{-1}$ of each of leupeptide, pepstatin and chymostatin and 15 mM NEM

2.2.2.13 Preparation of DNA substrates for in vitro *sumoylation*

Topo I buffer: 50 mM Tris-HCl pH 7.5, 50 mM KCl, 10 mM $MgCl_2$, 0.1 mM EDTA, 30 $\mu g \cdot \mu L^{-1}$ BSA and 0.5 mM DTT

Annealing buffer: 50 mM Tris-HCl pH 7.5 and 250 mM NaCl

2.2.2.14 Analysis of protein-DNA interactions

EMSA binding buffer: 50 mM Tris-HCl pH 7.4, 150 µM $ZnSO_4$, 4 mM DTT, 10% v/v glycerol

2.2.2.15 General methods for NMR spectroscopy

NMR dialysis buffer: 50 mM Tris-HCl pH 7.0, 200 mM NaCl, 150 µM $ZnSO_4$, 4mM [$^2H_6$] DTT

2.3 DNA oligonucleotides

DNA oligonucleotides were purchased from Sigma-Genosys, except for those that were biotinylated, which were instead obtained from Operon.

#	Name	Sequence	Sense/Use
453	^{Sc}SIZ1 KO down	AAGAAGACTCCAACTCAAACAGTTGAGTGTTCCA TATACATTCTGTTTCACGTACGCTGCAGGTCGAC	Sense, amplification of knockout cassettes
454	^{Sc}SIZ1 KO up	AAATATTTCATGAAAGAGCTGGACGGAACCGTCC AATTTTAGCCTCGTTTATCGATGAATTCGAGCTCG	Antisense, amplification of knockout cassettes
455	^{Sc}SIZ1 KO test	CTAGAACTACCATTTTAGAGC	Sense, testing of correct knockout
843	XO	GACGCTGCCGAATTCTACCAGTGCCTTGCTAGGA CATCTTTGCCCACCTGCAGGTTCACCC	*In vitro* DNA substrate
844	XO-c	GGGTGAACCTGCAGGTGGGCAAAGATGTCCTAG CAAGGCACTGGTAGAATTCGGCAGCGTC	Reverse complement to oHU843
888	^{Xl}SUMO1 PrSc down	CGCGGATCCCTGGAAGTTCTGTTCCAGGGGCCC ATGTCTGATCAGGAAGCTAAACCATC	Sense, amplification of ORF
889	^{Xl}SUMO1 up	GCGCTGCAGTTACCCCCCAGTCTGTTCCTG	Antisense, amplification of ORF
890	^{Xl}SUMO2 down	GCGCCCGGGCCCATGGCGGACGATAAGCCCAAG	Sense, amplification of ORF
891	^{Xl}SUMO2 up	GCGCTGCAGTTATCCACCCGTCTGCTGCTG	Antisense, amplification of ORF
896	^{Xl}MMS21 down	GCGCCCGGGCCCATGTCTGGCCGGTCAGCGCCT GTGG	Sense, amplification of ORF
897	^{Xl}MMS21 up	GCGCTGCAGTGTTCAATGACGGCCTTTCTGCTTG	Antisense, mutagenesis of ORF

972	pQE30 RGS-His_6 down	GCGCCATGGGAGGATCGCATCACCATCACC	Sense, amplification of vector sequence
973	pQE 3'UTR up	GTCCAAGCTCAGCTAATTAAGCTTGGC	Antisense, amplification of vector sequence
1022	^{Sc}SIZ2 KO down	CCACAAACGATACACTGATAATCAAGAAACGTATA AGGGAAAAGAGCACGCGTACGCTGCAGGTCGAC	Sense, amplification of knockout cassettes
1023	^{Sc}SIZ2 KO up	AAATAAAAATAGAATACAATCGGAAAGGAAAGAA ATCAAAAGACGGTTAAATCGATGAATTCGAGCTC G	Antisense, amplification of knockout cassettes
1024	^{Sc}SIZ2 KO test	GTGTTAATTTATCCATCCATTTTAG	Sense, testing of correct knockout
1048	^{Sc}ORC1 tag down	TAGAAGAAGCCAAAAGAGCCATGAATGAGGATGA GACATTGAGAAATTTACGTACGCTGCAGGTCGAC	Sense, amplification of tagging cassettes
1049	^{Sc}ORC1 tag up	TAGGTATATGTATGTGTATGCTAGGTCATGAATAA TAAAAACCGAATCTAATCGATGAATTCGAGCTCG	Antisense, amplification of tagging cassettes
1122	ssDNA-bio 25	ATGCTAGTACACTGCGTTTATGTAT	*In vitro* DNA substrate. 3' biotinylated
1123	ssDNA-bio 15	ACTGCGTTTATGTAT	*In vitro* DNA substrate. 3' biotinylated
1124	ssDNA-bio 8	TTATGTAT	*In vitro* DNA substrate. 3' biotinylated
1125	ssDNA 25	ATACATAAACGCAGTGTACTAGCAT	Reverse complement to oHU1122
1126	ssDNA 15	ATACATAAACGCAGT	Reverse complement to oHU1123
1127	ssDNA 8	ATACATAA	Reverse complement to oHU1124
1132	^{Sc}RAD54 tag down	CGAGCATCATTACAATGATATCAGTTTTGCATTTC AATATATTTCACATCGTACGCTGCAGGTCGAC	Sense, amplification of tagging cassettes
1133	^{Sc}RAD54 tag up	CGAATTCTACTTTTTGTTTTTGTTTTATAAGTACAT GTATGTAAGAGATCAATCGATGAATTCGAGCTCG	Antisense, amplification of tagging cassettes
1134	^{Sc}RAD54 tag test	CGTTGAAAGGTTGTTTAGTTC	Sense, testing of correct tagging
1135	^{Sc}RFC1 tag down	GACTGCCACCAGTAAACCTGGTGGTAGCAAAAAA AGGAAAACGAAAGCACGTACGCTGCAGGTCGAC	Sense, amplification of tagging cassettes
1136	^{Sc}RFC1 tag up	CAATGAGAAGAAAAGTGTAATTATAATCTTAGTGT ATGAATAAATCAATCGATGAATTCGAGCTCG	Antisense, amplification of tagging cassettes
1137	^{Sc}RFC1 tag test	GTGGATTCACGCGGAAATAC	Sense, testing of correct tagging
1138	^{Sc}ORC2 tag down	CACGTATGCGGAACTTGAAAAACTTCTGAAAACC GTTTTAAATACTCTACGTACGCTGCAGGTCGAC	Sense, amplification of tagging cassettes
1139	^{Sc}ORC2 tag up	GCTAGCAAGCCTAGTACTATTACAATTGTTCGTGA TATGTATACATTTAATCGATGAATTCGAGCTCG	Antisense, amplification of tagging cassettes
1140	^{Sc}ORC2 tag test	CCAAGAAGATGTATAAGTTGC	Sense, testing of correct tagging
1150	^{Sc}POL1 tag down	GGACGTCGCTACGTTGATATGACTAGCATATTTG ATTTCATGCTAAATCGTACGCTGCAGGTCGAC	Sense, amplification of tagging cassettes
1151	^{Sc}POL1 tag up	CTATATAGAATATTCATGAGATCACACAACACATA CAAAATACTTACCTAATCGATGAATTCGAGCTCG	Antisense, amplification of tagging cassettes
1152	^{Sc}POL1 tag test	GACAGCACATGCGGTATAG	Sense, testing of correct tagging
1185	^{Sc}ORC3 tag down	AAAGCACCAAGAGTTACGATCTGGTAGAAAAATG TGTCTGGAGAGGAATTCGTACGCTGCAGGTCGA C	Sense, amplification of tagging cassettes
1186	^{Sc}ORC3 tag up	ATATATGTATGGTTATTTATTTACTTATTTATCCGT GCATTCTTTATCTAATCGATGAATTCGAGCTCG	Antisense, amplification of tagging cassettes
1187	^{Sc}ORC3 tag test	GAGGCGAATATGACTATCAAC	Sense, testing of correct tagging

1188	^{Sc}ORC4 tag down	TAAGAAGAATTATCCCCAAATCTAATATGTACTAC TCCTGGACACAACTGCGTACGCTGCAGGTCGAC	Sense, amplification of tagging cassette
1189	^{Sc}ORC4 tag up	TCAGAGTTGCTACCGCCAATAAAATGTCTGTATAT TGTTCCCAAGATTCAATCGATGAATTCGAGCTCG	Antisense, amplification of tagging cassette
1190	^{Sc}ORC4 tag test	CGACAATACTATCAAACTATG	Sense, testing of correct tagging
1191	^{Sc}ORC5 tag down	CAGAATCTGTTCATTTCAATATCAGCGATTACTTC AGCGATATTCACGAACGTACGCTGCAGGTCGAC	Sense, amplification of tagging cassette
1192	^{Sc}ORC5 tag up	GTTGTTTCGAACGTATCCTGCCCTCTGGATACCT TCCAGGGAGATAATCAATCGATGAATTCGAGCTC G	Antisense, amplification of tagging cassette
1193	^{Sc}ORC5 tag test	CCCTATTCAAGGTAAGGCGG	Sense, testing of correct tagging
1194	^{Sc}ORC6 tag down	ATATTTGGAAGAAAAGAATTGAAATGGATTTGGCA TTAACAGAACCTTTACGTACGCTGCAGGTCGAC	Sense, amplification of tagging cassette
1195	^{Sc}ORC6 tag up	ATGTCAGGTATTGGTCAAATATATACTTTTAGTTA ATACTGGATATGTTAATCGATGAATTCGAGCTCG	Antisense, amplification of tagging cassette
1196	^{Sc}ORC6 tag test	GATGTGCAGCTTGATGTTGAC	Sense, testing of correct tagging
1199	^{Sc}ORC1 ORF down	GCGCCCGGGAAAAATGGCAAAAACGTTGAAGG	Sense, amplification of ORF
1200	^{Sc}ORC1 ORF up	GCGCACGTGCTCGAGCTATAAATTTCTCAATGTC TCATCC	Antisense, amplification of ORF
1203	^{Sc}ORC2 ORF down	GCGCCCGGGAAAAATGCTAAATGGGGAAGACTTT G	Sense, amplification of ORF
1204	^{Sc}ORC2 ORF up	GCCCTGCAGTTATAGAGTATTTAAAACGG	Antisense, amplification of ORF
1286	ARS1 down	GAGAGCTTACATTTTATGTTAGCTGG	Sense, amplification of *ARS1* from YCp family plasmids
1287	ARS1 up	[CACATGTTAAAATAGTGAAGG AGC	Antisense, amplification of *ARS1* from YCp family plasmids. 5' biotinylated
1288	^{Sc}ORC3 ORF down	CGCCCGGGAATGAGCGACCTTAACCAATCC	Sense, amplification of ORF
1289	^{Sc}ORC3 ORF up	CGCCTGCAGTCTAAATTCCTCTCCAGACAC	Antisense, mutagenesis of ORF
1291	^{Sc}ORC4 ORF down	CGCCCGGGAATGACTATAAGCGAAGCTCG	Sense, amplification of ORF
1292	^{Sc}ORC4 ORF up	GGGATCCTTCACAGTTGTGTCCAGGAG	Antisense, mutagenesis of ORF
1294	^{Sc}ORC5 ORF down	CGCCCGGGAATGAATGTGACCACTCCGG	Sense, amplification of ORF
1295	^{Sc}ORC5 ORF up	CGGATCCTCATTCGTGAATATCGCTGAAG	Antisense, mutagenesis of ORF
1297	^{Sc}ORC6 ORF down	CGCCCGGGAATGTCCATGCAACAAGTCC	Sense, amplification of ORF
1298	^{Sc}ORC6 ORF up	CGCCTGCAGGTTATAAAGGTTCTGTTAATG	Antisense, mutagenesis of ORF
1299	^{Sc}REP1 down	GCCAGAGGATGGCGAACC	Sense, for testing loss of 2-μ plasmid
1300	^{Sc}REP1 up	GCTCGCGTTGCATTTTCG	Antisense, for testing loss of 2-μ plasmid
1339	^{Hs}APLF up	TCATTTTCTTTTCATAAACCTTTTTGC	Antisense, amplification of ORF
1340	^{Hs}Aprataxin down	CACCATGAGTAACGTGAATTTGTCCGTC	Sense, amplification of ORF

1341	^{Hs}Aprataxin up	TTACTCTTGTGATTCTAGGAAGTATTCTG	Antisense, amplification of ORF
1343	^{Hs}BLC2 up	TTACTTGTGGCCCAGATAGGCACCCAGG	Antisense, amplification of ORF
1346	^{Hs}Caspase 3 down	CACCATGGAGAACACTGAAAACTCAGTGG	Sense, amplification of ORF
1347	^{Hs}Caspase 3 up	TCAGTGATAAAAATAGAGTTCTTTTGTGAGC	Antisense, amplification of ORF
1349	^{Hs}Caspase 7 up	TCATTGACTGAAGTAGAGTTCCTTGGTG	Antisense, amplification of ORF
1351	^{Hs}CENP-A up	TCAGCCGAGTCCCTCCTCAAGGCCCCG	Antisense, amplification of ORF
1353	^{Hs}CENP-B up	TCAGCTTTGATGTCCAAGACCTCGAAC	Antisense, amplification of ORF
1355	^{Hs}Ligase III up	TCAGCAGGGAGCTACCAGTCTCCGTTTCC	Antisense, amplification of ORF
1356	^{Hs}p21 down	CACCATGTCAGAACCGGCTGGGGATGTCC	Sense, amplification of ORF
1357	^{Hs}p21 up	TCAGGGCTTCCTCTTGGAGAAGATCAGC	Antisense, amplification of ORF
1358	^{Hs}p53 down	CACCATGGAGGAGCCGCAGTCAGATCC	Sense, amplification of ORF
1359	^{Hs}p53 up	TCAGTCTGAGTCAGGCCCTTCTGTCTTG	Antisense, amplification of ORF
1360	^{Hs}PARP1 down	CACCCATATGGCGGAGTCTTCGGATAAGCTC	Sense, amplification of ORF
1361	^{Hs}PARP1 up	TTAGGCGCCCCACAGGGAGGTCTTAAAATTG	Antisense, amplification of ORF
1365	^{Hs}PARP3 up	TCAGAGGTGGACCTCCAGCAGGTAGCG	Antisense, amplification of ORF
1367	^{Hs}PCNA up	TCAAGATCCTTCTTCATCCTCGATCTTGG	Antisense, amplification of ORF
1373	^{Hs}TRF2IP up	TCATTTCTTTCGAAATTCAATCCTCCG	Antisense, amplification of ORF
1374	^{Hs}WRN down	CACCATGAGTGAAAAAAAATTGGAAAC	Sense, amplification of ORF
1375	^{Hs}WRN up	TCAACTAAAAAGACCTCCCCTTTTCG	Antisense, amplification of ORF
1377	^{Hs}XRCC1 up	TCAGGCTTGCGGCACCACCCCATAGAGC	Antisense, amplification of ORF
1378	^{Xl}SUMO1 down	CACCGGCGCCCATATGTCTGATCAGGAAGCTAAACC	Sense, amplification of ORF
1379	^{Xl}SUMO1 up	CCTGCATATGGGCGCCAGTCTGTTCCTGATAAACTTC	Antisense, amplification of ORF
1380	^{Xl}SUMO2 down	CACCGGCGCCCATATGGCGGACGATAAGCCCAAGG	Sense, amplification of ORF
1381	^{Xl}SUMO2 up	CCTGCATATGGGCGCCCGTCTGCTGCTGGAAAACATC	Antisense, amplification of ORF
1382	PARP1^{K203R} up	CTTTCCTTCAGATCTGACTCCTGGGAGCTGC	Sense, mutagenesis of ORF
1383	^{Hs}PARP1^{K203R} down	GGAGTCAGATCTGAAGGAAAGAGAAAAGGC	Antisense, mutagenesis of ORF
1384	^{Hs}PARP1^{K486R} up	CTCTGCCCTCACCTCTGCCCCCCAAGGG	Sense, mutagenesis of ORF
1385	^{Hs}PARP1^{K486R} down	GGCAGAGGTGAGGGCAGAGCCTGTTGAAG	Antisense, mutagenesis of ORF
1411	^{Hs}WRN +980 up	CTGTTGTACTCCCCCAG	Antisense, amplification

			of partial ORF
1413	^{Hs}WRN +1960 up	TTGCTGGAGCAGGCCC	Antisense, amplification of partial ORF
1415	^{Hs}WRN +2930 up	ATTCCAAATTTTTCGCC	Antisense, amplification of partial ORF
1416	^{Hs}WRN seq7 +3880 up	CAGCTTTCACCGCTTGGG	Antisense, amplification of partial ORF
1449	^{Xl}SUMO1$^{K27/36/37R}$ down	CAGGAAGCTAGACCATCTAGTGAGGATCTAGGAGACAGAAGAGAAGGAGG	Sense, mutagenesis of ORF
1450	^{Xl}SUMO1$^{K27/36/37R}$ up	CCTCCTTCTCTTCTGTCTCCTAGATCCTCACTAGATGGTCTAGCTTCCTG	Antisense, mutagenesis of ORF
1451	^{Xl}SUMO2$^{K25/27/31R}$ down	GCGGACGATAGGCCCAGGGAAGGAGTTAGGACTGAGAAC	Sense, mutagenesis of ORF
1452	^{Xl}SUMO2$^{K25/27/31R}$ up	GTTCTCAGTCCTAACTCCTTCCCTGGGCCTATCGTCCGC	Antisense, mutagenesis of ORF
1453	^{Hs}APLF down	ATGTCCGGGGGCTTCGAGC	Sense, amplification of ORF
1454	^{Hs}CENP-A down	ATGGGCCCGCGCCGCCGG	Sense, mutagenesis of ORF
1455	^{Hs}Ligase III down	ATGGCTGAGCAACGGTTCTG	Sense, amplification of ORF
1458	^{Hs}PCNA down	ATGTTCGAGGCGCGCCTGG	Sense, amplification of ORF
1459	^{Hs}PARP-3 down	ATGGCTCCAAAGCCGAAGC	Sense, amplification of ORF
1470	BCL-2 down	ATGGCGCACGCTGGGAG	Sense, amplification of ORF
1471	^{Hs}Caspase 7 down	ATGGCAGATGATCAGGGC	Sense, amplification of ORF
1472	^{Hs}CENP-B down	ATGGGCCCCAAGAGGCGAC	Sense, amplification of ORF
1473	^{Hs}PARP-2 down	ATGGCGGCGCGGCGGCGACG	Sense, amplification of ORF
1474	^{Hs}TRF2IP down	ATGGCGGAGGCGATGG	Sense, amplification of ORF
1475	^{Hs}XRCC1 down	ATGCCGGAGATCCGCCTCC	Sense, amplification of ORF
1566	^{Hs}APLF up w/o STOP	TTTTCTTTTCATAAACCTTTTTGC	Antisense, amplification of ORF
1567	^{Hs}XRCC1 up w/o STOP	GGCTTGCGGCACCACCCCATAGAGC	Antisense, amplification of ORF
1593	^{Hs}PARP1^{M890V} down	CGTGACAGGCTACGTGTTTGGTAAAGGG	Sense, mutagenesis of ORF
1594	^{Hs}PARP1^{M890V} up	CCCTTTACCAAACACGTAGCCTGTCACG	Antisense, mutagenesis of ORF
1595	^{Hs}PARP1^{D899N} down	GATCTATTTCGCTAACATGGTCTCCAAG	Sense, mutagenesis of ORF
1596	^{Hs}PARP1^{D899N} up	CTTGGAGACCATGTTAGCGAAATAGATC	Antisense, mutagenesis of ORF
1605	^{Hs}SUMO1^{T95R} down	CAGGAACAAAGGGGGGGTCATTC	Sense, mutagenesis of ORF
1606	SUMO1^{T95R} up	GAATGACCCCCCCTTTGTTCCTG	Antisense, mutagenesis of ORF
-	Dumbbell DNA	CGGTCGATCGTAAGATCGACCGGCGCTGGAGGTTCCTCCAGCGC	*In vitro* DNA substrate, 5' phosphorylated
-	^{Hs}PARP-1^{R138I} down	GATAGAAAAGGGCCAGGTGATTCTGTCCAAGAAGATGGTGG	Sense, amplification of ORF

-	^{Hs}PARP-1^{R138I} up	CCACCATCTTCTTGGACAGAATCACCTGGCCCTTTTCTATC	Antisense, mutagenesis of ORF
-	^{Hs}PARP-1^{R122I} down	GTATGCCAAGTCCAACATTAGTACGTGCAAGGGGTG	Sense, amplification of ORF
-	^{Hs}PARP-1^{R122I} up	CACCCCTTGCACGTACTAATGTTGGACTTGGCATAC	Antisense, mutagenesis of ORF

Table 2.5 - A list of the DNA oligonucleotides used in this thesis. Sc = *S. cerevisiae*, Xl = *X. laevis*, Hs= *Homo sapiens*.

2.4 Plasmids

#	Plasmid name	Description/Origin/References
82	pGBT9	Yeast two-hybrid vector for production of *GAL4* DBD fusion constructs (Clontech)
145	pGAD424	Yeast two-hybrid vector for production of *GAL4* AD fusion constructs (Clontech)
150	pQE30	Overproduction in *Escherichia coli* (Qiagen)
229	pYM6	To create 9myc tagging cassettes carrying the *TRP1* marker, Knop *et al.* (1999)
233	pFA-HIS3MX6	To create knockout cassettes carrying the *HIS3MX6* marker, Wach *et al.* (1994)
273	pGAD424-^{Sc}UBC9	Yeast two-hybrid assay (In-house)
452	pFA-KanMX4	To create knockout cassettes carrying the *KanMX4* marker, Wach *et al.* (1994)
620	pGBT9-^{Sc}SMT3	Yeast two-hybrid assay (In-house)
654	YEp181-ADH/T	Constitutive production of a protein in yeast (In-house)
822	YEp181-CUP1-His_6-^{Sc}SMT3	Cu^{2+}-inducible production of His_6-Smt3 in yeast (In-house)
839	pET15b	Over-production in BL21(DE3) *E. coli* (Merck)
1037	pGAD424-^{Sc}SMT3ΔGG	Yeast two-hybrid assay (In-house)
1038	pGBT9-^{Sc}SMT3ΔGG	Yeast two-hybrid assay (In-house)
1237	pET23a-^{Mm}UBC9	Over-production of metazoan Ubc9 in *E. coli* (Frauke Melchior)
1238	pET11a-^{Hs}SUMO1ΔC4	Over-production of mature human SUMO1 in *E. coli* (Frauke Melchior)
1337	pET21(+)	Over-production in BL21(DE3) *E. coli* (Merck)
1338	pET-^{Xl}PCNA	Over-production of His_6-PCNA in *E. coli*, Leach and Michael (2005)
1551	pET21-^{Xl}ORC1-His_6	Over-production of ORC1-His_6 in *E. coli*, Tugal *et al.* (1998)
1558	pDK243	Plasmid stability assay in yeast (1× ARS1, Hogan and Koshland, 1992)
1559	pDK368-7	Plasmid stability assay in yeast (1× ARS1 + 7× H4 ARS, Hogan and Koshland, 1992)
1791	pGGWA	Gateway destination vector for over-production of N-terminally GST-tagged and C-terminally His_6-tagged proteins in *E. coli*, Busso *et al.* (2005)
1795	pDEST22	Gateway destination vector for the generation of *GAL4* AD fusions for use in the yeast two hybrid assay (Invitrogen)
1796	pDEST32	Gateway destination vector for the generation of *GAL4* BDB fusions for use in the yeast two hybrid assay (Invitrogen)

1797	pGAD424-GW	Gateway-compatible pGAD424, Albers *et al.* (2005)
1798	pGBT9-GW	Gateway-compatible pGBT9, Albers *et al.* (2005)
1800	pDEST10	Gateway destination BAC-to-BAC-compatible vector for the production of N-terminally His_6-tagged proteins in insect cells (Invitrogen)
1801	pDEST12.2	Gateway destination vector for the constitutive production of non-tagged proteins in mammalian cells (Invitrogen)
1802	pDEST/TO/FLAG/FRT	Gateway destination Flp-In-compatible vector for the Tet-inducible production of N-terminally FLAG-tagged proteins in mammalian cells (Simon Boulton)
1804	pDEST/N-$FLAG_3$/FRT	Gateway destination Flp-In-compatible vector for the constitutive production of N-terminally $FLAG_3$-tagged proteins in mammalian cells (Stephen West)
1805	pDEST-myc	Gateway destination vector for the constitutive production of N-terminally myc-tagged proteins in mammalian cells (Simon Boulton)
1809	pOG44	Constitutive production of ^{Sc}Flp1(F70L) in mammalian cells, O'Gorman *et al.* (1991). For use with Invitrogen's Flp-In System
2019	pBIS-GALkFLP(URA3)	Curing yeast of the 2-µm plasmid Tsalik and Gartenberg (1998)
2021	pET23a-^{Ms}UBC9(C93S)	Over-production of metazoan UBC9(C93S) in *E. coli* (Frauke Melchior)
2022	pDuet-1-^{Hs}Uba2, ^{Hs}Aos1	Over-production of human SUMO E1 in *E. coli* (Christopher Lima)
-	pDEST/C-$FLAG_3$/FRT-PARP-1	Constitutive production of the specified C-terminally $FLAG_3$-tagged PARP-1 construct in mammalian cells (Stephen West)
-	pDEST/C-$FLAG_3$/FRT-PARP-1^{K203}	
-	pDEST/C-$FLAG_3$/FRT-PARP-1^{K486R}	
-	pDEST/C-$FLAG_3$/FRT-PARP-1^{K233R}	
-	pDEST/C-$FLAG_3$/FRT-PARP-1^{K249R}	
-	pDEST/C-$FLAG_3$/FRT-PARP-1^{K512R}	
-	pDEST/C-$FLAG_3$/FRT-PARP-$1^{K203/486R}$	
-	pDEST/C-$FLAG_3$/FRT-PARP-$1^{K233/486R}$	
-	pDEST/C-$FLAG_3$/FRT-PARP-$1^{K249/486R}$	
-	pDEST/C-$FLAG_3$/FRT-PARP-$1^{K486/512R}$	
-	pDEST/C-$FLAG_3$/FRT-PARP-$1^{K305/486R}$	

-	pDEST/C-$FLAG_3$/FRT-PARP-$1^{K352/486R}$	
-	pDEST/C-$FLAG_3$/FRT-PARP-$1^{K442/486R}$	
-	pSG5-His_6-^{Hs}SUMO1	Constitutive over-production of mature His_6-SUMO1 in mammalian cells, Muller *et al.* (2000)

Table 2.6 - A list of the plasmids used in this thesis that were commercially available or were generated by others. Sc = *S. cerevisiae*, Xl = *X. laevis*, Hs= *H. sapiens*.

#	Name	Use/Construction
1284	pET15b-PrSc-^{Xl}SUMO1	Overproduction of His_6-PrSc-SUMO1 in *E. coli*. Reverse transcription (oHU888/oHU889) from frog egg RNA, cloned BamHI/PstI into pHU150. PCR (oHU972/oHU973) from this plasmid cloned NcoI/BlpI into pHU839
1285	pET21-PrSc-^{Xl}SUMO2	Overproduction of His_6-PrSc-SUMO2 in *E. coli*. Reverse transcription (oHU890/oHU891) from frog egg RNA, cloned BamHI/PstI into pHU150. His_6-PrSc-SUMO2 from this plasmid was cloned EcoRI/HindIII into pHU1337
1561	pGAD424-^{Sc}ORC1	Yeast two-hybrid analysis. PCR from genomic DNA (oHU1199/oHU1200), cloned SmaI/XhoI into pHU145
1562	pGBT9-^{Sc}ORC1	Yeast two-hybrid analysis. PCR from genomic DNA (oHU1199/oHU1200), cloned SmaI/XhoI into pHU82
1563	pGAD424-^{Sc}ORC2	Yeast two-hybrid analysis. PCR from genomic DNA (oHU1203/oHU1200), cloned SmaI/PstI into pHU145
1564	pGBT9-^{Sc}ORC2	Yeast two-hybrid analysis. PCR from genomic DNA (oHU1203/oHU1200), cloned SmaI/PstI into pHU82
1730	pENTR/D-TOPO-^{Hs}PARP-1	Gateway donor vector. PCR from GeneService IMAGE Clone 5193735 (oHU1360/oHU1361) TOPO-cloned into pENTR/D-TOPO
1731	pENTR/D-TOPO-PARP-1(K203R)	Gateway donor vector. Site-directed mutagenesis of pHU1730 (oHU1382/oHU1383)
1732	pENTR/D-TOPO-PARP-1(K486R)	Gateway donor vector. Site-directed mutagenesis of pHU1730 (oHU1384/oHU1385)
1733	pENTR/D-TOPO-PARP-$1^{K203/486R}$	Gateway donor vector. Site-directed mutagenesis of pHU1731 (oHU1384/oHU1385)
1735	pENTR/D-TOPO-PARP-$1^{M890V, D899N}$	Gateway donor vector. Site-directed mutagenesis of pHU1730 (oHU1593/1594 and oHU1595/1596)
1740	pENTR/D-TOPO-SUMO1-PARP-$1^{K203/486R}$	Gateway donor vector. PCR from pHU1284 (oHU1378/oHU1379) cloned with NdeI into pUH1733
1741	pENTR/D-TOPO-SUMO2-PARP-$1^{K203/486R}$	Gateway donor vector. PCR from pHU1285 (oHU1380/oHU1381) cloned with NdeI into pUH1733
1742	pENTR/D-TOPO-PARP-$1^{K203/486R}$-SUMO1	Gateway donor vector. PCR from pHU1284 (oHU1378/oHU1379) cloned with KasI into pUH1733
1743	pENTR/D-TOPO-PARP-$1^{K203/486R}$-SUMO2	Gateway donor vector. PCR from pHU1285 (oHU1380/oHU1381) cloned with KasI into pUH1733
1748	pENTR/D-TOPO-PARP-1^{C21G}	Gateway donor vector. Fragment from pDONR221-PARP-1^{C21G} (Stephen West) cloned ApaI/BsaBI into pHU1730
1749	pENTR/D-TOPO-PARP-$1^{R122/138I}$	Gateway donor vector. Site-directed mutagenesis of pHU1730 (oligonucleotides donated by Sebastian

		Eustermann)
1750	pENTR/D-TOPO-PARP-1^{C298A}	Gateway donor vector. Site-directed mutagenesis of pHU1730 (oHU1645/oHU1646)
1753	pENTR/D-TOPO-PARP-1$^{K203/486R, M890V, D899N}$	Gateway donor vector. Fragment from pHU1733 cloned NdeI/PstI into pHU1735
1754	pENTR/D-TOPO-PARP-1$^{K203/486R, M890V, D899N}$-SUMO1	Gateway donor vector. PCR from pHU1284 (oHU1378/oHU1379) cloned with KasI into pUH1735
1755	pENTR/D-TOPO-PARP-1$^{K203/486R, M890V, D899N}$-SUMO2	Gateway donor vector. PCR from pHU1285 (oHU1380/oHU1381) cloned with KasI into pUH1735
1756	pCR8/GW/TOPO-^{Hs}APLF	Gateway donor vector. PCR from GeneService IMAGE clone 6042653 (oHU1453/1339) TOPO-cloned into pCR8/GW/TOPO
1757	pENTR/D-TOPO-^{Hs}Aprataxin	Gateway donor vector. PCR from human cDNA (oHU1340/1341) TOPO-cloned into pENTR/D-TOPO
1758	pCR8/GW/TOPO-^{Hs}BCL2	Gateway donor vector. PCR from a plasmid donated by Julian Downward (oHU1470/1343) TOPO-cloned into pCR8/GW/TOPO
1760	pENTR/D-TOPO-^{Hs}Caspase 3	Gateway donor vector. PCR from human cDNA (oHU1346/1347) TOPO-cloned into pENTR/D-TOPO
1761	pCR8/GW/TOPO-^{Hs}Caspase 7	Gateway donor vector. PCR from human cDNA (oHU1471/1349) TOPO-cloned into pCR8/GW/TOPO
1762	pCR8/GW/TOPO-^{Hs}CENP-A	Gateway donor vector. PCR from GeneService IMAGE clone 3461992 (oHU1454/1351) TOPO-cloned into pCR8/GW/TOPO
1763	pCR8/GW/TOPO-^{Hs}CENP-B	Gateway donor vector. PCR from GeneService IMAGE clone 6470289 (oHU1472/1353) TOPO-cloned into pCR8/GW/TOPO
1764	pCR8/GW/TOPO-^{Hs}Ligase III	Gateway donor vector. PCR from a plasmid donated by Tomas Lindhal (oHU1455/1355) TOPO-cloned into pCR8/GW/TOPO
1765	pENTR/D-TOPO-^{Hs}p53	Gateway donor vector. PCR from human cDNA (oHU1358/1359) TOPO-cloned into pENTR/D-TOPO
1766	pCR8/GW/TOPO-^{Hs}PARP-3	Gateway donor vector. PCR from GeneService IMAGE clone 4763951 (oHU1459/1365) TOPO-cloned into pCR8/GW/TOPO
1767	pCR8/GW/TOPO-^{Hs}PCNA	Gateway donor vector. PCR from a plasmid donated by Svend Petersen-Mahrt (oHU1458/1367) TOPO-cloned into pCR8/GW/TOPO
1768	pENTR/D-TOPO-^{Xl}SUMO1	Gateway donor vector. PCR from pHU1284 (oHU1378/oHU1379) TOPO-cloned into pENTR/D-TOPO
1769	pENTR/D-TOPO-^{Xl}SUMO2	Gateway donor vector. PCR from pHU1285 (oHU1380/oHU1381) TOPO-cloned into pENTR/D-TOPO
1770	pCR8/GW/TOPO-^{Hs}TRF2IP	Gateway donor vector. PCR from GeneService IMAGE clone 5760351 with oHU1474 and 1373 and TOPO-cloned into pCR8/GW/TOPO
1771	pENTR/D-TOPO-^{Hs}WRN	Gateway donor vector. PCR from a plasmid donated by Ray Monnat (oHU1374/oHU1375) TOPO-cloned into pENTR/D-TOPO
1772	pCR8/GW/TOPO-^{Hs}XRCC1	Gateway donor vector. PCR from a plasmid donated by Tomas Lindhal (oHU1475/1377) TOPO-cloned into pCR8/GW/TOPO
1774	pCR8 APLF w/o STOP	Gateway donor vector. PCR from pHU1756 (oHU1453/oHU1566) TOPO-cloned into pCR8/GW/TOPO
1775	pCR8 XRCC1 w/o STOP	Gatewaty donor vector. PCR from pHU1772 (oHU1475/oHU1567) TOPO-cloned into pCR8/GW/TOPO
1806	pDEST-eGFP-myc	Gateway destination vector for the constitutive production of N-terminally eGFP-myc-tagged proteins in mammalian

		cells. eGFP from pEGFP-C1 (Clontech) cloned NdeI/HindIII into pHU1805
1810	pDEST12.2-PARP-1	Constitutive over-production in mammalian cells. LR recombination between pHU1730 and pHU1801
1811	pDEST12.2-PARP-1$^{K203/486R}$	Constitutive over-production in mammalian cells LR recombination between pHU1733 and pHU1801
1816	pDEST12.2-PARP-1$^{K203/486R}$-SUMO2	Constitutive over-production in mammalian cells. LR recombination between pHU1743 and pHU1801
1818	pDEST/TO/FLAG/FRT-PARP-1	Tet-inducible over-production in mammalian cells. LR recombination between pHU1730 and pHU1802
1819	pDEST/TO/FLAG/FRT-PARP-1$^{K203/486R}$	Tet-inducible over-production in mammalian cells. LR recombination between pHU1733 and pHU1802
1823	pDEST/TO/FLAG/FRT-PARP-1$^{K203/486R}$-SUMO2	Tet-inducible over-production in mammalian cells. LR recombination between pHU1743 and pHU1802
1824	pDEST/N-FLAG$_3$/FRT-PARP1	Constitutive over-production in mammalian cells. LR recombination between pHU1730 and pHU1804
1825	pDEST/N-FLAG$_3$/FRT-PARP-1$^{K203/486R}$	Constitutive over-production in mammalian cells. LR recombination between pHU1733 and pHU1804
1826	pDEST/N-FLAG$_3$/FRT-PARP-1$^{K203/486R}$-SUMO2	Constitutive over-production in mammalian cells. LR recombination between pHU1743 and pHU1804
1833	pDEST-eGFP-myc-PARP-1 WT	Constitutive over-production in mammalian cells. LR recombination between pHU1730 and pHU1806
1834	pDEST-eGFP-myc-PARP-1$^{K203/486R}$	Constitutive over-production in mammalian cells. LR recombination between pHU1733 and pHU1806
1836	pDEST-eGFP-myc-PARP-1$^{K203/486R}$-SUMO2	Constitutive over-production in mammalian cells. LR recombination between pHU1743 and pHU1806
1841	pDEST10-PARP-1	BAC-to-BAC-based bacmid cloning. LR recombination between pHU1730 and pHU1800
1842	pDEST10-PARP-1^{K203R}	BAC-to-BAC-based bacmid cloning. LR recombination between pHU1731 and pHU1800
1843	pDEST10-PARP-1^{K486R}	BAC-to-BAC-based bacmid cloning. LR recombination between pHU1732 and pHU1800
1844	pDEST10-PARP-1$^{K203/486R}$	BAC-to-BAC-based bacmid cloning. LR recombination between pHU1733 and pHU1800
1849	pDEST10-PARP-1$^{K203/486R}$-SUMO2	BAC-to-BAC-based bacmid cloning. LR recombination between pHU1743 and pHU1800
1850	pDEST10-PARP-1^{C21G}	BAC-to-BAC-based bacmid cloning. LR recombination between pHU1748 and pHU1800
1851	pDEST10-PARP-1$^{R122/138R}$	BAC-to-BAC-based bacmid cloning. LR recombination between pHU1749 and pHU1800
1852	pDEST10-PARP-1^{C298A}	BAC-to-BAC-based bacmid cloning. LR recombination between pHU1750 and pHU1800
1857	pGGWA-APLF	Over-production of GST-APLF-His$_6$ in *E. coli*. LR recombination between pHU1774 and pHU1791
1860	pGGWA-XRCC1	Over-production of GST-XRCC1-His$_6$ in *E. coli*. LR recombination between pHU1775 and pHU1791
1862	pDEST22-PARP-1	Yeast two-hybrid assay. LR recombination between pHU1730 and pHU1795
1863	pDEST22-PARP-1$^{K203/486R}$	Yeast two-hybrid assay. LR recombination between pHU1733 and pHU1795
1868	pDEST22-SUMO1-PARP-1$^{K203/486R}$	Yeast two-hybrid assay. LR recombination between pHU1740 and pHU1795
1869	pDEST22-SUMO2-PARP-1$^{K203/486R}$	Yeast two-hybrid assay. LR recombination between pHU1741 and pHU1795
1870	pDEST22-PARP-1$^{K203/486R}$-SUMO1	Yeast two-hybrid assay. LR recombination between pHU1742 and pHU1795
1871	pDEST22-PARP-1$^{K203/486R}$-	Yeast two-hybrid assay. LR recombination between

	SUMO2	pHU1743 and pHU1795
1872	pDEST22-APLF	Yeast two-hybrid assay. LR recombination between pHU1756 and pHU1795
1873	pDEST22-Aprataxin	Yeast two-hybrid assay. LR recombination between pHU1757 and pHU1795
1874	pDEST22-BCL2	Yeast two-hybrid assay. LR recombination between pHU1758 and pHU1795
1876	pDEST22-Caspase 3	Yeast two-hybrid assay. LR recombination between pHU1760 and pHU1795
1877	pDEST22-Caspase 7	Yeast two-hybrid assay. LR recombination between pHU1761 and pHU1795
1878	pDEST22-CENP-A	Yeast two-hybrid assay. LR recombination between pHU1762 and pHU1795
1879	pDEST22-CENP-B	Yeast two-hybrid assay. LR recombination between pHU1763 and pHU1795
1880	pDEST22-Ligase III	Yeast two-hybrid assay. LR recombination between pHU1764 and pHU1795
1881	pDEST22-p53	Yeast two-hybrid assay. LR recombination between pHU1765 and pHU1795
1882	pDEST22-PARP-3	Yeast two-hybrid assay. LR recombination between pHU1766 and pHU1795
1883	pDEST22-PCNA	Yeast two-hybrid assay. LR recombination between pHU1767 and pHU1795
1884	pDEST22-SUMO1	Yeast two-hybrid assay. LR recombination between pHU1768 and pHU1795
1885	pDEST22-SUMO2	Yeast two-hybrid assay. LR recombination between pHU1769 and pHU1795
1886	pDEST22-TRF2IP	Yeast two-hybrid assay. LR recombination between pHU1770 and pHU1795
1887	pDEST22-WRN	Yeast two-hybrid assay. LR recombination between pHU1771 and pHU1795
1888	pDEST22-XRCC1	Yeast two-hybrid assay. LR recombination between pHU1772 and pHU1795
1900	pDEST32-PARP1 WT	Yeast two-hybrid assay. LR recombination between pHU1730 and pHU1796
1901	pDEST32-PARP1$^{K203/486R}$	Yeast two-hybrid assay. LR recombination between pHU1733 and pHU1796
1906	pDEST32-SUMO1-PARP-1$^{K203/486R}$	Yeast two-hybrid assay. LR recombination between pHU1740 and pHU1796
1907	pDEST32-SUMO2-PARP-1$^{K203/486R}$	Yeast two-hybrid assay. LR recombination between pHU1741 and pHU1796
1908	pDEST32-PARP-1$^{K203/486R}$-SUMO1	Yeast two-hybrid assay. LR recombination between pHU1742 and pHU1796
1909	pDEST32-PARP-1$^{K203/486R}$-SUMO2	Yeast two-hybrid assay. LR recombination between pHU1743 and pHU1796
1910	pDEST32-APLF	Yeast two-hybrid assay. LR recombination between pHU1756 and pHU1796
1911	pDEST32-Aprataxin	Yeast two-hybrid assay. LR recombination between pHU1757 and pHU1796
1912	pDEST32-BCL2	Yeast two-hybrid assay. LR recombination between pHU1758 and pHU1796
1914	pDEST32-Caspase 3	Yeast two-hybrid assay. LR recombination between pHU1760 and pHU1796
1915	pDEST32-Caspase 7	Yeast two-hybrid assay. LR recombination between pHU1761 and pHU1796
1916	pDEST32-CENP-A	Yeast two-hybrid assay. LR recombination between pHU1762 and pHU1796

1917	pDEST32-Ligase III	Yeast two-hybrid assay. LR recombination between pHU1764 and pHU1796
1918	pDEST32-p53	Yeast two-hybrid assay. LR recombination between pHU1765 and pHU1796
1919	pDEST32-PARP-3	Yeast two-hybrid assay. LR recombination between pHU1766 and pHU1796
1920	pDEST32-PCNA	Yeast two-hybrid assay. LR recombination between pHU1767 and pHU1796
1921	pDEST32-SUMO1	Yeast two-hybrid assay. LR recombination between pHU1768 and pHU1796
1922	pDEST32-SUMO2	Yeast two-hybrid assay. LR recombination between pHU1769 and pHU1796
1923	pDEST32-TRF2IP	Yeast two-hybrid assay. LR recombination between pHU1770 and pHU1796
1924	pDEST32-WRN	Yeast two-hybrid assay. LR recombination between pHU1771 and pHU1796
1933	pGAD424-APLF	Yeast two-hybrid assay. LR recombination between pHU1756 and pHU1797
1934	pGAD424-XRCC1	Yeast two-hybrid assay. LR recombination between pHU1772 and pHU1797
1935	pGBT9-PARP-1 WT	Yeast two-hybrid assay. LR recombination between pHU1730 and pHU1798
1936	pGBT9-PARP-1$^{K203/486R}$	Yeast two-hybrid assay. LR recombination between pHU1733 and pHU1798
1941	pGBT9-PARP-1$^{K203/486R}$-SUMO1	Yeast two-hybrid assay. LR recombination between pHU1742 and pHU1798
1942	pGBT9-PARP-1$^{K203/486R}$-SUMO2	Yeast two-hybrid assay. LR recombination between pHU1743 and pHU1798
1943	pGBT9-PARP-1$^{M890V, D899N}$	Yeast two-hybrid assay. LR recombination between pHU1735 and pHU1798
1944	pGBT9-PARP-1$^{K203/486R, M890V, D899N}$	Yeast two-hybrid assay. LR recombination between pHU1753 and pHU1798
1945	pGBT9-PARP-1$^{K203/486R, M890V, D899N}$-SUMO1	Yeast two-hybrid assay. LR recombination between pHU1754 and pHU1798
1946	pGBT9-PARP-1$^{K203/486R, M890V, D899N}$-SUMO2	Yeast two-hybrid assay. LR recombination between pHU1755 and pHU1798
1954	pET11a-SUMO1^{T95R}	Over-production of SUMO1(T95R) in *E. coli*. Site-directed mutagenesis of pHU1238 (oHU1605/oHU1606)
2020	pCR4Blunt-^{Xl}MMS21	Reverse transcription from frog RNA (oHU896/oHU897) TOPO-cloned into pCR4Blunt-TOPO
2023	pGAD-^{Sc}ORC3	Yeast two-hybrid assay. PCR from genomic DNA (oHU1288/oHU1289) cloned SmaI/PstI into pHU145
2024	pGBT9-^{Sc}ORC3	Yeast two-hybrid assay. PCR from genomic DNA (oHU1288/oHU1289) cloned SmaI/PstI into pH82
2025	pGAD-^{Sc}ORC4	Yeast two-hybrid assay. PCR from genomic DNA (oHU1291/oHU1292) cloned SmaI/BamHI into pHU145
2026	pGBT9-^{Sc}ORC4	Yeast two-hybrid assay. PCR from genomic DNA (oHU1291/oHU1292) cloned SmaI/BamHI into pH82
2027	pGAD-^{Sc}ORC5	Yeast two-hybrid assay. PCR from genomic DNA (oHU1294/oHU1295) cloned SmaI/BamHI into pHU145
2028	pGBT9-^{Sc}ORC5	Yeast two-hybrid assay. PCR from genomic DNA (oHU1294 and oHU1295) cloned SmaI/BamHI into pH82
2029	pGAD-^{Sc}ORC6	Yeast two-hybrid assay. PCR from genomic DNA (oHU1297/oHU1298) cloned SmaI/PstI into pHU145
2030	pGBT9-^{Sc}ORC6	Yeast two-hybrid assay. PCR from genomic DNA (oHU1297/oHU1298) cloned SmaI/PstI into pH82

2031	pET15b-^{Xl}SUMO1$^{K27/36/37R}$	Over-production in *E. coli*. Site-directed mutagenesis of pHU1284 (oHU1449/oHU1450)
2032	pET21-^{Xl}SUMO2$^{K25/27/31R}$	Over-production in *E. coli*. Site-directed mutagenesis of pHU1285 (oHU1451/oHU1452)
2083	pDEST/N-FLAG$_3$/FRT-APLF	Constitutive over-production in mammalian cells. LR recombination between pHU1756 and pHU1804
2084	pDEST/N-FLAG$_3$/FRT-XRCC1	Constitutive over-production in mammalian cells. LR recombination between pHU1772 and pHU1804

Table 2.7 - A list of the plasmids that were constructed for this thesis. Sc = *S. cerevisiae*, Xl = *X. laevis*, Hs= *H. sapiens*.

2.5 Strains and cell lines

2.5.1 *Escherichia coli* strains

Name	Use	Source	Genotype
Top10	Propagation of most vectors and for DNA cloning	Invitrogen	F$^-$ *mcr*A Δ(*mrr-hsd*RMS-*mcr*BC) Φ80*lac*ZΔM15 Δ*lac*X74 *rec*A1 *ara*Δ139 Δ(*ara-leu*)7697 *gal*U *gal*K *rps*L (Str^R) *end*A1 *nup*G
DH10Bac	Production of recombinant baculovirus DNA	Invitrogen	F$^-$ *mcr*A Δ(*mrr-hsd*RMS-*mcrBC*) Φ80*lac*ZΔM15 Δ*lac*X74 *rec*A1 *end*A1 *ara*D139 Δ(*ara, leu*)7697 *gal*U *gal*K λ$^-$ *rps*L *nup*G/pMON14272/pMON7124
HB101	Propagation of pDK243 and pDK286	Douglas Koshland	F$^-$ *hsd*S20(r_B^- m_B^-) *xyl*5 λ$^-$ *rec*A13 *gal*K2 *ara*14 *sup*E44 *lac*Y1 *rps*L20(Str^R) *leu*B6 *mtl*-1 *thi*-1
ccdB Survival-T1R	Propagation of plasmids containing the *ccd*B gene	Invitrogen	F$^-$ *mcr*A Δ(*mrr-hsd*RMS-*mcrBC*) Φ80*lac*ZΔM15 Δ*lac*X74 *rec*A1 *ara*Δ139 Δ(*ara-leu*)7697 *gal*U *gal*K *rps*L (Str^R) *end*A1 *nup*G *ton*A::P_{trc}-*ccd*A
GM2163	Generation of plasmids devoid of methylation	New England Biolabs	*dam*-13::*Tn 9 dcm*-6 *hsd*R2 *leu*B6 *his*-4 *thi*-1 *ara*-14 *lac*Y1 *gal*K2 *gal*T22 *xyl*-5 *mtl*-1 *rpsL*136 *ton*A31 *tsx*-78 *sup*E44 *Mcr*A$^-$ *Mcr*B$^-$
BL21-CodonPlus (DE3)-RIL	Protein production	Stratagene	F$^-$ *omp*T *hsd*S(r_B^- m_B^-) *dcm*$^+$ Tet^R *gal* λ(DE3) *end*A Hte [*arg*U *ile*Y *leu*W Cam^R]

Table 2.8 - A list of the *E. coli* strains used in this thesis.

2.5.2 Yeast strains

All of the yeast (*S. cerevisiae*) strains used in this work were congenic with the haploid form of the wild type DF5 strain (Finley *et al.*, 1987), except for those employed for yeast two-hybrid analysis, which were derivatives of the strain PJ69-4 (James *et al.*,

1996). The introduction of an episomal plasmid in any such strains is indicated in the relevant figure legend.

#	Name	Genotype
3	DF5a	*MATa, his3-Δ200, leu2-3,2-112, lys2-801, trp1-1(am), ura3-52*
195	PJ69-4A	*MATa, trp1-901, leu2-3,112, ura3-52, his3-200, gal4Δ, gal80Δ, LYS2::GAL1-HIS3, GAL2-ADE2, met2::GAL7-lacZ*
196	PJ69-4α	*MATα, trp1-901, leu2-3,112, ura3-52, his3-200, gal4Δ, gal80Δ, LYS2::GAL1-HIS3, GAL2-ADE2, met2::GAL7-lacZ*
1630	rad53 sml1Δ bar1Δ from Adelina Davies	*MATα, his3-Δ200, leu2-3,2-112, lys2-801, trp1-1(am), ura3-52, sml1::hisG-URA3-hisG, bar1::HISMX6, rad53::KanMX*
2198	Orc1-9myc	*MATa, his3-Δ200, leu2-3,2-112, lys2-801, trp1-1(am), ura3-52, orc1-9myc::klTRP1*
2199	Orc2-9myc	*MATa, his3-Δ200, leu2-3,2-112, lys2-801, trp1-1(am), ura3-52, orc2-9myc::klTRP1*
2200	Orc3-9myc	*MATa, his3-Δ200, leu2-3,2-112, lys2-801, trp1-1(am), ura3-52, orc3-9myc::klTRP1*
2201	Orc4-9myc	*MATa, his3-Δ200, leu2-3,2-112, lys2-801, trp1-1(am), ura3-52, orc4-9myc::klTRP1*
2202	Orc5-9myc	*MATa, his3-Δ200, leu2-3,2-112, lys2-801, trp1-1(am), ura3-52, orc5-9myc::klTRP1*
2203	Orc6-9myc	*MATa, his3-Δ200, leu2-3,2-112, lys2-801, trp1-1(am), ura3-52, orc6-9myc::klTRP1*
2204	Rfc1-9myc	*MATa, his3-Δ200, leu2-3,2-112, lys2-801, trp1-1(am), ura3-52, rfc1-9myc::klTRP1*
2205	Rad54-9myc	*MATa, his3-Δ200, leu2-3,2-112, lys2-801, trp1-1(am), ura3-52, rad54-9myc::klTRP1*
2206	Pol1-9myc	*MATa, his3-Δ200, leu2-3,2-112, lys2-801, trp1-1(am), ura3-52, pol1-9myc::klTRP1*
2210	siz1Δ siz2Δ from Andrea Bucceri	*MATα, his3-Δ200, leu2-3,2-112, lys2-801, trp1-1(am), ura3-52, siz1::KanMX6, siz2::HIS3 MX6*
2219	DF5a cir^0	*MATa, his3-Δ200, leu2-3,2-112, lys2-801, trp1-1(am), ura3-52, cir^0*
2220	siz1Δ siz2Δ cir^0	*MATα, his3-Δ200, leu2-3,2-112, lys2-801, trp1-1(am), ura3-52, siz1::KanMX6, siz2::HIS3 MX6, cir^0*
2564	Orc5-9myc siz1Δ	*MATa, his3-Δ200, leu2-3,2-112, lys2-801, trp1-1(am), ura3-52, orc5-9myc::klTRP1, siz1::KanMX*
2565	Orc5-9myc siz2Δ	*MATa, his3-Δ200, leu2-3,2-112, lys2-801, trp1-1(am), ura3-52, orc5-9myc::klTRP1, siz2::HIS3*
2566	Orc5-9myc siz1Δ siz2Δ	*MATa, his3-Δ200, leu2-3,2-112, lys2-801, trp1-1(am), ura3-52, orc5-9myc::klTRP1, siz1::KanMX, siz2::HIS3*
2567	Orc6-9myc siz1Δ	*MATa, his3-Δ200, leu2-3,2-112, lys2-801, trp1-1(am), ura3-52, orc6-9myc::klTRP1, siz1::KanMX*
2568	Orc6-9myc siz2Δ	*MATa, his3-Δ200, leu2-3,2-112, lys2-801, trp1-1(am), ura3-52, orc6-9myc::klTRP1, siz2::HIS3*
2569	Orc6-9myc siz1Δ siz2Δ	*MATa, his3-Δ200, leu2-3,2-112, lys2-801, trp1-1(am), ura3-52, orc6-9myc::klTRP1, siz1::KanMX, siz2::HIS3*
2570	Orc5-9myc rad53Δ sml1Δ	*MATa, his3-Δ200, leu2-3,2-112, lys2-801, trp1-1(am), ura3-52, orc5-9myc::klTRP1, sml1::hisG-URA3-hisG, rad53::KanMX*

Table 2.9 - A list of the yeast strains used in this thesis.

2.5.3 Insect cell lines

Spodoptera frugiperda (Sf9) and *Trichoplusia ni* (Hi5) cells were maintained and propagated by the London Research Institute's Cell Production Services by standard culturing practices, as described by Richardson (1995).

2.5.4 Human cell lines

All cell lines were obtained from the London Research Institute's Cell Production Services who stored, propagated and regularly tested them for mycoplasma infection. All cells were maintained as monolayers and grown in a humidified incubator at 37°C and 5% v/v CO_2.

Cell line	Source	Antibiotics
Flp-In HEK293	Invitrogen	100 $\mu g \cdot mL^{-1}$ zeocin
HEK293	ATCC	
HeLa	ATCC	
Flp-In T-Rex HEK293	Invitrogen	100 $\mu g \cdot mL^{-1}$ zeocin 15 $\mu g \cdot mL^{-1}$ blasticidin
T-Rex HeLa + pcDNA4/TO/N-MRGS His_6-PrSUMO1	Gerrit Praefcke, Weisshaar *et al.* (2008)	150 $\mu g \cdot mL^{-1}$ zeocin 5 $\mu g \cdot mL^{-1}$ blasticidin
T-Rex HeLa + pcDNA4/TO/N-MRGS His_6-PrSUMO2		
T-Rex HeLa + pcDNA4/TO/N-MRGS His_6-PrSUMO3		
Flp-In T-Rex HEK293 + pDEST/TO/FLAG/FRT	Simon Boulton	150 $\mu g \cdot mL^{-1}$ hygromycin B 15 $\mu g \cdot mL^{-1}$ blasticidin
Flp-In T-Rex HEK293 + pDEST/TO/FLAG/FRT-PARP-1	This thesis	150 $\mu g \cdot mL^{-1}$ hygromycin B 15 $\mu g \cdot mL^{-1}$ blasticidin
Flp-In T-Rex HEK293 + pDEST/TO/FLAG/FRT-PARP-1$^{K203/486R}$		
Flp-In T-Rex HEK293 + pDEST/TO/FLAG/FRT-PARP-1$^{K203/486R}$-SUMO2		
Flp-In HEK293 + pDEST/N-$FLAG_3$/FRT-APLF	This thesis	150 $\mu g \cdot mL^{-1}$ hygromycin B
Flp-In HEK293 + pDEST/N-$FLAG_3$/FRT-XRCC1		
Flp-In HEK293 + pDEST/N-$FLAG_3$/FRT	Stephen West	150 $\mu g \cdot mL^{-1}$ hygromycin B

PARP-1$^{-/-}$ mouse embryonic fibroblast clone A11	Zhao-Qi Wang, Wang *et al.* (1997)	

Table 2.10 - A list of the mammalian cell lines used in this thesis.

2.6 Molecular biology methods for *E. coli*

2.6.1 Preparation of chemically-competent cells

A fresh overnight culture of *E. coli* was diluted 100-fold in LB medium, grown at 37°C to an OD_{600} of 0.5 to 0.8, chilled on ice for 15 min and then harvested at 4°C by centrifugation at 4,000 *g* for 15 min. The pellets were washed once in TfbI solution (×0.4 of the original culture volume) and once in TfbII solution (×0.04 of original volume) for 15 min each time. The cell suspension was distributed into 100 µL aliquots, flash-frozen and stored at -80°C.

2.6.2 Transformation of chemically-competent cells

Aliquots of chemically-competent cells were thawed on ice, mixed with DNA and incubated on ice for 10 min. Next, the cells were heat-shocked at 42°C for 1 min, put back on ice and resuspended with 1 mL of LB medium. When ampicillin was used as the selective antibiotic, the cells were immediately harvested by centrifugation at 3,000 *g*, resuspended in 100 µL of LB medium and then plated on LB agar plates supplemented with ampicillin. Otherwise, they were incubated at 37°C for 1 h before being plated as described above.

If HB101 cells were transformed with pDK243 or pDK368-7, they were incubated for 3 h at 37°C before being plated on M9 medium lacking leucine.

2.6.3 Isolation of plasmid DNA

Isolated clones of *E. coli* were inoculated in LB medium containing the relevant antibiotic. The cultures were grown overnight at 37°C with shaking and then used for plasmid isolation using Qiagen's plasmid purification kits according to the manufacturer's instructions.

2.7 Molecular biology methods for *X. laevis* egg extracts

2.7.1 Preparation of interphase egg extracts

X. laevis mature females were housed at 18°C in dechlorinated tap water at a density of one frog per litre. One week and eighteen hours prior to egg collection the frogs were primed with 50 units of pregnant mare serum gonadotrophin and 500 units of human chorionic gonadotrophin, respectively. Eggs were collected overnight in laying tanks containing 0.25× MMR buffer and subsequently transferred to a beaker. Hiro Mahbubani carried out these initial steps. “Bad” eggs (*i.e.* grey, white, spotted, unusually large, etc.) were removed with a large-tip pastette. The remaining eggs were de-jellied at room temperature for 5 min in De-jellying buffer supplemented with 5 mM DTT, washed 3 times in 0.25× MMR buffer, activated with 2 µL of 10 $mg \cdot mL^{-1}$ A23187 (Merck) for 5 min at room temperature, washed again 3 times in 0.25× MMR buffer and then 3 times with ice-cold S buffer supplemented with 2 mM β-ME and 10 $\mu g \cdot mL^{-1}$ of each of leupeptin, pepstatin and chymostatin. The eggs were packed by briefly centrifuging them up to 4,000 *g* in chilled 1.5 mL tubes and then removing the excess of liquid with a fine-tip pastette. Spinning the eggs at 16,000 *g* for 15 min at 4°C yielded a crude cytoplasmic extract, which was supplemented with 40 $\mu g \cdot mL^{-1}$ cytochalasin B (Merck), transferred to 1.5 mL polyallomer tubes (Beckman) and then centrifuged again at 250,000 *g* for 15 min at 4°C in a TLA100.3 rotor fitted to a table-top TL-100 TLX ultracentrifuge (Beckman). The cleared cytoplasmic and membrane phases were collected by pipetting with a severed 200 µL tip, leaving behind all the lipid and mitochondrial layers. The resulting extract was supplemented with 30 mM creatine phosphate (Merck), 150 $\mu g \cdot mL^{-1}$ phospho-creatine kinase (Roche) and 10 $\mu g \cdot mL^{-1}$ cycloheximide, and either used fresh or supplemented with glycerol to a final concentration of 3% v/v before being flash-frozen in liquid nitrogen in the form of 22 µL beads. These extracts were stored in liquid nitrogen.

2.7.2 Preparation of demembranated *X. laevis* sperm nuclei

X. laevis mature males were housed at 18°C in dechlorinated tap water at a density of one frog per litre. One week before the testes had to be removed the frogs were primed with 50 units of pregnant mare serum gonadotrophin. On the day of testes removal, the animals were anesthetized in 0.1% v/v tricaine and sacrificed by cervical dislocation. The testes were dissected out of the frog and cleaned of excess blood and fat with dissection forceps. Hiro Mahbubani carried out these initial steps. The clean testes

were transferred to a Petri dish containing 20 mL of ice-cold EB buffer, finely chopped and homogenized with a dounce homogenizer. The homogenate was filtered through a 25-µm mesh nylon membrane (Nitex) and then spun at 2,000 *g* in a swing out rotor for 5 min at 4°C. The pellet was resuspended in 2 mL of SuNaSp buffer kept at room temperature. Nuclei were incubated with lysolecithin to a final concentration of 100 $\mu g \cdot mL^{-1}$ until when more than 95% of nuclei had been demembranated, as judged by Hoechst 33258 staining. Quenching of lysolecithin was accomplished by the addition of 2 mL of ice-cold SuNaSp buffer containing 3% w/v BSA. The sperm nuclei were washed twice by sequential centrifugation (2,000 *g* for 5 min in a swing out rotor) and resuspension in ice-cold SuNaSp buffer supplemented with 3% w/v BSA, resuspended in 400-500 µl of EB buffer supplemented with glycerol to a final concentration of 30% v/v, flash-frozen and stored at -80°C. The sperm count of these preparations was determined by means of a haemocytometer.

2.7.3 Handling of interphase egg extracts

Unless otherwise stated in the relevant figure legend, interphase extracts were always supplemented with 2,000-3,000 sperm nuclei$\cdot \mu L^{-1}$ of extract and incubated at 23°C with gentle mixing by pipetting every 10-15 min to avoid clumping of the DNA.

2.7.4 Testing the replication competence of interphase frog egg extracts

The ability of interphase egg extracts to replicate was assessed by supplementing them (20 µL) with 2,500 sperm nuclei$\cdot \mu L^{-1}$ of extract and 20 pmol of Cy3-dCTP (Invitrogen). Following incubation at 23°C for 30 min, 1 µl of extract was mixed with 1 µL of Fixation buffer and analyzed by fluorescence microscopy. Only extracts that showed properly condensed nuclei and a strong nuclear Cy3 signal were used for downstream applications.

2.7.5 DNA replication assay

The extent of DNA replication was determined by measuring the incorporation of [α-^{32}P]dCMP (GE Healthcare) into sperm DNA as described by Dasso and Newport (1990). 20 µl of extract was supplemented with 2,500 sperm nuclei$\cdot \mu L^{-1}$ of extract and ~ 1 µCi of [α-^{32}P]dCTP, and incubated at 23°C. After the desired amount of time, 5 µL of extract was mixed with 5 µL of STOP buffer, supplemented with proteinase K to a final concentration of 2 $\mu g \cdot \mu L^{-1}$, incubated at 37°C for 2 h, and then loaded on a 1% w/v agarose gel made in 1× TBE buffer (see 2.11.2). This gel was run at 100 V until when

the dye front had migrated approximately $^2/_3$ of its total length. Next it was fixed in 30% w/v TCA for 30 min, dried in a gel dryer (Bio-Rad) and exposed to a storage phosphor screen (GE Healthcare). The screen was imaged on a Typhoon 9400 scanner using the ImageQuant TL software (GE healthcare).

2.7.6 Chromatin binding assay

Extracts (50 µL) were mixed with 250 µL ice-cold ELB buffer supplemented with 0.25 M sucrose and 1 mM DTT, layered on top of a 1 ml sucrose cushion (0.9 M sucrose in ELB buffer) and centrifuged at 10,000 *g* for 2 min at 4°C in a swing out rotor. After aspirating all but 50-100 µL of the supernatant the "pellet" was mixed with 200 µL of ELB buffer supplemented with 0.25 M sucrose, 0.6% v/v Triton X-100 and 1 mM DTT. This sample was layered on top of a second 1 mL sucrose cushion and treated as described above. All but 10 µL of the supernatant was removed by aspiration and it was used either as native chromatin or mixed with 40 µL of 1.5× NuPAGE LDS Sample Buffer (Invitrogen). Smaller or larger chromatin preparations were carried out by scaling up or down this basic procedure.

2.8 Molecular biology and genetic methods for yeast

2.8.1 Chemical transformation of yeast cells

For a single transformation, 3 OD_{600} equivalents of exponentially growing yeast cells were harvested by centrifugation at 800 *g* for 3 min, resuspended in 100 µL of LiT buffer, transferred to a 1.5 mL tube, supplemented with 10 µL of HT DNA solution and the relevant transforming DNA (100-400 ng of plasmid or 5-10 µg of an integrative cassette), and mixed. Following the addition of 500 µL LiT/PEG solution, the cells were vortexed and incubated at room temperature for 20 min with rotation. Next, they were supplemented with 50 µL of DMSO, mixed and heat-shocked at 42°C for 15 min. The cells were eventually collected by centrifugation at 800 *g* for 30 s, resuspended in 100 µL of water and plated on the relevant selective medium.

2.8.2 Induction of His_6-SUMO production

Transformants (a pool of three isolated colonies) obtained by chemical transformation of pHU822 into the relevant strains were grown to saturation in medium lacking leucine and then switched to an equivalent broth containing 100 µM $CuSO_4$ as well, to induce production of His_6-SUMO from the *CUP1* copper inducible promoter. After an overnight

incubation, the cells were diluted to an OD_{600} of 0.2-0.3 in selective medium supplemented with 100 µM $CuSO_4$ and subsequently grown to exponential phase.

2.8.3 Colony PCR

A minute amount of cells was collected from isolated colonies by means of a 10 µL tip, transferred to PCR tubes that contained 50 µL of freshly prepared Zymolyase solution, and then incubated for 15 min at room temperature. The resulting spheroblasts were collected by centrifugation in a Rotilabo microcentrifuge fitted with a butterfly-rotor (Roth) for 5 min. After the supernatant had been removed, the pellets were boiled at 95°C for 5 min, resuspended in a PCR reaction mix and subjected to PCR amplification (see 2.12.1).

2.8.4 Preparation of total yeast cell extracts

2.8.4.1 Alkaline lysis method

Exponentially growing yeast cells (1 OD_{600} equivalent) were washed once in water and then resuspended in 500 µL of ice-cold water supplemented with 75 µL NaOH/β−ME solution. After 15 min on ice, the lysate was mixed with 75 µL of 55% w/v TCA and incubated for an additional 10 min. The precipitates were collected by centrifugation at 16,000 *g* for 10 min at 4°C. After removing most of the supernatant by aspiration, the pellets were centrifuged again for 30 s to get rid of any remaining traces of it, resuspended in 50 µL of HU buffer and incubated at 65°C for 15 min.

2.8.4.2 Mechanical lysis method

Exponentially growing yeast cells (40-50 OD_{600} equivalents) were washed once in water, resuspended in 500-600 µL of the appropriate lysis buffer and then mixed with 500-600 µL of zirconia/silica beads (Thistle Scientific) in a 1.5 mL screw-cap tube. Lysis was brought about by ultra-vortexing in a FastPrep-24 instrument (MP Biomedicals) with eight 30 s pulses at 5.5 $m \cdot s^{-1}$, and 1 min rest time on ice. This crude lysate was cleared of beads by puncturing the bottom of the tube containing it with a white-hot needle and then spinning it up to 1,500 *g* into a 2 mL collection tube. Next, it was sonicated in a Branson Sonifier with five 10 s pulses at 20% power and 1 min rest time on ice and then cleared by centrifugation at 100,000 *g* and 4°C for 15 min in a table-top TL-100 TLX ultracentrifuge fitted with a TLA100.3 rotor (Beckman). The resulting extract was used for the desired downstream applications.

2.8.5 Cell synchronization and cell cycle analysis

Exponentially growing *MATa* cells (OD_{600} ~ 0.7) were arrested at the G_1 phase by incubating them for 1.5 h at 30°C with 10 $\mu g \cdot mL^{-1}$ of α factor, and then one more hour with an additional 5 $\mu g \cdot mL^{-1}$. To release the cells from this G_1-phase block, they were washed twice in a solution of 1M sorbitol and 25 mM EDTA, before being resuspended in the appropriate growth medium, which was supplemented with either 200 mM HU or 15 $\mu g \cdot mL^{-1}$ nocodazole to stop the cells in either S or G_2 phase, respectively. Cells were collected at the time indicated in the relevant figure legend, immediately killed by the addition of 1 $mg \cdot mL^{-1}$ sodium azide to the medium and then harvested by centrifugation.

2.8.6 Flow cytometry

Approximately 1 OD_{600} equivalent of cells was washed once in ice-cold water and fixed in 70% v/v ethanol for 1 h at 4°C. The pellets were washed twice in 50 mM Citrate buffer pH 7.0, resuspended in 1 mL of the same solution containing 250 µg of RNase A and incubated for 1 h at 50°C. Next, they were supplemented with proteinase K (3,000 U), incubated for an additional 1 h at 50°C and then sonicated on a Branson sonifier for 1-2 s at 10% power. Finally, the cell suspensions (250 µL) were mixed with 1 mL of Propidium Iodide Stock solution and analyzed on a FACSCalibur flow cytometer using the FACStation software (BD Biosciences, FSC-H threshold = 10, P1 (FSC) = E01, P2 (SSC) = default, P4 = 830).

2.8.7 Elimination of the 2-µm plasmid

Cells were cured of the 2-µm plasmid as described by Tsalik and Gartenberg (1998). In summary, the relevant wild type or mutant cells were chemically transformed with pBIS-GALkFLP(URA3). Transformants were selected by growth on plates lacking uracil and then re-streaked on galactose-containing medium to induce the production of $Flp1^{H305L}$ from pBIS-GALkFLP(URA3). This mutant Flp1 protein forms stable covalent complexes with the 2-µm circle, thus causing it to be lost from cells at very high frequencies. Single colonies from these plates were streaked on 5-FOA medium to obtain clones that had been cured of pBIS-GALkFLP(URA3) as well the 2-µm plasmid, which was confirmed by colony PCR (see 2.8.3) using oligonucleotides oHU1299 and oHU1300.

2.8.8 Plasmid stability assay

The mitotic loss rate of pDK243 and pDK368-7 was measured as previously described by Marahrens and Stillman (1992). The plasmids were transformed into the desired strains by chemical transformation (see 2.8.1). Transformants were selected on medium lacking leucine and individually inoculated in ~ 3 mL of selective broth. After 30 h at 30°C, the cultures were diluted to an OD_{600} of 0.0003 in liquid YPD medium and grown for an additional 30 h at 30°C. The resulting cultures were plated in triplicate on both YPD agar and selective medium lacking leucine at a dilution that produced 200-300 colonies on the YPD plates.

2.8.9 Yeast two-hybrid analysis

Yeast plasmids carrying the *GAL4* activation (AD) or DNA-binding (BD) domain fused to relevant genes were chemically transformed into the reporter strains PJ69-4A (*MATa*) and PJ69-4α (*MATα*), respectively. Since the strains carrying the *GAL4* AD and BD domain-fusion proteins were of different mating types, mixing them together yielded diploid cells carrying both plasmids. A loopful of transformants (10-20 medium-sized colonies) was resuspended in 100 µL of liquid YPD medium, mixed together in the relevant combinations and then spotted (3.5 µL) on solid YPD medium. Following an overnight incubation at 30°C, the cells were replicated onto medium lacking tryptophan and leucine, and grown for an additional 24 h at 30°C. Approximately 1-2 mm^3 of the cells that grew on such selective plates were inoculated in 100 µL of water and then plated (3.5 µL) on medium lacking different amino acids. The presence of both the *GAL4* AD and BD plasmids was confirmed by growth on plates lacking leucine and tryptophan. Positive interactions were determined by growth on plates lacking leucine, tryptophan and histidine, whereas stronger interactions were detected on plates lacking adenine as well.

2.8.10 Construction of mutants by mating and tetrad dissection

Fresh colonies or liquid cultures of the relevant haploid mutant strains of opposite mating types were mixed, spotted on YPD agar and incubated for 3-5 h at 30 °C. Next, zygotes were picked using a MSM micromanipulator (Singer), allowed to grow for 2 days at 30°C, resuspended in 1 mL of 1% w/v KOAc and then incubated for an additional 2-3 days at 30°C with shaking. The cell suspension (10 µL) was combined with 10 µL of STE-Zymolyase solution, incubated at room temperature for 15 min and then streaked on YPD agar. Tetrads were dissected using a MSM micromanipulator.

By testing the ability of the germinated spores to grow on certain selective media, those carrying the desired set of markers/mutations were identified.

2.9 Molecular biology methods for insect cells and baculoviruses

2.9.1 Generation of recombinant bacmids

Invitrogen's BAC-to-BAC system was used to generate recombinant bacmids as described by the manufacturer. In summary, chemically-competent DH10Bac *E. coli* cells (Invitrogen) were transformed with 100-400 ng of pDEST10 vector carrying the relevant PARP-1 construct and then plated on LB agar supplemented with 50 $\mu g \cdot mL^{-1}$ kanamycin, 7 $\mu g \cdot mL^{-1}$ gentamycin, 10 $\mu g \cdot mL^{-1}$ tetracycline, 100 $\mu g \cdot mL^{-1}$ BluO-gal (Invitrogen) and 40 $\mu g \cdot mL^{-1}$ IPTG. After incubating the plates for 2 days at 37°C, successful transposition of the pDEST10 vectors into the bacmid DNA carried by the DH10Bac strain resulted in white, rather than blue, colonies due to disruption of the *lacZ* gene present in such a DNA. These colonies were re-streaked on fresh LB agar plates containing the same supplements as those described above to obtain isolated clones, which were then inoculated in 200 mL of liquid LB medium supplemented with 50 $\mu g \cdot mL^{-1}$ kanamycin, 7 $\mu g \cdot mL^{-1}$ gentamycin and 10 $\mu g \cdot mL^{-1}$ tetracycline, and grown overnight at 37°C. The recombinant baculovirus DNA was isolated using Qiagen's Plasmid MIDI Kit following the manufacturer's instructions. To confirm integration of the PARP-1 gene into the recombinant bacmid, PCR amplification (see 2.12.1) was employed using a primer annealing to the bacmid itself (M13 forward -20, Invitrogen) and one to the 5' end of the PARP-1 gene (oHU1482). Positive clones generated a product of ~2.5 kbp.

2.9.2 Generation of the P_0 baculovirus stocks

Approximately $6 \cdot 10^6$ exponentially growing Sf9 cells were seeded into a 100 mm ∅ dish and allowed to adhere for 1 h. For each transfection, 45 µL of Cellfectin II (Invitrogen) and 6 µg of DNA were diluted in 0.5 mL of plain Grace's medium. The diluted DNA and Cellfectin II were combined, mixed gently, and incubated for 20 min at room temperature. In the meanwhile, the cells were washed once with plain Grace's medium and supplemented with 5 mL of the same medium. DNA-lipid complexes were added to the plates drop-wise and allowed to be taken up by the cells for 5 h before replacing the transfection mixture with 10 mL of Grace's medium supplemented with

10% v/v heat-inactivated foetal bovine serum, 50 $\mu g \cdot mL^{-1}$ gentamycin and 250 $ng \cdot mL^{-1}$ amphotericin B. After incubating the cells for 4 days at 27°C to allow accumulation of the virus in the culture medium, the cells' supernatant was collected, centrifuged at 2,000 *g* for 5 min, filtered through a low-protein binding 0.22-µm PES filter (Millipore), and stored away from light at 4°C in a plastic container. The titre of this P_0 virus stock was assumed to be $1 \cdot 10^6$ $pfu \cdot mL^{-1}$.

2.9.3 Amplification of the P_0 virus stocks

About 1.5 ml of a P_0 virus stock was added to $1.8 \cdot 10^7$ exponentially growing Sf9 cells seeded in 150 mm ∅ plates in a total volume of 30 mL of complete Grace's medium. After 3 days at 27°C, the budded viruses were collected as described in 2.9.1 and used for either further virus amplification or for protein production. The titre of this P_1 stock was estimated by the end-point dilution assay. Briefly, $1 \cdot 10^6$ exponentially growing Hi5 cells were seeded in each well of a 6-well plate in 2 mL of complete Grace's medium. 100, 10, 1 or 0 µL of the virus stock was added to each well, in duplicate. Often, 10 µL of virus supernatant was sufficient to produce a synchronous infection (*i.e.* uniformly large cells), after a 2-day incubation at 27°C. The titre of this P_1 stock was therefore estimated to be approximately $1\text{-}5 \cdot 10^8$ $pfu \cdot mL^{-1}$.

2.10 Molecular biology methods for human cells

2.10.1 Passaging and harvesting cells

Cells were passaged when sub-confluent, or every 3-4 days, by incubating them with 0.2 mL per 10 cm^2 of Trypsin/Versene solution for 2-3 min. Upon cell detachment, trypsin was neutralized by adding a two-fold volume excess of complete DMEM. The resulting cell suspension was inoculated into a new flask at a dilution ratio of between 1:8 and 1:15 or subjected to centrifugation at 200 *g* for 5 min to harvest the cells. Alternatively, harvesting was achieved by gently scraping a cell monolayer that had been rinsed in ice-cold PBS with a rubber policeman.

2.10.2 Cell counting

The cell count of cell suspensions prepared by trypsinization as described in 2.10.1 was determined with a Countess Automated Cell Counter (Invitrogen), using default parameters and following the manufacturer's instructions.

2.10.3 Total cell extracts for western blotting analysis

Usually, 5-10 µL of cells was resuspended in 50-150 µL of a solution of 8 M urea and 100 mM Tris-HCl pH 6.8. The lysate was sonicated for 2-3 s on a Branson sonifier at 10% power, analyzed by the Bradford assay (2.13.4.3) and adjusted to 1.5 µg of protein per µL of extract. Next, the extracts were mixed at a 3:1 ratio with 3× NuPAGE LDS Sample Buffer supplemented with a reducing agent and incubated at 65°C for 15 min. Generally, 5-15 µL were loaded onto a gel for western blotting analysis.

2.10.4 Transient transfection

Cells were transfected with either Lipofectamine 2000 (Invitrogen) or Fugene HD (Roche) according the manufacturer's instructions, using OptiMEM I reduced-serum medium (Invitrogen) as a dilution agent. The exact cell confluency, amounts of DNA and transfection reagent and post-transfection harvesting time used for each transfection are indicated in the relevant figure legend.

2.10.5 Stable transfection

Invitrogen's Flp-In system was used to generate clones of the Flp-In 293 and Flp-In T-Rex 293 cells lines that were stably integrated with the relevant expression plasmid, according to the manufacturer's manual. The cells were grown in 60 mm ∅ dishes to 90% confluence and co-transfected with pHU1809 (0.5 µg, Invitrogen) and the relevant Flp-In-compatible expression plasmid (3.5 µg) using Fugene HD (16 µL), as described in 2.10.4. After 24 h, the cells were transferred to a 150 mm ∅ plate containing complete DMEM supplemented with 200 $\mu g \cdot mL^{-1}$ hygromycin B and, when appropriate, 15 $\mu g \cdot mL^{-1}$ blasticidin. After a week, isolated colonies were handpicked, individually grown in 6-well plates and then tested for transgene expression by western blotting (see 2.13.5). Three clones that produced similar levels of the relevant recombinant protein were pooled together and submitted to the London Research Institute's Cell Production Services for maintenance, mycoplasma testing and storage.

2.10.6 Indirect immunofluorescence

For localization studies, cells were handled in 8-well CultureSlides (BD Biosciences). The cells were fixed in 4% v/v paraformaldehyde in PBS for 10 min, washed in PBS-Tx for 2 min, permeabilized in PBS supplemented with 0.5 % Triton X-100 for 3 min, and then washed twice more in PBS-Tx for 5 min. The slides were blocked for 1 h at room temperature in 3% w/v BSA in PBS and then washed once in PBS-Tx for 5 min. Next,

100 µL of PBS-Tx supplemented with 0.3% w/v BSA and the relevant primary antibodies (**Table 2.2**) was added to each well of the slide. Following an overnight incubation at 4°C in a humid chamber, the slides were washed three times for 5 min in PBS-Tx before being incubated with the appropriate secondary antibodies (**Table 2.3**) in 100 µL of PBS-Tx supplemented with 0.3% w/v BSA and 0.1 $\mu g \cdot mL^{-1}$ DAPI. At last, the cells were washed in PBS-Tx four more times for 5 min and then mounted with 10 µL of ProLong Gold Antifade Reagent (Invitrogen). Images were captured at multiple Z-sections using the Volocity 4.3.2 software (Improvision) on a Zeiss Axio Imager M1 microscope fitted with a Plan APOCHROMAT 100×/1.4 oil objective (Zeiss) and attached to an ORCA-ER camera (Hamamatsu).

2.10.7 Cellular fractionation

Cellular fractionation analysis was carried out by Rajvee Shah. Cells harvested from a confluent 35 mm ∅ dish were washed once in PBS and then resuspend in 1 mL of ice-cold PBS. The resulting cell suspension (100 µL) was mixed with 100 µL of 2× NuPAGE LDS Sample Buffer supplemented with a reducing agent and immediately boiled at 95°C for 5 min ("Input" sample). The cells present in the remaining 900 µL of the suspension were collected by centrifugations (200 *g* for 5 min), resuspended in 180 µL of Cell fractionation buffer A, supplemented with Triton X-100 to a final concentration of 0.1% v/v, mixed by inversion and incubated on ice for 5 min in order to dissolve the plasma membrane. The nuclei were precipitated by centrifugation at 1,300 *g* for 5 min at 4°C. The resulting supernatant was clarified at 16,000 *g* for 15 min at 4°C, 100 µL of it was mixed with 100 µL of 2× NuPAGE LDS Sample Buffer supplemented with a reducing agent before being boiled at 95°C for 5 min ("Cytoplasm" sample). The pellet was washed once in 200 µL of Cell fractionation buffer A, gently resuspended in 180 µL of Cell fractionation buffer B, incubated on ice for 30 min to lyse the nuclei and then centrifuged at 1,700 *g* for 5 min at 4°C to precipitate the chromatin. The resulting supernatant (100 µL) was mixed with 100 µL of 2× NuPAGE LDS Sample Buffer supplemented with a reducing agent and immediately boiled at 95°C for 5 min ("Nucleoplasm" sample). The pellet was instead washed once with 200 µL of Cell fractionation buffer B, resuspended in 200 µL of 2× NuPAGE LDS Sample Buffer supplemented with a reducing agent and immediately boiled at 95°C for 5 min ("Chromatin" sample). All samples (15 µL) were subjected to western blotting analysis as described in 2.13.5.

2.10.8 Preparation of extracts from *PARP-1*$^{-/-}$ mouse embryonic fibroblasts

Cell extracts from *PARP-1*$^{-/-}$ mouse embryonic fibroblasts were prepared exactly as described by Vodenicharov *et al.* (2000).

2.10.9 Cycloheximide chase experiment

The relevant stably-transfected clones of FLP-In T-Rex 293 cells (~$5 \cdot 10^5$ cells) were seeded in 60 mm ∅ plates. After 24 h, the medium was supplemented with 1 $\mu g \cdot mL^{-1}$ doxycycline and incubated for an additional 24 h. Next, the cells were washed in PBS and supplemented with complete DMEM containing 50 $\mu g \cdot mL^{-1}$ cycloheximide with or without 30 μM MG132. Cells were harvested at the relevant times by scraping, and processed for western blotting analysis (see 2.13.5).

2.11 General methods for DNA manipulation

2.11.1 Determination of DNA concentration

The concentration of ssDNA or dsDNA in solution was determined by measuring the OD_{260} on a Nanodrop ND-1000 spectrophotometer (Thermo Scientific) and making the assumption that a solution of 33 $\mu g \cdot mL^{-1}$ ssDNA or 50 $\mu g \cdot mL^{-1}$ dsDNA would yield an absorbance of 1 at 260 nm.

2.11.2 Native agarose gel electrophoresis

Agarose gels contained 0.5-2% w/v UltraPure agarose (Invitrogen) in 1× TAE or 1× TBE buffers. DNA samples were mixed at 5:1 ratio with 6× DNA Loading buffer and run at 80 V (~ 5 $V \cdot cm^{-1}$) in a Jencons Scientific horizontal gel electrophoresis apparatus. New England Biolabs' 100 bp and 1 kbp DNA ladders were used as size standards.

2.11.3 Native and denaturing PAGE

Native (1× TBE) or denaturing (8 M urea in 1× TBE) polyacrylamide gels were prepared using Invitrogen's X-Cell SureLock Mini-Cells as described by Sambrook and Russell (2001). DNA samples were mixed at a 5:1 ratio either with 6× DNA Loading buffer, for native PAGE, or 100% v/v formamide and incubated at 65°C for 10 min, for denaturing PAGE, and then run in 1× TBE buffer at 80 V for 2.5 h.

2.12 General methods for molecular cloning

2.12.1 Polymerase chain reaction (PCR)

DNA products were generated with Phusion DNA polymerase (Finnzymes), according to the manufacturer's manual, typically using 1 pmol of template and the following thermal cycling protocol: an initial denaturing step at 98°C for 1 min and then 30 cycles of 98°C for 20 s, 50-65°C (depending on the melting temperature of the oligonucleotides employed) for 20 s and 72°C for 20 s·kbp^{-1}. A final 5 min incubation at 72°C was included in order to polish the ends of the resulting PCR products. All PCR reactions were performed in a DYAD Thermal Cycler (MJ Research).

2.12.2 Site-directed mutagenesis

Site-directed mutagenesis was carried out using the same procedure as that described in Stratagene's QuikChange II Site-Directed Mutagenesis Kit with the only difference that Phusion DNA polymerase (Finnzymes) was used instead of *Pfu* DNA polymerase.

2.12.3 Cut-and-paste cloning

For a typical cut-and-paste cloning procedure 1-2 µg of plasmid or PCR product was digested for 3 h in a 50 µL reaction supplemented with 20-30 U of the relevant restriction endonuclease and the corresponding reaction buffer. Whenever needed, 1 µL of calf intestinal phosphatase was added to the reaction during the last hour of incubation. The products were resolved by agarose gel electrophoresis (see 2.11.2) and extracted using the JETSORB Gel Extraction kit (Genomed) according to the manufacturer's instructions. Ligation reactions were performed using 25 ng of vector DNA and a 3-fold molar excess of insert in total volume of 10 µL supplemented with 0.5 µL of QuickStick ligase and 2.5 µL of 4× QuickStick buffer (Bioline) for 15 min at 25°C.

2.12.4 TOPO cloning

Blunt PCR products were cloned into pCR-Blunt II-TOPO or pENTR/D-TOPO (Invitrogen) following the manufacturer's instructions. For cloning into the TA-based cloning vector pCR8/GW/TOPO (Invitrogen), 3' "A overhangs" had to be added to the PCR products generated by Phusion DNA polymerase. In order to do so, these DNA fragments were resolved by agarose gel electrophoresis (see 2.11.2), purified from the gel using JETSORB Gel Extraction kit and then incubated (1 pmol) at 72°C for 30 with 0.2 mM dATP, 1× *Taq* polymerase buffer (Thermo Scientific), 2 U of *Taq* DNA

polymerase (Thermo Scientific) in a total volume of 50 µL. The resulting products were used in a standard TOPO cloning reaction as described by the manufacturer.

2.12.5 Gateway cloning

Site-directed recombination between a Gateway Donor vector (attP1/2) and a Gateway Destination vector (attR1/2) was achieved by combining 70 ng of each plasmid and 0.5 µL of the Gateway LR Clonase II enzyme mix (Invitrogen) in a total volume of 4 µL and incubating it for 1 h at 25°C. Next, the reaction was supplemented with 0.5 µL of the Proteinase K solution provided with the LR Gateway LR Clonase II kit (Invitrogen) and incubated for 15 min at 37°C.

2.12.6 DNA sequencing

Sequencing reactions consisted of 3-4 fmol of template, 3.2 pmol of oligonucleotide, 3.5 µL of 5× BigDye Sequencing buffer (Applied Biosystems) and 0.5 µL of BigDye Terminator Ready v3.1 Reaction mix (Applied Biosystems). They were carried out in a DYAD Thermal Cycler using the thermal cycling protocol recommended by Applied Biosystems. The resulting products were purified using DyeEx 2.0 columns (Qiagen), dried in an Eppendorf's Vacufuge and finally run on an ABI3730 DNA Analyzer (Applied Biosystems) by the London Research Institute's Equipment Park team.

2.12.7 Visualization of DNA by ethidium bromide, SYBR green and SYBR Safe staining

For agarose gels, ethidium bromide (0.5 $\mu g \cdot mL^{-1}$, Seven Biotech), SYBR Green I (1×, Invitrogen) or SYBR Safe (1×, Invitrogen) was added to the gel before it solidified. Electrophoresed polyacrylamide gels were instead soaked for 30 min in 1× TBE buffer supplemented with the same concentrations of the above-mentioned stains. DNA was visualized by exposing the gel to UV light at 254 nm in a BioDoc_it UV transilluminator (UVP) for ethidium bromide, or visible light at 460nm in a LAS-3000 scanner (Fujifilm) using the AIDA software (Raytest), for SYBR Green and SYBR Safe.

2.13 General methods of protein manipulation

2.13.1 SDS-PAGE

SDS-PAGE was carried out using either 4-12% NuPAGE Novex gels in 1× MOPS running buffer (Invitrogen), according to the manufacturer's instructions, or Tris-Glycine

polyacrylamide gels prepared as described by Sambrook and Russell (2001) in Bio-Rad's Mini-PROTEAN system or Invitrogen's X-Cell SureLock Mini-Cells. For both systems the protein samples were mixed either with NuPAGE LDS Sample Buffer containing a reducing agent (Invitrogen), and boiled at 95°C for 5 min, or with HU buffer, and incubated at 65°C for 15 min. Pre-stained peqGOLD Protein-Markers IV (PeqLab) were used as molecular weight standards.

2.13.2 Coomassie blue staining

Electrophoresed gels were incubated on an orbital shaker for 15 min with 5-10 mL of the Coomassie Blue-based stain InstantBlue (Novexin). Alternatively, they were soaked for either 2-3 h or overnight in Coomassie Blue Staining solution and then de-stained through several washes in Coomassie Blue De-staining solution. In both cases, the gels were immersed in a Gel Drying solution for 1 h before being imaged on a LAS-3000 scanner.

2.13.3 SYPRO Ruby staining

Electrophoresed gels were washed twice for 30 min in SYPRO Fixing solution, to fix them, and then incubated overnight on an orbital shaker with 10-20 mL of SYPRO Ruby Protein Gel Stain (Invitrogen) at room temperature. Next, the gels were washed once in SYPRO Wash solution and once in water before being imaged on Typhoon 9400 scanner using the ImageQuant TL software.

2.13.4 Determination of protein concentration

2.13.4.1 Absorbance at 280 nm (OD_{280})

The extinction coefficient (ε) of a protein was calculated using the following formula:

$\varepsilon = 5690 \times (\#\text{ of Try}) + 1280 \times (\#\text{ Tyr}) + 120 \times (\#\text{ of Cys})\ M^{-1} \cdot cm^{-1}$

The OD_{280} of a protein sample was measured on a Nanodrop ND-1000 spectrophotometer (Labtech International) and then used to calculate its protein concentration by means of Beer's law:

$\text{Concentration} = OD_{280}/(\text{Path length} \cdot \varepsilon)$

2.13.4.2 Comparison by Coomassie staining

Different volumes of a relevant protein sample and known amounts of BSA were resolved by SDS-PAGE (see 2.13.1) on the same gel and subsequently subjected to

Coomassie staining (see 2.13.2). An image of this gel was acquired on a LAS-3000 scanner and then used to quantify the intensity of the stained bands by means of the AIDA software. The amount of protein of interest loaded onto the gel was determined by comparing the intensity of its corresponding bands to those of known amounts of BSA.

2.13.4.3 Bradford's method

Bio-Rad's Protein Assay was used to determine protein amounts by the Bradford's method (Bradford, 1976), according to the manufacturer's instructions. The OD_{595} was measured in Eppendorf's Biophotometer. The amount of protein present in a certain solution was determined by comparing its OD_{595} to that of known amounts of BSA.

2.13.5 Western blotting by the semi-dry transfer method

Electrophoresed gels were blotted onto a 45 µm Immobilon-P PVDF membrane (Millipore) by the semi-dry transfer method as follows. The filter was activated in methanol for 30 s and then equilibrated in Blotting buffer II for 5-10 min. In the meanwhile, two pieces of gel blotting paper (GB003, Whatman) pre-wetted in Blotting buffer I were set onto the anode plate of a semi-dry transfer cassette (Roth) and overlaid with another piece, which had been immersed in Blotting buffer II. The PVDF membrane was placed on top of these three layers, followed by the gel and three additional pieces of blotting paper soaked in Blotting buffer III. The resulting transfer stack was covered with the cathode plate of the transfer cassette. Proteins were electro-blotted onto the membrane at a maximum voltage of 25 V and at a constant current of either 40 mA for 1 h, for Bio-Rad's Mini-PROTEAN gels, or 50 mA for 1.5 h, for Invitrogen's NuPAGE Novex gels. Next, the membrane was rinsed in PBS, blocked for 1 h at room temperature in Blocking solution and incubated with a primary antibody (**Table 2.2**) either overnight at 4°C or for 2 h at room temperature. After four 5-10 min washes in PBS-T, the membrane was incubated in Blocking solution containing the relevant secondary antibody (**Table 2.3**) for 1 h at room temperature, and then washed again in PBS-T for three additional times. Finally, the membrane was developed using PerkinElmer's ECL Western Lightning Plus kit, according to the manufacturer's instructions, and imaged either on a LAS-3000 scanner (Fujifilm) or by exposure to Hyperfilm ECL (GE Healthcare) followed by chemical development in an X-Ray film processor (JP-33, Jungwon Precision Industry). When needed, the membrane was stripped of bound antibodies by washing it three times, for 10 min each, with Gentle

Stripping solution at room temperature or once with Harsh Stripping solution at 50°C for 30 min. In both cases, the membrane was rinsed extensively with PBS before being blocked and probed again as described above.

2.14 Protein purification

2.14.1 Protein production and purification in *E. coli*

2.14.1.1 Induction of gene expression and lysate preparation

Chemically-competent BL21-CodonPlus (DE3)-RIL *E. coli* cells (Stratagene) were transformed with the desired expression plasmid (**Table 2.6** and **Table 2.7**). Single clones were inoculated in liquid LB medium supplemented with the relevant antibiotic and propagated overnight at 37°C with shaking. The resulting saturated culture was diluted 100-fold typically in 2 L of liquid LB medium supplemented with the relevant antibiotic and grown at 37°C to an OD_{600} of 0.5-0.8. Transgene expression was induced by adding 1 mM IPTG (MP Biomedicals) to the culture and subsequently incubating it for 3 h at 37°C, in the case of SUMO, UBC9 or ORC1 over-production, or for 5 h at 25°C to produce the SUMO E1, APLF and XRCC1. Cells were harvested by centrifugation at 3,000 *g* for 10 min at 4°C, resuspended in 50 mL of the appropriate lysis buffer devoid of any reducing agent or protease inhibitors and flash-frozen in liquid nitrogen. On the day of purification, the cells were quickly thawed at 37°C, supplemented with 1 mM DTT (or 2 mM β-ME) and 1× Complete Protease Inhibitors, lysed by five 30 s pulses of sonication on a Branson sonifier at 50% output, with 2 min rest on ice, and finally centrifuged at 100,000 *g* for 1 h at 4°C to yield a cleared lysate.

2.14.1.2 Purification of AOS1/UBA2 (SUMO E1)

The SUMO E1 was purified essentially as described by Yunus and Lima (2009a). The cleared lysate was incubated with 4 mL of pre-equilibrated Ni^{2+}-NTA (Qiagen) for 2 h at 4°C with rotation. The bound proteins were washed with 60 mL of Ni^{2+}-NTA Wash buffer and eluted with 20 mL of Ni^{2+}-NTA elution buffer. The fractions containing the E1 enzyme were pooled, concentrated to 2 mL in a centrifugal concentrator (30,000 MWCO, Vivaspin) and applied to a HiLoad 16/60 Superdex 200 gel filtration column (GE Healthcare) equilibrated in E1 Gel Filtration buffer. The fractions that included the E1 enzyme were combined, diluted with an equal volume of E1 Gel Filtration buffer devoid of any salt and applied to an anion exchange column (Mono Q HR 5/5, 1 mL, GE Healthcare). The protein was eluted on a 50-500 mM NaCl gradient over 20 column

volumes. E1 enzyme-containing fractions were pooled, dialyzed overnight at 4°C against Protein Storage solution, concentrated to 1-2 $\mu g \cdot \mu L^{-1}$ and flash-frozen in liquid nitrogen.

2.14.1.3 Purification of UBC9 (SUMO E2)

UBC9 was purified essentially as described by Werner *et al.* (2009). The cleared lysate was applied to 10 mL of pre-equlibrated HiTrap SP HP resin (GE Healthcare). The bound proteins were washed with 100-120 mL of E2 Lysis buffer and eluted with 30 mL of E2 elution buffer. The fractions containing UBC9 were combined, concentrated to 2 mL in a centrifugal concentrator (3,000 MWCO, Vivaspin) and applied to a HiLoad 16/60 Superdex 200 gel filtration column equilibrated in Protein Storage buffer. UBC9-containing fractions were pooled, concentrated to 2-5 $\mu g \cdot \mu L^{-1}$ and flash-frozen in liquid nitrogen.

2.14.1.4 Purification of His_6-SUMO and Orc1-His_6

His_6-tagged SUMO1, SUMO2 and Orc1 were purified using fundamentally the same protocol as that employed to isolate the SUMO E1 enzyme (see 2.14.1.2), with the exception that the anion exchange step was omitted and the protein was concentrated to 1-2 $\mu g \cdot \mu L^{-1}$, in the case of Orc1, or 5-10 $\mu g \cdot \mu L^{-1}$, for SUMO, before being stored.

2.14.1.5 Purification of non-tagged SUMO

The cleared lysates prepared in Ni^{2+}-NTA Lysis buffer devoid of imidazole were ultrafiltered twice through a centrifugal concentrator (30,000 MWCO, Vivaspin). The resulting flow-through was concentrated to 1 mL in a centrifugal concentrator (3,000 MWCO, Vivaspin) and then applied to a Superdex 75 HR 10/30 gel filtration column (GE Healthcare) equilibrated in Protein Storage buffer. The fractions containing SUMO were combined, concentrated to 5-10 $\mu g \cdot \mu L^{-1}$ and finally flash-frozen in liquid nitrogen.

2.14.1.6 Purification of APLF and XRCC1

The lysate of cells producing N-terminally GST-tagged and C-terminally His_6-tagged APLF and XRCC1 were incubated with 3 mL of pre-equilibrated Ni^{2+}-NTA resin and handled thereafter essentially as described in 2.14.1.2. Imidazole was removed from the eluate by repetitively concentrating it in a centrifugal concentrator (10,000 MWCO, Vivaspin) and diluting it with a solution devoid of any imidazole. The resulting preparation was incubated with 3 mL of glutathione sepharose 4B (GE Healthcare) for 1 h at 4°C. Bound proteins were washed with 40 mL of GST Wash buffer and eluted

with 15 mL of GST Elution buffer. The fractions containing the relevant protein were combined, dialyzed against PBS supplemented with 1 mM DTT and 10% v/v glycerol, concentrated to 1-2 $\mu g \cdot \mu L^{-1}$ and flash-frozen in liquid nitrogen.

2.14.2 Protein production and purification in insect cells

2.14.2.1 Over-production of PARP-1

Exponentially growing Sf9 or Hi5 cells ($\sim 1 \cdot 10^9$) were harvested by centrifugation at 200 *g* for 5 min and typically mixed with 25-50 mL, or a volume large enough to give a MOI of 3, of the relevant virus stock and plain Grace's medium to a final volume of 100 mL, and then incubated for 1h to allow the virus to bind to the cells. Next, the suspension was diluted with 900 mL of Grace's medium supplemented with 10% v/v heat-inactivated foetal bovine serum and grown in suspension for 48-72 h at 27°C. Finally the cells were harvested by centrifugation at 1,000 *g* for 10 min, washed in ice-cold PBS, resuspended in 20 mL of PARP-1 Lysis buffer, flash-frozen in liquid nitrogen and stored at -80°C.

2.14.2.2 Preparation of 3-AB resin

The competitive PARP-1 inhibitor 3-aminobenzamide (3-AB) was covalently coupled to ECH Sepharose 4B (GE Healthcare) exactly as described by Dantzer *et al.* (2006).

2.14.2.3 Purification of PARP-1

PARP-1 was purified using a modified version of the original purification strategy described by Dantzer *et al.* (2006). Cleared lysates were prepared from frozen cell suspensions freshly supplemented with 1× Complete Protease Inhibitors and 5 mM β-ME essentially as described in 2.14.1.2. Next, they were supplemented with 1 $\mu g \cdot \mu L^{-1}$ protamine sulfate, centrifuged at 50,000 *g* for 15 min, slowly diluted with an equal volume of PARP-1 Lysis buffer devoid of salt and then incubated with 4 mL of pre-equilibrated 3-AB resin for 2 h at 4°C with rotation. The bound proteins were washed sequentially with 40 mL of each of PARP-1 Lysis buffer and equivalent solutions containing 500 or 800 mM NaCl. PARP-1 was eluted with 25 mL of PARP-1 Lysis buffer freshly supplemented with 1 mM 3-methoxybenzamide, mixed with an equal volume of PARP-1 Lysis buffer devoid of salt and applied to a HiTrap Heparin HP column (1 mL, GE Healthcare) pre-equilibrated in PARP-1 Heparin buffer. Proteins were eluted on a 100-1000 mM NaCl gradient over 20 column volumes. PARP-1-containing fractions were pooled, concentrated to 2 mL in a centrifugal concentrator

(30,000 MWCO, Vivaspin), applied to a HiLoad 16/60 Superdex 200 gel filtration column pre-equilibrated in Protein Storage buffer. The fractions that included PARP-1 were combined, concentrated to 1-2 $\mu g \cdot \mu L^{-1}$ and flash-frozen in liquid nitrogen.

2.15 Generation and affinity purification of polyclonal antibodies

2.15.1 Anti-SUMO rabbit polyclonal serum

Recombinant His_6-SUMO was used to immunize four rabbits by Harlan Sera-Lab UK, using 200 µg of protein for the initial immunization and 100 µg for the subsequent five boosts for each animal. The terminal bleed sera of rabbits ADA-11 (His_6-SUMO1) and HU-4 (His_6-SUMO2) were used for all downstream applications because they showed the highest affinity and specificity for the epitope against which they had been raised, as determined by western blotting analysis.

2.15.2 Preparation of SUMO1 and SUMO2 affinity resins

His_6-SUMO was covalently coupled overnight at 4°C to CNBr-activated Sepharose 4B (GE Healthcare) at a ratio of 2 mg of protein per mL of pre-swollen resin according the manufacturer's instructions with the only exception that after inactivation of the reactive groups the beads were also washed with 200 mM glycine pH 2.5. The conjugated resin was stored in PBS supplemented with 0.02% w/v sodium azide.

2.15.3 Affinity purification of antibodies

The SUMO-sepharose resin (1 mL) was initially washed three times in PBS and then incubated overnight with 10 mL of the appropriate serum at 4°C with rotation. Next, the beads were washed with 20 mL of PBS and then eluted with 10 mL of Antibody Elution buffer I and 10 mL of Antibody Elution buffer II as 1 mL aliquots in tubes containing 200 µL of Neutralization buffer. These fractions were pooled, dialyzed overnight at 4°C against PBS plus 1 mM DTT and concentrated in a centrifugal concentrator (3,000 MWCO, Vivaspin). The resulting preparations were supplemented with 50% v/v glycerol, flash frozen in liquid nitrogen and stored at -80°C (long-term) or -20°C (short-term).

2.16 Analysis of protein sumoylation

2.16.1 Denaturing Ni^{2+}-NTA pull down method

His_6-SUMO-modified species were isolated from frog sperm chromatin (2.7.6, ~ $1.5 \cdot 10^6$ nuclei), total yeast cell extracts prepared by the alkaline lysis method (2.8.4.1, 50-100 OD_{600} equivalents of cell) or mammalian cell pellets (1.0-$1.5 \cdot 10^7$ cells) by essentially the same procedure. They were resuspended in 1 mL of Ni^{2+}-NTA buffer A supplemented with 15 mM imidazole and 0.15 mM Tween 20 and incubated at room temperature for 1 h with rotation. The resulting preparations were sonicated for 20 s on a Branson Sonifier at 20% power to reduce the viscosity of the resulting lysate, in the case of frog sperm chromatin and mammalian cells, or centrifuged at 16,000 *g* for 10 min to clear it of large particulates, in the case of the yeast cell pellets. Next, 20 µL of Ni^{2+}-NTA resin pre-equilibrated in Ni^{2+}-NTA buffer A was added to the lysates and incubated overnight at room temperature with rotation. The resin was washed, by rounds of centrifugation (800 *g* for 15 s) and resuspension, in Ni^{2+}-NTA buffer A supplemented with 20 mM imidazole for three times, and twice more in Ni^{2+}-NTA buffer C, adjusted to either pH 6.3 or pH 8.0 and also supplemented with 35 mM imidazole. Excess of buffer was removed from the resin, which was finally resuspended in 35 µL of 1.5× NuPAGE LDS Sample Buffer supplemented with a reducing agent.

2.16.2 Immunoprecipitation method

Total cell extracts from either yeast (2.8.4.2, ~ 50 OD_{600} equivalents) or mammalian cells (2.18.1, ~ $5 \cdot 10^6$ cells) were prepared in RIPA buffer and then subjected to a common immunoprecipitation protocol. The exact amounts of cell extract and antibody used for a specific experiment are reported in the relevant figure legend. Generally, total cell extracts (2-4 mg of protein in 1-2 ml of RIPA buffer) were initially pre-cleared by incubating them with ~ 500 µL of plain Sepharose 4B resin (GE Healthcare) for 30 min at 4°C with rotation. Next, the extracts were separated from the resin by centrifugation at 3,000 *g* for 30 s, subjected to the Bradford's assay (see 2.13.4.3) and adjusted to the desired volume and protein concentration. The extracts were then transferred to silicon-coated 1.5 mL tubes, supplemented with the relevant antibody (usually 5-10 µg) and incubated with rotation at 4°C. After 2 h, the lysate-antibody mixture was spun at 16,000 *g* for 15 min, to remove any particulate that might have formed, and then transferred into new silicon-coated 1.5 mL tubes containing 15 µL of pre-equilibrated protein A/G resin (protein A for rabbit polyclonal antibodies, and

protein G for mouse monoclonal ones), which had been previously blocked with 10 $mg \cdot mL^{-1}$ BSA in PBS. Following an additional 1 h at 4°C with rotation, the resin was washed through subsequent rounds of centrifugation (800 *g* for 15 s) and resuspension in the following solutions: 1) RIPA buffer, 2) the same as RIPA buffer but containing 500 mM NaCl, 3) the same as RIPA buffer but containing 0.1% w/v SDS instead of 0.1% w/v sodium deoxycholate, 4) the same as RIPA buffer but containing 125 mM NaCl and no detergents. Finally, the beads were resuspended in 30 µL of 1.5× NuPAGE LDS Sample Buffer supplemented with a reducing agent.

2.17 Enzymatic reactions

2.17.1 Sumoylation reactions

Sumoylation reactions were typically carried out in 20 µL of Sumoylation buffer containing: 25 nM SUMO E1 (either His_6-tagged or untagged), 150 nM SUMO E2, 300 nM SUMO1 or SUMO2 (either His_6-tagged or untagged), 150 nM of the relevant SUMO substrate and 2 mM ATP. These reactions were allowed to proceed for 2 h at 30°C before being used to either purify a sumoylated substrate under native conditions (2.17.1.1 and 2.17.1.2) or to determine the extent of its modification by western blotting analysis (3-4 µL of the reaction). Any departures from this basic protocol are indicated in the relevant figure legend.

2.17.1.1 Purification of sumoylated PARP-1's DBD

PARP-1's DBD was sumoylated in a large-scale reaction using a buffer devoid of any BSA or Tween 20 and in the presence of His_6-SUMO containing a rhinovirus 3C protease cleavage site between the tag and the modifier, and a supercoiled plasmid (250 ng per 20 µl of reaction). The final volume of the reaction is reported in the relevant figure legend. Once the reaction was complete, it was slowly supplemented with NaCl and imidazole to a final concentration of 500 mM and 20 mM, respectively, and then applied to a 1 mL HisTrap HP column (GE Healthcare). The bound proteins were washed with 20 mL of Su-DBD Wash buffer, which was subsequently exchanged for 3C Cleavage buffer over five column volumes. A GST-tagged version of the rhinovirus 3C protease was added to 1.1 mL of such a solution at a protease:SUMO molar ratio of 1:40, injected into the column and then incubated overnight at 4°C. Next, the HisTrap HP column was connected in series to a 1 mL GSTrap HP one (GE Healthcare) and then slowly washed with 15 mL of 3C Cleavage buffer to "elute" the

sumoylated proteins and simultaneously remove the protease. The eluate was concentrated to 0.5 mL in a centrifugal concentrator (3,000 MWCO, Vivaspin) and applied to a Superdex 75 HR 10/30 gel filtration column pre-equilibrated in Su-DBD gel filtration buffer. The fractions containing the sumoylated PARP-1's DBD were pooled, concentrated to 1-2 $\mu g \cdot \mu L^{-1}$ and stored at 4°C.

2.17.1.2 Purification of sumoylated full-length PARP-1

His_6-PARP-1 was sumoylated in a large-scale reaction using a buffer devoid of any BSA or Tween 20 and in the presence of untagged SUMO E1, untagged SUMO1 and a supercoiled plasmid (250 ng per 20 µl of reaction). The final volume of the reaction is reported in the relevant figure legend. Once the reaction was complete, it was slowly supplemented with NaCl and imidazole to a final concentration of 500 mM and 20 mM, respectively. The sumoylated His_6-PARP-1 was captured onto 50 µL of Ni^{2+}-NTA resin, washed four times with 1 mL of Su-PARP-1 Wash buffer and eluted four times with 200 µL of Su-PARP-1 elution buffer. The eluate was dialyzed against either 100 mM ammonium acetate, before being concentrated to 50 µL for mass spectrometry analysis (see 2.21), or Protein Storage buffer, before being concentrated to 50 µL and flash-frozen in liquid nitrogen.

2.17.2 Parylation reactions

A complete parylation reaction contained 17.5 nM PARP-1 and 40 ng of DNase I-activated calf thymus DNA in a 20 µL total volume of either Auto-parylation buffer, if the polymerase was the only protein present in the reaction, or in Extract buffer if a cell extract (25 µg) was also included. The reactions were incubated at 25°C for the required lengths of time, stopped by the addition of 10 µL of 3× NuPAGE LDS Sample Buffer supplemented with a reducing agent, boiled for 5 min at 95°C and subjected to western blotting (10 µL, see 2.13.5).

2.18 Analysis of protein-protein interactions

2.18.1 Anti-FLAG co-immunoprecipitation

Frozen pellets of cells (100 µL) that had been transfected as indicate in the relevant figure legend were resuspended in 500 µL of Hypotonic buffer and incubated for 10 min on ice. The resulting lysates were supplemented with KCl to a final concentration of 150 mM, set on ice for an additional 5 minutes, subjected to two 5 s sonication pulses on a Branson sonifier at 10% power and then cleared by centrifugation at 16,000 *g* for

10 min at 4°C. Next, the extracts were subjected to the Bradford assay (see 2.13.4.3) and then adjusted to 1.5 $\mu g \cdot \mu L^{-1}$ of total protein. FLAG M2 agarose (30 µL, SIGMA) was added to 1 mL of this lysate and incubated overnight at 4°C with rotation. Finally, the resin was washed four times with Co-immunoprecipitation Wash buffer before being resuspended in 35 µL of 1.2× NuPAGE LDS Sample Buffer supplemented with a reducing agent.

2.18.2 Glutathione pull-down assays

Typically, defined amounts of a GST-tagged polypeptide (the bait) and a second protein (the prey), as indicated in the relevant figure legends, were combined in 100 µL final volume of PBS-Tx supplemented with 1 mM DTT. The reactions were mixed and incubated at 4°C for 2 h. Next, 10 µL of glutathione resin (GE Healthcare) was added to the tubes and incubated for an additional 1 h at 4°C with rotation. The beads were washed four times with PBS-Tx plus 1 mM DTT before being resuspended in 30 µL of 1.2× NuPAGE LDS Sample Buffer and a reducing agent.

2.19 Preparation of DNA substrates for sumoylation reactions

2.19.1 Preparation of digested, nicked and relaxed pHU2020

Double- or single-stranded breaks were inflicted on pHU2020 (11 µg) by incubating it in a total volume of 120 µL with 110 U of PstI, EcoRV or EcoRI for 3 h at 37°C, or Nb.BsrDI (New England Biolabs) for 3 h at 65°C. Supercoiling was released from pHU2020 (5 µg) in the presence of 5 U of topoisomerase I (Invitrogen) for 3h at 37°C in 500 µL of Topo I buffer. The resulting DNA was purified using Qiagen's QIAquick Spin columns according to the manufacturer's instructions. Successful digestion was confirmed by agarose gel electrophoresis (see 2.11.2).

2.19.2 Annealing of oligonucleotides

Double-stranded DNA oligonucleotides were generated by combining the appropriate pair of ssDNA oligonucleotides in Annealing buffer to a final concentration of 50 µM, boiling the resulting mixture at 98°C for 3 min and then allowing it to cool to room temperature in 2°C steps every 2 min, with a 2 min rest time, at a rate of $0.1°C \cdot s^{-1}$ in a DYAD Thermal Cycler. Sebastian Eustermann created the nicked dumbbell substrate by diluting the corresponding ssDNA oligonucleotide to a concentration of 50 µM in

Annealing buffer, incubating it on boiling water for 3 min and then allowing it to slowly cool down to room temperature.

2.19.3 Ligation of nicked dumbbell

The nicked dumbbell (20 µM) was ligated in a total volume of 40 µL containing 2,000 U of T4 DNA ligase for 16 h at 25°C. The reaction was terminated by incubating it at 65°C for 5 min. Successful ligation of the nicked dumbbell was assessed by comparing its migrating patterns to that of a mock-ligated substrate by denaturing PAGE (see 2.11.3).

2.20 Analysis of protein-DNA interactions

Analysis of protein-DNA interactions was carried out by Sebastian Eustermann.

2.20.1 Electrophoretic mobility shift assay

DNA ligand (400nM) was mixed with PARP-1's DBD (200 nM, 400, nM, 800 nM, 1600 nM) in EMSA binding buffer in a total volume of 10 µL and incubated for 30 min at room temperature. The samples were resolved by native PAGE as described in 2.11.3.

2.21 General methods of mass spectrometry

Mass spectrometry analysis was carried out by the Protein Analysis and Proteomics team of the London Research Institute.

2.21.1 Sample preparation

Poly-acrylamide gel slices or proteins in solution (resuspended in 4 M urea and 50 mM ammonium bicarbonate) were prepared for mass spectrometry analysis using the Janus Liquid Handling System (PerkinElmer). The samples were placed in a 96-well microtitre plate and destained with 50% v/v acetonitrile and 50 mM ammonium bicarbonate, reduced with 10 mM DTT and then alkylated with 55 mM iodoacetamide. An additional 2 µl of 10 mM DTT was added to the samples to neutralize excess iodoacetamide and subsequently incubated overnight at 37°C with 6 $ng \cdot \mu L^{-1}$ of trypsin. In the case of gel slices, the peptides were extracted in a solution of 2% v/v formic acid and 2% v/v acetonitrile.

2.21.2 Peptide analysis by LC-MS/MS

The peptides were separated at a flow of 300 $nL \cdot min^{-1}$ with a gradient of acetonitrile on a nanoACQUITY UPLC system (Waters) attached to a C_{18} Symmetry µ-Precolumn (5

μm, 180 μm × 20 mm, Waters) in series with a C_{18} BEH130 analytical UPLC column (1.7 μm, 75 μm × 100 mm, Waters). The column outlet was directly interfaced with an LTQ Orbitrap XL/ETD instrument (Thermo Scientific) via a modified nano-flow electrospray ionisation source. Data-dependent analysis was performed using a resolution of 30,000 for the full MS spectrum, followed by eight MS/MS spectra in the linear ion trap. MS spectra were acquired with an automatic target gain control of $5 \cdot 10^5$ and a maximum injection fill-time of 100 ms over an m/z range of 300-2,000. MS/MS scans were collected using an automatic gain control value of $4 \cdot 10^4$ and a threshold energy of 35 for collision-induced dissociation. The data were analyzed against the UniProt database by means of the MASCOT algorithm (Matrix Science) using the following parameters: a precursor tolerance of 5 ppm, a fragment ion mass tolerance of 0.8 Da, one missed trypsin cleavage site and variable modifications for oxidized methionine, carbamidomethyl cysteine, pyroglutamic acid, phosphorylated serine, threonine and tyrosine. MS/MS data were manually curated and validated using the Scaffold programme (Proteome Software).

2.22 General methods of NMR spectroscopy

NRM spectroscopy was carried out by Sebastian Eustermann. ^{15}N- and ^{13}C-labelled SUMO-PARP-1's DBD (see 2.17.1.1) was dialyzed against NMR dialysis buffer and 5% v/v D_2O. NMR data were acquired on a DMX600 spectrometer (Bruker) fitted with a triple resonance ($^1H/^{15}N/^{13}C$) cryoprobe. Experiments were performed at 300K and ^1H, ^{15}N and ^{13}C chemical shifts (δ) were calibrated using sodium 3,3,3-trimethylsilylpropionate as an external ^1H reference. Spectra were processed using either the program TOPSPIN (Bruker) or SPARKY (Goddard T.D. and Kneller D.G., University of California, San Francisco). Resonance assignments of PARP-1 residues were made using a standard suite of triple resonance NMR experiments. $^{15}N,^1H$ resonances of protein backbone amide groups of PARP-1's DBD in the context of the sumoylated domain were assigned by comparing its ($^{15}N,^1H$) heteronuclear single quantum coherence spectrum to that of the unmodified PARP-1's DBD. A large majority of resonances were found at closely corresponding peak positions so that perturbed signals could be unambiguously identified and assigned. Amide group chemical shift perturbation between PARP-1's DBD and SUMO-PARP-1's DBD was calculated as follows, $\Delta\delta = \sqrt{((\delta^1H)^2 + (\delta^{15}N/5)^2)}$.

Chapter 3. Results I: Isolation and identification of sumoylated proteins from normal and challenged replicating chromatin

3.1 Introduction

Sumoylation plays an important role in the maintenance of genome stability. In both budding and fission yeasts, mutations within the members of the sumoylation pathway lead to hypersensitivity to different genotoxins (Andrews *et al.*, 2005; Ho and Watts, 2003; Maeda *et al.*, 2004; Zhao and Blobel, 2005), accumulation of chromosomal rearragements (Motegi *et al.*, 2006), defective chromatid segregation (Tanaka *et al.*, 1999), failure to properly retain mini-chromosomes (Takahashi *et al.*, 2006) and telomeric defects (Rog *et al.*, 2009; Tanaka *et al.*, 1999; Xhemalce *et al.*, 2004; Zhao and Blobel, 2005). In human cells, disrupting the normal regulation of sumoylation also leads to the accumulation of damaged DNA and impairs its repair (Galanty *et al.*, 2009; Li *et al.*, 2000; Morris *et al.*, 2009; Potts and Yu, 2005). In addition, proteins involved in controlling DNA metabolism, and therefore also genome integrity, have been found to be sumoylated, including members of nucleotide excision repair (*e.g.* XPC and XRCC4, Wang *et al.*, 2005b; Yurchenko *et al.*, 2006), BER (*e.g.* thymine DNA glycosylase, see 1.3.4), homologous recombination (*e.g.* Rad52, PCNA, BRCA1 and the RECQ family of DNA helicases, Eladad *et al.*, 2005; Galanty *et al.*, 2009; Hoege *et al.*, 2002; Kawabe *et al.*, 2000; Morris *et al.*, 2009; Sacher *et al.*, 2006), non-homologous end joining (*e.g.* Ku70, Zhao and Blobel, 2005), topoisomerase I (Horie *et al.*, 2002; Mao *et al.*, 2000b), topoisomerase II (Azuma *et al.*, 2003; Bachant *et al.*, 2002; Mao *et al.*, 2000a) and proteins involved in telomere protection (Potts and Yu, 2005).

Although our understanding of how sumoylation impinges on biological processes has improved considerably, the exact mechanisms by which SUMO protects cells against DNA damage remain largely unknown because it has often not been possible to correlate a specific phenotype to the modification of a certain protein by specific E3 ligases. When I started my research work several proteomic studies had been carried out in both yeast and vertebrates with the aim of identifying possible targets of sumoylation (Denison *et al.*, 2005; Hannich *et al.*, 2005; Rosas-Acosta *et al.*, 2005; Vertegaal *et al.*, 2006; Vertegaal *et al.*, 2004; Wohlschlegel *et al.*, 2004; Zhao *et al.*, 2004b; Zhou *et al.*, 2004). Amongst the candidates that were found, proteins involved in DNA replication and repair appeared to be somewhat under-represented in

comparison to, for example, transcription factors, probably because their sumoylation levels were too small in comparison to the entire “sumoylome” of a cell to be efficiently detected by mass spectrometry. I reasoned that if I could identify proteins that were sumoylated during S phase and/or after challenge with genotoxic stress then I could gain more insight on how sumoylation controls genome stability. Towards this goal, I decided to identify SUMO conjugates during unchallenged replication or in the presence of genotoxins from chromatin, because it should be enriched for proteins with established roles in DNA metabolism.

As a source of chromatin for these experiments I decided to use sperm DNA incubated in *X. laevis* egg interphase extracts for several reasons. Firstly, several published studies had already shown that frog egg extracts could be successfully used to identify sumoylated species from mitotic chromosomes as well as to study diverse aspects of sumoylation, often in a target-specific manner (Azuma *et al.*, 2003; Leach and Michael, 2005; Lee *et al.*, 1998; Saitoh *et al.*, 1998). Secondly, in frog egg extracts chromosomes are rapidly, synchronously and efficiently replicated under the same controls that exist *in vivo*: only once per cell cycle by semi-conservative DNA synthesis. Since such extracts can be extensively manipulated in a biochemically-tractable manner, they have been instrumental to exploring the mechanics of DNA replication under normal conditions and in the presence of DNA damage (Blow and Laskey, 1986; Coleman *et al.*, 1996; Costanzo *et al.*, 2001; Costanzo *et al.*, 2004).

For all the studies presented in this chapter I used interphase extracts supplemented with cycloheximide. These extracts consist of essentially pure egg cytoplasm and membranes that are obtained by centrifuging mature frog eggs, which are naturally arrested at metaphase of the second meiotic division (Walter and Newport, 1999). The addition of calcium to the eggs activates them, that is, it leads to degradation of mitotic cyclins, the subsequent exit from metaphase and entry into interphase. When hyper-condensed sperm chromatin is added to the extracts it undergoes a series of remodelling events that include decondensation, exchange of sperm protamines for egg histones and packaging into structures that resemble interphase nuclei before being replicated (Blow, 1996). The addition of cycloheximide to the extracts inhibits the *de novo* synthesis of proteins such as mitotic cyclins, which are required for mitotic entry, thus ensuring that they do not progress past the end of DNA replication (Solomon *et al.*, 1990).

The aim of this part of my study was: 1) to show that chromatin isolated from frog egg extract associates with sumoylated proteins during DNA replication and in response to genotoxic stress, 2) to isolate and identify such SUMO conjugates and 3) to confirm the sumoylation of such proteins.

3.2 Results

3.2.1 Generation of anti-SUMO1- and anti-SUMO2-specific antibodies

Towards the end of identifying sumoylated species from DNA that is being replicated, I initially wanted to confirm that sumoylated species do indeed associate with replicating chromatin. For this purpose, and because I discovered that the specificity of commercially-available antibodies against SUMO1 or SUMO2 leaves a lot to be desired, I set out to generate antibodies that specifically recognized either one SUMO paralogue. Since the primary sequence of the mature forms of SUMO2 and SUMO3 differ only by three amino acids, I assumed that a polyclonal antibody raised against SUMO2 would recognize SUMO3 as well. The antibodies against SUMO1 or SUMO2 were generated in rabbits by five subsequent injections of either His_6-SUMO1 or His_6-SUMO2. The SUMO-specific antibodies were captured from terminal-bleed sera on a resin produced by cross-linking either His_6-SUMO1 or His_6-SUMO2 to activated

Figure 3.1 - Characterization of anti-SUMO1 and anti-SUMO2 antibodies. A) Increasing amounts of His_6-SUMO1 or His_6-SUMO2 were spotted onto a nitrocellulose membrane and probed overnight at 4°C with 1 µg of anti-SUMO1 and anti-SUMO2 antibodies per mL of 5% w/v milk in PBS + 0.1% v/v Tween 20. Detection was carried out by chemiluminescence. B) Interphase extracts (10 µL) were supplemented with His_6-SUMO1 or His_6-SUMO2 to a final concentration of 0, 2, 5, 10, 20 or 40 µM and incubated for 1 h at 23°C. For western blotting, 1 µL of extract was analyzed against SUMO1 or SUMO2.

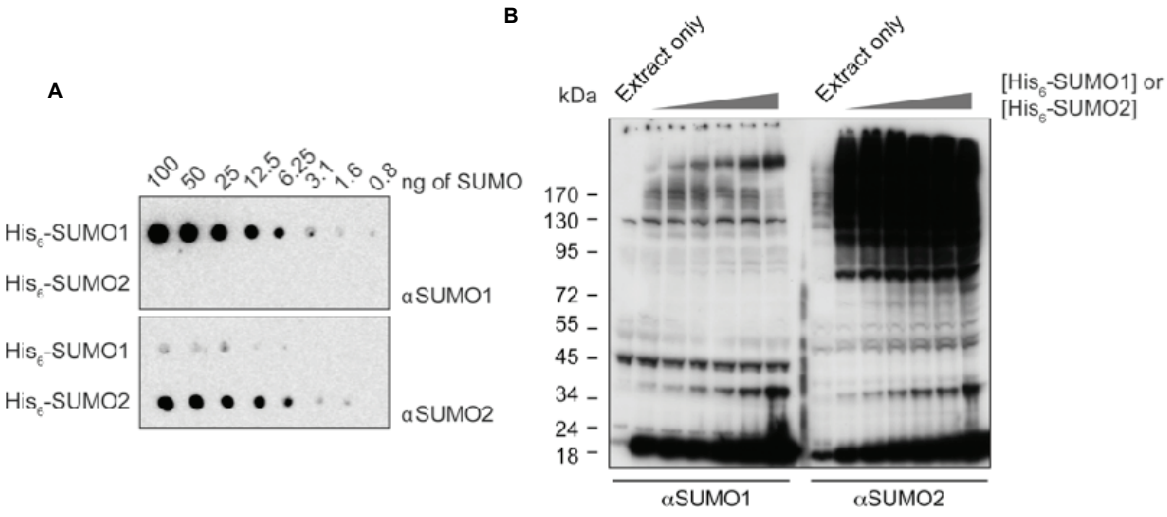

sepharose, and isolated by acid elution. To estimate the affinity and test the specificity of these antibodies, I analyzed them by western blotting on a filter spotted with increasing amounts of purified His_6-SUMO1 or His_6-SUMO2. **Figure 3.1**A shows both the anti-SUMO1 and anti-SUMO2 antibodies specifically recognized the relevant SUMO paralogue against which they were raised and purified. The data also indicate that the antibodies must have minimal cross-reactivity towards the His_6 tag because both recombinant SUMOs spotted on the membrane carried it. Although other types of cross-reactivity in total cell extracts cannot be excluded, these results suggest that they are not likely. Western blotting analysis of egg extracts supplemented with increasing amounts of His_6-SUMO1 or His_6-SUMO2 also showed a dose-dependent rise in the levels of several species spanning a range of molecular weights, which in all likelihood represent SUMO conjugates (**Figure 3.1**B).

Altogether, these data indicate that I generated specific antibodies against SUMO1 and SUMO2. Importantly, they also demonstrate that the His_6-tagged SUMO1 and SUMO2 I added to the extracts were functional, that is, they could be actively conjugated to proteins.

3.2.2 SUMO conjugates associate with chromatin during interphase

Having generated antibodies that recognize SUMO1 and SUMO2, I used them to verify that SUMO conjugates associate with DNA during interphase. I isolated chromatin at mid-S phase from extracts that were supplemented with sperm nuclei alongside a control buffered solution, SUMO1, SUMO2 or their respective His_6-tagged versions before being allowed to replicate, and analyzed them by western blotting. I added recombinant SUMO to the extracts because I wanted to inspect the behaviour of sumoylated species under the same conditions that I would be using in subsequent experiments to generate SUMO conjugates that bear a His_6 tag and can therefore be captured under denaturing conditions. **Figure 3.2** shows that replicating chromatin associated with both SUMO1 and SUMO2 conjugates. Expectedly, supplementing the extracts with recombinant untagged SUMO enhanced the levels of such species. The addition of His_6-SUMO afforded a similar increase and resulted in the incorporation of the tagged protein into high-molecular weight species, which must have been generated by *de novo* sumoylation. These observations also suggest that the His_6 tag does not significantly impair the conjugation of SUMO to its targets. The SUMO adducts shown in **Figure 3.2** were *bona fide* DNA-binding proteins because they were not detected in a mock isolation carried out on extracts devoid of chromatin.

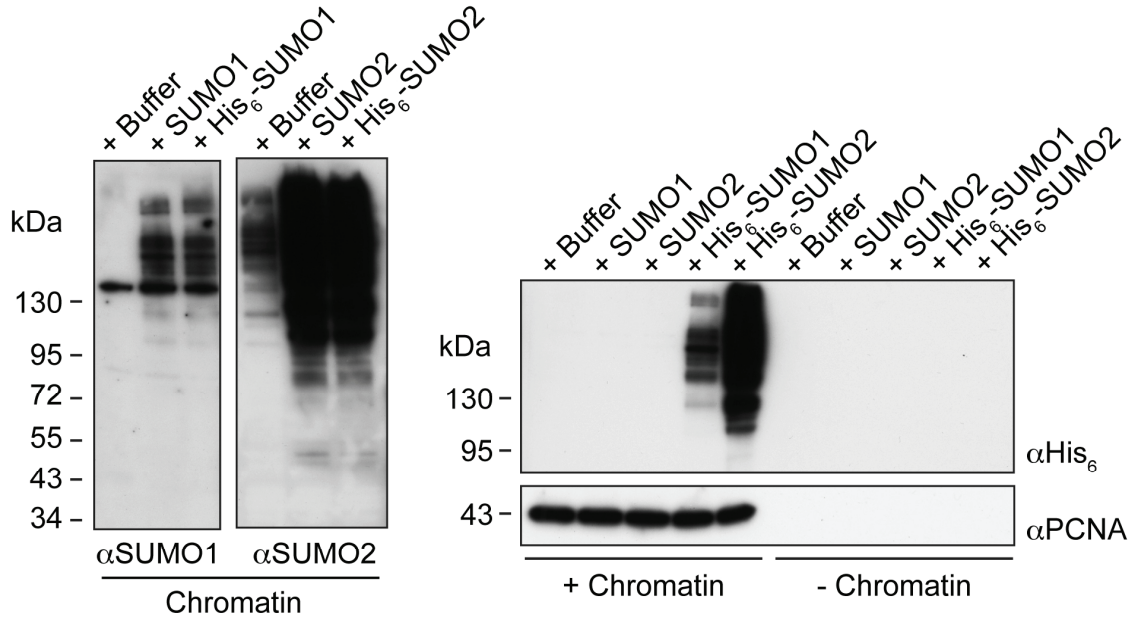

Figure 3.2 - SUMO1- and SUMO2-modified species associate with chromatin during interphase. Interphase extracts (25 µL) were supplemented with either a control buffer, untagged SUMO1/2 or His_6-SUMO1/2 to a final concentration of 20 µM. Where indicated, sperm nuclei (2,500 nuclei·µL^{-1} of extract) were added. Chromatin was isolated from the extracts after an incubation of 1 h at 23°C and analyzed by western blotting against SUMO1, SUMO2, His_6 and PCNA (loading control).

3.2.3 The levels of chromatin-associated SUMO1 conjugates change during and depend on entry into S phase

Having found SUMO1- and SUMO2-conjugated species on replicating chromatin, I was interested in determining whether their levels changed during the course of DNA replication. Interphase extracts were supplemented with sperm nuclei and either His_6-SUMO1 or His_6-SUMO2 prior to replication. Chromatin was isolated from these extracts at three time-points: soon after addition of nuclei (0 h), during DNA replication (1 h) or after replication was completed (2 h) and analyzed by western blotting against the His_6 tag. The amount of PCNA loaded on the chromatin was used as a rough estimate to monitor progression through S phase. **Figure 3.3**A shows that the levels of both SUMO1 and SUMO2 species on DNA peaked during S phase and disappeared thereafter.

To confirm that such a trend depended on DNA replication and it was not simply a time-dependent effect of the incorporation of the His_6-SUMO into conjugates, I repeated the above-described experiment in the absence or presence of recombinant geminin (a gift from Vincenzo Costanzo). Geminin is normally absent at the G_1 phase

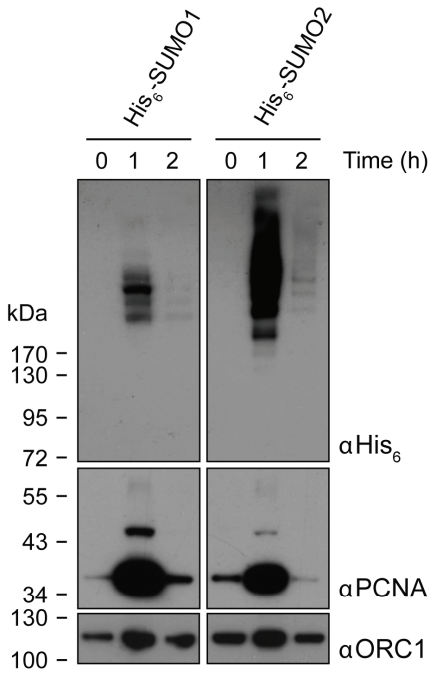

Figure 3.3 - The levels of chromatin-associated SUMO1- and SUMO2-modified species change during interphase. Interphase extracts (25 µL) were supplemented with 2,500 nuclei·µL^{-1} of extract and either His_6-SUMO1 or His_6-SUMO2 to a final concentration of 20 µM. Chromatin was isolated from the extracts at the indicated times and analyzed by western blotting against His_6, PCNA and ORC1 (loading control).

and it accumulates during S and G_2 phases, when it blocks the loading of the MCM2-7 helicase on replication origins by binding to and inhibiting the essential replication factor CDT1, thus preventing re-replication of DNA (McGarry and Kirschner, 1998; Tada *et al.*, 2001; Wohlschlegel *et al.*, 2000). If exogenous geminin is added to egg extracts before replication origins fire, it inhibits DNA replication. For this experiment, I isolated DNA at increasing time points from interphase extracts supplied with His_6-SUMO1 and analyzed it by western blotting against the His_6 tag. The kinetics of replication was followed by quantifying the incorporation of [α-^{32}P]dCMP into genomic DNA (**Figure 3.4**C). In the absence of geminin, the levels or extent of modification of sumoylated proteins on DNA appeared to follow, although with a delay, the course of S phase (**Figure 3.4**A, left panel). In the absence of chromosomal replication, that is, in the presence of geminin, very little on-chromatin sumoylation was observed (**Figure 3.4**A, middle panel). To exclude an inhibitory effect of geminin itself on sumoylation, I examined the dynamics of modification in the soluble fraction of the extracts. Although geminin did slightly inhibit sumoylation in this fraction (**Figure 3.4**B), the effect was almost an order of magnitude smaller than what I observed for DNA-associated proteins.

Altogether these results indicate that progression through S phase is critical for the presence of sumoylated species on the chromatin and suggest that sumoylation may play an important role during DNA replication.

3.2.4 Genotoxic stress does not visibly alter the modification of chromatin-associated proteins by SUMO1

I was interested in determining whether the pattern of sumoylation of chromatin-associated proteins changed in response to genotoxic stress. In that case, the modification of certain proteins might be important in maintaining genome stability. As a source of genotoxic stress I used aphidicolin, which inhibits replicative DNA polymerases, leading to the accumulation of ssDNA and activation of several pathways of DNA damage detection and repair such as the DNA damage checkpoint (Lupardus *et al.*, 2002), homologous recombination (Saintigny *et al.*, 2001) and post-replication repair (Chang *et al.*, 2006).

I isolated DNA at increasing time-points from interphase extracts supplemented with His_6-SUMO1 in the absence or presence of aphidicolin and examined it for sumoylation by western blotting. **Figure 3.4**A, right panel, shows that analogously to the addition of geminin, although to a lesser extent, the presence of aphidicolin reduced the level of sumoylated species on the chromatin. The conjugates that however did appear accumulated with similar kinetics to those observed for the untreated sample (**Figure 3.4**A, left panel), but did not disappear at the later time-point. Taking into account that progression through S phase seems to be required for the presence of sumoylated species on DNA (**Figure 3.4**A, left and middle panel) and that aphidicolin arrests DNA replication at an early stage, this observation is likely to reflect the inability of the extract to complete S phase. The slightly higher levels of sumoylated species observed on the DNA of the aphidicolin-treated extract compared to the geminin-treated one, where progression through S phase is prevented by inhibiting origin licensing and not DNA replication, suggests that between these two events some proteins may become sumoylated. Unfortunately, I also observed that the distribution and the relative intensities of the SUMO1 conjugates from the extracts treated with aphidicolin appeared very similar to those observed in the non-damaged extracts, thus indicating that replicative stress does not noticeably alter the sumoylation of the bulk of chromatin-associated proteins. I, however, reasoned that given the relatively low abundance of individual sumoylated species, small changes in their modification could

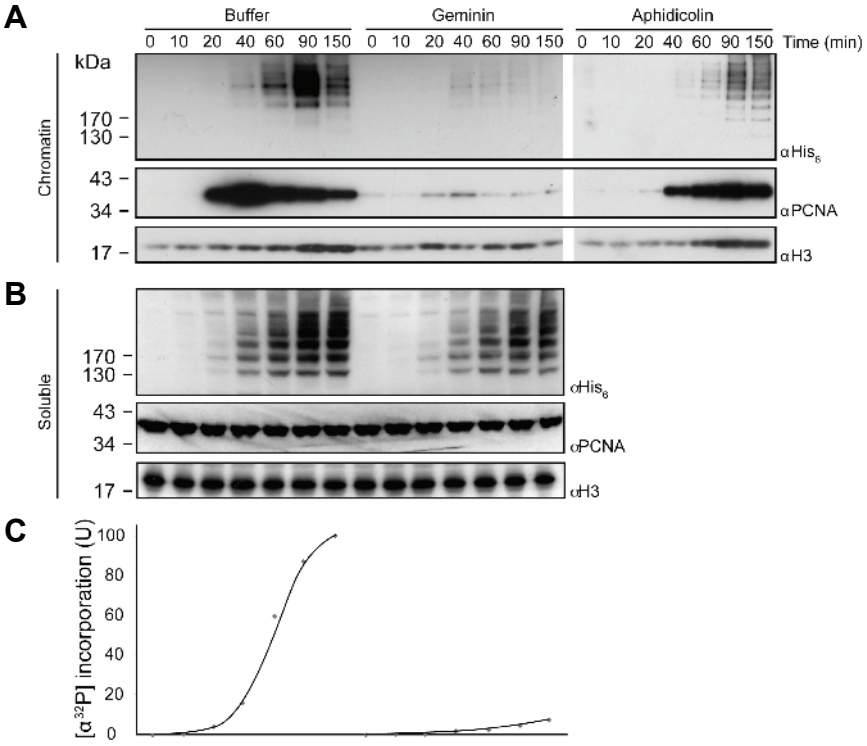

Figure 3.4 - Progression through S phase, but not genotoxic stress, affects the sumoylation of chromatin-associated proteins in interphase extracts. A) Interphase extracts (25 µL) were supplemented with 2,500 nuclei·µL^{-1} of extract and His_6-SUMO1 to a final concentration of 20 µM. Where indicated a control buffer, geminin (8 nM) or aphidicolin (40 µM) were also added. Chromatin was isolated from the extracts at the indicated times and analyzed by western blotting against His_6, PCNA and histone H3 (loading control). B) The soluble fractions of the extracts prepared as described in A) were analyzed by western blotting against His_6, PCNA and H3 (loading control). C) DNA replication was analyzed as described in 2.7.5. U = % of [α-^{32}P]dCMP incorporation. 100% was defined as the amount of [α-^{32}P]dCMP incorporated in the genomic DNA of the control sample at 150 min.

not be excluded because they may be hard to discern in blots like those shown in **Figure 3.4**, where discrete bands are not obvious.

3.2.5 Identification of SUMO conjugates from replicating chromatin by mass spectrometry and western blotting

To identify the SUMO conjugates that I observed in **Figure 3.4**, I devised the following strategy. Chromatin was isolated during S phase from a large preparation of undamaged or aphidicolin-treated interphase extracts that were supplemented with His_6-SUMO1 or His_6-SUMO2. The covalent nature of the bond between SUMO and its targets and the ability of the His_6 tag to bind to a Ni^{2+}NTA matrix even in the presence of 6 M guanidine HCl allowed me to capture sumoylated species by denaturing affinity chromatography (**Figure 3.5**A). By using this tactic, I expected to inactivate SUMO

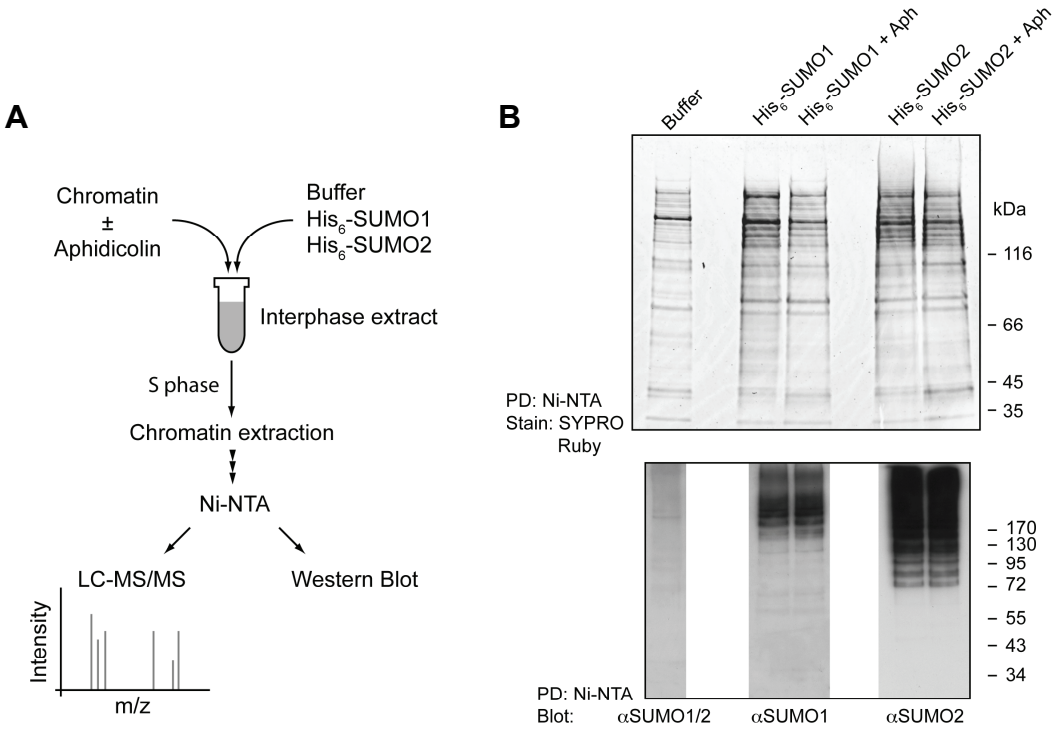

Figure 3.5 - Isolation of sumoylated species from replicating chromatin under normal conditions and in the presence of genotoxic stress. A) Experimental strategy used to isolate and identify chromatin-associated substrates of sumoylation. B) Interphase extracts (1 mL) were supplemented with 2,500 nuclei·μL^{-1} of extract and His_6-SUMO1 or His_6-SUMO2 to a final concentration of 20 μM. Where indicated aphidicolin (Aph, 40 μM) or just DMSO was also added. Chromatin was isolated from the extracts after 1 h and resuspended in 1 mL of a buffered solution containing 6 M guanidine HCl. His_6-SUMO1/2-modified species were captured as described in 2.16.1 at room temperature with 50 μL of Ni^{2+}-NTA resin. Affinity purified proteins were subjected to SDS-PAGE followed by SYPRO Ruby staining or western blotting against SUMO1/2. PD = Ni^{2+}-NTA pull-down.

isopeptidases and therefore minimize the loss of sumoylated species that may otherwise occur during the enrichment procedure (Vertegaal *et al.*, 2006; Vertegaal *et al.*, 2004). I also expected to disrupt most non-covalent interactions, thus ensuring that only proteins covalently linked to SUMO would be isolated. To account for the recognized non-specific affinity of the Ni^{2+}NTA resin towards the many histidine-rich proteins present in eukaryotes, a control mock purification was also performed using chromatin isolated from extracts supplied only with a buffered solution.

The proteins extracted by the above-described procedure were resolved by SDS-PAGE and visualized by SYPRO Ruby staining. **Figure 3.5**B shows that, with the exception of some discrete bands and a stronger "general" staining observed specifically in the experimental samples, the protein patterns of the mock and experimental purifications were similar. However, when such samples were analyzed by western blotting against SUMO1 and SUMO2, I observed a significant enrichment of

Table 3.1 - Identification of sumoylated species from replicating chromatin under normal conditions and in the presence of genotoxic stress by mass spectrometry. Sumoylated proteins isolated as described in Figure 3.5B were analyzed by LC-MS/MS. * Maximum number of peptides detected within one band for proteins identified in two or more bands.

	Identified Protein	Uniprot Accession	# peptides				Modification by SUMO1/2	Aphidicolin dependence?
			SUMO1	SUMO1 + Aph	SUMO2	SUMO2+ Aph		
DNA replication and repair	Aprataxin	Q7T287	-	-	5	3	SUMO2	No
	ATR	Q9DE14	-	9	-	5	Both	Yes
	DNA pol α (catalytic subunit)	Q9DE46	-	8*	-	19*	Both	Yes
	PARP-1	P31669	-	-	14	-	SUMO2	Yes
	PCNA	P18248	-	-	-	2	SUMO2	Yes
	PLK1	P34331	-	-	-	2	SUMO2	Yes
	RAD50	Q92878	2	2	-	-	SUMO1	No
	RAD52	P39022	-	-	-	2	SUMO2	Yes
	RAD54B	Q9DG67	6*	-	2*	-	Both	No
	RFC1	P35251	-	2	-	3	Both	Yes
	RTEL1	Q9NZ71	-	-	-	4	SUMO2	Yes
	TOP2A	O42130	5	-	28*	17*	Both	No
	TOP2B	O42131	-	4	9*	9*	Both	No
	WDHD1	O13046	-	-	-	4*	SUMO2	Yes
Chromatin remodeling	CHD1	O14646	9	8*	9*	4*	Both	No
	CHD3	Q12873	-	7	12*	4*	Both	No
	CHD4	Q14839	-	-	21	11	SUMO2	No
	CHD6	Q8TD26	4	9*	5*	9*	Both	No
	CHD7	Q9P2D1	7*	26*	28*	25*	Both	No
	HDAC1	Q91695	-	-	9	4	SUMO2	No
	ISW1	Q24368	-	-	5*	-	SUMO2	Yes
	ISW2	Q8RWY3	-	2	5*	4*	Both	No
	JHD2C	Q15652	2	5	5*	6*	Both	No
	N-COR1	O75376	-	-	2	-	SUMO2	Yes
	N-COR2	Q9Y618	-	5	6	5	Both	No
	RBBP4	Q3MHL3	-	-	2*	8*	SUMO2	No
	RBBP7	Q9I8G9	4	-	2*	2*	Both	No
	SNF2	O60264	-	-	6*	4	SUMO2	No
	TRRAP	Q9Y4A5	3	4	8	-	Both	No
Transcription	ARID5B	Q14865	-	2	-	-	SUMO1	Yes
	CTBP1	Q13363	2	3	9*	12*	Both	No
	HIC 2	Q15652	-	-	2	2	SUMO2	No
	RBM39	Q14498	-	2	-	-	SUMO1	Yes
	SAL-like protein 1	Q9NSC2	-	3	8*	12	Both	No
	SAL-like protein 4	Q9UJQ4	-	-	4	-	SUMO2	Yes
	SIN3A	Q96ST3	-	9	9*	7	Both	No
	Transcription repressor p66	Q86YP4	5*	2	5*	3*	Both	No

	Zn finger protein 143	P52747	-	-	11*	4	SUMO2	No
	Zn finger protein 462	Q96JM2	-	5	7*	-	Both	No
	Zn finger protein 687	Q8N1G0	-	-	3*	-	SUMO2	Yes
Other/Cytoplasmic	CDK11	Q9BWU1	-	-	-	3*	SUMO2	Yes
	Afadin	P55196	-	-	-	3	SUMO2	Yes
	BAT2	P48634	-	4	2	4	Both	No
	BRE1	Q60YN5	2	-	-	-	SUMO1	Yes
	CAM kinase II γ chain	Q13555	-	-	4*	5*	SUMO2	No
	Cyclin T1	Q6T8E9	-	-	3	-	SUMO2	Yes
	GPR27	Q9NS67	2	-	-	-	SUMO1	Yes
	LIS1	P43033	-	-	-	7*	SUMO2	Yes
	NOL3	O60936	-	-	-	3*	SUMO2	Yes
	Phenylalanyl-tRNA synthetase β chain	Q1971	6	-	-	-	SUMO1	No
	PP1 subunit 10	Q6GLQ4	2	-	4	5	Both	

sumoylated species from 40 kDa to over 190 kDa in size specifically in the experimental samples (**Figure 3.5**B). No free SUMO1 or SUMO2 were found bound to the chromatin, indicating that these proteins do not bind on their own to DNA (data not shown). Because I could not discern discrete band in the western blotting shown in **Figure 3.5**B, but also to ensure that only targets of sumoylation were identified and all the possible contaminants were excluded, the experimental and control lanes of the gel were divided into 40 bands, each of which was subjected to in-gel trypsin digestion. The resulting peptides were extracted and analyzed by the Protein Analysis and Proteomics team of the London Research Institute on a ThermoScientific LTQ Orbitrap XL/ETD mass spectrometer coupled to a Waters NanoACQUITY UPLC system (LC MS/MS), both in terms of their mass (MS) and their sequence (MS/MS). This information was used by the Mascot algorithm to identify the proteins which the peptides came from by searching the Swiss-Prot database. Only metazoan proteins were included in such searches. For the experimental samples a hit was defined as a protein identified by two tryptic peptides with an Xcorr value greater than 10.0. I used looser screening criteria to establish hits within the control sample, a single tryptic peptide with an Xcorr value of 5.0, to guarantee that all the possible contaminants were included in the analysis. Upon comparison of the control and experimental samples, I found several proteins to be unique to the His_6-SUMO purifications; a list of such proteins is included in **Table 3.1** and its features are discussed in detail below.

Protein identified	Uniprot accession
Cortactin	Q01406
Actin	Multiple
Amplaxin	Q14247
Bromodomain-containing protein 3	Q15059
EF2	P29691
Gephyrin	Q9NQX3
IL8	P08317
Lamin A	P11048
Lamin A/C	Q3ZD69
LIMA1	Q9UHB6
MCM2	P49736
MCM3	P49739
Myosin 11	P10587
ORC4	O93479
PINK1	Q9BXM7
Protein polybromo 1	Q86U86
Supervillin	O95425
Triadin	Q13061
Ubiquitin protein ligase E3B	Q7Z3V4

Table 3.2 - Proteins identified in the Ni^{2+}-NTA pull-down that was carried out on chromatin isolated from extracts devoid of His_6-SUMO.

Comparing the datasets described in other sumoylation-centred proteomic studies with each other reveals that relatively limited overlap exists amongst the SUMO targets identified. This means that such studies did not find all of the SUMO substrates in a cell, but in fact only a few. To examine whether the proteomic approach I carried out also missed some sumoylation targets, I analyzed the His_6-SUMO1 and control purifications by western blotting with antibodies available at the Clare Hall Laboratories that could recognize the *Xenopus* orthologues of proteins involved in DNA metabolism, such as ORC1, MCM7 and RPA70. PCNA was used as a positive control because it had been previously reported to be sumoylated on chromatin during S phase in frog egg extracts (Leach and Michael, 2005). **Figure 3.6** confirms that PCNA was sumoylated in this system. In addition, it shows that ORC1, and possibly RPA70, were also modified since a slow-migrating form of the proteins was observed solely in the His_6-SUMO1 affinity purifications. No modification of MCM7 was detected. These results indicate that the proteomic approach described here did not identify the complete cohort of chromatin-associated targets of SUMO in frog egg extracts.

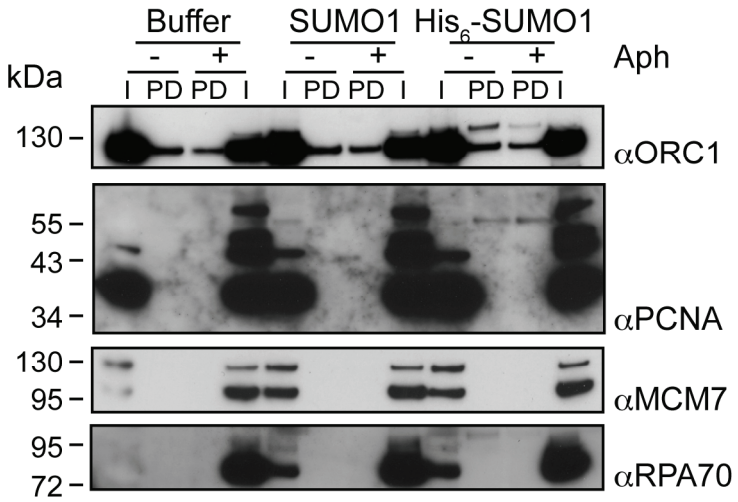

Figure 3.6 - Identification of sumoylated species from replicating chromatin under normal conditions and in the presence of genotoxic stress by western blotting. Sumoylated *Xenopus* proteins isolated as described in Figure 3.5B were analyzed by western blotting with antibodies against ORC1, PCNA, MCM7 and RPA70. I = Input chromatin, PD = Ni^{2+}-NTA pull-down.

3.2.6 Validation of sumoylation substrates in frog egg extracts and budding yeast

To validate the proteomic approach described in the previous paragraph, I needed to confirm by western blotting the modification of some of the novel sumoylation targets that were identified. The catalytic subunit of DNA polymerase α (Pol α) was an interesting candidate because it was detected only in the presence of aphidicolin and I found a commercially available antibody that could recognize the *Xenopus* orthologue of this protein. When chromatin-associated His_6-SUMO1 conjugates were analyzed by western blotting to visualize Pol α, a distinct slow-migrating form of the protein was detected only in the presence of genotoxic stress (**Figure 3.7**A). However, the observation that under such conditions the quantity of Pol α bound to the DNA was greatly increased in comparison to the untreated extract raised the possibility that this result originated from a difference in the amounts of the polymerase present in the input material. To address this issue, I analyzed the amount of sumoylated polymerase present in His_6-SUMO1 conjugates isolated from a quantity of untreated and aphidicolin-treated chromatin that contained equivalent levels of Pol α. I observed that, even under these experimental conditions, in the presence of genotoxic stress the levels of the sumoylated Pol α were increased (**Figure 3.7**B). However, I also noticed that when the extracts were treated with aphidicolin the non-specific binding to the Ni^{2+}

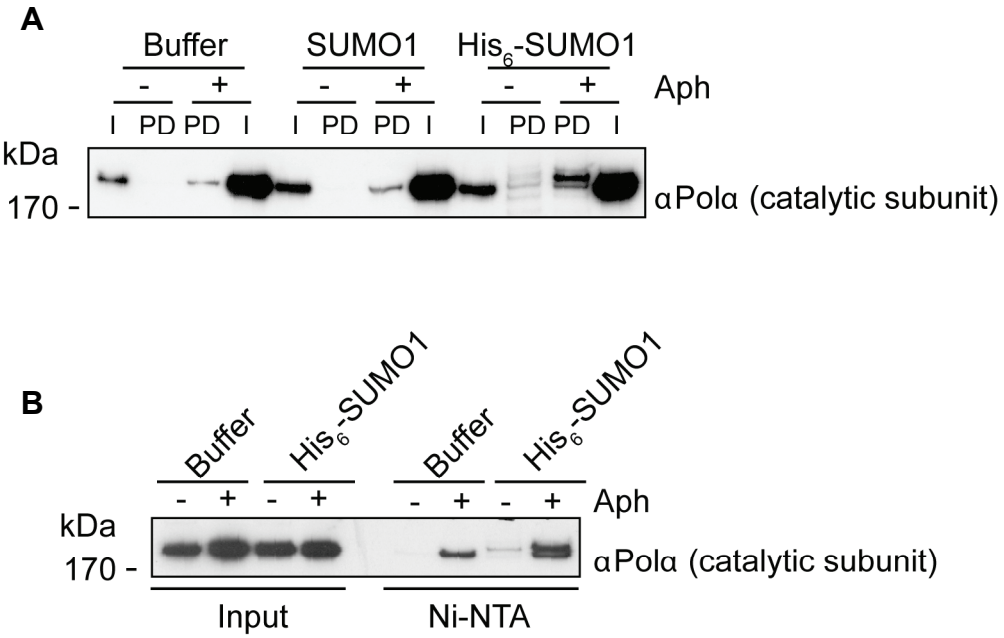

Figure 3.7 - The catalytic subunit of DNA polymerase α bound to interphase chromatin is sumoylated. A) Sumoylated *Xenopus* proteins isolated as described in Figure 3.5B were analyzed by western blotting with antibodies against the catalytic subunit of Pol α. I = Input chromatin, PD = Ni^{2+}-NTA pull-down. B) The experiment described in A) was repeated using amounts of chromatin that contained equivalent levels of Pol α. Aph = aphidicolin.

resin of the unmodified Pol α itself was enhanced (**Figure 3.7**B). These data indicate that although Pol α is likely to be sumoylated in frog egg extracts, this modification appears to be largely independent on genotoxic stress.

To further substantiate the validity of the proteomic approach I employed, I needed to confirm that those sumoylated proteins identified by means of adding exogenous SUMO to the extracts were also modified in the presence of endogenous levels of the modifier. Towards this end, I attempted to immunoprecipitate Pol α from untreated and aphidicolin-treated chromatin that had been solubilized by sonication. Unfortunately, the antibody was unable to efficiently isolate enough protein to analyze the immunoprecipitate by western blotting against SUMO1 and/or SUMO2 (data not shown).

To circumvent these limitations and provide stronger evidence of the validity of the above-described screen, I decided to explore the possibility that particularly interesting hits amongst the proteins reported in **Table 3.1** may be sumoylated beyond *X. laevis*. As a matter of fact, many of them are well-conserved throughout evolution and show orthologues in lower organisms such as *S. cerevisiae*. If the sumoylation of these

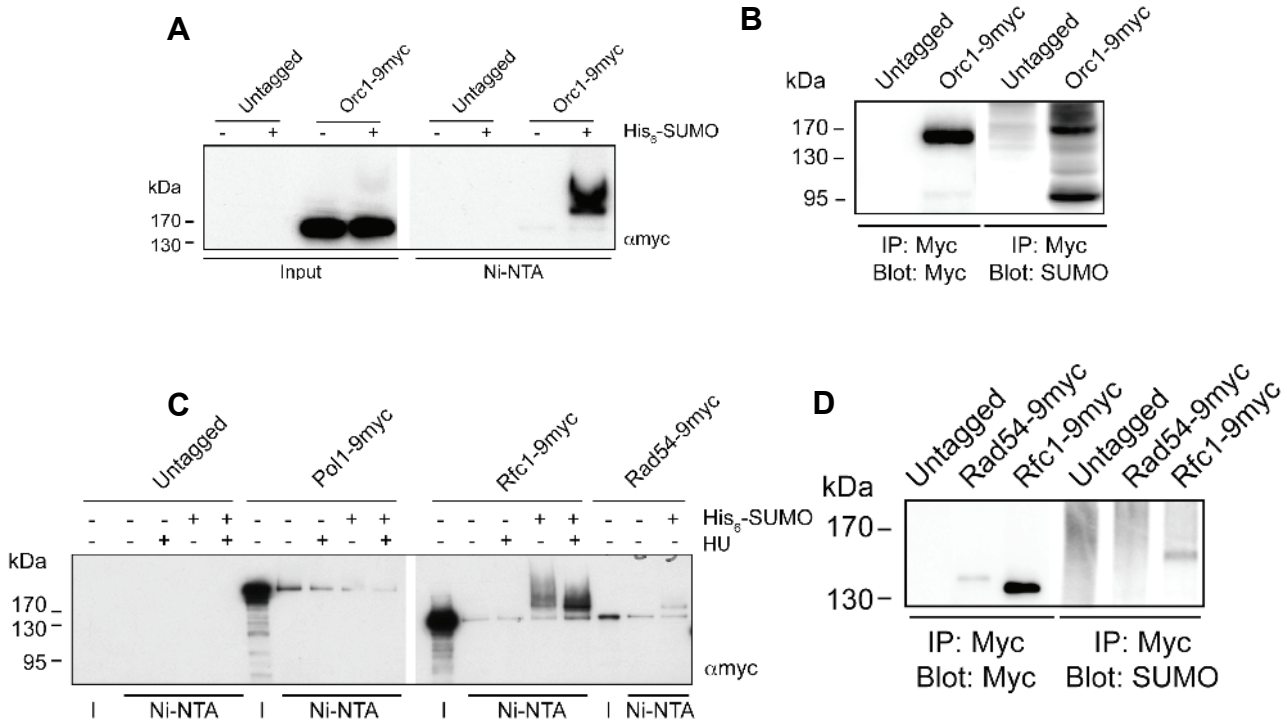

Figure 3.8 - Orc1, Rfc1 and Rad54 are sumoylated in *S. cerevisiae*. A) and C) Exponentially growing cells (75 OD_{600}) transformed with a control or a His_6-SUMO expression plasmid were lysed under alkaline conditions (2.8.4.1). His_6-SUMO-modified species were captured as described in 2.16.1 and subjected to western blotting against the 9myc tag. I = input, HU = hydroxyurea, 200 mM for 1.5 h. B) and D) Extracts (2 mg of total protein in 1 ml of RIPA buffer) of exponentially growing cells (75 OD_{600}) were obtained by mechanical lysis in RIPA buffer followed by centrifugation (2.8.4.2). An anti-Myc antibody (8 µg) was incubated with the extracts for 3 h at 4°C and then captured as described in 2.16.2. Immunoprecipitated proteins were analyzed by western blotting against the 9myc tag and SUMO. IP = immunoprecipitation.

proteins were conserved among different species, I could take advantage of the strengths of each system to investigate the modification's functions. Consequently, I created yeast strains in which the orthologues of *Xenopus* ORC1, RAD54B, RFC1 and Pol α (*POL1*) were C-terminally fused to the 9myc tag at their endogenous locus. *MEC1*, the yeast orthologue of ATR, was not included in this analysis because all my attempts to append a tag to it were unsuccessful. These strains were transformed with either a control or a His_6-SUMO expression plasmid, which allowed me to isolate their SUMO conjugates by denaturing Ni^{2+}-NTA affinity chromatography. Since RFC1 and the catalytic subunit of Pol α were identified only from the chromatin of aphidicolin-treated frog egg extracts, the strains carrying Rfc1-9myc and Pol1-9myc were also treated with hydroxyurea, which causes problems similar to those of aphidicolin in yeast cells and it is able to cross their cell wall. Western blotting of such purifications showed the presence of slow-migrating forms of Orc1-9myc, Rad54-9myc and Rfc1-

9myc, but not Pol1-9myc (**Figure 3.8**A and C) only in those strains expressing His_6-SUMO, thus showing that they are sumoylated. In addition, the presence of hydroxyurea did not significantly alter the extent of Rfc1p-9myc sumoylation. To confirm that the 9myc-fusions of Orc1, Rad54 and Rfc1 were modified even in the absence of His_6-SUMO, I isolated them from native lysates prepared from strains expressing normal SUMO levels, by means of an anti-Myc antibody, and analyzed them by western blotting against SUMO itself. **Figure 3.8**B and D show that even after stringent washing of the immunoprecipitates Orc1-9myc and Rfc1-9myc co-purified with sumoylated species of the expected size for a covalent SUMO conjugate of such proteins, thus demonstrating that they are *bona fide* sumoylation targets in yeast. Unfortunately, the endogenous levels of Rad54-9myc were too low to isolate enough protein for detection of sumoylation products, thus it remains to be determined whether Rad54p is a genuine SUMO target in budding yeast.

3.3 Discussion

Although sumoylation clearly plays an important role in controlling DNA metabolism and therefore in maintaining genome stability, to date the modification of only a handful of proteins has been shown to be stimulated by genotoxic stress and/or linked to this biological process. To overcome such shortcomings, I decided to identify and compare the population of sumoylated species that bind to chromatin during unperturbed and challenged replication. Using frog egg interphase extracts as a model system, I initially confirmed the presence of sumoylated proteins on replicating DNA and then studied their abundance throughout S phase. Having observed a population of SUMO conjugates on the chromatin whose abundance largely depended on entry in S phase but was not visibly affected by genotoxic stress, I isolated such species and identified them by both mass spectrometry and western blotting. Interestingly, a few novel sumoylation targets were identified exclusively in the presence of genotoxic stress.

3.3.1 Is the proteomic dataset valid?

Given the initial aims of this part of my research (see 3.1), I evaluated the validity of the proteomic dataset presented here against three criteria: 1) the complexity of the dataset, that is, the enrichment of proteins that associate with DNA versus those that do not, 2) the likelihood of the identified proteins to be true SUMO substrates, and 3) the probability of those hits detected only in the presence of genotoxic stress to be *bona fide* DNA damage-induced SUMO.

3.3.1.1 Dataset complexity

The overall complexity of the dataset seems to be satisfactory. Most of the identified candidates fall within one of three functional categories, which mainly encompass proteins important for DNA metabolism, such as: DNA replication and repair, chromatin remodelling and transcription. A few proteins (11 out of 51) that are known not to associate with DNA were detected in the experimental samples (**Table 3.1**). The most obvious example of these is RANGAP1, which is one of the most abundant SUMO1 substrate in higher eukaryotes and therefore it may not be an unexpected contaminant (Mahajan *et al.*, 1997; Saitoh *et al.*, 1997). Comparing the functional distribution of the sumoylation targets that were detected in the present analysis with those from previous proteomic studies also indicates that I enriched for chromatin-associated proteins. In such studies, 40-50% of the hypothetical SUMO substrates identified fall within one of the three above-mentioned categories (Denison *et al.*, 2005; Rosas-Acosta *et al.*, 2005), this percentage rises to 80% in the current dataset. Additionally, several proteins involved in processes other than DNA metabolism were identified in those studies, such as cell metabolism, cell cycle, apoptosis, signalling, translation, mRNA processing and nucleocytoplasmic transport (Golebiowski *et al.*, 2009; Rosas-Acosta *et al.*, 2005; Vertegaal *et al.*, 2006; Zhao *et al.*, 2004b), which were instead barely detected in the present analysis. It must be mentioned that a few proteins involved in cell metabolism and cell cycle were identified only in the experimental samples but these were not included in **Table 3.1** because they were detected by a single low-confidence peptide. Interestingly, in contrast to previous proteomic studies where transcription factors often represented a significant proportion of the identified SUMO substrates (Golebiowski *et al.*, 2009; Rosas-Acosta *et al.*, 2005; Vertegaal *et al.*, 2006), the present analysis discovered relatively few of them. It is possible that the sumoylated forms of some of these factors may not be associated with the chromatin, *de facto* excluding them from the current analysis. Alternatively, transcription factors themselves may not be an abundant population of proteins that associates with chromatin in frog egg extracts, where in fact very little transcription occurs (Masui and Wang, 1998).

3.3.1.2 Are the identified hits true SUMO targets?

The likelihood of the identified hits being true SUMO substrates is also good. Many of them have meanwhile been reported to be sumoylated in other proteomic studies or more directly by pull-down experiments and western blotting, from budding yeast to

human cells. With respect to proteins involved in DNA metabolism, this includes PCNA (Arakawa *et al.*, 2006; Hoege *et al.*, 2002; Leach and Michael, 2005), RAD52 (Sacher *et al.*, 2006), PARP1 (Blomster *et al.*, 2009; Golebiowski *et al.*, 2009; Martin *et al.*, 2009; Messner *et al.*, 2009; Rosas-Acosta *et al.*, 2005) and topoisomerase II (Azuma *et al.*, 2003; Bachant *et al.*, 2002; Mao *et al.*, 2000a). Recently a thorough quantitative proteomic approach also showed that the sumoylation of the catalytic subunit of Pol α, RFC1 and RAD54B is increased after heat shock in human cells (Golebiowski *et al.*, 2009). Several factors involved in chromatin remodelling and transcription have also been shown elsewhere to be modified by SUMO, such as HDAC1 (David *et al.*, 2002), NCOR1/2 (Tiefenbach *et al.*, 2006), SALL1 (Netzer *et al.*, 2002), SALL4 (Golebiowski *et al.*, 2009), SIN3A (Pungaliya *et al.*, 2007), TRRAP (Golebiowski *et al.*, 2009), RBBP7 (Golebiowski *et al.*, 2009) and p66 (Gong *et al.*, 2006). It is conceivable that some of the remaining hits may represent false positives, that is, proteins that are not truly sumoylated, which could arise when a protein that spuriously binds to the Ni^{2+}-NTA resin is not detected in the control purification. To minimize the occurrence of false positive, I analyzed the raw data against stringent filtering criteria, as described earlier, and lowered the threshold for identifications from two peptides for the SUMO purification to one peptide for the control purification.

3.3.1.3 SUMO substrates from intact and aphidicolin-treated chromatin

Amongst the proteins with a role in genome stability that were identified in the present proteomic analysis, some were exclusively detected within the samples of intact (RAD54B and PARP1) or aphidicolin-treated chromatin (the catalytic subunit of Pol α, RFC1, ATR, RTEL1, WDHD1, PLK1 and PCNA), while others in both of them (aprataxin, RAD50 and topoisomerase IIα/β). I was particularly interested in verifying that the hits present in the second category were true DNA-damage-induced SUMO substrates. As a prototypical example I studied the sumoylation of the catalytic subunit of Pol α. **Figure 3.7** strongly suggests that the sumoylated form of this protein was detected exclusively from aphidicolin-treated chromatin because Pol α itself is heavily enriched on DNA under such conditions. These observations illustrate an important limitation of the strategy used in the current proteomic study. The big changes in protein composition that chromatin undergoes throughout replication and upon certain stimuli (Khoudoli *et al.*, 2008) makes it hard to distinguish between a factor that is specifically sumoylated during replication or after DNA damage from one, for instance,

that is either constitutively modified but associates with DNA only in the presence of genotoxins or one that is not normally sumoylated but becomes conjugated to SUMO when it binds to DNA, irrespectively of whether it is damaged or not. The second one of these three scenarios is likely to be true for Pol α and possibly ATR, which has been previously shown to preferentially interact with damaged DNA (Costanzo *et al.*, 2003). Given the limited quantitative nature of the proteomic approach I employed, a firm conclusion about the DNA-damage dependency of those SUMO substrates detected in the aphidicolin-treated chromatin only by two peptides, such as PCNA and PLK1, is also hard to draw. In fact, the sumoylation of PCNA was not enhanced by aphidicolin when this was analyzed by western blotting (**Figure 3.6**). On the other hand, RAD54 and PARP1 were identified only during unperturbed replication (**Table 3.1**). Although it is possible that aphidicolin may inhibit the sumoylation of these proteins, it is also not improbable that it could lead to a transient loss of RAD54B and PARP1 from the chromatin. In conclusion, the chromatin-associated SUMO substrates that were identified only in response to genotoxic stress represent an interesting group of proteins whose modification could be linked to damaged DNA. In the future, it will be useful to prove that these findings are true on an individual basis.

Although only a few proteins with a role in genome stability were identified in both normal and aphidicolin-treated DNA (see above), most chromatin remodeling and transcription factors fell in this category, thus suggesting that their sumoylation may be related to a process that is unaffected by genotoxic stress.

3.3.2 Is the proteomic dataset complete?

The proteomic dataset described in this chapter is unlikely to represent the complete cohort of SUMO substrates that bind to the chromatin during normal and disrupted replication for at least two reasons. Firstly, using western blotting I could identify sumoylated proteins on the chromatin that were not detected by mass spectrometry, such as ORC1 (**Figure 3.6**). These proteins may have been missed because they do not bind well to the affinity resin or because they are modified at such low levels that they cannot be detected by mass spectrometry. As a matter of fact, the sensitive proteomic approach used by Golebiowski *et al.* (2009) allowed them to identify several proteins with a role in genome stability that were not detected in the current study. Although I cannot exclude that such proteins may be sumoylated away from DNA, at least some of them are likely to be modified on chromatin. The presence of false positives, that is, those proteins that are truly sumoylated but were not included in

Table 3.1 because they were identified in both the control and SUMO purifications, also contributes to limiting the completeness of the dataset presented. This may have been, for instance, the case of MCM2 and MCM3, which were identified in both the control and His_6-SUMO2 purifications, but they are in fact likely to be true SUMO2 substrates because they have been detected in another proteomic study (Golebiowski *et al.*, 2009). Although the modification of MCM2 and MCM3 were not directly confirmed in such report, the highly stringent tandem affinity purification they used to isolate sumoylated proteins argues in favour of such hits being true SUMO targets rather than common contaminants of Ni^{2+}-NTA-based SUMO-enriching protocols.

3.3.3 Modification by SUMO1 *vs.* SUMO2

Although the proteomic strategy described here is mostly qualitative, it allowed me to notice some differences with respect to the levels and distribution of SUMO1- and SUMO2-modified proteins. Overall, more peptides and proteins were identified from the SUMO2 purifications compared to those of SUMO1 (**Table 3.1**). Only six proteins were identified exclusively as a SUMO1 substrate, while 23 hits were detected only from the SUMO2 purifications. The 22 remaining SUMO1 substrates were also modified by SUMO2. Interestingly, when equivalent amounts of His_6-SUMO1 and His_6-SUMO2 were added to interphase extracts, His_6-SUMO2 species appeared to be more abundant than those conjugated to His_6-SUMO1 on the chromatin (**Figure 3.2**).

The exclusive, or near exclusive, identification of many chromatin-associated proteins only in the His_6-SUMO2 purifications suggests that even when SUMO1 is added in excess to the extract a certain degree of paralogue-specific modification may be maintained. For example, topoisomerase II, which is a prototypical chromatin-associated substrate of SUMO2 (Azuma *et al.*, 2005; Azuma *et al.*, 2003), was mostly modified by SUMO2 (**Table 3.1**). Given that topoisomerase II was originally identified as a SUMO1 substrate in frog egg extracts, it was not unexpected to detect some modification of this protein also by SUMO1 (Azuma *et al.*, 2003). On the other hand, the identification of topoisomerase II itself as a SUMO substrate on replicating chromatin was surprising because this modification event normally occurs in mitosis (Azuma *et al.*, 2005; Azuma *et al.*, 2003). Although it cannot be excluded that even if cycloheximide-treated interphase extracts were used some nuclei may have “leaked” into mitosis, thus providing the ideal conditions for topoisomerase II sumoylation, it is possible that the addition of exogenous SUMO to the extract may have loosened the cell cycle-dependence or paralogue-specificity of this modification event.

Interestingly, SUMO2 was detected in the His_6-SUMO1 purifications, thus suggesting that some of the identified proteins may be either simultaneously sumoylated by SUMO1 and SUMO2 at different sites, such that when His_6-SUMO1 is immobilized SUMO2 is carried over, or conjugated to a mixed SUMO2/1 chain where the SUMO1 moiety may act as a termination signal (Golebiowski *et al.*, 2009; Matic *et al.*, 2008). The latter possibility in turn suggests that those proteins identified in both the SUMO1 and SUMO2 purifications may not be species that are directly conjugated to SUMO1. Conversely, why SUMO1 was not detected in the His_6-SUMO2 purifications is harder to explain, but it may be because of the small amounts of this modifier in such samples.

The good size-resolution of the dataset presented here, achieved by slicing the control and experimental lanes in many bands, revealed that several of those proteins identified in the His_6-SUMO2 purifications, and only a few in the His_6-SUMO1 samples, were detected in two or more bands (**Table 3.1**). For instance, topoisomerase II, CHD1 and CHD7 were detected in up to seven or eight bands (data not shown). The good correlation between the size of the identified hits and their positions on the gel (data not shown) argues in favour of them being modified by either single SUMO2 moieties at multiple sites, or more likely, by a SUMO2 chain, rather than representing partial degradation of sumoylated proteins.

3.3.4 Advantages and limitations of the proteomic approach employed

I identified advantages and disadvantages for three key aspects of the proteomic approach described in this chapter: the model system and the tag that I used to purify sumoylated species and the mass spectrometry technique employed to identify them.

The innate ability of DNA added to frog egg extracts to replicate synchronously means that in this system replicating chromatin can be caught more easily than in mammalian or yeast cells where time-consuming synchronization techniques are otherwise needed. Chromatin can be isolated in just a few minutes from egg extracts, with very little contamination from cyto- and nucleoplasmic proteins. Much lengthier and difficult protocols have to be used to isolate chromatin from yeast or mammalian cells, thus increasing the chance of SUMO isopeptidases acting on their substrates. As I discussed earlier, identifying sumoylated species from replicating DNA also helped to enrich for those proteins whose modification could be important in DNA metabolism. On the other hand, using frog egg extracts and chromatin as a model system was disadvantageous for two reasons. Firstly, the significant changes in protein composition that chromatin experiences throughout S phase and in response to certain stimuli

(Khoudoli *et al.*, 2008) makes it a rather heterogeneous input material to work with. The recent development of a strategy to isolate significant amounts of highly purified sumoylated species from total cell extracts (Golebiowski *et al.*) could be a solution to this problem because the total levels of a certain protein is unlikely to change in response to DNA damage in total cell extracts as much as it would do in the chromatin fraction. Secondly, only a relatively small amount of chromatin can be isolated from interphase extracts, even when large preparations are used, in comparison to what could be obtained from large volumes of yeast or mammalian cell cultures. For example, Golebiowski *et al.* (2009) used fifty dishes (∅ = 150 mm) of HeLa cells per condition they tested in their recent proteomic survey. If the cells were collected when they were 80-90% confluent (~$2 \cdot 10^7$ cells per dish), it follows that they must have used ~ $1 \cdot 10^9$ cells per condition. In frog egg extracts, sperm nuclei are typically used at a concentration of 2,000-3,000 units per µL of extract to ensure that DNA replication proceeds at a "normal" rate and is properly controlled. Thus, to isolate ~ $1 \cdot 10^9$ replicating frog nuclei one would need to use between 300 mL and 500 mL of *Xenopus* egg extracts. This is likely to be a conservative estimate because it does not take into account the difference in size between a diploid human genome (~ 6 pg) and that of a haploid frog nucleus (~ 3 pg). A good batch of eggs normally yields 2-3 mL of extract.

By using His_6-tagged SUMO, I was able to isolate sumoylated species by metal affinity chromatography under stringent denaturing conditions, thus minimizing the activity of SUMO isopeptidases and the chance of co-purifiying proteins that non-covalently interact either with SUMO itself or with a sumoylated protein because, for example, they are part of the same complex. The small size of the His_6 tag fused to SUMO also reduced the chance of compromising the sumoylation of certain substrates, which has been reported when bigger tags are used (Wohlschlegel *et al.*, 2004). On the other hand, as it has been described in previous proteomic studies (Vertegaal *et al.*, 2004; Wohlschlegel *et al.*, 2004), the non-specific affinity of the Ni^{2+} resin for highly abundant and/or histidine-rich proteins combined with the low abundance of sumoylated species means that although His_6-SUMO purifications are enriched for SUMO conjugates, they unavoidably contain contaminants. I have taken several steps towards eliminating such proteins, as described in 3.2.5. In other proteomic studies, these limitations have been partly circumvented by using different types of tandem-affinity purification tags (Denison *et al.*, 2005; Golebiowski *et al.*, 2009; Hannich *et al.*, 2005; Zhou *et al.*, 2004), which do yield much cleaner preparations of SUMO conjugates but they have to be used under native conditions. An interesting alternative to both denaturing and native

approaches could be the use of a biotinylated form of SUMO, which can be captured on a streptavidin support under partially denaturing conditions (Li *et al.*, 2004b).

The employment of LC MS/MS and Orbitrap technologies was another important advantage of the proteomic study presented here. Its high sensitivity, accuracy and specificity compared to other spectrometric techniques was instrumental in identifying and sequencing complex mixtures of low-abundance peptides such as those obtained from a pool of sumoylated protein. Additionally, the very good mass accuracy of the instrument employed (<2 ppm) gave us confidence in the relevance of even those proteins detected by only one or two peptides. The low abundance of chromatin-associated species that are sumoylated, and consequently of the peptides derived from them, made it difficult to quantify differences between the different populations of modified proteins, even if using semi-quantitative approaches such as comparing the signal intensity or the number of fragment spectra of peptides belonging to a certain protein. The employment of more quantitative spectrometric techniques, rather than simply scoring for the presence or absence of a protein in a sample, could have yielded more information, especially with respect to those species for which genotoxic stress upregulated, rather than absolutely induced, their sumoylation. The development of highly comparative and quantitative spectrometric techniques such as stable isotope labelling with amino acids in cell culture (SILAC), which has been successfully used to identify heat shock-induced targets of sumoylation (Blomster *et al.*, 2009; Golebiowski *et al.*, 2009), may be a solution to this problem.

Chapter 4. Results II: Sumoylation of ORC in frog egg extracts and *S. cerevisiae*

4.1 Introduction

Amongst the targets of sumoylation that were identified in the screen I described in the previous chapter, I analyzed further the modification of ORC1 for several reasons. ORC1, as part of the origin recognition complex (ORC), plays a central role in the initiation of DNA replication (see below). Although it has been shown that sumoylation can protect replication forks during S phase in the presence of DNA damage (Branzei *et al.*, 2006) and that SUMO chain formation is important for the response to DNA replication arrest (Skilton *et al.*, 2009), little is known about whether SUMO normally impinges on DNA replication. Additionally, the finding that ORC1 is sumoylated in both yeast and frog egg extracts raised the possibility that this modification might play an important role throughout evolution.

ORC was originally identified in budding yeast as a six-subunit complex (Orc1-6) that specifically bound to an origin of DNA replication (Bell and Stillman, 1992). Since then, evolutionarily related six-membered complexes have been identified in and/or purified from various organisms, including the fruit fly (Gossen *et al.*, 1995), frog egg extracts (Tugal *et al.*, 1998) and humans (Dhar and Dutta, 2000). With the exception of ORC6, which is poorly conserved throughout evolution, orthologues of the yeast Orc1-5 have been found in all eukaryotes. These proteins share a conserved AAA+ ATPase fold that contains Walker A and Walker B motifs, which are absent from ORC6. ORC1-5 are therefore thought to have a common evolutionary origin (Duncker *et al.*, 2009).

In all the organisms analyzed to date, ORC is essential for the initiation of DNA replication. Its principal function is to bind origins of replication and act as a landing pad for the ordered recruitment of several factors collectively known as the pre-replication complex (pre-RC), reviewed by Takeda and Dutta (2005). During late mitosis and early G_1 phase, the ORC bound to replication origins becomes competent to recruit CDC6 to the DNA, thus allowing CDT1 to load the replicative helicase MCM2-7 at such locations and producing a pre-RC. As cells progress into S phase, pre-RCs are converted into replication forks through a series of steps. CDC6 and CDT1 leave the pre-RC, MCM10 binds to it and the activities of DBF4-dependent (DDK) and cyclin-dependent kinases (CDK) increase, which lead to the recruitment of CDC45, Dbp11 (TOPBP1 in higher eukaryotes), SLD2/3 and GINS. These events allow unwinding of the DNA around the

origin of replication and the subsequent loading of the ssDNA-binding protein RPA and DNA polymerase α, which initiates DNA synthesis (Mimura *et al.*, 2000). Once origins of replications have fired, they are prevented from doing so again until the next cell cycle through various mechanisms. These safeguards ensure that genomic DNA is not re-replicated, which could otherwise lead to genome instability, reviewed by Blow and Dutta (2005). The increase in CDK activity that occurs from the beginning of S phase until the end of mitosis leads to inactivation of the pre-RC through the phosphorylation of CDC6 and CDT1, which are consequently exported from the nucleus or degraded depending on the organism examined. MCM2-7 and ORC are also phosphorylated by CDKs and thereby inactivated. The drop in CDK activity that occurs at the end of mitosis allows the assembly of new pre-RCs. In higher eukaryotes, an additional mechanism has evolved to prevent DNA re-replication, which depends on the protein geminin. Geminin, which is absent in the G_1 phase but accumulates throughout the cell cycle, binds to CDT1 and prevents it from interacting with MCM2-7.

Although the essential functions of ORC appear to be conserved throughout evolution, the way in which the complex recognizes origins of replication and is regulated during the cell cycle can vary between organisms. In budding yeast, all origins of replication contain an 11 bp consensus sequence, which is essential for ORC binding, plus additional elements that also contribute to this event (Bell and Stillman, 1992; Rao and Stillman, 1995; Rowley *et al.*, 1995). In fission yeast, origins do not share any consensus but they often contain two or more asymmetric AT-rich sequences (Okuno *et al.*, 1999; Segurado *et al.*, 2003), which are recognized by AT-hook motifs found within the Orc4 subunit (Chuang and Kelly, 1999). In human cells, origins can localize to defined genomic loci (Giacca *et al.*, 1994; Heintz and Hamlin, 1982), yet any sequence can act as one, provided it is long enough (Heinzel *et al.*, 1991). Factors other than sequence therefore appear to define the location of our origins, such as transcriptional activity (Lin *et al.*, 2005), epigenetic mechanisms (DNA methylation, histone acetylation and chromatin compaction, Goren *et al.*, 2008; Mechali, 2001; Rein *et al.*, 1999), the presence of specific DNA binding elements (Danis *et al.*, 2004) and nuclear organization (Li *et al.*, 2001). Transcription may also be responsible for those changes in origin specification that are observed in early embryonic systems such as frog and fly embryos. During the first few cleavages after fertilization, origins occur apparently randomly along the DNA but are nevertheless evenly spaced; when zygotic transcription starts at the mid-blastula transition the locations of origins become more specific (Hyrien *et al.*, 1995).

In addition to having different modes of defining replication origins, the ORCs from yeast, frog egg extracts and mammalian cells are regulated in somewhat different ways with respect to their post-translational modifications and binding to chromatin during the cell cycle. In budding yeast, ORC remains bound to origins throughout the cell cycle (Liang and Stillman, 1997). Orc2 and Orc6 are phosphorylated by CDKs from S phase until mitosis, which helps to prevent the re-assembly of pre-RCs until the next G_1 phase (Nguyen *et al.*, 2001). In interphase frog egg extracts, ORC quickly binds to sperm chromatin during interphase and it is released from it only at mitosis, probably due to its CDK-dependent phosphorylation. The recruitment of MCM2-7 to pre-RCs also leads to a weakening of the binding of ORC to chromatin, which is detected as a change in its patterns of salt extraction from the DNA (Rowles *et al.*, 1999). In mammalian cells, a core ORC2-5 complex remains bound to chromatin throughout the cell cycle (Ohta *et al.*, 2003). ORC1 also stably associates with DNA during the G_1 phase, but as cells progress through to S phase this binding weakens, which causes ORC1 to be selectively released from the chromatin and subsequently ubiquitylated (Li and DePamphilis, 2002). Depending on the cell line tested the ubiquitylated ORC1 may or may not be degraded by the proteasome (Li and DePamphilis, 2002; Mendez *et al.*, 2002). In those cells where ORC1 persists throughout the cell cycle, it becomes phosphorylated during mitosis, which may prevent its re-association with ORC2-5 (Li *et al.*, 2004a). Once this phase is completed ORC1 is re-synthesized and/or becomes competent to bind chromatin again (Mendez *et al.*, 2002).

Even though the main function of ORC is in DNA replication, this complex, or parts of it, have been shown to play roles in other processes as well. Some of these alternative functions, such as the regulation of the S phase checkpoint and the attachment of properly condensed chromosome to the mitotic spindle (Gibson *et al.*, 2006), are likely to be secondary effects of disturbing ORC's role in replication and therefore will not be described here (Sasaki and Gilbert, 2007). ORC plays a conserved role in establishing transcriptionally inert chromatin. In budding yeast, Orc1 interacts with Sir1, which mediates the formation of silent chromatin at the mating type loci *HMR* and *HML* (Bell *et al.*, 1993; Triolo and Sternglanz, 1996). In both the fruit fly and human cells, ORC interacts with and is important for the correct localization of HP1 (Lidonnici *et al.*, 2004; Pak *et al.*, 1997), which represents the fundamental unit of heterochromatin packaging in higher eukaryotes. Additionally, ORC also appears to play a role in establishing sister chromatid cohesion in budding yeast (Shimada and Gasser, 2007). Depleting Orc2 after the firing of replication origins causes signs of precocious separation of

sister chromatids, the activation of the spindle assembly checkpoint and mitotic arrest with normal levels of chromatid-loaded cohesin. Re-expressing *ORC2* at the G_2/M transition rescues this phenotype, thus indicating that ORC mediates cohesion independently of cohesin or replication. Finally, an intriguing function of ORC6 has been uncovered in fly and mammalian cells, where the protein localizes to the cleavage furrow during cytokinesis (Chesnokov *et al.*, 2003; Prasanth *et al.*, 2002). Knocking down ORC6 in such systems leads to the accumulation of multi-nucleated cells, which probably originate from cells that completed mitosis but not cytokinesis.

The aim of this part of my thesis was: 1) to confirm that ORC1 is a true target of sumoylation in frog egg extracts and yeast, 2) to explore whether this modification event is controlled at the spatial and/or temporal levels, as this information could provide clues about the roles it may have, and finally 3) to investigate its possible functions.

4.2 Results

4.2.1 ORC1 is a *bona fide* sumoylation target in frog egg extracts

The results presented in **Figure 3.6** indicated that in frog egg extracts ORC1 might be a target of sumoylation, possibly on the chromatin only. To further confirm this finding, I studied the sumoylation of this protein in more detail by multiple approaches.

Firstly, I asked whether ORC1 could be sumoylated in an *in vitro* sumoylation reaction. Recombinant His_6-ORC1 or a more native source of the protein, *i.e.* chromatin isolated from interphase extracts, was mixed with SUMO1, SUMO conjugating enzymes and ATP, incubated, and then analyzed by western blotting against ORC1. **Figure 4.1**A shows that only when all the required reagents were present both the recombinant and chromatin-associated ORC1 proteins were sumoylated. I also noticed that the SUMO-modified ORC1 produced in the complete reaction supplemented with chromatin ran at the same size as a slow-migrating, and very weak, form of ORC1 that was present in the control reactions.

This result prompted me to explore the possibility that such slow-migrating form of ORC1 may represent sumoylation on the chromatin. I separated chromatin-associated proteins from the soluble fraction of the extracts at mid S phase and then analyzed them by western blotting against ORC1. **Figure 4.1**B shows that in addition to a major ~130 kDa species, the soluble ORC1 displayed two slow-migrating forms. These bands may be ubiquitylated forms of such protein, which have been previously detected in the

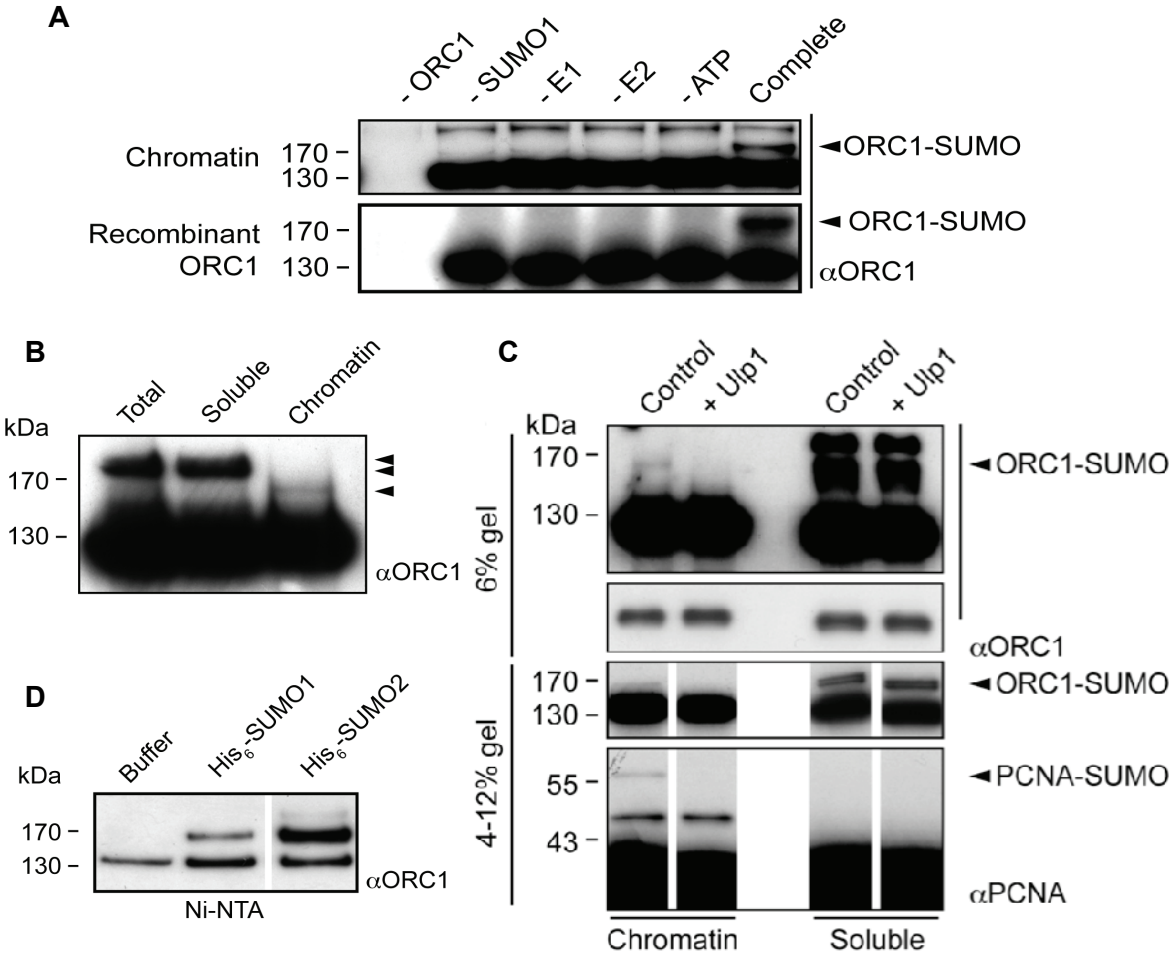

Figure 4.1 - ORC1 is a true substrate of sumoylation in frog egg extracts. A) Recombinant ORC1-His_6 (~3 pmol) and interphase chromatin (~30,000 nuclei) were sumoylated *in vitro* in standard reactions (see 2.17.1) containing all the required components or lacking individual ones and then analyzed by western blotting against ORC1. B) Interphase extracts were supplemented with 2,500 nuclei·μL^{-1} and incubated for 20 min at 23°C before being separated into soluble and chromatin fractions. For western blotting analysis, I loaded ~20,000 nuclei of the chromatin fraction and 0.4 µL of the total and soluble ones (~15 µg). C) Soluble (~15 µg) and chromatin fractions (~20,000 nuclei) prepared as described in B) were incubated in the presence or absence of 50 nM of the catalytic domain of Ulp1 in a total volume of 20 µL for 1 h at 30°C. The products of the reactions were resolved on both 4-12% and 6% gels and then analyzed by western blotting against ORC1 and PCNA (loading control). D) Sumoylated proteins isolated as described in Figure 3.5B were analyzed by western blotting against ORC1.

non-chromatin-associated fraction of extracts prepared from mammalian cells (Li and DePamphilis, 2002). Conversely, the chromatin-associated ORC1 was resolved as one major and one retarded band only, the latter running at a smaller size than those observed in the soluble fraction. To determine whether any of these putative modified forms of ORC1 was a SUMO conjugate, I immunoprecipitated chromatin-associated and soluble ORC1 from plain interphase extracts and analyze them by western blotting against SUMO. I did not detect any sumoylated species in the anti-ORC1

immunoprecipitate prepared from the soluble fraction of the extracts (data not shown). Unfortunately the anti-ORC1 antibody failed to precipitate an amount of chromatin-associated ORC1 that would be sufficient to detect sumoylated species. To circumvent this problem I incubated the soluble and chromatin-associated fractions obtained from plain extracts with the catalytic domain of the desumoylating enzyme Ulp1 (a gift from Dale Wigley) and then analyzed them by western blotting against ORC1. **Figure 4.1**C shows that Ulp1 converted all of the modified ORC1 in the chromatin fraction directly into the ~110 kDa form. Conversely, treatment with Ulp1 did not alter the abundance of any of the modified ORC1 species observed in the soluble fraction.

Finally, I examined whether ORC1 is modified by SUMO1 only, or whether it can also be conjugated to SUMO2. Chromatin-bound sumoylated species were isolated by Ni^{2+}-NTA affinity chromatography from interphase extracts supplied with His_6-SUMO1, His_6-SUMO2 or just a buffer solution as a control, and analyzed by western blotting against ORC1. **Figure 4.1**D shows that ORC1 was modified both by both SUMO1 and SUMO2.

Altogether these data show that ORC1 is a *bona fide* sumoylation target in *Xenopus* egg extracts and suggest that this modification may occur specifically on the chromatin.

4.2.2 ORC is sumoylated in budding yeast

In addition to having shown that ORC1 is sumoylated in frog egg extracts, I observed that an Orc1-9myc fusion was also modified in budding yeast (**Figure 3.8**A). **Figure 3.8**B also revealed that Orc1-9myc co-precipitated with sumoylated species other than itself even after stringent washing of the immunoprecipitate with a buffered solution containing 500 mM NaCl and 0.1% v/v SDS. Since Orc1 is part of ORC, which is a complex that is stable over a range of salt concentrations, I investigated whether such species could represent sumoylated Orc2-6. Towards this end, the yeast *ORC2-ORC6* genes were tagged with the 9myc epitope at their C terminus and tested for sumoylation by denaturing Ni^{2+}-NTA chromatography and immunoprecipitation as described in 3.2.6. **Figure 4.2**A and **Figure 4.2**B show that 9myc-tagged Orc2-Orc6 were also sumoylated. In addition, they show that multiple sumoylated species were detected for Orc2, Orc4, Orc5 and Orc6, thus indicating that these proteins could be either modified at multiple sites or by a short SUMO chain. The absence of detectable amounts of sumoylated species in the immunoprecipitate of Orc1-9myc and Orc3-9myc reported in **Figure 4.2**B can be possibly explained by the minute modification

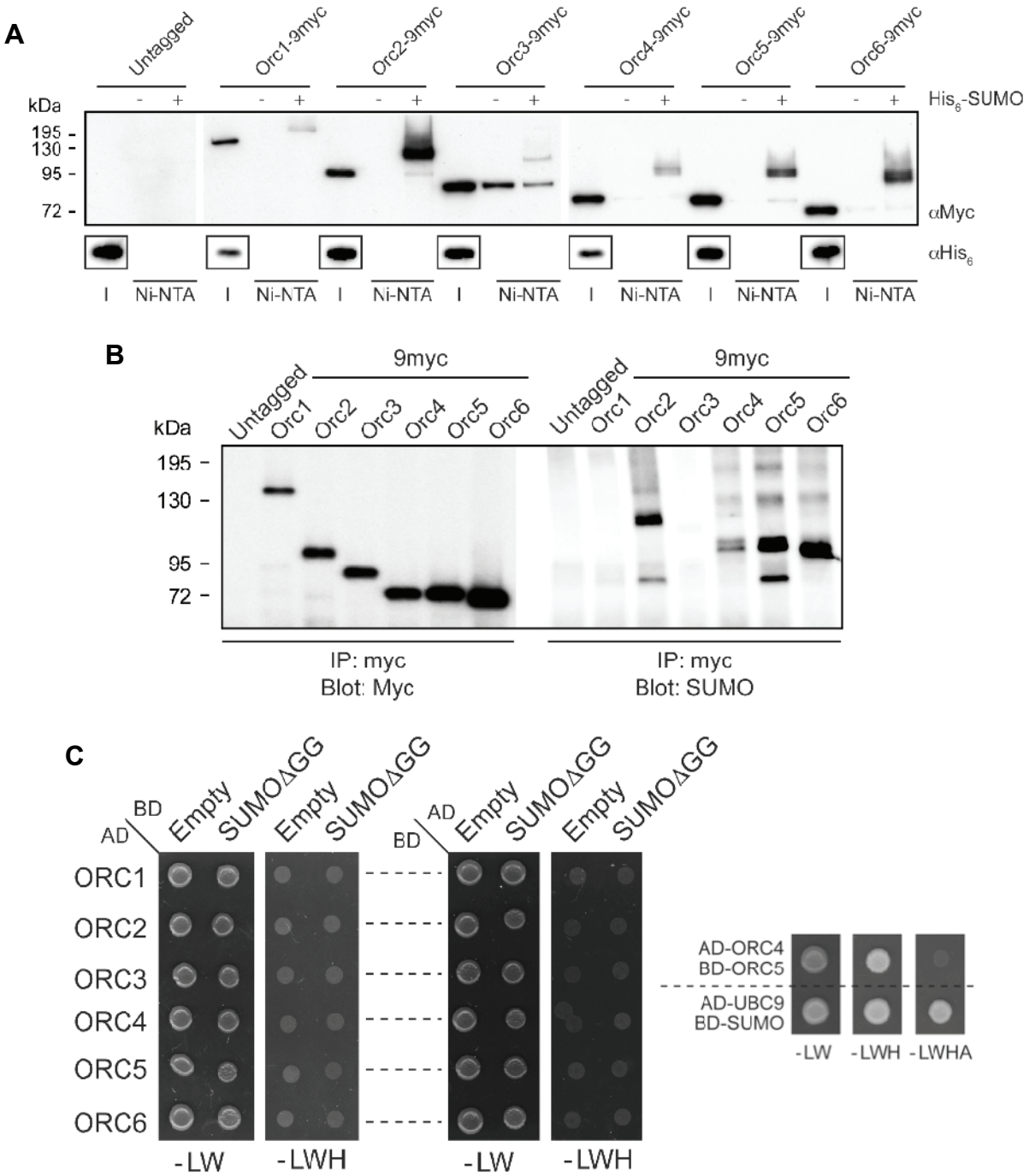

Figure 4.2 - Orc1-6 are sumoylated in *S. cerevisiae*. A) Sumoylated proteins isolated from strains carrying 9myc-tagged ORC subunits were analyzed by western blotting against the His_6 and 9myc tags, as described in Figure 3.8A. I = input. B) Orc1-6 tagged with the 9myc-epitope were immunoprecipitated and analyzed by western blotting against the 9myc-tag and SUMO, as described in Figure 3.8B. C) *ORC1-6* and an unconjugatable *smt3* mutant (SUMOΔGG) were expressed as fusions of Gal4 DNA-binding (BD) or activation (AD) domain in the yeast two-hybrid reporter strain PJ69-4A as described in 2.8.9. -LW = medium lacking leucine and tryptophan, -HLW medium lacking leucine, tryptophan and histidine, -HLWA = medium lacking leucine, tryptophan, histidine and adenine. Since Ubc9 and SUMO as well as Orc4 and Orc5 have been previously shown to interact with each other in the yeast two-hybrid assay (Matsuda *et al.*, 2007; Uetz *et al.*, 2000), I used them as positive controls. They are shown separately from the other interactions for presentation purposes only, in fact they were grown on the same plates.

levels of these ORC subunits in comparison to the others, as shown in **Figure 4.2**A. Although the immunoprecipitates obtained from this experiment were washed very stringently, it was possible that some of the sumoylated species observed in **Figure 4.2**B could have been isolated with the epitope-tagged ORC subunits as a result of their ability to non-covalently interact with SUMO. To address this issue, I examined whether any of the six ORC subunits could bind to an unconjugatable form of SUMO using the yeast two-hybrid system. **Figure 4.2**C shows that Orc1-6 did not appear to interact with SUMO non-covalently. Overall, these data show that in budding yeast the whole of ORC is sumoylated.

The results presented in **Figure 4.2** led me to hypothesize that besides ORC1 other ORC subunits may be sumoylated in frog egg extracts as well. Having found an antibody against the frog ORC2, I explored the possibility that this protein may also be modified by SUMO. In preliminary experiments analogous to those described in 4.2.1, I did not detect any slow-migrating forms of ORC2 (data not shown). Since the modification of ORC1 was hardly detectable when I analyzed the chromatin isolated from frog egg extracts (**Figure 4.1**C), to exclude the possibility that the extent of ORC2 sumoylation may be even lower, I isolated sumoylated species by denaturing pull-down from extracts supplemented with His_6-SUMO1 or His_6-SUMO2 and analyzed them by western blotting against ORC2. Unfortunately, this experiment was inconclusive because the anti-ORC2 antibody I used heavily cross-reacted with the His_6 tag.

4.2.3 The budding yeast ORC is sumoylated through Siz1 and Siz2

Since the addition of SUMO to a substrate *in vivo* often depends on a SUMO ligase and the bulk of sumoylation in budding yeast relies upon the E3 enzymes Siz1 and Siz2 (Johnson and Gupta, 2001), I investigated which one of them aids ORC sumoylation. I tested the extent of modification of Orc5-9myc and Orc6-9myc, the two subunits of ORC that showed the strongest sumoylation (**Figure 4.2**A), by denaturing Ni^{2+}-NTA chromatography in wild type cells and in the single and double *siz1Δ siz2Δ* mutants expressing His_6-SUMO. Consistent with the evidence that both Siz1 and Siz2 often contribute to the modification of the same SUMO target in budding yeast (Reindle *et al.*, 2006), I found that the modification of Orc5-9myc and Orc6-9myc was reduced in both the *siz1Δ* and *siz2Δ* single mutants and it was completely abolished in the double *siz1Δ siz2Δ* mutant (**Figure 4.3**A).

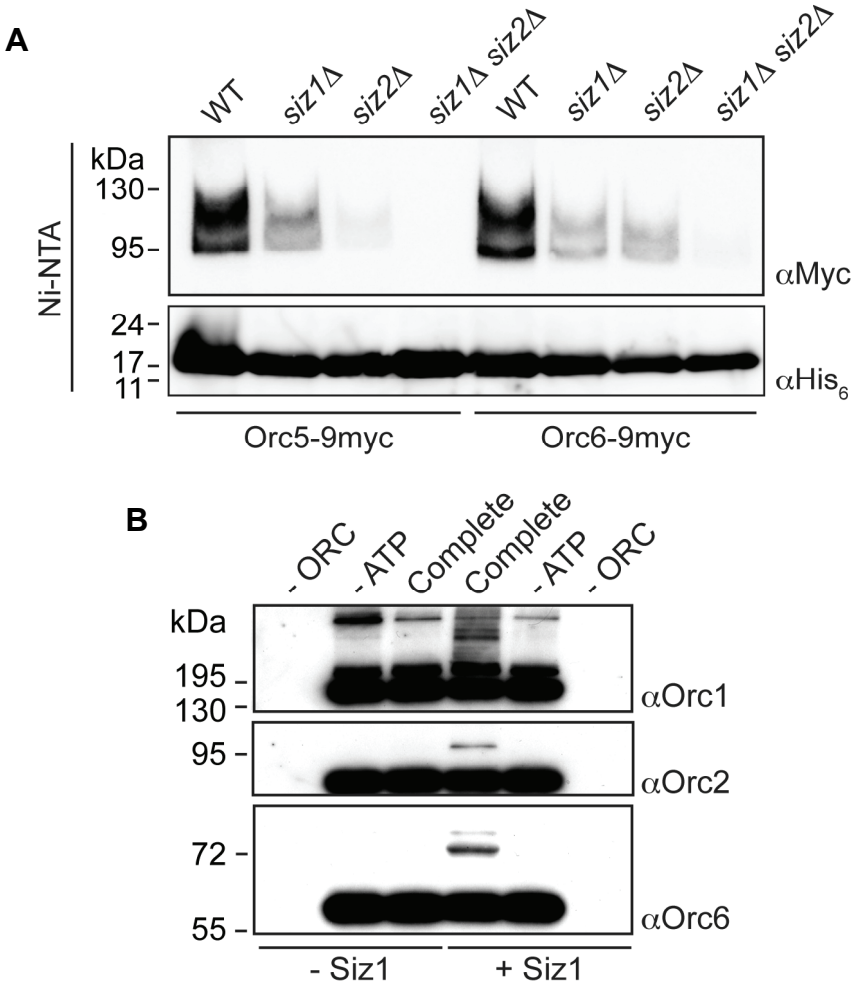

Figure 4.3 - ORC is sumoylated through Siz1 and Siz2 in budding yeast. A) Sumoylated proteins isolated from strains carrying Orc5-9myc or Orc6-9myc, His_6-tagged Smt3 and a deletion of *SIZ1*, *SIZ2* or both were analyzed by western blotting against the His_6 and 9myc tags, as described in Figure 3.8A. B) Recombinant yeast ORC (~0.5 pmol) was sumoylated *in vitro* in standard reactions (see 2.17.1) containing all the required components or lacking individual ones, both in the presence or absence of Siz1 (aa 1-508), and then analyzed by western blotting against Orc1, Orc2 and Orc6. When Siz1 was included a reaction only 25 nM of Ubc9 was used instead of 150 nM, which was normally employed for mixtures devoid of an E3.

To further substantiate these results I asked whether the budding yeast ORC could be sumoylated in a Siz1-dependent manner *in vitro*. The recombinant ORC (a gift from John Diffley) was incubated with all the essential sumoylation reagents and in the presence or absence of Siz1 (aa 1-508). Western blotting analysis of these reactions (**Figure 4.3**B) with antibodies against Orc1, Orc2 and Orc6 showed that these subunits were sumoylated only in the presence of Siz1. I did not analyze whether Orc3, Orc4 and Orc5 were also modified due to the lack of antibodies against these proteins.

Altogether these results strongly suggest that the yeast ORC is a Siz1- and Siz2-dependent sumoylation target.

4.2.4 Sumoylation of the budding yeast ORC is not significantly enhanced in the presence of origin DNA

The evidence presented here that ORC could be a substrate of SUMO in both budding yeast and frog egg extracts put forward the possibility that this modification event may be controlled by a common mechanism in both systems. Although the way in which ORC recognizes origins in different species varies, binding to DNA is a critical property of the complex in all the organisms analyzed to date. Since the frog ORC1 appeared to be sumoylated in its chromatin-associated state (**Figure 4.1**) and the modification of other DNA-associated proteins has been shown to depend on DNA binding (Parker *et al.*, 2008), I asked whether the sumoylation of ORC may be modulated by the presence of DNA. Being able to sumoylate the yeast ORC *in vitro* (**Figure 4.3**) allowed me to address this question directly. The recombinant complex was incubated with a 841 bp DNA fragment containing the prototypical ORC binding sequence, *ARS1*, and ATP, which is necessary for binding of ORC to DNA (Speck *et al.*, 2005), before proceeding to the addition of the relevant sumoylation reaction mix. **Figure 4.4** shows that in the

Figure 4.4 - *In vitro* sumoylation of the budding yeast ORC is not significantly enhanced in the presence of a replication origin. Recombinant yeast ORC (~0.5 pmol) was incubated at 25°C for 20 min with ATP (1 mM) in the presence or absence an 841 bp PCR product (~0.5 pmol) containing the *ARS1* sequence. These samples were sumoylated *in vitro* in standard reactions (see 2.17.1) supplemented with wild type Siz1 (aa 1-508) or one mutated within its SAP domain (G55A/K57A/L60A, SAP*) and then analyzed by western blotting against Orc1, Orc2 and Orc6. When Siz1 was included in a reaction only 25 nM of Ubc9 was used instead of 150 nM, which was normally employed for mixtures devoid of an E3.

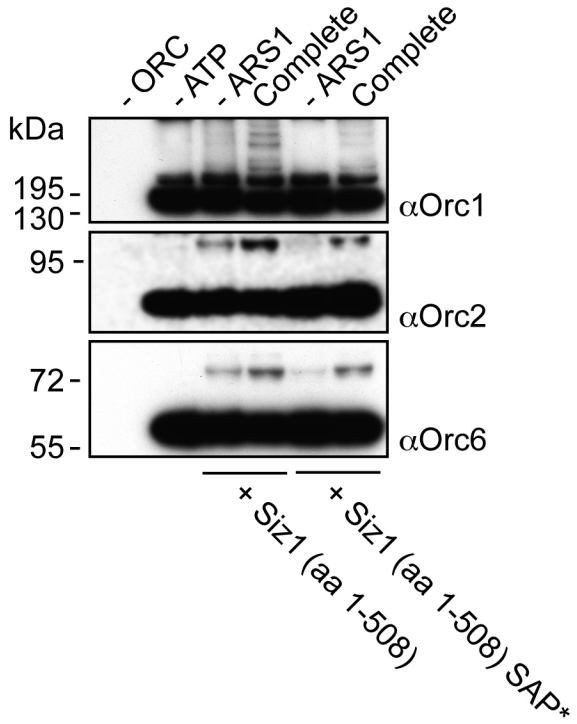

presence of *ARS1*-containing DNA, the ORC complex was sumoylated slightly more efficiently than its absence. This effect was not dependent on the ability of Siz1 (aa 1-508) to bind to DNA through its SAP domain because although mutating it did cause some loss of ORC sumoylation, this effect probably originated from the lower activity of the mutant Siz1 (aa 1-508) compared to the wild type protein (Parker *et al.*, 2008).

4.2.5 Sumoylation of the frog ORC1 and yeast Orc5-9myc appear to be cell cycle-regulated but the latter does not depend on origin firing

In addition to DNA binding, another important and conserved property of ORC is that its activity is tightly linked to DNA replication and the cell cycle. Thus I explored whether the extent of ORC sumoylation may change during DNA replication in both frog egg extracts and budding yeast.

In *Xenopus*, I isolated chromatin at increasing time points from interphase extracts supplemented with a control solution or His_6-SUMO1, to enhance the low levels of ORC1 modification, and analyzed it by western blotting against ORC1 and PCNA. Although the overall modification levels were low, I noticed that sumoylated ORC1 accumulated just prior to or at the beginning of S phase, it then disappeared as the extracts progressed through full-blown replication and it eventually re-appeared as S phase was completed (**Figure 4.5**A).

To determine whether this phenomenon may be conserved in budding yeast, I examined the levels of Orc5-9myc sumoylation in synchronized cells as they progressed through DNA replication from an α factor-induced G_1-arrest. These cells were released into medium containing the microtubule-destabilizing drug nocodazole to stop them at the G_2-M phase. At each time point, cells were analyzed by flow cytometry, to confirm they progressed through the cell cycle, and processed to isolate sumoylated species by denaturing Ni^{2+}-NTA chromatography. Western blotting analysis of such samples showed that, similarly to what I observed for the sumoylation of the frog ORC1, the amount of sumoylated Orc5-9myc dipped as the cells progressed into S phase but it rose again as they accumulated at the G_2-M boundary (**Figure 4.5**B). Conversely, the levels of sumoylated PCNA, a prototypical S phase-specific SUMO substrate (Hoege *et al.*, 2002), peaked as cells replicated their DNA.

Having observed that the sumoylation of both ORC1 in frog egg extracts and Orc5-9myc in budding yeast disappeared or decreased as the genome started being

Figure 4.5 - Sumoylation of the frog ORC1 and yeast Orc5-9myc during DNA replication and origin firing. A) Interphase extracts (25 µL) were supplemented with 2,500 nuclei·µL^{-1} of extract and either a control solution or His_6-SUMO1 to a final concentration of 20 µM. Chromatin was isolated from the extracts at the indicated times and analyzed by western blotting against ORC1 and PCNA. B) and C) Wild type and *rad53Δ sml1Δ* strains carrying the 9myc-tagged *ORC5* were synchronized in G_1 phase with an α factor peptide (10 µg·mL^{-1} for 2.5 h) and then released into fresh medium containing nocodazole (15 µg·mL^{-1}). Cells were collected at the indicated time points and analyzed by flow cytometry (see 2.8.6). Sumoylated species were isolated as described in Figure 3.8A and analyzed by western blotting against the His_6 and 9myc tags and PCNA (loading control). A = asynchronous, α = α factor-arrested D) Wild type and *rad53Δ sml1Δ* strains carrying the 9myc-tagged *ORC5* were synchronized in G_1 phase with an α factor peptide (10 µg·mL^{-1} for 2.5 h) and then released into fresh medium containing HU (200 mM for 1.5 h). Cells were processed as described in B).

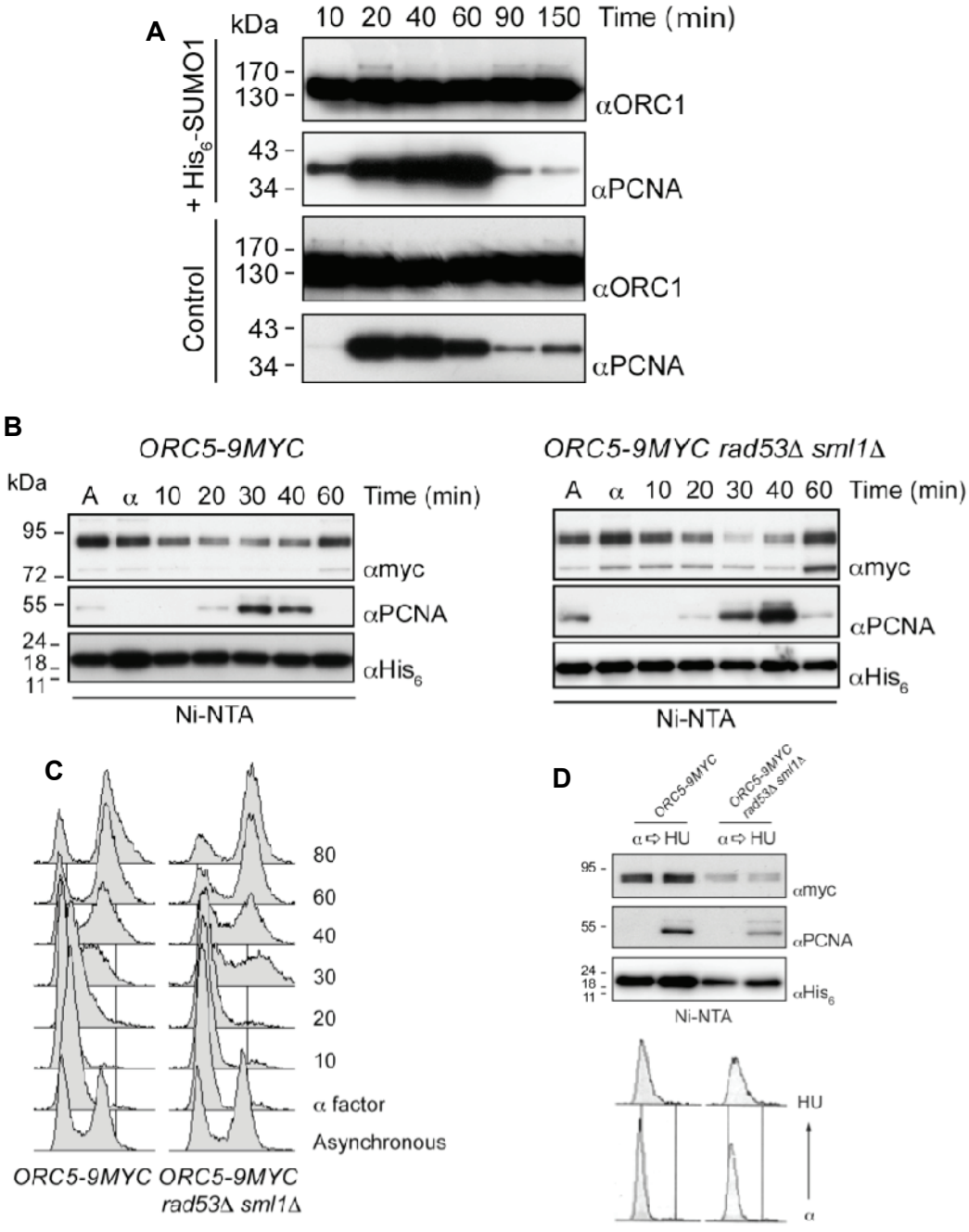

replicated, I asked whether this phenomenon may depend on the firing of replication origins. To address this question, I examined the levels of Orc5-9myc sumoylation in wild type and *rad53Δ sml1Δ* cells released from a G_1-arrest into medium containing hydroxyurea (HU). During an unperturbed S phase, DNA is duplicated from many replication origins, some of which are activated at the onset of S phase (early-firing origin) and others later on (late-firing origin). In wild type yeast, the checkpoint kinase Rad53 ensures that the firing of late replication origins is inhibited in the presence of genotoxins such as hydroxyurea. Deleting *RAD53* relieves this inhibition, thus allowing late replication origins to fire early (Santocanale and Diffley, 1998). It follows that if the firing of replication origins were responsible for reducing the levels of ORC sumoylation, then releasing G_1-arrested cells into a medium containing hydroxyurea should afford a larger decrease in ORC sumoylation in the *rad53Δ sml1Δ* mutant than in the wild type, because more origins fire in the former case. First of all, since *RAD53* plays a role in the initiation of DNA replication that is independent of its checkpoint functions (Dohrmann and Sclafani, 2006), I examined whether knocking it out by itself affected the cell cycle-related changes in Orc5-9myc sumoylation I described earlier. **Figure 4.5**B shows that, like in the wild type, the sumoylated Orc5-9myc disappeared during S phase in the *rad53Δ sml1Δ* mutant. I also observed that there was no significant difference in the levels of Orc5-9myc sumoylation between wild type and *rad53Δ sml1Δ* cells upon their release into HU-containing medium from a G_1-arrest, which could not be explained by the smaller amount of His_6-SUMO pulled down from the mutant (**Figure 4.5**D). Additionally, in both the wild type and the *rad53Δ sml1Δ* mutant there was no difference in the amount of sumoylated Orc5-9myc between the G_1-arrested cells and those that had fired replication origins (HU).

Altogether these data suggest that ORC sumoylation could be cell cycle-regulated in both frog egg extracts and budding yeast, but this phenomenon is unlikely to depend on the firing of replication origins, at least in the latter system.

4.2.6 Sumoylation does not noticeably alter the association with chromatin of the frog ORC1

Sumoylation has been shown to modulate the association with chromatin of proteins such as topoisomerase II (Azuma *et al.*, 2003), TDG (Hardeland *et al.*, 2002) and some transcription factors (Goodson *et al.*, 2001; Tsuruzoe *et al.*, 2006). In the case of topoisomerase II, abolishing its modification by adding a dominant negative mutant of

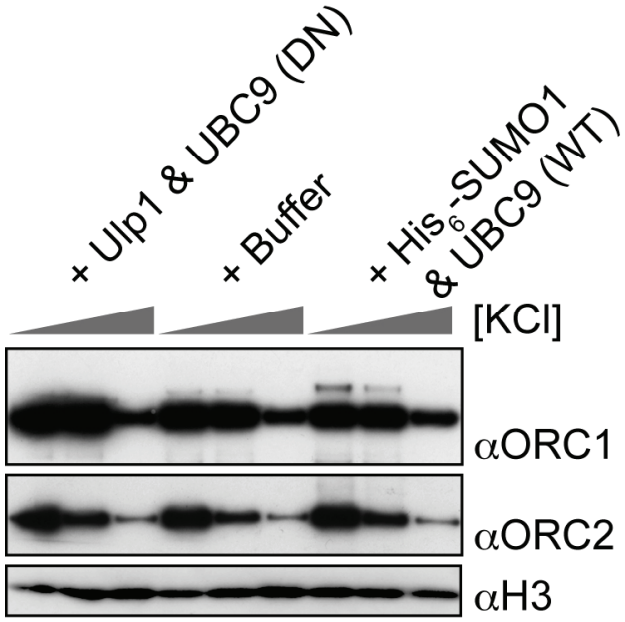

Figure 4.6 - Changing the normal levels of sumoylation in egg extracts does not alter the association of ORC1 with chromatin. Interphase extracts (25 µL) were supplemented with 2,500 nuclei·µL^{-1} of extract and the following proteins: 20 µM UBC9 (C93S) and 2 µM Ulp1 (catalytic domain) to reduce sumoylation, a buffered solution to preserve normal sumoylation levels in the extract or 20 µM wild type UBC9 and 20 µM His_6-SUMO1 to enhance normal sumoylation levels. The extracts were incubated for 20 min at 23°C. Chromatin was isolated through sucrose cushions containing 50, 100 and 150 mM KCl and analyzed by western blotting against ORC1, ORC2, PCNA and histone H3 (loading control). DN = dominant negative.

UBC9 to egg extracts led to an increase in the amount of enzyme that remained tightly bound to chromosomes (Azuma *et al.*, 2003). Thus, I asked whether this may also be the case for the frog ORC1.

To address this question, I isolated chromatin through sucrose cushions containing increasing concentrations of KCl from three kinds of interphase extracts: one supplemented with a dominant negative mutant of UBC9 and the catalytic domain of Ulp1 to reduce sumoylation, one supplemented with wild type UBC9 and His_6-SUMO1 to induce hyper-sumoylation and one supplemented with a buffered solution, where normal levels of sumoylation should be maintained. **Figure 4.6** shows that at the lowest salt concentration a slow-migrating form of ORC1 was detected in the control sample. This band increased in intensity after the addition of the wild type UBC9 and His_6-SUMO1 to the extract and it disappeared when the dominant negative UBC9 and Ulp1 were used, indicating that it represents sumoylated ORC1. I also observed that the salt-extraction patterns of the unmodified ORC1, and another ORC subunit, ORC2, did not differ in the three kinds of extracts described above. Additionally in both the control extracts and those supplemented with the wild type UBC9 and His_6-SUMO1, the

sumoylated and the unmodified ORC1 were released from the chromatin by similar salt concentrations.

Overall, these results suggest that sumoylation does not noticeably alter the association of ORC1 with chromatin in frog egg extracts.

4.2.7 Influencing the normal levels of sumoylation in frog egg extracts and budding yeast has no major effect on the efficiency of DNA replication

ORC is essential for DNA replication from yeast to humans. Thus, if sumoylation impinged on the structure or function of this complex, then abolishing or enhancing it should have an impact on DNA replication. Since changing the modification of ORC exclusively was not a trivial task, I explored whether altering the levels of the bulk of sumoylation may regulate DNA replication.

To address this question in *Xenopus*, I measured the kinetics of DNA replication in extracts prepared as described in 4.2.6. These extracts were supplemented with [α^{32}-P]dCTP and the extent of replication was determined by measuring the incorporation of the labelled nucleotide into the genomic DNA isolated at multiple time-points. **Figure 4.7**A and **Figure 4.7**B show that the control extracts behaved similarly to the hypo- and hyper-sumoylated extracts with respect to the length of the initial lag phase, when the sperm chromatin is remodelled, ORC binds to DNA and forms pre-RCs, the rate of DNA replication and the amplitude of the final plateau phase, which represents the total amount of replicated DNA. Similarly, Simona Fiorani and Vincenzo Costanzo (Clare Hall Laboratories) did not detect any reproducible difference in the replication kinetics of somatic nuclei, as well as sperm chromatin, incubated in the three kinds of interphase extracts describe earlier (personal communication).

To determine whether a different situation may apply to budding yeast, I measured the transmission fidelity of mini-chromosomes containing different numbers of replication origins in wild type and a *siz1Δ siz2Δ* cells. I reasoned that if Siz1- and Siz2-dependent sumoylation played a role in DNA replication through the modification of either ORC (**Figure 4.3**) or possibly other proteins, then deleting such SUMO ligases should affect the efficiency of the initiation of DNA replication and consequently the rate of mini-chromosome loss. Adding extra replication origins to a mini-chromosome increases its chance of being replicated and transmitted to daughter cells and therefore it can be used to distinguish a phenotype that is caused by a problem with chromosome

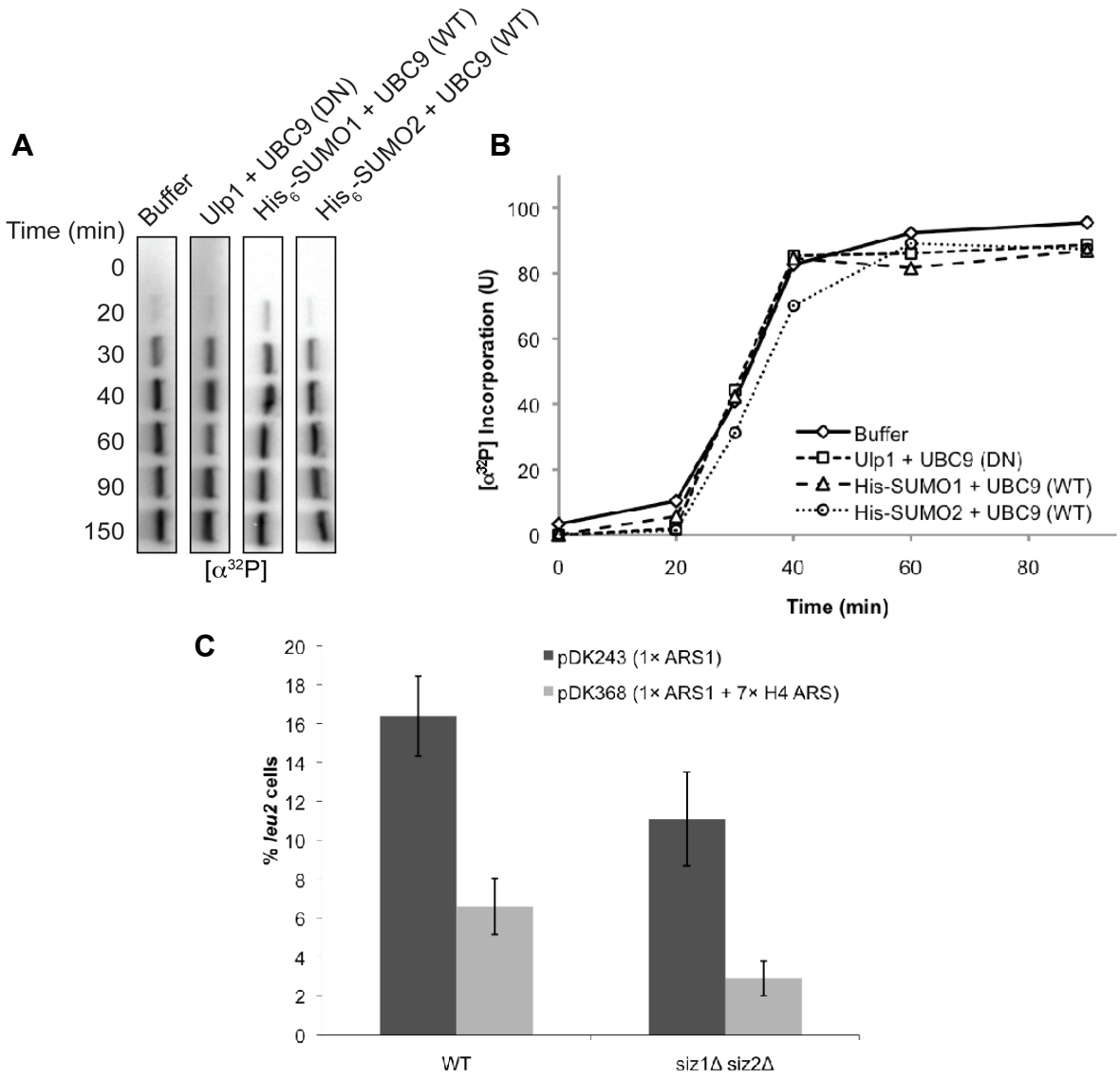

Figure 4.7 - Normal levels of sumoylation are not critical for efficient replication in budding yeast and frog egg extracts. A) DNA replication was analyzed as described in 2.7.5. U = % of [α-^{32}P]dCMP incorporation. 100% was defined as the amount of [α-^{32}P]dCMP incorporated in the genomic DNA of the control sample at 90 min. C) Wild type *cir^{0}* and *siz1Δ siz2Δ cir^{0}* cells were transformed with either pDK243 (1× ARS1) or pDK368-7 (1× ARS1 + 7× H4 ARS). Three colonies per condition were cultured as described in 2.8.8. Eighteen plates (9 YPD and 9 devoid of leucine) containing between 100 and 300 colonies were counted per condition. The graph shown is a representative example of multiple experiments that yielded similar results. Error bars represent the standard deviations calculated from nine plates in one experimental replicate. DN = dominant negative.

segregation rather from one that instead involves replication (Hogan and Koshland, 1992). For the experiments described below, I used strains that were cured of the naturally occurring 2-µm plasmid (*cir^{0}*) because it accumulates at such massive levels in the *siz1Δ siz2Δ* mutant that it causes cells to grow slowly and form "nibbled" colonies on solid medium (Chen *et al.*, 2005), which I found difficult to reliably count. Thus, wild type *cir^{0}* and *siz1Δ siz2Δ cir^{0}* cells transformed with mini-chromosomes containing either one or eight replication origins were propagated in selective medium to maintain

the plasmids, diluted and grown for 30 h in non-selective medium, to allow loss of the plasmids, and then spread on plates of either selective or non-selective media, to determine the percentage of cells that lost the plasmids. **Figure 4.7**C shows that mini-chromosome stability was slightly enhanced in the *siz1Δ siz2Δ* mutant compared to the wild type, however this difference is not statistically significant. As expected, the plasmid containing eight origins of replication was maintained more efficiently than that harbouring one only, however this effect was very similar between the wild type and *siz1Δ siz2Δ* mutant.

Altogether these data show that altering the normal homeostasis of sumoylation in frog egg extracts or budding yeast has no considerable effect on the efficiency of DNA replication, thus indicating that ORC sumoylation is unlikely to control this process.

4.3 Discussion

4.3.1 ORC as a conserved target of sumoylation

Figure 4.1 and **Figure 4.2** show that ORC1 in frog egg extracts and each one of the six subunits of the budding yeast complex are *bona fide* targets of SUMO. Interestingly, ORC1, ORC2, ORC3, ORC5 and ORC6 have also been identified as SUMO2 targets in a recent proteomic analysis of sumoylation substrates from human cells (Golebiowski *et al.*, 2009). Although formal proof will be required, these observations suggest that ORC, as a whole, is likely to be a target of sumoylation from yeast, through frogs, to humans. This is not a completely unexpected finding since other proteins for which orthologues exist in lower and higher eukaryotes have been identified as conserved SUMO substrates. For one these proteins, topoisomerase II, a large number of studies have confirmed that its sumoylation plays analogous functions and is similarly regulated at the temporal and spatial level in both lower and higher eukaryotes (Lee and Bachant, 2009). Thus it is possible that the sumoylation of ORC may also have an evolutionarily conserved role.

4.3.2 Spatio-temporal regulation of ORC sumoylation

The data presented in **Figure 4.1** and **Figure 4.5** provide some evidence in favour of the possibility that the sumoylation of ORC may be regulated both at the spatial and temporal level.

By separating chromatin-bound proteins from soluble ones in frog egg extracts, I noticed that only the ORC1 associated to chromatin was sumoylated. However, since

both the recombinant and the chromatin-associated ORC1 were modified to a similar extent *in vitro* and the sumoylation of the yeast ORC was not significantly enhanced by the presence of origin DNA *in vitro*, it is likely that factors other than the physical binding of the complex to the DNA may promote its sumoylation. These factors may include a DNA-associated E3 or another post-translational modification of ORC, such as phosphorylation, which can stimulate the sumoylation of certain proteins (see 1.2.5). However, given that the way ORC recognizes DNA varies in different organisms, I cannot categorically exclude that DNA may not affect the modification of the complex in other systems.

The sumoylation of ORC1 in frog egg extracts and that of Orc5-9myc in yeast also seemed to disappear as DNA was being replicated (**Figure 4.5**). In yeast, this phenomenon was not dependent on the firing of replication origins, thus indicating that other processes could be involved. Sumoylation of ORC could therefore be regulated at level of the cell cycle stage. This possibility could be tested in budding yeast by mutating the protein kinase Cdc7. Under the appropriate conditions, a *cdc7* mutant progresses from a G_1-arrest through the cell cycle with normal changes in CDK levels but fails to initiate DNA replication (Hartwell, 1973). Since the addition of geminin has a similar effect on DNA replication and cell cycle progression in frog egg extracts, it could be used to explore whether or not the cell cycle controls ORC1 sumoylation in this system. It has to be mentioned that although the loss of Orc5-9myc sumoylation during DNA replication was reproducible, the quantity of unmodified Orc5-9myc that non-specifically bound to the affinity resin followed a similar pattern, indicating that Orc5-9myc itself may undergo small changes in amount throughout replication. Analogously, although I did observe a similar loss of sumoylated ORC1 during replication in various experiments, I cannot rule out that a small decrease in the amount of protein recovered with chromatin during replication may be disproportionately enhanced with respect to the modified ORC1, given its paucity. If the loss of sumoylated ORC1 from replicating DNA were a real effect then it would be unlikely to be linked to the weakening of binding that ORC experiences upon pre-RC firing, because this phenomenon has been shown to persist until mitosis, when the complex leaves the chromatin (Rowles *et al.*, 1999), while sumoylated ORC1 re-appeared at the end of DNA replication (**Figure 4.5**).

4.3.3 What are the possible functions of ORC sumoylation?

The observations that I described in this chapter do not allow me to conclude what the function of ORC sumoylation is, however they do help ruling out what this modification may not be doing.

The data collected from many proteomic studies aimed at identifying large numbers of SUMO targets have revealed that these proteins very often cluster within well-defined multi-subunit complexes (Denison *et al.*, 2005; Golebiowski *et al.*, 2009; Wohlschlegel *et al.*, 2004). ORC appears to abide to such pattern. Although the mechanisms underlying this phenomenon are unknown, it has been proposed that multiple sumoylation events within the same protein complex may act as a "molecular glue" to facilitate their assembly and/or to maintain their structures (Matunis *et al.*, 2006). This hypothesis comes from the observation that the assembly of PML nuclear bodies requires the sumoylation of PML itself but also its ability to interact non-covalently with SUMO through a SIM (Shen *et al.*, 2006b). Thus, PML bodies may be held together by a network of interactions between the SUMO moiety conjugated to a sumoylated PML and a SIM on another. The presence of SIMs in other proteins, such as the transcriptional repressor DAXX, can also mediate their recruitment in or out of PML nuclear bodies (Lin *et al.*, 2006). Whether or not SUMO may also be important for keeping ORC together is an interesting possibility, but perhaps an unlikely one for several reasons. Firstly, an unconjugatable mutant of SUMO did not bind to any of the yeast ORC subunits in the yeast two-hybrid system, which means that these protein are unlikely to interact with each other, at least strongly. Very weak interactions between SUMO and ORC that fall below the detection threshold of the yeast two-hybrid assay cannot be however excluded. Secondly, I did not detect any sumoylated species in the preparation of recombinant ORC purified from yeast cells (data not shown). This loss of ORC modification can be probably explained by the isopeptidase-mediated removal of SUMO during the purification procedure, which in turn suggests that sumoylation is not necessary to maintain the structure of the complex. It remains to be determined whether the *in vivo* assembly, rather than the maintenance, of ORC and/or its interactions with other proteins may be controlled by SUMO.

Another intriguing consideration from the observations presented here is that although the Orc6 protein from budding yeast and fission yeast/metazoans bear so little sequence similarity that they may in fact have different evolutionary origins (Duncker *et al.*, 2009), they are both targets of SUMO. In humans, ORC6 is somewhat of a puzzle

because even though its depletion causes defects in DNA replication (Prasanth *et al.*, 2002) and it is part of ORC *in vivo* (Siddiqui and Stillman, 2007), it binds weakly to the rest of the complex. A similar behaviour applies to the human ORC1, which associates with the rest of ORC non-stoichiometrically (Vashee *et al.*, 2001) and it is able to independently dissociate from chromatin upon entry into S phase (Li and DePamphilis, 2002). It is therefore possible that the subunit composition of the human ORC, and potentially that of complexes from other organisms, may change during the cell cycle to define unique ensembles with different functions. Since SUMO is conjugated to all of the six subunits of ORC in both budding yeast and probably in humans, I hypothesize that this modification event may be important in a conserved role of ORC that requires the complex to exist as a six-subunit entity. It follows that sumoylation is unlikely to play a role in those functions of ORC that depend on either a single subunit within the intact complex, such as the establishment of transcriptionally silent chromatin, which is mediated through ORC1 in both budding yeast and *Drosophila* (Pak *et al.*, 1997; Triolo and Sternglanz, 1996), or an ORC subunit on its own, such as the regulation of cytokinesis by ORC6 (Chesnokov *et al.*, 2003; Prasanth *et al.*, 2002).

If SUMO impinged on the initiation of DNA replication by modifying ORC, or possibly other proteins, then altering the normal levels of sumoylation in a cell should have an impact on such a process. Surprisingly, I found that abolishing the sumoylation of ORC in yeast by deleting *SIZ1* and *SIZ2* did not significantly alter the transmission efficiency of mini-chromosomes with different numbers of replication origins in comparison to the wild type (**Figure 4.7**). This result was somewhat unexpected because the *siz1Δ siz2Δ* mutant had been previously reported to lose mini-chromosomes more easily than the wild type, in a manner that depended on topoisomerase II sumoylation (Takahashi *et al.*, 2006). The use of different yeast backgrounds, strains that lack or harbour the 2-μm circle and different ways of scoring for those cells that lost the plasmid could have accounted for such discrepancy. In fact, altering the normal levels of sumoylation had no significant impact on the kinetics of DNA replication in frog egg extracts either. Additionally, a similar phenotype was observed for a temperature sensitive mutant of *UBC9* (*ubc9-1*) in budding yeast: *ubc9-1* cells grown at a semi-permissive temperature progressed through S phase from a G_2-M arrest and a brief incubation in HU as well as the wild type, but they accumulated at the G_2 phase after a few duplications (Branzei *et al.*, 2006). The *ubc9-1* mutation leads to an almost complete loss of the protein at the restrictive temperature, but only a small decrease at the semi-permissive temperature (Betting and Seufert, 1996). It is therefore possible that in the *ubc9-1* mutant some

proteins may remain sufficiently sumoylated at the semi-permissive temperature to carry out their normal functions.

The presence of residual amounts of protein sumoylation has also been used to explain why the almost complete loss of SUMO conjugation in the *siz1 siz2Δ* mutant causes only a mild phenotype, after removal of the 2-μm plasmid (Chen *et al.*, 2005; Johnson and Gupta, 2001), while *UBC9* and *SMT3* are essential genes in budding yeast. It has been proposed that even in the absence of *SIZ1* and *SIZ2* indispensable sumoylation events must still occur, which could be mediated either by Ubc9 directly or possibly by another E3 ligase (Johnson and Gupta, 2001), such as Mms21. Although I cannot categorically exclude that residual amounts of ORC sumoylation in the *siz1Δ siz2Δ* mutant may have allowed the complex to show a wild type-like behaviour with respect to the rate of mini-chromosome loss, I deem it an unlikely possibility because deleting these E3 ligases reduced the modification of at least two ORC subunits to undetectable levels, even after a prolonged exposure of the western blot membrane (**Figure 4.3** and data not shown). Similarly, if the sumoylation of ORC1 modulated DNA replication in frog egg extracts, even at severely reduced levels, then I cannot exclude that the comparable replication kinetics observed for the hypo-sumoylated extracts (**Figure 4.7**) may have arisen because of the incomplete removal of SUMO from ORC1, which was hard to assess given the minute extent of this modification event. Even by taking these problems into account, the observations that I have discussed in this paragraph still indicate that under conditions whereby the sumoylation of ORC is reduced to undetectable levels in two different experimental systems, DNA replication is not significantly affected. By inference, this suggests that the sumoylation of ORC may not play an essential or general role in the establishment of pre-RCs.

At the moment, what the sumoylation of ORC does remains an open question. Since this modification event is very likely to be conserved and therefore to have an important function, I believe that it is a very interesting, but certainly not an easy, problem to explore for several reasons. Firstly, deleting E3 ligases or over-producing SUMO proteases to abolish the sumoylation of ORC and then to study the consequences on processes that the complex is involved in is a good way to quickly screen for a positive phenotype. However, when one such phenotype is found, confirming that it specifically depends on the sumoylation of ORC would involve showing that a sumoylation-deficient mutant of the complex exhibits similar problems. In the case of ORC, this is an enormous undertaking because each subunit of the complex is sumoylated, probably at multiple locations (**Figure 4.2**), which means that 8-10 sites would need to be identified

in a ~400 kDa complex. To complicate this problem further, some ORC subunits do not even have any obvious sumoylation consensus motifs, and mutating lysines targeted by SUMO can activate cryptic sumoylation sites (Jacobs *et al.*, 2007; Onishi *et al.*, 2009). Secondly, even if all the possible sumoylation sites within ORC are identified and mutated, thereafter resulting in a phenotype, the question remains of whether introducing so many mutations by itself may "damage" the complex, independently of sumoylation. Thirdly, studying the functions of ORC sumoylation in frog egg extracts is a major technical challenge because of the need to deplete ORC from the extract and then reconstitute it with either a wild type or a sumoylation-deficient complex produced from a recombinant source. By taking into account these problems and the fact that the modification of ORC is barely detectable *in vivo*, I decided to shift the focus of my attention to studying the modification of another SUMO target I identified earlier, that is, PARP-1. The choice fell on this protein because preliminary experiments revealed that its ability to bind DNA might be important for its modification. From this starting point, I studied the role of DNA in PARP-1 sumoylation further and I also investigated what the functions of this modification may be.

As I discussed above, studying the roles of ORC sumoylation is a tough problem to address experimentally. Being able to easily introduce mutations in one or multiple genes in budding yeast makes it an ideal system to explore this question *in vivo*. Additionally, the availability of conditional ORC mutants in *S. cerevisiae*, such as *orc2-1* (Foss *et al.*, 1993), would allow studying how sumoylation impinges on the functions of the complex when its integrity is compromised. In fact, this stratagem may be neccesary to see any effect given that the roles of the sumoylation of other proteins, such as PCNA and Rad52 (Papouli *et al.*, 2005; Pfander *et al.*, 2005; Torres-Rosell *et al.*, 2007), became apparent only in certain mutant backgrounds. The very recent reconstitution of a pre-RC that can load Mcm2-7 onto DNA using only purified proteins (Remus *et al.*, 2009), together with the fact that ORC can be sumoylated *in vitro* (**Figure 4.3**), open the possibility to study whether sumoylation directly affects any step in the assembly of pre-RCs.

Chapter 5. Results III: The sumoylation of PARP-1 *in vivo*

5.1 Introduction

PARP-1 is another one of the potential targets of sumoylation I identified from replicating chromatin incubated in frog egg extracts (**Table 3.1**). It is a very abundant chromatin-bound protein that is the founding member of a large superfamily of enzymes that catalyze the transfer of ADP-ribose moieties from NAD^+ onto certain target proteins to form long poly(ADP-ribose) chains (see 1.4). PARP-1 is best known for its ability to recognize DNA breaks, which strongly activate it, and for playing roles in genome stability, apoptosis and transcription (see 1.5). As I will describe in more detail in Chapter 6, *in vitro* PARP-1 sumoylation is strongly stimulated by DNA. This finding prompted me to characterize such a modification event *in vivo* as well. I decided to address this problem using mammalian cells as a model system for three reasons. Firstly, this choice meant that I could take advantage of an established range of tools and assays that had been designed to study the properties of PARP-1 in such an experimental system. Secondly, almost all of what is known about PARP-1 has been gathered from mammalian cells. Lastly, others had also identified PARP-1 as a possible target of SUMO in human cells (Gocke *et al.*, 2005; Rosas-Acosta *et al.*, 2005; Stephen West, personal communication).

The aim of this part of my thesis was: 1) to confirm that PARP-1 is a true sumoylation target *in vivo*, 2) to map its sumoylation sites, 3) to study the possible roles of this modification event by taking into account the known functions of SUMO and PARP-1, and 4) to verify *in vivo* the *in vitro* data described in Chapter 6 about the interplay between PARP-1 sumoylation and DNA.

5.2 Results

5.2.1 PARP-1 is a *bona fide* sumoylation target in human cells that is preferentially modified by SUMO3

Although in frog egg extracts PARP-1 was identified only within a pool of chromatin-associated proteins modified by SUMO2, but not SUMO1 (**Table 3.1**), in human cells it had been reported in proteomic studies as a possible target of SUMO1 (Gocke *et al.*, 2005; and Stephen West, personal communication), SUMO2 (Blomster *et al.*, 2009;

Golebiowski *et al.*, 2009), and SUMO3 (Rosas-Acosta *et al.*, 2005). It was therefore important to confirm that PARP-1 was sumoylated *in vivo*, and by which paralogue of SUMO, by alternative means than mass spectrometry. Thus I isolated sumoylated species from HeLa cells that conditionally produced His_6-tagged SUMO1, SUMO2 or SUMO3 (a gift from Gerrit Praefcke) by denaturing Ni^{2+}-NTA chromatography. Western blotting analysis of these purifications (**Figure 5.1**A) showed the presence of at least two slow-migrating forms of PARP-1, one significantly more abundant than the other, only in the cells that produced His_6-tagged SUMO (+ DOX). This figure also revealed that the SUMO3-modified PARP-1 was more abundant than the corresponding SUMO1 or SUMO2 conjugates.

Figure 5.1 - PARP-1 is sumoylated in human cells, preferentially by SUMO3. A) HeLa cells producing His_6-SUMO1/2/3 under the control of a doxycycline-inducible promoter were incubated in the presence or absence of doxycycline for 24 h. The cells (~10^7) were subjected to denaturing Ni^{2+}-NTA pull-down experiments, as described in 2.16.1, and analyzed by western blotting against PARP-1 and the His_6 tag. DOX = doxycycline. B) Total extracts (1.5 mg of total protein in 1 ml of RIPA buffer) of untreated or H_2O_2-challenged (10 mM for 5 min) HEK293 cells were incubated with 2-3 µg of each of three anti-PARP-1 antibodies (F2, F1-23 and C2-10) or 8-9 µg of anti-FLAG antibody for 3 h at 4°C and then processed as described in section 2.16.2. The immunocaptured proteins were eluted and subjected to western blotting analysis against PARP-1 (7.5% of the eluate) and SUMO2/3 (75% of the eluate). IP = immunoprecipitation.

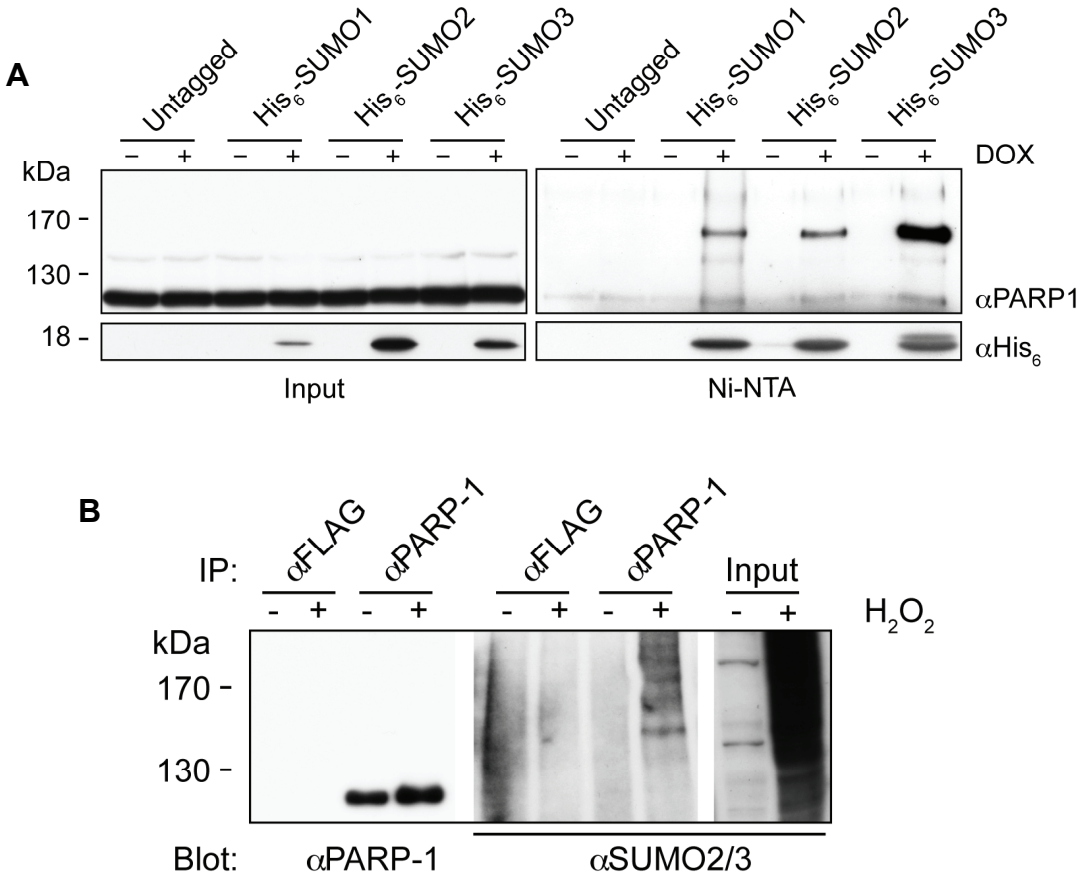

To confirm that PARP-1 was also sumoylated in cells expressing normal levels of SUMO, I subjected total cell extracts from HEK293 cells to immunoprecipitation using an anti-FLAG antibody, as a control, or an anti-PARP-1 antibody. These immunoprecipitates were analyzed by western blotting against SUMO2/3 and PARP-1. **Figure 5.1**B shows that, under these conditions, I could not detect any SUMO2/3-modified forms of PARP-1. This result was not completely unexpected, given that I estimated the sumoylated PARP-1 to represent considerably less than 1% of the total amount of this enzyme. To overcome these limitations, I repeated the above-described experiment, but this time I immunoprecipitated PARP-1 from extracts of cells that had also been exposed to H_2O_2 for a short period of time. This treatment stimulates the general modification of proteins by SUMO2/3, without the need to artificially overproduce any protein (Saitoh and Hinchey, 2000). Indeed, **Figure 5.1**B shows that in the presence of H_2O_2 PARP-1 co-immunoprecipitated with several sumoylated species, which were of the appropriate sizes for a multiply sumoylated PARP-1.

In conclusion, these results show that PARP-1 is a *bona fide* target of sumoylation in human cells and they also indicate that, at least in our system, the polymerase is preferentially modified by SUMO3.

5.2.2 PARP-1 sumoylation is enhanced by oxidative stress, and possibly other environmental stimuli, but not DNA damage

Having observed that PARP-1 was preferentially modified by SUMO3 prompted me to investigate whether the extent of this modification event may be affected by certain environmental cues because the conjugation of SUMO2/3 to proteins has been shown to increase in response to various stimuli (Saitoh and Hinchey, 2000). To answer this question, I isolated sumoylated species by denaturing Ni^{2+}-NTA chromatography from His_6-SUMO3-producing HeLa cells that were subjected to heat (42°C), osmotic (0.7 M NaCl), metabolic (7% EtOH) or oxidative (10 mM H_2O_2) shock, and then analyzed them by western blotting against PARP-1, SUMO2/3 and the His_6-tag. **Figure 5.2**A shows that the levels of sumoylated PARP-1 were enhanced in response to oxidative stress and, to a lesser degree, to osmotic shock as well. The extent of this upregulation correlated well with the increase in the total levels of SUMO2/3-modified species seen under the same conditions. Consistently, I also observed that heat or metabolic shocks did not appreciably alter the sumoylation of PARP-1, nor did they visibly enhance the overall levels of SUMO2/3 conjugates.

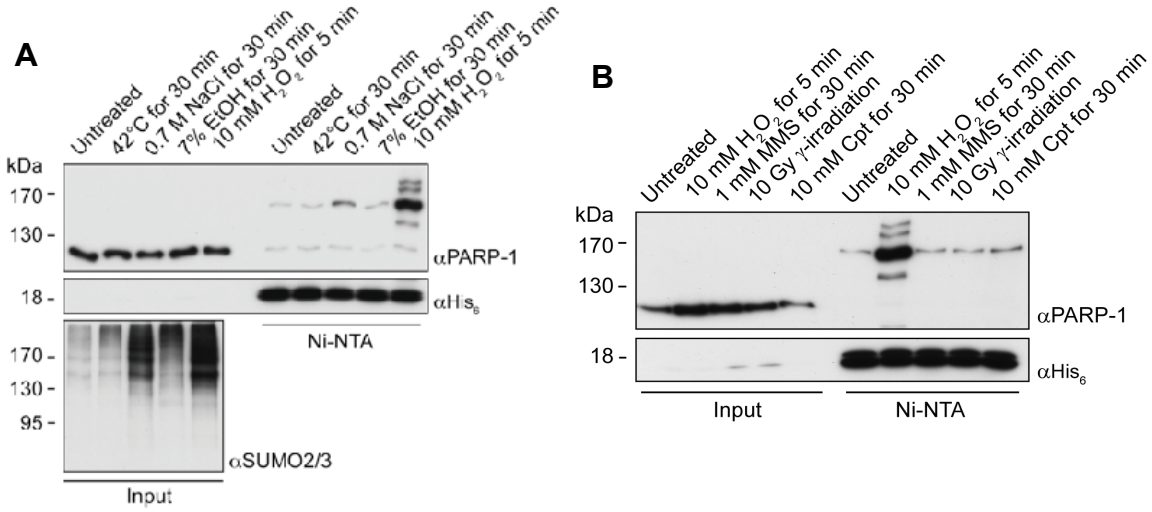

Figure 5.2 - PARP-1 sumoylation is enhanced by environmental stimuli but not DNA damage. HeLa cells producing His_6-SUMO3 (Figure 5.1A) were subjected to various environmental shocks A) or DNA-damaging agents B), as specified in the figure itself. His_6-SUMO-modified species were captured and analyzed as described in Figure 5.1A. Cpt = Camptothecin.

These data strongly suggested that the H_2O_2-dependent increase in PARP-1 sumoylation arose simply because of the general stimulatory effect that such a treatment has on SUMO2/3 conjugation, rather than being exclusive for PARP-1. Nonetheless, a specific role for H_2O_2 in triggering the modification of the polymerase could have been possible because this chemical introduces single-stranded breaks in the DNA, which strongly activate PARP-1 (Dantzer *et al.*, 2006). Thus, to explore whether this possibility was true or whether DNA damage might in fact have an inhibitory effect on the modification of PARP-1, I analyzed the extent of PARP-1 sumoylation in cells that were mock-treated or exposed to various DNA damaging agent (γ-irradiation, MMS, H_2O_2 and camptothecin), which are known to activate PARP-1 (see 1.5.2). **Figure 5.2**B shows that the levels of sumoylated PARP-1 isolated from the mock-treated cells and those incubated in the presence of genotoxins were comparable.

Altogether, these data indicate that damaging DNA does not directly affect PARP-1 sumoylation, which instead seems to be stimulated by the same environmental stimuli that enhance the general levels of SUMO2/3 conjugates in a cell.

5.2.3 PARP-1 is mainly sumoylated at K203 and K486

Having demonstrated that PARP-1 was a new target of sumoylation, I was interested in exploring the possible functions of this modification event. This question is best

A

Position	Sequence	Score	Type
203	QLPG VKSE GKRK	2.445	Consensus
233	KDKD SKLE KALK	3.676	Non-consensus
249	LIWN IKDE LKKV	1.142	Consensus
486	WGAE VKAE PVEV	4.479	Consensus
512	SKGQ VKEE GINK	2.299	Consensus

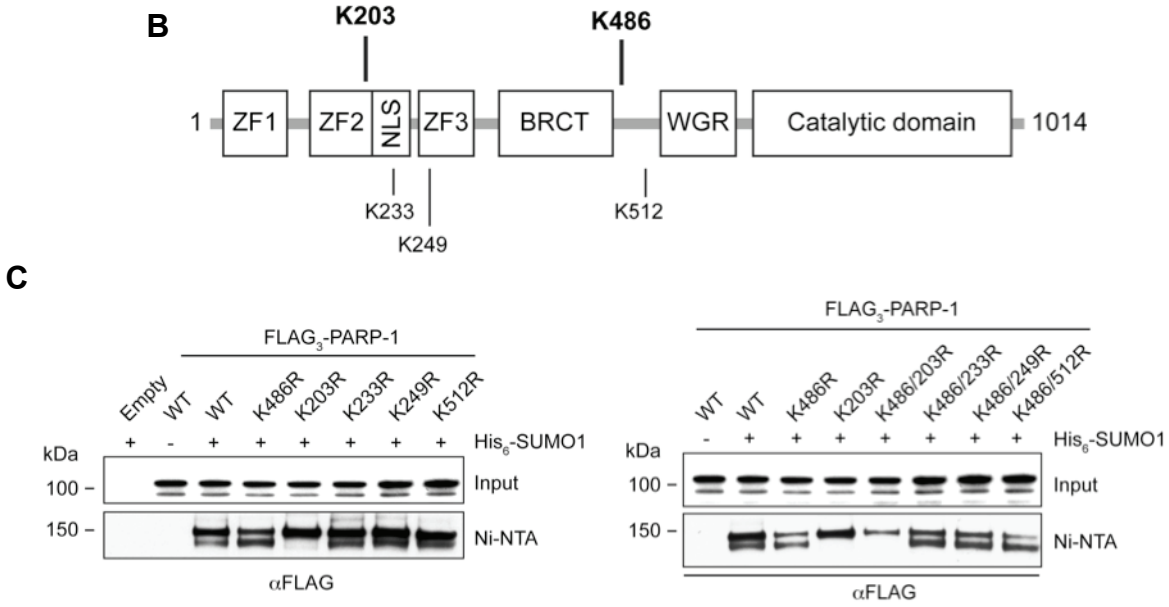

Figure 5.3 - PARP-1 is mainly sumoylated at K203 and K486. A) By using the SUMOsp 2.0 algorithm (http://sumosp.biocuckoo.org/), I identified several potential sumoylation sites in PARP-1. The table contains a selection of such lysines including their neighbouring sequence, a score representing their likelihood of being true sumoylation sites and whether or not they conform to the classical ΨKXD/E sumoylation consensus site. Shading = confirmed sumoylation sites. B) The positions of the hypothetical sumoylation sites identified in A) were mapped onto a graphical representation of PARP-1's domain structure. ZF = zinc finger, NLS = nuclear localization signal, bold font = confirmed sumoylation sites. C) HEK293 cells (35 mm ∅ dish, 60% confluent) were co-transfected by lipofection (6 µL of Fugene HD) with a plasmid encoding His_6-SUMO1 and another encoding C-terminally $FLAG_3$-tagged PARP-1 WT or the indicated mutants (1 µg of each). After 48 h, His_6-SUMO-modified species were captured and analyzed by western blotting against the FLAG tag, as described in Figure 5.1A.

addressed by comparing the properties of a wild type protein to those of a mutant in which the SUMO attachment sites have been mutated to prevent their modification.

Sumoylation often, but not always, targets lysines that are found within the consensus sequence ΨKXD/E (see 1.2.5). A bioinformatics analysis of PARP-1's primary sequence using the SUMOsp 2.0 algorithm (Ren *et al.*, 2009) identified several residues as potential sumoylation sites. From this pool of lysines, the five highest-scoring ones (K486, K233, K203, K512, K249), that is, those that were most likely to be true sumoylation sites, were tested for whether they could be sumoylated *in vivo*.

Rajvee Shah transfected HEK293 cells transiently producing His_6-SUMO1 with plasmids encoding C-terminally $FLAG_3$-tagged constructs of the wild type PARP-1 or mutants in which an hypothetical SUMO acceptor lysine was mutated to arginine. Sumoylated species were enriched for by denaturing Ni^{2+}-NTA chromatography and then analyzed by western blotting against the FLAG-tag. **Figure 5.3**B shows that mutating K203 resulted in the loss of one of the two main sumoylated forms of PARP-1, while changing K486 to arginine significantly reduced the levels of the other one. Individually mutating K233, K249 or K512 did not appreciably alter the sumoylation of PARP-1 in comparison to the wild type protein. Interestingly, I also noticed that abolishing the conjugation of SUMO to K203 enhanced the levels of sumoylation of K486, and/or possibly that of another site, and *vice versa*. These observations suggested that there must be a third minor sumoylation site in PARP-1 whose modification could become obvious/relevant only when K486 is mutated. Consistently, although the K203/486R mutant of PARP-1 was almost completely devoid of sumoylation, some residual modification could still be detected (**Figure 5.3**C). Next, the possibility that K233, K249 or K512 may actually represent the third sumoylation site of PARP-1, but this event may become experimentally detectable only when K486 is mutated was explored. Rajvee Shah analyzed the modification patterns of PARP-1 K486R mutants that also carried a second mutation at one of the above-mentioned lysines. **Figure 5.3**C shows that all of the tested double mutants exhibited a pattern of sumoylation essentially identical to that of PARP-1 K486R, thus indicating that none of them was likely to be the exclusive third sumoylation site. This of course does not exclude a redundancy between individual sites.

Altogether these data show that PARP-1 is mainly sumoylated at K203 and K486, but they also suggest that at least one more minor and/or cryptic modification site may exist as well. These *in vivo* results were also confirmed *in vitro* (see 6.2.6 and **Figure 6.7**).

5.2.4 APLF and XRCC1 preferentially interact with PARP-1-SUMO in the yeast two-hybrid system

Although sumoylation can affect the properties of proteins as diverse as activity, localization or stability, it is becoming increasingly clear that these functional consequences are often brought about by factors that specifically recognize the sumoylated forms of such proteins (see 1.3). Conversely, in a few cases sumoylation has been shown or proposed to disrupt the interactions between partner proteins

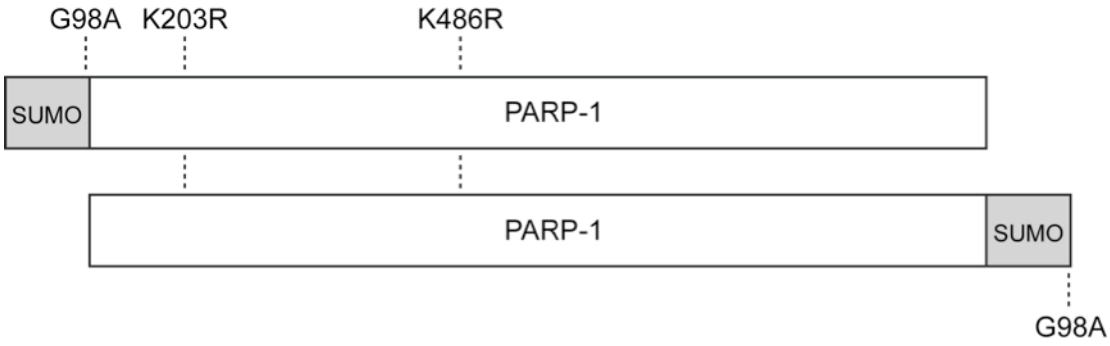

Figure 5.4 - Schematic representation of the linear SUMO-PARP-1 fusion constructs used in this chapter.

(Mohan *et al.*, 2007; Moldovan *et al.*, 2006). Thus, if I identified receptors specific for the sumoylated PARP-1 then I could use this information to narrow down the range of roles that this modification event might play. To tackle this question, I initially covalently fused SUMO to either the N- or C-terminus of PARP-1 to create fusion constructs that may behave as mimics of the truly sumoylated PARP-1 (**Figure 5.4**). Then, I analyzed how well these constructs interacted with known partners of the polymerase in comparison to the wild type PARP-1, the K203/486R mutant, SUMO1 and SUMO2 alone, using the yeast two-hybrid assay. The complete list of known PARP-1-interacting proteins, and the relevant references, can be accessed using GeneID 142 at the National Center for Biotechnology Information's Entrez Gene database (http://www.ncbi.nlm.nih.gov/sites/entrez?db=gene). Given the important role of PARP-1 in genome stability, I included several partners of the polymerase that had established functions in such a biological process – DNA repair (PARP-3, XRCC1, Ligase III, Aprataxin, APLF, TERF2IP) and replication (PCNA, p21, Werner's helicase). Since PARP-1 has an important function in apoptosis as well, I also included proteins with a role in this process that had been reported to interact with the polymerase (p53, Caspase 3, Caspase 7 and BCL2). In addition, the centromere factors CENP-A and CENP-B were also added to this analysis because they had been shown to interact with PARP-1 and to be parylated in response to DNA damage (Saxena *et al.*, 2002).

Figure 5.5 - APLF and PARP-1 preferentially interact with PARP-1-SUMO in the yeast two-hybrid assay. A), B and D) Yeast two-hybrid analysis was carried out as described in 2.8.9. BD = Gal4 DNA-binding domain, AD = Gal4 activation domain. - LW = lacking leucine and tryptophan, - LWH = lacking leucine, tryptophan and histidine, - LWHA = lacking leucine, tryptophan and adenine, WRN = Werner's helicase, PARP-1* = PARP-1 M890V/D899N. C) and E) Total extracts were prepared as described in 2.8.4.1 from cells carrying yeast two-hybrid plasmids that encoded for the BD fusions of the indicated PARP-1 constructs and analyzed by western blotting against PARP-1, PAR and PGK (loading control).

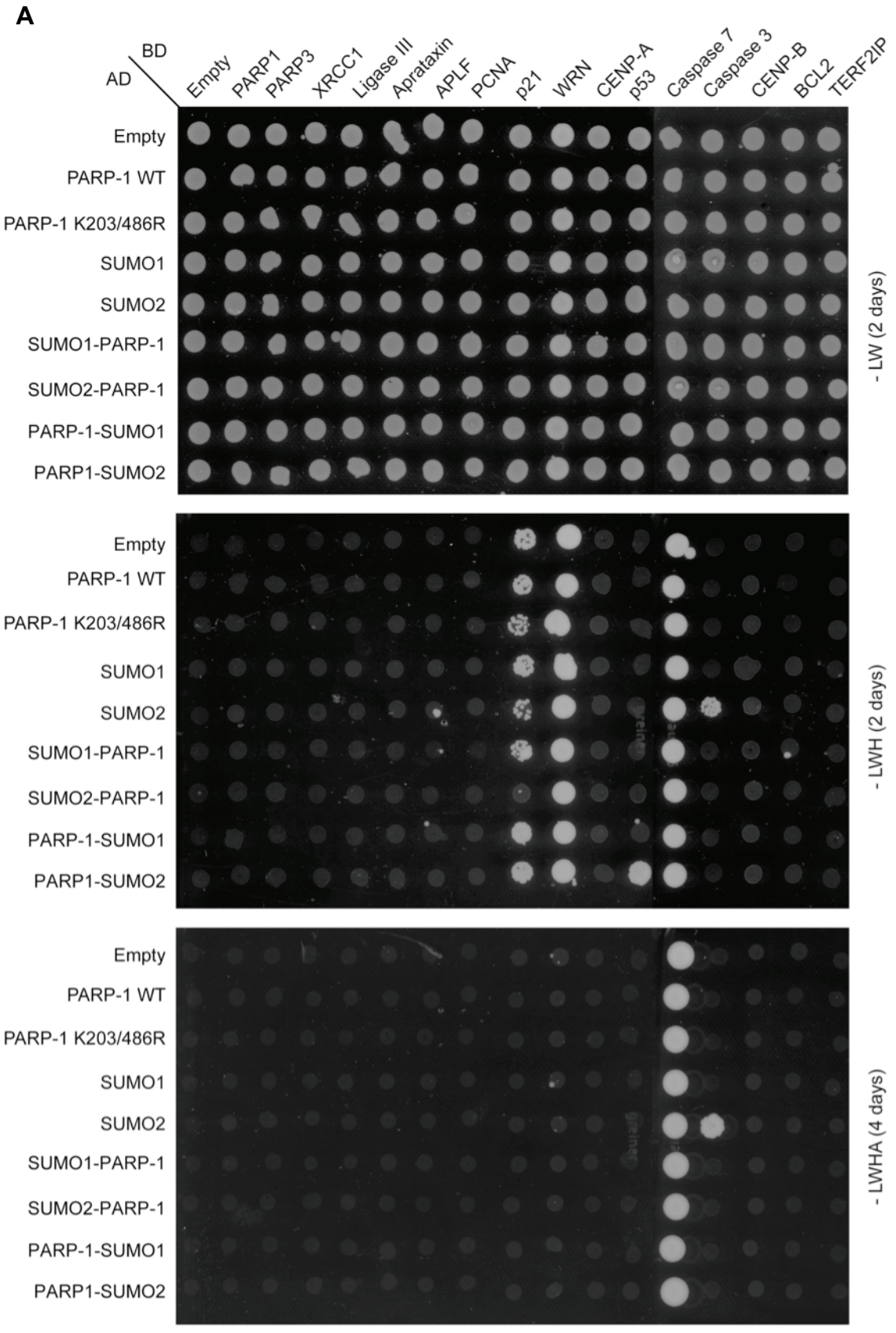
A
BD
AD
Empty
PARP1
PARP3
XRCC1
Ligase III
Aprataxin
APLF
PCNA
p21
WRN
CENP-A
p53
Caspase 7
Caspase 3
CENP-B
BCL2
TERF2IP
Empty
PARP-1 WT
PARP-1 K203/486R
SUMO1
SUMO2
SUMO1-PARP-1
SUMO2-PARP-1
PARP-1-SUMO1
PARP1-SUMO2
- LW (2 days)
- LWH (2 days)
- LWHA (4 days)

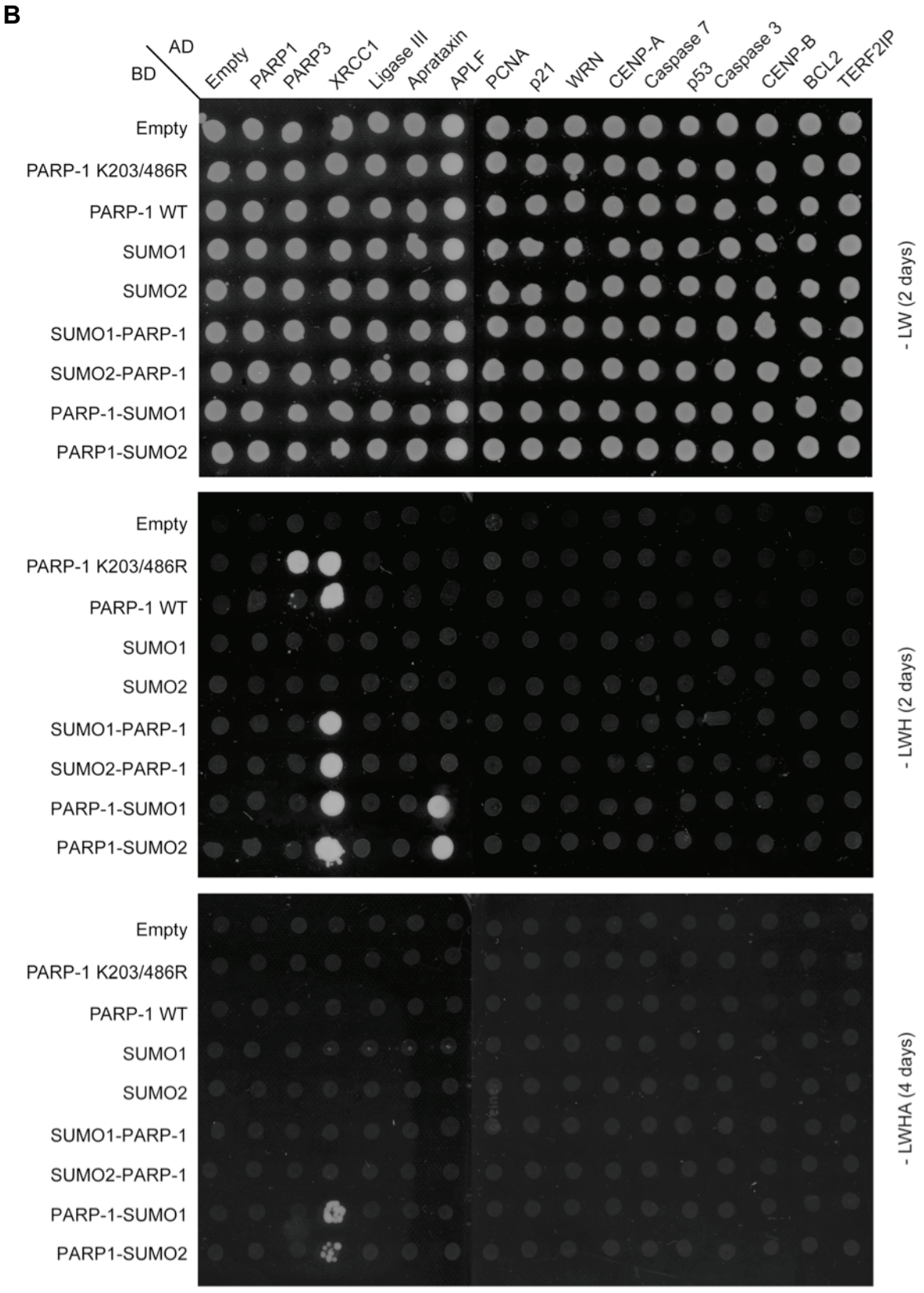
B
AD
BD
Empty
PARP1
PARP3
XRCC1
Ligase III
Aprataxin
APLF
PCNA
p21
WRN
CENP-A
Caspase 7
p53
Caspase 3
CENP-B
BCL2
TERF2IP
Empty
PARP-1 K203/486R
PARP-1 WT
SUMO1
SUMO2
SUMO1-PARP-1
SUMO2-PARP-1
PARP-1-SUMO1
PARP1-SUMO2
- LW (2 days)
- LWH (2 days)
- LWHA (4 days)

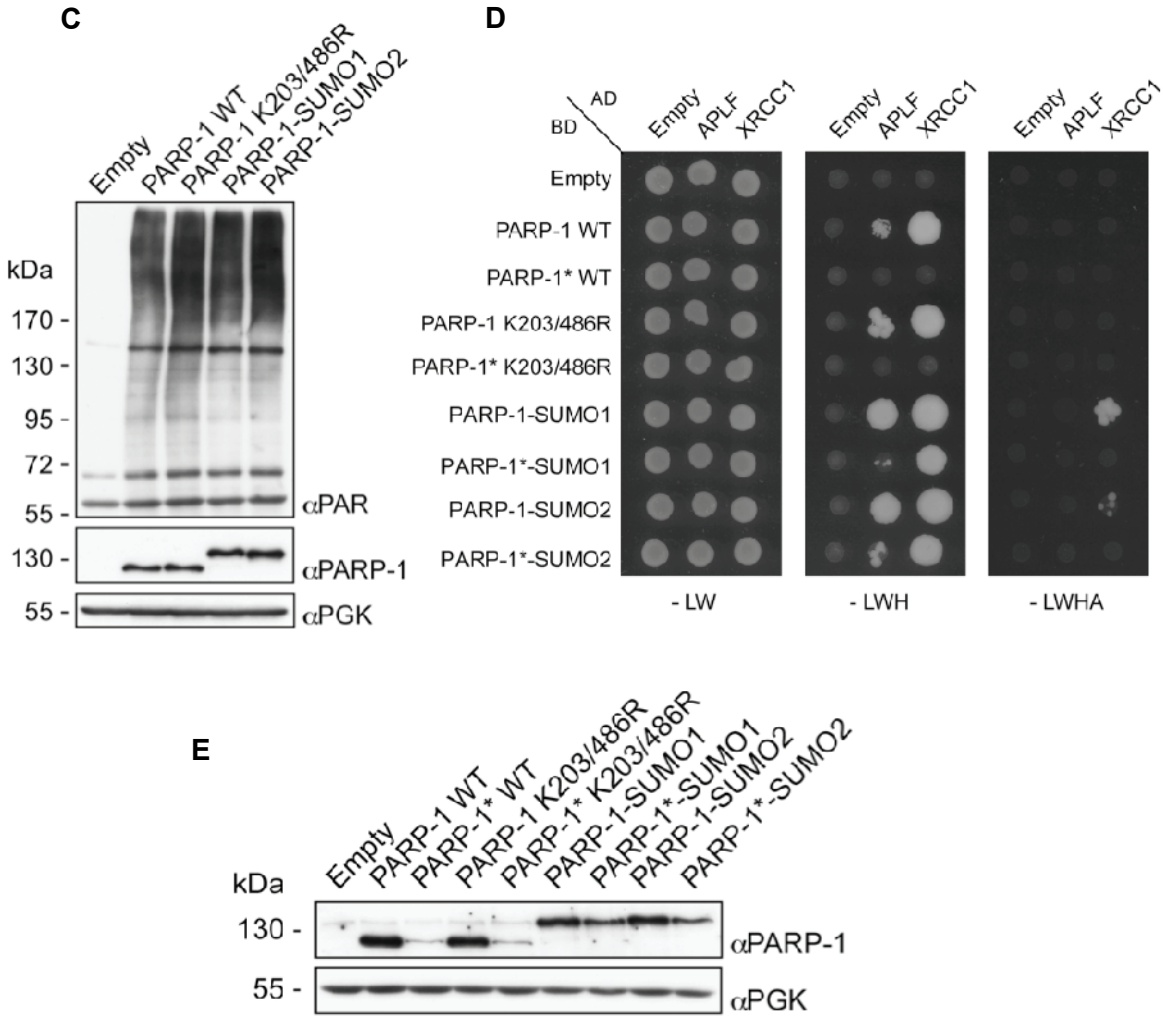

On the other hand, even though PARP-1 plays a role in transcription and it had been shown to interact with transcription factors (Kraus, 2008), with the exception of p53 I did not include such proteins in this analysis because how, or more importantly if, PARP-1 directly binds to them and affects their functions is not clear in most cases. **Figure 5.5**A and **Figure 5.5**B show the results of this large interaction analysis. The most striking observation from these data was that, in this type of yeast two-hybrid assay, neither the wild type PARP-1 nor the K203/486R mutant was able to interact with any of the tested baits, except for XRCC1. Even in this instance, XRCC1 interacted with PARP-1 in one direction of the yeast two-hybrid system only (BD-PARP-1 × AD-XRCC1). The examined baits did not interact with SUMO1 or SUMO2 alone either, except for Caspase 7 (AD-SUMO2 × BD-Caspase 7). Interestingly, I also observed that APLF and XRCC1 interacted with the PARP-1-SUMO1/2 fusions, but not the SUMO1/2-PARP-1 constructs, better than they did with either PARP-1 or SUMO1/2 alone. p53 exclusively interacted with the PARP-1-SUMO2 construct in the orientation

opposite to the APLF and XRCC1 interactions (AD-PARP-1-SUMO2 × BD-p53). The signals obtained with the GAL4 AD fusions of p21, Werner's helicase and Caspase 7, were certainly false-positives caused by the auto-activation of the relevant reporter genes by these constructs, as they were also detected in the presence of the empty GAL4 BD vector.

When PARP-1 is ectopically produced in budding yeast, it constitutively parylates itself even in the absence of DNA damage (Kaiser *et al.*, 1992). APLF and XRCC1 interact with PAR (Ahel *et al.*, 2008; Pleschke *et al.*, 2000). It was therefore possible that their preferential binding to PARP-1-SUMO1/2 could have been the result of an increased auto-parylation activity of the fusion constructs in comparison to the unmodified PARP-1. To investigate this possibility, I transformed yeast cells with an empty two-hybrid vector or the equivalent plasmids encoding wild type PARP-1, the K203/486R mutant or the PARP-1-SUMO fusions. I prepared total extracts from such cells and then analyzed them by western blotting against PARP-1, PAR and PGK (loading control). **Figure 5.5**C shows that all of the examined PARP-1 constructs were produced at similar levels and generated comparable amounts of PAR.

To corroborate these results I also examined the interaction of APLF and XRCC1 with catalytically deficient PARP-1 mutants. Two point mutations (M890V and D899N) were introduced into PARP-1, which have been shown to individually reduce catalytic activity to less than 1% of that of the wild type protein (Rolli *et al.*, 1997). **Figure 5.5**D shows that although abrogating the enzymatic activity of PARP-1 weakened the binding of APLF and XRCC1 to the PARP-1-SUMO1/2 fusions, the interactions were still stronger than those detected in the presence of the "non-sumoylated" PARP-1 M890V/D899N mutants. A possible explanation for these results was that, in addition to inactivating PARP-1, mutating M890 and D899 could also destabilize the protein, hence reducing its steady-state levels in comparison to the wild type polymerase. Indeed, when total extracts from yeast cells producing the PARP-1 M890V/D899N constructs or the corresponding wild type counterparts were analyzed by western blotting the levels of the former were significantly lower than those of the latter (**Figure 5.5**E).

Altogether these results show that, by yeast two-hybrid analysis, APLF and XRCC1 interacted better with PARP-1-SUMO than they did with PARP-1, independently of the enzyme's catalytic activity.

5.2.5 Interactions of APLF and XRCC1 with sumoylated PARP-1 *in vitro*

Since I observed that appending SUMO to PARP-1 affected its interactions with APLF and XRCC1 in the yeast two-hybrid system, it was important to confirm this finding by a more biochemically tractable method. I therefore carried out *in vitro* binding assay using recombinant proteins. GST alone, N-terminally GST-tagged APLF or XRCC1 were mixed with equal amounts of His_6-PARP-1 K203/486R and His_6-PARP-1-SUMO2, incubated, captured on glutathione resin and then analyzed by western blotting against PARP-1. After this analysis the membrane was stained with Coomassie to confirm the even loading of the GST-tagged proteins in the pull-down samples and the comparable amounts of PARP-1 and the PARP-SUMO2 fusion in the input material (**Figure 5.6**A). This experiment revealed that both APLF and XRCC1 interacted with PARP-1-SUMO2 almost as well as they did with PARP-1 alone.

Although the PARP-1-SUMO2 construct used in this experiment was a useful and easy-to-handle tool, it nevertheless remained an artificial mimic of PARP-1 modified at K203 and K486. It was therefore important to demonstrate that a "truly" sumoylated PARP-1 could behave similarly to the fusion construct with respect to the way it interacted with APLF and XRCC1. To address this question, I subjected PARP-1 to two kinds of *in vitro* sumoylation reactions. Both of them contained His_6-PARP-1 and AOS1/His_6-UBA2, SUMO2 K25/27/31R, which was used to reduce chain formation, and plasmid DNA, which was added to enhance the otherwise low levels of the modification (see 6.2). One reaction was supplemented with the wild type UBC9 while the control one with the catalytically inactive UBC9 C93S mutant. Following incubation at 30°C for 2 h, the polymerase was purified by metal affinity chromatography under

Figure 5.6 - Interactions of APLF and XRCC1 with sumoylated PARP-1 *in vitro*. A) GST, GST-APLF and GST-XRCC1 (20 pmol) were mixed with His_6-PARP1 (30 pmol) and His_6-PARP1-SUMO2 (30 pmol) in a final volume of 100 µL PBS + 0.1% Triton X-100 and subjected to pull-down analysis as described in 2.18.2. The western blotting membrane was also stained with Coomassie. B) His_6-PARP-1 (450 pmol) was subjected to a 3 mL sumoylation reaction supplemented with SUMO2 K25/27/31R, a supercoiled plasmid (18 µg) and either UBC9 WT or UBC9 C93S. All subsequent stages were performed as described in 2.17.1.2. C) GST, GST-APLF and GST-XRCC1 (20 pmol) were combined with a mix of the mock modified and sumoylated PARP-1 proteins (60 pmol of PARP-1 in total) and then analyzed by pull-down analysis as described in A). D) GST, GST-APLF and GST-XRCC1 (30 pmol) were mixed with His_6-tagged PARP-1 (90 pmol), His_6-SUMO1 or His_6-SUMO2 (1 nmol) and then subjected to pull-down analysis as described in A). E) HEK293 cells stably producing $FLAG_3$-APLF or $FLAG_3$-XRCC1 (90% confluent, 60 mm ∅ dish) were transfected with a plasmid (8 µg) encoding for PARP-1-SUMO2 by lipofection (20 µL of lipofectamine 2000). After 24 h, total extracts (1.75 mg in 1 mL of RIPA buffer) were prepared and subjected to anti-FLAG immunoprecipitation as described in 2.16.2. Immunoprecipitated proteins were eluted and then analyzed by western blotting against PARP-1 (75% of the eluate) and the $FLAG_3$ tag (7.5% of the eluate).

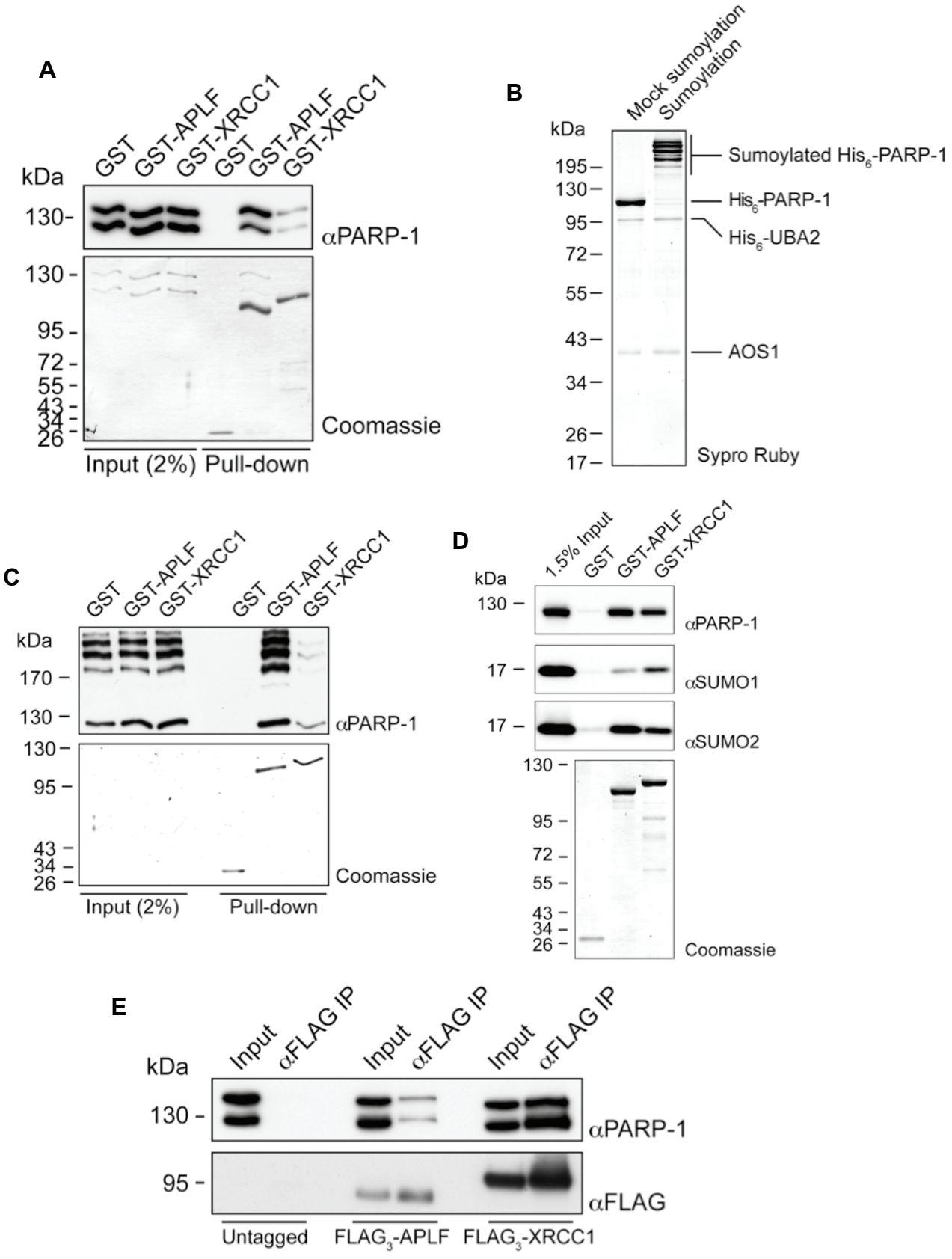
A
GST
GST-APLF
GST-XRCC1
GST
GST-APLF
GST-XRCC1
kDa
130
αPARP-1
130
95
72
55
43
34
26
Coomassie
Input (2%)
Pull-down
B
Mock sumoylation
Sumoylation
kDa
195
130
95
72
55
43
34
26
17
Sumoylated His6-PARP-1
His6-PARP-1
His6-UBA2
AOS1
Sypro Ruby
C
GST
GST-APLF
GST-XRCC1
GST
GST-APLF
GST-XRCC1
kDa
170
130
αPARP-1
130
95
43
34
26
Coomassie
Input (2%)
Pull-down
D
1.5% Input
GST
GST-APLF
GST-XRCC1
kDa
130
αPARP-1
17
αSUMO1
17
αSUMO2
130
95
72
55
43
34
26
Coomassie
E
Input
αFLAG IP
Input
αFLAG IP
Input
αFLAG IP
kDa
130
αPARP-1
95
αFLAG
Untagged
FLAG3-APLF
FLAG3-XRCC1

stringent ionic conditions to remove the DNA and the other proteins present in the reaction, except for negligible amounts of the SUMO activating enzyme, which was also His_6-tagged. The purified proteins were resolved by SDS-PAGE and visualized by SYPRO Ruby staining (**Figure 5.6**B). As expected, the His_6-PARP-1 isolated from the reaction containing UBC9 C93S appeared as a tight single band that ran at the right size for an unmodified polymerase (~120 kDa). Conversely, when the wild type UBC9 was used in the reaction, the purified His_6-PARP-1 was converted into multiple slow-migrating bands, which mainly correspond to sumoylation of K203 and K486 (**Figure 6.7**B). With these protein preparations in hand, I repeated the above-described pull-down experiment, but this time the GST-tagged APLF and XRCC1 were incubated with a mix of the mock-modified and sumoylated PARP-1. **Figure 5.6**C shows that APLF and XRCC1 interacted with the modified forms of PARP-1 essentially as well as they did with the mock-sumoylated polymerase.

A noteworthy observation transpiring from these results was that the preferential binding of APLF and XRRC1 to the sumoylated PARP-1 *in vitro* was minimal in comparison to that observed in the yeast two-hybrid system (**Figure 5.5**B). I therefore wondered whether APLF and XRCC1 bound PARP-1 somewhat better when it was sumoylated simply because this conjugation event led to the addition of their individual affinities for PARP-1 and SUMO, instead of a “synergistic” effect, which would have been instead expected for a true receptor of sumoylated PARP-1. To partly address this question I looked at how well APLF and XRCC1 interacted with SUMO1 and SUMO2 in comparison to PARP-1 by *in vitro* pull-down analysis. GST alone, GST-tagged APLF or XRCC1 were mixed with His_6-tagged SUMO1, SUMO2 or PARP-1, incubated, captured on glutathione resin and then analyzed by western blotting against SUMO1, SUMO2 and PARP-1. **Figure 5.6**D shows that, as expected, both APLF and XRCC1 interacted with PARP-1 and that they were able to bind SUMO1 and, somewhat preferentially, SUMO2. In addition, it was evident that APLF and XRCC1 bound comparable amounts of SUMO and PARP-1. Since I used ten times more SUMO than PARP-1 in such binding assays, these results suggested that APLF and XRCC1 probably interact more weakly with SUMO than they do with PARP-1. By a very rough estimate, the strength of interaction between APLF/XRCC1 and SUMO was in the same order of magnitude as the minimal increase in binding affinity that such two proteins exhibited towards the sumoylated PARP-1 in comparison to the unmodified protein (**Figure 5.6**A and **Figure 5.6**C). In addition, I also observed that APLF and XRCC1 interacted with PARP-1-SUMO2 essentially as well as they did with PARP-1

alone when they were immunoprecipitated from extracts of HEK293 cells that produced PARP-1-SUMO2 at endogenous PARP-1 levels (**Figure 5.6**E).

Altogether these data indicate that *in vitro* APLF and XRCC1 do not probably have any significant preference for the sumoylated PARP-1 *vs.* the unmodified polymerase that cannot be traced back to the simple addition of two protein-protein interaction events (APLF/XRCC1 ⇔ SUMO and APLF/XRCC1 ⇔ PARP-1), which probably occured when SUMO was conjugated to PARP-1.

5.2.6 Sumoylation of PARP-1 does not significantly alter its enzymatic activity

Sumoylation has been shown to affect the enzymatic activity of certain proteins (Hardeland *et al.*, 2002; Morris *et al.*, 2009; Vethantham *et al.*, 2008). Having isolated a recombinant form of PARP-1 that had been sumoylated at K203 and K486 enabled me to determine whether SUMO may impinge on PARP-1's catalytic activity. To answer this question, I initially examined the auto-parylation of PARP-1 by mixing the mock-modified and sumoylated forms of this protein with DNase I-activated calf thymus DNA, to stimulate their catalytic activity, and NAD^+, which is used by the enzyme as a source of ADP-ribose. Samples of these reactions were collected at increasing time points and analyzed by western blotting against PAR. **Figure 5.7**A shows that the unmodified PARP-1 and its sumoylated counterpart were auto-parylated with similar kinetics and to similar extents.

The above-described data showed that sumoylation did not directly affect the auto-parylation activity of PARP-1, at least when it was analyzed in a minimalistic *in vitro* assay. However, they did not exclude the possibility that under more "physiological" conditions a difference may have become more apparent. This situation could have occurred by means of, for instance, regulatory proteins that specifically recognize the sumoylated polymerase. Factors that influence the activity of PARP-1, such as ERK2 and histones, have been identified (Cohen-Armon *et al.*, 2007; Kun *et al.*, 2004). Therefore, it would have been ideal to analyze the enzymatic activity of the unmodified and physiologically sumoylated PARP-1 *in vivo*. Given the extremely low levels of the latter, this type of experiment proved technically unfeasible. As an alternative, I measured the levels of PAR in cells depleted of the endogenous PARP-1 by RNA interference and reconstituted with recombinant PARP-1 or the PARP-1-SUMO constructs. Unfortunately, I was never able to reliably detect a reproducible PAR signal in these experiments. I therefore opted for a "hybrid" *in vitro/in vivo* approach whereby I

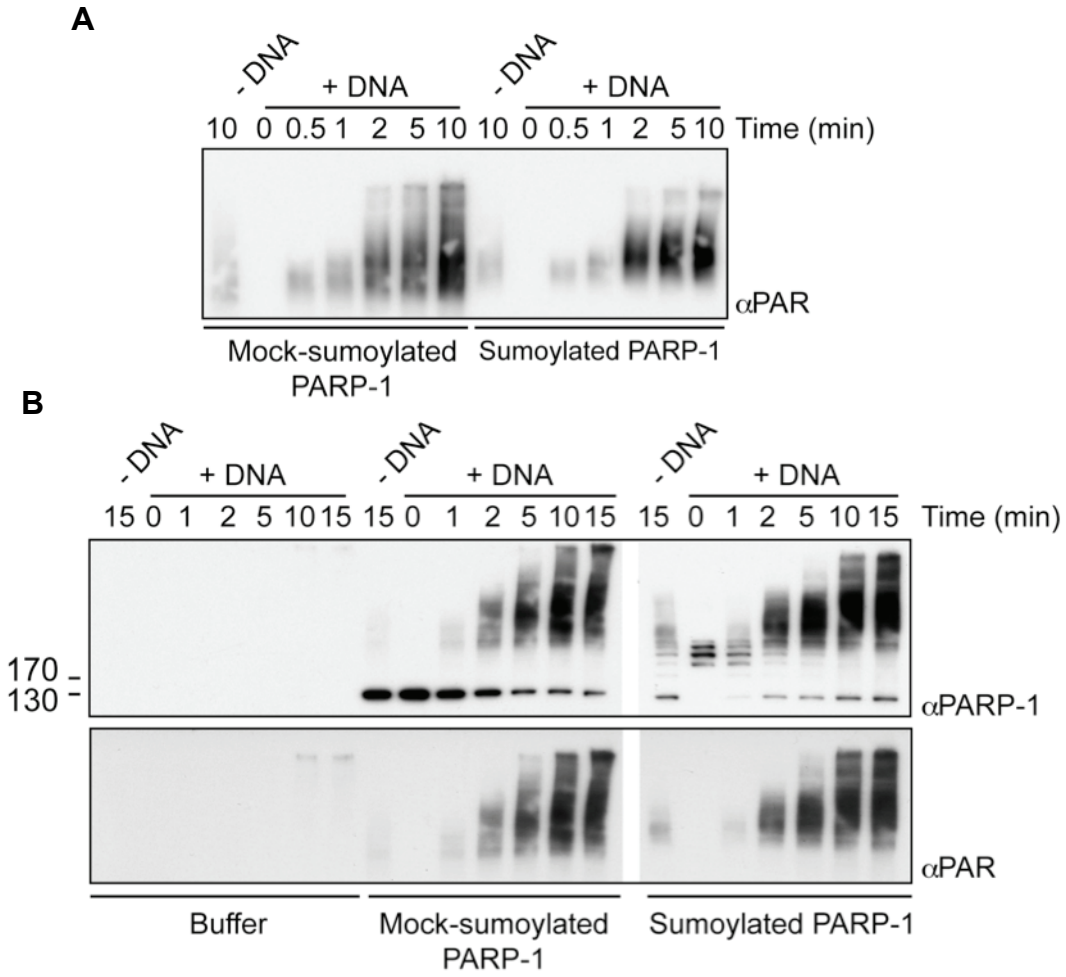

Figure 5.7 - Sumoylation does not affect the parylation activity of PARP-1. A) Parylation reactions in the presence of mock-modified or sumoylated His_6-PARP-1 (40 ng) were carried out under standard conditions as described in 2.17.2. B) As in A) but in the presence of nuclear extracts prepared from *PARP-1*$^{-/-}$ mouse embryonic fibroblasts (25 µg) as described in 2.10.8.

assayed the activity of the unmodified and sumoylated His_6-PARP-1 in nuclear extracts prepared from *PARP-1*$^{-/-}$ mouse embryonic fibroblasts (a gift from Zhao-Qi Wang). These extracts were used under reaction conditions that had been previously shown to support DNA repair (Vodenicharov *et al.*, 2000). They were supplemented with either ~ 0.45 pmol of modified or unmodified PARP-1 per 30 µg of extract, which is equivalent to the quantity of the polymerase present in the same amount of *PARP-1*$^{+/+}$ nuclear extracts (Vodenicharov *et al.*, 2000), or with a buffered solution to account for background PAR activity from PARP-2 (Schreiber *et al.*, 2002). In these reactions PARP-1 activity was analyzed in the presence of DNase I-activated calf thymus DNA and NAD^+. Samples were collected at increasing time points and analyzed by western blotting against PARP-1 and PAR. **Figure 5.7**B shows that even under these

conditions the unmodified and sumoylated His_6-PARP-1 catalyzed similar levels of PAR with similar kinetics. This polymer was specifically produced by the recombinant His_6-PARP-1 because almost no PAR was detected in the reactions supplemented with a buffered solution only.

Overall these data show that SUMO does not significantly alter the enzymatic activity of PARP-1.

5.2.7 Sumoylation of PARP-1 does not alter its subcellular localization

SUMO controls the subcellular localization of certain proteins in both lower and higher eukaryotes (Dawlaty *et al.*, 2008; Liu and Gerace, 2009; Mahajan *et al.*, 1997; Matunis *et al.*, 1998; Takahashi and Strunnikov, 2008; Yurchenko *et al.*, 2006; Zhu *et al.*, 2009). For some of these factors, artificially fusing them to SUMO has been shown to mimic their physiological modification. For example, fusing SUMO to XRCC4 rescues the localization phenotype of the corresponding unsumoylatable mutant (Yurchenko *et al.*, 2006), and a SUMO-topoisomerase II fusion is correctly targeted to its biologically relevant subcellular address (Dawlaty *et al.*, 2008). PARP-1 is mainly a chromatin-associated nuclear protein, although it has been recently detected in mitochondria as well (Rossi *et al.*, 2009). Within the nucleus, PARP-1 is somewhat enriched in transcriptionally active nucleoli (Meder *et al.*, 2005), at least at specific stages of the cell cycle (Sugimura *et al.*, 2008). To examine whether sumoylation may affect the subcellular localization of PARP-1, I transfected HeLa cells with plasmids encoding eGFP alone, as a control, or N-terminally eGFP-tagged wild type PARP-1, the K203/486R mutant, or the C-terminal SUMO fusions. The cells were fixed and the localization of the eGFP-tagged proteins was determined by fluorescence microscopy. **Figure 5.8**A shows that fusing the wild type PARP-1 to eGFP restricted to the nucleus the pan-cellular signal observed in the cells producing this tag alone, which indicated that eGFP-tagging of PARP-1 did not disrupt its proper subcellular localization. Additionally, it showed that the PARP-1 K203/486R mutant and the PARP-1-SUMO constructs also localized exclusively to the nucleus, with distribution patterns comparable to those seen for the wild type protein.

In order to corroborate these results, and also to explore whether sumoylation may control the association of PARP-1 to chromatin without affecting its nuclear retention, the subcellular distribution of the wild type PARP-1 was compared to that of the K203/486R mutant and the PARP-1-SUMO2 fusion by cellular fractionation. I transfected HEK293 cells with plasmids encoding an N-terminally $FLAG_3$-tagged

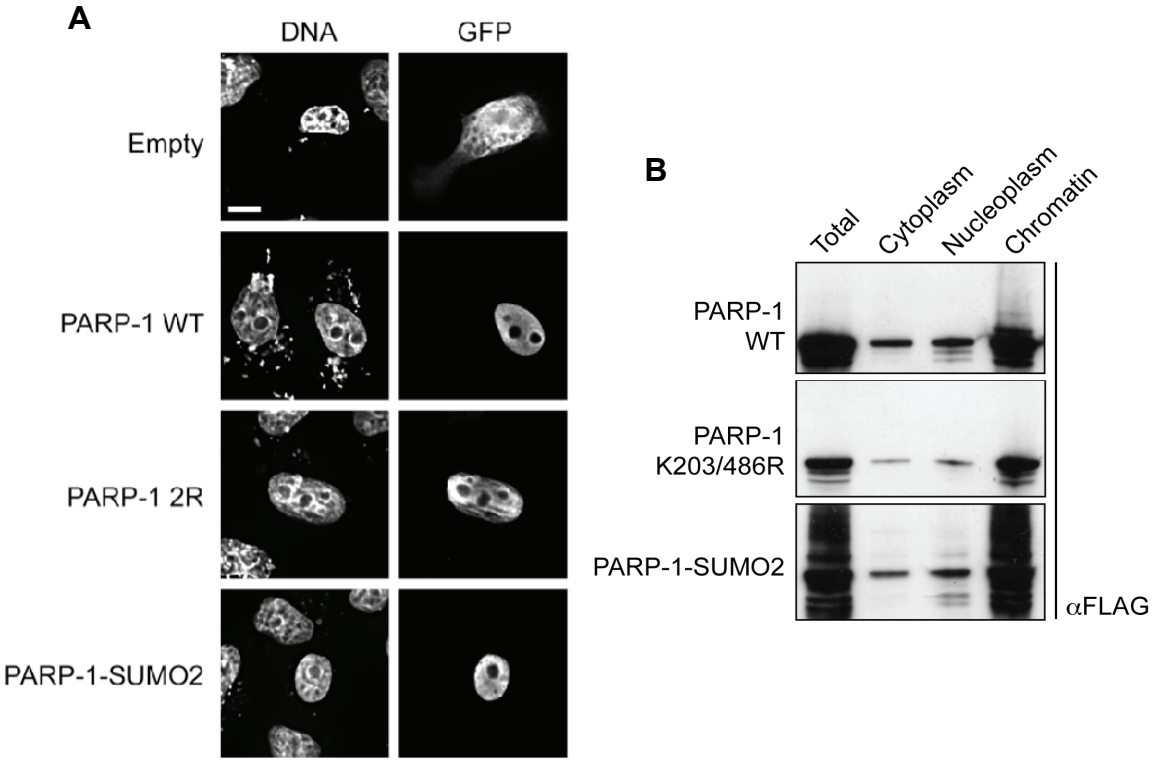

Figure 5.8 - Sumoylation does not affect the subcellular localization of PARP-1. HeLa cells (60% confluent, 8-well Cultureslide) were transfected with plasmids (250 ng) encoding for eGFP alone or the indicated N-terminally eGFP-tagged PARP-1 constructs by lipofection (1 µL of Fugene HD). After 24 h, the cells were fixed and subjected to immunofluorescence as described in 2.10.6. B) HEK293 cells (90% confluent, 100 mm ∅ dish) were transfected with plasmids (10 µg) encoding the specified N-terminally $FLAG_3$-tagged constructs of PARP-1 by lipofection (40 µL of Fugene HD). After 24 h, total extracts prepared from these cells were fractionated into cytoplasmic, nucleoplasmic and chromatin phases, as described in 2.10.7, and analyzed by western blotting against the FLAG tag.

version of the above-mentioned constructs. Rajvee Shah prepared total extracts from these cells, fractionated them into cytoplasmic, nucleoplasmic and chromatin phases and then analyzed them by western blotting against the $FLAG_3$ tag. **Figure 5.8**B shows that the distribution patterns of the $FLAG_3$-PARP-1 K203/486R mutant and the $FLAG_3$-PARP-1-SUMO2 fusion were very similar to that of the wild type protein, in fact, all of them were almost completely associated with the chromatin.

Altogether these results indicate that, at least under unchallenged growth, SUMO does not appreciably affect the subcellular localization of PARP-1.

5.2.8 The PARP-1-SUMO fusion proteins are poly-sumoylated *in vivo*

Interestingly, the cell fractionation experiments shown in **Figure 5.8**B revealed that $FLAG_3$-PARP-1-SUMO2 was resolved as one main band, which expectedly ran somewhat more slowly than the wild type polymerase, and several slower-migrating

forms. This finding was exciting because it suggested that appending SUMO2 to PARP-1 led to the further post-translational modification of this protein. By inference, it was possible that sumoylating PARP-1 at K203 and K486 could also trigger a similar effect. Crosstalk between sumoylation and other types of post-translational modifiers has been reported before (Desterro *et al.*, 1998; Mohan *et al.*, 2007; Prudden *et al.*, 2007; Sun *et al.*, 2007; Wu and Chiang, 2009). In addition PARP-1 can be conjugated to SUMO, PAR, ubiquitin (Wang *et al.*, 2008b) and acetyl groups (Hassa *et al.*, 2005) *in vivo*. It was interesting to determine whether any of these modifiers was specifically conjugated to PARP-1-SUMO2. Towards this end, Rajvee Shah transfected HEK293 cells with plasmids carrying the eGFP-PARP-1 constructs described in 5.2.7 or the empty eGFP vector as a control. She prepared total extracts from these cells and then captured the eGFP-tagged proteins with an anti-GFP antibody under conditions of high ionic strength. These immunoprecipitates were analyzed by western blotting against GFP, ubiquitin and PAR. In addition, they were probed for SUMO1 to determine whether fusing SUMO2 to PARP-1 stimulated the attachment of polymeric SUMO chains to this construct. Although only SUMO2/3 appear to be able to make chains *in vivo* (Matic *et al.*, 2008; Tatham *et al.*, 2008), I used an anti-SUMO1 antibody to explore this issue for two reasons. Firstly, if I employed an anti-SUMO2/3 antibody then I would have not been able to distinguish between the western blotting signal from the SUMO2 moiety artificially fused to PARP-1, in the PARP-1-SUMO2, construct and that from true polymeric SUMO chains that may be conjugated to it. Secondly, although SUMO1 does not seem to form chains *in vivo*, it can be part of the naturally occurring SUMO2/3 polymers as a termination signal (Matic *et al.*, 2008; Tatham *et al.*, 2008). **Figure 5.9**A showed that, in comparison to the wild type protein, appending SUMO2 to PARP-1 did not significantly alter its low background levels of auto-parylation in the absence of DNA damage or the extent to which it was ubiquitylated. Nevertheless, the average size of the ubiquitylated PARP-1-SUMO2 was larger than that of the ubiquitylated wild type enzyme. Conversely, the PARP-1-SUMO2 fusion was heavily conjugated to SUMO1. Such a modification event did not depend on which tag was appended to the fusion construct because it was detected for both the eGFP- (**Figure 5.9**A) and $FLAG_3$-tagged (**Figure 5.8**B) versions. In addition, I also observed this phenomenon when untagged PARP-1-SUMO2 was ectopically produced in *PARP-1*$^{-/-}$ mouse embryonic fibroblasts (data not shown). Last but not least, the identity of the SUMO paralogue fused to PARP-1 did not significantly affect the ability of the resulting construct to be further modified (**Figure 5.9**B).

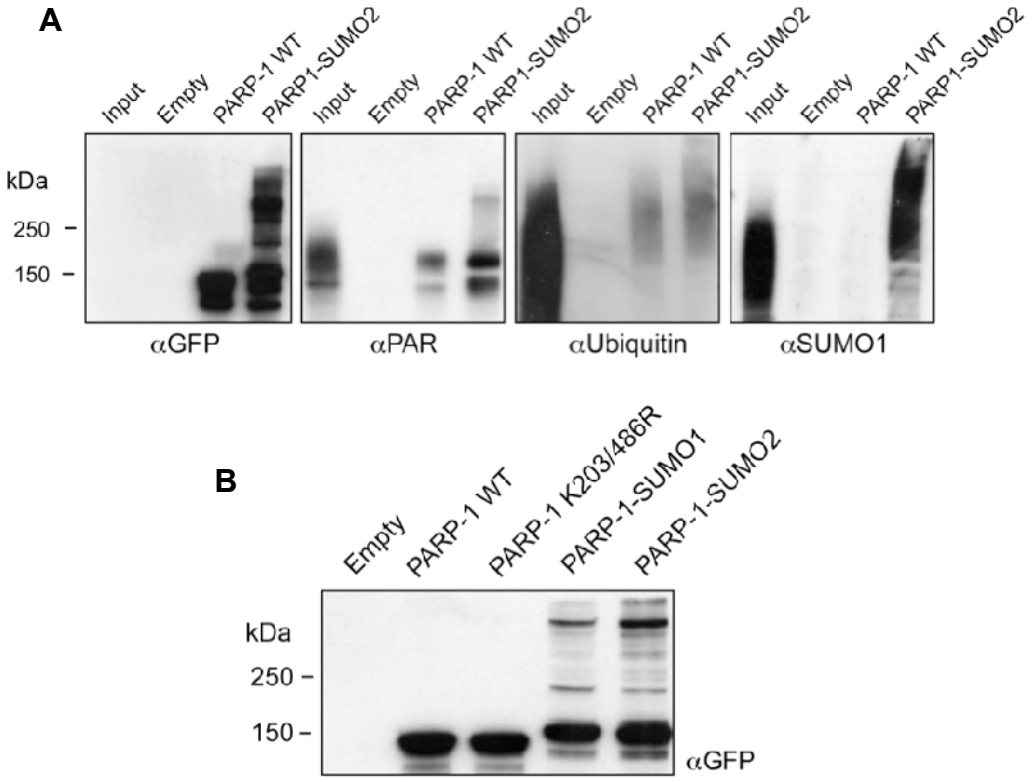

Figure 5.9 - The PARP-1-SUMO constructs are poly-sumoylated *in vivo*. A) HEK293 cells (60% confluent, 100 mm ∅ dish) were transfected with plasmids (10 µg) encoding for eGFP alone or the indicated N-terminally eGFP-tagged PARP-1 constructs by lipofection (40 µL of Fugene HD). After 48 h, total extracts (1 mg in 1 mL of RIPA buffer) from these cells were subjected to overnight immunoprecipitation as described in section 2.16.2 in the presence of anti-GFP resin (10 µL). The immunocaptured proteins were analyzed by western blotting against GFP, PAR, ubiquitin and SUMO1 (10% of eluate). B) Total extracts from HEK293 cells transfected as described in A) were subjected to western blotting analysis against GFP.

In conclusion, these data show that appending SUMO to PARP-1 stimulates its poly-sumoylation, most likely through SUMO2/3 chains bearing a SUMO1 moiety at their very ends.

5.2.9 Proteasomal inhibition leads to further post-translational modification of the sumoylated PARP-1

Through the action of specific SUMO-targeted ubiquitin ligases, polymeric SUMO chains have been shown to tag proteins for poly-ubiquitylation and subsequent proteasome-mediated degradation (see 1.2.6). Having found that the PARP-1-SUMO fusions were heavily polysumoylated *in vivo*, I was curious to explore whether this phenomenon might lead to their poly-ubiquitylation and destruction. Thus, I incubated HEK293 cells producing N-terminally FLAG-tagged wild type PARP-1, the K203/486R

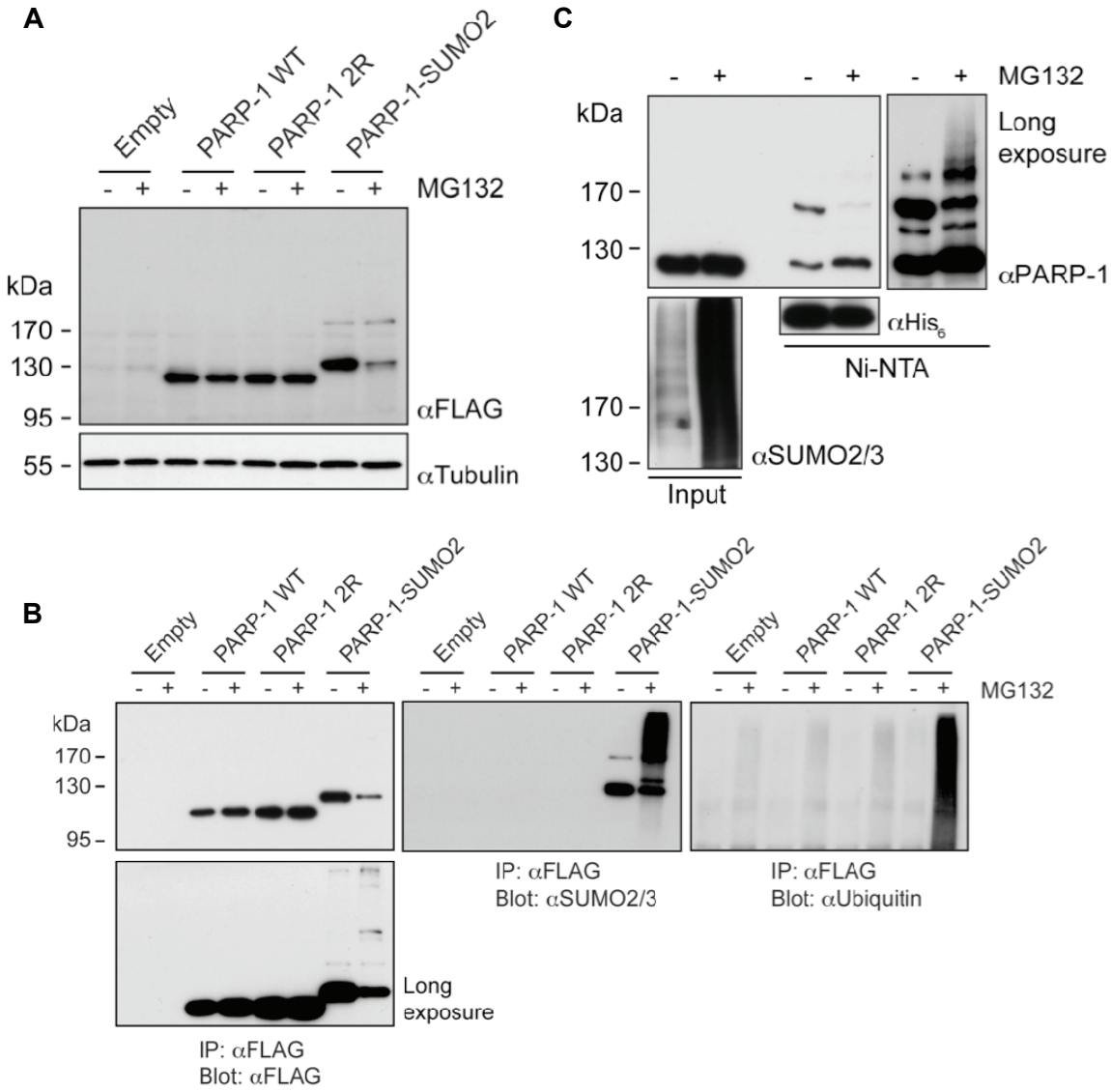

Figure 5.10 - PARP-1-SUMO2 becomes further modified following proteasomal inhibition. A) HEK293 producing FLAG-tagged constructs of PARP-1 WT, the K203/486R mutant or the PARP-1-SUMO2 fusion were incubated with MG132 (30 μM), or an equivalent volume of DMSO. After 5 h, total extracts made from these cells were analyzed by western blotting against the FLAG tag and tubulin (loading control). B) Total extracts (750 μg in 0.75 mL of RIPA buffer) prepared from cells treated as described in A) were subjected to an overnight immunoprecipitation with an anti-FLAG resin (30 μL) as described in 2.16.2. The immunoprecipitated proteins were analyzed by western blotting against the FLAG tag (7.5% of the eluate), ubiquitin (30% of the eluate) and SUMO2/3 (30% of the eluate). C) HeLa cells producing His_6-SUMO3 (Figure 5.1A) were incubated for 5 h in the presence of MG132 (30 μM) or an equivalent volume of DMSO before proceeding to the isolation of sumoylated species as described in Figure 5.1A.

mutant or the PARP-1-SUMO2 fusion in the presence of the proteasome inhibitor MG132 or DMSO. I prepared total extracts from these cells and analyzed them by western blotting against the FLAG tag or tubulin. **Figure 5.10**A shows that the steady-state levels of the wild type PARP-1 and the K203/486R mutant were largely

unaffected by treatment with MG132. On the other hand, proteasomal inhibition led to an almost complete loss of the signal for PARP1-SUMO2.

This last observation was rather counter-intuitive unless I assumed that inhibiting the proteasome might have led to the accumulation of long ubiquitin chains on a protein, *i.e.* PARP1-SUMO2, that was already being heavily poly-sumoylated. Such a substantial amount of modification could have potentially converted the PARP-1-SUMO2 fusion into a range of high-molecular weight conjugates so wide that their signal seemingly disappeared due to a "dilution effect", or their sheer size. To substantiate this hypothesis, I repeated the above-described experiment, but this time I immunoprecipitated the recombinant PARP-1 constructs by means of an anti-FLAG antibody. Western blotting analysis of these preparations showed that inhibiting the proteasome apparently reduced the amount of immunoprecipitated PARP-1-SUMO2 but it also led to the accumulation of several slow-migrating forms of this protein (Fig. **Figure 5.10**B). Analysis of these immunoprecipitates with an anti-SUMO2/3 antibody also revealed that proteasomal inhibition converted the unmodified PARP-1-SUMO2 construct into a smear of greater signal intensity, which migrated all the way up to the well of the gel. Given these results, I was not surprised to observe that in the presence of MG132 PARP-1-SUMO2 also co-isolated with ubiquitylated species.

The above-presented data showed that inhibiting the proteasome boosted the poly-sumoylation of PARP-1-SUMO2 and its association with poly-ubiquitylated species, probably through covalent interactions. I was therefore interested in establishing whether the sumoylation of PARP-1 at K203 and K486 was also susceptible to proteasomal inhibition. To address this problem, I isolated sumoylated species by denaturing Ni^{2+}-NTA chromatography from His_6-SUMO3-expressing HeLa cells that were incubated in the presence of MG132 or DMSO. Western blotting analysis of these purifications, **Figure 5.10**C, showed that proteasomal inhibition led to the apparent loss of the main sumoylated forms of PARP-1. From a longer exposure of this same western blotting membrane I noticed that the MG132-depedent loss of the (mono)-sumoylated PARP-1 was accompanied by the appearance of a faint but noticeable high-molecular weight smear. This observation strongly suggested that inhibiting the proteasome led to further modification of the sumoylated PARP-1.

Altogether these data indicate that upon proteasomal inhibition both the PARP-1-SUMO2 fusion construct and the physiologically sumoylated PARP-1 were further conjugated to SUMO and/or ubiquitin.

5.2.10 Proteasomal inhibition leads to the accrual of PARP1-SUMO2 into nuclear foci that do not co-localize with PML nuclear bodies

The unexpected finding that PARP-1-SUMO2 specifically associated with ubiquitylated species of lower molecular weight than PARP-1 itself (**Figure 5.10**B) put forward the possibilities that some of them might have been generated by partial proteolysis of the ubiquitylated fusion protein. Alternatively, they could have been ubiquitylated proteins isolated through non-covalent interactions with PARP-1-SUMO2. Such a phenomenon could have occurred if, for instance, the fusion construct relocalized to, and thereby became entrapped in, PML nuclear bodies. These nuclear structures are heavily enriched in species conjugated to SUMO and/or ubiquitin and they have been proposed to act as degradation factories (Bailey and O'Hare, 2005). To explore this possibility, I transfected HeLa cells with the eGFP constructs described in 5.2.7 and then treated them with MG132 or DMSO only. The cells were fixed, subjected to indirect immunofluorescence against PML and finally analyzed by fluorescence microscopy. **Figure 5.11** shows that upon proteasomal inhibition eGFP-PARP-1-SUMO2 accrued into well-defined nuclear foci in more than 30% of the transfected cells. These foci did not co-localize with PML nuclear bodies and were not detected for

Figure 5.11 - PARP-1-SUMO2 accrues into nuclear foci that do not co-localize with PML nuclear bodies, upon inhibition of the proteasome. A) HeLa cells were transfected and processed for immunofluorescence as described in Figure 5.8A, but before being fixed they were incubated in the presence of MG132 (30 μM) or an equivalent volume of DMSO for 5 h. B) Quantification of the percentage of the GFP-positive HeLa cells that displayed 5 or more nuclear PARP-1 foci.

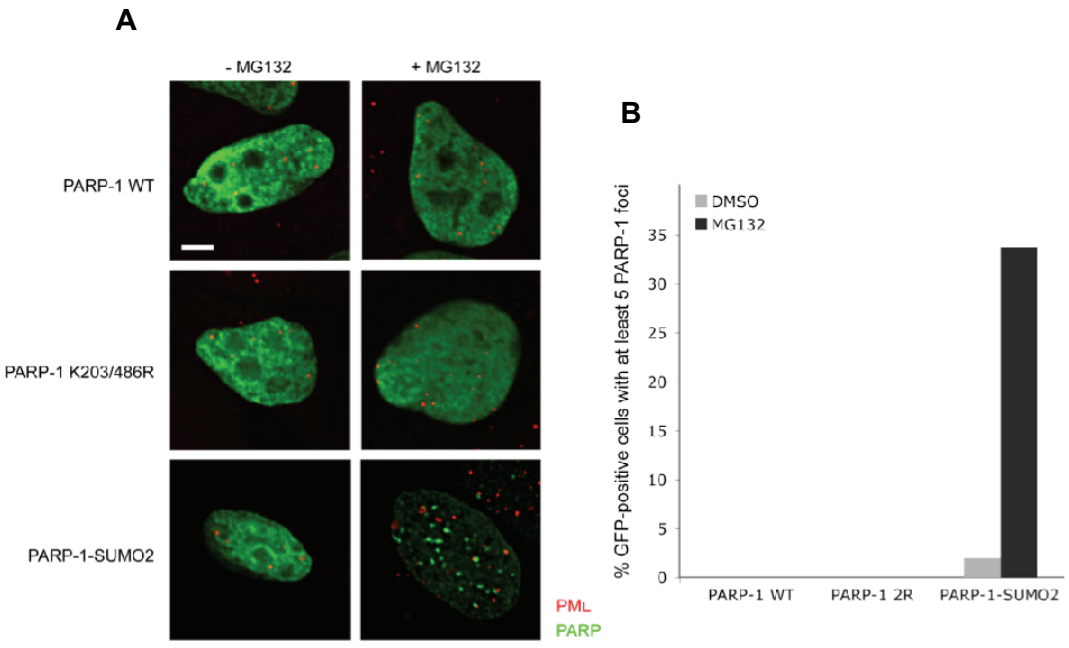

the eGFP-tagged wild type PARP-1 or the K203/486R mutant.

These data, together with those presented in the previous paragraph, show that when PARP-1-SUMO2 becomes further modified by SUMO and possibly ubiquitin, it relocalizes to nuclear structures that do not correspond to PML nuclear bodies.

5.2.11 Sumoylation of PARP-1 is a signal for proteasome-mediated degradation

The data presented above suggested that both the physiologically sumoylated PARP-1 and the PARP-1-SUMO2 fusion could be ubiquitylated. Consequently, it was possible that they might be degraded by the proteasome. To address this question, I compared the stability of the wild type PARP-1, the K203/486R mutant and the PARP-1-SUMO2 fusion in a cycloheximide chase experiment. HEK293 cells producing N-terminally FLAG-tagged versions of such constructs (**Figure 5.10**) were incubated in the presence of cycloheximide alone or cycloheximide and MG132. I harvested these cells at increasing time points, prepared total extracts and then analyzed them by western blotting against the FLAG tag and tubulin. **Figure 5.12** shows that inhibiting the proteasome drastically reduced the moderately fast degradation rate of the wild type PARP-1. Mutating the two main sumoylation sites of the polymerase afforded a similar stabilization effect, thus indicating that sumoylation of PARP-1 controls its stability. Since appending SUMO2 to PARP-1 enabled the polymerase to become further modified by SUMO and ubiquitin (**Figure 5.9** and **Figure 5.10**), I expected that the PARP-1-SUMO2 fusion would behave similarly to the wild type protein, with respect to its stability. Instead, I found that it was as stable as the K203/486R mutant in the presence of cycloheximide only. When MG132 was also present in the medium, such a

Figure 5.12 - Sumoylation targets PARP-1 for proteasomal degradation. HEK293 cells producing PARP-1 WT, the K203/486R mutant or the PARP-1-SUMO2 construct (Figure 5.10A) were subjected to cycloheximide-chase analysis as described in 2.10.9. Total extracts were prepared from them and analyzed by western blotting against the FLAG tag and tubulin (loading control). CHX = cycloheximide.

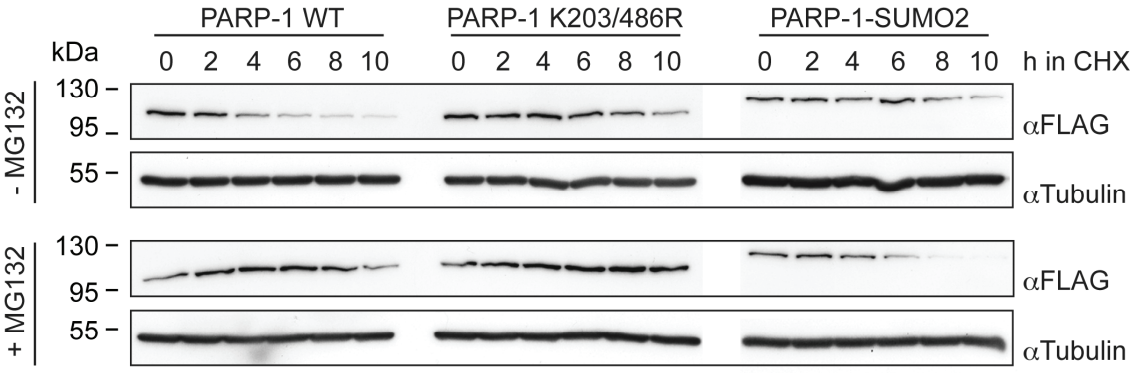

construct disappeared at a rate similar to that at which the wild type PARP-1 was degraded, probably because such fusion was heavily modified under these conditions (**Figure 5.10**).

On one hand, these data indicate that PARP-1 must be sumoylated at K203 and K486 in untreated cells and that this event leads to its degradation by the proteasome. On the other hand, they also reveal that the PARP-1-SUMO2 construct is probably not targeted for proteasome-mediated degradation, or at least not as fast as the wild type protein.

5.3 Discussion

While I was completing the experiments presented in this part of my thesis, four other groups reported PARP-1 as a target of sumoylation (Blomster *et al.*, 2009; Martin *et al.*, 2009; Messner *et al.*, 2009; Ryu *et al.*, 2010). Like I did, they uncovered many of the properties of this modification event, including the identity of the modification sites, the signals that trigger it and its possible functions. I will therefore discuss several of my results in light of such studies.

5.3.1 PARP-1 as a target of sumoylation

Here, I demonstrated that PARP-1 is a true sumoylation substrate in human cells by 1) isolating sumoylated species under denaturing conditions from cells producing His_6-SUMO and 2) immunoprecipitating PARP-1 from cells expressing endogenous levels of the modifier (**Figure 5.1**). I also showed that the polymerase was preferentially conjugated to SUMO3, in comparison to SUMO1 or SUMO2 (**Figure 5.1**A). The latter observation was unexpected because it is widely believed that the mature forms of SUMO2 and SUMO3, being essentially identical, cannot be distinguished even *in vivo* (Wang and Dasso, 2009). Yet, it is possible that SUMO2 and SUMO3 could target different subsets of proteins because this hypothesis has never been examined and at least one other protein besides PARP-1, *i.e.* the transcriptional repressor p66, has also reported to be preferentially modified by SUMO3 over SUMO2 (Liu and Warbrick, 2006).

This phenomenon could have potentially arisen by controlling the sumoylation of PARP-1 in at least four different ways. Firstly, it is possible that it may have been simply caused by higher overall levels of SUMO3 in the cells compared to those of the other modifiers. Alternatively, it could have stemmed from the presence of a SUMO3-specific SIM in the target of sumoylation. In fact, not only can SIMs aid the modification

of the proteins that carry them (Knipscheer *et al.*, 2008; Zhu *et al.*, 2008), but, being able to discriminate between SUMO1 and SUMO2/3, they can also specify which SUMO paralogue will be attached to a polypeptide (Hecker *et al.*, 2006; Meulmeester *et al.*, 2008; Ouyang *et al.*, 2009; Zhu *et al.*, 2008). This scenario, however, appears unlikely since Messner *et al.* (2009) did not detect any non-covalent interaction between PARP-1 and any of the SUMO paralogues. In addition, a SIM that can dinstinguish between SUMO2 and SUMO3 probably does not exist because these two SUMO paralogues interact with known SIMs through a region that is identical between them. Thirdly, the preferential conjugation of SUMO3 to PARP-1 could depend on a SUMO ligase that has a preference for SUMO3. PIASy seems to be the relevant E3 enzyme for PARP-1 sumoylation because depleting it abolishes this modification event *in vivo* and it can also stimulate the modification of the polymerase *in vitro* by SUMO1 or SUMO2 (Martin *et al.*, 2009). PIASy has been shown to mediate the modification of several other proteins by either SUMO1 or SUMO2 (Azuma *et al.*, 2005; Dahle *et al.*, 2003; Subramanian *et al.*, 2003). It therefore seems unlikely that this SUMO ligase may able to distinguish amongst SUMO paralogues and consequently promote the sumoylation of PARP-1 specifically by SUMO3. In the future it will be however important to directly prove this issue in the context of PARP-1. Lastly, the preferential modification of PARP-1 by SUMO3 could depend on the action of a SENP that is able to remove SUMO1 and SUMO2 from PARP-1 more efficiently than SUMO3. Although no such protein has been reported, it might nevertheless exist. Some SENPs can actually deconjugate SUMO1 and SUMO2/3 with different efficiencies (**Table 1.1**). They can also process the immature forms of SUMO1 and SUMO2 better than that of SUMO3, because of the different extensions that they bear after their di-glycine motifs (Bailey and O'Hare, 2004; Gong *et al.*, 2000; Gong and Yeh, 2006; Kolli *et al.*, 2010; Mikolajczyk *et al.*, 2007; Shen *et al.*, 2009).

It is also possible that PARP-1 is preferentially modified by SUMO3 because this particular form of the protein is functionally distinct from those conjugated to SUMO1 or SUMO2. There is in fact some evidence suggesting that SUMO3 may control processes that are distinct, at least partly, from those mediated by SUMO1 and/or SUMO2: depleting SUMO3 from cells impairs the formation of PML nuclear bodies, which can only be rescued by ectopically over-producing SUMO3 but not SUMO1 or SUMO2 (Fu *et al.*, 2005). This scenario, however, seems unlikely because SUMO1/2/3 are attached to the same lysine residues within PARP-1 (**Figure 5.3**, Martin *et al.*, 2009; Messner *et al.*, 2009).

Martin *et al.* (2009), Messner *et al.* (2009) and I have identified K486 and K203 as the main sumoylation sites of PARP-1, with a third one also likely to exist (**Figure 5.3**). The observation that individually mutating PARP-1's K203 or K486 (or K482 in *X. laevis*) enhances the sumoylation of other residues in human cells (**Figure 5.3**), *in vitro* (**Figure 6.7**) and also in frog egg extracts (Ryu *et al.*, 2010) raises the possibility that the third sumoylation site of PARP-1 may be very minor or cryptic. It therefore could become relevant only when the main sumoylated lysines are not accessible, which is a phenomenon that has been shown for other sumoylation substrates (Jacobs *et al.*, 2007; Onishi *et al.*, 2009).

5.3.2 Regulation of PARP-1 sumoylation

The observations presented in this thesis, together with those reported in other studies (Martin *et al.*, 2009; Messner *et al.*, 2009; Ryu *et al.*, 2010), demonstrate that *in vivo* the sumoylation of PARP-1 is not a static event but it changes under different conditions.

5.3.2.1 Regulation of PARP-1 sumoylation by environmental stimuli

In human cells, PARP-1 appears to be only mono-sumoylated at low levels during normal growth (**Figure 5.1**, Blomster *et al.*, 2009; Martin *et al.*, 2009; Messner *et al.*, 2009), but it becomes more heavily mono-sumoylated and also poly-sumoylated in response to acute heat (Blomster *et al.*, 2009; Martin *et al.*, 2009). This phenomenon would be consistent with the evidence that upon heat shock PARP-1 K203/486R does not activate *HSP70.1* transcription as well as the wild type protein (Martin *et al.*, 2009). Nevertheless, I found that PARP-1 sumoylation was also upregulated in response to osmotic and metabolic stresses (**Figure 5.2**), which, like excessive heat, are known to boost the overall levels of SUMO2/3-modified species in a cell (Saitoh and Hinchey, 2000). The extent of such increase correlated well with the degree to which PARP-1 sumoylation was enhanced under the same conditions (**Figure 5.2**). These results therefore suggest that the increase in sumoylation that PARP-1 experiences in response to a variety of environmental stimuli is not a specific event, instead it is probably the consequence of their ability to boost the general levels of SUMO2/3 conjugates. In support of this view, PARP-1 sumoylation has been shown to impinge on the roles of the polymerase in transcription not only following heat shock, but also after hypoxia (Messner *et al.*, 2009), which can also stimulate the overall levels of SUMO2/3 conjugates *in vivo* (van Hagen *et al.*, 2010).

5.3.2.2 Regulation of PARP-1 sumoylation by the cell cycle

PARP-1 sumoylation also seems to be controlled at the level of the cell cycle, at least in frog egg extracts, where it occurs specifically at mitosis (Ryu *et al.*, 2010). Since in *Xenopus* egg extracts, SUMO2/3 conjugates accumulate on the chromatin during mitosis (Azuma *et al.*, 2003), it is possible that this phenomenon may not be specific for PARP-1 either. In order to corroborate the importance of this result, it will therefore be useful to examine the cell cycle patterns of PARP-1 sumoylation in human cells because, unlike frog egg extracts, here the levels of SUMO2/3 conjugates drop at beginning of metaphase but then progressively grow throughout mitosis (Zhang *et al.*, 2008).

Although the increase in sumoylation that PARP-1 experiences in response to environmental cues and at specific cell cycle stages may not be PARP-1-specific, this does not mean that they are functionally relevant. They could in fact elicit a downstream process that is important to deal with all of these situations, such as controlling gene transcription/expression, in which PARP-1 sumoylation actually seems to play a role (Martin *et al.*, 2009; Messner *et al.*, 2009). These speculations raise the possibility that the poly-sumoylated PARP-1 is observed only under stressful conditions (**Figure 5.2**, Blomster *et al.*, 2009; Martin *et al.*, 2009) because it has different functions, *e.g.* promote degradation, compared to the mono-sumoylated polymerase. Although this scenario may not seem very likely, it has been demonstrated for other modification events, such as the mono- and poly-ubiquitylation of PCNA (see 1.3.3). Whether this situation also applies to PARP-1 should be investigated further, as could be the way in which the balance between the mono and poly-sumoylated forms of PARP-1 is controlled. In order to do so, it will be useful to study PARP-1 sumoylation in cells that produce SUMO2/3 mutants that are unable to form chains.

5.3.3 Are the PARP-1-SUMO fusion constructs functionally relevant mimics of the sumoylated PARP-1?

5.3.3.1 A rationale for using SUMO-PARP-1 fusions as mimics of the physiologically sumoylated PARP-1

Recognizing the biological consequences of a sumoylation event is difficult because they cannot be generally predicted and only a tiny amount of a protein is usually modified at any time. It therefore follows that being able to quantitatively sumoylate a protein could facilitate this endeavour. Although achieving this goal *in vivo* is technically

impossible at present, it has been shown that artificially fusing SUMO to an unsumoylatable version of certain proteins can restore their wild type-like behaviour, and in some cases drive it even further (Carter and Vousden, 2008; Dawlaty *et al.*, 2008; Hishida *et al.*, 2006; Ross *et al.*, 2002; Sugimura *et al.*, 2008; Takahashi and Strunnikov, 2008; Takahashi *et al.*, 2006; Yurchenko *et al.*, 2006). This phenomenon seems to occur because the exact residues to which a modifier is attached within a protein may not matter at all to trigger a physiologically relevant event (Ross *et al.*, 2002; Sacher *et al.*, 2006). For these reasons I decided to investigate the function of PARP-1 sumoylation by using, in addition to the K203/486R mutant, SUMO-PARP-1 fusion constructs whenever I could not use a PARP-1 protein that had been sumoylated at K203 and K486.

To create these SUMO-PARP-1 constructs I recombinantly fused SUMO to either the N- or C-terminus of the PARP-1 K203/486R mutant. Importantly, the C-terminal di-glycine motif of these SUMO appendages, which would normally be required for their conjugation and deconjugation to/from proteins, was mutated to GA for two reasons. Firstly, to prevent the SUMO protease-mediated desumoylation of the N-terminal SUMO fusion constructs. Secondly, to avoid the enzymatic attachment of the SUMO moiety appended at the C-terminus of PARP-1 to other polypeptides, which has been reported for other SUMO-fused proteins (Carter and Vousden, 2008). Instead of fusing SUMO3 to PARP-1, which would have been the ideal choice (**Figure 5.1**A), I used either SUMO1 or SUMO2 because when I created and analyzed the fusion constructs I only knew that 1) PARP-1 was likely to be modified by SUMO1, SUMO2 and SUMO3 and 2) a significant difference in the extent to which PARP-1 was modified by SUMO2 *vs.* SUMO3 seemed improbable, given that they had been deemed indistinguishable in most situations (Wang and Dasso, 2009). The properties of PARP-1 fused to SUMO1 or SUMO2, which are only 45% identical, are nevertheless noteworthy because whenever one of them displayed a specific property the other behaved exactly the same way. These results therefore indicate that such effects must have arisen by appending a SUMO moiety to PARP-1, regardless of its exact identity.

The results presented in this part of my thesis showed that fusing SUMO to PARP-1 changed the properties of the polymerase in at least two different ways: 1) how it interacted with some of its partners, and 2) how it was post-translationally modified. The features and biological relevance of these two phenomena will be discussed below.

5.3.3.2 Fusing SUMO to PARP-1 affects its interactions with APLF and XRCC1

The main question that arises from the data indicating that APLF and XRCC1 preferentially interact with the sumoylation mimics of PARP-1 is whether APLF and XRCC1 are actually genuine "downstream effectors" of the physiologically sumoylated polymerase.

5.3.3.2.1 Yeast two-hybrid system

By means of the yeast two-hybrid system, I found that two known partners of PARP-1, that is, the DNA break repair factors APFL and XRCC1 (Brem and Hall, 2005; Iles *et al.*, 2007), interacted with the PARP-1-SUMO constructs drastically better than they did with either SUMO or PARP-1 on their own (**Figure 5.5**). The fact that this phenomenon occurred only when SUMO was fused to the C-terminus of PARP-1, but not its N-terminus, was slightly surprising because the two known sumoylation sites of PARP-1 are located within the first half of the protein (**Figure 5.3**). One possible explanation for such an occurrence is that the SUMO moiety attached to the C-terminus of PARP-1 adopted at a more physiological position than that fused to the N-terminal, probably thanks to PARP-1's large size and modular structure. An alternative scenario is that the PARP-1-SUMO constructs may be able to accommodate a greater variety of conformations than the SUMO-PARP-1 fusions. This situation is possible because in the PARP-1-SUMO constructs the polymerase and SUMO's core domain are separated by a linker, *i.e.* the N-terminal tail of the modifier, which is long and highly flexible (Melchior, 2000). Instead, in the N-terminal fusions SUMO is attached to PARP-1 through its shorter C-terminal conjugation tail. To study the latter one of these two possibilities one could examine the affinities of APLF and XRCC1 for the SUMO-PARP-1 constructs where the modifier flexible N-terminal tail is removed from the C-terminal fusions and/or a long flexible linker is added to the N-terminal constructs.

Given that PARP-1 is constitutively active when ectopically produced in budding yeast (**Figure 5.5**, Kaiser *et al.*, 1992) and that APLF and XRCC1 bind PAR (Ahel *et al.*, 2008; Pleschke *et al.*, 2000), it follows that their ability to preferentially recognize the PARP-SUMO constructs could have arisen from a SUMO-dependent increase in the autoparylation activity of such constructs. I excluded this possibility by showing that APLF and XRCC1 preferentially interacted with the PARP-SUMO fusions even when their PARP-1 moieties were catalytically inactive (**Figure 5.5**D). In addition, I demonstrated that the wild type PARP-1 and the SUMO fusion constructs produced

similar levels of PAR (**Figure 5.5**C) and that ligase III, which is also a PAR-binding protein (Ahel *et al.*, 2008; Pleschke *et al.*, 2000), did not show the same preference for PARP-1-SUMO as APLF and XRCC1 did (**Figure 5.5**B).

5.3.3.2.2 *In vitro* and *in vivo*

Surprisingly, the significantly higher affinity that APLF and XRCC1 displayed towards the PARP-1-SUMO constructs in the yeast two-hybrid system could not be recapitulated *in vitro*, using purified proteins, or *in vivo* (**Figure 5.6**).

The reasons for why APLF and XRCC1 did not interact with the PARP-1-SUMO constructs with the same degree of preference in all the three employed experimental systems are unclear. Many of the biological properties of PARP-1, possibly including the way in which it interacts with its partners, are heavily influenced by DNA (Soldatenkov and Potaman, 2004). I can therefore speculate that the above-described discrepancies may have originated from the different forms in which DNA was present in the different experiments: chromatin-packaged intact DNA in the yeast two-hybrid system, no DNA in the *in vitro* pull-down assays and solubilized chromatin in the mammalian cell extracts. A possible way to address this issue would be to assess how inactivating PARP-1's DNA binding activity in the yeast two-hybrid system or including different kinds of DNA molecules in the *in vitro* binding assays affects the interactions between PARP-1-SUMO and APLF/XRCC1.

In vitro APLF and XRCC1 were able to weakly interact with SUMO alone (**Figure 5.6**D). By a very rough estimate, the strength of this interaction seems to be in the same order of magnitude as the very minimal increase in affinity that these proteins demonstrate for the sumoylated PARP-1 (**Figure 5.6**A). Thus, such phenomenon may have simply been the result of the mathematical addition of the individual affinities of APLF and XRCC1 themselves for SUMO and PARP-1 independently, which may have occurred as a result fusing/conjugating them together. It therefore follows that APLF and XRCC1 are unlikely to be true receptors/effectors of the sumoylated PARP-1 because such a protein should recognize a PARP-1-SUMO conjugate with an affinity that is higher than the sum of its individual affinities for PARP-1 and SUMO alone. As a matter of fact, a function for APLF or XRCC1, which play a role in the repair of SSBs (Brem and Hall, 2005; Iles *et al.*, 2007), downstream of sumoylated PARP-1 would be inconsistent with the findings that 1) SSBs inhibit PARP-1 sumoylation *in vitro* (see 6.2), and 2) the sumoylation of PARP-1 appears to have a role in controlling transcription rather than DNA repair (Martin *et al.*, 2009; Messner *et al.*, 2009).

Even though the results discussed above may not reflect physiologically relevant interactions, they nevertheless uncovered the previously unknown finding that APLF and XRCC1 can non-covalently interact with SUMO, albeit weakly. The amino acids responsible for these interactions should be located within the first BRCT motif of XRCC1 (aa 170-428) and the C-terminal domain of APLF (aa 360-511) because such regions also preferentially recognize the PARP-1-SUMO constructs in the yeast two-hybrid system (data not shown). Both of these protein fragments contain a hypothetical SIM that conforms to classic consensus sequences (see 1.3.1). Mutating such motifs did not however affect the binding between APLF/XRCC1 and PARP-1-SUMO (data not shown), thus suggesting that other types of SUMO-interacting sequence must be involved in these interaction events.

5.3.3.3 Fusing SUMO to PARP-1 affects its post-translational modification

Another intriguing property of the PARP-1-SUMO constructs was that they became heavily conjugated to SUMO when ectopically produced in mouse or human cells (**Figure 5.9** and data not shown). Such conjugates almost certainly represent SUMO chains because their number was simply too big to have been produced by multiple mono-sumoylation events (**Figure 5.9**). Having said that, I cannot categorically exclude that they may have originated from a mixture of mono- and poly-sumoylation events. Showing that the number and/or abundance of these sumoylated species are reduced by over-producing SUMO1 or SUMO2/3 mutants that are unable to form chains could help to confirm these deductions.

5.3.3.3.1 <u>On the specificity of PARP-SUMO sumoylation</u>

The ability of the PARP-1-SUMO fusion constructs to become poly-sumoylated appears to be a specific event in at least three respects.

Firstly, with regard to which organisms it happened in. In fact, I detected it only in mammalian cells but not in budding yeast (**Figure 5.5**C), where no orthologues of PARP-1 exist, or in insect cells (data not shown), where only one PARP protein is present (Uchida *et al.*, 1993).

The second level of specificity relates to PARP-1 itself. Poly-sumoylation has not been reported for several other proteins over-produced as SUMO fusions in mammalian cells, whether or not they are known SUMO substrates (Babic *et al.*, 2006; Liu *et al.*, 2008; Muromoto *et al.*, 2006; Peroutka *et al.*, 2008; Tan *et al.*, 2008).

Thirdly, with respect to the part of the PARP-1-SUMO construct that was poly-sumoylated. SUMO appears to be a better candidate than PARP-1 because while the polymerase employed to generate the fusion constructs had its sumoylation sites mutated, their SUMO moieties contained residues that could be used to form SUMO chains. That said, this assumption is inconsistent with the fact that both the SUMO1 and the SUMO2 fusions of PARP-1 were poly-sumoylated equally well (**Figure 5.9**), even though only SUMO2/3 is capable of forming chains efficiently *in vivo* (Tatham *et al.*, 2001).

On the basis of these speculations two scenarios are conceivable to explain how the PARP-1-SUMO constructs may have been poly-sumoylated. On the one hand, it is possible that fusing SUMO to PARP-1 facilitated the recruitment of the sumoylation machinery to the polymerase, thus boosting the modification of its third sumoylation site. On the other hand, given that SUMO1 can potentially form chains (Pichler *et al.*, 2002; Yang *et al.*, 2006a), it is imaginable that appending it to PARP-1 could have placed the modifier at an ideal position, *e.g.* next to a chromatin-bound SUMO ligase, to be further modified. A possible way to distinguish between these two possibilities could be to examine the consequences of depleting PIASy and/or mutating all of the lysines within the SUMO moiety of the PARP-SUMO fusions on the poly-sumoylation of these constructs. Interestingly, there is some evidence in support of the latter scenario: after heat shock, UBC9, PIASy and PARP-1 become heavily enriched at the same chromatin region, *i.e.* at the promoter of the *HSP70.1* gene (Martin *et al.*, 2009). Although at present there is no data on whether this recruitment phenomenon also occurs during normal cell growth, this possibility seems likely because: 1) PARP-1 and PARP-1-SUMO are modified during normal growth conditions (**Figure 5.1**, Martin *et al.*, 2009; Messner *et al.*, 2009) and 2) inhibiting the sumoylation of the polymerase affects *HSP70.1* transcription even in non-stressed cells (Martin *et al.*, 2009). In the future, it will be therefore interesting to corroborate these observations by chromatin immunoprecipitation (ChIP) analysis of PARP-1, PIASy and UBC9, against either known PARP-1-bound and -free regions or, preferably, the entire genome.

5.3.3.3.2 On the physiological relevance PARP-1-SUMO sumoylation

In addition to being specific, the conjugation of SUMO2/3 chains to PARP-1-SUMO appears to be physiologically relevant because the wild type polymerase has also been observed to be poly-sumoylated *in vivo* (**Figure 5.2**, Blomster *et al.*, 2009; Martin *et al.*, 2009). That said, while poly-sumoylated PARP-1 was exclusively detected under

conditions of cellular stress, poly-sumoylated PARP-1-SUMO was also visible during normal growth (**Figure 5.9**). This difference probably arose because appending SUMO to PARP-1 increased the "sumoylation potential" of the resulting fusion enough to allow it to become poly-sumoylated even in non-stressed cells. It therefore follows that some poly-sumoylated PARP-1 may also exist in untreated cells but we may not be able to detect it because it is not very abundant. This hypothesis is realistic as poly-SUMO chains can lead to the poly-ubiquitylation of their targets and their subsequent proteasome-mediated degradation (Lallemand-Breitenbach *et al.*, 2008; Tatham *et al.*, 2008; Uzunova *et al.*, 2007). Consistently with this scenario I found that under normal growth conditions mutating the sumoylation sites of PARP-1 prevented its proteasome-mediated degradation (**Figure 5.12**). In the presence of MG132, sumoylated and ubiquitylated species also accumulated so heavily on both the physiologically sumoylated PARP-1 and the PARP-1-SUMO2 constructs that they were apparently depleted (**Figure 5.10**). On the one hand, these observations indicate that sumoylation is indeed likely to target PARP-1 for ubiquitylation and subsequent proteasome-mediated degradation. On the other hand, they further corroborate the physiological relevance of the polymeric SUMO chains that form on the PARP-1-SUMO constructs.

If these SUMO chains truly mimicked the degradative functions of those polymerized on the wild type PARP-1, then the PARP-1-SUMO constructs should have been turned over as well as the wild type protein, if not better. Instead, I found that PARP-1-SUMO2, which carries the K203/486R mutations, was as stable as the unmodified PARP-1 K203/486R mutant and consequently more so than the wild type protein (**Figure 5.12**). How can these apparently contradictory findings be reconciled? It is possible that PARP-1-SUMO2 could actually be degraded better than the K203/486R mutant, but maybe not quickly and/or efficiently enough to be detected during the relatively short cycloheximide-chase assay I performed. In this respect, it is worthwhile to mention that when the C- and N-terminal SUMO fusion constructs of PARP1 were transiently produced in mammalian cells, the former was always produced at higher levels than the latter (data not shown). In the future, it will be interesting to examine whether this phenomenon occurred simply because appending SUMO to the N-terminus of PARP-1 had an intrinsic destabilizing effect on the polymerase or because such a construct was in fact a better mimic of the sumoylated PARP-1 than PARP-1-SUMO2, and it was therefore degraded more quickly.

5.3.3.3.3 Do the SUMO chains conjugated to PARP-SUMO have different functions than those polymerized on the wild type polymerase?

The above-discussed considerations suggest that the SUMO chains attached to the wild type PARP-1 may not carry out the same function as those conjugated to the PARP-1-SUMO constructs. Such a possibility is based on the conclusion that poly-sumoylation targets PARP-1 for proteasome-mediated degradation, which could have actually been incorrectly drawn from the presented data. The increase in PARP-1's half-life caused by mutating K203 and K486 (**Figure 5.12**) may have not been the result of abolishing its SUMO-dependent poly-ubiquitylation, but rather its direct poly-ubiquitylation. PARP-1 is in fact poly-ubiquitylated at a site within its DBD (Wang *et al.*, 2008b), which includes K203, hence suggesting that the polymerase could be sumoylated and ubiquitylated at the same lysine. Thus, in order to convincingly demonstrate that SUMO affects the stability of PARP-1, it will be necessary to show that abolishing its sumoylation by mutating other residues than the lysine within the ΨKXE motifs in which K203 and K486 are found also stabilizes the polymerase. That said, there is evidence supporting the possibility that sumoylated PARP-1 is actually a target of ubiquitylation and degradation because it appears to be a substrate of the SUMO-targeted ubiquitin ligase RNF4 (Martin *et al.*, 2009). Although interesting, this conclusion needs to be taken with caution because, except for a minor increase in the levels of sumoylated PARP-1 upon RNF4 depletion, it is backed up only by experiments that involved over-producing RNF4 in cells where PARP-1 was also hyper-sumoylated. Under such artificial conditions these two proteins may have been forced to interact, even though they would not normally do so, simply because RNF4 can bind and ubiquitylate any poly-sumoylated protein (Tatham *et al.*, 2008). Thus, in order to confirm that PARP-1 is indeed a target of RNF4, it will be important to demonstrate that the half-life of PARP-1 also increases in the absence of RNF4 and that this effect is epistatic with that caused by abolishing PARP-1 sumoylation.

5.3.4 Cross-talk between PARP-1 sumoylation and other post-translational modification events

PARP-1 is not only sumoylated and ubiquitylated (Wang *et al.*, 2008b), but it is also parylated, acetylated (Hassa *et al.*, 2005) and phosphorylated (Kauppinen *et al.*, 2006). It is therefore possible that the ability of the sumoylated PARP-1 to cross-talk with other modification events may not be limited to ubiquitin. As a matter of fact, Messner *et al.* (2009) have shown that sumoylating PARP-1 at K486 impairs its binding to the acetyl-

transferase CBP/p300, thereby reducing its acetylation. Given that such a SUMO-dependent inhibition of acetylation seems to be common amongst proteins that are targeted by both post-translational modifiers (Gregoire and Yang, 2005; Mohan *et al.*, 2007; Shalizi *et al.*, 2006; Zhang *et al.*, 2008), it is possible that sumoylation may act as a general inhibitor of acetylation. Conversely, as it has meanwhile been shown by others (Messner *et al.*, 2009; Ryu *et al.*, 2010), I found that sumoylation does not significantly alter the catalytic activity of PARP-1 (**Figure 5.7**).

Chapter 6. Results IV: DNA controls the sumoylation of PARP-1 *in vitro*

6.1 Introduction

The possibility that PARP-1 could be a target of sumoylation encouraged Sebastian Eustermann (MRC-LMB, Cambridge), who works on PARP-1's DBD, and I to examine the relevance of a hypothetical sumoylation consensus motif found within such a domain, that is, ^{202}V<u>K</u>SE$_{205}$. We reasoned that if K203 were truly sumoylated *in vivo*, a hypothesis that has now been proven (**Figure 5.3** and Martin *et al.*, 2009), then its proximity to a domain critical for DNA binding resembled what had already been described for another target of SUMO, *i.e.* TDG (see 1.3.4). This enzyme is sumoylated near its DNA-binding/catalytic domain and, as a result, it undergoes a conformational change that reduces its affinity for, and hence allows it to disassociate from, the DNA. We were therefore curious to explore whether sumoylation may also impinge on the DNA-binding properties of PARP-1, especially in the context of its DBD. Since Sebastian Eustermann, and several other scientists, have developed many tools and assays to analyze this aspect of PARP-1's biology *in vitro*, we decided to address the above-described question in a test-tube. Using this type of experimental approach meant that I had to be able to generate a fair amount of sumoylated protein to use in downstream functional assays. In order to efficiently modify a protein *in vitro* almost always requires the presence of the relevant E3 enzyme in the reaction. At the start of this project, very little was known about PARP-1 sumoylation, let alone which SUMO ligase specifically enhanced it. I therefore tried to modify PARP-1's DBD (aa 1-214, **Figure 1.6**) *in vitro* in the presence AOS1/UBA2 and UBC9 only, but, as expected, this reaction proved to be very inefficient (**Figure 6.1**A). While testing several conditions in the hope to improve the modification of PARP-1's DBD, I observed that mixing a heavily digested plasmid with this domain enhanced its sumoylation (**Figure 6.1**A). This preliminary result was very interesting because it put forward the possibility that DNA may play a role in the modification of PARP-1.

Following up on these observations, the aim of this part of my thesis was: 1) to characterize the roles of DNA in the sumoylation of PARP-1 with respect to which features of the DNA and PARP-1 itself underlain it, and 2) to explore whether the conjugation of SUMO to PARP-1's DBD may bring about structural changes that could alter its ability to bind DNA.

6.2 Results

6.2.1 Sumoylation of PARP-1's DBD is enhanced in the presence of a plasmid, but not when it contains single-stranded breaks

Having observed that in the presence of a digested plasmid the sumoylation of PARP-1's DBD was strongly enhanced (**Figure 6.1**A), I wanted to ensure that this phenomenon was specific for such a domain and it was not caused simply by a plasmid-induced increase in the overall rate of sumoylation. In the reactions presented here, the rate of sumoylation must depend on AOS1/UBA2 and UBC9, which also mediate the formation of SUMO1 polymers *in vitro* (Pichler *et al.*, 2002; Tatham *et al.*, 2001; Yang *et al.*, 2006a). It therefore follows that if a plasmid non-specifically boosted the rate of sumoylation then I should be able to detect it as an increase in the amount of SUMO1 chains, in addition to that of the sumoylated DBD in the reactions shown in **Figure 6.1**A. When these samples were analyzed by western blotting against SUMO1 (**Figure 6.1**A, right panel), I found that in the presence of a plasmid the formation of SUMO1 chains was certainly not enhanced, instead it was somewhat reduced, probably because of the increased attachment of the modifier to PARP-1's DBD. Similarly, in reactions that contained only AOS1/UBA2, UBC9 and SUMO1, but no PARP-1's DBD, a plasmid did not stimulate the formation of SUMO1 chains (**Figure 6.1**B).

An intact supercoiled plasmid does not activate PARP-1's catalytic activity *in vitro*; conversely, those that contain either blunt breaks or free DNA ends bearing 3' or 5' single-stranded overhangs can do so, yet with different efficiencies (Benjamin and Gill, 1980). Since the plasmid I used to stimulate the sumoylation of PARP-1's DBD in **Figure 6.1**A harboured a heterogeneous mixture of DSBs, I was curious to explore whether this phenomenon may have been triggered by DNA interruptions and, if so, by what kind. To address this question, I digested a supercoiled plasmid with restriction endonucleases that produced the three types of DSBs described above. Each enzyme cut the plasmid twice, hence generating four free ends per plasmid molecule (**Figure 6.1**C). Since PARP-1 also binds to nicks or gaps in a DNA duplex, I treated the plasmid with a nicking endonuclease that was expected to inflict five SSBs per molecule (**Figure 6.1**C). Subsequently, I assessed how well these preparations of damaged DNAs, alongside that of the intact supercoiled plasmid as a control, stimulated the sumoylation of PARP-1's DBD. **Figure 6.1**D shows that the plasmids bearing DSBs enhanced the sumoylation of PARP-1's DBD as well as the intact template.

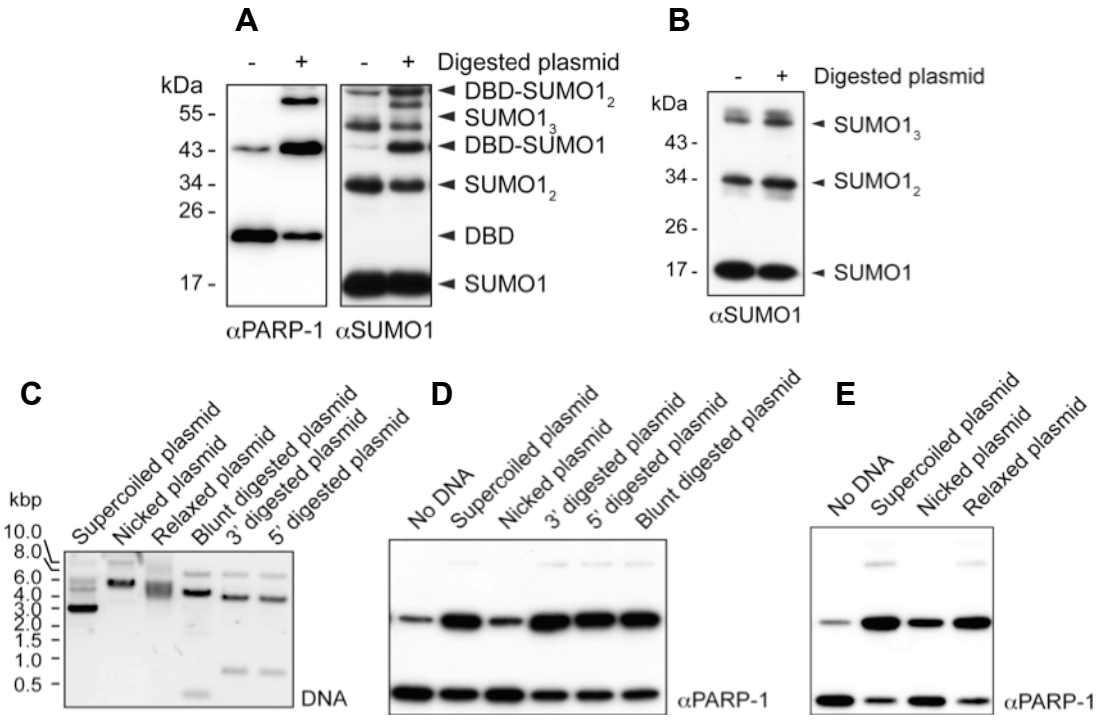

Figure 6.1 - PARP-1's DBD is strongly sumoylated in the presence of a plasmid, but not when it carries nicks. A), E) and F) PARP-1's DBD (3 pmol) was subjected to *in vitro* sumoylation reactions under standard conditions (see 2.17.1) in the absence or presence of the relevant plasmid (240 ng), and then analyzed by western blotting against PARP-1 or SUMO1. B) Sumoylation reactions containing SUMO E1/E2, His_6-SUMO1 and ATP were carried under standard conditions in the presence or absence of intact plasmid (240 ng), and then analyzed by western blotting against SUMO1. C) The plasmids used in D) and E) were enzymatically treated as described in 2.19.1, resolved by agarose gel electrophoresis (2.11.2) and then stained with SYBR Safe (2.12.7). Unless otherwise stated, the same plasmid backbone was used for all the relevant reactions shown in this chapter, pHU2020 (Table 2.7). Digested plasmid = various restriction endonucleases, Nicked = Nb.BsrDI, 5' digested = PstI, Blunt digested = EcoRV, 3' digested = EcoRI, Relaxed = topoisomerase I.

On the other hand, I observed that the nicked plasmid stimulated the modification of PARP-1's DBD less than the intact supercoiled template.

Nicking a supercoiled plasmid introduces breaks in its backbone but it also relieves the torsional strain that it is under. The binding of PARP-1 to a plasmid is affected by its superhelical state: the enzyme interacts with a supercoiled template better than a relaxed one, probably because it recognizes some secondary DNA structures, such as loops and cruciforms, which can be extruded from DNA molecules as a consequence of supercoiling (Gradwohl *et al.*, 1987). Thus, the nicked plasmid might have been unable to enhance the sumoylation of PARP-1's DBD as well as the supercoiled template either because it contained nicks or because it was relaxed. To distinguish between these two possibilities, I studied how well a plasmid that had been almost

completely relaxed with topoisomerase I (**Figure 6.1**C), and therefore should contain no SSBs, stimulated the modification of PARP-1's DBD in comparison to the nicked and intact templates. **Figure 6.1**E shows that the supercoiled and relaxed plasmids enhanced the modification of PARP-1's DBD equally well and considerably more than the nicked template.

Altogether the results presented in this paragraph demonstrate that the sumoylation of PARP-1's DBD is specifically stimulated by DNA in the form of an intact or digested plasmid, but not when it carries SSBs.

6.2.2 The length of a plasmid, rather than its sequence or methylation state, may play a role in the sumoylation of PARP-1's DBD at K203

Having observed that DNA stimulated the modification of PARP-1's DBD, it was important to study this phenomenon further with respect to where the sumoylation occurred within the domain and what properties of the plasmid triggered it.

The data presented elsewhere in this thesis (**Figure 5.3**) and those reported by Martin *et al.* (2009) show that PARP-1 is sumoylated at K203 and K486 *in vivo*. Since K203 falls within the DBD of PARP-1 and it is also part of a sumoylation consensus motif, it was the most likely site of modification in the reactions described above. In order to corroborate this hypothesis, I sumoylated PARP-1's DBD *in vitro* in the presence of a plasmid and then purified the modified protein as shown in **Figure 6.2**A. This SUMO conjugate was trypsinized in solution and analyzed by the Protein Analysis and Proteomics team of the London Research Institute on a ThermoScientific LTQ Orbitrap XL/ETD mass spectrometer coupled to a Waters NanoACQUITY UPLC system (LC MS). From this analysis, only one triply charged ion peptide bearing a SUMO1-specific mass signature was identified, which corresponded to sumoylated K203 (**Figure 6.2**C).

Figure 6.1D indicates that properties other than supercoiling must enable a plasmid to enhance the sumoylation of PARP-1's DBD. I therefore analyzed how three additional features of a plasmid influenced this modification phenomenon. Firstly, I asked whether the sequence of the template mattered because PARP-1 is able to recognize DNA in a sequence-specific and/or sequence-selective manner (see 1.5.2.2). I compared how well three plasmids of similar sizes, but carrying little sequence identity, stimulated the sumoylation of PARP-1's DBD. **Figure 6.3**A shows that this modification event was enhanced equally well by all three templates. Secondly, I realized that since the plasmids I used for the reactions shown above were isolated from a common *E. coli*

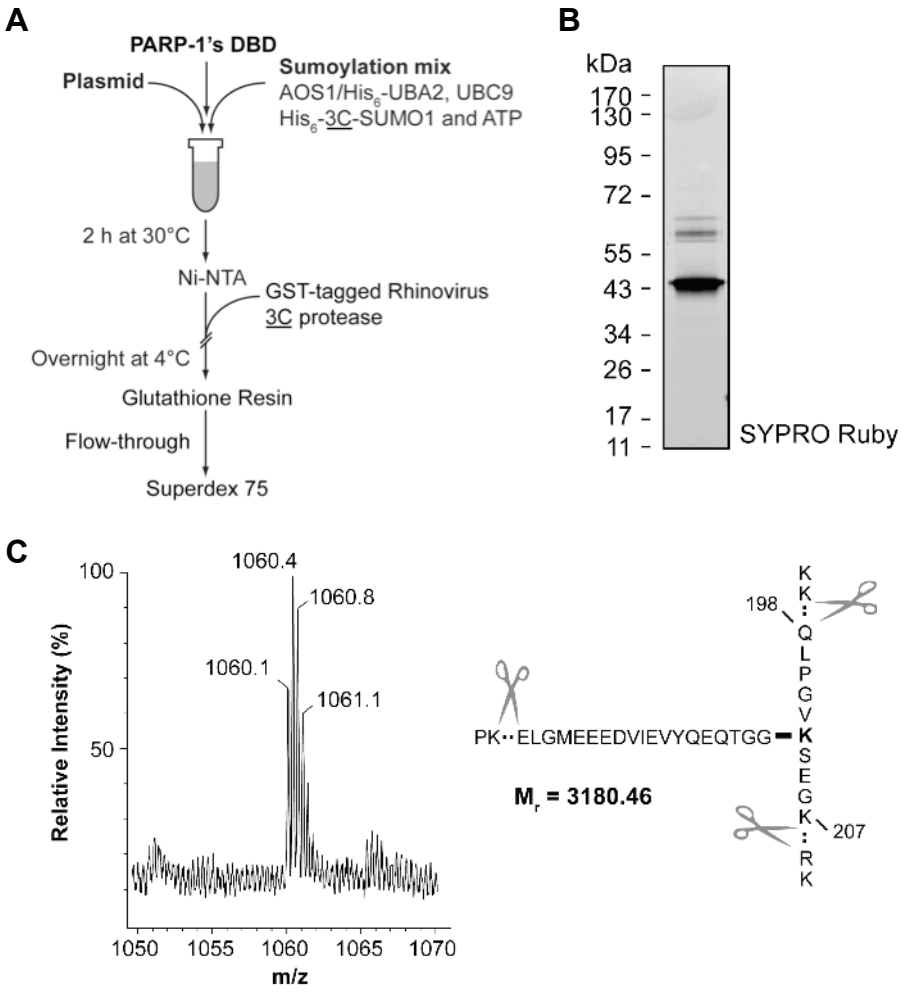

Figure 6.2 - PARP-1's DBD is sumoylated at K203. A) Scheme for the purification of sumoylated PARP-1's DBD. B) PARP-1's DBD (6.75 nmol) was sumoylated *in vitro* in a final volume of 45 mL in the presence of a supercoiled plasmid (330 µg) and then purified as shown in A) and described in 2.17.1.1. A sample of the purified SUMO conjugate was resolved by SDS-PAGE and visualized by SYPRO Ruby staining. C) The purified DBD-SUMO1 conjugate was trypsinized in solution and analyzed by mass spectrometry. The graph reports the identification of a triply charged ion with an average mass-to-charge ratio (m/z) of ~ 1060.5. This value matches the molecular weight (M_r), based on the average isotopic masses of the occurring amino acids, of large branched peptide that would be generated by trypsinization (scissors) of SUMO1-modified K203 (3180.46/3 = 1060.15).

strain, they must have been methylated at the N^6 position of the adenine and C^5 position of the cytosine that are found within certain sequences (Marinus and Morris, 1973). In mammals DNA is also modified at the C^5 position of a cytosine, but only within a CpG (Siegfried and Cedar, 1997). PARP-1 can influence the patterns of DNA methylation in mammalian cells (Caiafa *et al.*, 2009), but how it behaves towards methylated DNA has never been addressed. These considerations raised the possibility that the methylation state of DNA may control PARP-1 sumoylation. Accordingly, I evaluated the ability of methylated and non-methylated plasmids to

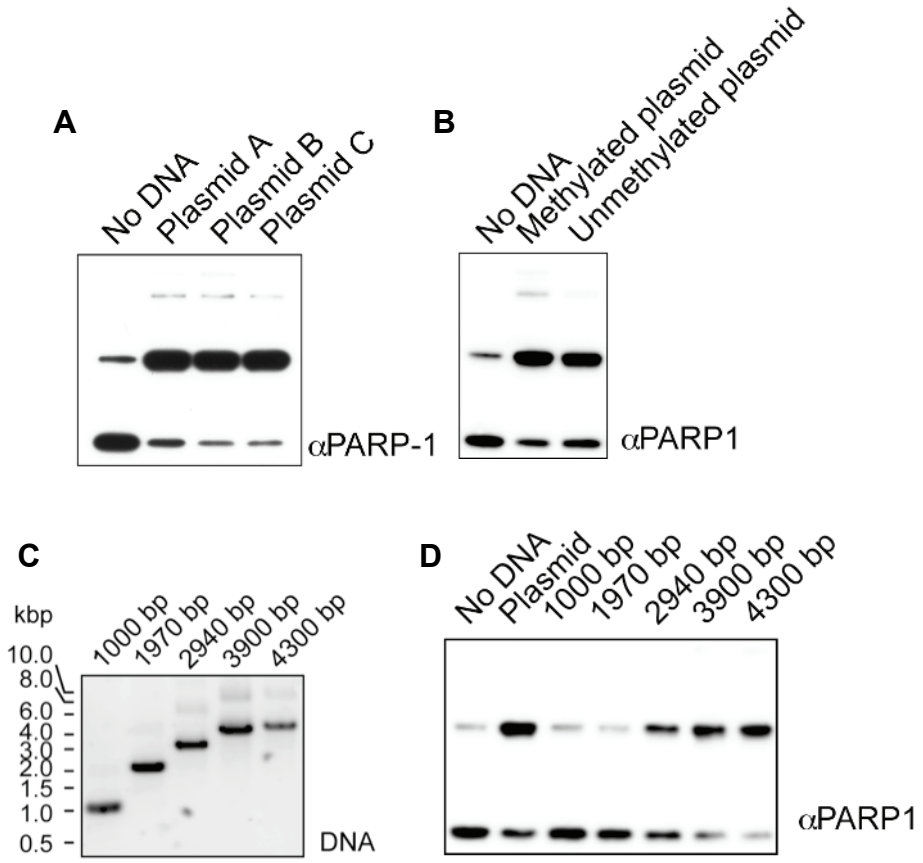

Figure 6.3 - The sumoylation of PARP-1's DBD is stimulated by a plasmid probably due to its size rather than because it carries certain sequences or it is methylated. PARP-1's DBD (3 pmol) was sumoylated *in vitro* in the presence of: A) three different plasmids (240 ng of pHU2020, 4.8 kbp, pHU1338, 5.3 kbp, or pHU1916, 5.5 kbp), B) an *E. coli*, *i.e.* Dam and Dcm, methylated or a non-methylated version of pHU2020 (240 ng), or D) dsDNA molecules of increasing lengths generated by PCR using pHU1771 as a template and oHU1374 together with oHU1411 (994 bp, 53 ng), oHU1413 (1969 bp, 105 ng), oHU1415 (2940 bp, 157 ng), oHU1416 (3896 bp, 208 ng) or oHU1375 (4300 bp, 229 ng). The products of these PCR amplifications were resolved by agarose gel electrophoresis, visualized with SYBER Green (2.12.7), extracted from the gel and then used in sumoylation reactions. The reaction products were analyzed by western blotting against PARP-1.

stimulate the modification of PARP-1's DBD. **Figure 6.3**B shows that this domain was sumoylated to a similar extent in the presence of either type of plasmid. Lastly, I analyzed whether the length of the DNA influenced the sumoylation of PARP-1's DBD. In order to do so, I sumoylated the protein in the presence of progressively longer dsDNA fragments (**Figure 6.3**C). Since these DNA duplexes were linear and therefore bore free ends, which PARP-1's DBD is able to recognize (Pion *et al.*, 2003), I used the same number of molecules in each reaction to maintain the number of DSBs constant. **Figure 6.3**D shows that the sumoylation of PARP-1's DBD was progressively enhanced as the size of the DNA incubated with it increased.

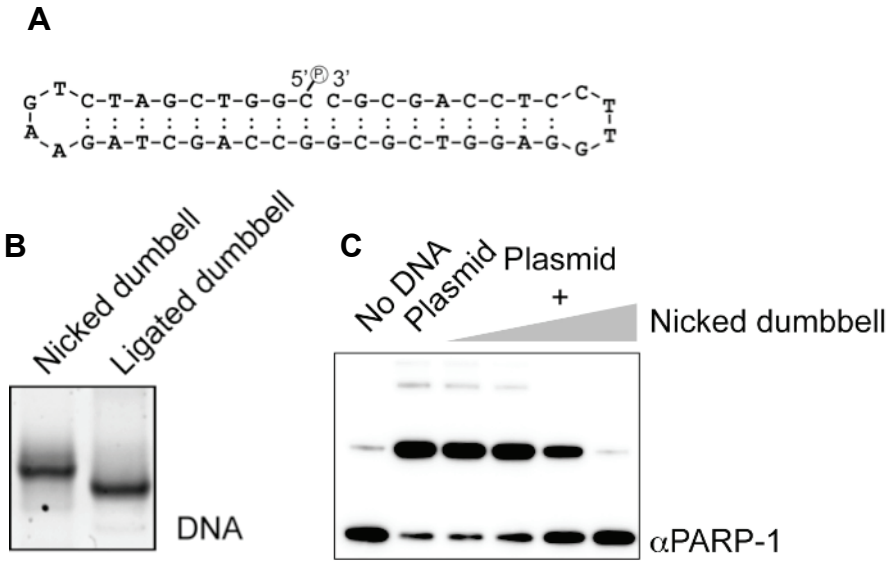

Figure 6.4 - Sumoylation of PARP-1's DBD is inhibited in the presence of nicked DNA. A) Structure of the nicked dumbbell. B) A sample of the nicked and ligated dumbbells (see 2.19.3) was resolved by denaturing PAGE (2.11.3) and visualized with ethidium bromide (2.12.7). C) PARP-1's DBD (3 pmol) was sumoylated *in vitro* in the presence of a supercoiled plasmid (240 ng) and increasing amounts (0.6, 1.5, 3 and 6 pmol) of the nicked dumbbell. The products of these reactions were analyzed by western blotting against PARP-1.

These data indicate that PARP-1's DBD is sumoylated at K203 in the presence of a plasmid, not because it contains certain sequences or is methylated but probably because it is a rather long piece of DNA.

6.2.3 PARP-1's DBD cannot be sumoylated in the presence of nicked DNA

The finding that introducing nicks in a plasmid reduced its ability to stimulate the sumoylation of PARP-1's DBD (**Figure 6.1**D) put forward the possibility that when this domain is bound to nicked DNA it cannot be sumoylated. To address this problem, I studied how the plasmid-stimulated modification of PARP-1's DBD was affected by adding increasing amounts of SSBs to the reaction. The nicked DNA consisted of a 44 nt long oligonucleotide that folds onto itself to form 18 bp of double-stranded DNA with a nick in the middle and a tight hairpin at either end so that no DSBs are exposed ("dumbbell", **Figure 6.4**A). Ligating this molecule produces an "intact" piece of DNA (**Figure 6.4**B). **Figure 6.4**C shows that the sumoylation of PARP-1's DBD was progressively inhibited by increasing amounts of the nicked dumbbell, hence indicating that nicked DNA specifically inhibits the modification of this domain of PARP-1.

6.2.4 Sumoylation of PARP-1's DBD relies upon its second zinc finger

PARP-1 recognizes SSBs in the DNA mainly through its second zinc finger (Gradwohl *et al.*, 1990; Ikejima *et al.*, 1990). I was therefore curious to determine whether the inhibitory action of nicked DNA on the modification of PARP-1's DBD depended on the second zinc finger of the protein. To address this hypothesis, I initially examined how well a construct that consisted of only the second zinc finger of PARP-1, including K203, was sumoylated in the presence of a plasmid, nicked DNA or DNA duplexes of increasing lengths. **Figure 6.5**A, left panel, and **Figure 6.5**B show that the sumoylation of such a protein was also enhanced by a plasmid or DNA molecules of increasing lengths and inhibited by DNA carrying a SSB (**Figure 6.5**C). Introducing a point mutation (R122I) in the second zinc finger of PARP-1 that impairs its ability to bind DNA but preserves its natural fold (Sebastian Eustermann, personal communication) completely abolished its ability to be preferentially sumoylated in the presence of DNA (**Figure 6.5**A, right panel). Interestingly, the extent to which PARP-1's second zinc finger was sumoylated under the conditions described in **Figure 6.1** was similar to that observed for equivalent experiments where the "full" DBD was used instead (**Figure 6.5**A).

Figure 6.5 - The second zinc finger of PARP-1's DBD is necessary and sufficient for DNA-stimulated sumoylation. A) A wild type or mutant (R122I) construct of the second zinc finger of PARP-1 (aa 103-214, 3 pmol) was subjected to *in vitro* sumoylation in the presence of: A) a supercoiled plasmid (240 ng), B) dsDNA molecules of increasing sizes as described in Figure 6.3D, or C) a supercoiled plasmid (240 ng) and two amounts of the nicked dumbbell (3 and 6 pmol). The products of these reactions were analyzed by western blotting against PARP-1.

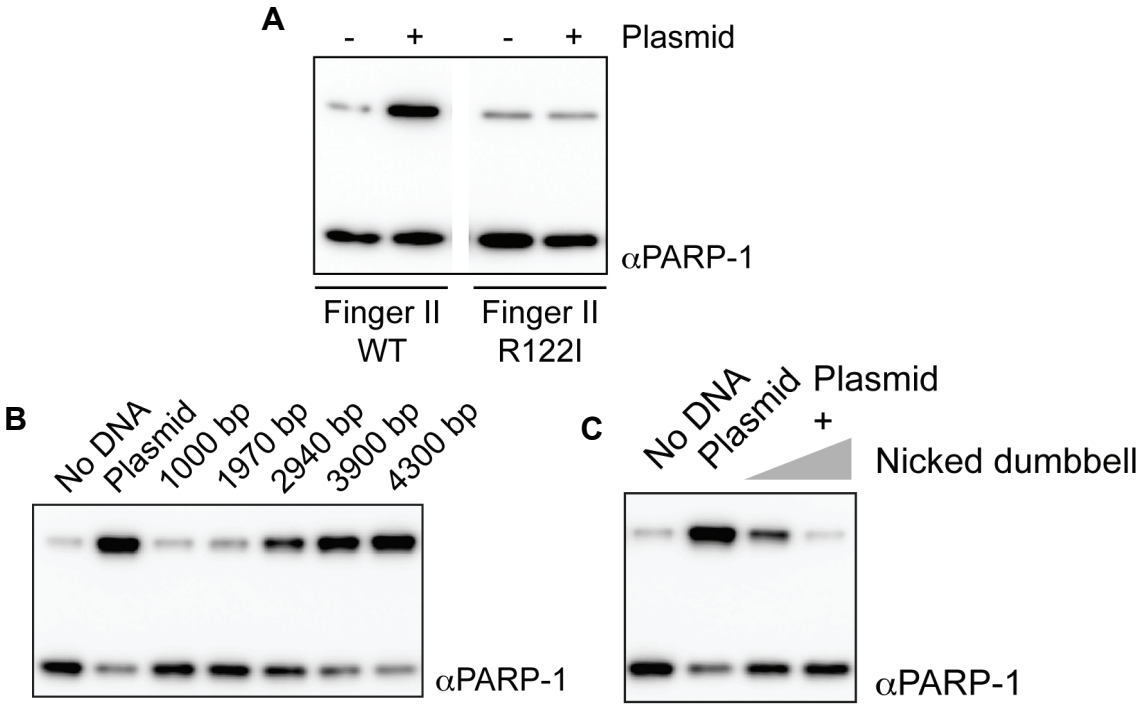

Altogether these observations show that the DNA-dependent sumoylation of PARP-1's DBD is mainly mediated through its second zinc finger.

6.2.5 Sumoylation does not significantly affect the structure of PARP-1's DBD or its ability to recognize nicked DNA

The evidence provided here that DNA affects the sumoylation of PARP-1's DBD persuaded us to find out whether the reverse may be also happening: does the attachment of SUMO to this domain of PARP-1 change its structure and thereby alter its ability to recognize DNA? We decided to address this question by comparing the tertiary structure of the unmodified DBD to that of the sumoylated form. For this part of my research I collaborated with Sebastian Eustermann, who had extensive experience in studying the solution structure of PARP-1's DBD by NMR. Towards this end, I modified and purified an ^{15}N- and ^{13}C-labelled version of the DBD with a non-labelled His_6-SUMO1 using an analogous strategy to that I already described in the caption of **Figure 6.2**. **Figure 6.6**A shows a sample of PARP-1's DBD before and after being sumoylated and purified. Sebastian Eustermann measured the chemical shifts produced by the backbone NH groups of the DBD conjugated to SUMO1 by ^{1}H ^{15}N heteronuclear single quantum coherence NMR and compared them to those of the unmodified domain. If the SUMO1 moiety that was attached to the DBD affected the overall structure of this domain by interacting non-covalently with some of its residues, then we expected the chemical shifts produced by these amino acids to differ between the unmodified and sumoylated proteins, because they would be in different local magnetic field environments. For this experiment, the SUMO1 conjugated to PARP-1's DBD was not labelled to avoid the appearance of SUMO1-specific chemical shifts in the NMR spectrum, which would have significantly complicated its analysis.

Figure 6.6B shows the changes in the chemical shift for each amino acid within PARP-1's DBD between its unmodified and sumoylated forms. We observed the highest degree of chemical shift perturbations around K203, which was expected given that SUMO is conjugated to such residue. Besides this obvious difference, sumoylation caused only small changes in the chemical shifts of only a few other residues of PARP-1's DBD, suggesting that SUMO1 does not significantly contact any residues in PARP-1's DBD nor changes its structure. As a matter of fact, the data favour a "bead on a string" model where PARP-1's DBD and SUMO1 move more or less freely with respect

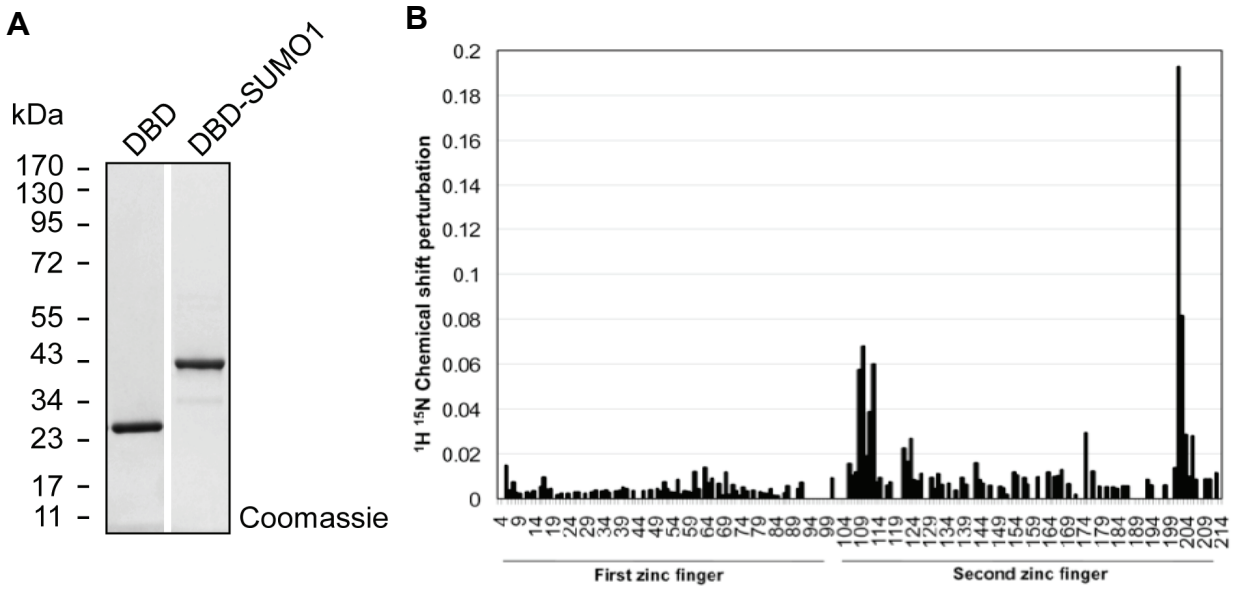

Figure 6.6 - The structure of PARP-1's DBD or its ability to recognize nicked DNA. A) A^{15}N- and ^{13}C-labelled version of PARP-1's DBD (~200 nmol) was sumoylated *in vitro* under standard conditions in the presence of a supercoiled plasmid (~10 mg) in a total volume of ~1.4 L. After 6 h the sumoylated DBD was purified essentially as described in Figure 6.2A and Figure 6.2B. Approximately ~ 1 µg of unmodified and sumoylated PARP-1's DBD were resolved by SDS-PAGE and stained with Coomassie. Although the two proteins samples were resolved on the same gel, they are shown separately for presentation purposes only. B) The SUMO1-DBD conjugate obtained in A) was subjected to ^{1}H ^{15}N heteronuclear single quantum coherence NMR to measure the chemical shifts produced by the backbone amide groups of its DBD moiety. These chemical shifts were compared against those yielded by the unmodified PARP-1's DBD to determine the extent of chemical shift perturbation (Y axis) that sumoylating such a domain induced at each one of its amino acids (X axis), as described in 2.22.

to each other. Yet, we noticed some small differences in the chemical shifts around L110, which indicates that SUMO1 may have some preference in the way it positions itself with respect to the second zinc finger of PARP-1. To corroborate these structural data, Sebastian Eustermann assayed the affinity of the unmodified and sumoylated DBDs for the nicked dumbbell (**Figure 6.3**A) by electrophoretic mobility shift analysis. The DBD of PARP-1 and the nicked dumbbell were mixed together at various molar ratios, incubated and loaded onto an poly-acrylamide gel. After electrophoresis, the DNA was visualized with ethidium bromide. Sebastian Eustermann observed that the unmodified and sumoylated DBDs associated with the nicked dumbbell at similar protein:DNA molar ratios (personal communication).

These data indicate that the conjugation of SUMO1 to K203 of PARP-1's DBD does not significantly affect its structure or ability to recognize nicked DNA.

6.2.6 DNA enhances the sumoylation of the full-length PARP-1 at K203 and K486

The finding that DNA stimulated the sumoylation of K203 within PARP-1's DBD raised the question of whether this phenomenon was specific for such a domain or a similar effect also occurred at sites located elsewhere in PARP-1. This is a relevant issue because, in the presence of DNA damage, the DBD of PARP-1 is able to interact with and activate its catalytic domain even when these two regions are physically separated from each other (Altmeyer *et al.*, 2009). These results therefore suggest that DNA may bring about changes in PARP-1 that go beyond its DBD. The identification of a second sumoylation site in PARP-1 provided a means to address the above-mentioned problem because it is located in its auto-modification domain (^{485}V<u>K</u>AE$_{488}$, **Figure 5.3**, Martin *et al.*, 2009; Messner *et al.*, 2009) and it falls within a sumoylation consensus motif, which meant that it should be recognized by UBC9 alone *in vitro*. Purified full-length wild type His$_6$-PARP-1 was sumoylated in the absence or presence of a supercoiled plasmid and analyzed by western blotting analysis. **Figure 6.7**A shows that His$_6$-PARP-1 was completely converted into multiple slow-migrating forms in the presence of DNA, which must represent SUMO1-modified species because they are recognized by an anti-SUMO1 antibody. This effect was independent of supercoiling because the polymerase was modified equally well by non-saturating amounts of relaxed and supercoiled plasmids (**Figure 6.7**B). In contrast, in the absence of DNA I barely detected any sumoylation of the polymerase. Although I cannot exclude that a few of the PARP-1-SUMO1 species shown in **Figure 6.7**A represented SUMO chains conjugated to K203, their number and electrophoretic mobilities strongly suggested that DNA enhanced the modification of the full-length PARP-1 at more than one lysine residue. To test this hypothesis, I created mutants of the full-length His$_6$-PARP-1 where its two known sites of sumoylation, *i.e.* K203 and K486, were individually changed to arginines and then I sumoylated them in the absence or presence of a plasmid. **Figure 6.7**C confirms that His$_6$-PARP-1 was sumoylated at the relevant sites in the *in vitro* reactions described here and it shows that DNA stimulated not only the modification of K203 but also that of K486. Surprisingly, a K203/486R mutant of His$_6$-PARP-1 was also efficiently sumoylated in the presence of DNA (**Figure 6.7**C), which means that *in vitro* a third lysine of PARP-1 can be sumoylated. Since the data reported elsewhere in this thesis (**Figure 5.3**) and by Martin *et al.* (2009) indicate that *in vivo* there may be a third sumoylation site in PARP-1, I sumoylated His$_6$-PARP-1 *in vitro* in the presence

Figure 6.7 - PARP-1 is sumoylated at K203 and K486 in the presence of DNA. A) His_6-PARP-1 (3 pmol) was sumoylated *in vitro* in the presence of A) a supercoiled plasmid (240 ng) or B) a supercoiled or a relaxed plasmid (20 ng). C) Wild type, K203R, K486R, or K203/486R His_6-PARP-1 (3 pmol) were sumoylated *in vitro* in the presence of a supercoiled plasmid (240 ng). D) His_6-PARP-1 (3 pmol) was subjected to *in vitro* sumoylation in the presence of a supercoiled plasmid (240 ng) and equivalent amounts of either wild type SUMO1 or SUMO1 T95R. The reaction products were analyzed by western blotting against PARP-1. E) His_6-PARP-1 (200 pmol) was modified in a 1.3 mL sumoylation reaction supplemented with an untagged version of the SUMO1 E1 enzyme, SUMO1 T95R and a supercoiled plasmid (15.6 µg) and purified as described in 2.17.1.2. The isolated protein was dialyzed against 100 mM ammonium acetate before being vacuum concentrated to approximately 50 µL, trypsinized in solution and then analyzed by mass spectrometry. The graph shows the mass-to-charge ratio (m/z) distribution of the b- (red and green) and y-series (blue) ions generated by fragmenting a precursor peptide that included K512 of PARP-1 and showed a 114 Da mass signature, which corresponds to the addition of GG "tag" to the peptide.

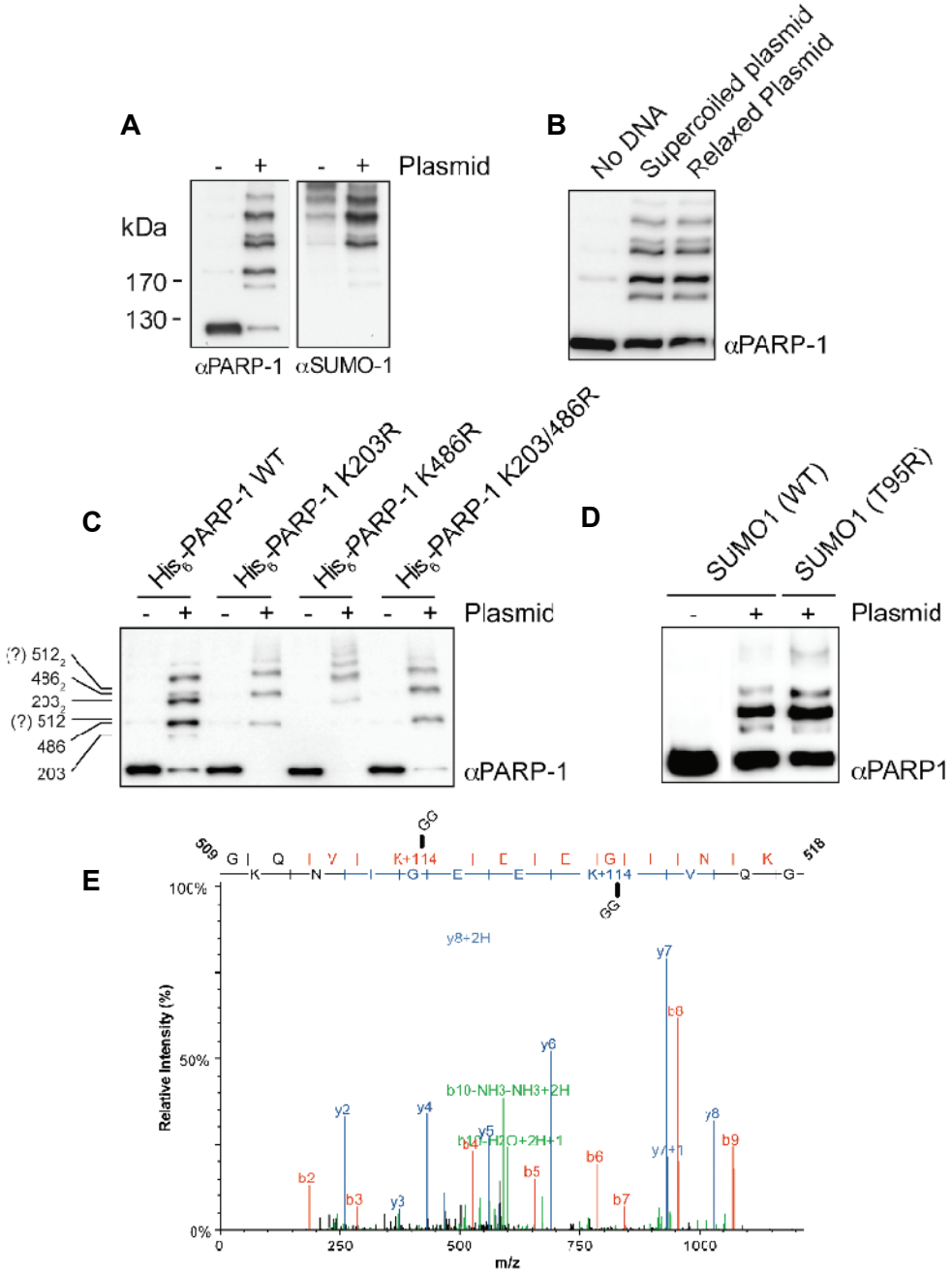

of a plasmid and SUMO-1 T95R. This mutant of SUMO-1 facilitates the identification of sumoylated residues by mass spectrometry because, after trypsinization, the peptides conjugated to it would bear a smaller and more easily detectable mass addition (a GG "tag") than those attached to the wild type modifier (Knuesel *et al.*, 2005). Sumoylated His_6-PARP-1 was captured by metal affinity chromatography, as described in more detail in the caption of **Figure 6.7**E, and analyzed by the Protein Analysis and Proteomics team of the London Research Institute on a ThermoScientific LTQ Orbitrap XL/ETD mass spectrometer coupled to a Waters NanoACQUITY UPLC system (LC MS/MS). Sumoylating His_6-PARP-1 in the presence of wild type SUMO1 or the T95R mutant resulted in essentially identical modification patterns (**Figure 6.7**D), indicating that this mutation in SUMO1 does not appreciably distort the *in vitro* modification of the polymerase. Mass spectrometric analysis of the sumoylated His_6-PARP-1 identified and sequenced two unique peptides that bore a di-glycine mass signature, which corresponded to sumoylated K486 and K512 (**Figure 6.7**E). These data therefore suggest that when K203 and K486 are mutated in PARP-1, the sumoylation machinery may preferentially target K512 *in vitro*. Since K512 does not appear to be a relevant modification site of PARP-1 *in vivo* (**Figure 5.3**), I decided not to confirm this result by mutagenesis because K512 was probably modified *in vitro* by virtue of the fact that it falls within a sumoylation consensus motif ($^{511}V\underline{K}EE_{514}$).

Altogether these findings show that the ability of DNA to stimulate the sumoylation of PARP-1 is not limited to the modification of its DBD but it also happens at sites located elsewhere in the polymerase, and even on sites that may not be physiologically relevant.

6.2.7 A minimal DNA substrate stimulates the sumoylation of the full-length PARP-1 through the second zinc finger

Having observed that a plasmid stimulated the sumoylation of the full-length PARP-1, I wondered whether the second zinc finger of this protein and nicked DNA also played a role in such a modification event, as I showed for the DBD alone. For the experiments described in this paragraph I used the intact dumbbell to enhance the sumoylation of PARP-1 because, unlike the DBD alone, this minimal DNA substrate was sufficiently long to trigger the modification of the full-length polymerase and it did not bear free ends (**Figure 6.8**A). In order to address the above-described question, I tested how the nicked and intact dumbbells affected the sumoylation of wild type His_6-PARP-1 or that of a mutant carrying a defective second zinc finger (R122/138I). **Figure 6.8**A, top

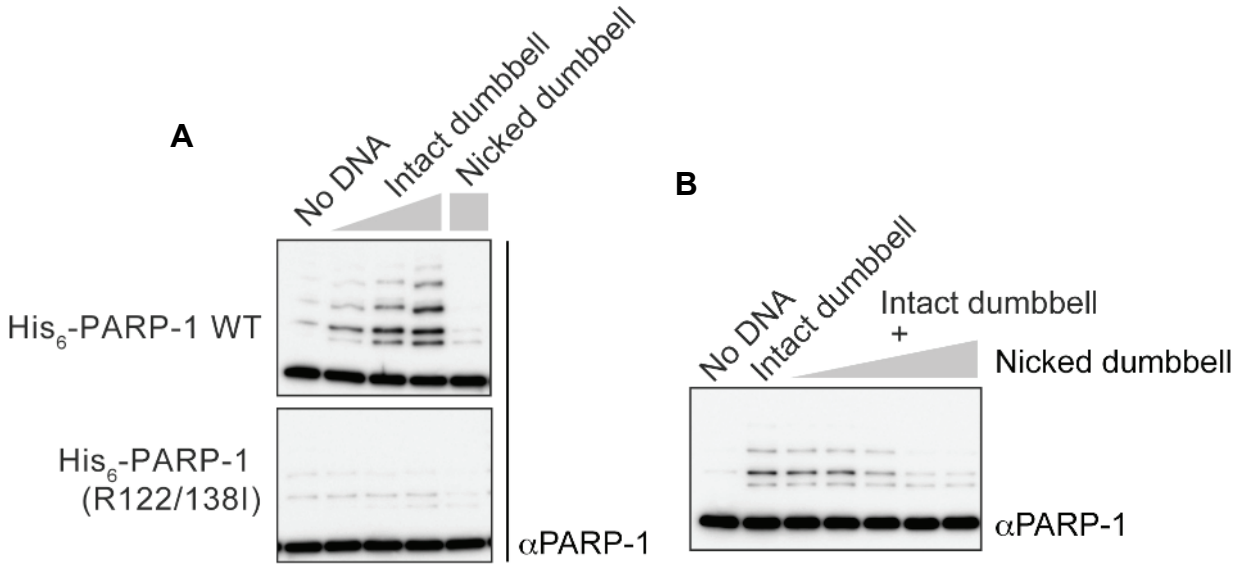

Figure 6.8 - Sumoylation of PARP-1 in the presence of a minimal DNA substrate depends on its second zinc finger. A) His_6-PARP-1 (wild type or R122/138I, 3 pmol) were subjected to *in vitro* sumoylation in the presence of increasing amounts of the intact dumbbell (1.5, 3 or 6 pmol) or the nicked one (6 pmol). B) His_6-PARP-1 was sumoylated *in vitro* in the presence of the intact dumbbell (3 pmol) and increasing amounts of the nicked one (0.38, 0.75, 1.5, 3 or 6 pmol). The reaction products were analyzed by western blotting against PARP-1.

panel, shows that the intact dumbbell stimulated the sumoylation of the wild type His_6-PARP-1 in a dose-dependent manner. The nicked substrate did not afford such an effect; on the contrary, it counteracted the ability of the intact dumbbell to enhance PARP-1 sumoylation (**Figure 6.8**B). Mutating the second zinc finger of the polymerase completely abolished these DNA-dependent effects (**Figure 6.8**A, bottom panel).

Altogether the results presented here show that a short intact DNA molecule stimulates the sumoylation of the full-length PARP-1 by means of its second zinc finger, but one that carries a SSB has instead the opposite effect.

6.2.8 DNA length defines two types of PARP-1 sumoylation

Although the data described in the previous paragraph show that nicked DNA can inhibit PARP-1 sumoylation, I found that this phenomenon did not happen when the modification of the polymerase was brought about by a plasmid (**Figure 6.9**A), instead of the intact dumbbell. This was the case even if I used an amount of plasmid that was equivalent, with respect to the number of nucleotides, to the quantity of intact dumbbell employed for the experiments shown in **Figure 6.8**A. Such an unusual observation made me think about the differences that exist between a plasmid and the intact dumbbell, which could explain it. The different lengths of these DNA molecules could

have been the determining factor. To explore this hypothesis, I compared the ability of the nicked dumbbell to inhibit the enhancement of PARP-1 sumoylation triggered by short or long dsDNA oligonucleotides. The shorter DNA molecule was 15 bp long, which is the smallest DNA substrate that can stimulate the sumoylation of PARP-1 (**Figure 6.9**A and **Figure 6.9**F), while the longer one was 61 bp long. **Figure 6.9**B shows that the nicked dumbbell hindered the capacity of the 15 bp long oligonucleotide, but not that of the 61 bp long one, to stimulate the sumoylation of His_6-PARP-1. This difference could have stemmed from the different amounts of DNA present in the two sets of reactions, as both the 15 and 61 bp long oligonucleotides were used at a protein:DNA molar ratio of 1:1, but one is four times as long as the other. I therefore tested the inhibitory activity of the nicked dumbbell on PARP-1 sumoylation in reactions supplemented with the 61 bp long oligonucleotide at a protein:DNA molar ratio of 1:0.25. **Figure 6.9**B shows that even under these conditions the nicked DNA did not significantly inhibit the modification of PARP-1.

The ability of nicked DNA to inhibit PARP-1 sumoylation was not the only property of this modification event that was affected by length of the DNA used to stimulate it. I found that while the sumoylation of the wild type polymerase was enhanced by a dsDNA as short as 15 bp, that of the R122/138I mutant happened only in the presence of the 61 bp long oligonucleotide (**Figure 6.9**C). Titrating increasing amounts of either the 15 or 61 bp long oligonucleotide in sumoylation reactions containing the wild type His_6-PARP-1 showed that, at equivalent molar amount, the longer DNA stimulated the sumoylation of this protein more efficiently than the shorter one (**Figure 6.9**D). Additionally, I found that the extent to which PARP-1 sumoylation grew with increasing amounts of the 61 bp long DNA did not change significantly between the wild type His_6-PARP-1 and the R122/138I mutant (**Figure 6.9**D). Likewise, these two versions of the polymerase were modified equally well and with similar kinetics in the presence of a non-saturating amount of a plasmid (**Figure 6.9**E).

The possibility that the phenomena described above were simply the consequence of adding any double-stranded oligonucleotide to PARP-1 can be excluded because the sumoylation of the polymerase could not be stimulated by either 15-25 nt long single-stranded DNA molecules (**Figure 6.9**F) or a 21 bp long dsRNA (**Figure 6.9**G). **Figure 6.9**F did however show that a 61 nt long oligonucleotide could actually stimulate the modification of PARP-1, which probably occurred because this DNA substrate was long enough to form double-stranded DNA secondary structures.

Figure 6.9 - DNA length defines two types of PARP-1 sumoylation. His_6-PARP-1 (3 pmol) was sumoylated *in vitro* in the presence of increasing amounts of the nicked dumbbell (0.38, 0.75, 1.5, 3 or 6 pmol) and a constant amount of either A) a plasmid DNA (20 ng) or B) dsDNA oligonucleotides of different lengths (15 bp long dsDNA, 3 pmol; 61 bp long dsDNA, 3 or 0.75 pmol). C) His_6-PARP-1 (wild type or R122/138I, 3 pmol) was subjected to *in vitro* sumoylation in the presence of C) 8, 15, 25 and 61 bp long oligonucleotides (3 pmol), D) 0.38, 0.75, 1.5, 3 or 6 pmol of either the 15 or the 61 bp long dsDNAs, or E) 20 ng of supercoiled plasmid for the indicated lengths of time. His_6-PARP-1 (3 pmol) was sumoylated *in vitro* in the presence of F) 3 pmol of the indicated double-stranded or single-stranded DNA oligonucleotides or G) 1 pmol of either the 25 bp long dsDNA or a 21 bp long dsRNA.

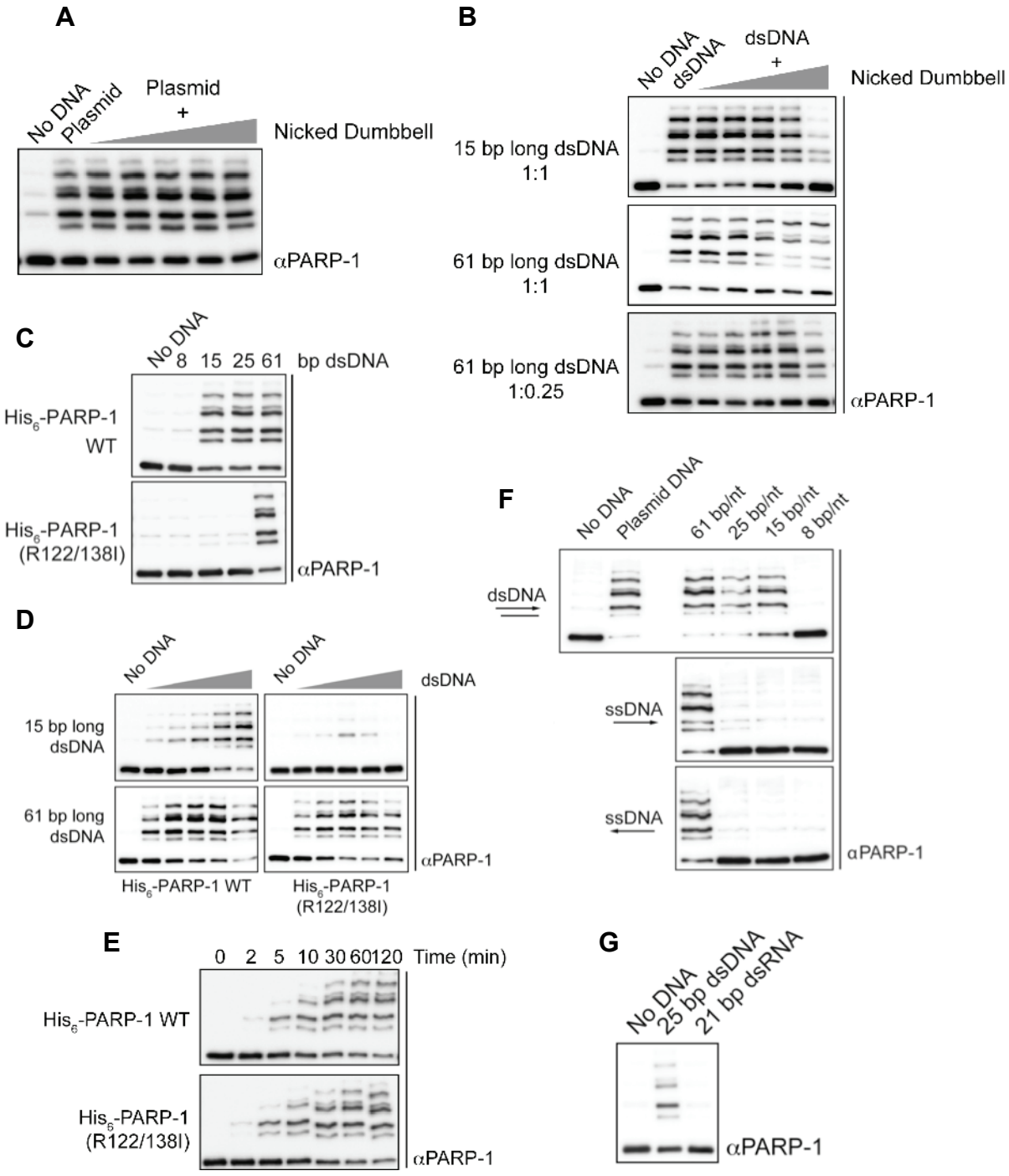

These data, together with those presented in the previous paragraph, demonstrate that the length of the DNA used to stimulate PARP-1 sumoylation determines how sensitive this modification event is to SSBs and inactivating the second zinc finger of the polymerase. These two factors can in fact inhibit the modification of the polymerase only when it is brought about by DNA substrates of a minimal length, but not longer ones.

6.2.9 The third zinc finger is not important for the DNA-dependent sumoylation of PARP-1

In addition to showing that the second zinc finger of PARP-1 is essential for triggering the sumoylation of this protein in the presence of short DNA molecules, the data presented above suggested that when the length of DNA is not limiting other features within the polymerase become relevant in stimulating its modification. Thus, I set out to explore whether the other two zinc fingers located within the N-terminal DNA-binding domain of PARP-1 also played a role in such a phenomenon. Even though I had already shown that deleting the first zinc finger from PARP-1's DBD did not significantly affect its sumoylation (**Figure 6.5**), I decided to study the consequences of inactivating it in the full-length protein. In fact, in such a context the first zinc finger of PARP-1 could have possibly played a role in stimulating its sumoylation by, for instance, interacting with regions located outside the DBD. Additionally, I was curious to establish whether the third zinc finger of PARP-1 played a role in its modification because although it does not seem to bind DNA on its own (Tao *et al.*, 2008), it has been shown that features C-terminal to the first two zinc fingers of PARP-1 are important for binding to intact DNA (Ikejima *et al.*, 1990). In order to address the question described above, I created His_6-PARP-1 mutants where either the first (C21G) or the third (C298A) zinc finger was inactivated. Unfortunately, although I was able to purify the His_6-PARP-1 C21G mutant through several chromatographic steps, it eluted from a gel filtration column in the void volume (data not shown), which suggested that it was heavily aggregated and it was therefore unusable. The His_6-PARP-1 C298A mutant also had a slight tendency to aggregate; yet, I recovered a significant amount of it that had the same elution profile as that of the wild type His_6-PARP-1 over gel filtration (data not shown). These observations are consistent with Langelier *et al.* (2008), who on such basis proposed that the C298A mutation destabilizes the structure of PARP-1 only locally. Since the His_6-PARP-1 C298A mutant appeared to be well behaved, I examined how efficiently it was sumoylated in the presence of a plasmid, the intact

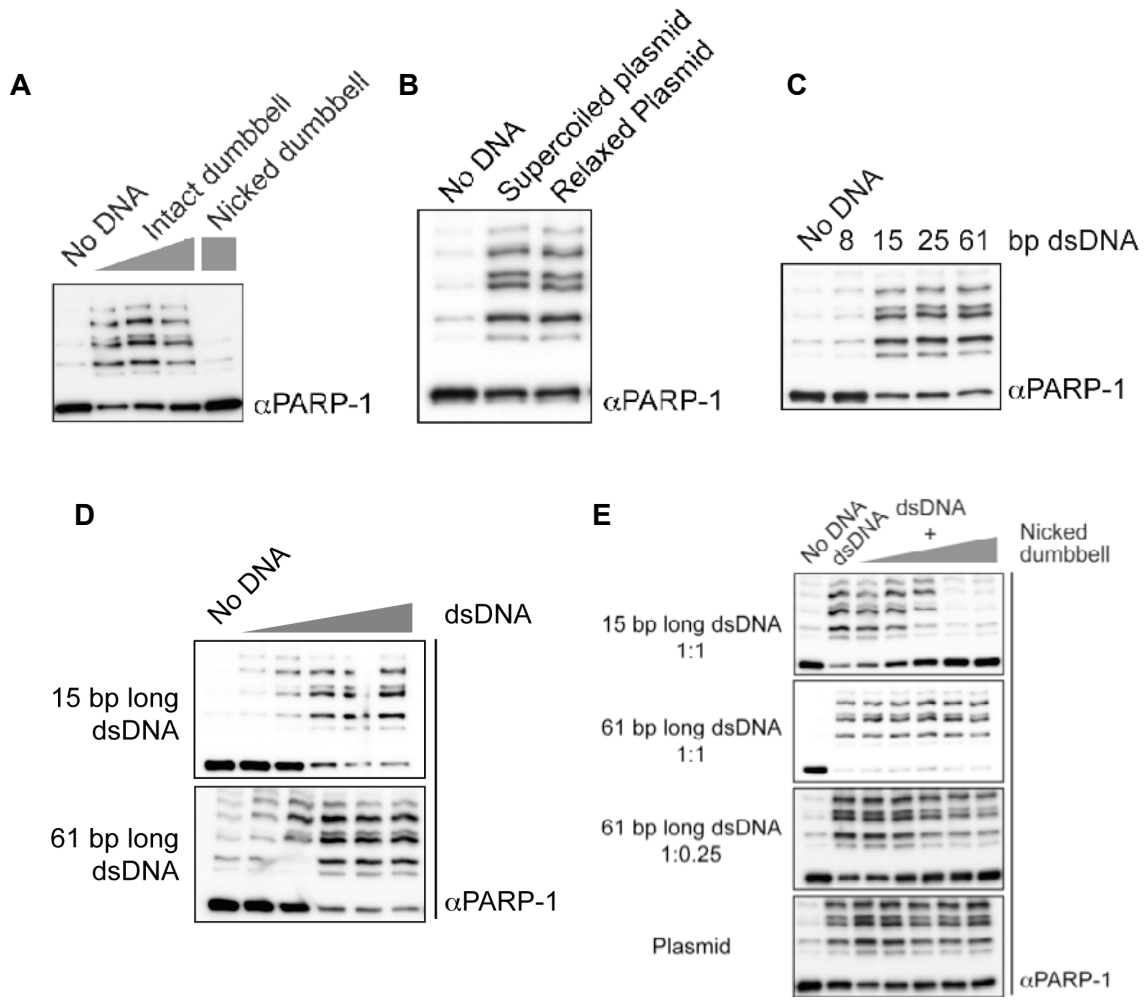

Figure 6.10 - The third zinc finger does not play a significant role in the DNA-dependent sumoylation of PARP-1. All the reactions shown in this figure were carried out under the same experimental conditions as the equivalent ones shown in Figures 6.7 and Figure 6.8, but in this case using His_6-PARP-1 C298A instead. The reaction products were analyzed by western blotting against PARP-1.

dumbbell or oligonucleotides of different lengths. In addition, I also studied the extent to which the nicked DNA inhibited the enhancement of His_6-PARP-1 C298A modification triggered by the intact dumbbell, the 15 and 61 bp long dsDNAs or the plasmid DNA. **Figure 6.10**A-E show that the His_6-PARP-1 C298A mutant behaved similarly to the wild type protein (**Figure 6.10** and **Figure 6.9**) with respect to the way it was sumoylated under the conditions tested here. In fact, the only difference between the two proteins was that the mutant seemed to be sumoylated somewhat more efficiently than the wild type protein.

Altogether these data show that the third zinc finger of PARP-1 does not play a significant role in the DNA-dependent sumoylation of this protein, at least when it is individually mutated.

6.2.10 Small changes in salt concentration considerably affect plasmid-stimulated PARP-1 sumoylation

As I mentioned above, Ikejima *et al.* (1990) showed that the first two zinc fingers of PARP-1 and unknown features C-terminal to them are important for the binding of this protein to an intact supercoiled plasmid. This interaction was detected at a very low salt concentration, *i.e.* 2 mM magnesium acetate, and it was found to be fairly weak because it was significantly, but not completely, reduced in the presence of as little as 100 mM KCl (Ikejima *et al.*, 1990). Conversely, PARP-1, or at least its DBD encompassing all three zinc fingers, can bind to single- or double-stranded breaks at much higher salt concentrations (Lilyestrom *et al.*, 2010). By taking into account these observations and the evidence provided here that intact DNA stimulates the sumoylation of PARP-1, I hypothesized that this modification phenomenon should be sensitive to small changes in the salt concentrations used for the sumoylation reactions. Thus, I set out to test how well a plasmid enhanced the modification of His_6-PARP-1 in the presence of increasing concentrations of different salts. The *in vitro* sumoylation reactions described in this part of my thesis were routinely carried out in a buffered solution containing 110 mM potassium acetate as a source of salt, which in terms of ionic strength corresponds to a 50-60 mM NaCl/KCl solution. I therefore chose to examine the extent of PARP-1 sumoylation in reaction mixtures containing 110, 180 and 230 mM potassium acetate or 50, 100 and 150 mM NaCl/KCl because they have corresponding ionic strengths. Importantly, since the intrinsic activities of the SUMO activating and conjugating enzymes are only mildly affected across this range of salt concentrations (**Figure 6.11**, lower panel), it follows that any major changes in the plasmid-stimulated sumoylation of PARP-1 under these conditions should stem from alterations in the interaction between the polymerase and DNA or, perhaps less likely, between the polymerase and UBC9. **Figure 6.11**, upper panel, shows that, for all of the three salts used, the DNA-induced sumoylation of His_6-PARP-1 was almost complete at the lowest concentrations, it was reduced to half of that amount at the intermediate ones and it was nearly abolished at the highest.

These results suggest that the interaction between a plasmid and PARP-1 that must happen to trigger its sumoylation is weak and it is similar to the strength of binding that PARP-1 exhibits towards a supercoiled plasmid (Ikejima *et al.*, 1990).

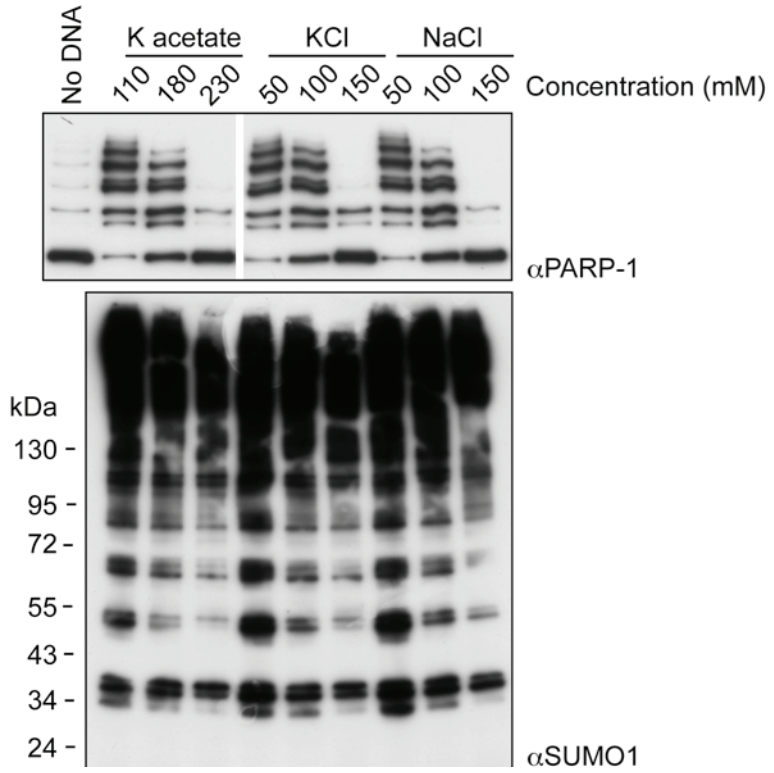

Figure 6.11 - The plasmid-triggered sumoylation of PARP-1 is inhibited by small changes in salt concentration. His_6-PARP-1 (3 pmol) was sumoylated *in vitro* in the presence of a supercoiled plasmid (240 ng) and a reaction solution in which the type and concentration of salt it normally contained, *i.e.* 110 mM potassium acetate, were varied as indicated in the figure itself. The solutions supplemented with potassium acetate also contained 2 mM magnesium acetate, while those prepared with NaCl or KCl also included 2 mM $MgCl_2$. The reaction products were analyzed by western blotting against PARP-1.

6.2.11 DNA packaged into chromatin can stimulate PARP-1 sumoylation

For many of the reactions shown in this part of my thesis I used a recombinant plasmid, or some other form of naked DNA, to stimulate the sumoylation of PARP-1. However, this protein may never see DNA in this form in a eukaryotic cell because there DNA is packaged into chromatin. In addition, PARP-1 itself has a role in chromatin compaction both *in vivo* and *in vitro* (Kraus, 2008). Thus, I wondered whether PARP-1 sumoylation also occurred in the context of chromatin. To address this question I examined how well PARP-1's DBD and the full-length protein were sumoylated in the presence of a chromatin mimic. This mimic consisted of a freshly reconstituted nucleosomal array that contained 60 nucleosomes evenly spaced along an ~11 kbp DNA molecule (a gift from Daniela Rhodes). It consisted of a tandemly repeated high affinity histone octamer binding sequence that was 187 bp long (Lowary and Widom, 1998).

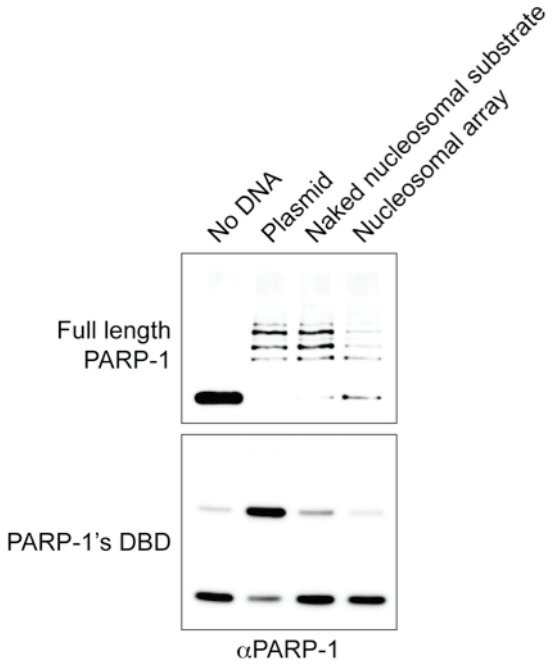

Figure 6.12 - Chromatin-packaged DNA can stimulate the sumoylation of PARP-1. Full-length His_6-PARP-1 or PARP-1's DBD (3 pmol) were subjected to *in vitro* sumoylation reactions in the absence of any DNA or in the presence of 240 ng of intact plasmid or 240 ng of an ~11 kbp DNA molecule consisting of sixty tandemly repeated high affinity histone octamer binding sequences. The latter DNA substrate was used either naked or in a complex with histones. The products of these reactions were analyzed by western blotting against PARP-1.

Figure 6.12 shows that the nucleosome array was able to stimulate the sumoylation of the full-length His_6-PARP-1, perhaps to a slightly lesser extent than the naked 11 kbp DNA, which was used as a control. Conversely, neither the chromatin mimic nor the control substrate enhanced the sumoylation of PARP-1's DBD.

These results strongly suggest that even when DNA is packaged in the form of chromatin it can stimulate the sumoylation of the full-length PARP-1.

6.3 Discussion

The main finding of this part of my research is that *in vitro* DNA regulates the sumoylation of PARP-1 in at least two different ways, which will be discussed below.

6.3.1 Intact DNA stimulates PARP-1 sumoylation

Classic B-form DNA appeared to stimulate PARP-1 modification, regardless of its sequence. In fact, in the presence of a supercoiled intact plasmid the modification of both the full-length PARP-1 and its DBD alone were specifically enhanced (**Figure 6.1** and **Figure 6.7**). Relaxing the plasmid did not affect this stimulatory phenomenon, thus

indicating that it cannot have been triggered by unusual supercoiling-induced DNA structures such as hairpins, cruciforms, bent DNA and base unpaired regions, to which PARP-1 can specifically bind (Jorgensen *et al.*, 2009; Lonskaya *et al.*, 2005; Potaman *et al.*, 2005; Sastry and Kun, 1990; Soldatenkov *et al.*, 2008). The latter observation also argues against the possibility that the plasmid-induced sumoylation of PARP-1 may have stemmed from its ability to recognize non-covalent DNA crossovers (Chasovskikh *et al.*, 2005). Although PARP-1 apparently does so on both supercoiled and relaxed plasmids (Chasovskikh *et al.*, 2005), the former should contain more of these structures, as it carries supercoiling nodes, than the latter, where such structures probably occur only stochastically. In addition, these considerations also suggest that the ability of the intact dumbbell to enhance the sumoylation of the full-length PARP-1 was not mediated through the hairpins that this DNA substrate carried but rather by the intact stretch of DNA found between them. In order to undoubtedly prove this point it will be useful to show that another type of short intact DNA molecule, such as a double-stranded oligonucleotide whose free ends have been occluded with streptavidin, stimulates the modification of like the intact dumbbell does.

6.3.1.1 Can PARP-1 bind intact DNA?

The above-discussed observations provide strong evidence that intact DNA stimulates PARP-1 sumoylation. Yet, they do not prove that it does so by productively binding to the polymerase. This is an issue that I did not directly examine but which could be addressed to undoubtedly confirm the validity of such a stimulatory phenomenon, especially in the light that it is still unclear whether PARP-1 can recognize, at least in a physiologically relevant manner, intact B-form DNA (see 1.5.2.2). The data reported by Ikejima *et al.* (1990) indicate that the apparent binding of PARP-1 to unbroken DNA was actually the major interaction they detected in their assays. Deleting the first two zinc fingers of PARP-1 did not affect this generalized affinity for intact DNA, except for making it weaker. Consistent with these data suggesting that PARP-1 binds intact DNA weakly, I found that the ability of a plasmid to stimulate PARP-1 sumoylation was significantly affected by small changes in salt concentration (**Figure 6.11**).

If PARP-1 cannot normally bind intact DNA, how/why would it stimulate the sumoylation of this protein? In the reactions presented above PARP-1 was sumoylated under relatively low ionic conditions (110 mM KOAc ~ 50 mM NaCl), which could however be defined as “standard” given that they have been commonly used elsewhere for this type of assay (Werner *et al.*, 2009). There is therefore the chance

that at this low salt concentration, PARP-1's recognized affinity for broken or unusual forms of DNA may have been enhanced enough to allow it to associate with intact DNA as well, probably in an abnormal manner. Such a non-physiological type of DNA binding might have destabilized the polymerase, causing it to amass into large complexes, which could be better substrates for sumoylation. In fact, a similar mechanism has been shown to underlie the increased sumoylation that PML experiences in response to arsenic trioxide (Zhang *et al.*, 2010). This drug can directly bind PML, causing it to forms oligomers that are recognized by UBC9 better than the monomeric PML (Zhang *et al.*, 2010). The apparent susceptibility of a fragment of PARP-1, spanning from its N-terminus to the BRCT domain, to form high molecular weight complexes in the presence of DNA under particular, sub-optimal, conditions would argue in favour of this model (Lilyestrom *et al.*, 2010).

6.3.2 Single-stranded breaks inhibit PARP-1 sumoylation

Unlike intact DNA, SSBs inhibited the sumoylation of both the full-length PARP-1 and its DBD alone *in vitro* (**Figure 6.3** and **Figure 6.8**). Such a phenomenon is more easily explainable than the one described above because it is well established that PARP-1 recognizes and is activated by this type of DNA breaks (D'Silva *et al.*, 1999; Gradwohl *et al.*, 1990; Ikejima *et al.*, 1990; Pion *et al.*, 2005). Yet, PARP-1 sumoylation was not appreciably inhibited *in vivo* by exposing cells to drugs, such as MMS or H_2O_2, which introduce SSBs in their DNA (**Figure 5.2**). It is unlikely that this incongruence may have arisen from an insufficient number of SSBs in the cells because the employed amounts of, and length of exposure to, the relevant drugs should have produced enough lesions to outnumber the quantity of PARP-1 molecules found in a nucleus. An alternative scenario to explain the incongruence described above could be envisioned on the basis of the proposed model that PARP-1 binds to damaged DNA very dynamically, through rapid cycles of biding to DNA lesions, auto-parylation, disassociation from the DNA, de-parylation and re-binding to the damaged DNA (Haince *et al.*, 2008; Woodhouse and Dianov, 2008). This model therefore suggests that *in vivo* the binding of PARP-1 to DNA nicks may be too transient to produce a visible drop in its sumoylation levels. Consistent with this idea, both Rajvee Shah and I found that even PARP-1 auto-parylation, an event that is directly coupled to the polymerase recognizing damaged DNA, could not be easily detected and, even when it was, it was very transitory.

6.3.2.1 Stoichiometric vs. non-stoichiometric effects of nicked DNA on PARP-1 sumoylation

Although it is evident that SSBs negatively affect the *in vitro* sumoylation of PARP-1, two observations presented here suggest that the mechanisms underlying this phenomenon may not be as simple as a nick-induced change in the conformation of the polymerase.

Firstly, it still remains unclear why the nicks carried within the dumbbell substrate inhibited the plasmid-induced sumoylation of PARP-1's DBD at roughly stoichiometric ratios (**Figure 6.4**), while those present in the plasmid DNA afforded a higher inhibitory effect than expected, that is, about 50% even though the ratio of SSBs to DBD molecules present in the reaction was only 1:6. Since the full-length PARP-1 can impart considerable changes on the structure of DNA (Chasovskikh *et al.*, 2005), it is possible that when its DBD binds to SSBs within a plasmid it could alter the properties of the intact DNA flanking them enough to make it unable to stimulate sumoylation. In this way, a nick would inhibit the sumoylation of PARP-1's DBD not only by directly binding to it but also by prevent it from interacting with the intact DNA surrounding such SSBs. Alternatively, this phenomenon could be explained by assuming that PARP-1's DBD binds long intact DNA cooperatively (see 6.3.5.1) and that introducing nicks in it disrupts this mode of binding locally to the site of lesion. This situation could occur if PARP-1's DBD adopted different conformations when bound to different types of DNA, which in fact seems to be the case (Lilyestrom *et al.*, 2010). Conversely, the nicked dumbbell might have inhibited the sumoylation of PARP-1's DBD in a stoichiometric manner because these two molecules can form a 1:1 complex (Sebastian Eustermann, personal communication), which, in addition to being refractory to sumoylation, would also be distinct and independent from the plasmid and its ability to stimulate the modification of PARP-1's DBD.

Secondly, I observed that the nicked dumbbell could hinder the sumoylation of the full-length PARP-1 only when short DNA molecules were used to stimulate this modification event in the first place. As a matter of fact, it seems that DNA size can affect various other aspects of the *in vitro* sumoylation of PARP-1, which will be discussed in more detail below (see 6.3.5).

6.3.3 A role for the second zinc finger of PARP-1 in its sumoylation

The evidence that SSBs can inhibit PARP-1 sumoylation *in vitro* suggested that this phenomenon relied upon its second zinc finger motif because it directly recognizes this type of DNA lesion (Gradwohl *et al.*, 1990). Unfortunately I could not directly prove this hypothesis because mutating such a domain completely abrogated the ability of the intact dumbbell or a plasmid to stimulate the sumoylation of the full-length protein or its DBD alone, respectively (**Figure 6.4** and **Figure 6.8**). These stimulatory events had in fact to occur in the first place in order to detect the inhibitory effect that SSBs exert on PARP-1 sumoylation. That said, I believe that nicked DNA does indeed inhibit the modification of PARP-1 through its second zinc finger because such a type of DNA lesion hindered the plasmid-induced modification of a fragment of the polymerase encompassing just this domain (**Figure 6.4**). For lack of evidence proving otherwise, I cannot however categorically exclude that other domains of PARP-1 may also be involved in this process (see 6.3.4).

The fact that mutating the second zinc finger of PARP-1 abolished its ability to become sumoylated in the presence of intact DNA indicated that this finger motif must also be involved in recognizing intact DNA. This observation was interesting because such a domain had been generally viewed as a nick sensor. Yet, it was not completely unexpected provided that in at least one other instance, *i.e.* Ligase III, a PARP-type zinc finger that was thought to specifically bind nicked DNA was also found to bind intact DNA, albeit at relatively low salt concentrations (Cotner-Gohara *et al.*, 2008). Consistent with the idea that the second zinc finger of PARP-1 may also bind intact DNA, Ikejima *et al.* (1990) showed that deleting the DBD from this protein led to a significant weakening of the pervasive binding to intact DNA that the full-length polymerase demonstrated in their assays.

6.3.4 A role for other domains of PARP-1 in its sumoylation

Interestingly, except for its inability to be sumoylated in the presence of the intact dumbbell, or other short DNA molecules (**Figure 6.8** and **Figure 6.9**), the finger II mutant of the full-length PARP-1's behaved identically to the wild type protein in all of the presented assays. Instead, mutating such a domain in PARP-1's DBD completely abolished its plasmid-induced sumoylation (**Figure 6.5**). It therefore seems likely that in addition to the second zinc finger other motifs within the full-length PARP-1 must be involved in stimulating the sumoylation of this protein in the presence of DNA.

The fact that the roles of such unknown determinants in the modification of PARP-1 is detectable only on long DNA molecules suggests that only these DNA substrates provide enough surface for binding to such structures, probably together with the finger II motif. If this scenario were true, it would explain why the second zinc finger of PARP-1 played a role in its sumoylation only in the presence of very short DNA substrates. Since the enhancement of PARP-1 sumoylation afforded by the finger II domain of the polymerase appeared to be much less pronounced than that mediated through the unknown determinants, it is possible that the former event could have become detectable only when the latter was prevented. This situation could have happened if, for instance, the finger II motif of PARP-1, but not the other unknown determinants, were able to recognize the very short DNA substrates used to stimulate the modification of the polymerase. Such a hypothesis would predict that the second zinc finger of PARP-1 should be able to bind relatively short DNA substrates, like the dumbbell (18 bp), on its own without leaving too much unexposed DNA. In fact, it has been shown that, at least on nicked DNA, PARP-1 protects 7 bp pairs of DNA on both sides of a SSB, apparently through its second zinc finger (Gradwohl *et al.*, 1990; Le Cam *et al.*, 1994).

Although it is clear that the second zinc finger of PARP-1 plays a role in the DNA-dependent sumoylation of the polymerase, the identity of the other domains that are likely to be involved in such a modification event remains an open question. I will, however, propose two possibilities.

6.3.4.1 The first and third zinc fingers of PARP-1

The first scenario envisions that the first and third zinc fingers of PARP-1 could be the answer to the question mentioned above. I partly addressed this issue by examining the consequence of individually mutating these motifs on PARP-1 sumoylation.

As far as the first zinc finger was concerned, my attempt to inactive it by mutating one of its zinc-coordinating residues (C21) led to the heavy aggregation of the resulting mutant protein (data not shown), thus rendering it unusable. Although this finding was rather disappointing, it is an important one because it questions the validity of those functions that have been ascribed to the first zinc finger of PARP-1 by means of mutating its C21 residue (Hassa *et al.*, 2005; Mortusewicz *et al.*, 2007; Trucco *et al.*, 1996; Wacker *et al.*, 2007). The authors of these studies assumed that such a mutation specifically inactivated the first zinc finger of PARP-1, without affecting the overall integrity of the protein, which I have shown it is not the case. Despite these practical

limitations, the evidence that the DNA-stimulated sumoylation of PARP-1's DBD (finger I + finger II) was not significantly affected by deleting its finger I domain indicates that such a motif is not likely to be involved in this modification event (compare **Figure 6.3** with **Figure 6.5**).

The third zinc finger of PARP-1 is unique in comparison to its finger I and II motifs because it does not seem to bind DNA, at least on its own (Tao *et al.*, 2008), but instead it appears to relay the conformational changes that the DBD undergoes when it binds DNA to the catalytic domain, thereby activating it (Altmeyer *et al.*, 2009; Langelier *et al.*, 2010; Langelier *et al.*, 2008; Tao *et al.*, 2008). On the one side, this information argues against the possibility that the finger III motif of PARP-1 would be involved in stimulating its sumoylation, at least by directly recognizing DNA. On the other hand, it suggests that such a domain could have mediated the enhancement of modification that PARP-1 experiences in the presence of DNA at K486, which is located far away from the DBD. This scenario would be consistent with the evidence that some of the pervasive binding to intact DNA that PARP-1 exhibits in the assays reported by Ikejima *et al.* (1990) depends on features C-terminal to its first two finger domains. I however found that the sumoylation patterns of a PARP-1 mutant carrying an inactive finger III domain were essentially undistinguishable from those of the wild type protein (**Figure 6.10**), thus indicating that such a motif does not play a major role in this modification event.

The observations discussed above provide compelling evidence that neither the first nor the third zinc finger of PARP-1 play a major role in the DNA-stimulated sumoylation that this protein undergoes *in vitro*. This conclusion could be, however, somewhat flawed because it was reached by studying the consequences of inactivating such motifs individually. It has been shown that neighbouring zinc fingers, like those found in PARP-1, can collaborate with each other to bring about a common function, so that when only one of them is inactivated a specific phenotype may not be readily detectable (Green *et al.*, 1988). Although it is not known whether this phenomenon actually applies to PARP-1's zinc fingers, it is a possibility that would explain why individually mutating such motifs did not noticeably affect its sumoylation. Thus, it will be important to examine how inactivating combinations of such domains impinges on the modification of the polymerase. In order to carry out these experiments, it will be necessary to isolate mutations that specifically abolish the functions of PARP-1's zinc fingers without affecting their structures or that of the polymerase itself. One such type of mutant has already been identified for the finger II motif of PARP-1, and has been

used in this thesis, while another has been recently reported for the finger III domain (Langelier *et al.*, 2010).

6.3.4.2 Other domains of PARP-1

The second scenario envisages that domains of the full-length PARP-1 other than its finger I, II or III motifs may contribute to its DNA-dependent sumoylation. There is some evidence in favour of this hypothesis as it has been shown that a fragment of PARP-1 including its third zinc finger and AD domains can still bind DNA, although in a length-dependent manner. In addition fusing this polypeptide to the C-terminal portion of PARP-1 containing its WGR and catalytic domains increased its affinity for DNA (Thibodeau *et al.*, 1993). Interestingly, the WRG motif has been proposed to bind nucleic acids (Nagashima *et al.*, 2005).

6.3.5 The effects of DNA length on PARP-1 sumoylation

One of the most surprising features about the *in vitro* sumoylation of PARP-1 presented here was that it was affected by the length of the DNA molecules used as stimulating cofactors. Another was that the way in which DNA length affected the modification of the full-length PARP-1 and that of its DBD alone differed. At present I do not have a definitive answer to the questions of why or how these phenomena took place. I will nevertheless propose possible explanations on the basis of the presented data as well as published work.

6.3.5.1 The effects of DNA length on the stimulation of PARP-1 sumoylation

I observed that PARP-1's DBD was efficiently sumoylated only in the presence of very long DNA molecules (**Figure 6.3**). Since linear DNA duplexes were used to carry out this experiment, I decided to supplement each reaction with the same number of DNA molecules, regardless of their lengths. This is an important experimental detail because it ensured that all of the reactions contained the same number of free DNA ends. Conversely, if I used the same amount of DNA in each reaction, then they would have not only contained molecules of different lengths but also different amounts of DSBs. Since PARP-1's DBD recognizes such a type of break (Pion *et al.*, 2003), it follows that any phenotype observed under the latter experimental conditions could have been triggered by a change in either the number of DNA breaks or the length of the molecules present in the reactions, thus making it inconclusive. Keeping the number of DNA molecules constant in all reactions ensured that they carried the same number of

DSBs, yet, it also meant that the reactions supplemented with the longer DNA molecules contained a greater total amount of DNA than those containing the shorter DNA duplexes. It is therefore possible that PARP-1's DBD might have been preferentially sumoylated in the reactions supplemented with the longer DNA substrates simply because they contained more DNA. This option seems, however, very unlikely because the sumoylation of PARP-1's DBD was not enhanced the least in the presence of an amount of intact dumbbell that in the case of a plasmid would greatly stimulate it (data not shown). Thus, in order to substantiate these speculations it will be useful to show that PARP-1's DBD is also preferentially modified in sumoylation reactions supplemented with the same amount of increasingly long DNA substrates whose ends have been occluded, for instance, with streptavidin.

Should these experiments confirm that PARP-1's DBD indeed requires long DNA molecules to be efficiently sumoylated, they would not, however, answer the question of why such a phenomenon occured. This is an important issue because the fact that long stretches of naked DNA do not probably exist *in vivo* would question the physiological validity of this observation. I believe that PARP-1's DBD required long DNA duplexes to be proficiently sumoylated simply because it was a sub-optimal substrate for this type of modification event. It is in fact possible that such a domain, being only a small portion of the full-length PARP-1, lacked structures important for allowing it to be sumoylated in the presence of more biologically relevant DNA cofactors (see 6.3.4). Consistently, I found that the full-length PARP-1 was efficiently modified also in the presence of short DNA duplexes (15 bp dsDNA and intact dumbbell, **Figure 6.8** and **Figure 6.9**).

If it was indeed specific motifs within the full-length PARP-1 that enabled this protein, as opposed to its DBD alone, to be sumoylated in the presence of short DNA molecules, how did such structures bring about this difference? Two likely scenarios can be envisioned. Firstly, it is possible that the second zinc finger of PARP-1 may actually require the help of these unknown determinants to efficiently promote sumoylation. Consequently, in their absence, *i.e.* as in PARP-1's DBD, the sumoylation-potential of such a finger could have been reduced to such an extent that it made it necessary to use very long DNA molecule to promote its modification. This hypothesis is consistent with the evidence that although both the full-length PARP-1 and its DBD alone contained the finger II motif, only in the context of the former protein was this domain able/necessary to stimulate sumoylation in the presence of short DNA molecules (**Figure 6.5** and **Figure 6.8**). Secondly, it is possible that PARP-1 may need

to dimerize on DNA and/or cooperatively bind to it to be efficiently sumoylated, and that these molecular events preferentially occur in the context of the full-length PARP-1. It has in fact been reported for at least three targets of sumoylation that dimerization is an essential pre-requisite for their modification (Kim *et al.*, 2005; Kirsh *et al.*, 2002; Mascle *et al.*, 2007). There is also some evidence in favour of PARP-1 being able to dimerize specifically on DNA (Altmeyer *et al.*, 2009; Mendoza-Alvarez and Alvarez-Gonzalez, 1993; Pion *et al.*, 2003; Pion *et al.*, 2005). The catalytic domain of PARP-1 alone can also form dimers in a DNA-independent manner (Mendoza-Alvarez and Alvarez-Gonzalez, 2004). Finally, PARP-1 has also been proposed to bind DNA cooperatively, yet, this property has not been observed in all studies (Lilyestrom *et al.*, 2010; Pion *et al.*, 2003; Pion *et al.*, 2005).

6.3.5.2 The effects of DNA length on the inhibition of PARP-1 sumoylation

The inhibitory activity that SSBs had on the sumoylation of the full-length PARP-1 could only be detected when this modification event was stimulated by a short DNA substrate (15 bp dsDNA or the intact dumbbell, **Figure 6.8** and **Figure 6.9**), but not a longer one (61 bp dsDNA or plasmid, **Figure 6.9**). This observation is strikingly similar to how inactivating the second finger of the polymerase abolished its DNA-dependent sumoylation only on a minimal DNA substrate. Earlier, I proposed that the latter of these two phenomena occurred probably because in the presence of short DNA duplexes the DNA-stimulated sumoylation of PARP-1 is exclusively dependent on the activity of its second zinc finger, while on longer duplexes other motifs may come into play. A similar model could have explained a partial reduction in the ability of nicked DNA to inhibit the PARP-1 sumoylation stimulated by short *vs.* long DNA substrates; yet, a complete loss of this ability is much harder to rationalize. At present, I cannot propose any hypothetical, yet realistic, explanations for this phenomenon because I was unable to study in more detail the interplay between PARP-1 and DNA. This process remains in fact to date poorly understood. Once its underlying properties are uncovered, examining how they impinge on the DNA-dependent sumoylation of PARP-1 should shed light on the causes of the observations described above.

6.3.6 The effects of free DNA ends on PARP-1 sumoylation

The data reported in **Figure 6.8** and **Figure 6.9** indicated that the intact dumbbell stimulated the sumoylation of the full-length PARP-1 less efficiently than a DNA

substrate of equivalent length but bearing free ends (15 bp dsDNA). The simplest explanation for this phenomenon is that the enhancement of PARP-1 sumoylation afforded by intact DNA is further increased in the presence of DSBs. PARP-1 directly binds to this type of DNA lesion, thus in their presence the polymerase may adopt a conformation that makes it an even better substrate for sumoylation than that it acquires when it is bound to intact DNA. That said, I cannot find a reason for why the modification of PARP-1's DBD, unlike that of the full-length protein, was not stimulated by DSBs, given that both proteins can recognize DSBs (Ikejima *et al.*, 1990; Lilyestrom *et al.*, 2010). Such a discrepancy could be potentially explained by the same models I proposed earlier to rationalize the other differences in sumoylation behaviour between the full-length PARP-1 and its DBD alone (see 6.3.4 and 6.3.5).

Since DSBs seemed to enhance the sumoylation of the full-length PARP-1 *in vitro*, I would have expected them to be able to trigger a similar effect *in vivo*. On the contrary, the levels of sumoylated PARP-1 did not significantly change when this kind of DNA lesion was introduced in cells by exposing them to γ-rays (**Figure 5.2**). This phenomenon is reminiscent of how nicked DNA inhibited PARP-1 sumoylation *in vitro* but did not apparently do so *in vivo*. It is therefore reasonable to propose that both phenomena could have been underlain by the same molecular mechanisms, which I discussed in 6.3.1.

In the future, in order to undoubtedly prove that DSBs do indeed stimulate the sumoylation of the full-length PARP-1, it will be necessary to show that occluding the ends of linear DNA molecules with streptavidin reduces the ability of these DNA substrates to stimulate the modification of the polymerase. A partial, but not complete, loss of such stimulatory effect would also further corroborate the conclusion that PARP-1 sumoylation is also triggered by intact DNA. A positive finding from these experiments would open new research avenues; yet, it would also add an extra layer of complexity to a biological process, the interplay between PARP-1 sumoylation and DNA, that is already quite complex. In particular, such a finding would make it quite challenging to explain why both intact DNA and a DSBs can stimulate PARP-1 sumoylation, while another form of DNA damage, *i.e.* SSBs, would inhibit it. I will present a tentative model to rationalize all these events in Chapter 7.

Chapter 7. Conclusions and future directions

The work presented in this thesis aimed at uncovering mechanisms by which sumoylation interplays with DNA to regulate processes important for DNA metabolism, in the hope to ultimately provide insight on how SUMO helps maintaining genome stability.

Provided that when I started working on this project only a few proteins with a role in DNA metabolism had been shown to be sumoylated, I initially used frog egg extracts, mass spectrometry and western blotting to systematically identify proteins conjugated to SUMO that associated with chromatin during unperturbed or disrupted DNA replication (Chapter 3), because under these conditions such cellular fraction should be enriched for factors with a role in DNA metabolism. This analysis, in fact, identified only a few hypothetical SUMO substrates that did not have DNA-related roles, while the majority were involved in DNA replication, repair and recombination as well as chromatin remodelling and gene transcription. It also indicated that SUMO2-modified species were probably more abundant than those conjugated to SUMO1, at least on replicating frog sperm chromatin, and that their abundance was not affected by DNA damage but required progression through S phase. Amongst the new targets of sumoylation I identified, the modification of a few of them was confirmed by western blotting in *Xenopus* egg extracts, and it was also shown to occur for the corresponding orthologous proteins in *S. cerevisiae*. The observation that some of the sumoylation events reported here are conserved in yeast and frogs, and possibly also in human cells (Golebiowski *et al.*, 2009), puts forward the possibility that they play evolutionarily conserved, and therefore possibly important, roles. Since many of them concern proteins that are involved in the maintenance of genome stability and Helle Ulrich is interested in understanding how sumoylation impinges on this biological process, she is keen on exploring further their possible functions.

Amongst the conserved targets of sumoylation that I identified in the screen described in Chapter 3, I investigated in more detail the modification of the largest subunit of the six-membered origin recognition complex, ORC1 (Chapter 4). In *S. cerevisiae*, I found that all of the six subunits of this complex were sumoylated in a Siz1- and Siz2-dependent manner. Golebiowski *et al.* (2009) also recently showed that ORC is sumoylated in human cells, hence indicating that this modification event is probably evolutionary conserved in all eukaryotes. In frog egg extracts, the sumoylation of ORC1 appeared to occur specifically on chromatin, yet the modification of a recombinant

yeast ORC was not significantly affected by origin DNA *in vitro*, which suggests that other determinants may be involved in this phenomenon. In both *Xenopus* egg extracts and yeast cells, ORC sumoylation seemed to disappear following the initiation of DNA replication, until the start of the G_2 phase. This observation suggested that such a modification event probably played a role during S phase, which would have been consistent with the recognized functions of ORC. That said, I found that altering the general levels of sumoylation in both experimental systems did not appreciably affect the efficiency of DNA replication, hence implying that SUMO does not significantly affect the essential roles of ORC in such a process. It has been proposed for other protein complexes in which all or most of their components are sumoylated that these modification events may work as a molecular glue during their biogenesis or to keep the complexes together (Matunis *et al.*, 2006). This is unlikely to be the case for the sumoylation of ORC because this complex can be recombinantly produced in a variety of different systems, apparently in the absence of SUMO. Although the ways in which sumoylation impinges on the properties of ORC remain unknown, it is likely that, if this modification event actually has a role, it probably concerns a function that this complex performs as a whole, rather than one that is specifically carried out by ORC sub-complexes or even by some of its subunits on their own. Thus, in order to gain insight in the roles of ORC sumoylation it will be necessary to create, and study the phenotypes of, an unsumoylatable mutant of the complex. Since this task may not be technically or biologically feasible at present, an alternative could be to study the consequences of hyper-sumoylating ORC *in vivo* by UBC9 fusion-dependent sumoylation (UFDS, Niedenthal, 2009) and/or how sumoylating ORC *in vitro* affects its roles in pre-replication complex formation, which has been recently reconstituted in a test-tube (Remus *et al.*, 2009).

Having appreciated that exploring the functions of ORC sumoylation was probably too challenging of a project for the tools I had available, I decided to focus my attention to the modification of another protein that was identified in Chapter 3, *i.e.* PARP-1. Not only was this protein known to play important roles in DNA metabolism but also preliminary data indicated that a digested plasmid could stimulate the sumoylation of its DBD. Further analysis revealed that the modification of PARP-1's DBD 1) was not affected by whether a plasmid contained DSBs or specific DNA sequences, was supercoiled or methylated but 2) it instead occurred in the presence of DNA molecules that carried a relatively long stretch of intact DNA and 3) in a manner that depended on the second zinc finger of this protein being functional (Chapter 6). The sumoylation of

the full-length PARP-1 was also stimulated by an intact plasmid; yet, DNA molecules of minimal length could trigger this modification phenomenon as well. It is therefore possible that PARP-1's DBD was efficiently sumoylated only in the presence of long DNA molecules because it lacked features, instead present in the full-length PARP-1, which should have allowed it to recognize short DNA substrates. The participation of at least two regions within the full-length PARP-1 in its DNA-dependent sumoylation, *i.e.* the second zinc finger and other unknown determinants, could also explain why inactivating the former one of these two domains abolished the modification of the full-length polymerase only by DNA substrates of minimal length, but not longer ones. These results have two important implications for the PARP-1 field. Firstly, not only do they imply that PARP-1 can recognize intact B-form DNA, which is an event that remains poorly understood and rather controversial (see 1.5.2), but they also assign a functional consequence to it, that is, the stimulation of PARP-1 sumoylation. Secondly, these results imply that the polymerase recognizes intact DNA, at least partly, through its second zinc finger, which is a domain that has been generally considered as a DNA nick sensor (see 1.5) That said, the ability of such a domain to recognize nicked DNA probably underlies the ability of SSBs to inhibit PARP-1 sumoylation. It therefore appears that DNA structures that normally trigger the catalytic activity of PARP-1, *e.g.* DNA nicks, inhibit its sumoylation, while those that normally activate the polymerase, *e.g.* intact DNA, actually stimulate its conjugation to SUMO.

In order to place the rather mechanistic results described above in a more functional context, after having identified PARP-1 as a preferential target of SUMO3 and mapped its two main modification sites (K203 and K486), I investigated the possible roles of PARP-1 sumoylation *in vivo* (Chapter 5). Towards this end I used an unsumoylatable PARP-1 mutant, an *in vitro* sumoylated PARP-1 and/or PARP-1-SUMO fusion, to mimic a constitutively sumoylated polymerase. I found that SUMO did not affect PARP-1's catalytic activity, localization, association with intact chromatin or binding to nicked DNA. Conversely, mutating the sumoylation sites of the polymerase increased PARP-1's half-life in a proteasome-dependent manner under normal growth conditions, hence indicating that SUMO probably targets PARP-1 for proteasomal degradation. This process is likely to occur through a poly-sumoylation-triggered poly-ubiquitylation event because the PARP-1-SUMO fusions were found to be specifically poly-sumoylated under normal growth conditions, as was the endogenous PARP-1 following specific environmental signals. In addition, both types of sumoylated proteins were converted into high molecular weight ubiquitylated species upon proteasomal inhibition. At

present, I cannot however explain why even though the PARP-1-SUMO constructs were poly-sumoylated and poly-ubiquitylated, they apparently were as stable as the unsumoylatable PARP-1 mutant.

These observations are consistent with the results that have been meanwhile reported by Martin *et al.* (2009), which suggest that PARP-1 could be a substrate of the SUMO-targeted ubiquitin ligase RNF4. They proposed that RNF4 could mediate the degradation of the poly-sumoylated PARP-1 that is produced upon heat shock, hence allowing its removal from the *HSP70.1* promoter under such stressful conditions (Martin *et al.*, 2009). This phenomenon is likely to be linked to the activation of the *HSP70.1* gene itself because an unsumoylatable PARP-1 mutant failed to trigger the expression of such a gene following heat shock as well as the wild type protein (Martin *et al.*, 2009). A role for PARP-1 sumoylation in controlling transcription is, however, unlikely to be specific for heat shock and heat shock-responsive genes because I found that other environmental cues, which like heat shock can boost the general levels of sumoylation in a cell, also up-regulated the modification of PARP-1. Additionally, the modification of PARP-1 also affects the activation of hypoxia-responsive genes after hypoxia, which can enhance general sumoylation levels as well (Messner *et al.*, 2009).

In the light of the results described above and the current knowledge concerning sumoylation and PARP-1, I will put forward a tentative model for how the modification of the polymerase could work (**Figure 7.1**). I propose that sumoylation is used as a means of differentially labelling two functionally-distinct populations of PARP-1. The first one is engaged in DNA repair, *e.g.* PARP-1 bound to nicked DNA, and therefore should not be sumoylated and degraded because this could compromise cell survival. The other population is involved in some other aspect of PARP-1 biology, such as transcription regulation, where the removal of the polymerase from certain regions of intact DNA, through sumoylation and subsequent degradation, may be important to trigger specific downstream events. This phenomenon must occur under normal growth conditions because inhibiting the sumoylation of PARP-1 affects its stability even under undisturbed growth (Chapter 5). PARP-1 could instead be removed from specific genomic regions under particular conditions by the increased sumoylation it undergoes in response to certain environmental signals, possibly also in cooperation with its DNA-stimulated modification.

An issue that has been puzzling scientists working on PARP-1 is how this protein can function in both DNA sensing/repair and transcription regulation. More and more

evidence suggests that this functional duality probably depends on PARP-1's ability to control chromatin structure, yet, how this dichotomy is controlled remains unclear. The model described above suggests that sumoylation may be involved in this process. Such a model is however clearly incomplete because, for instance, it would not be able to explain the likely stimulatory role of DSBs on PARP-1 sumoylation (Chapter 6). Thus further work will be necessary to fine-tune it. Firstly, it will be important to show that PARP-1 bound to nicked DNA cannot be not sumoylated *in vivo* because this result will confirm that 1) sumoylation is used to differentiate between two populations of the polymerase and 2) SSBs are inhibitory to PARP-1 sumoylation also in a cell. Being able to capture PARP-1 molecules that are associated with a DNA nick is technically challenging *in vivo* because this enzyme turns over DNA breaks extremely quickly. I reasoned, however, that since PARP-1 is the main acceptor of PAR in a cell and SSBs induce its auto-modification, then sumoylated PARP-1 should not be parylated, if the polymerase bound to nicked DNA cannot be sumoylated. All my attempts to determine whether this prediction were true were unfortunately hindered by the fact that I could never reliably detect PARP-1 auto-parylation following DNA damage, in the cells I employed. These experiments are now being trialled by our collaborator Jacob Seeler. Secondly, it will be useful to confirm that sumoylation plays a more general role in clearing promoters, or possibly other DNA regions, from PARP-1 under normal growth conditions and/or specifically in response to environmental cues. This issue could be addressed by comparing the distribution of PARP-1 along the entire genome between cells that produce wild type PARP-1, an unsumoylatable PARP-1 mutant or the PARP-1-SUMO fusions, during unperturbed growth and in response to specific stimuli. These results could be then used to explore how sumoylation-dependent changes in the occupancy by PARP-1 of a specific DNA region impinges on the expression of the relevant genes, if such a region corresponds to a promoter, or other biological processes, if it corresponds to other functional DNA sequence, *e.g.* centromeres, telomeres, introns *vs.* exons *etc.*

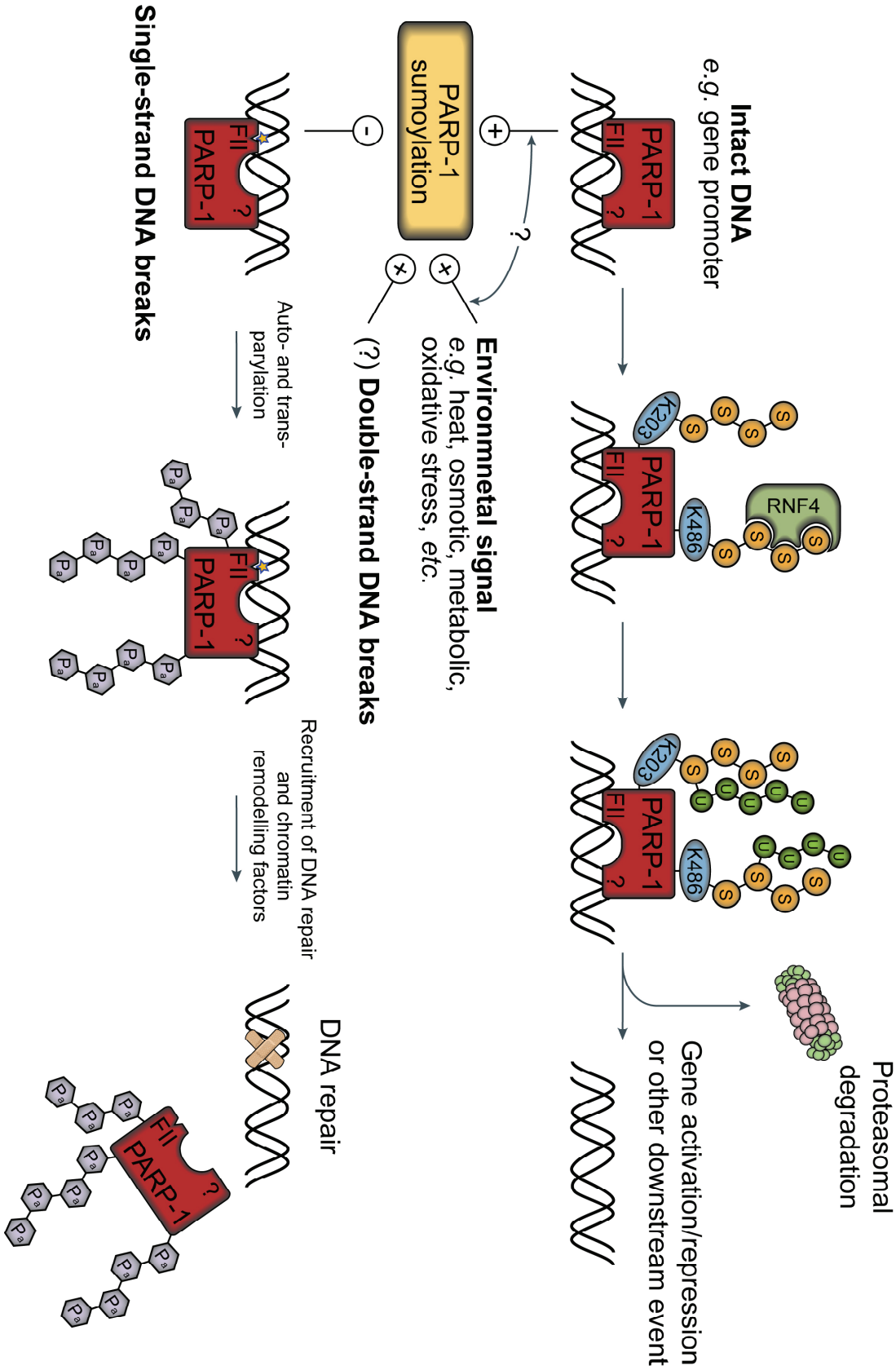

Figure 7.1 - A possible model for how the sumoylation of PARP-1 could function. See main text for details. FII = PARP-1's second zinc finger, ? = unanswered questions, P_a = PAR, S = SUMO, U = ubiquitin.

References

Agostinho, M., Santos, V., Ferreira, F., Costa, R., Cardoso, J., Pinheiro, I., Rino, J., Jaffray, E., Hay, R.T., and Ferreira, J. (2008). Conjugation of human topoisomerase 2α with small ubiquitin-like modifiers 2/3 in response to topoisomerase inhibitors: cell cycle stage and chromosome domain specificity. Cancer Res *68*, 2409-2418.

Aguiar, R.C., Takeyama, K., He, C., Kreinbrink, K., and Shipp, M.A. (2005). B-aggressive lymphoma family proteins have unique domains that modulate transcription and exhibit poly(ADP-ribose) polymerase activity. J Biol Chem *280*, 33756-33765.

Aguiar, R.C., Yakushijin, Y., Kharbanda, S., Salgia, R., Fletcher, J.A., and Shipp, M.A. (2000). BAL is a novel risk-related gene in diffuse large B-cell lymphomas that enhances cellular migration. Blood *96*, 4328-4334.

Ahel, D., Horejsi, Z., Wiechens, N., Polo, S.E., Garcia-Wilson, E., Ahel, I., Flynn, H., Skehel, M., West, S.C., Jackson, S.P.*, et al.* (2009). Poly(ADP-ribose)-dependent regulation of DNA repair by the chromatin remodeling enzyme ALC1. Science *325*, 1240-1243.

Ahel, I., Ahel, D., Matsusaka, T., Clark, A.J., Pines, J., Boulton, S.J., and West, S.C. (2008). Poly(ADP-ribose)-binding zinc finger motifs in DNA repair/checkpoint proteins. Nature *451*, 81-85.

Akiyama, T., Takasawa, S., Nata, K., Kobayashi, S., Abe, M., Shervani, N.J., Ikeda, T., Nakagawa, K., Unno, M., Matsuno, S.*, et al.* (2001). Activation of Reg gene, a gene for insulin-producing β-cell regeneration: poly(ADP-ribose) polymerase binds Reg promoter and regulates the transcription by autopoly(ADP-ribosyl)ation. Proc Natl Acad Sci USA *98*, 48-53.

Alano, C.C., Ying, W., and Swanson, R.A. (2004). Poly(ADP-ribose) polymerase-1-mediated cell death in astrocytes requires NAD^+ depletion and mitochondrial permeability transition. J Biol Chem *279*, 18895-18902.

Albers, M., Kranz, H., Kober, I., Kaiser, C., Klink, M., Suckow, J., Kern, R., and Koegl, M. (2005). Automated yeast two-hybrid screening for nuclear receptor-interacting proteins. Mol Cell Proteomics *4*, 205-213.

Allinson, S.L., Dianova, II, and Dianov, G.L. (2003). Poly(ADP-ribose) polymerase in base excision repair: always engaged, but not essential for DNA damage processing. Acta Biochim Pol *50*, 169-179.

Altmeyer, M., Messner, S., Hassa, P.O., Fey, M., and Hottiger, M.O. (2009). Molecular mechanism of poly(ADP-ribosyl)ation by PARP1 and identification of lysine residues as ADP-ribose acceptor sites. Nucleic Acids Res *37*, 3723-3738.

Alvarez-Gonzalez, R., and Althaus, F.R. (1989). Poly(ADP-ribose) catabolism in mammalian cells exposed to DNA-damaging agents. Mutat Res *218*, 67-74.

Alvarez-Gonzalez, R., and Jacobson, M.K. (1987). Characterization of polymers of adenosine diphosphate ribose generated *in vitro* and *in vivo*. Biochemistry *26*, 3218-3224.

Alvarez-Gonzalez, R., and Mendoza-Alvarez, H. (1995). Dissection of ADP-ribose polymer synthesis into individual steps of initiation, elongation, and branching. Biochimie *77*, 403-407.

Alvarez-Gonzalez, R., Pacheco-Rodriguez, G., and Mendoza-Alvarez, H. (1994). Enzymology of ADP-ribose polymer synthesis. Mol Cell Biochem *138*, 33-37.

Ambrose, H.E., Papadopoulou, V., Beswick, R.W., and Wagner, S.D. (2007). Poly-(ADP-ribose) polymerase-1 (Parp-1) binds in a sequence-specific manner at the Bcl-6 locus and contributes to the regulation of Bcl-6 transcription. Oncogene *26*, 6244-6252.

Ame, J.C., Fouquerel, E., Gauthier, L.R., Biard, D., Boussin, F.D., Dantzer, F., de Murcia, G., and Schreiber, V. (2009). Radiation-induced mitotic catastrophe in PARG-deficient cells. J Cell Sci *122*, 1990-2002.

Ame, J.C., Rolli, V., Schreiber, V., Niedergang, C., Apiou, F., Decker, P., Muller, S., Hoger, T., Menissier-de Murcia, J., and de Murcia, G. (1999). PARP-2, A novel mammalian DNA damage-dependent poly(ADP-ribose) polymerase. J Biol Chem *274*, 17860-17868.

Ame, J.C., Spenlehauer, C., and de Murcia, G. (2004). The PARP superfamily. Bioessays *26*, 882-893.

Amiri, K.I., Ha, H.C., Smulson, M.E., and Richmond, A. (2006). Differential regulation of CXC ligand 1 transcription in melanoma cell lines by poly(ADP-ribose) polymerase-1. Oncogene *25*, 7714-7722.

Andrews, E.A., Palecek, J., Sergeant, J., Taylor, E., Lehmann, A.R., and Watts, F.Z. (2005). Nse2, a component of the Smc5-6 complex, is a SUMO ligase required for the response to DNA damage. Mol Cell Biol *25*, 185-196.

Arakawa, H., Moldovan, G.L., Saribasak, H., Saribasak, N.N., Jentsch, S., and Buerstedde, J.M. (2006). A role for PCNA ubiquitination in immunoglobulin hypermutation. PLoS Biol *4*, e366.

Arito, M., Horiba, T., Hachimura, S., Inoue, J., and Sato, R. (2008). Growth factor-induced phosphorylation of sterol regulatory element-binding proteins inhibits sumoylation, thereby stimulating the expression of their target genes, low density lipoprotein uptake, and lipid synthesis. J Biol Chem *283*, 15224-15231.

Ariumi, Y., Masutani, M., Copeland, T.D., Mimori, T., Sugimura, T., Shimotohno, K., Ueda, K., Hatanaka, M., and Noda, M. (1999). Suppression of the poly(ADP-ribose) polymerase activity by DNA-dependent protein kinase *in vitro*. Oncogene *18*, 4616-4625.

Atorino, L., Di Meglio, S., Farina, B., Jones, R., and Quesada, P. (2001). Rat germinal cells require PARP for repair of DNA damage induced by gamma-irradiation and H_2O_2 treatment. Eur J Cell Biol *80*, 222-229.

Audebert, M., Salles, B., and Calsou, P. (2004). Involvement of poly(ADP-ribose) polymerase-1 and XRCC1/DNA ligase III in an alternative route for DNA double-strand breaks rejoining. J Biol Chem *279*, 55117-55126.

Audebert, M., Salles, B., Weinfeld, M., and Calsou, P. (2006). Involvement of polynucleotide kinase in a poly(ADP-ribose) polymerase-1-dependent DNA double-strand breaks rejoining pathway. J Mol Biol *356*, 257-265.

Augustin, A., Spenlehauer, C., Dumond, H., Menissier-De Murcia, J., Piel, M., Schmit, A.C., Apiou, F., Vonesch, J.L., Kock, M., Bornens, M.*, et al.* (2003). PARP-3 localizes preferentially to the daughter centriole and interferes with the G_1/S cell cycle progression. J Cell Sci *116*, 1551-1562.

Azuma, Y., Arnaoutov, A., Anan, T., and Dasso, M. (2005). PIASy mediates SUMO-2 conjugation of Topoisomerase-II on mitotic chromosomes. EMBO J *24*, 2172-2182.

Azuma, Y., Arnaoutov, A., and Dasso, M. (2003). SUMO-2/3 regulates topoisomerase II in mitosis. J Cell Biol *163*, 477-487.

Baba, D., Maita, N., Jee, J.G., Uchimura, Y., Saitoh, H., Sugasawa, K., Hanaoka, F., Tochio, H., Hiroaki, H., and Shirakawa, M. (2005). Crystal structure of thymine DNA glycosylase conjugated to SUMO-1. Nature *435*, 979-982.

Baba, D., Maita, N., Jee, J.G., Uchimura, Y., Saitoh, H., Sugasawa, K., Hanaoka, F., Tochio, H., Hiroaki, H., and Shirakawa, M. (2006). Crystal structure of SUMO-3-modified thymine-DNA glycosylase. J Mol Biol *359*, 137-147.

Babic, I., Cherry, E., and Fujita, D.J. (2006). SUMO modification of Sam68 enhances its ability to repress cyclin D1 expression and inhibits its ability to induce apoptosis. Oncogene *25*, 4955-4964.

Bachant, J., Alcasabas, A., Blat, Y., Kleckner, N., and Elledge, S.J. (2002). The SUMO-1 isopeptidase Smt4 is linked to centromeric cohesion through SUMO-1 modification of DNA topoisomerase II. Mol Cell *9*, 1169-1182.

Bailey, D., and O'Hare, P. (2004). Characterization of the localization and proteolytic activity of the SUMO-specific protease, SENP1. J Biol Chem *279*, 692-703.

Bailey, D., and O'Hare, P. (2005). Comparison of the SUMO1 and ubiquitin conjugation pathways during the inhibition of proteasome activity with evidence of SUMO1 recycling. Biochem J *392*, 271-281.

Barnes, D.E., and Lindahl, T. (2004). Repair and genetic consequences of endogenous DNA base damage in mammalian cells. Annu Rev Genet *38*, 445-476.

Bauer, P.I., Kenesi, E., Mendeleyev, J., and Kun, E. (2005). The influence of ATP on poly(ADP-ribose) metabolism. Int J Mol Med *16*, 321-324.

Bell, S.P., Kobayashi, R., and Stillman, B. (1993). Yeast origin recognition complex functions in transcription silencing and DNA replication. Science *262*, 1844-1849.

Bell, S.P., and Stillman, B. (1992). ATP-dependent recognition of eukaryotic origins of DNA replication by a multiprotein complex. Nature *357*, 128-134.

Benjamin, R.C., and Gill, D.M. (1980). Poly(ADP-ribose) synthesis *in vitro* programmed by damaged DNA. A comparison of DNA molecules containing different types of strand breaks. J Biol Chem *255*, 10502-10508.

Berger, N.A. (1985). Poly(ADP-ribose) in the cellular response to DNA damage. Radiat Res *101*, 4-15.

Berger, N.A., Sims, J.L., Catino, D.M., and Berger, S.J. (1983). Poly(ADP-ribose) polymerase mediates the suicide response to massive DNA damage: studies in normal and DNA-repair defective cells. Princess Takamatsu Symp *13*, 219-226.

Bergink, S., and Jentsch, S. (2009). Principles of ubiquitin and SUMO modifications in DNA repair. Nature *458*, 461-467.

Bernier-Villamor, V., Sampson, D.A., Matunis, M.J., and Lima, C.D. (2002). Structural basis for E2-mediated SUMO conjugation revealed by a complex between ubiquitin-conjugating enzyme Ubc9 and RanGAP1. Cell *108*, 345-356.

Betting, J., and Seufert, W. (1996). A yeast Ubc9 mutant protein with temperature-sensitive *in vivo* function is subject to conditional proteolysis by a ubiquitin- and proteasome-dependent pathway. J Biol Chem *271*, 25790-25796.

Blomster, H.A., Hietakangas, V., Wu, J., Kouvonen, P., Hautaniemi, S., and Sistonen, L. (2009). Novel proteomics strategy brings insight into the prevalence of SUMO-2 target sites. Mol Cell Proteomics *8*, 1382-1390.

Blomster, H.A., Imanishi, S.Y., Siimes, J., Kastu, J., Morrice, N.A., Eriksson, J.E., and Sistonen, L. (2010). *In vivo* identification of sumoylation sites by a signature tag and cysteine-targeted affinity purification. J Biol Chem *285*, 19324-19329.

Blow, J.J. (1996). Chromosome replication in *Xenopus* egg extracts. In Eukaryotic DNA Replication, J.J. Blow, ed. (IRL Press), pp. 143-159.

Blow, J.J., and Dutta, A. (2005). Preventing re-replication of chromosomal DNA. Nat Rev Mol Cell Biol *6*, 476-486.

Blow, J.J., and Laskey, R.A. (1986). Initiation of DNA replication in nuclei and purified DNA by a cell-free extract of *Xenopus* eggs. Cell *47*, 577-587.

Bohren, K.M., Nadkarni, V., Song, J.H., Gabbay, K.H., and Owerbach, D. (2004). A M55V polymorphism in a novel SUMO gene (SUMO-4) differentially activates heat shock transcription factors and is associated with susceptibility to type I diabetes mellitus. J Biol Chem *279*, 27233-27238.

Bossis, G., and Melchior, F. (2006). Regulation of SUMOylation by reversible oxidation of SUMO conjugating enzymes. Mol Cell *21*, 349-357.

Boulton, S., Pemberton, L.C., Porteous, J.K., Curtin, N.J., Griffin, R.J., Golding, B.T., and Durkacz, B.W. (1995). Potentiation of temozolomide-induced cytotoxicity: a comparative study of the biological effects of poly(ADP-ribose) polymerase inhibitors. Br J Cancer *72*, 849-856.

Bowman, K.J., White, A., Golding, B.T., Griffin, R.J., and Curtin, N.J. (1998). Potentiation of anti-cancer agent cytotoxicity by the potent poly(ADP-ribose) polymerase inhibitors NU1025 and NU1064. Br J Cancer *78*, 1269-1277.

Bradford, M.M. (1976). A rapid and sensitive method for the quantitation of microgram quantities of protein utilizing the principle of protein-dye binding. Anal Biochem *72*, 248-254.

Branzei, D., Sollier, J., Liberi, G., Zhao, X., Maeda, D., Seki, M., Enomoto, T., Ohta, K., and Foiani, M. (2006). Ubc9- and mms21-mediated sumoylation counteracts recombinogenic events at damaged replication forks. Cell *127*, 509-522.

Braun, S.A., Panzeter, P.L., Collinge, M.A., and Althaus, F.R. (1994). Endoglycosidic cleavage of branched polymers by poly(ADP-ribose) glycohydrolase. Eur J Biochem *220*, 369-375.

Brem, R., and Hall, J. (2005). XRCC1 is required for DNA single-strand break repair in human cells. Nucleic Acids Res *33*, 2512-2520.

Brochu, G., Duchaine, C., Thibeault, L., Lagueux, J., Shah, G.M., and Poirier, G.G. (1994). Mode of action of poly(ADP-ribose) glycohydrolase. Biochim Biophys Acta *1219*, 342-350.

Bryant, H.E., and Helleday, T. (2006). Inhibition of poly (ADP-ribose) polymerase activates ATM which is required for subsequent homologous recombination repair. Nucleic Acids Res *34*, 1685-1691.

Bryant, H.E., Schultz, N., Thomas, H.D., Parker, K.M., Flower, D., Lopez, E., Kyle, S., Meuth, M., Curtin, N.J., and Helleday, T. (2005). Specific killing of BRCA2-deficient tumours with inhibitors of poly(ADP-ribose) polymerase. Nature *434*, 913-917.

Buki, K.G., Bauer, P.I., Hakam, A., and Kun, E. (1995). Identification of domains of poly(ADP-ribose) polymerase for protein binding and self-association. J Biol Chem *270*, 3370-3377.

Burgess, R.C., Rahman, S., Lisby, M., Rothstein, R., and Zhao, X. (2007). The Slx5-Slx8 complex affects sumoylation of DNA repair proteins and negatively regulates recombination. Mol Cell Biol *27*, 6153-6162.

Burzio, L.O., Riquelme, P.T., and Koide, S.S. (1979). ADP-ribosylation of rat liver nucleosomal core histones. J Biol Chem *254*, 3029-3037.

Busso, D., Delagoutte-Busso, B., and Moras, D. (2005). Construction of a set Gateway-based destination vectors for high-throughput cloning and expression screening in Escherichia coli. Anal Biochem *343*, 313-321.

Butler, A.J., and Ordahl, C.P. (1999). Poly(ADP-ribose) polymerase binds with transcription enhancer factor 1 to MCAT1 elements to regulate muscle-specific transcription. Mol Cell Biol *19*, 296-306.

Bylebyl, G.R., Belichenko, I., and Johnson, E.S. (2003). The SUMO isopeptidase Ulp2 prevents accumulation of SUMO chains in yeast. J Biol Chem *278*, 44113-44120.

Caiafa, P., Guastafierro, T., and Zampieri, M. (2009). Epigenetics: poly(ADP-ribosyl)ation of PARP-1 regulates genomic methylation patterns. FASEB J *23*, 672-678.

Cande, C., Vahsen, N., Kouranti, I., Schmitt, E., Daugas, E., Spahr, C., Luban, J., Kroemer, R.T., Giordanetto, F., Garrido, C*., et al.* (2004). AIF and cyclophilin A cooperate in apoptosis-associated chromatinolysis. Oncogene *23*, 1514-1521.

Capili, A.D., and Lima, C.D. (2007). Structure and analysis of a complex between SUMO and Ubc9 illustrates features of a conserved E2-Ubl interaction. J Mol Biol *369*, 608-618.

Carbia-Nagashima, A., Gerez, J., Perez-Castro, C., Paez-Pereda, M., Silberstein, S., Stalla, G.K., Holsboer, F., and Arzt, E. (2007). RSUME, a small RWD-containing protein, enhances SUMO conjugation and stabilizes HIF-1α during hypoxia. Cell *131*, 309-323.

Carter, S., and Vousden, K.H. (2008). p53-Ubl fusions as models of ubiquitination, sumoylation and neddylation of p53. Cell Cycle *7*, 2519-2528.

Cayuela, M.L., Carrillo, A., Ramirez, P., Parrilla, P., and Yelamos, J. (2001). Genomic instability in a PARP-1$^{-/-}$ cell line expressing PARP-1 DNA-binding domain. Biochem Biophys Res Commun *285*, 289-294.

Cazzalini, O., Dona, F., Savio, M., Tillhon, M., Maccario, C., Perucca, P., Stivala, L.A., Scovassi, A.I., and Prosperi, E. (2010). p21/CDKN1A participates in base excision repair by regulating the activity of poly(ADP-ribose) polymerase-1. DNA Repair (Amst) *9*, 627-635.

Chang, D.J., Lupardus, P.J., and Cimprich, K.A. (2006). Monoubiquitination of proliferating cell nuclear antigen induced by stalled replication requires uncoupling of DNA polymerase and mini-chromosome maintenance helicase activities. J Biol Chem *281*, 32081-32088.

Chang, P., Coughlin, M., and Mitchison, T.J. (2005a). Tankyrase-1 polymerization of poly(ADP-ribose) is required for spindle structure and function. Nat Cell Biol *7*, 1133-1139.

Chang, W., Dynek, J.N., and Smith, S. (2005b). NuMA is a major acceptor of poly(ADP-ribosyl)ation by tankyrase 1 in mitosis. Biochem J *391*, 177-184.

Chasovskikh, S., Dimtchev, A., Smulson, M., and Dritschilo, A. (2005). DNA transitions induced by binding of PARP-1 to cruciform structures in supercoiled plasmids. Cytometry A *68*, 21-27.

Chatterjee, S., and Berger, N.A. (1998). Poly(ADP-Ribose) polymerase in response to DNA damage. In DNA damage and repair, J.A. Nickoloff, and M.F. Hoekstra, eds. (Totowa, USA, Humana Press Inc.), pp. 487-515.

Chen, X.L., Reindle, A., and Johnson, E.S. (2005). Misregulation of 2-μm circle copy number in a SUMO pathway mutant. Mol Cell Biol *25*, 4311-4320.

Cheng, C.H., Lo, Y.H., Liang, S.S., Ti, S.C., Lin, F.M., Yeh, C.H., Huang, H.Y., and Wang, T.F. (2006a). SUMO modifications control assembly of synaptonemal complex and polycomplex in meiosis of *Saccharomyces cerevisiae*. Genes Dev *20*, 2067-2081.

Cheng, J., Bawa, T., Lee, P., Gong, L., and Yeh, E.T. (2006b). Role of desumoylation in the development of prostate cancer. Neoplasia *8*, 667-676.

Chesnokov, I.N., Chesnokova, O.N., and Botchan, M. (2003). A cytokinetic function of *Drosophila* ORC6 protein resides in a domain distinct from its replication activity. Proc Natl Acad Sci USA *100*, 9150-9155.

Chiang, Y.J., Hsiao, S.J., Yver, D., Cushman, S.W., Tessarollo, L., Smith, S., and Hodes, R.J. (2008). Tankyrase 1 and tankyrase 2 are essential but redundant for mouse embryonic development. PLoS ONE *3*, e2639.

Chiang, Y.J., Nguyen, M.L., Gurunathan, S., Kaminker, P., Tessarollo, L., Campisi, J., and Hodes, R.J. (2006). Generation and characterization of telomere length maintenance in tankyrase 2-deficient mice. Mol Cell Biol *26*, 2037-2043.

Cho, S.H., Goenka, S., Henttinen, T., Gudapati, P., Reinikainen, A., Eischen, C.M., Lahesmaa, R., and Boothby, M. (2009). PARP-14, a member of the B aggressive lymphoma family, transduces survival signals in primary B cells. Blood *113*, 2416-2425.

Chou, H.Y., Chou, H.T., and Lee, S.C. (2006). CDK-dependent activation of poly(ADP-ribose) polymerase member 10 (PARP10). J Biol Chem *281*, 15201-15207.

Chuang, R.Y., and Kelly, T.J. (1999). The fission yeast homologue of Orc4p binds to replication origin DNA via multiple AT-hooks. Proc Natl Acad Sci USA *96*, 2656-2661.

Chupreta, S., Holmstrom, S., Subramanian, L., and Iniguez-Lluhi, J.A. (2005). A small conserved surface in SUMO is the critical structural determinant of its transcriptional inhibitory properties. Mol Cell Biol *25*, 4272-4282.

Cohen-Armon, M., Visochek, L., Rozensal, D., Kalal, A., Geistrikh, I., Klein, R., Bendetz-Nezer, S., Yao, Z., and Seger, R. (2007). DNA-independent PARP-1 activation by phosphorylated ERK2 increases Elk1 activity: a link to histone acetylation. Mol Cell *25*, 297-308.

Coleman, T.R., Carpenter, P.B., and Dunphy, W.G. (1996). The *Xenopus* Cdc6 protein is essential for the initiation of a single round of DNA replication in cell-free extracts. Cell *87*, 53-63.

Cook, B.D., Dynek, J.N., Chang, W., Shostak, G., and Smith, S. (2002). Role for the related poly(ADP-Ribose) polymerases tankyrase 1 and 2 at human telomeres. Mol Cell Biol *22*, 332-342.

Cortes, U., Tong, W.M., Coyle, D.L., Meyer-Ficca, M.L., Meyer, R.G., Petrilli, V., Herceg, Z., Jacobson, E.L., Jacobson, M.K., and Wang, Z.Q. (2004). Depletion of the 110-kilodalton isoform of poly(ADP-ribose) glycohydrolase increases sensitivity to genotoxic and endotoxic stress in mice. Mol Cell Biol *24*, 7163-7178.

Costanzo, V., Robertson, K., Bibikova, M., Kim, E., Grieco, D., Gottesman, M., Carroll, D., and Gautier, J. (2001). Mre11 protein complex prevents double-strand break accumulation during chromosomal DNA replication. Mol Cell *8*, 137-147.

Costanzo, V., Robertson, K., and Gautier, J. (2004). *Xenopus* cell-free extracts to study the DNA damage response. Methods Mol Biol *280*, 213-227.

Costanzo, V., Shechter, D., Lupardus, P.J., Cimprich, K.A., Gottesman, M., and Gautier, J. (2003). An ATR- and Cdc7-dependent DNA damage checkpoint that inhibits initiation of DNA replication. Mol Cell *11*, 203-213.

Cotner-Gohara, E., Kim, I.K., Tomkinson, A.E., and Ellenberger, T. (2008). Two DNA-binding and nick recognition modules in human DNA ligase III. J Biol Chem *283*, 10764-10772.

D'Amours, D., Desnoyers, S., D'Silva, I., and Poirier, G.G. (1999). Poly(ADP-ribosyl)ation reactions in the regulation of nuclear functions. Biochem J *342 (Pt 2)*, 249-268.

D'Cunha, J., Ramanujam, S., Wagner, R.J., Witt, P.L., Knight, E., Jr., and Borden, E.C. (1996). *In vitro* and *in vivo* secretion of human ISG15, an IFN-induced immunomodulatory cytokine. J Immunol *157*, 4100-4108.

D'Silva, I., Pelletier, J.D., Lagueux, J., D'Amours, D., Chaudhry, M.A., Weinfeld, M., Lees-Miller, S.P., and Poirier, G.G. (1999). Relative affinities of poly(ADP-ribose) polymerase and DNA-dependent protein kinase for DNA strand interruptions. Biochim Biophys Acta *1430*, 119-126.

Dahle, O., Andersen, T.O., Nordgard, O., Matre, V., Del Sal, G., and Gabrielsen, O.S. (2003). Transactivation properties of c-Myb are critically dependent on two SUMO-1 acceptor sites that are conjugated in a PIASy enhanced manner. Eur J Biochem *270*, 1338-1348.

Danis, E., Brodolin, K., Menut, S., Maiorano, D., Girard-Reydet, C., and Mechali, M. (2004). Specification of a DNA replication origin by a transcription complex. Nat Cell Biol *6*, 721-730.

Dantzer, F., Ame, J.C., Schreiber, V., Nakamura, J., Menissier-de Murcia, J., and de Murcia, G. (2006). Poly(ADP-ribose) polymerase-1 activation during DNA damage and repair. Methods Enzymol *409*, 493-510.

Dantzer, F., de La Rubia, G., Menissier-De Murcia, J., Hostomsky, Z., de Murcia, G., and Schreiber, V. (2000). Base excision repair is impaired in mammalian cells lacking Poly(ADP-ribose) polymerase-1. Biochemistry *39*, 7559-7569.

Dantzer, F., Nasheuer, H.P., Vonesch, J.L., de Murcia, G., and Menissier-de Murcia, J. (1998). Functional association of poly(ADP-ribose) polymerase with DNA polymerase α-primase

complex: a link between DNA strand break detection and DNA replication. Nucleic Acids Res *26*, 1891-1898.

Dasso, M., and Newport, J.W. (1990). Completion of DNA replication is monitored by a feedback system that controls the initiation of mitosis *in vitro*: studies in *Xenopus*. Cell *61*, 811-823.

David, G., Neptune, M.A., and DePinho, R.A. (2002). SUMO-1 modification of histone deacetylase 1 (HDAC1) modulates its biological activities. J Biol Chem *277*, 23658-23663.

Davidovic, L., Vodenicharov, M., Affar, E.B., and Poirier, G.G. (2001). Importance of poly(ADP-ribose) glycohydrolase in the control of poly(ADP-ribose) metabolism. Exp Cell Res *268*, 7-13.

Dawlaty, M.M., Malureanu, L., Jeganathan, K.B., Kao, E., Sustmann, C., Tahk, S., Shuai, K., Grosschedl, R., and van Deursen, J.M. (2008). Resolution of sister centromeres requires RanBP2-mediated SUMOylation of topoisomerase IIα. Cell *133*, 103-115.

de Capoa, A., Febbo, F.R., Giovannelli, F., Niveleau, A., Zardo, G., Marenzi, S., and Caiafa, P. (1999). Reduced levels of poly(ADP-ribosyl)ation result in chromatin compaction and hypermethylation as shown by cell-by-cell computer-assisted quantitative analysis. FASEB J *13*, 89-93.

de Murcia, G., Huletsky, A., Lamarre, D., Gaudreau, A., Pouyet, J., Daune, M., and Poirier, G.G. (1986). Modulation of chromatin superstructure induced by poly(ADP-ribose) synthesis and degradation. J Biol Chem *261*, 7011-7017.

de Murcia, J.M., Niedergang, C., Trucco, C., Ricoul, M., Dutrillaux, B., Mark, M., Oliver, F.J., Masson, M., Dierich, A., LeMeur, M.*, et al.* (1997). Requirement of poly(ADP-ribose) polymerase in recovery from DNA damage in mice and in cells. Proc Natl Acad Sci USA *94*, 7303-7307.

Denison, C., Rudner, A.D., Gerber, S.A., Bakalarski, C.E., Moazed, D., and Gygi, S.P. (2005). A proteomic strategy for gaining insights into protein sumoylation in yeast. Mol Cell Proteomics *4*, 246-254.

Desmarais, Y., Menard, L., Lagueux, J., and Poirier, G.G. (1991). Enzymological properties of poly(ADP-ribose)polymerase: characterization of automodification sites and NADase activity. Biochim Biophys Acta *1078*, 179-186.

Desterro, J.M., Rodriguez, M.S., and Hay, R.T. (1998). SUMO-1 modification of IκBα inhibits NF-κB activation. Mol Cell *2*, 233-239.

Desterro, J.M., Rodriguez, M.S., Kemp, G.D., and Hay, R.T. (1999). Identification of the enzyme required for activation of the small ubiquitin-like protein SUMO-1. J Biol Chem *274*, 10618-10624.

Desterro, J.M., Thomson, J., and Hay, R.T. (1997). Ubch9 conjugates SUMO but not ubiquitin. FEBS Lett *417*, 297-300.

Deyrieux, A.F., Rosas-Acosta, G., Ozbun, M.A., and Wilson, V.G. (2007). Sumoylation dynamics during keratinocyte differentiation. J Cell Sci *120*, 125-136.

Dhar, S.K., and Dutta, A. (2000). Identification and characterization of the human ORC6 homolog. J Biol Chem *275*, 34983-34988.

Diaz-Martinez, L.A., Gimenez-Abian, J.F., Azuma, Y., Guacci, V., Gimenez-Martin, G., Lanier, L.M., and Clarke, D.J. (2006). PIASy is required for faithful chromosome segregation in human cells. PLoS ONE *1*, e53.

Dittmar, G.A., Wilkinson, C.R., Jedrzejewski, P.T., and Finley, D. (2002). Role of a ubiquitin-like modification in polarized morphogenesis. Science *295*, 2442-2446.

Dohrmann, P.R., and Sclafani, R.A. (2006). Novel role for checkpoint Rad53 protein kinase in the initiation of chromosomal DNA replication in *Saccharomyces cerevisiae*. Genetics *174*, 87-99.

Dominguez-Bendala, J., Masutani, M., and McWhir, J. (2006). Down-regulation of PARP-1, but not of Ku80 or DNA-PKcs', results in higher gene targeting efficiency. Cell Biol Int *30*, 389-393.

Dong, F., Soubeyrand, S., and Hache, R.J. (2010). Activation of PARP-1 in response to bleomycin depends on the Ku antigen and protein phosphatase 5. Oncogene *29*, 2093-2103.

Donigian, J.R., and de Lange, T. (2007). The role of the poly(ADP-ribose) polymerase tankyrase1 in telomere length control by the TRF1 component of the shelterin complex. J Biol Chem *282*, 22662-22667.

Dou, H., Huang, C., Singh, M., Carpenter, P.B., and Yeh, E.T. (2010). Regulation of DNA repair through deSUMOylation and SUMOylation of replication protein A complex. Mol Cell *39*, 333-345.

Duncker, B.P., Chesnokov, I.N., and McConkey, B.J. (2009). The origin recognition complex protein family. Genome Biol *10*, 214.

Durkacz, B.W., Irwin, J., and Shall, S. (1981). Inhibition of (ADP-ribose)n biosynthesis retards DNA repair but does not inhibit DNA repair synthesis. Biochem Biophys Res Commun *101*, 1433-1441.

Durkacz, B.W., Omidiji, O., Gray, D.A., and Shall, S. (1980). $(ADP\text{-}ribose)_n$ participates in DNA excision repair. Nature *283*, 593-596.

Duval, D., Duval, G., Kedinger, C., Poch, O., and Boeuf, H. (2003). The 'PINIT' motif, of a newly identified conserved domain of the PIAS protein family, is essential for nuclear retention of PIAS3L. FEBS Lett *554*, 111-118.

Earle, E., Saxena, A., MacDonald, A., Hudson, D.F., Shaffer, L.G., Saffery, R., Cancilla, M.R., Cutts, S.M., Howman, E., and Choo, K.H. (2000). Poly(ADP-ribose) polymerase at active centromeres and neocentromeres at metaphase. Hum Mol Genet *9*, 187-194.

El-Khamisy, S.F., Masutani, M., Suzuki, H., and Caldecott, K.W. (2003). A requirement for PARP-1 for the assembly or stability of XRCC1 nuclear foci at sites of oxidative DNA damage. Nucleic Acids Res *31*, 5526-5533.

Eladad, S., Ye, T.Z., Hu, P., Leversha, M., Beresten, S., Matunis, M.J., and Ellis, N.A. (2005). Intra-nuclear trafficking of the BLM helicase to DNA damage-induced foci is regulated by SUMO modification. Hum Mol Genet *14*, 1351-1365.

Everett, R.D., Lomonte, P., Sternsdorf, T., van Driel, R., and Orr, A. (1999). Cell cycle regulation of PML modification and ND10 composition. J Cell Sci *112 (Pt 24)*, 4581-4588.

Fakan, S., Leduc, Y., Lamarre, D., Brunet, G., and Poirier, G.G. (1988). Immunoelectron microscopical distribution of poly(ADP-ribose)polymerase in the mammalian cell nucleus. Exp Cell Res *179*, 517-526.

Farmer, H., McCabe, N., Lord, C.J., Tutt, A.N., Johnson, D.A., Richardson, T.B., Santarosa, M., Dillon, K.J., Hickson, I., Knights, C.*, et al.* (2005). Targeting the DNA repair defect in BRCA mutant cells as a therapeutic strategy. Nature *434*, 917-921.

Farrar, D., Rai, S., Chernukhin, I., Jagodic, M., Ito, Y., Yammine, S., Ohlsson, R., Murrell, A., and Klenova, E. (2010). Mutational analysis of the poly(ADP-ribosyl)ation sites of the transcription factor CTCF provides an insight into the mechanism of its regulation by poly(ADP-ribosyl)ation. Mol Cell Biol *30*, 1199-1216.

Farzaneh, F., Panayotou, G.N., Bowler, L.D., Hardas, B.D., Broom, T., Walther, C., and Shall, S. (1988). ADP-ribosylation is involved in the integration of foreign DNA into the mammalian cell genome. Nucleic Acids Res *16*, 11319-11326.

Ferraris, D.V. (2010). Evolution of poly(ADP-ribose) polymerase-1 (PARP-1) inhibitors. From concept to clinic. J Med Chem *53*, 4561-4584.

Ferro, A.M., and Olivera, B.M. (1982). Poly(ADP-ribosylation) *in vitro*. Reaction parameters and enzyme mechanism. J Biol Chem *257*, 7808-7813.

Fink, S.L., and Cookson, B.T. (2005). Apoptosis, pyroptosis, and necrosis: mechanistic description of dead and dying eukaryotic cells. Infect Immun *73*, 1907-1916.

Finley, D., Ozkaynak, E., and Varshavsky, A. (1987). The yeast polyubiquitin gene is essential for resistance to high temperatures, starvation, and other stresses. Cell *48*, 1035-1046.

Fisher, A.E., Hochegger, H., Takeda, S., and Caldecott, K.W. (2007). Poly(ADP-ribose) polymerase 1 accelerates single-strand break repair in concert with poly(ADP-ribose) glycohydrolase. Mol Cell Biol *27*, 5597-5605.

Fong, P.C., Boss, D.S., Yap, T.A., Tutt, A., Wu, P., Mergui-Roelvink, M., Mortimer, P., Swaisland, H., Lau, A., O'Connor, M.J.*, et al.* (2009). Inhibition of poly(ADP-ribose) polymerase in tumors from BRCA mutation carriers. N Engl J Med *361*, 123-134.

Foss, M., McNally, F.J., Laurenson, P., and Rine, J. (1993). Origin recognition complex (ORC) in transcriptional silencing and DNA replication in S. cerevisiae. Science *262*, 1838-1844.

Frizzell, K.M., Gamble, M.J., Berrocal, J.G., Zhang, T., Krishnakumar, R., Cen, Y., Sauve, A.A., and Kraus, W.L. (2009). Global analysis of transcriptional regulation by poly(ADP-ribose) polymerase-1 and poly(ADP-ribose) glycohydrolase in MCF-7 human breast cancer cells. J Biol Chem *284*, 33926-33938.

Fu, C., Ahmed, K., Ding, H., Ding, X., Lan, J., Yang, Z., Miao, Y., Zhu, Y., Shi, Y., Zhu, J.*, et al.* (2005). Stabilization of PML nuclear localization by conjugation and oligomerization of SUMO-3. Oncogene *24*, 5401-5413.

Galande, S., and Kohwi-Shigematsu, T. (1999). Poly(ADP-ribose) polymerase and Ku autoantigen form a complex and synergistically bind to matrix attachment sequences. J Biol Chem *274*, 20521-20528.

Galanty, Y., Belotserkovskaya, R., Coates, J., Polo, S., Miller, K.M., and Jackson, S.P. (2009). Mammalian SUMO E3-ligases PIAS1 and PIAS4 promote responses to DNA double-strand breaks. Nature *462*, 935-939.

Gao, G., Guo, X., and Goff, S.P. (2002). Inhibition of retroviral RNA production by ZAP, a CCCH-type zinc finger protein. Science *297*, 1703-1706.

Gao, H., Coyle, D.L., Meyer-Ficca, M.L., Meyer, R.G., Jacobson, E.L., Wang, Z.Q., and Jacobson, M.K. (2007). Altered poly(ADP-ribose) metabolism impairs cellular responses to genotoxic stress in a hypomorphic mutant of poly(ADP-ribose) glycohydrolase. Exp Cell Res *313*, 984-996.

Geiss-Friedlander, R., and Melchior, F. (2007). Concepts in sumoylation: a decade on. Nat Rev Mol Cell Biol *8*, 947-956.

Giacca, M., Zentilin, L., Norio, P., Diviacco, S., Dimitrova, D., Contreas, G., Biamonti, G., Perini, G., Weighardt, F., Riva, S.*, et al.* (1994). Fine mapping of a replication origin of human DNA. Proc Natl Acad Sci USA *91*, 7119-7123.

Gibson, D.G., Bell, S.P., and Aparicio, O.M. (2006). Cell cycle execution point analysis of ORC function and characterization of the checkpoint response to ORC inactivation in *Saccharomyces cerevisiae*. Genes Cells *11*, 557-573.

Giraud, M.F., Desterro, J.M., and Naismith, J.H. (1998). Structure of ubiquitin-conjugating enzyme 9 displays significant differences with other ubiquitin-conjugating enzymes which may reflect its specificity for sumo rather than ubiquitin. Acta Crystallogr D Biol Crystallogr *54*, 891-898.

Glass, C.K., and Rosenfeld, M.G. (2000). The coregulator exchange in transcriptional functions of nuclear receptors. Genes Dev *14*, 121-141.

Gocke, C.B., Yu, H., and Kang, J. (2005). Systematic identification and analysis of mammalian small ubiquitin-like modifier substrates. J Biol Chem *280*, 5004-5012.

Goenka, S., and Boothby, M. (2006). Selective potentiation of Stat-dependent gene expression by collaborator of Stat6 (CoaSt6), a transcriptional cofactor. Proc Natl Acad Sci USA *103*, 4210-4215.

Golebiowski, F., Matic, I., Tatham, M.H., Cole, C., Yin, Y., Nakamura, A., Cox, J., Barton, G.J., Mann, M., and Hay, R.T. (2009). System-wide changes to SUMO modifications in response to heat shock. Sci Signal *2*, ra24.

Golebiowski, F., Tatham, M.H., Nakamura, A., and Hay, R.T. (2010). High-stringency tandem affinity purification of proteins conjugated to ubiquitin-like moieties. Nat Protoc *5*, 873-882.

Gong, L., Millas, S., Maul, G.G., and Yeh, E.T. (2000). Differential regulation of sentrinized proteins by a novel sentrin-specific protease. J Biol Chem *275*, 3355-3359.

Gong, L., and Yeh, E.T. (2006). Characterization of a family of nucleolar SUMO-specific proteases with preference for SUMO-2 or SUMO-3. J Biol Chem *281*, 15869-15877.

Gong, Z., Brackertz, M., and Renkawitz, R. (2006). SUMO modification enhances p66-mediated transcriptional repression of the Mi-2/NuRD complex. Mol Cell Biol *26*, 4519-4528.

Goodson, M.L., Hong, Y., Rogers, R., Matunis, M.J., Park-Sarge, O.K., and Sarge, K.D. (2001). Sumo-1 modification regulates the DNA binding activity of heat shock transcription factor 2, a promyelocytic leukemia nuclear body associated transcription factor. J Biol Chem *276*, 18513-18518.

Goren, A., Tabib, A., Hecht, M., and Cedar, H. (2008). DNA replication timing of the human β-globin domain is controlled by histone modification at the origin. Genes Dev *22*, 1319-1324.

Gossen, M., Pak, D.T., Hansen, S.K., Acharya, J.K., and Botchan, M.R. (1995). A *Drosophila* homolog of the yeast origin recognition complex. Science *270*, 1674-1677.

Gottschalk, A.J., Timinszky, G., Kong, S.E., Jin, J., Cai, Y., Swanson, S.K., Washburn, M.P., Florens, L., Ladurner, A.G., Conaway, J.W.*, et al.* (2009). Poly(ADP-ribosyl)ation directs recruitment and activation of an ATP-dependent chromatin remodeler. Proc Natl Acad Sci USA *106*, 13770-13774.

Grabbe, C., and Dikic, I. (2009). Functional roles of ubiquitin-like domain (ULD) and ubiquitin-binding domain (UBD) containing proteins. Chem Rev *109*, 1481-1494.

Gradwohl, G., Mazen, A., and de Murcia, G. (1987). Poly(ADP-ribose) polymerase forms loops with DNA. Biochem Biophys Res Commun *148*, 913-919.

Gradwohl, G., Menissier de Murcia, J.M., Molinete, M., Simonin, F., Koken, M., Hoeijmakers, J.H., and de Murcia, G. (1990). The second zinc-finger domain of poly(ADP-ribose) polymerase determines specificity for single-stranded breaks in DNA. Proc Natl Acad Sci USA *87*, 2990-2994.

Green, S., Kumar, V., Theulaz, I., Wahli, W., and Chambon, P. (1988). The N-terminal DNA-binding 'zinc finger' of the oestrogen and glucocorticoid receptors determines target gene specificity. EMBO J *7*, 3037-3044.

Gregoire, S., Tremblay, A.M., Xiao, L., Yang, Q., Ma, K., Nie, J., Mao, Z., Wu, Z., Giguere, V., and Yang, X.J. (2006). Control of MEF2 transcriptional activity by coordinated phosphorylation and sumoylation. J Biol Chem *281*, 4423-4433.

Gregoire, S., and Yang, X.J. (2005). Association with class IIa histone deacetylases upregulates the sumoylation of MEF2 transcription factors. Mol Cell Biol *25*, 2273-2287.

Grewal, S.I., and Moazed, D. (2003). Heterochromatin and epigenetic control of gene expression. Science *301*, 798-802.

Griesenbeck, J., Oei, S.L., Mayer-Kuckuk, P., Ziegler, M., Buchlow, G., and Schweiger, M. (1997). Protein-protein interaction of the human poly(ADP-ribosyl)transferase depends on the functional state of the enzyme. Biochemistry *36*, 7297-7304.

Guastafierro, T., Cecchinelli, B., Zampieri, M., Reale, A., Riggio, G., Sthandier, O., Zupi, G., Calabrese, L., and Caiafa, P. (2008). CCCTC-binding factor activates PARP-1 affecting DNA methylation machinery. J Biol Chem *283*, 21873-21880.

Guo, D., Han, J., Adam, B.L., Colburn, N.H., Wang, M.H., Dong, Z., Eizirik, D.L., She, J.X., and Wang, C.Y. (2005). Proteomic analysis of SUMO4 substrates in HEK293 cells under serum starvation-induced stress. Biochem Biophys Res Commun *337*, 1308-1318.

Guo, D., Li, M., Zhang, Y., Yang, P., Eckenrode, S., Hopkins, D., Zheng, W., Purohit, S., Podolsky, R.H., Muir, A.*, et al.* (2004). A functional variant of SUMO4, a new IκBα modifier, is associated with type 1 diabetes. Nat Genet *36*, 837-841.

Hagan, M.P., Yacoub, A., and Dent, P. (2007). Radiation-induced PARP activation is enhanced through EGFR-ERK signaling. J Cell Biochem *101*, 1384-1393.

Haince, J.F., McDonald, D., Rodrigue, A., Dery, U., Masson, J.Y., Hendzel, M.J., and Poirier, G.G. (2008). PARP1-dependent kinetics of recruitment of MRE11 and NBS1 proteins to multiple DNA damage sites. J Biol Chem *283*, 1197-1208.

Hanahan, D., and Weinberg, R.A. (2000). The hallmarks of cancer. Cell *100*, 57-70.

Hanai, S., Kanai, M., Ohashi, S., Okamoto, K., Yamada, M., Takahashi, H., and Miwa, M. (2004). Loss of poly(ADP-ribose) glycohydrolase causes progressive neurodegeneration in *Drosophila melanogaster*. Proc Natl Acad Sci USA *101*, 82-86.

Hang, J., and Dasso, M. (2002). Association of the human SUMO-1 protease SENP2 with the nuclear pore. J Biol Chem *277*, 19961-19966.

Hannich, J.T., Lewis, A., Kroetz, M.B., Li, S.J., Heide, H., Emili, A., and Hochstrasser, M. (2005). Defining the SUMO-modified proteome by multiple approaches in *Saccharomyces cerevisiae*. J Biol Chem *280*, 4102-4110.

Hardeland, U., Steinacher, R., Jiricny, J., and Schar, P. (2002). Modification of the human thymine-DNA glycosylase by ubiquitin-like proteins facilitates enzymatic turnover. Embo J *21*, 1456-1464.

Hartwell, L.H. (1973). Three additional genes required for deoxyribonucleic acid synthesis in *Saccharomyces cerevisiae*. J Bacteriol *115*, 966-974.

Hassa, P.O., Haenni, S.S., Buerki, C., Meier, N.I., Lane, W.S., Owen, H., Gersbach, M., Imhof, R., and Hottiger, M.O. (2005). Acetylation of poly(ADP-ribose) polymerase-1 by p300/CREB-binding protein regulates coactivation of NF-kappaB-dependent transcription. J Biol Chem *280*, 40450-40464.

Hassa, P.O., Haenni, S.S., Elser, M., and Hottiger, M.O. (2006). Nuclear ADP-ribosylation reactions in mammalian cells: where are we today and where are we going? Microbiol Mol Biol Rev *70*, 789-829.

Hassa, P.O., and Hottiger, M.O. (1999). A role of poly (ADP-ribose) polymerase in NF-κB transcriptional activation. Biol Chem *380*, 953-959.

Hatakeyama, K., Nemoto, Y., Ueda, K., and Hayaishi, O. (1986). Purification and characterization of poly(ADP-ribose) glycohydrolase. Different modes of action on large and small poly(ADP-ribose). J Biol Chem *261*, 14902-14911.

Hayashi, K., Tanaka, M., Shimada, T., Miwa, M., and Sugimura, T. (1983). Size and shape of poly(ADP-ribose): examination by gel filtration, gel electrophoresis and electron microscopy. Biochem Biophys Res Commun *112*, 102-107.

Heacock, M.L., Stefanick, D.F., Horton, J.K., and Wilson, S.H. (2010). Alkylation DNA damage in combination with PARP inhibition results in formation of S-phase-dependent double-strand breaks. DNA Repair (Amst) *9*, 929-936.

Hecker, C.M., Rabiller, M., Haglund, K., Bayer, P., and Dikic, I. (2006). Specification of SUMO1- and SUMO2-interacting motifs. J Biol Chem *281*, 16117-16127.

Heintz, N.H., and Hamlin, J.L. (1982). An amplified chromosomal sequence that includes the gene for dihydrofolate reductase initiates replication within specific restriction fragments. Proc Natl Acad Sci USA *79*, 4083-4087.

Heinzel, S.S., Krysan, P.J., Tran, C.T., and Calos, M.P. (1991). Autonomous DNA replication in human cells is affected by the size and the source of the DNA. Mol Cell Biol *11*, 2263-2272.

Helleday, T. (2010). Homologous recombination in cancer development, treatment and development of drug resistance. Carcinogenesis *31*, 955-960.

Hengartner, C., Lagueux, J., and Poirier, G.G. (1991). Analysis of the activation of poly(ADP-ribose) polymerase by various types of DNA. Biochem Cell Biol *69*, 577-580.

Henrie, M.S., Kurimasa, A., Burma, S., Menissier-de Murcia, J., de Murcia, G., Li, G.C., and Chen, D.J. (2003). Lethality in PARP-1/Ku80 double mutant mice reveals physiological synergy during early embryogenesis. DNA Repair (Amst) *2*, 151-158.

Hicke, L., and Dunn, R. (2003). Regulation of membrane protein transport by ubiquitin and ubiquitin-binding proteins. Annu Rev Cell Dev Biol *19*, 141-172.

Hietakangas, V., Ahlskog, J.K., Jakobsson, A.M., Hellesuo, M., Sahlberg, N.M., Holmberg, C.I., Mikhailov, A., Palvimo, J.J., Pirkkala, L., and Sistonen, L. (2003). Phosphorylation of serine 303 is a prerequisite for the stress-inducible SUMO modification of heat shock factor 1. Mol Cell Biol *23*, 2953-2968.

Hietakangas, V., Anckar, J., Blomster, H.A., Fujimoto, M., Palvimo, J.J., Nakai, A., and Sistonen, L. (2006). PDSM, a motif for phosphorylation-dependent SUMO modification. Proc Natl Acad Sci USA *103*, 45-50.

Hishida, T., Ohya, T., Kubota, Y., Kamada, Y., and Shinagawa, H. (2006). Functional and physical interaction of yeast Mgs1 with PCNA: impact on RAD6-dependent DNA damage tolerance. Mol Cell Biol *26*, 5509-5517.

Ho, J.C., and Watts, F.Z. (2003). Characterization of SUMO-conjugating enzyme mutants in *Schizosaccharomyces pombe* identifies a dominant-negative allele that severely reduces SUMO conjugation. Biochem J *372*, 97-104.

Hochegger, H., Dejsuphong, D., Fukushima, T., Morrison, C., Sonoda, E., Schreiber, V., Zhao, G.Y., Saberi, A., Masutani, M., Adachi, N.*, et al.* (2006). Parp-1 protects homologous recombination from interference by Ku and Ligase IV in vertebrate cells. EMBO J *25*, 1305-1314.

Hoege, C., Pfander, B., Moldovan, G.L., Pyrowolakis, G., and Jentsch, S. (2002). *RAD6*-dependent DNA repair is linked to modification of PCNA by ubiquitin and SUMO. Nature *419*, 135-141.

Hogan, E., and Koshland, D. (1992). Addition of extra origins of replication to a minichromosome suppresses its mitotic loss in cdc6 and cdc14 mutants of *Saccharomyces cerevisiae*. Proc Natl Acad Sci USA *89*, 3098-3102.

Hori, T., Osaka, F., Chiba, T., Miyamoto, C., Okabayashi, K., Shimbara, N., Kato, S., and Tanaka, K. (1999). Covalent modification of all members of human cullin family proteins by NEDD8. Oncogene *18*, 6829-6834.

Horie, K., Tomida, A., Sugimoto, Y., Yasugi, T., Yoshikawa, H., Taketani, Y., and Tsuruo, T. (2002). SUMO-1 conjugation to intact DNA topoisomerase I amplifies cleavable complex formation induced by camptothecin. Oncogene *21*, 7913-7922.

Horsman, M.R., Brown, D.M., Hirst, D.G., and Brown, J.M. (1986). Changes in the response of the RIF-1 tumour to melphalan *in vivo* induced by inhibitors of nuclear ADP-ribosyl transferase. Br J Cancer *53*, 247-254.

Hsiao, S.J., and Smith, S. (2008). Tankyrase function at telomeres, spindle poles, and beyond. Biochimie *90*, 83-92.

Huang, D.T., Ayrault, O., Hunt, H.W., Taherbhoy, A.M., Duda, D.M., Scott, D.C., Borg, L.A., Neale, G., Murray, P.J., Roussel, M.F.*, et al.* (2009). E2-RING expansion of the NEDD8 cascade confers specificity to cullin modification. Mol Cell *33*, 483-495.

Huang, D.T., Hunt, H.W., Zhuang, M., Ohi, M.D., Holton, J.M., and Schulman, B.A. (2007). Basis for a ubiquitin-like protein thioester switch toggling E1-E2 affinity. Nature *445*, 394-398.

Hyrien, O., Maric, C., and Mechali, M. (1995). Transition in specification of embryonic metazoan DNA replication origins. Science *270*, 994-997.

Ichimura, Y., Kirisako, T., Takao, T., Satomi, Y., Shimonishi, Y., Ishihara, N., Mizushima, N., Tanida, I., Kominami, E., Ohsumi, M.*, et al.* (2000). A ubiquitin-like system mediates protein lipidation. Nature *408*, 488-492.

Ii, T., Fung, J., Mullen, J.R., and Brill, S.J. (2007a). The yeast Slx5-Slx8 DNA integrity complex displays ubiquitin ligase activity. Cell Cycle *6*, 2800-2809.

Ii, T., Mullen, J.R., Slagle, C.E., and Brill, S.J. (2007b). Stimulation of *in vitro* sumoylation by Slx5-Slx8: evidence for a functional interaction with the SUMO pathway. DNA Repair (Amst) *6*, 1679-1691.

Ikejima, M., Noguchi, S., Yamashita, R., Ogura, T., Sugimura, T., Gill, D.M., and Miwa, M. (1990). The zinc fingers of human poly(ADP-ribose) polymerase are differentially required for the recognition of DNA breaks and nicks and the consequent enzyme activation. Other structures recognize intact DNA. J Biol Chem *265*, 21907-21913.

Iles, N., Rulten, S., El-Khamisy, S.F., and Caldecott, K.W. (2007). APLF (C2orf13) is a novel human protein involved in the cellular response to chromosomal DNA strand breaks. Mol Cell Biol *27*, 3793-3803.

Itahana, Y., Yeh, E.T., and Zhang, Y. (2006). Nucleocytoplasmic shuttling modulates activity and ubiquitination-dependent turnover of SUMO-specific protease 2. Mol Cell Biol *26*, 4675-4689.

Jackson, S.P. (2002). Sensing and repairing DNA double-strand breaks. Carcinogenesis *23*, 687-696.

Jacobs, A.M., Nicol, S.M., Hislop, R.G., Jaffray, E.G., Hay, R.T., and Fuller-Pace, F.V. (2007). SUMO modification of the DEAD box protein p68 modulates its transcriptional activity and promotes its interaction with HDAC1. Oncogene *26*, 5866-5876.

Jagtap, P., and Szabo, C. (2005). Poly(ADP-ribose) polymerase and the therapeutic effects of its inhibitors. Nat Rev Drug Discov *4*, 421-440.

James, P., Halladay, J., and Craig, E.A. (1996). Genomic libraries and a host strain designed for highly efficient two-hybrid selection in yeast. Genetics *144*, 1425-1436.

Jentsch, S., and Pyrowolakis, G. (2000). Ubiquitin and its kin: how close are the family ties? Trends Cell Biol *10*, 335-342.

Johnson, E.S. (2004). Protein modification by SUMO. Annu Rev Biochem *73*, 355-382.

Johnson, E.S., and Blobel, G. (1999). Cell cycle-regulated attachment of the ubiquitin-related protein SUMO to the yeast septins. J Cell Biol *147*, 981-994.

Johnson, E.S., and Gupta, A.A. (2001). An E3-like factor that promotes SUMO conjugation to the yeast septins. Cell *106*, 735-744.

Johnson, E.S., Schwienhorst, I., Dohmen, R.J., and Blobel, G. (1997). The ubiquitin-like protein Smt3p is activated for conjugation to other proteins by an Aos1p/Uba2p heterodimer. EMBO J *16*, 5509-5519.

Jorgensen, T.J., Chen, K., Chasovskikh, S., Roy, R., Dritschilo, A., and Uren, A. (2009). Binding kinetics and activity of human poly(ADP-ribose) polymerase-1 on oligo-deoxyribonucleotide substrates. J Mol Recognit *22*, 446-452.

Ju, B.G., Lunyak, V.V., Perissi, V., Garcia-Bassets, I., Rose, D.W., Glass, C.K., and Rosenfeld, M.G. (2006). A topoisomerase IIβ-mediated dsDNA break required for regulated transcription. Science *312*, 1798-1802.

Ju, B.G., Solum, D., Song, E.J., Lee, K.J., Rose, D.W., Glass, C.K., and Rosenfeld, M.G. (2004). Activating the PARP-1 sensor component of the groucho/ TLE1 corepressor complex mediates a CaMKinase IIdelta-dependent neurogenic gene activation pathway. Cell *119*, 815-829.

Juarez-Salinas, H., Levi, V., Jacobson, E.L., and Jacobson, M.K. (1982). Poly(ADP-ribose) has a branched structure *in vivo*. J Biol Chem *257*, 607-609.

Kagey, M.H., Melhuish, T.A., Powers, S.E., and Wotton, D. (2005). Multiple activities contribute to Pc2 E3 function. EMBO J *24*, 108-119.

Kagey, M.H., Melhuish, T.A., and Wotton, D. (2003). The polycomb protein Pc2 is a SUMO E3. Cell *113*, 127-137.

Kaiser, P., Auer, B., and Schweiger, M. (1992). Inhibition of cell proliferation in *Saccharomyces cerevisiae* by expression of human NAD^+ ADP-ribosyltransferase requires the DNA binding domain ("zinc fingers"). Mol Gen Genet *232*, 231-239.

Kameshita, I., Matsuda, M., Nishikimi, M., Ushiro, H., and Shizuta, Y. (1986). Reconstitution and poly(ADP-ribosyl)ation of proteolytically fragmented poly(ADP-ribose) synthetase. J Biol Chem *261*, 3863-3868.

Kameshita, I., Matsuda, Z., Taniguchi, T., and Shizuta, Y. (1984). Poly (ADP-Ribose) synthetase. Separation and identification of three proteolytic fragments as the substrate-binding domain, the DNA-binding domain, and the automodification domain. J Biol Chem *259*, 4770-4776.

Karras, G.I., Kustatscher, G., Buhecha, H.R., Allen, M.D., Pugieux, C., Sait, F., Bycroft, M., and Ladurner, A.G. (2005). The macro domain is an ADP-ribose binding module. EMBO J *24*, 1911-1920.

Kaufmann, S.H., Brunet, G., Talbot, B., Lamarr, D., Dumas, C., Shaper, J.H., and Poirier, G. (1991). Association of poly(ADP-ribose) polymerase with the nuclear matrix: the role of intermolecular disulfide bond formation, RNA retention, and cell type. Exp Cell Res *192*, 524-535.

Kaufmann, S.H., Desnoyers, S., Ottaviano, Y., Davidson, N.E., and Poirier, G.G. (1993). Specific proteolytic cleavage of poly(ADP-ribose) polymerase: an early marker of chemotherapy-induced apoptosis. Cancer Res *53*, 3976-3985.

Kauppinen, T.M., Chan, W.Y., Suh, S.W., Wiggins, A.K., Huang, E.J., and Swanson, R.A. (2006). Direct phosphorylation and regulation of poly(ADP-ribose) polymerase-1 by extracellular signal-regulated kinases 1/2. Proc Natl Acad Sci USA *103*, 7136-7141.

Kawabe, Y., Seki, M., Seki, T., Wang, W.S., Imamura, O., Furuichi, Y., Saitoh, H., and Enomoto, T. (2000). Covalent modification of the Werner's syndrome gene product with the ubiquitin-related protein, SUMO-1. J Biol Chem *275*, 20963-20966.

Kawaichi, M., Ueda, K., and Hayaishi, O. (1981). Multiple autopoly(ADP-ribosyl)ation of rat liver poly(ADP-ribose) synthetase. Mode of modification and properties of automodified synthetase. J Biol Chem *256*, 9483-9489.

Keil, C., Grobe, T., and Oei, S.L. (2006). MNNG-induced cell death is controlled by interactions between PARP-1, poly(ADP-ribose) glycohydrolase, and XRCC1. J Biol Chem *281*, 34394-34405.

Kerscher, O. (2007). SUMO junction-what's your function? New insights through SUMO-interacting motifs. EMBO Rep *8*, 550-555.

Khoudoli, G.A., Gillespie, P.J., Stewart, G., Andersen, J.S., Swedlow, J.R., and Blow, J.J. (2008). Temporal profiling of the chromatin proteome reveals system-wide responses to replication inhibition. Curr Biol *18*, 838-843.

Kickhoefer, V.A., Siva, A.C., Kedersha, N.L., Inman, E.M., Ruland, C., Streuli, M., and Rome, L.H. (1999). The 193-kD vault protein, VPARP, is a novel poly(ADP-ribose) polymerase. J Cell Biol *146*, 917-928.

Kim, H., Jacobson, M.K., Rolli, V., Menissier-de Murcia, J., Reinbolt, J., Simonin, F., Ruf, A., Schulz, G., and de Murcia, G. (1997). Photoaffinity labelling of human poly(ADP-ribose) polymerase catalytic domain. Biochem J *322 (Pt 2)*, 469-475.

Kim, M.Y., Mauro, S., Gevry, N., Lis, J.T., and Kraus, W.L. (2004). NAD^+-dependent modulation of chromatin structure and transcription by nucleosome binding properties of PARP-1. Cell *119*, 803-814.

Kim, Y.E., Kim, D.Y., Lee, J.M., Kim, S.T., Han, T.H., and Ahn, J.H. (2005). Requirement of the coiled-coil domain of PML-RARα oncoprotein for localization, sumoylation, and inhibition of monocyte differentiation. Biochem Biophys Res Commun *330*, 746-754.

Kirsh, O., Seeler, J.S., Pichler, A., Gast, A., Muller, S., Miska, E., Mathieu, M., Harel-Bellan, A., Kouzarides, T., Melchior, F.*, et al.* (2002). The SUMO E3 ligase RanBP2 promotes modification of the HDAC4 deacetylase. EMBO J *21*, 2682-2691.

Klein, U.R., Haindl, M., Nigg, E.A., and Muller, S. (2009). RanBP2 and SENP3 function in a mitotic SUMO2/3 conjugation-deconjugation cycle on Borealin. Mol Biol Cell *20*, 410-418.

Kleine, H., Poreba, E., Lesniewicz, K., Hassa, P.O., Hottiger, M.O., Litchfield, D.W., Shilton, B.H., and Luscher, B. (2008). Substrate-assisted catalysis by PARP10 limits its activity to mono-ADP-ribosylation. Mol Cell *32*, 57-69.

Knipscheer, P., Flotho, A., Klug, H., Olsen, J.V., van Dijk, W.J., Fish, A., Johnson, E.S., Mann, M., Sixma, T.K., and Pichler, A. (2008). Ubc9 sumoylation regulates SUMO target discrimination. Mol Cell *31*, 371-382.

Knipscheer, P., van Dijk, W.J., Olsen, J.V., Mann, M., and Sixma, T.K. (2007). Noncovalent interaction between Ubc9 and SUMO promotes SUMO chain formation. EMBO J *26*, 2797-2807.

Knop, M., Siegers, K., Pereira, G., Zachariae, W., Winsor, B., Nasmyth, K., and Schiebel, E. (1999). Epitope tagging of yeast genes using a PCR-based strategy: more tags and improved practical routines. Yeast *15*, 963-972.

Knuesel, M., Cheung, H.T., Hamady, M., Barthel, K.K., and Liu, X. (2005). A method of mapping protein sumoylation sites by mass spectrometry using a modified small ubiquitin-like modifier 1 (SUMO-1) and a computational program. Mol Cell Proteomics *4*, 1626-1636.

Koh, D.W., Lawler, A.M., Poitras, M.F., Sasaki, M., Wattler, S., Nehls, M.C., Stoger, T., Poirier, G.G., Dawson, V.L., and Dawson, T.M. (2004). Failure to degrade poly(ADP-ribose) causes increased sensitivity to cytotoxicity and early embryonic lethality. Proc Natl Acad Sci USA *101*, 17699-17704.

Kolli, N., Mikolajczyk, J., Drag, M., Mukhopadhyay, D., Moffatt, N., Dasso, M., Salvesen, G., and Wilkinson, K.D. (2010). Distribution and paralog specificity of mammalian deSUMOylating enzymes. Biochem J.

Kosoy, A., Calonge, T.M., Outwin, E.A., and O'Connell, M.J. (2007). Fission yeast Rnf4 homologs are required for DNA repair. J Biol Chem *282*, 20388-20394.

Kotaja, N., Karvonen, U., Janne, O.A., and Palvimo, J.J. (2002). PIAS proteins modulate transcription factors by functioning as SUMO-1 ligases. Mol Cell Biol *22*, 5222-5234.

Kotova, E., Jarnik, M., and Tulin, A.V. (2010). Uncoupling of the transactivation and transrepression functions of PARP1 protein. Proc Natl Acad Sci USA *107*, 6406-6411.

Koyama, Y., Katagiri, S., Hanai, S., Uchida, K., and Miwa, M. (1999). Poly(ADP-ribose) polymerase interacts with novel *Drosophila* ribosomal proteins, L22 and l23a, with unique histone-like amino-terminal extensions. Gene *226*, 339-345.

Kraus, W.L. (2008). Transcriptional control by PARP-1: chromatin modulation, enhancer-binding, coregulation, and insulation. Curr Opin Cell Biol *20*, 294-302.

Kraus, W.L., and Lis, J.T. (2003). PARP goes transcription. Cell *113*, 677-683.

Krishnakumar, R., Gamble, M.J., Frizzell, K.M., Berrocal, J.G., Kininis, M., and Kraus, W.L. (2008). Reciprocal binding of PARP-1 and histone H1 at promoters specifies transcriptional outcomes. Science *319*, 819-821.

Kubota, Y., Nash, R.A., Klungland, A., Schar, P., Barnes, D.E., and Lindahl, T. (1996). Reconstitution of DNA base excision-repair with purified human proteins: interaction between DNA polymerase β and the XRCC1 protein. EMBO J *15*, 6662-6670.

Kun, E., Kirsten, E., Mendeleyev, J., and Ordahl, C.P. (2004). Regulation of the enzymatic catalysis of poly(ADP-ribose) polymerase by dsDNA, polyamines, Mg^{2+}, Ca^{2+}, histones H1 and H3, and ATP. Biochemistry *43*, 210-216.

Kupper, J.H., de Murcia, G., and Burkle, A. (1990). Inhibition of poly(ADP-ribosyl)ation by overexpressing the poly(ADP-ribose) polymerase DNA-binding domain in mammalian cells. J Biol Chem *265*, 18721-18724.

Kupper, J.H., Muller, M., Jacobson, M.K., Tatsumi-Miyajima, J., Coyle, D.L., Jacobson, E.L., and Burkle, A. (1995). trans-dominant inhibition of poly(ADP-ribosyl)ation sensitizes cells against gamma-irradiation and N-methyl-N'-nitro-N-nitrosoguanidine but does not limit DNA replication of a polyomavirus replicon. Mol Cell Biol *15*, 3154-3163.

Lallemand-Breitenbach, V., Jeanne, M., Benhenda, S., Nasr, R., Lei, M., Peres, L., Zhou, J., Zhu, J., Raught, B., and de The, H. (2008). Arsenic degrades PML or PML-RARα through a SUMO-triggered RNF4/ubiquitin-mediated pathway. Nat Cell Biol *10*, 547-555.

Lallemand-Breitenbach, V., Zhu, J., Puvion, F., Koken, M., Honore, N., Doubeikovsky, A., Duprez, E., Pandolfi, P.P., Puvion, E., Freemont, P.*, et al.* (2001). Role of promyelocytic leukemia (PML) sumolation in nuclear body formation, 11S proteasome recruitment, and As_2O_3-induced PML or PML/retinoic acid receptor α degradation. J Exp Med *193*, 1361-1371.

Langelier, M.F., Ruhl, D.D., Planck, J.L., Kraus, W.L., and Pascal, J.M. (2010). The Zn3 domain of human poly(ADP-ribose) polymerase-1 (PARP-1) functions in both DNA-dependent poly(ADP-ribose) synthesis activity and chromatin compaction. J Biol Chem.

Langelier, M.F., Servent, K.M., Rogers, E.E., and Pascal, J.M. (2008). A third zinc-binding domain of human poly(ADP-ribose) polymerase-1 coordinates DNA-dependent enzyme activation. J Biol Chem *283*, 4105-4114.

Larkin, M.A., Blackshields, G., Brown, N.P., Chenna, R., McGettigan, P.A., McWilliam, H., Valentin, F., Wallace, I.M., Wilm, A., Lopez, R.*, et al.* (2007). Clustal W and Clustal X version 2.0. Bioinformatics *23*, 2947-2948.

Lazebnik, Y.A., Kaufmann, S.H., Desnoyers, S., Poirier, G.G., and Earnshaw, W.C. (1994). Cleavage of poly(ADP-ribose) polymerase by a proteinase with properties like ICE. Nature *371*, 346-347.

Le Cam, E., Fack, F., Menissier-de Murcia, J., Cognet, J.A., Barbin, A., Sarantoglou, V., Revet, B., Delain, E., and de Murcia, G. (1994). Conformational analysis of a 139 base-pair DNA fragment containing a single-stranded break and its interaction with human poly(ADP-ribose) polymerase. J Mol Biol *235*, 1062-1071.

Leach, C.A., and Michael, W.M. (2005). Ubiquitin/SUMO modification of PCNA promotes replication fork progression in *Xenopus* laevis egg extracts. J Cell Biol *171*, 947-954.

Lee, D., Kim, J.W., Kim, K., Joe, C.O., Schreiber, V., Menissier-De Murcia, J., and Choe, J. (2002). Functional interaction between human papillomavirus type 18 E2 and poly(ADP-ribose) polymerase 1. Oncogene *21*, 5877-5885.

Lee, G.W., Melchior, F., Matunis, M.J., Mahajan, R., Tian, Q., and Anderson, P. (1998). Modification of Ran GTPase-activating protein by the small ubiquitin-related modifier SUMO-1 requires Ubc9, an E2-type ubiquitin-conjugating enzyme homologue. J Biol Chem *273*, 6503-6507.

Lee, I., and Schindelin, H. (2008). Structural insights into E1-catalyzed ubiquitin activation and transfer to conjugating enzymes. Cell *134*, 268-278.

Lee, M.T., and Bachant, J. (2009). SUMO modification of DNA topoisomerase II: trying to get a CENse of it all. DNA Repair (Amst) *8*, 557-568.

Leidel, S., Pedrioli, P.G., Bucher, T., Brost, R., Costanzo, M., Schmidt, A., Aebersold, R., Boone, C., Hofmann, K., and Peter, M. (2009). Ubiquitin-related modifier Urm1 acts as a sulphur carrier in thiolation of eukaryotic transfer RNA. Nature *458*, 228-232.

Leist, M., Single, B., Kunstle, G., Volbracht, C., Hentze, H., and Nicotera, P. (1997). Apoptosis in the absence of poly-(ADP-ribose) polymerase. Biochem Biophys Res Commun *233*, 518-522.

Leppard, J.B., Dong, Z., Mackey, Z.B., and Tomkinson, A.E. (2003). Physical and functional interaction between DNA ligase IIIα and poly(ADP-Ribose) polymerase 1 in DNA single-strand break repair. Mol Cell Biol *23*, 5919-5927.

Li, C.J., and DePamphilis, M.L. (2002). Mammalian Orc1 protein is selectively released from chromatin and ubiquitinated during the S-to-M transition in the cell division cycle. Mol Cell Biol *22*, 105-116.

Li, C.J., Vassilev, A., and DePamphilis, M.L. (2004a). Role for Cdk1 (Cdc2)/cyclin A in preventing the mammalian origin recognition complex's largest subunit (Orc1) from binding to chromatin during mitosis. Mol Cell Biol *24*, 5875-5886.

Li, F., Chen, J., Izumi, M., Butler, M.C., Keezer, S.M., and Gilbert, D.M. (2001). The replication timing program of the Chinese hamster β-globin locus is established coincident with its repositioning near peripheral heterochromatin in early G_1 phase. J Cell Biol *154*, 283-292.

Li, S.J., and Hochstrasser, M. (1999). A new protease required for cell-cycle progression in yeast. Nature *398*, 246-251.

Li, S.J., and Hochstrasser, M. (2000). The yeast ULP2 (SMT4) gene encodes a novel protease specific for the ubiquitin-like Smt3 protein. Mol Cell Biol *20*, 2367-2377.

Li, S.J., and Hochstrasser, M. (2003). The Ulp1 SUMO isopeptidase: distinct domains required for viability, nuclear envelope localization, and substrate specificity. J Cell Biol *160*, 1069-1081.

Li, T., Evdokimov, E., Shen, R.F., Chao, C.C., Tekle, E., Wang, T., Stadtman, E.R., Yang, D.C., and Chock, P.B. (2004b). Sumoylation of heterogeneous nuclear ribonucleoproteins, zinc finger proteins, and nuclear pore complex proteins: a proteomic analysis. Proc Natl Acad Sci USA *101*, 8551-8556.

Li, W., Hesabi, B., Babbo, A., Pacione, C., Liu, J., Chen, D.J., Nickoloff, J.A., and Shen, Z. (2000). Regulation of double-strand break-induced mammalian homologous recombination by UBL1, a RAD51-interacting protein. Nucleic Acids Res *28*, 1145-1153.

Liang, C., and Stillman, B. (1997). Persistent initiation of DNA replication and chromatin-bound MCM proteins during the cell cycle in cdc6 mutants. Genes Dev *11*, 3375-3386.

Lidonnici, M.R., Rossi, R., Paixao, S., Mendoza-Maldonado, R., Paolinelli, R., Arcangeli, C., Giacca, M., Biamonti, G., and Montecucco, A. (2004). Subnuclear distribution of the largest subunit of the human origin recognition complex during the cell cycle. J Cell Sci *117*, 5221-5231.

Lilyestrom, W., van der Woerd, M.J., Clark, N., and Luger, K. (2010). Structural and biophysical studies of human PARP-1 in complex with damaged DNA. J Mol Biol *395*, 983-994.

Lima, C.D., and Reverter, D. (2008). Structure of the human SENP7 catalytic domain and poly-SUMO deconjugation activities for SENP6 and SENP7. J Biol Chem *283*, 32045-32055.

Lin, D.Y., Huang, Y.S., Jeng, J.C., Kuo, H.Y., Chang, C.C., Chao, T.T., Ho, C.C., Chen, Y.C., Lin, T.P., Fang, H.I*., et al.* (2006). Role of SUMO-interacting motif in Daxx SUMO modification, subnuclear localization, and repression of sumoylated transcription factors. Mol Cell *24*, 341-354.

Lin, H.B., Dijkwel, P.A., and Hamlin, J.L. (2005). Promiscuous initiation on mammalian chromosomal DNA templates and its possible suppression by transcription. Exp Cell Res *308*, 53-64.

Liu, B., Yang, Y., Chernishof, V., Loo, R.R., Jang, H., Tahk, S., Yang, R., Mink, S., Shultz, D., Bellone, C.J*., et al.* (2007). Proinflammatory stimuli induce IKKα-mediated phosphorylation of PIAS1 to restrict inflammation and immunity. Cell *129*, 903-914.

Liu, G., and Warbrick, E. (2006). The p66 and p12 subunits of DNA polymerase delta are modified by ubiquitin and ubiquitin-like proteins. Biochem Biophys Res Commun *349*, 360-366.

Liu, G.H., and Gerace, L. (2009). Sumoylation regulates nuclear localization of lipin-1α in neuronal cells. PLoS ONE *4*, e7031.

Liu, L., Spurrier, J., Butt, T.R., and Strickler, J.E. (2008). Enhanced protein expression in the baculovirus/insect cell system using engineered SUMO fusions. Protein Expr Purif *62*, 21-28.

Liu, Y., Snow, B.E., Kickhoefer, V.A., Erdmann, N., Zhou, W., Wakeham, A., Gomez, M., Rome, L.H., and Harrington, L. (2004). Vault poly(ADP-ribose) polymerase is associated with mammalian telomerase and is dispensable for telomerase function and vault structure *in vivo*. Mol Cell Biol *24*, 5314-5323.

Lois, L.M., and Lima, C.D. (2005). Structures of the SUMO E1 provide mechanistic insights into SUMO activation and E2 recruitment to E1. EMBO J *24*, 439-451.

Long, J., Zuo, D., and Park, M. (2005). Pc2-mediated sumoylation of Smad-interacting protein 1 attenuates transcriptional repression of E-cadherin. J Biol Chem *280*, 35477-35489.

Lonskaya, I., Potaman, V.N., Shlyakhtenko, L.S., Oussatcheva, E.A., Lyubchenko, Y.L., and Soldatenkov, V.A. (2005). Regulation of poly(ADP-ribose) polymerase-1 by DNA structure-specific binding. J Biol Chem *280*, 17076-17083.

Loseva, O., Jemth, A.S., Bryant, H.E., Schuler, H., Lehtio, L., Karlberg, T., and Helleday, T. (2010). PARP-3 is a mono-ADP-ribosylase that activates PARP-1 in the absence of DNA. J Biol Chem *285*, 8054-8060.

Lowary, P.T., and Widom, J. (1998). New DNA sequence rules for high affinity binding to histone octamer and sequence-directed nucleosome positioning. J Mol Biol *276*, 19-42.

Ludwig, A., Behnke, B., Holtlund, J., and Hilz, H. (1988). Immunoquantitation and size determination of intrinsic poly(ADP-ribose) polymerase from acid precipitates. An analysis of the *in vivo* status in mammalian species and in lower eukaryotes. J Biol Chem *263*, 6993-6999.

Lupardus, P.J., Byun, T., Yee, M.C., Hekmat-Nejad, M., and Cimprich, K.A. (2002). A requirement for replication in activation of the ATR-dependent DNA damage checkpoint. Genes Dev *16*, 2327-2332.

Ma, Q., Baldwin, K.T., Renzelli, A.J., McDaniel, A., and Dong, L. (2001). TCDD-inducible poly(ADP-ribose) polymerase: a novel response to 2,3,7,8-tetrachlorodibenzo-p-dioxin. Biochem Biophys Res Commun *289*, 499-506.

Maeda, D., Seki, M., Onoda, F., Branzei, D., Kawabe, Y., and Enomoto, T. (2004). Ubc9 is required for damage-tolerance and damage-induced interchromosomal homologous recombination in *S. cerevisiae*. DNA Repair (Amst) *3*, 335-341.

Mahajan, R., Delphin, C., Guan, T., Gerace, L., and Melchior, F. (1997). A small ubiquitin-related polypeptide involved in targeting RanGAP1 to nuclear pore complex protein RanBP2. Cell *88*, 97-107.

Malorni, W., Rivabene, R., Straface, E., Rainaldi, G., Monti, D., Salvioli, S., Cossarizza, A., and Franceschi, C. (1995). 3-Aminobenzamide protects cells from UV-B-induced apoptosis by acting on cytoskeleton and substrate adhesion. Biochem Biophys Res Commun *207*, 715-724.

Mao, Y., Desai, S.D., and Liu, L.F. (2000a). SUMO-1 conjugation to human DNA topoisomerase II isozymes. J Biol Chem *275*, 26066-26073.

Mao, Y., Sun, M., Desai, S.D., and Liu, L.F. (2000b). SUMO-1 conjugation to topoisomerase I: A possible repair response to topoisomerase-mediated DNA damage. Proc Natl Acad Sci USA *97*, 4046-4051.

Marahrens, Y., and Stillman, B. (1992). A yeast chromosomal origin of DNA replication defined by multiple functional elements. Science *255*, 817-823.

Marinus, M.G., and Morris, N.R. (1973). Isolation of deoxyribonucleic acid methylase mutants of Escherichia coli K-12. J Bacteriol *114*, 1143-1150.

Marsischky, G.T., Wilson, B.A., and Collier, R.J. (1995). Role of glutamic acid 988 of human poly-ADP-ribose polymerase in polymer formation. Evidence for active site similarities to the ADP-ribosylating toxins. J Biol Chem *270*, 3247-3254.

Martin, N., Schwamborn, K., Schreiber, V., Werner, A., Guillier, C., Zhang, X.D., Bischof, O., Seeler, J.S., and Dejean, A. (2009). PARP-1 transcriptional activity is regulated by sumoylation upon heat shock. EMBO J *28*, 3534-3548.

Martin, S.A., Lord, C.J., and Ashworth, A. (2008). DNA repair deficiency as a therapeutic target in cancer. Curr Opin Genet Dev *18*, 80-86.

Mascle, X.H., Germain-Desprez, D., Huynh, P., Estephan, P., and Aubry, M. (2007). Sumoylation of the transcriptional intermediary factor 1β (TIF1β), the Co-repressor of the KRAB Multifinger proteins, is required for its transcriptional activity and is modulated by the KRAB domain. J Biol Chem *282*, 10190-10202.

Masson, M., Menissier-de Murcia, J., Mattei, M.G., de Murcia, G., and Niedergang, C.P. (1997). Poly(ADP-ribose) polymerase interacts with a novel human ubiquitin conjugating enzyme: hUbc9. Gene *190*, 287-296.

Masson, M., Niedergang, C., Schreiber, V., Muller, S., Menissier-de Murcia, J., and de Murcia, G. (1998). XRCC1 is specifically associated with poly(ADP-ribose) polymerase and negatively regulates its activity following DNA damage. Mol Cell Biol *18*, 3563-3571.

Masui, Y., and Wang, P. (1998). Cell cycle transition in early embryonic development of *Xenopus* laevis. Biol Cell *90*, 537-548.

Masutani, M., Nozaki, T., Nishiyama, E., Shimokawa, T., Tachi, Y., Suzuki, H., Nakagama, H., Wakabayashi, K., and Sugimura, T. (1999). Function of poly(ADP-ribose) polymerase in response to DNA damage: gene-disruption study in mice. Mol Cell Biochem *193*, 149-152.

Matic, I., Schimmel, J., Hendriks, I.A., van Santen, M.A., van de Rijke, F., van Dam, H., Gnad, F., Mann, M., and Vertegaal, A.C. (2010). Site-Specific Identification of SUMO-2 Targets in Cells Reveals an Inverted SUMOylation Motif and a Hydrophobic Cluster SUMOylation Motif. Mol Cell *39*, 641-652.

Matic, I., van Hagen, M., Schimmel, J., Macek, B., Ogg, S.C., Tatham, M.H., Hay, R.T., Lamond, A.I., Mann, M., and Vertegaal, A.C. (2008). *In vivo* identification of human small ubiquitin-like modifier polymerization sites by high accuracy mass spectrometry and an *in vitro* to *in vivo* strategy. Mol Cell Proteomics *7*, 132-144.

Matsuda, K., Makise, M., Sueyasu, Y., Takehara, M., Asano, T., and Mizushima, T. (2007). Yeast two-hybrid analysis of the origin recognition complex of *Saccharomyces cerevisiae*: interaction between subunits and identification of binding proteins. FEMS Yeast Res *7*, 1263-1269.

Matsuo, R., Murayama, A., Saitoh, Y., Sakaki, Y., and Inokuchi, K. (2000). Identification and cataloging of genes induced by long-lasting long-term potentiation in awake rats. J Neurochem *74*, 2239-2249.

Matunis, M.J., Coutavas, E., and Blobel, G. (1996). A novel ubiquitin-like modification modulates the partitioning of the Ran-GTPase-activating protein RanGAP1 between the cytosol and the nuclear pore complex. J Cell Biol *135*, 1457-1470.

Matunis, M.J., Wu, J., and Blobel, G. (1998). SUMO-1 modification and its role in targeting the Ran GTPase-activating protein, RanGAP1, to the nuclear pore complex. J Cell Biol *140*, 499-509.

Matunis, M.J., Zhang, X.D., and Ellis, N.A. (2006). SUMO: the glue that binds. Dev Cell *11*, 596-597.

McGarry, T.J., and Kirschner, M.W. (1998). Geminin, an inhibitor of DNA replication, is degraded during mitosis. Cell *93*, 1043-1053.

Mechali, M. (2001). DNA replication origins: from sequence specificity to epigenetics. Nat Rev Genet *2*, 640-645.

Meder, V.S., Boeglin, M., de Murcia, G., and Schreiber, V. (2005). PARP-1 and PARP-2 interact with nucleophosmin/B23 and accumulate in transcriptionally active nucleoli. J Cell Sci *118*, 211-222.

Melchior, F. (2000). SUMO - Non-classical ubiquitin. Annu Rev Cell Dev Biol *16*, 591-626.

Mendez, J., Zou-Yang, X.H., Kim, S.Y., Hidaka, M., Tansey, W.P., and Stillman, B. (2002). Human origin recognition complex large subunit is degraded by ubiquitin-mediated proteolysis after initiation of DNA replication. Mol Cell *9*, 481-491.

Mendoza-Alvarez, H., and Alvarez-Gonzalez, R. (1993). Poly(ADP-ribose) polymerase is a catalytic dimer and the automodification reaction is intermolecular. J Biol Chem *268*, 22575-22580.

Mendoza-Alvarez, H., and Alvarez-Gonzalez, R. (1999). Biochemical characterization of mono(ADP-ribosyl)ated poly(ADP-ribose) polymerase. Biochemistry *38*, 3948-3953.

Mendoza-Alvarez, H., and Alvarez-Gonzalez, R. (2004). The 40 kDa carboxy-terminal domain of poly(ADP-ribose) polymerase-1 forms catalytically competent homo- and heterodimers in the absence of DNA. J Mol Biol *336*, 105-114.

Menissier de Murcia, J., Ricoul, M., Tartier, L., Niedergang, C., Huber, A., Dantzer, F., Schreiber, V., Ame, J.C., Dierich, A., LeMeur, M.*, et al.* (2003). Functional interaction between PARP-1 and PARP-2 in chromosome stability and embryonic development in mouse. EMBO J *22*, 2255-2263.

Menissier-de Murcia, J., Molinete, M., Gradwohl, G., Simonin, F., and de Murcia, G. (1989). Zinc-binding domain of poly(ADP-ribose)polymerase participates in the recognition of single strand breaks on DNA. J Mol Biol *210*, 229-233.

Merrill, J.C., Melhuish, T.A., Kagey, M.H., Yang, S.H., Sharrocks, A.D., and Wotton, D. (2010). A role for non-covalent SUMO interaction motifs in Pc2/CBX4 E3 activity. PLoS ONE *5*, e8794.

Messner, S., Altmeyer, M., Zhao, H., Pozivil, A., Roschitzki, B., Gehrig, P., Rutishauser, D., Huang, D., Caflisch, A., and Hottiger, M.O. (2010). PARP1 ADP-ribosylates lysine residues of the core histone tails. Nucleic Acids Res.

Messner, S., Schuermann, D., Altmeyer, M., Kassner, I., Schmidt, D., Schar, P., Muller, S., and Hottiger, M.O. (2009). Sumoylation of poly(ADP-ribose) polymerase 1 inhibits its acetylation and restrains transcriptional coactivator function. FASEB J *23*, 3978-3989.

Meulmeester, E., Kunze, M., Hsiao, H.H., Urlaub, H., and Melchior, F. (2008). Mechanism and consequences for paralog-specific sumoylation of ubiquitin-specific protease 25. Mol Cell *30*, 610-619.

Meyer, R.G., Meyer-Ficca, M.L., Whatcott, C.J., Jacobson, E.L., and Jacobson, M.K. (2007). Two small enzyme isoforms mediate mammalian mitochondrial poly(ADP-ribose) glycohydrolase (PARG) activity. Exp Cell Res *313*, 2920-2936.

Meyer-Ficca, M.L., Meyer, R.G., Coyle, D.L., Jacobson, E.L., and Jacobson, M.K. (2004). Human poly(ADP-ribose) glycohydrolase is expressed in alternative splice variants yielding isoforms that localize to different cell compartments. Exp Cell Res *297*, 521-532.

Miknyoczki, S.J., Jones-Bolin, S., Pritchard, S., Hunter, K., Zhao, H., Wan, W., Ator, M., Bihovsky, R., Hudkins, R., Chatterjee, S.*, et al.* (2003). Chemopotentiation of temozolomide, irinotecan, and cisplatin activity by CEP-6800, a poly(ADP-ribose) polymerase inhibitor. Mol Cancer Ther *2*, 371-382.

Mikolajczyk, J., Drag, M., Bekes, M., Cao, J.T., Ronai, Z., and Salvesen, G.S. (2007). Small ubiquitin-related modifier (SUMO)-specific proteases: profiling the specificities and activities of human SENPs. J Biol Chem *282*, 26217-26224.

Mimura, S., Masuda, T., Matsui, T., and Takisawa, H. (2000). Central role for cdc45 in establishing an initiation complex of DNA replication in *Xenopus* egg extracts. Genes Cells *5*, 439-452.

Minty, A., Dumont, X., Kaghad, M., and Caput, D. (2000). Covalent modification of p73α by SUMO-1. Two-hybrid screening with p73 identifies novel SUMO-1-interacting proteins and a SUMO-1 interaction motif. J Biol Chem *275*, 36316-36323.

Miramar, M.D., Costantini, P., Ravagnan, L., Saraiva, L.M., Haouzi, D., Brothers, G., Penninger, J.M., Peleato, M.L., Kroemer, G., and Susin, S.A. (2001). NADH oxidase activity of mitochondrial apoptosis-inducing factor. J Biol Chem *276*, 16391-16398.

Mitchell, J., Smith, G.C., and Curtin, N.J. (2009). Poly(ADP-Ribose) polymerase-1 and DNA-dependent protein kinase have equivalent roles in double strand break repair following ionizing radiation. Int J Radiat Oncol Biol Phys *75*, 1520-1527.

Miyamoto, T., Kakizawa, T., and Hashizume, K. (1999). Inhibition of nuclear receptor signalling by poly(ADP-ribose) polymerase. Mol Cell Biol *19*, 2644-2649.

Mizushima, N., Noda, T., Yoshimori, T., Tanaka, Y., Ishii, T., George, M.D., Klionsky, D.J., Ohsumi, M., and Ohsumi, Y. (1998). A protein conjugation system essential for autophagy. Nature *395*, 395-398.

Mohan, R.D., Rao, A., Gagliardi, J., and Tini, M. (2007). SUMO-1-dependent allosteric regulation of thymine DNA glycosylase alters subnuclear localization and CBP/p300 recruitment. Mol Cell Biol *27*, 229-243.

Mohideen, F., Capili, A.D., Bilimoria, P.M., Yamada, T., Bonni, A., and Lima, C.D. (2009). A molecular basis for phosphorylation-dependent SUMO conjugation by the E2 UBC9. Nat Struct Mol Biol *16*, 945-952.

Moldovan, G.L., Pfander, B., and Jentsch, S. (2006). PCNA controls establishment of sister chromatid cohesion during S phase. Mol Cell *23*, 723-732.

Molinete, M., Vermeulen, W., Burkle, A., Menissier-de Murcia, J., Kupper, J.H., Hoeijmakers, J.H., and de Murcia, G. (1993). Overproduction of the poly(ADP-ribose) polymerase DNA-binding domain blocks alkylation-induced DNA repair synthesis in mammalian cells. EMBO J *12*, 2109-2117.

Morris, J.R., Boutell, C., Keppler, M., Densham, R., Weekes, D., Alamshah, A., Butler, L., Galanty, Y., Pangon, L., Kiuchi, T.*, et al.* (2009). The SUMO modification pathway is involved in the BRCA1 response to genotoxic stress. Nature *462*, 886-890.

Morrison, C., Smith, G.C., Stingl, L., Jackson, S.P., Wagner, E.F., and Wang, Z.Q. (1997). Genetic interaction between PARP and DNA-PK in V(D)J recombination and tumorigenesis. Nat Genet *17*, 479-482.

Mortusewicz, O., Ame, J.C., Schreiber, V., and Leonhardt, H. (2007). Feedback-regulated poly(ADP-ribosyl)ation by PARP-1 is required for rapid response to DNA damage in living cells. Nucleic Acids Res *35*, 7665-7675.

Mosgoeller, W., Steiner, M., Hozak, P., Penner, E., and Wesierska-Gadek, J. (1996). Nuclear architecture and ultrastructural distribution of poly(ADP-ribosyl)transferase, a multifunctional enzyme. J Cell Sci *109 (Pt 2)*, 409-418.

Mossessova, E., and Lima, C.D. (2000). Ulp1-SUMO crystal structure and genetic analysis reveal conserved interactions and a regulatory element essential for cell growth in yeast. Mol Cell *5*, 865-876.

Motegi, A., Kuntz, K., Majeed, A., Smith, S., and Myung, K. (2006). Regulation of gross chromosomal rearrangements by ubiquitin and SUMO ligases in *Saccharomyces cerevisiae*. Mol Cell Biol *26*, 1424-1433.

Mueller-Dieckmann, C., Kernstock, S., Lisurek, M., von Kries, J.P., Haag, F., Weiss, M.S., and Koch-Nolte, F. (2006). The structure of human ADP-ribosylhydrolase 3 (ARH3) provides insights into the reversibility of protein ADP-ribosylation. Proc Natl Acad Sci USA *103*, 15026-15031.

Mukhopadhyay, D., Ayaydin, F., Kolli, N., Tan, S.H., Anan, T., Kametaka, A., Azuma, Y., Wilkinson, K.D., and Dasso, M. (2006). SUSP1 antagonizes formation of highly SUMO2/3-conjugated species. J Cell Biol *174*, 939-949.

Mullen, J.R., and Brill, S.J. (2008). Activation of the Slx5-Slx8 ubiquitin ligase by poly-small ubiquitin-like modifier conjugates. J Biol Chem *283*, 19912-19921.

Mullen, J.R., Kaliraman, V., Ibrahim, S.S., and Brill, S.J. (2001). Requirement for three novel protein complexes in the absence of the Sgs1 DNA helicase in *Saccharomyces cerevisiae*. Genetics *157*, 103-118.

Muller, S., Berger, M., Lehembre, F., Seeler, J.S., Haupt, Y., and Dejean, A. (2000). c-Jun and p53 activity is modulated by SUMO-1 modification. J Biol Chem *275*, 13321-13329.

Muromoto, R., Ishida, M., Sugiyama, K., Sekine, Y., Oritani, K., Shimoda, K., and Matsuda, T. (2006). Sumoylation of Daxx regulates IFN-induced growth suppression of B lymphocytes and the hormone receptor-mediated transactivation. J Immunol *177*, 1160-1170.

Nagashima, T., Hayashi, F., and Yokoyama, S. (2005). RIKEN Structural Genomics/Proteomics Initiative (RSGI).

Nagata, T., Nakamura, M., Kawauchi, H., and Tanigawa, Y. (1998). Conjugation of ubiquitin-like polypeptide to intracellular acceptor proteins. Biochim Biophys Acta *1401*, 319-328.

Nakamura, M., and Tanigawa, Y. (2003). Characterization of ubiquitin-like polypeptide acceptor protein, a novel pro-apoptotic member of the Bcl2 family. Eur J Biochem *270*, 4052-4058.

Nathan, D., Ingvarsdottir, K., Sterner, D.E., Bylebyl, G.R., Dokmanovic, M., Dorsey, J.A., Whelan, K.A., Krsmanovic, M., Lane, W.S., Meluh, P.B.*, et al.* (2006). Histone sumoylation is a negative regulator in *Saccharomyces cerevisiae* and shows dynamic interplay with positive-acting histone modifications. Genes Dev *20*, 966-976.

Netzer, C., Bohlander, S.K., Rieger, L., Muller, S., and Kohlhase, J. (2002). Interaction of the developmental regulator SALL1 with UBE2I and SUMO-1. Biochem Biophys Res Commun *296*, 870-876.

Nguyen, V.Q., Co, C., and Li, J.J. (2001). Cyclin-dependent kinases prevent DNA re-replication through multiple mechanisms. Nature *411*, 1068-1073.

Nie, J., Sakamoto, S., Song, D., Qu, Z., Ota, K., and Taniguchi, T. (1998). Interaction of Oct-1 and automodification domain of poly(ADP-ribose) synthetase. FEBS Lett *424*, 27-32.

Niedenthal, R. (2009). Enhanced detection of *in vivo* SUMO conjugation by Ubc9 fusion-dependent sumoylation (UFDS). Methods Mol Biol *497*, 63-79.

Niere, M., Kernstock, S., Koch-Nolte, F., and Ziegler, M. (2008). Functional localization of two poly(ADP-ribose)-degrading enzymes to the mitochondrial matrix. Mol Cell Biol *28*, 814-824.

Nirodi, C., NagDas, S., Gygi, S.P., Olson, G., Aebersold, R., and Richmond, A. (2001). A role for poly(ADP-ribose) polymerase in the transcriptional regulation of the melanoma growth stimulatory activity (CXCL1) gene expression. J Biol Chem *276*, 9366-9374.

Noel, G., Giocanti, N., Fernet, M., Megnin-Chanet, F., and Favaudon, V. (2003). Poly(ADP-ribose) polymerase (PARP-1) is not involved in DNA double-strand break recovery. BMC Cell Biol *4*, 7.

Nozaki, T., Fujihara, H., Watanabe, M., Tsutsumi, M., Nakamoto, K., Kusuoka, O., Kamada, N., Suzuki, H., Nakagama, H., Sugimura, T.*, et al.* (2003). Parp-1 deficiency implicated in colon and liver tumorigenesis induced by azoxymethane. Cancer Sci *94*, 497-500.

Nusinow, D.A., Hernandez-Munoz, I., Fazzio, T.G., Shah, G.M., Kraus, W.L., and Panning, B. (2007). Poly(ADP-ribose) polymerase 1 is inhibited by a histone H2A variant, MacroH2A, and contributes to silencing of the inactive X chromosome. J Biol Chem *282*, 12851-12859.

O'Gorman, S., Fox, D.T., and Wahl, G.M. (1991). Recombinase-mediated gene activation and site-specific integration in mammalian cells. Science *251*, 1351-1355.

Oei, S.L., Griesenbeck, J., Schweiger, M., Babich, V., Kropotov, A., and Tomilin, N. (1997). Interaction of the transcription factor YY1 with human poly(ADP-ribosyl) transferase. Biochem Biophys Res Commun *240*, 108-111.

Ogino, H., Nozaki, T., Gunji, A., Maeda, M., Suzuki, H., Ohta, T., Murakami, Y., Nakagama, H., Sugimura, T., and Masutani, M. (2007). Loss of Parp-1 affects gene expression profile in a genome-wide manner in ES cells and liver cells. BMC Genomics *8*, 41.

Ohta, S., Tatsumi, Y., Fujita, M., Tsurimoto, T., and Obuse, C. (2003). The ORC1 cycle in human cells: II. Dynamic changes in the human ORC complex during the cell cycle. J Biol Chem *278*, 41535-41540.

Oka, J., Ueda, K., Hayaishi, O., Komura, H., and Nakanishi, K. (1984). ADP-ribosyl protein lyase. Purification, properties, and identification of the product. J Biol Chem *259*, 986-995.

Oka, S., Kato, J., and Moss, J. (2006). Identification and characterization of a mammalian 39-kDa poly(ADP-ribose) glycohydrolase. J Biol Chem *281*, 705-713.

Okayama, H., Honda, M., and Hayaishi, O. (1978). Novel enzyme from rat liver that cleaves an ADP-ribosyl histone linkage. Proc Natl Acad Sci USA *75*, 2254-2257.

Okubo, S., Hara, F., Tsuchida, Y., Shimotakahara, S., Suzuki, S., Hatanaka, H., Yokoyama, S., Tanaka, H., Yasuda, H., and Shindo, H. (2004). NMR structure of the N-terminal domain of SUMO ligase PIAS1 and its interaction with tumor suppressor p53 and A/T-rich DNA oligomers. J Biol Chem *279*, 31455-31461.

Okuno, Y., Satoh, H., Sekiguchi, M., and Masukata, H. (1999). Clustered adenine/thymine stretches are essential for function of a fission yeast replication origin. Mol Cell Biol *19*, 6699-6709.

Olabisi, O.A., Soto-Nieves, N., Nieves, E., Yang, T.T., Yang, X., Yu, R.Y., Suk, H.Y., Macian, F., and Chow, C.W. (2008). Regulation of transcription factor NFAT by ADP-ribosylation. Mol Cell Biol *28*, 2860-2871.

Olsen, S.K., Capili, A.D., Lu, X., Tan, D.S., and Lima, C.D. (2010). Active site remodelling accompanies thioester bond formation in the SUMO E1. Nature *463*, 906-912.

Onishi, A., Peng, G.H., Hsu, C., Alexis, U., Chen, S., and Blackshaw, S. (2009). Pias3-dependent SUMOylation directs rod photoreceptor development. Neuron *61*, 234-246.

Ono, T., Kasamatsu, A., Oka, S., and Moss, J. (2006). The 39-kDa poly(ADP-ribose) glycohydrolase ARH3 hydrolyzes O-acetyl-ADP-ribose, a product of the Sir2 family of acetyl-histone deacetylases. Proc Natl Acad Sci USA *103*, 16687-16691.

Ouararhni, K., Hadj-Slimane, R., Ait-Si-Ali, S., Robin, P., Mietton, F., Harel-Bellan, A., Dimitrov, S., and Hamiche, A. (2006). The histone variant mH2A1.1 interferes with transcription by down-regulating PARP-1 enzymatic activity. Genes Dev *20*, 3324-3336.

Ouyang, J., Shi, Y., Valin, A., Xuan, Y., and Gill, G. (2009). Direct binding of CoREST1 to SUMO-2/3 contributes to gene-specific repression by the LSD1/CoREST1/HDAC complex. Mol Cell *34*, 145-154.

Owerbach, D., McKay, E.M., Yeh, E.T., Gabbay, K.H., and Bohren, K.M. (2005). A proline-90 residue unique to SUMO-4 prevents maturation and sumoylation. Biochem Biophys Res Commun *337*, 517-520.

Pak, D.T., Pflumm, M., Chesnokov, I., Huang, D.W., Kellum, R., Marr, J., Romanowski, P., and Botchan, M.R. (1997). Association of the origin recognition complex with heterochromatin and HP1 in higher eukaryotes. Cell *91*, 311-323.

Panse, V.G., Kuster, B., Gerstberger, T., and Hurt, E. (2003). Unconventional tethering of Ulp1 to the transport channel of the nuclear pore complex by karyopherins. Nat Cell Biol *5*, 21-27.

Panzeter, P.L., Zweifel, B., Malanga, M., Waser, S.H., Richard, M., and Althaus, F.R. (1993). Targeting of histone tails by poly(ADP-ribose). J Biol Chem *268*, 17662-17664.

Papouli, E., Chen, S., Davies, A.A., Huttner, D., Krejci, L., Sung, P., and Ulrich, H.D. (2005). Crosstalk between SUMO and ubiquitin on PCNA is mediated by recruitment of the helicase Srs2p. Mol Cell *19*, 123-133.

Park, Y., Park, S., Kang, J., Yang, S., and Kim, D. (2005). Assessing the validity of the association between the SUMO4 M55V variant and risk of type 1 diabetes. Nat Genet *37*, 112; author reply 112-113.

Parker, J.L., Bucceri, A., Davies, A.A., Heidrich, K., Windecker, H., and Ulrich, H.D. (2008). SUMO modification of PCNA is controlled by DNA. EMBO J *27*, 2422-2431.

Parnas, O., Zipin-Roitman, A., Pfander, B., Liefshitz, B., Mazor, Y., Ben-Aroya, S., Jentsch, S., and Kupiec, M. (2010). Elg1, an alternative subunit of the RFC clamp loader, preferentially interacts with SUMOylated PCNA. EMBO J.

Parsons, J.L., Dianova, II, Allinson, S.L., and Dianov, G.L. (2005). Poly(ADP-ribose) polymerase-1 protects excessive DNA strand breaks from deterioration during repair in human cell extracts. FEBS J *272*, 2012-2021.

Pavri, R., Lewis, B., Kim, T.K., Dilworth, F.J., Erdjument-Bromage, H., Tempst, P., de Murcia, G., Evans, R., Chambon, P., and Reinberg, D. (2005). PARP-1 determines specificity in a retinoid signaling pathway via direct modulation of mediator. Mol Cell *18*, 83-96.

Pedrioli, P.G., Raught, B., Zhang, X.D., Rogers, R., Aitchison, J., Matunis, M., and Aebersold, R. (2006). Automated identification of SUMOylation sites using mass spectrometry and SUMmOn pattern recognition software. Nat Methods *3*, 533-539.

Peroutka, R.J., Elshourbagy, N., Piech, T., and Butt, T.R. (2008). Enhanced protein expression in mammalian cells using engineered SUMO fusions: secreted phospholipase A2. Protein Sci *17*, 1586-1595.

Petrucco, S., and Percudani, R. (2008). Structural recognition of DNA by poly(ADP-ribose)polymerase-like zinc finger families. FEBS J *275*, 883-893.

Pfander, B., Moldovan, G.L., Sacher, M., Hoege, C., and Jentsch, S. (2005). SUMO-modified PCNA recruits Srs2 to prevent recombination during S phase. Nature *436*, 428-433.

Pichler, A., Gast, A., Seeler, J.S., Dejean, A., and Melchior, F. (2002). The nucleoporin RanBP2 has SUMO1 E3 ligase activity. Cell *108*, 109-120.

Pichler, A., Knipscheer, P., Oberhofer, E., van Dijk, W.J., Korner, R., Olsen, J.V., Jentsch, S., Melchior, F., and Sixma, T.K. (2005). SUMO modification of the ubiquitin-conjugating enzyme E2-25K. Nat Struct Mol Biol *12*, 264-269.

Pichler, A., Knipscheer, P., Saitoh, H., Sixma, T.K., and Melchior, F. (2004). The RanBP2 SUMO E3 ligase is neither HECT- nor RING-type. Nat Struct Mol Biol *11*, 984-991.

Pion, E., Bombarda, E., Stiegler, P., Ullmann, G.M., Mely, Y., de Murcia, G., and Gerard, D. (2003). Poly(ADP-ribose) polymerase-1 dimerizes at a 5' recessed DNA end *in vitro*: a fluorescence study. Biochemistry *42*, 12409-12417.

Pion, E., Ullmann, G.M., Ame, J.C., Gerard, D., de Murcia, G., and Bombarda, E. (2005). DNA-induced dimerization of poly(ADP-ribose) polymerase-1 triggers its activation. Biochemistry *44*, 14670-14681.

Pleschke, J.M., Kleczkowska, H.E., Strohm, M., and Althaus, F.R. (2000). Poly(ADP-ribose) binds to specific domains in DNA damage checkpoint proteins. J Biol Chem *275*, 40974-40980.

Plummer, R., Lorigan, P., Evans, J., Steven, N., Middleton, M., Wilson, R., Snow, K., Dewji, R., and Calvert, H. (2006). First and final report of a phase II study of the poly(ADP-ribose) polymerase (PARP) inhibitor, AG014699, in combination with temozolomide (TMZ) in patients with metastatic malignant melanoma (MM). J Clin Oncol (Meeting Abstracts) *24*, 8013-.

Poirier, G.G., de Murcia, G., Jongstra-Bilen, J., Niedergang, C., and Mandel, P. (1982). Poly(ADP-ribosyl)ation of polynucleosomes causes relaxation of chromatin structure. Proc Natl Acad Sci USA *79*, 3423-3427.

Potaman, V.N., Shlyakhtenko, L.S., Oussatcheva, E.A., Lyubchenko, Y.L., and Soldatenkov, V.A. (2005). Specific binding of poly(ADP-ribose) polymerase-1 to cruciform hairpins. J Mol Biol *348*, 609-615.

Potts, P.R., and Yu, H. (2005). Human MMS21/NSE2 is a SUMO ligase required for DNA repair. Mol Cell Biol *25*, 7021-7032.

Prasad, R., Lavrik, O.I., Kim, S.J., Kedar, P., Yang, X.P., Vande Berg, B.J., and Wilson, S.H. (2001). DNA polymerase β-mediated long patch base excision repair. Poly(ADP-ribose)polymerase-1 stimulates strand displacement DNA synthesis. J Biol Chem *276*, 32411-32414.

Prasanth, S.G., Prasanth, K.V., and Stillman, B. (2002). Orc6 involved in DNA replication, chromosome segregation, and cytokinesis. Science *297*, 1026-1031.

Prudden, J., Pebernard, S., Raffa, G., Slavin, D.A., Perry, J.J., Tainer, J.A., McGowan, C.H., and Boddy, M.N. (2007). SUMO-targeted ubiquitin ligases in genome stability. EMBO J *26*, 4089-4101.

Pungaliya, P., Kulkarni, D., Park, H.J., Marshall, H., Zheng, H., Lackland, H., Saleem, A., and Rubin, E.H. (2007). TOPORS functions as a SUMO-1 E3 ligase for chromatin-modifying proteins. J Proteome Res *6*, 3918-3923.

Purnell, M.R., and Whish, W.J. (1980). Novel inhibitors of poly(ADP-ribose) synthetase. Biochem J *185*, 775-777.

Qu, H., Bharaj, B., Liu, X.Q., Curtis, J.A., Newhook, L.A., Paterson, A.D., Hudson, T.J., and Polychronakos, C. (2005). Assessing the validity of the association between the SUMO4 M55V variant and risk of type 1 diabetes. Nat Genet *37*, 111-112; author reply 112-113.

Raasi, S., Schmidtke, G., de Giuli, R., and Groettrup, M. (1999). A ubiquitin-like protein which is synergistically inducible by interferon-γ and tumor necrosis factor-α. Eur J Immunol *29*, 4030-4036.

Raasi, S., Schmidtke, G., and Groettrup, M. (2001). The ubiquitin-like protein FAT10 forms covalent conjugates and induces apoptosis. J Biol Chem *276*, 35334-35343.

Rajendra, R., Malegaonkar, D., Pungaliya, P., Marshall, H., Rasheed, Z., Brownell, J., Liu, L.F., Lutzker, S., Saleem, A., and Rubin, E.H. (2004). Topors functions as an E3 ubiquitin ligase with specific E2 enzymes and ubiquitinates p53. J Biol Chem *279*, 36440-36444.

Ramelot, T.A., Cort, J.R., Yee, A.A., Semesi, A., Edwards, A.M., Arrowsmith, C.H., and Kennedy, M.A. (2003). Solution structure of the yeast ubiquitin-like modifier protein Hub1. J Struct Funct Genomics *4*, 25-30.

Rao, H., and Stillman, B. (1995). The origin recognition complex interacts with a bipartite DNA binding site within yeast replicators. Proc Natl Acad Sci USA *92*, 2224-2228.

Raval-Fernandes, S., Kickhoefer, V.A., Kitchen, C., and Rome, L.H. (2005). Increased susceptibility of vault poly(ADP-ribose) polymerase-deficient mice to carcinogen-induced tumorigenesis. Cancer Res *65*, 8846-8852.

Reale, A., Matteis, G.D., Galleazzi, G., Zampieri, M., and Caiafa, P. (2005). Modulation of DNMT1 activity by ADP-ribose polymers. Oncogene *24*, 13-19.

Realini, C.A., and Althaus, F.R. (1992). Histone shuttling by poly(ADP-ribosylation). J Biol Chem *267*, 18858-18865.

Rein, T., Kobayashi, T., Malott, M., Leffak, M., and DePamphilis, M.L. (1999). DNA methylation at mammalian replication origins. J Biol Chem *274*, 25792-25800.

Reindle, A., Belichenko, I., Bylebyl, G.R., Chen, X.L., Gandhi, N., and Johnson, E.S. (2006). Multiple domains in Siz SUMO ligases contribute to substrate selectivity. J Cell Sci *119*, 4749-4757.

Remus, D., Beuron, F., Tolun, G., Griffith, J.D., Morris, E.P., and Diffley, J.F. (2009). Concerted loading of Mcm2-7 double hexamers around DNA during DNA replication origin licensing. Cell *139*, 719-730.

Ren, J., Gao, X., Jin, C., Zhu, M., Wang, X., Shaw, A., Wen, L., Yao, X., and Xue, Y. (2009). Systematic study of protein sumoylation: Development of a site-specific predictor of SUMOsp 2.0. Proteomics *9*, 3409-3412.

Reverter, D., and Lima, C.D. (2004). A basis for SUMO protease specificity provided by analysis of human Senp2 and a Senp2-SUMO complex. Structure *12*, 1519-1531.

Reverter, D., and Lima, C.D. (2005). Insights into E3 ligase activity revealed by a SUMO-RanGAP1-Ubc9-Nup358 complex. Nature *435*, 687-692.

Reverter, D., and Lima, C.D. (2006). Structural basis for SENP2 protease interactions with SUMO precursors and conjugated substrates. Nat Struct Mol Biol *13*, 1060-1068.

Richardson, C.D., ed. (1995). Baculovirus Expression Protocols (New York, Springer).

Riquelme, P.T., Burzio, L.O., and Koide, S.S. (1979). ADP ribosylation of rat liver lysine-rich histone *in vitro*. J Biol Chem *254*, 3018-3028.

Robert, T., Dervins, D., Fabre, F., and Gangloff, S. (2006). Mrc1 and Srs2 are major actors in the regulation of spontaneous crossover. EMBO J *25*, 2837-2846.

Rodriguez, M.S., Dargemont, C., and Hay, R.T. (2001). SUMO-1 conjugation *in vivo* requires both a consensus modification motif and nuclear targeting. J Biol Chem *276*, 12654-12659.

Rog, O., Miller, K.M., Ferreira, M.G., and Cooper, J.P. (2009). Sumoylation of RecQ helicase controls the fate of dysfunctional telomeres. Mol Cell *33*, 559-569.

Rolli, V., O'Farrell, M., Menissier-de Murcia, J., and de Murcia, G. (1997). Random mutagenesis of the poly(ADP-ribose) polymerase catalytic domain reveals amino acids involved in polymer branching. Biochemistry *36*, 12147-12154.

Rosas-Acosta, G., Russell, W.K., Deyrieux, A., Russell, D.H., and Wilson, V.G. (2005). A universal strategy for proteomic studies of SUMO and other ubiquitin-like modifiers. Mol Cell Proteomics *4*, 56-72.

Roscic, A., Moller, A., Calzado, M.A., Renner, F., Wimmer, V.C., Gresko, E., Ludi, K.S., and Schmitz, M.L. (2006). Phosphorylation-dependent control of Pc2 SUMO E3 ligase activity by its substrate protein HIPK2. Mol Cell *24*, 77-89.

Ross, S., Best, J.L., Zon, L.I., and Gill, G. (2002). SUMO-1 modification represses Sp3 transcriptional activation and modulates its subnuclear localization. Mol Cell *10*, 831-842.

Rossi, M.N., Carbone, M., Mostocotto, C., Mancone, C., Tripodi, M., Maione, R., and Amati, P. (2009). Mitochondrial localization of PARP-1 requires interaction with mitofilin and is involved in the maintenance of mitochondrial DNA integrity. J Biol Chem *284*, 31616-31624.

Rouleau, M., McDonald, D., Gagne, P., Ouellet, M.E., Droit, A., Hunter, J.M., Dutertre, S., Prigent, C., Hendzel, M.J., and Poirier, G.G. (2007). PARP-3 associates with polycomb group bodies and with components of the DNA damage repair machinery. J Cell Biochem *100*, 385-401.

Rouleau, M., Patel, A., Hendzel, M.J., Kaufmann, S.H., and Poirier, G.G. (2010). PARP inhibition: PARP1 and beyond. Nat Rev Cancer *10*, 293-301.

Rowles, A., Tada, S., and Blow, J.J. (1999). Changes in association of the *Xenopus* origin recognition complex with chromatin on licensing of replication origins. J Cell Sci *112 (Pt 12)*, 2011-2018.

Rowley, A., Cocker, J.H., Harwood, J., and Diffley, J.F. (1995). Initiation complex assembly at budding yeast replication origins begins with the recognition of a bipartite sequence by limiting amounts of the initiator, ORC. EMBO J *14*, 2631-2641.

Rudat, V., Bachmann, N., Kupper, J.H., and Weber, K.J. (2001). Overexpression of the DNA-binding domain of poly(ADP-ribose) polymerase inhibits rejoining of ionizing radiation-induced DNA double-strand breaks. Int J Radiat Biol *77*, 303-307.

Ruf, A., Mennissier de Murcia, J., de Murcia, G., and Schulz, G.E. (1996). Structure of the catalytic fragment of poly(AD-ribose) polymerase from chicken. Proc Natl Acad Sci USA *93*, 7481-7485.

Rytinki, M.M., and Palvimo, J.J. (2009). SUMOylation attenuates the function of PGC-1α. J Biol Chem *284*, 26184-26193.

Ryu, H., Al-Ani, G., Deckert, K., Kirkpatrick, D., Gygi, S.P., Dasso, M., and Azuma, Y. (2010). PIASy mediates SUMO-2/3 conjugation of poly(ADP-ribose) polymerase 1 (PARP1) on mitotic chromosomes. J Biol Chem *285*, 14415-14423.

Sacher, M., Pfander, B., Hoege, C., and Jentsch, S. (2006). Control of Rad52 recombination activity by double-strand break-induced SUMO modification. Nat Cell Biol *8*, 1284-1290.

Saintigny, Y., Delacote, F., Vares, G., Petitot, F., Lambert, S., Averbeck, D., and Lopez, B.S. (2001). Characterization of homologous recombination induced by replication inhibition in mammalian cells. Embo J *20*, 3861-3870.

Saitoh, H., and Hinchey, J. (2000). Functional heterogeneity of small ubiquitin-related protein modifiers SUMO-1 versus SUMO-2/3. J Biol Chem *275*, 6252-6258.

Saitoh, H., Pizzi, M.D., and Wang, J. (2002). Perturbation of SUMOlation enzyme Ubc9 by distinct domain within nucleoporin RanBP2/Nup358. J Biol Chem *277*, 4755-4763.

Saitoh, H., Pu, R., Cavenagh, M., and Dasso, M. (1997). RanBP2 associates with Ubc9p and a modified form of RanGAP1. Proc Natl Acad Sci USA *94*, 3736-3741.

Saitoh, H., Sparrow, D.B., Shiomi, T., Pu, R.T., Nishimoto, T., Mohun, T.J., and Dasso, M. (1998). Ubc9p and the conjugation of SUMO-1 to RanGAP1 and RanBP2. Curr Biol *8*, 121-124.

Sambrook, J., and Russell, D.W. (2001). Molecular Cloning: A Laboratory Manual, Third edn (New York, Cold Spring Harbour Laboratory Press).

Santocanale, C., and Diffley, J.F. (1998). A Mec1- and Rad53-dependent checkpoint controls late-firing origins of DNA replication. Nature *395*, 615-618.

Sapetschnig, A., Rischitor, G., Braun, H., Doll, A., Schergaut, M., Melchior, F., and Suske, G. (2002). Transcription factor Sp3 is silenced through SUMO modification by PIAS1. EMBO J *21*, 5206-5215.

Sasaki, T., and Gilbert, D.M. (2007). The many faces of the origin recognition complex. Curr Opin Cell Biol *19*, 337-343.

Sastry, S.S., Buki, K.G., and Kun, E. (1989). Binding of adenosine diphosphoribosyltransferase to the termini and internal regions of linear DNAs. Biochemistry *28*, 5670-5680.

Sastry, S.S., and Kun, E. (1988). Molecular interactions between DNA, poly(ADP-ribose) polymerase, and histones. J Biol Chem *263*, 1505-1512.

Sastry, S.S., and Kun, E. (1990). The interaction of adenosine diphosphoribosyl transferase (ADPRT) with a cruciform DNA. Biochem Biophys Res Commun *167*, 842-847.

Satoh, M.S., and Lindahl, T. (1992). Role of poly(ADP-ribose) formation in DNA repair. Nature *356*, 356-358.

Satoh, M.S., Poirier, G.G., and Lindahl, T. (1993). NAD^+-dependent repair of damaged DNA by human cell extracts. J Biol Chem *268*, 5480-5487.

Saxena, A., Saffery, R., Wong, L.H., Kalitsis, P., and Choo, K.H. (2002). Centromere proteins Cenpa, Cenpb, and Bub3 interact with poly(ADP-ribose) polymerase-1 protein and are poly(ADP-ribosyl)ated. J Biol Chem *277*, 26921-26926.

Schimmel, J., Balog, C.I., Deelder, A.M., Drijfhout, J.W., Hensbergen, P.J., and Vertegaal, A.C. (2010). Positively charged amino acids flanking a sumoylation consensus tetramer on the 110kDa tri-snRNP component SART1 enhance sumoylation efficiency. J Proteomics *73*, 1523-1534.

Schreiber, V., Ame, J.C., Dolle, P., Schultz, I., Rinaldi, B., Fraulob, V., Menissier-de Murcia, J., and de Murcia, G. (2002). Poly(ADP-ribose) polymerase-2 (PARP-2) is required for efficient base excision DNA repair in association with PARP-1 and XRCC1. J Biol Chem *277*, 23028-23036.

Schreiber, V., Dantzer, F., Ame, J.C., and de Murcia, G. (2006). Poly(ADP-ribose): novel functions for an old molecule. Nat Rev Mol Cell Biol *7*, 517-528.

Schreiber, V., Molinete, M., Boeuf, H., de Murcia, G., and Menissier-de Murcia, J. (1992). The human poly(ADP-ribose) polymerase nuclear localization signal is a bipartite element functionally separate from DNA binding and catalytic activity. EMBO J *11*, 3263-3269.

Schultz, N., Lopez, E., Saleh-Gohari, N., and Helleday, T. (2003). Poly(ADP-ribose) polymerase (PARP-1) has a controlling role in homologous recombination. Nucleic Acids Res *31*, 4959-4964.

Schwamborn, K., Knipscheer, P., van Dijk, E., van Dijk, W.J., Sixma, T.K., Meloen, R.H., and Langedijk, J.P. (2008). SUMO assay with peptide arrays on solid support: insights into SUMO target sites. J Biochem *144*, 39-49.

Schwartz, D.C., Felberbaum, R., and Hochstrasser, M. (2007). The Ulp2 SUMO protease is required for cell division following termination of the DNA damage checkpoint. Mol Cell Biol *27*, 6948-6961.

Segurado, M., de Luis, A., and Antequera, F. (2003). Genome-wide distribution of DNA replication origins at A+T-rich islands in *Schizosaccharomyces pombe*. EMBO Rep *4*, 1048-1053.

Shalizi, A., Gaudilliere, B., Yuan, Z., Stegmuller, J., Shirogane, T., Ge, Q., Tan, Y., Schulman, B., Harper, J.W., and Bonni, A. (2006). A calcium-regulated MEF2 sumoylation switch controls postsynaptic differentiation. Science *311*, 1012-1017.

Shall, S., and de Murcia, G. (2000). Poly(ADP-ribose) polymerase-1: what have we learned from the deficient mouse model? Mutat Res *460*, 1-15.

Shao, W., Fanelli, M., Ferrara, F.F., Riccioni, R., Rosenauer, A., Davison, K., Lamph, W.W., Waxman, S., Pelicci, P.G., Lo Coco, F.*, et al.* (1998). Arsenic trioxide as an inducer of apoptosis and loss of PML/RARα protein in acute promyelocytic leukemia cells. J Natl Cancer Inst *90*, 124-133.

Shen, L., Tatham, M.H., Dong, C., Zagorska, A., Naismith, J.H., and Hay, R.T. (2006a). SUMO protease SENP1 induces isomerization of the scissile peptide bond. Nat Struct Mol Biol *13*, 1069-1077.

Shen, L.N., Geoffroy, M.C., Jaffray, E.G., and Hay, R.T. (2009). Characterization of SENP7, a SUMO-2/3-specific isopeptidase. Biochem J *421*, 223-230.

Shen, T.H., Lin, H.K., Scaglioni, P.P., Yung, T.M., and Pandolfi, P.P. (2006b). The mechanisms of PML-nuclear body formation. Mol Cell *24*, 331-339.

Shieh, W.M., Ame, J.C., Wilson, M.V., Wang, Z.Q., Koh, D.W., Jacobson, M.K., and Jacobson, E.L. (1998). Poly(ADP-ribose) polymerase null mouse cells synthesize ADP-ribose polymers. J Biol Chem *273*, 30069-30072.

Shimada, K., and Gasser, S.M. (2007). The origin recognition complex functions in sister-chromatid cohesion in *Saccharomyces cerevisiae*. Cell *128*, 85-99.

Shiokawa, D., Maruta, H., and Tanuma, S. (1997). Inhibitors of poly(ADP-ribose) polymerase suppress nuclear fragmentation and apoptotic-body formation during apoptosis in HL-60 cells. FEBS Lett *413*, 99-103.

Siddiqui, K., and Stillman, B. (2007). ATP-dependent assembly of the human origin recognition complex. J Biol Chem *282*, 32370-32383.

Siegfried, Z., and Cedar, H. (1997). DNA methylation: a molecular lock. Curr Biol *7*, R305-307.

Simbulan-Rosenthal, C.M., Haddad, B.R., Rosenthal, D.S., Weaver, Z., Coleman, A., Luo, R., Young, H.M., Wang, Z.Q., Ried, T., and Smulson, M.E. (1999). Chromosomal aberrations in PARP(-/-) mice: genome stabilization in immortalized cells by reintroduction of poly(ADP-ribose) polymerase cDNA. Proc Natl Acad Sci USA *96*, 13191-13196.

Simbulan-Rosenthal, C.M., Ly, D.H., Rosenthal, D.S., Konopka, G., Luo, R., Wang, Z.Q., Schultz, P.G., and Smulson, M.E. (2000). Misregulation of gene expression in primary fibroblasts lacking poly(ADP-ribose) polymerase. Proc Natl Acad Sci USA *97*, 11274-11279.

Simbulan-Rosenthal, C.M., Rosenthal, D.S., Iyer, S., Boulares, A.H., and Smulson, M.E. (1998). Transient poly(ADP-ribosyl)ation of nuclear proteins and role of poly(ADP-ribose) polymerase in the early stages of apoptosis. J Biol Chem *273*, 13703-13712.

Simbulan-Rosenthal, C.M., Rosenthal, D.S., Luo, R., Samara, R., Espinoza, L.A., Hassa, P.O., Hottiger, M.O., and Smulson, M.E. (2003). PARP-1 binds E2F-1 independently of its DNA binding and catalytic domains, and acts as a novel coactivator of E2F-1-mediated transcription during re-entry of quiescent cells into S phase. Oncogene *22*, 8460-8471.

Simonin, F., Menissier-de Murcia, J., Poch, O., Muller, S., Gradwohl, G., Molinete, M., Penning, C., Keith, G., and de Murcia, G. (1990). Expression and site-directed mutagenesis of the catalytic domain of human poly(ADP-ribose)polymerase in *Escherichia coli*. Lysine 893 is critical for activity. J Biol Chem *265*, 19249-19256.

Skilton, A., Ho, J.C., Mercer, B., Outwin, E., and Watts, F.Z. (2009). SUMO chain formation is required for response to replication arrest in *S. pombe*. PLoS ONE *4*, e6750.

Smith, L.M., Willmore, E., Austin, C.A., and Curtin, N.J. (2005). The novel poly(ADP-Ribose) polymerase inhibitor, AG14361, sensitizes cells to topoisomerase I poisons by increasing the persistence of DNA strand breaks. Clin Cancer Res *11*, 8449-8457.

Smith, S., and de Lange, T. (2000). Tankyrase promotes telomere elongation in human cells. Curr Biol *10*, 1299-1302.

Smith, S., Giriat, I., Schmitt, A., and de Lange, T. (1998). Tankyrase, a poly(ADP-ribose) polymerase at human telomeres. Science *282*, 1484-1487.

Smulson, M.E., Simbulan-Rosenthal, C.M., Boulares, A.H., Yakovlev, A., Stoica, B., Iyer, S., Luo, R., Haddad, B., Wang, Z.Q., Pang, T.*, et al.* (2000). Roles of poly(ADP-ribosyl)ation and PARP in apoptosis, DNA repair, genomic stability and functions of p53 and E2F-1. Adv Enzyme Regul *40*, 183-215.

Smyth, D.J., Howson, J.M., Lowe, C.E., Walker, N.M., Lam, A.C., Nutland, S., Hutchings, J., Tuomilehto-Wolf, E., Tuomilehto, J., Guja, C.*, et al.* (2005). Assessing the validity of the association between the SUMO4 M55V variant and risk of type 1 diabetes. Nat Genet *37*, 110-111; author reply 112-113.

Soldatenkov, V.A., Chasovskikh, S., Potaman, V.N., Trofimova, I., Smulson, M.E., and Dritschilo, A. (2002). Transcriptional repression by binding of poly(ADP-ribose) polymerase to promoter sequences. J Biol Chem *277*, 665-670.

Soldatenkov, V.A., and Potaman, V.N. (2004). DNA-binding properties of poly(ADP-ribose) polymerase: a target for anticancer therapy. Curr Drug Targets *5*, 357-365.

Soldatenkov, V.A., Vetcher, A.A., Duka, T., and Ladame, S. (2008). First evidence of a functional interaction between DNA quadruplexes and poly(ADP-ribose) polymerase-1. ACS Chem Biol *3*, 214-219.

Solomon, M.J., Glotzer, M., Lee, T.H., Philippe, M., and Kirschner, M.W. (1990). Cyclin activation of p34cdc2. Cell *63*, 1013-1024.

Song, J., Durrin, L.K., Wilkinson, T.A., Krontiris, T.G., and Chen, Y. (2004). Identification of a SUMO-binding motif that recognizes SUMO-modified proteins. Proc Natl Acad Sci USA *101*, 14373-14378.

Song, J., Zhang, Z., Hu, W., and Chen, Y. (2005). Small ubiquitin-like modifier (SUMO) recognition of a SUMO binding motif: a reversal of the bound orientation. J Biol Chem *280*, 40122-40129.

Speck, C., Chen, Z., Li, H., and Stillman, B. (2005). ATPase-dependent cooperative binding of ORC and Cdc6 to origin DNA. Nat Struct Mol Biol *12*, 965-971.

Stankovic-Valentin, N., Deltour, S., Seeler, J., Pinte, S., Vergoten, G., Guerardel, C., Dejean, A., and Leprince, D. (2007). An acetylation/deacetylation-SUMOylation switch through a phylogenetically conserved ΨKXEP motif in the tumor suppressor HIC1 regulates transcriptional repression activity. Mol Cell Biol *27*, 2661-2675.

Steinacher, R., and Schar, P. (2005). Functionality of human thymine DNA glycosylase requires SUMO-regulated changes in protein conformation. Curr Biol *15*, 616-623.

Stelter, P., and Ulrich, H.D. (2003). Control of spontaneous and damage-induced mutagenesis by SUMO and ubiquitin conjugation. Nature *425*, 188-191.

Stros, M. (2010). HMGB proteins: interactions with DNA and chromatin. Biochim Biophys Acta *1799*, 101-113.

Su, H.L., and Li, S.S. (2002). Molecular features of human ubiquitin-like SUMO genes and their encoded proteins. Gene *296*, 65-73.

Subramanian, L., Benson, M.D., and Iniguez-Lluhi, J.A. (2003). A synergy control motif within the attenuator domain of CCAAT/enhancer-binding protein α inhibits transcriptional synergy

through its PIASy-enhanced modification by SUMO-1 or SUMO-3. J Biol Chem *278*, 9134-9141.

Sugimura, K., Takebayashi, S., Taguchi, H., Takeda, S., and Okumura, K. (2008). PARP-1 ensures regulation of replication fork progression by homologous recombination on damaged DNA. J Cell Biol *183*, 1203-1212.

Sun, H., Leverson, J.D., and Hunter, T. (2007). Conserved function of RNF4 family proteins in eukaryotes: targeting a ubiquitin ligase to SUMOylated proteins. EMBO J *26*, 4102-4112.

Susin, S.A., Lorenzo, H.K., Zamzami, N., Marzo, I., Snow, B.E., Brothers, G.M., Mangion, J., Jacotot, E., Costantini, P., Loeffler, M*., et al.* (1999). Molecular characterization of mitochondrial apoptosis-inducing factor. Nature *397*, 441-446.

Suzuki, H., Quesada, P., Farina, B., and Leone, E. (1986). *In vitro* poly(ADP-ribosyl)ation of seminal ribonuclease. J Biol Chem *261*, 6048-6055.

Suzuki, R., Shindo, H., Tase, A., Kikuchi, Y., Shimizu, M., and Yamazaki, T. (2009). Solution structures and DNA binding properties of the N-terminal SAP domains of SUMO E3 ligases from *Saccharomyces cerevisiae* and *Oryza sativa*. Proteins *75*, 336-347.

Tada, S., Li, A., Maiorano, D., Mechali, M., and Blow, J.J. (2001). Repression of origin assembly in metaphase depends on inhibition of RLF-B/Cdt1 by geminin. Nat Cell Biol *3*, 107-113.

Takahashi, H., Hatakeyama, S., Saitoh, H., and Nakayama, K.I. (2005). Noncovalent SUMO-1 binding activity of thymine DNA glycosylase (TDG) is required for its SUMO-1 modification and colocalization with the promyelocytic leukemia protein. J Biol Chem *280*, 5611-5621.

Takahashi, Y., and Kikuchi, Y. (2005). Yeast PIAS-type Ull1/Siz1 is composed of SUMO ligase and regulatory domains. J Biol Chem *280*, 35822-35828.

Takahashi, Y., and Strunnikov, A. (2008). *In vivo* modeling of polysumoylation uncovers targeting of Topoisomerase II to the nucleolus via optimal level of SUMO modification. Chromosoma *117*, 189-198.

Takahashi, Y., Yong-Gonzalez, V., Kikuchi, Y., and Strunnikov, A. (2006). *SIZ1*/*SIZ2* control of chromosome transmission fidelity is mediated by the sumoylation of topoisomerase II. Genetics *172*, 783-794.

Takeda, D.Y., and Dutta, A. (2005). DNA replication and progression through S phase. Oncogene *24*, 2827-2843.

Tan, J.A., Sun, Y., Song, J., Chen, Y., Krontiris, T.G., and Durrin, L.K. (2008). SUMO conjugation to the matrix attachment region-binding protein, special AT-rich sequence-binding protein-1 (SATB1), targets SATB1 to promyelocytic nuclear bodies where it undergoes caspase cleavage. J Biol Chem *283*, 18124-18134.

Tanaka, K., Nishide, J., Okazaki, K., Kato, H., Niwa, O., Nakagawa, T., Matsuda, H., Kawamukai, M., and Murakami, Y. (1999). Characterization of a fission yeast SUMO-1 homologue, Pmt3p, required for multiple nuclear events, including the control of telomere length and chromosome segregation. Mol Cell Biol *19*, 8660-8672.

Tao, Z., Gao, P., Hoffman, D.W., and Liu, H.W. (2008). Domain C of human poly(ADP-ribose) polymerase-1 is important for enzyme activity and contains a novel zinc-ribbon motif. Biochemistry *47*, 5804-5813.

Tao, Z., Gao, P., and Liu, H.W. (2009). Identification of the ADP-ribosylation sites in the PARP-1 automodification domain: analysis and implications. J Am Chem Soc *131*, 14258-14260.

Tatham, M.H., Chen, Y., and Hay, R.T. (2003a). Role of two residues proximal to the active site of Ubc9 in substrate recognition by the Ubc9.SUMO-1 thiolester complex. Biochemistry *42*, 3168-3179.

Tatham, M.H., Geoffroy, M.C., Shen, L., Plechanovova, A., Hattersley, N., Jaffray, E.G., Palvimo, J.J., and Hay, R.T. (2008). RNF4 is a poly-SUMO-specific E3 ubiquitin ligase required for arsenic-induced PML degradation. Nat Cell Biol *10*, 538-546.

Tatham, M.H., Jaffray, E., Vaughan, O.A., Desterro, J.M., Botting, C.H., Naismith, J.H., and Hay, R.T. (2001). Polymeric chains of SUMO-2 and SUMO-3 are conjugated to protein substrates by SAE1/SAE2 and Ubc9. J Biol Chem *276*, 35368-35374.

Tatham, M.H., Kim, S., Jaffray, E., Song, J., Chen, Y., and Hay, R.T. (2005). Unique binding interactions among Ubc9, SUMO and RanBP2 reveal a mechanism for SUMO paralog selection. Nat Struct Mol Biol *12*, 67-74.

Tatham, M.H., Kim, S., Yu, B., Jaffray, E., Song, J., Zheng, J., Rodriguez, M.S., Hay, R.T., and Chen, Y. (2003b). Role of an N-terminal site of Ubc9 in SUMO-1, -2, and -3 binding and conjugation. Biochemistry *42*, 9959-9969.

Taylor, D.L., Ho, J.C., Oliver, A., and Watts, F.Z. (2002). Cell-cycle-dependent localisation of Ulp1, a *Schizosaccharomyces pombe* Pmt3 (SUMO)-specific protease. J Cell Sci *115*, 1113-1122.

Tentori, L., and Graziani, G. (2005). Chemopotentiation by PARP inhibitors in cancer therapy. Pharmacol Res *52*, 25-33.

Tentori, L., Orlando, L., Lacal, P.M., Benincasa, E., Faraoni, I., Bonmassar, E., D'Atri, S., and Graziani, G. (1997). Inhibition of O6-alkylguanine DNA-alkyltransferase or poly(ADP-ribose) polymerase increases susceptibility of leukemic cells to apoptosis induced by temozolomide. Mol Pharmacol *52*, 249-258.

Thibodeau, J., Potvin, F., Kirkland, J.B., and Poirier, G. (1993). Expression in *Escherichia coli* of the 36 kDa domain of poly(ADP-ribose) polymerase and investigation of its DNA binding properties. Biochim Biophys Acta *1163*, 49-53.

Tiefenbach, J., Novac, N., Ducasse, M., Eck, M., Melchior, F., and Heinzel, T. (2006). SUMOylation of the corepressor N-CoR modulates its capacity to repress transcription. Mol Biol Cell *17*, 1643-1651.

Timinszky, G., Till, S., Hassa, P.O., Hothorn, M., Kustatscher, G., Nijmeijer, B., Colombelli, J., Altmeyer, M., Stelzer, E.H., Scheffzek, K.*, et al.* (2009). A macrodomain-containing histone rearranges chromatin upon sensing PARP1 activation. Nat Struct Mol Biol *16*, 923-929.

Tini, M., Benecke, A., Um, S.J., Torchia, J., Evans, R.M., and Chambon, P. (2002). Association of CBP/p300 acetylase and thymine DNA glycosylase links DNA repair and transcription. Mol Cell *9*, 265-277.

Tong, W.M., Cortes, U., Hande, M.P., Ohgaki, H., Cavalli, L.R., Lansdorp, P.M., Haddad, B.R., and Wang, Z.Q. (2002). Synergistic role of Ku80 and poly(ADP-ribose) polymerase in suppressing chromosomal aberrations and liver cancer formation. Cancer Res *62*, 6990-6996.

Tong, W.M., Hande, M.P., Lansdorp, P.M., and Wang, Z.Q. (2001). DNA strand break-sensing molecule poly(ADP-Ribose) polymerase cooperates with p53 in telomere function, chromosome stability, and tumor suppression. Mol Cell Biol *21*, 4046-4054.

Torres-Rosell, J., Sunjevaric, I., De Piccoli, G., Sacher, M., Eckert-Boulet, N., Reid, R., Jentsch, S., Rothstein, R., Aragon, L., and Lisby, M. (2007). The Smc5-Smc6 complex and SUMO modification of Rad52 regulates recombinational repair at the ribosomal gene locus. Nat Cell Biol *9*, 923-931.

Triolo, T., and Sternglanz, R. (1996). Role of interactions between the origin recognition complex and SIR1 in transcriptional silencing. Nature *381*, 251-253.

Trucco, C., Flatter, E., Fribourg, S., de Murcia, G., and Menissier-de Murcia, J. (1996). Mutations in the amino-terminal domain of the human poly(ADP-ribose) polymerase that affect its catalytic activity but not its DNA binding capacity. FEBS Lett *399*, 313-316.

Trucco, C., Oliver, F.J., de Murcia, G., and Menissier-de Murcia, J. (1998). DNA repair defect in poly(ADP-ribose) polymerase-deficient cell lines. Nucleic Acids Res *26*, 2644-2649.

Tsalik, E.L., and Gartenberg, M.R. (1998). Curing *Saccharomyces cerevisiae* of the 2-µm plasmid by targeted DNA damage. Yeast *14*, 847-852.

Tsuruzoe, S., Ishihara, K., Uchimura, Y., Watanabe, S., Sekita, Y., Aoto, T., Saitoh, H., Yuasa, Y., Niwa, H., Kawasuji, M.*, et al.* (2006). Inhibition of DNA binding of Sox2 by the SUMO conjugation. Biochem Biophys Res Commun *351*, 920-926.

Tsutsumi, M., Masutani, M., Nozaki, T., Kusuoka, O., Tsujiuchi, T., Nakagama, H., Suzuki, H., Konishi, Y., and Sugimura, T. (2001). Increased susceptibility of poly(ADP-ribose) polymerase-1 knockout mice to nitrosamine carcinogenicity. Carcinogenesis *22*, 1-3.

Tugal, T., Zou-Yang, X.H., Gavin, K., Pappin, D., Canas, B., Kobayashi, R., Hunt, T., and Stillman, B. (1998). The Orc4p and Orc5p subunits of the *Xenopus* and human origin recognition complex are related to Orc1p and Cdc6p. J Biol Chem *273*, 32421-32429.

Tulin, A., Naumova, N.M., Menon, A.K., and Spradling, A.C. (2006). *Drosophila* poly(ADP-ribose) glycohydrolase mediates chromatin structure and SIR2-dependent silencing. Genetics *172*, 363-371.

Tulin, A., and Spradling, A. (2003). Chromatin loosening by poly(ADP)-ribose polymerase (PARP) at *Drosophila* puff loci. Science *299*, 560-562.

Uchida, K., Hanai, S., Ishikawa, K., Ozawa, Y., Uchida, M., Sugimura, T., and Miwa, M. (1993). Cloning of cDNA encoding *Drosophila* poly(ADP-ribose) polymerase: leucine zipper in the auto-modification domain. Proc Natl Acad Sci USA *90*, 3481-3485.

Uetz, P., Giot, L., Cagney, G., Mansfield, T.A., Judson, R.S., Knight, J.R., Lockshon, D., Narayan, V., Srinivasan, M., Pochart, P.*, et al.* (2000). A comprehensive analysis of protein-protein interactions in *Saccharomyces cerevisiae*. Nature *403*, 623-627.

Ulrich, H.D. (2005). The *RAD6* pathway: control of DNA damage bypass and mutagenesis by ubiquitin and SUMO. Chembiochem *6*, 1735-1743.

Uzunova, K., Gottsche, K., Miteva, M., Weisshaar, S.R., Glanemann, C., Schnellhardt, M., Niessen, M., Scheel, H., Hofmann, K., Johnson, E.S., *et al.* (2007). Ubiquitin-dependent proteolytic control of SUMO conjugates. J Biol Chem *282*, 34167-34175.

van Hagen, M., Overmeer, R.M., Abolvardi, S.S., and Vertegaal, A.C. (2010). RNF4 and VHL regulate the proteasomal degradation of SUMO-conjugated Hypoxia-Inducible Factor-2α. Nucleic Acids Res *38*, 1922-1931.

van Holde, K., and Zlatanova, J. (1994). Unusual DNA structures, chromatin and transcription. Bioessays *16*, 59-68.

Vashee, S., Simancek, P., Challberg, M.D., and Kelly, T.J. (2001). Assembly of the human origin recognition complex. J Biol Chem *276*, 26666-26673.

Venkitaraman, A.R. (2002). Cancer susceptibility and the functions of BRCA1 and BRCA2. Cell *108*, 171-182.

Venkitaraman, A.R. (2009). Linking the cellular functions of BRCA genes to cancer pathogenesis and treatment. Annu Rev Pathol *4*, 461-487.

Vertegaal, A.C., Andersen, J.S., Ogg, S.C., Hay, R.T., Mann, M., and Lamond, A.I. (2006). Distinct and overlapping sets of SUMO-1 and SUMO-2 target proteins revealed by quantitative proteomics. Mol Cell Proteomics *5*, 2298-2310.

Vertegaal, A.C., Ogg, S.C., Jaffray, E., Rodriguez, M.S., Hay, R.T., Andersen, J.S., Mann, M., and Lamond, A.I. (2004). A proteomic study of SUMO-2 target proteins. J Biol Chem *279*, 33791-33798.

Vethantham, V., Rao, N., and Manley, J.L. (2008). Sumoylation regulates multiple aspects of mammalian poly(A) polymerase function. Genes Dev *22*, 499-511.

Virag, L., Salzman, A.L., and Szabo, C. (1998a). Poly(ADP-ribose) synthetase activation mediates mitochondrial injury during oxidant-induced cell death. J Immunol *161*, 3753-3759.

Virag, L., Scott, G.S., Cuzzocrea, S., Marmer, D., Salzman, A.L., and Szabo, C. (1998b). Peroxynitrite-induced thymocyte apoptosis: the role of caspases and poly (ADP-ribose) synthetase (PARS) activation. Immunology *94*, 345-355.

Vodenicharov, M.D., Ghodgaonkar, M.M., Halappanavar, S.S., Shah, R.G., and Shah, G.M. (2005). Mechanism of early biphasic activation of poly(ADP-ribose) polymerase-1 in response to ultraviolet B radiation. J Cell Sci *118*, 589-599.

Vodenicharov, M.D., Sallmann, F.R., Satoh, M.S., and Poirier, G.G. (2000). Base excision repair is efficient in cells lacking poly(ADP-ribose) polymerase 1. Nucleic Acids Res *28*, 3887-3896.

von Kobbe, C., Harrigan, J.A., May, A., Opresko, P.L., Dawut, L., Cheng, W.H., and Bohr, V.A. (2003). Central role for the Werner syndrome protein/poly(ADP-ribose) polymerase 1 complex in the poly(ADP-ribosyl)ation pathway after DNA damage. Mol Cell Biol *23*, 8601-8613.

Wach, A., Brachat, A., Pohlmann, R., and Philippsen, P. (1994). New heterologous modules for classical or PCR-based gene disruptions in *Saccharomyces cerevisiae*. Yeast *10*, 1793-1808.

Wacker, D.A., Ruhl, D.D., Balagamwala, E.H., Hope, K.M., Zhang, T., and Kraus, W.L. (2007). The DNA binding and catalytic domains of poly(ADP-ribose) polymerase 1 cooperate in the regulation of chromatin structure and transcription. Mol Cell Biol *27*, 7475-7485.

Walden, H., Podgorski, M.S., and Schulman, B.A. (2003). Insights into the ubiquitin transfer cascade from the structure of the activating enzyme for NEDD8. Nature *422*, 330-334.

Waldman, B.C., and Waldman, A.S. (1990). Illegitimate and homologous recombination in mammalian cells: differential sensitivity to an inhibitor of poly(ADP-ribosylation). Nucleic Acids Res *18*, 5981-5988.

Wallace, J.A., and Felsenfeld, G. (2007). We gather together: insulators and genome organization. Curr Opin Genet Dev *17*, 400-407.

Walter, J.C., and Newport, J.W. (1999). The use of *Xenopus laevis* interphase egg extracts to study genomic dna replication. In Eukaryotic DNA replication: A practical approach, S. Cotterill, ed. (Oxford, Oxford University Press), pp. 201-221.

Wang, H., Rosidi, B., Perrault, R., Wang, M., Zhang, L., Windhofer, F., and Iliakis, G. (2005a). DNA ligase III as a candidate component of backup pathways of nonhomologous end joining. Cancer Res *65*, 4020-4030.

Wang, J., Bian, C., Li, J., Couch, F.J., Wu, K., and Zhao, R.C. (2008a). Poly(ADP-ribose) polymerase-1 down-regulates BRCA2 expression through the BRCA2 promoter. J Biol Chem *283*, 36249-36256.

Wang, J., and Chen, Y. (2010). Role of the Zn^{2+} motif of E1 in SUMO adenylation. J Biol Chem *285*, 23732-23738.

Wang, J., Hu, W., Cai, S., Lee, B., Song, J., and Chen, Y. (2007). The intrinsic affinity between E2 and the Cys domain of E1 in ubiquitin-like modifications. Mol Cell *27*, 228-237.

Wang, M., Wu, W., Rosidi, B., Zhang, L., Wang, H., and Iliakis, G. (2006). PARP-1 and Ku compete for repair of DNA double strand breaks by distinct NHEJ pathways. Nucleic Acids Res *34*, 6170-6182.

Wang, Q.E., Zhu, Q., Wani, G., El-Mahdy, M.A., Li, J., and Wani, A.A. (2005b). DNA repair factor XPC is modified by SUMO-1 and ubiquitin following UV irradiation. Nucleic Acids Res *33*, 4023-4034.

Wang, T., Simbulan-Rosenthal, C.M., Smulson, M.E., Chock, P.B., and Yang, D.C. (2008b). Polyubiquitylation of PARP-1 through ubiquitin K48 is modulated by activated DNA, NAD^+, and dipeptides. J Cell Biochem *104*, 318-328.

Wang, Y., and Dasso, M. (2009). SUMOylation and deSUMOylation at a glance. J Cell Sci *122*, 4249-4252.

Wang, Z.Q., Auer, B., Stingl, L., Berghammer, H., Haidacher, D., Schweiger, M., and Wagner, E.F. (1995). Mice lacking ADPRT and poly(ADP-ribosyl)ation develop normally but are susceptible to skin disease. Genes Dev *9*, 509-520.

Wang, Z.Q., Stingl, L., Morrison, C., Jantsch, M., Los, M., Schulze-Osthoff, K., and Wagner, E.F. (1997). PARP is important for genomic stability but dispensable in apoptosis. Genes Dev *11*, 2347-2358.

Watts, F.Z., Skilton, A., Ho, J.C., Boyd, L.K., Trickey, M.A., Gardner, L., Ogi, F.X., and Outwin, E.A. (2007). The role of *Schizosaccharomyces pombe* SUMO ligases in genome stability. Biochem Soc Trans *35*, 1379-1384.

Weger, S., Hammer, E., and Heilbronn, R. (2005). Topors acts as a SUMO-1 E3 ligase for p53 *in vitro* and *in vivo*. FEBS Lett *579*, 5007-5012.

Weisshaar, S.R., Keusekotten, K., Krause, A., Horst, C., Springer, H.M., Gottsche, K., Dohmen, R.J., and Praefcke, G.J. (2008). Arsenic trioxide stimulates SUMO-2/3 modification leading to RNF4-dependent proteolytic targeting of PML. FEBS Lett *582*, 3174-3178.

Welchman, R.L., Gordon, C., and Mayer, R.J. (2005). Ubiquitin and ubiquitin-like proteins as multifunctional signals. Nat Rev Mol Cell Biol *6*, 599-609.

Werner, A., Moutty, M.-C., Möller, U., and Melchior, F. (2009). Performing *in vitro* sumoylation reactions using recombinant enzymes. In SUMO Protocols, H.D. Ulrich, ed. (New York, Human Press), pp. 167-186.

Whatcott, C.J., Meyer-Ficca, M.L., Meyer, R.G., and Jacobson, M.K. (2009). A specific isoform of poly(ADP-ribose) glycohydrolase is targeted to the mitochondrial matrix by a N-terminal mitochondrial targeting sequence. Exp Cell Res *315*, 3477-3485.

Wielckens, K., George, E., Pless, T., and Hilz, H. (1983). Stimulation of poly(ADP-ribosyl)ation during Ehrlich ascites tumor cell "starvation" and suppression of concomitant DNA fragmentation by benzamide. J Biol Chem *258*, 4098-4104.

Wohlschlegel, J.A., Dwyer, B.T., Dhar, S.K., Cvetic, C., Walter, J.C., and Dutta, A. (2000). Inhibition of eukaryotic DNA replication by geminin binding to Cdt1. Science *290*, 2309-2312.

Wohlschlegel, J.A., Johnson, E.S., Reed, S.I., and Yates, J.R., 3rd (2004). Global analysis of protein sumoylation in *Saccharomyces cerevisiae*. J Biol Chem *279*, 45662-45668.

Woodhouse, B.C., and Dianov, G.L. (2008). Poly ADP-ribose polymerase-1: an international molecule of mystery. DNA Repair (Amst) *7*, 1077-1086.

Woodhouse, B.C., Dianova, II, Parsons, J.L., and Dianov, G.L. (2008). Poly(ADP-ribose) polymerase-1 modulates DNA repair capacity and prevents formation of DNA double strand breaks. DNA Repair (Amst) *7*, 932-940.

Wu, S.Y., and Chiang, C.M. (2009). Crosstalk between sumoylation and acetylation regulates p53-dependent chromatin transcription and DNA binding. EMBO J *28*, 1246-1259.

Xhemalce, B., Seeler, J.S., Thon, G., Dejean, A., and Arcangioli, B. (2004). Role of the fission yeast SUMO E3 ligase Pli1p in centromere and telomere maintenance. Embo J *23*, 3844-3853.

Xie, Y., Kerscher, O., Kroetz, M.B., McConchie, H.F., Sung, P., and Hochstrasser, M. (2007). The yeast Hex3-Slx8 heterodimer is a ubiquitin ligase stimulated by substrate sumoylation. J Biol Chem *282*, 34176-34184.

Xirodimas, D.P., Saville, M.K., Bourdon, J.C., Hay, R.T., and Lane, D.P. (2004). Mdm2-mediated NEDD8 conjugation of p53 inhibits its transcriptional activity. Cell *118*, 83-97.

Xu, Z., and Au, S.W. (2005). Mapping residues of SUMO precursors essential in differential maturation by SUMO-specific protease, SENP1. Biochem J *386*, 325-330.

Yamanaka, H., Penning, C.A., Willis, E.H., Wasson, D.B., and Carson, D.A. (1988). Characterization of human poly(ADP-ribose) polymerase with autoantibodies. J Biol Chem *263*, 3879-3883.

Yang, M., Hsu, C.T., Ting, C.Y., Liu, L.F., and Hwang, J. (2006a). Assembly of a polymeric chain of SUMO1 on human topoisomerase I *in vitro*. J Biol Chem *281*, 8264-8274.

Yang, N., Gong, F., Sun, L., Yang, D., Han, X., Ma, C., and Sun, Y. (2010). Poly (ADP-ribose) polymerase-1 binds to BCL2 major breakpoint region and regulates BCL2 expression. J Cell Biochem *110*, 1208-1218.

Yang, S.H., Galanis, A., Witty, J., and Sharrocks, A.D. (2006b). An extended consensus motif enhances the specificity of substrate modification by SUMO. EMBO J *25*, 5083-5093.

Yang, S.H., and Sharrocks, A.D. (2010). The SUMO E3 ligase activity of Pc2 is coordinated through a SUMO interaction motif. Mol Cell Biol *30*, 2193-2205.

Yang, X.J., and Gregoire, S. (2006). A recurrent phospho-sumoyl switch in transcriptional repression and beyond. Mol Cell *23*, 779-786.

Yang, Y.G., Cortes, U., Patnaik, S., Jasin, M., and Wang, Z.Q. (2004). Ablation of PARP-1 does not interfere with the repair of DNA double-strand breaks, but compromises the reactivation of stalled replication forks. Oncogene *23*, 3872-3882.

Yeh, E.T. (2009). SUMOylation and De-SUMOylation: wrestling with life's processes. J Biol Chem *284*, 8223-8227.

Yoshihara, K. (1972). Complete dependency of poly)ADP-ribose) synthesis on DNA and its inhibition by actinomycin D. Biochem Biophys Res Commun *47*, 119-125.

Yu, M., Schreek, S., Cerni, C., Schamberger, C., Lesniewicz, K., Poreba, E., Vervoorts, J., Walsemann, G., Grotzinger, J., Kremmer, E.*, et al.* (2005). PARP-10, a novel Myc-interacting protein with poly(ADP-ribose) polymerase activity, inhibits transformation. Oncogene *24*, 1982-1993.

Yu, S.W., Andrabi, S.A., Wang, H., Kim, N.S., Poirier, G.G., Dawson, T.M., and Dawson, V.L. (2006). Apoptosis-inducing factor mediates poly(ADP-ribose) (PAR) polymer-induced cell death. Proc Natl Acad Sci USA *103*, 18314-18319.

Yu, S.W., Wang, H., Poitras, M.F., Coombs, C., Bowers, W.J., Federoff, H.J., Poirier, G.G., Dawson, T.M., and Dawson, V.L. (2002). Mediation of poly(ADP-ribose) polymerase-1-dependent cell death by apoptosis-inducing factor. Science *297*, 259-263.

Yu, W., Ginjala, V., Pant, V., Chernukhin, I., Whitehead, J., Docquier, F., Farrar, D., Tavoosidana, G., Mukhopadhyay, R., Kanduri, C.*, et al.* (2004). Poly(ADP-ribosyl)ation regulates CTCF-dependent chromatin insulation. Nat Genet *36*, 1105-1110.

Yung, T.M., Parent, M., Ho, E.L., and Satoh, M.S. (2004). Camptothecin-sensitive relaxation of supercoiled DNA by the topoisomerase I-like activity associated with poly(ADP-ribose) polymerase-1. J Biol Chem *279*, 11992-11999.

Yunus, A.A., and Lima, C.D. (2009a). Purification of SUMO conjugating enzymes and kinetic analysis of substrate conjugation In SUMO Protocols, H.D. Ulrich, ed. (New York, Human Press), pp. 167-186.

Yunus, A.A., and Lima, C.D. (2009b). Structure of the Siz/PIAS SUMO E3 ligase Siz1 and determinants required for SUMO modification of PCNA. Mol Cell *35*, 669-682.

Yurchenko, V., Xue, Z., and Sadofsky, M.J. (2006). SUMO modification of human XRCC4 regulates its localization and function in DNA double-strand break repair. Mol Cell Biol *26*, 1786-1794.

Zaniolo, K., Desnoyers, S., Leclerc, S., and Guerin, S.L. (2007). Regulation of poly(ADP-ribose) polymerase-1 (PARP-1) gene expression through the post-translational modification of Sp1: a nuclear target protein of PARP-1. BMC Mol Biol *8*, 96.

Zhang, C., Roberts, T.M., Yang, J., Desai, R., and Brown, G.W. (2006). Suppression of genomic instability by SLX5 and SLX8 in *Saccharomyces cerevisiae*. DNA Repair (Amst) *5*, 336-346.

Zhang, X.D., Goeres, J., Zhang, H., Yen, T.J., Porter, A.C., and Matunis, M.J. (2008). SUMO-2/3 modification and binding regulate the association of CENP-E with kinetochores and progression through mitosis. Mol Cell *29*, 729-741.

Zhang, X.W., Yan, X.J., Zhou, Z.R., Yang, F.F., Wu, Z.Y., Sun, H.B., Liang, W.X., Song, A.X., Lallemand-Breitenbach, V., Jeanne, M.*, et al.* (2010). Arsenic trioxide controls the fate of the PML-RARα oncoprotein by directly binding PML. Science *328*, 240-243.

Zhang, Z., Hildebrandt, E.F., Simbulan-Rosenthal, C.M., and Anderson, M.G. (2002). Sequence-specific binding of poly(ADP-ribose) polymerase-1 to the human T cell leukemia virus type-I tax responsive element. Virology *296*, 107-116.

Zhao, X., and Blobel, G. (2005). A SUMO ligase is part of a nuclear multiprotein complex that affects DNA repair and chromosomal organization. Proc Natl Acad Sci USA *102*, 4777-4782.

Zhao, X., Wu, C.Y., and Blobel, G. (2004a). Mlp-dependent anchorage and stabilization of a desumoylating enzyme is required to prevent clonal lethality. J Cell Biol *167*, 605-611.

Zhao, Y., Kwon, S.W., Anselmo, A., Kaur, K., and White, M.A. (2004b). Broad spectrum identification of cellular small ubiquitin-related modifier (SUMO) substrate proteins. J Biol Chem *279*, 20999-21002.

Zheng, N., Wang, P., Jeffrey, P.D., and Pavletich, N.P. (2000). Structure of a c-Cbl-UbcH7 complex: RING domain function in ubiquitin-protein ligases. Cell *102*, 533-539.

Zhou, W., Ryan, J.J., and Zhou, H. (2004). Global analyses of sumoylated proteins in *Saccharomyces cerevisiae*. Induction of protein sumoylation by cellular stresses. J Biol Chem *279*, 32262-32268.

Zhu, G., Chang, P., and Lippard, S.J. (2010). Recognition of platinum-DNA damage by poly(ADP-ribose) polymerase-1. Biochemistry *49*, 6177-6183.

Zhu, J., Zhu, S., Guzzo, C.M., Ellis, N.A., Sung, K.S., Choi, C.Y., and Matunis, M.J. (2008). Small ubiquitin-related modifier (SUMO) binding determines substrate recognition and paralog-selective SUMO modification. J Biol Chem *283*, 29405-29415.

Zhu, L., Santos, N.C., and Kim, K.H. (2009). Small ubiquitin-like modifier-2 modification of retinoic acid receptor-α regulates its subcellular localization and transcriptional activity. Endocrinology *150*, 5586-5595.

Zong, W.X., Ditsworth, D., Bauer, D.E., Wang, Z.Q., and Thompson, C.B. (2004). Alkylating DNA damage stimulates a regulated form of necrotic cell death. Genes Dev *18*, 1272-1282.